Metabolic environment and epigenetic programming of the early embryo in rabbit

Romina Via y Rada

université PARIS-SACLAY

Metabolic environment and epigenetic programming of the early embryo in rabbit

Environnement métabolique et programmation épigénétique de l'embryon pré-implantatoire chez le lapin

Thèse de doctorat de l'université Paris-Saclay

École doctorale n°568 : signalisations et réseaux intégratifs en biologie (Biosigne)
Spécialité de doctorat : Aspect moléculaire et cellulaire de la biologie
Graduate School : Life Sciences and Health. Référent : Faculté de médecine

Thèse préparée dans l'unité de recherche **BREED (Université Paris-Saclay, UVSQ, INRAE)** sous la direction de **Véronique DURANTHON**, directrice de recherche, le co-encadrement de **Sophie CALDERARI**, chargée de recherche

Thèse soutenue à Paris-Saclay, le 06 décembre 2022, par

Romina VIA Y RADA

Composition du Jury

Jamileh MOVASSAT Professseure, HDR, Université Paris Cité	Présidente
Isabelle DONNAY Professseure, Université Catholique de Louvain	Rapporteur & examinatrice
Marc-André SIRARD Professseur, Université Laval	Rapporteur & examinateur
Nathalie BEAUJEAN Directrice de recherche, HDR, INRAE, Université de Lyon	Examinatrice
Hervé ACLOQUE Chargé de recherche, HDR, INRAE, Université Paris-Saclay	Examinateur

THESE DE DOCTORAT

NNT : 2022UPASL078

université PARIS-SACLAY

ÉCOLE DOCTORALE
Signalisations et réseaux intégratifs en biologie (BIOSIGNE)

Titre : Environnement métabolique et programmation épigénétique de l'embryon pré-implantatoire chez le lapin

Mots clés : environnement, épigénétique, programmation, embryon, métabolisme

Résumé : La prévalence mondiale des maladies métaboliques est en constante augmentation. De plus en plus de femmes commencent leur grossesse avec une mauvaise santé métabolique. L'exposition à des signaux environnementaux tels qu'une hyperglycémie et/ou l'hyperinsulinémie pendant le développement est associée à la programmation d'une mauvaise santé chez la descendance, étudiée par les Origines Développementales de la Santé et des Maladies (DOHaD). L'objectif de cette thèse était d'étudier les effets d'un taux élevé de glucose et/ou d'insuline au cours du développement préimplantatoire, précisément dans la masse cellulaire interne (MCI) progéniteur de l'embryon proprement dit, et le trophectoderme (TE) progéniteur du futur placenta, chez le lapin. L'analyse transcriptomique par RNA-seq a montré des changements mineurs dans la MCI et le TE des embryons exposés à une insuline élevée. Le glucose élevé, seul ou en combinaison avec l'insuline élevée, a entraîné des changements dans l'expression des gènes liés au métabolisme énergétique, à la signalisation cellulaire, à la régulation de l'expression des gènes et à la spécification de la MCI. En outre, une perturbation de l'homéostasie du nombre de cellules a été détectée dans la MCI et le TE des embryons exposés. L'analyse de la chromatine accessible par ATAC-seq a révélé des modifications spécifiques à chaque lignée, en particulier lors de l'exposition à un taux élevé de glucose et d'insuline.

Par conséquent, l'exposition à un taux élevé de glucose et/ou d'insuline pendant le développement préimplantatoire chez le lapin entraîne des réponses communes et spécifiques à chaque lignée qui pourraient compromettre le développement du futur individu et du placenta.

Title : Metabolic environment and epigenetic programming of the early embryo in rabbit

Keywords : environment, epigenetic, programming, embryo, metabolism

Abstract : The worldwide prevalence of metabolic diseases is continuously increasing leading to more women entering pregnancy with poor metabolic health. Exposure to environmental cues such as hyperglycemia and/or hyperinsulinemia during development is associated with programming to poor health in the offspring, as studied by the Developmental Origins of Health and Disease (DOHaD). The aim of this thesis was to investigate the effects of high glucose and/or high insulin during preimplantation development, precisely in the inner cell mass (ICM), progenitor of the embryo proper, and the trophectoderm (TE), progenitor of the future placenta, using the rabbit. Transcriptomic analysis by RNA-seq showed minor changes in the ICM and TE of embryos exposed to high insulin. High glucose alone or in combination with high insulin resulted in gene expression changes related to energy metabolism, cell signaling, gene expression regulation and, lineage commitment in the ICM. In addition, perturbation of cell number homeostasis was detected in the ICM and TE of exposed embryos. Accessible chromatin profiling by ATAC-seq further revealed lineage-specific chromatin changes, especially upon exposure to high glucose and high insulin.

Hence, exposure to high glucose and/or high insulin during preimplantation development in the rabbit results in common and lineage-specific responses that could compromise the development of the future individual and placenta.

REMERCIEMENTS

Je tiens tout d'abord à remercier aux membres de mon jury qui ont accepté d'évaluer mon travail de thèse. Je remercie **Isabelle Donnay** et **Marc-André Sirard** d'avoir accepté d'être les rapporteurs de mon manuscrit de thèse, et à **Jamileh Movassat**, ainsi qu'à **Nathalie Beaujean** et **Hervé Acloque** d'avoir accepté d'être les examinateurs de ce travail. De la même manière, je tiens à remercier aux membres de mon comité de suivi **Delphine Rousseau-Ralliard**, **Patrice Humblot** et **Bertrand Duvillié** pour vos conseils et suggestions sur ce travail.

Je voudrais remercier à **l'école doctorale Biosigne** pour avoir m'avoir accordé une bouse de thèse qui m'a permis faire ce travail. Je voudrais également remercier au **Département Phase de l'INRAE**, qui suite au contexte sanitaire m'ont financé deux mois pour rattraper un peu le retard, et au **LabEx Revive** pour avoir financé ma quatrième de thèse, une quatrième année indispensable pour achever les deux dernières objectives de cette thèse.

Je tiens à remercier à la direction de l'unité, à **Corinne Cotinot** pendant mes premières années de thèse et à **Pascale Chavatte-Palmer** pour la deuxième partie, merci pour votre l'accueil au sein de l'unité.

Je voudrais remercier énormément à mes directrices de thèse **Véronique Duranthon** et **Sophie Calderari**. Véronique, je te remercie pour les discussions scientifiques, les hypothèses partagées et pour tous tes conseils sur ce travail, spécialement avec la relecture de notre article. Merci également pour tes mots d'encouragement ces dernières semaines. Sophie, un immense merci à toi. Merci pour ton encadrement, pour avoir cru en moi depuis ce matin quand je suis arrivée au labo pour un entretien de stage M2. Quatre ans et demi se sont passés depuis, et je veux sincèrement te remercier pour ton soutien dans le plan professionnel mais aussi humain. Pour m'avoir enseigné, pour m'aider à reconnaitre mes forces et mes faiblesses. Merci de m'avoir permis d'avoir de l'autonomie dans cette thèse, notamment avec l'ATAC-seq, merci d'avoir cru que j'étais capable de le faire, même quand je n'y croyais pas. J'ai appris énormément et je t'en suis très reconnaissante.

Je voudrais remercier à l'ensemble de l'équipe **EPEE** : Alice, Cathy, Bernadette, Thierry, Fabienne, Laurent, Emilie, Gilles, Olivier, Martine, Amélie, Pierre, et aux restes des membres de l'équipe.
Un petit mot spécialement pour **Bernadette Banrezes**, merci pour tes petits mots d'encouragement, ils m'ont donné un coup d'énergie quand j'en avais besoin ! **Amélie Bonnet-Garnier**, merci pour ta bonne humeur, pour les moments de détente, pour tes petites attentions et pour tes conseils et discussions scientifiques. **Cathy Archilla**, Cathy !!! merci pour ta gentillesse, ta bienveillance, pour veiller sur nous « les étudiantes », pour nous rappeler ce qui est important, pour ton aide, tes conseils et ta bonne humeur. Travailler avec toi va énormément me manquer ! Merci aussi de m'avoir beaucoup aidé quand le RER C m'abandonnait ! **Alice Jouneau**, merci énormément pour tes mots d'encouragement ces dernières mois, pour les pauses café, pour me rappeler qu'il faut se reposer…et merci énormément pour tes conseils et m'avoir permis de travailler avec tes cellules et dans ton labo ! je n'aurai jamais pu avancer si vite sur mes manips ATAC-seq sans ton aide ! **Laurent Boulanger**, merci pour ta bonne humeur, pour les moments de rigolade, pour le petit lapin imprimé en 3D que je garderai avec moi comme un souvenir de ma thèse, merci pour les *n* chocolats que tu as partagés avec Mél et moi, et je suis désolée encore une fois de t'avoir « volé » tes petits flacons tous neuf et propres (Ils sont dans le labo 01 paillasse du

milieu…si jamais). **Emilie Trautmann**, merci pour ton aide lors des derniers manip's d'immunochirugie et par ta bonne humeur. **Olivier Dubois,** merci pour ces petites discussions du couloir, pour tes conseils, ta bonne humeur, pour avoir adopté le p'tit chat, j'aurais aimé avoir plus de temps pour prendre des pauses café avec toi ! **Gilles Charpigny**, merci pour tout le temps et travail que tu as accordé aux analyses statistiques sur nos données, et merci d'avoir pris le temps pour m'enseigner à les faire. **Pierre Adenot**, merci pour tes conseils et ton aide avec l'apotome.

Je voudrais également remercier **aux anciens EPEE**. **Vincent Brochard**, ou « Mr.20cents » merci énormément pour ton aide, surtout avec les mille problèmes administratifs que j'ai pu rencontrer (pas de remerciement pour la sous-préfecture de Palaiseau), ou avec mes déménagements, ou tellement choses ! merci pour ta bonne humeur, pour les moments de rigolade avec Mél, ce sont de loin les meilleurs souvenirs que je garderais de cette période ! **Nathalie Daniel**, Nath !! merci pour ta gentillesse, ton empathie et bienveillance, et merci de m'avoir enseigné à travailler sur l'embryon (le labo n'est plus le même sans toi !). Merci pour ton aide lors de manip's, pour tes conseils, pour me sauver quand il n'y avait plus de RER C, pour m'avoir énormément aidé lors de mon petit problème de santé. **Nathalie Peynot**, merci pour tes conseils et ton aide lors de manip's. **Eugénie Canon**, merci pour ta gentillesse et pour me « prêter » des kits pour mes manip's d'ATAC-seq ! (Je te dois des chocolats il me semble…), **Michelle Halstead**, merci pour tes conseils sur mes manip's d'ATAC-seq, et pour m'avoir donné les bases d'UNIX. J'en peux plus m'en passer ! Je voudrais également remercier à **Pierre Midrouillet**, qui a fait son stage de BTS avec moi et Sophie. Pierre, c'était un vrai plaisir de t'enseigner et d'apprendre avec toi.

Je voudrais remercier du fond du cœur à **Mélanie Pailles.** Mél, ma bbf, partner-in-lab, psy, cheerleader, chef 5 étoiles, traductrice EN<FR, et je pourrais continuer. Je ne sais pas comment te remercier en quelques lignes tout ce que ton amitié et ton soutien ont été pour moi. Tu as été la meilleure « partner in thèse » que j'ai pu avoir. Je suis sure et certaine que notre expérience en thèse est le début d'une longue amitié. Merci énormément pour tous ces pauses café, ces moments de rigolade et complicité, pour tous tes petites attentions quand j'en pouvais plus, pour m'écouter parler des mèmes problèmes mille fois, pour être heureuse de mes réussites et pour me soutenir dans les moments les plus difficiles. Je garde précieusement tous nos aventures au labo et en dehors <3.

Je voudrais remercier à **Luc Jouneau** et **Anne Frambourg**, merci énormément pour votre aide, pour m'avoir accordé du temps, pour répondu à toutes mes doutes, pour m'avoir enseigné et aidé avec l'analyse des données.

Je voudrais également remercier à tous les membres du **secrétariat de l'unité BREED**. Merci de m'avoir aidé avec les démarches administratives, parfois si compliqués. Merci spécialement à **Katia Tarassenko** et **Corinne Ferreira**, merci énormément de m'avoir aidé pour trouver des solutions avec les milles problèmes des demandes de visa, salaire, etc.

Je voudrais remercier à mes chères amis **Andreina** et **Alvaro**, ma vénézuélienne et espagnol préférés. *Andre, Al, no sé cómo agradecerles por tanto, por escucharme, por darme palabras de aliento, por creer en mí, por estar siempre, así sea con un mensajito. Gracias por todas nuestras salidas, por sacarme de la rutina del laboratorio, del estrés y llenarme de alegría con sus ocurrencias. Son uno de los regalos mas hermosos que mi vida en Francia me ha dado <3.*

Je voudrais remercier du fond du cœur à ma meilleure amie, **Valeria**.
Vale, hermana de la vida, ni la distancia ni la vida han cambiado ni un poquito esta hermosa amistad que compartimos. En estos últimos años, a pesar de estar tan lejos y tan ocupadas, ha sido la mejor amiga que uno puede desear. Gracias por alentarme, por escuchar mis audios de mil minutos y nunca quejarte, gracias por acompañarme en este periodo, por estar pendiente de mí, y creer en mí <3.

Faire une thèse, c'est beaucoup beaucoup du travail, et faire une thèse loin de ces proches, et encore plus difficile. Je n'aurais jamais pu être en train d'écrire ces lignes sans le soutien de ma famille. Il y a un peu plus de 6 ans, j'ai pris une décision assez difficile, je suis partie de mon pays et de ma zone de confort pour continuer ma formation scientifique en France. Ma famille, malgré la distance, le décalage horaire, la langue, m'a toujours accompagnée.
Mami, papi, hermani, *GRACIAS es una palabra que queda corta comparada a todo lo que han significado para mí en este periodo. Gracias por ser mi pilar, mi punto de encuentro cuando me siento perdida, gracias por acompañarme en cada decisión, aunque eso significara que estaría lejos de Uds. Gracias por cada mensaje de aliento, cada llamada, por cuidarme, por alegrarse por mí y celebrar cada paso que doy. Espero que este trabajo los haga sentirse orgullosos de mí, como lo soy yo de ser su hija <3.*

Et finalement, je dois remercier du fond du cœur à la personne qui m'a le plus soutenue et qui a célébré et souffert chaque petite expérience de cette thèse avec moi, **Rémi**. Mon amour, je ne pense pas pouvoir jamais te remercier tout ce que ton amour, soutien, douceur et bienveillance ont signifié pour moi en cette période, et spécialement pendant la rédaction de ce manuscrit. Merci de m'accompagner dans chaque expérience, chaque manip' réussi, chaque manip' qui partait à la poubelle, merci de m'avoir soutenu dans les moments les plus durs, de m'aider pour gérer mon stress, merci d'avoir pris soin de notre petit chez nous ces derniers mois, merci pour tes petits soins et attentions pour que je travaille dans les meilleures conditions. Merci de m'avoir écouté parler sans arrêt des ICM et TE pendant ces années sans jamais te plaindre, je pense que tu pourrais soutenir cette thèse à ma place maintenant ! Merci énormément mi amor, je ne serais pas arrivée jusqu'ici sans toi à mes côtés *<3*.

TABLE OF CONTENTS

LIST OF TABLES

INTRODUCTION

Chapter 1

Chapter 3

LIST OF FIGURES

INTRODUCTION

Chapter 1

Chapter 2

Chapter 3

RESULTS

Part I

Part II

DISCUSSION

LIST OF APPENDICES

LIST OF ABBREVIATIONS

5mC	5-methylcytosine
5hmC	5-hydroxymethylcitosine
3PG	3-phosphoglycerate

AA	Amino acids
ADA	American Diabetes Association
Acetyl-coA	Acetyl coenzyme A
ACLY	ATP-citrate lyase
ART	assisted reproductive technology
BB	Bio-breeding
bp	Base pair
BMI	Body mass index
cAMP	Cyclic adenosine monophosphate
CNTRL	Control
CVD	Cardiovascular disease
dpf	Days postfertilization
DARs	Differentially accessible regions
DEGs	Differentially expressed genes
DMRs	Differentially methylated regions
DOHaD	Developmental origins of health and disease
EGA	Embryonic genome activation
ESCs	Embryonic stem cells
EPC	Ectoplacental cone
ETC	Electron transport chain
ExE	Extraembryonic ectoderm
FAD	Flavin adenine dinucleotide
FASN	Fatty acid synthase
FATP4	Fatty acid transport protein 4
Fgf4	Fibroblast growth factor 4
FOAD	Fetal Origins of Adult Disease
FOXO	Forkhead box class O
FOXO1	Forkhead box O1
G6P	Glucose-6-phosphate
GDM	Gestational diabetes mellitus
GlcNAc	β-N-acetylglucosamine
GK	Goto Kakizaki
GLUTs	Glucose transporters
GLUT-1	Glucose transporter 1
GLUT-2	Glucose transporter 2
GLUT-4	Glucose transporter 4
GSIS	Glucose-stimulated insulin secretion
GSK3	Glycogen synthase kinase 3
GlyT	Glycogen trophoblast
HAT	Histone acetyltransferase
HbA1c	Hemoglobin A1c
HBP	Hexosamine biosynthetic pathway
HDAC	Histone deacetylases
HDMT	Histone demethylases

HFD	High fat diet
HG	High glucose
HGI	High glucose and high insulin
HK	Hexokinase
HMT	Histone methyltransferase
HPA	Hypothalamic-pituitary-adrenal
h.p.c.	Hours post-coïtum
ICM	Inner cell mass
ICRs	Imprinting control regions
IGF1	Insulin-like growth factor 1
IGF2	Insulin-like growth factor 2
IGF1R	Insulin-like growth factor 1 receptor
IGFR2	Insulin-like growth factor 2 receptor
IR	Insulin receptor
IRS	Insulin receptor substrates
IDF	International Diabetes Federation
JHDMs	Jumonji-domain-containing demethylases
LGA	Large for gestational age
LPD	Low protein diet
MAPK	Mitogenic-activated protein kinase
MBD	Methyl-CpG binding domain MBD
MCTs	Monocarboxylate transporters
MetS	Metabolic syndrome
MODY	Maturity onset diabetes of the young
mESCs	Mouse embryonic stem cells
miRNA	microRNA
mRNA	messenger RNA
mTORC1	Mechanistic target of rapamycin complex 1
mTORC2	Mechanistic target of rapamycin complex 2
MZT	Maternal to zygotic transition
ncRNAs	non-coding RNAs
NCD	Non-communicable diseases
NOD	Non-obese diabetic
NPD	Normal protein diet
OXPHOS	Oxidative phosphorylation
PC	Pyruvate carboxylase
PCOS	Polycystic ovarian syndrome
PDH	Pyruvate dehydrogenase complex
PDK1	Phosphoinositide-dependent kinase 1
Pdx1	Pancreatic and duodenal homeobox 1
PEPCK	Phosphoenolpyruvate carboxylase
PPARα	Peroxisome proliferator-activated receptor alpha
PFK-1	Phosphofructokinase 1
PFK-2	Phosphofructokinase 2

PFK	Phosphofructokinase
PGD	Pre-gestational diabetes
PI3K	PI3-kinase
PIP_2	Phosphatidylinositol 4,5-biphosphate
PIP_3	Phosphatidylinositol 3,4,5-triphosphate
piRNA	Piwi-interacting RNA
PKB	Protein kinase B
PKC	Protein kinase C
PPP	Pentose Phosphate Pathway
PTM	Post-translational modification
PVP	Polyvinylpyrrolidone
RER	Rough endoplasmic reticulum
RISC	RNA-induced silencing complex
ROS	Reactive oxygen species
RPKM	Reads Per Kilobase Million
RPM	Reads Per Million
S6K	S6 kinase
siRNA	Small interfering RNA
SAM	S-adenosylmethionine
SGA	Small for gestational age
SGLTs	Sodium-glucose transporters
SOS	Son-of-sevenless
SpT	Spongiotrophoblast
SREBP1	Sterol-regulatory element binding protein 1
STB	Syncytiotrophoblast
T1D	Type 1 diabetes
T2D	Type 2 diabetes
TBC1D4	TBC1 domain family member 4
TCA	Tricarboxylic acid
TE	Trophectoderm
TET	Ten-eleven translocation
TGCs	Trophoblast giant cells
TGF-β	Transforming growth factor beta
TNF	Tumor necrosis factor
TSS	Transcription start sites
TET3	TET methylcytosine dioxygenase 3
Xist	X-inactive specific transcript

PREAMBLE

The worldwide prevalence of metabolic diseases such as type 2 diabetes (T2D) is continuously increasing. In addition, nearly half of people, mostly with T2D, are undiagnosed and, therefore untreated. This increasing prevalence has resulted in more women entering pregnancy with poor metabolic health. Early signs of metabolic imbalances, often asymptomatic, such as hyperglycemia and/or hyperinsulinemia, are increasingly detected in women of childbearing age. In 2021, the International Diabetes Federation (IDF) established that one in six live births is affected by hyperglycemia in pregnancy.

The Developmental Origins of Health and Disease (DOHaD) concept highlights that early life exposures to environmental insults, such as suboptimal maternal metabolic status, are associated with short- and long-term consequences in the offspring, including a high risk of non-communicable diseases later in life. Extensive human epidemiological and animal experimentation studies have further supported the DOHaD concept. These studies have described critical developmental windows as particularly sensitive to environmental cues and programming. One of these developmental windows corresponds to the preimplantation period.

The preimplantation embryo is particularly vulnerable to environmental cues. During the first days of embryonic development, finely-tuned critical events involving epigenetic mechanisms take place. These include the reprogramming of parental genomes from specialized cells to a totipotent embryo, the transcriptional activation of the embryonic genome, and the first lineage specification giving rise to the inner cell mass (ICM) and the trophectoderm (TE), progenitors of the embryo proper and the future placenta, respectively. In addition, the oviduct and uterine fluid, in strict dependence on the maternal metabolic status, constitute the surrounding environment of the developing embryo. The oviduct and uterine fluid supply embryos with the energy substrates and growth factors necessary to support their development. Therefore, an altered composition, as demonstrated in animal models of diabetes, may influence preimplantation development.
Furthermore, preimplantation embryos have been shown to be sensitive to changes in their surrounding environment. Nutritional challenges, assisted reproductive technology (ART) have been associated with embryo molecular and cellular changes, altered phenotype at different periods of development, and disease risk. Notably, animal experimentation has highlighted that exposure exclusively during preimplantation development is sufficient to induce long-lasting irreversible adaptations leading to the progressive development of disease risk in adulthood.

Pre-gestational diabetes, that is, overt diabetes before conception, is associated with adverse outcomes and developmental programming in the offspring, especially in case of poor glycemic control during the first trimester. Preimplantation development takes place during a period when women are not yet aware of the pregnancy. Therefore, women with poor metabolic health may not receive the necessary interventions, exposing the developing embryo to metabolic imbalances.

The mechanisms by which hyperglycemia and/or hyperinsulinemia may affect preimplantation development and contribute to developmental programming are not fully understood. Animal models,

especially *in vitro* embryo culture strategies, offer a great opportunity to investigate the effects of hyperglycemia and/or hyperinsulinemia exclusively during the preimplantation period.

The aim of this thesis was to evaluate the effects of high glucose, high insulin, and both during preimplantation development. Thus, an *in vitro* model consisting of one-cell stage embryos developed to the blastocyst stage with high glucose and/or high insulin supplementation was developed in the rabbit. Furthermore, during preimplantation development, two lineages are specified: the ICM and the TE, each with specific epigenetic, transcriptomic, and metabolic signatures. Hence, this thesis aimed to evaluate the effects of high glucose and/or high insulin in the ICM and TE separately to identify possible lineage-specific responses. Thus, to determine the effects of high glucose and/or high insulin on the ICM and TE gene expression program of exposed embryos, we performed transcriptomic analysis by RNA-seq.

Transcriptome analysis provided evidence of changes in gene expression in both lineages, especially in embryos exposed to high glucose alone or in combination with high insulin. This work has been published in the journal *Cells*. In addition, the transcriptome of exposed embryos showed altered expression of genes implicated in epigenetic mechanisms, especially in the TE exposed to high glucose, while the ICM showed gene expression changes suggestive of perturbed lineage specification. Therefore, to investigate whether high glucose alone or in combination with high insulin may have altered the epigenetic landscapes of the ICM and TE of exposed embryos, we performed chromatin accessibility profiling by ATAC-seq. This second part of my thesis work will mostly correspond to preliminary results. The implementation of a suitable ATAC-seq protocol in our model was significantly delayed due to the COVID-19 pandemic. As a consequence, ATAC-seq libraries were send for sequencing earlier this year and were recently received and analyzed.

To better introduce my thesis work, I have organized the bibliographical introduction section into three chapters. In the first chapter, I describe the physiological bases of energy metabolism with a focus on glucose-insulin axis, followed by the context of diabetes, its increasing incidence and prevalence in younger populations worldwide, the diabetes types, and the context of diabetes in pregnancy. In the second chapter, I introduce the concept of DOHaD, the critical windows in development susceptible to programming, the potential role of epigenetic mechanisms, followed by the different environmental cues associated with programming in human and animal studies, with special attention to suboptimal maternal metabolic status, as is the context of prediabetes/diabetes. In the third chapter, I will describe the periconceptional period in the context of DOHaD, followed by the development of the preimplantation embryo and the key milestones that take place, its metabolism throughout development, the surrounding environment of preimplantation embryos, and end presenting current knowledge about preimplantation development in a prediabetic/diabetic *in vivo* and *in vitro* environment in the context of DOHaD.

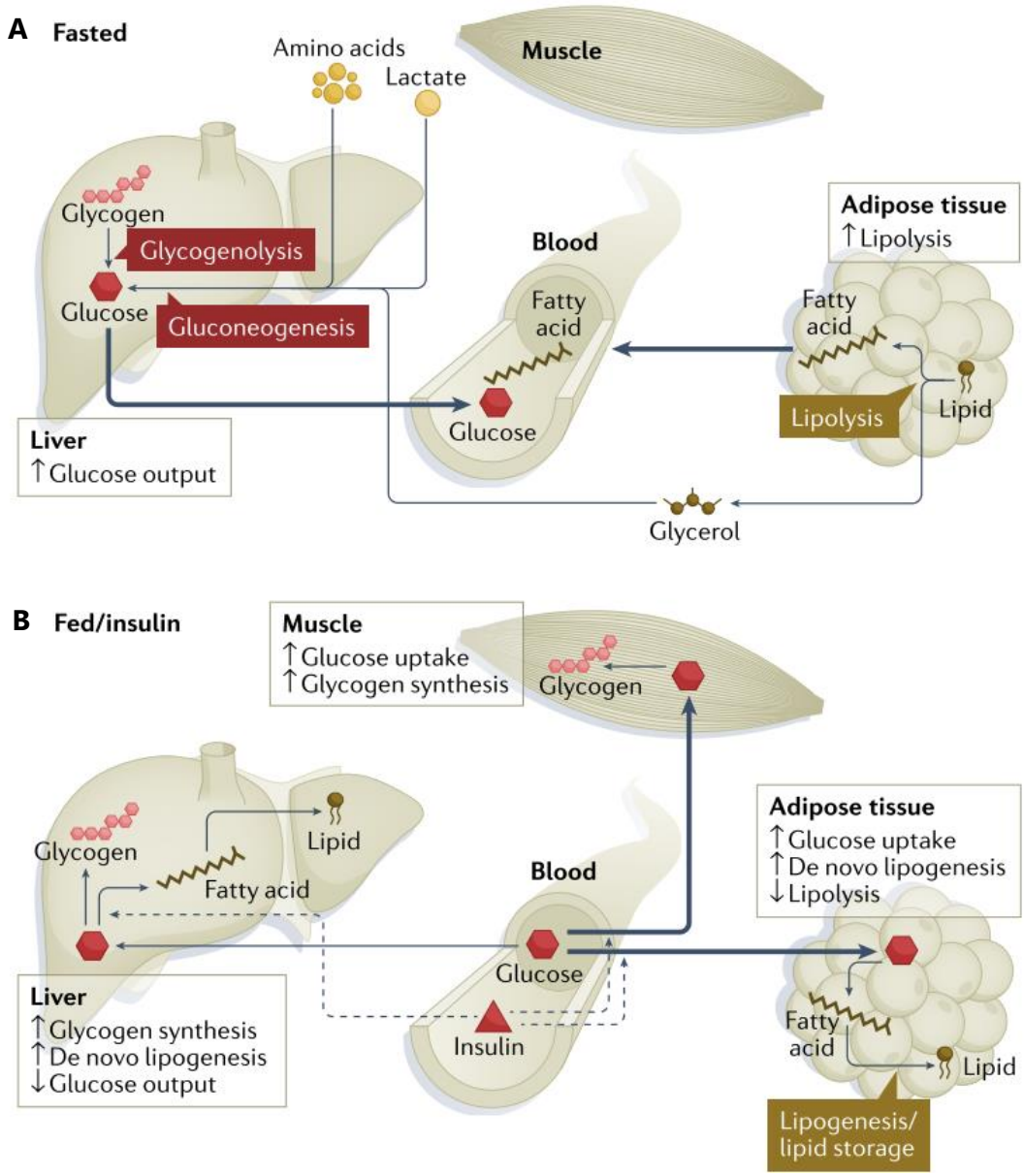

Figure 1: Tissue-specific insulin action on energy metabolism. Maintenance of steady circulating glucose levels is accomplished by the action of insulin and glucagon through glycogenolysis and gluconeogenesis. A) During fasting, circulating glucose levels are low, thus to maintain blood glucose levels pancreatic α-cells secrete glucagon (not shown), which stimulates glycogenolysis and gluconeogenesis in the liver, while the adipose tissue increases lipolysis. B) After feeding, circulating glucose levels rise triggering insulin production and secretion by pancreatic β-cells (not shown). In the liver, insulin suppresses gluconeogenesis and glycogenolysis, and rather stimulates glycogenesis and *de novo* lipogenesis. In the muscle, insulin stimulates glucose uptake as glycogen via glycogenesis. In the adipose tissue, insulin suppresses lipolysis and stimulates glucose uptake and *de novo* lipogenesis. From James et al., 2021.

INTRODUCTION

Chapter 1: Energy metabolism in health and disease

1. Physiological aspects of energy metabolism: the glucose-insulin axis

Every living organism needs energy to survive and carry out essential processes such as nutrition, growth, development, and reproduction. A fine-tuned cellular metabolism enables energy production and biosynthesis of macromolecules and metabolites essential for all cellular processes (Bar-Even et al., 2012). Key metabolic processes include glucose as a catabolic and anabolic substrate and insulin as the main regulator of whole-body energy homeostasis, especially in target tissues such as the liver, skeletal muscle, and adipose tissue (Tokarz et al., 2018). In target tissues, insulin influences glucose uptake, metabolism and storage, protein synthesis, lipogenesis, and cell growth (Boucher et al., 2014).

To better understand the influence of a disrupted glucose-insulin axis in pathophysiological contexts such as diabetes, it is necessary to understand the glucose-insulin axis in a physiological context. Therefore, this chapter will be divided into two parts. In the first part, I will summarize the glucose-insulin axis in a physiological context, and in the second part, I will describe the context of diabetes.

1.1 Role of insulin on energy metabolism

Glucose is the most important energy source for virtually all forms of life. In humans, circulating glucose is derived from intestinal absorption after feeding, from glycogenolysis, i.e., the breakdown of glycogen, the storage form of glucose, or from gluconeogenesis, i.e., the *de novo* synthesis of glucose from lactate and amino acids (AAs) (Aronoff et al., 2004). Glucose cannot be stored as is because high concentration of glucose would disturb the osmotic balance of the cell; consequently, glucose is stored in the form of glycogen via glycogenesis (Aronoff et al., 2004).

The maintenance of blood glucose levels throughout our fed and fasting cycles is finely regulated (Figure 1). Glycogenolysis and gluconeogenesis activity is critical for maintaining steady blood glucose levels (around 5.5 mM) (Chandel, 2021a).

After feeding, glucose levels rise, triggering insulin production and secretion by β-cells of the pancreas to lower circulating plasma glucose levels, known as the glucose-stimulated insulin secretion (GSIS) (Andrali et al., 2008; Campbell & Newgard, 2021; Tokarz et al., 2018). In addition, glucose stimulates the transcription and translation of insulin in β-cells (Andrali et al., 2008).
Insulin secretion and arrival to the liver through the portal vein suppresses gluconeogenesis and glycogenolysis, triggers glucose storage by glycogenesis, and stimulates *de novo* lipogenesis (Chandel, 2021a; James et al., 2021; Tokarz et al., 2018). Insulin similarly arrives at the muscle and adipose tissue, where it stimulates glucose uptake for storage, as glycogen via glycogenesis and triglycerides via *de novo* lipogenesis, respectively (Leto & Saltiel, 2012; Tokarz et al., 2018). Insulin also inhibits lipolysis in the adipose tissue (James et al., 2021). Myocytes are responsible for 90% of the insulin-stimulated glucose uptake, whereas adipocytes are in charge of the remaining 10% (Leto & Saltiel, 2012). Altogether, these insulin-triggered responses lower circulating glucose levels in the bloodstream (Figure

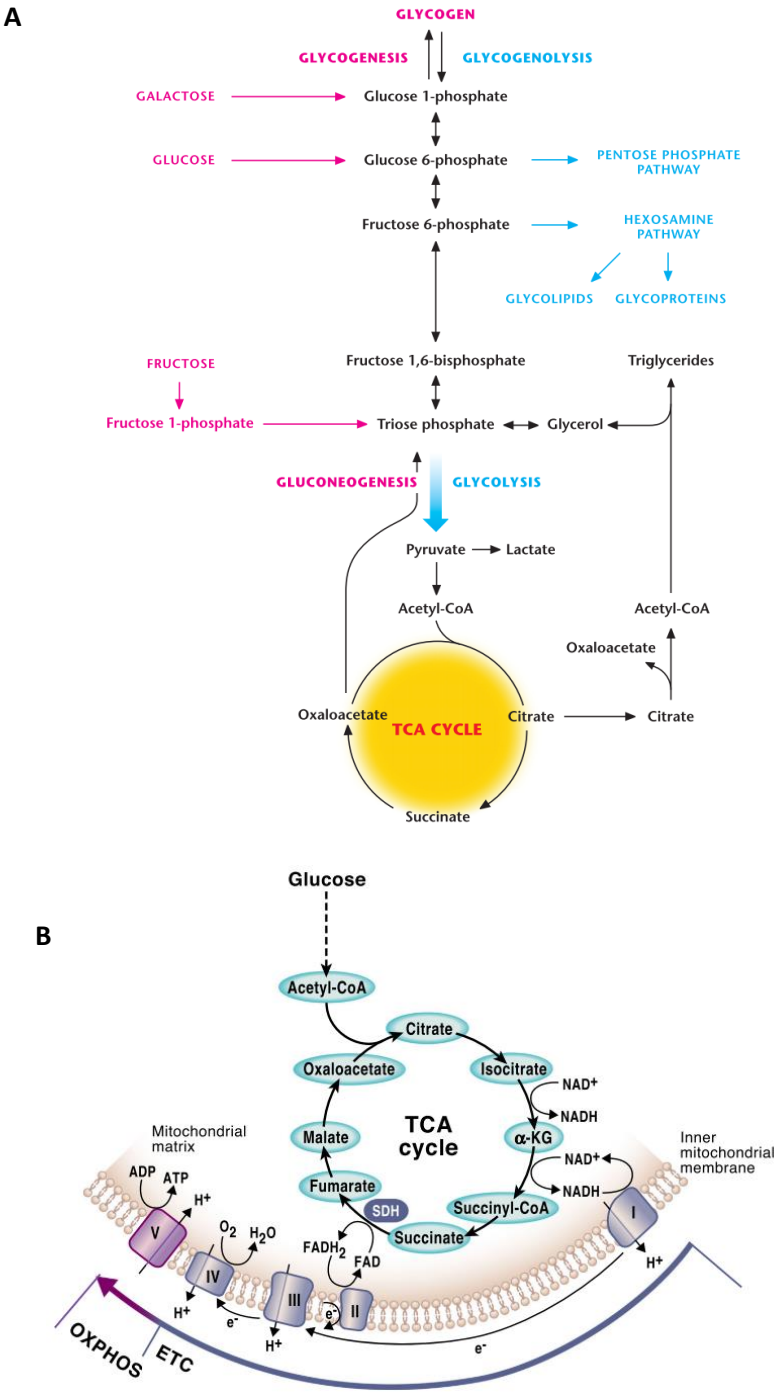

Figure 2. Overview of glucose metabolism. A) After entry to the cell, glucose is metabolized through glycolysis. Glycolysis results in the production of pyruvate. In the presence of oxygen, pyruvate can be used to generate acetyl-CoA, which feeds the TCA cycle by its conversion to citrate. In the absence of oxygen, pyruvate is reduced to lactate. Intermediates of glycolysis can feed the pentose phosphate pathway (PPP), hexosamine biosynthetic pathway (HBP) or enable the synthesis of triglycerides. The TCA-cycle intermediate oxaloacetate can be directed toward *de novo* glucose production via gluconeogenesis. Glucose can be converted to glycogen via glycogenesis and vice versa via glycogenolysis. B) TCA cycle generates NADH and $FADH_2$, which act as electron donors to the mitochondrial electron transport chain (ETC), generating energy in the form of ATP, a process is known as oxidative phosphorylation (OXPHOS). From Chandel, 2021; Martínez-Reyes & Chandel, 2020**.**

1). A few hours after feeding, we enter the fasting state. Circulating glucose levels decrease, which reduces insulin secretion, leading to pancreatic α-cells secretion of glucagon to stimulate liver gluconeogenesis (S. Guo, 2014). It should be noted that insulin is secreted continuously at low concentrations to maintain cellular functions but in a pulsatile manner to preserve insulin sensitivity because constant insulin secretion could result in insulin resistance (Seshadri & Doucette, 2021; Thomas et al., 2019).
In the fasting state, insulin levels decrease, and thus insulin-driven glucose uptake in muscle and adipose tissue is similarly reduced to maintain blood glucose levels and avoid hypoglycemia (Chandel, 2021a). In the adipose tissue, free fatty acids and glycerol are released via lipolysis to provide energy for the heart, muscle, and liver (Figure 1) (James et al., 2021). In the liver, glucagon inhibits glycogenesis, stimulates glycogenolysis, suppresses glycolysis, and stimulates gluconeogenesis through increased production of cyclic AMP (cAMP) to activate cAMP-dependent protein kinase A and convert phosphofructokinase-2 (PFK2) to fructose-2,6-biphosphatase (F-2,6-BPase) (Chandel, 2021a).
Upon re-entering the post-prandial state, glucose levels rise, and GSIS is stimulated (Chandel, 2021a). Glucagon immediately decreases, and cAMP is degraded, resulting in the activation of phosphofructokinase-1 (PFK1) and the stimulation of glycolysis, and the inhibition of gluconeogenesis (Chandel, 2021a). Thus, the metabolic events that regulate blood glucose levels are reinitiated (Chandel, 2021a) (Figure 1).

At the cellular level, glucose enters the cell, is phosphorylated, and, depending on the cellular context, is catabolized to provide energy in the form of ATP or used for anabolic functions, such as fatty acids production (Figure 2) (Chandel, 2021a).
Once in the cytoplasm, the breakdown of glucose through glycolysis, a ten-reactions metabolic pathway, produces two molecules of pyruvate, two molecules of ATP, and two molecules of NADH per molecule of glucose (Figure 2A) (Chandel, 2021b; Kaneko, 2016).
Further, the fate of glycolysis-derived pyruvate depends on the cell type and the availability of oxygen (Kaneko, 2016). In the presence of oxygen (aerobic glycolysis), pyruvate enters the mitochondria, where it is converted to acetyl-CoA by the pyruvate dehydrogenase complex (PDH), producing NADH and CO_2 (Bouché et al., 2004; Kaneko, 2016). Then, acetyl-CoA feeds the TCA cycle, which generates CO_2 and reduces NADH and $FADH_2$ (Figure 2B) (Bouché et al., 2004; Kaneko, 2016). In the mitochondria, NADH and $FADH_2$ are used as electron donors in the ETC, which produces 30 molecules of ATP and reactive oxygen species (ROS), a process referred to as oxidative phosphorylation (OXPHOS) (Figure 2B) (Chandel, 2021b; Kaneko, 2016). In the absence of oxygen, pyruvate and NADH are reduced into lactate and NAD^+ by the enzyme lactate dehydrogenase (Kaneko, 2016). The production of NAD^+ further stimulates the glycolytic flux (Kaneko, 2016).

The metabolic network of a cell is quite complex, and different substrates can feed metabolic pathways. During glucose metabolism, in addition to ATP generation, glycolytic intermediates can fuel multiple biosynthetic pathways (Chandel, 2021b). For example, glucose 6-phosphate (G6P) can enter the pentose phosphate pathway (PPP), generating ribose-5-phosphate (R5P), a precursor for nucleotide synthesis and NADPH, a reduction molecule essential in redox homeostasis (Chandel, 2021b; Kaneko, 2016). Dihydroxyacetone phosphate can generate glycerol 3-phosphate to synthesize lipids, whereas fructose 6-phosphate can be directed towards the hexosamine biosynthetic pathway (HBP), important for protein

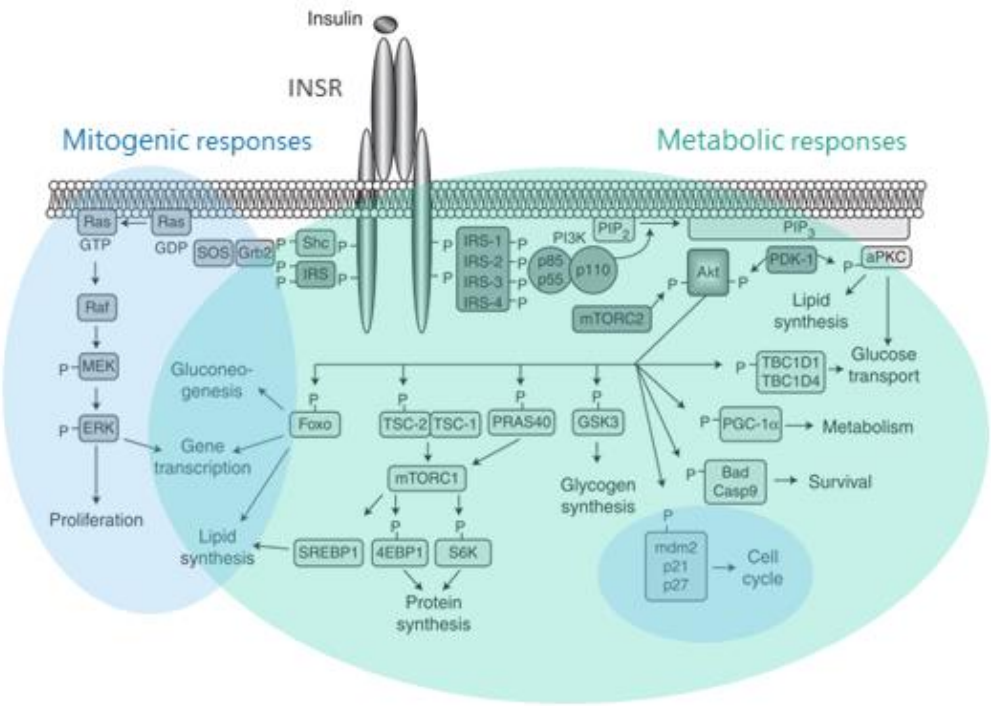

Figure 3: The insulin signaling pathway.

The cellular responses of the insulin signaling pathway can be simplified into two branches: the metabolic and the mitogenic responses. Insulin binding to its receptors triggers its autophosphorylation and activation. Activated INSR activates IRS proteins, which lead to the activation of the mitogenic branch through the phosphorylation cascade Shc-Grb2-SOS-Ras-GTP-Raf, MEK, ERK. Metabolic responses of insulin are mediated by the IRS recruitment of PI3K, leading to the formation of PIP3, phosphorylation, and activation of Akt, which itself is phosphorylated by PDK1 and mTORC2. Activated Akt drives several responses such as glucose transport, glycogen synthesis and contributes to cell cycle regulation and survival signals. INSR, insulin receptor; IRS, insulin receptor substrates. Adapted from Boucher et al., 2014.

glycosylation and synthesis of glycolipids, proteoglycans, and glycosylphosphatidylinositol anchors proteins Figure 2A) (Chandel, 2021a, 2021b).

1.2 The insulin signaling pathway

The insulin signaling pathway is constituted of a series of phosphorylation events that regulate the physiological responses to insulin, including glucose uptake, protein synthesis, metabolism, and growth (Boucher et al., 2014).

Insulin signaling initiates with insulin binding to the insulin receptor (IR) (Figure 3). The IR, situated on the plasma membrane of target cells, is constituted of a tyrosine kinase tetrameric protein formed by two extracellular α subunits and two transmembrane β subunits bound by disulfide bonds (Boucher et al., 2014). Furthermore, the tissue-specific alternative splicing of the exon-11 on the IR gene dictates the synthesis of isoforms IRa and IRb (M. F. White, 2003). These isoforms, together with the insulin-like growth factor 1 receptor (IGF1R), can form the heterodimer IR/IGF1R and bind insulin, insulin-like growth factor 1 (IGF-1), or insulin-like growth factor 2 (IGF-2) with different selectivity and affinity (M. F. White, 2003).

The binding of insulin to the extracellular α subunits of the IR triggers a conformational change, autophosphorylation, and activation of the tyrosine kinase activity of the β subunits (Boucher et al., 2014). Activation of the IR leads to the recruitment and phosphorylation of its substrates, such as insulin receptor substrates (IRS) and the Shc proteins (Boucher et al., 2014). From here, the insulin pathway can be divided into two main inter-connected pathways: the PI3-kinase (PI3K)/Akt pathway driving most of the metabolic effects of insulin, and the Raf/Ras/MEK/MAPK pathway driving mitogenic responses of insulin (Boucher et al., 2014). The PI3K/AKT pathway initiates with activated IRS leading to the recruitment, binding, and activation of PI3K heterodimers p85 or p55, resulting in the activation of the p110 catalytic subunit of PI3K (Boucher et al., 2014; Petersen & Shulman, 2018). Activation of PI3K catalyzes the generation of phosphatidylinositol 3,4,5-triphosphate (PIP_3) from membrane-bound phosphatidylinositol 4,5-biphosphate (PIP_2) (Boucher et al., 2014). Thereafter, PIP_3 recruits the serine/threonine kinase Akt, also known as Protein Kinase B (PKB), which is phosphorylated and activated by the phosphoinositide-dependent kinase 1 (PDK1) and mechanistic target of rapamycin complex 2 (mTORC2) (Boucher et al., 2014). Activated AKT phosphorylates several targets, including mechanistic target of rapamycin complex 2 (mTORC1), triggering its signaling cascade involved in the regulation of protein synthesis, glycogen synthase kinase 3 (GSK3) involved in the regulation of glycogenesis, the inhibition of forkhead box class O (FoxO) subfamily of transcription factors, such as FoxO1, involved in the regulation of gluconeogenic and lipogenic genes, and AS160 also known as TBC1 domain family member 4 (TBC1D4), involved in the regulation of GLUT-4 translocation for glucose uptake (Figure 3) (Boucher et al., 2014; Haeusler et al., 2017).

On the other hand, the mitogenic responses of insulin are mediated mainly by the Grb2-SOS-RaS-MAPK pathway. The IRS and Shc proteins are bound by Grb2, which is bound by son-of-sevenless (SOS) protein. SOS mediates the activation of Ras-GDP to Ras-GTP active form, which enables the consecutive activation of downstream effectors Raf, MEK, ERK1/2 (Figure 3) (Boucher et al., 2014). Phosphorylated ERK1/2 translocates to the nucleus and phosphorylates various targets, including transcription factors

GLUTs		
Member	**Preferred substrate (affinity in K_m)**	**Cell-type or tissue expression**
Class I		
GLUT-1	Glucose (~2 mM)	Erythrocytes, endothelial cells of blood-brain barrier, placenta, preimplantation embryos
GLUT-2	Glucose (~17-20 mM)	Pancreatic β-cells, hepatocytes, intestinal and kidney epithelial cells
GLUT-3	Glucose (1-2 mM)	Brain, sperm, placenta, immune cells, placenta
GLUT-4	Glucose (5 mM)	Heart, skeletal muscle, adipose tissue, placenta
GLUT-14	Glucose most likely	Testes, preimplantation embryos
Class II		
GLUT-5	Fructose and with lower affinity for glucose	Intestinal epithelial cells, kidney, sperm and in lower levels in muscle and adipose tissue
GLUT-7	Controversial. Low affinity for glucose and fructose	Small intestine, colon, testis and prostate
GLUT-9	Urate, glucose and fructose in lesser extent in kidney	Liver, kidney, preimplantation embryo, intestine, chondrocytes, placenta
GLUT-11	Glucose and fructose	Skeletal muscle and heart
Class III		
GLUT-6	Unknown, low affinity for glucose and fructose	Lymphocytes, spleen, brain
GLUT-8	Glucose and fructose	Testis, spermatozoa, blastocyst, heart, brain, lactating mammary gland alveolar cells, placenta
GLUT-10	Ascorbic acid	Liver, endocrine pancreas, vascular smooth muscle
GLUT-12	Glucose, fructose	Adipose tissue, heart, skeletal muscle, mammary gland alveolar cells, placenta
GLUT-13	Myoinositol	Brain
SGLTs		
SGLT1	Glucose, galactose	Small intestine and kidney
SGLT2	Glucose	Kidney
SGLT3	Glucose sensor	Enteric nervous system, muscle

Table 1: Glucose transporters expressed in human tissues.

GLUTs, glucose transporters; SGLTs, sodium-glucose transporters. References: Holman, 2020; Pizzagalli et al., 2021; Purcell & Moley, 2009; Stanirowski et al., 2018; Thorens & Mueckler, 2010; Wright et al., 2011.

involved in cell growth, survival, and cell differentiation (Taniguchi et al., 2006). Noteworthy, the metabolic actions of insulin are triggered with lower concentrations of insulin than the mitogenic responses (Petersen & Shulman, 2018).

1.3 Glucose transport and uptake

Glucose entry into the cell is mediated by two families of transporters: the GLUT family through facilitative diffusion (energy-independent) and the sodium-glucose transporters (SGLTs) through active transport against its concentration gradient (energy-dependent) (Table 1) (Purcell & Moley, 2009; Thorens & Mueckler, 2010).

The solute carrier 2 (SLC2) gene subfamily members facilitate the membrane transport of nutrients (Holman, 2020). Within the SLC2 subfamily lie 14 members classified into three classes of GLUTs proteins (Holman, 2020). The GLUTs members are characterized by different affinity and specificity to hexoses, tissue distribution, subcellular localization, and physiological function Table 1) (Leto & Saltiel, 2012).
Class 1 includes GLUT-1, GLUT-2, GLUT-3, GLUT-4, and GLUT-14, and are the most extensively studied GLUTs in the context of glucose homeostasis Table 1) (Holman, 2020). Class 2 includes GLUT-5, GLUT-7, GLUT-9, and GLUT-11, and class 3 includes GLUT-6, GLUT-8, GLUT-10, GLUT-12, and GLUT-13 Table 1) (Holman, 2020). The substrate of preference for class 2 GLUTs is fructose rather than glucose, but transport of alternative non-hexose substrates may also be involved (Holman, 2020).

The SGLTs proteins belong to the SLC5 subfamily and include 12 members (Pizzagalli et al., 2021). However, not all members have been reported to transport glucose (Pizzagalli et al., 2021). Among SGLTs proteins implicated in glucose transport, there is SLC5A1 (SGLT1) which transports glucose but also galactose in the small intestine and kidneys, and SLC5A2 (SGLT2), which is implicated in glucose reabsorption in the kidney cortex Table 1) (Pizzagalli et al., 2021). Interestingly, SLC5A4 (SGLT3) has been described as a glucose sensor in the plasma membrane of tissues rather than in glucose transport (Pizzagalli et al., 2021).

Among GLUT members, a few are responsive to insulin, such as GLUT-4, the master insulin-dependent transporter, GLUT-8 in preimplantation embryos (blastocysts), and GLUT-12 (Wood & Trayhurn, 2003). The rest of GLUTs, such as GLUT-2 are not dependent on insulin stimuli and allow glucose entry through facilitated diffusion (Petersen & Shulman, 2018).
GLUT-4 is a high-affinity insulin-dependent glucose transporter, mainly expressed in myocytes and adipocytes (Leto & Saltiel, 2012). In the absence of insulin, GLUT-4 is mainly found in the intracellular space between endosomes, the trans-Golgi network, and within GLUT-4 storage vesicles (Leto & Saltiel, 2012). In the post-prandial state, insulin stimulates glucose uptake in the muscle and adipose tissue, triggering the rapid trafficking of GLUT4 from intracellular stores to the plasma membrane to take up circulating glucose (Leto & Saltiel, 2012).

At the cellular level, insulin signaling activates PI3K and synthesis of PIP3 (Leto & Saltiel, 2012). PIP3 acts as the docking site of several kinases implicated in glucose uptake, including PDK1 and AKT (Leto & Saltiel, 2012). PDK1 and mTORC2 phosphorylate and activate AKT, and AKT orchestrates GLUT4 trafficking (Leto & Saltiel, 2012). Indeed, as shown by functional studies, IRS and AKT core members of

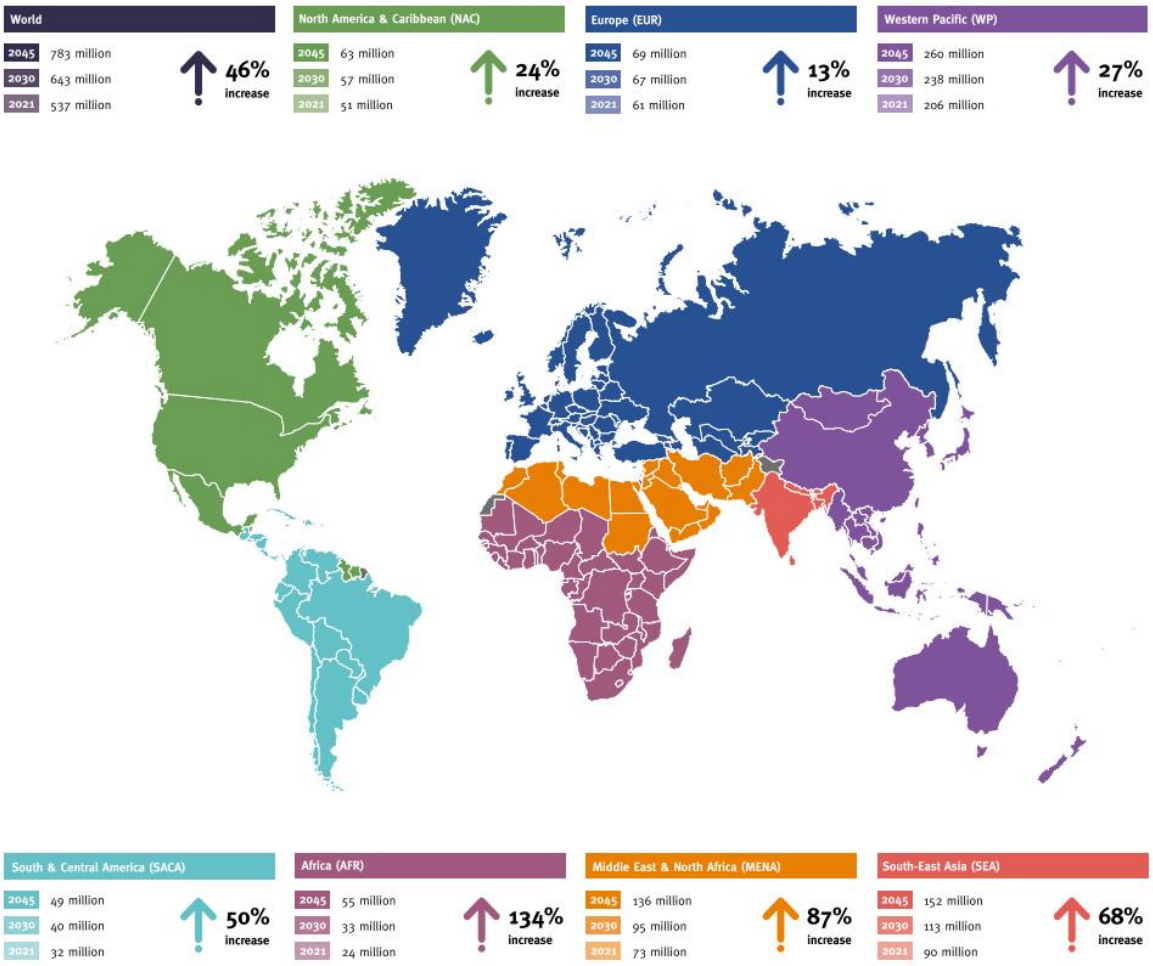

Figure 4: Global estimates of diabetes prevalence in adults (20-79 years) in 2021 and estimated projections to 2045. In 2021, approximately 537 million adults (20-79 years) had diabetes. Estimates for 2045 indicate a 46% increase in the prevalence of diabetes. Africa IDF region estimates indicate a 134% increase for 2045, followed by the middle East and North Africa region with 87%. In Europe, in 2021, 61 million people had diabetes, estimated to increase by 13% by 2045. From the IDF, 2021.

the insulin signaling pathway are necessary for insulin-stimulated glucose uptake (Leto & Saltiel, 2012). AKT mediates GLUT-4 exocytosis via several actors, including small GTPases (Leto & Saltiel, 2012).
Overall GLUT-4 translocation requires three main steps: the transit of GLUT-4 from the intracellular space, the recognition of GLUT-4-containing vesicles at the cell membrane, and the fusion of the two at the cell membrane (Leto & Saltiel, 2012). Nevertheless, in adipocytes, PI3K-dependent and independent mechanisms may take place in glucose uptake (Petersen & Shulman, 2018).
In the absence of insulin, GLUT4 is rapidly endocytosed through clathrin-mediated endocytosis and cholesterol-dependent endocytosis (Leto & Saltiel, 2012). The rapid GLUT-4 endocytosis and slow exocytosis prevent hypoglycemia (Leto & Saltiel, 2012).

2. Diabetes: pathological aspects of energy metabolism

Diabetes mellitus, more frequently known as diabetes, is a group of chronic metabolic diseases associated with elevated glucose levels or hyperglycemia and impaired insulin secretion and/or insulin resistance (International Diabetes Federation, 2021).

Diabetes constitutes a major health, social and economic burden. Diabetes is a chronic condition requiring lifelong follow-up, lifestyle changes that often extend to family members, and significant direct healthcare expenditures. In terms of global healthcare expenditure alone, the burden of diabetes has accounted for a 316% increase over fifteen years and is projected to continue to rise (International Diabetes Federation, 2021).
The prevalence of diabetes is alarmingly increasing worldwide (Figure 4). As the 2021 report of the IDF recently stated, diabetes is "one of the fastest growing global health emergencies of the 21st century" (International Diabetes Federation, 2021). More than one in ten adults live with diabetes (International Diabetes Federation, 2021). Approximately 537 million adults between the ages of 20 and 79 have some form of diabetes, representing 10.5% of the global population in this age group (International Diabetes Federation, 2021). In addition, projections from 2021 to 2045 indicate an alarming 46% increase in people with diabetes worldwide, including diagnosed and undiagnosed diabetes (Figure 4) (International Diabetes Federation, 2021). Furthermore, the prevalence of diabetes in the younger population, i.e., in children and adolescents up to 19 years old, is also increasing yearly (International Diabetes Federation, 2021).

Diabetes is a group of metabolic diseases and is classified by its etiology and pathophysiology into type 1 diabetes (T1D), type 2 diabetes (T2D), and other rare forms of diabetes, including monogenic diabetes (International Diabetes Federation, 2021). Additionally, gestational diabetes mellitus (GDM) is another type of diabetes exclusively developed during pregnancy.

Pregnancy can be affected by diabetes, either in the form of GDM, or by pre-gestational diabetes (PGD), i.e. overt diabetes diagnosed prior to conception. To better address diabetes in pregnancy, both GDM and PGD will be detailed at the end of this chapter.

2.1 Type 1 diabetes

Type 1 diabetes is characterized by a severe deficiency in insulin secretion and resultant hyperglycemia (Katsarou et al., 2017). Consequently, people with T1D depend on exogenous daily insulin

administration to mimic insulin release and maintain glycemic control (International Diabetes Federation, 2021).

In 70-90% of T1D cases, impaired insulin secretion is caused by the autoimmune destruction of the pancreatic β cells (Katsarou et al., 2017). However, the etiology of T1D is not fully understood. It is considered that a combination of factors, including genetic predisposition, viral infections, gut microbiota, nutrition, and other environmental triggers, may play a part in the destruction of β cells and the onset of T1D (Ilonen et al., 2019; Katsarou et al., 2017). To date, type 1 diabetes cannot be prevented (International Diabetes Federation, 2021).

Since the discovery of insulin in 1921, T1D is a treatable disease (DiMeglio et al., 2018). However, tight glycemic control is crucial in people with T1D to avoid or reduce the risk of complications and life-threatening conditions (DiMeglio et al., 2018). Type 1 diabetes most common complications include hypoglycemia, diabetic ketoacidosis, i.e., a life-threatening condition characterized by the buildup of ketone bodies; microvascular complications such as retinopathy, nephropathy, cognitive function, and macrovascular complications such as atherosclerosis, thrombosis in the heart, peripheral arteries and brain (DiMeglio et al., 2018).

2.1.1 Epidemiology of type 1 diabetes

Type 1 diabetes represents 10-15% of all cases of diabetes (Katsarou et al., 2017). Its incidence and prevalence are increasing by 2-3% per year worldwide (DiMeglio et al., 2018). In France, the incidence of T1D increases by 4% per year (Piffaretti et al., 2019).

Type 1 diabetes can develop at any age, but it is most frequent in children, adolescents, and young adults, with the highest incidence peak around 10-14 years old (DiMeglio et al., 2018). In 2017, global prevalence estimates showed that 9 million people, mostly from high-income countries, had T1D (World Health Organization, 2021a). In the younger population, the 2021 global estimates revealed that 2.61 billion children and adolescents had T1D (International Diabetes Federation, 2021).

The worldwide incidence of T1D in children and adolescents up until 19 years old revealed 149,500 new T1D cases per year (International Diabetes Federation, 2021).
The incidence of T1D varies between countries. The countries with the highest incidence of T1D in children and adolescents up until 19 years old in 2021 were India, followed by USA and Brazil (International Diabetes Federation, 2021). In addition, incidence estimates per 100,000 people in children up to 14 years old showed the highest incidence rates in Finland, followed by Sweden and Kuwait (International Diabetes Federation, 2021).
However, the estimation of T1D incidence rates in adults is more complicated because T1D is often misdiagnosed as T2D (DiMeglio et al., 2018). Incidence estimates per 100,000 people showed the highest incidence rates of T1D in adults in Eritrea, Sweden, and Ireland (International Diabetes Federation, 2021).

A comparison of incidence trends between boys and girls shows a similar overall trend, but the incidence peak in girls appears to precede the one in boys (Katsarou et al., 2017). This difference in the timing of

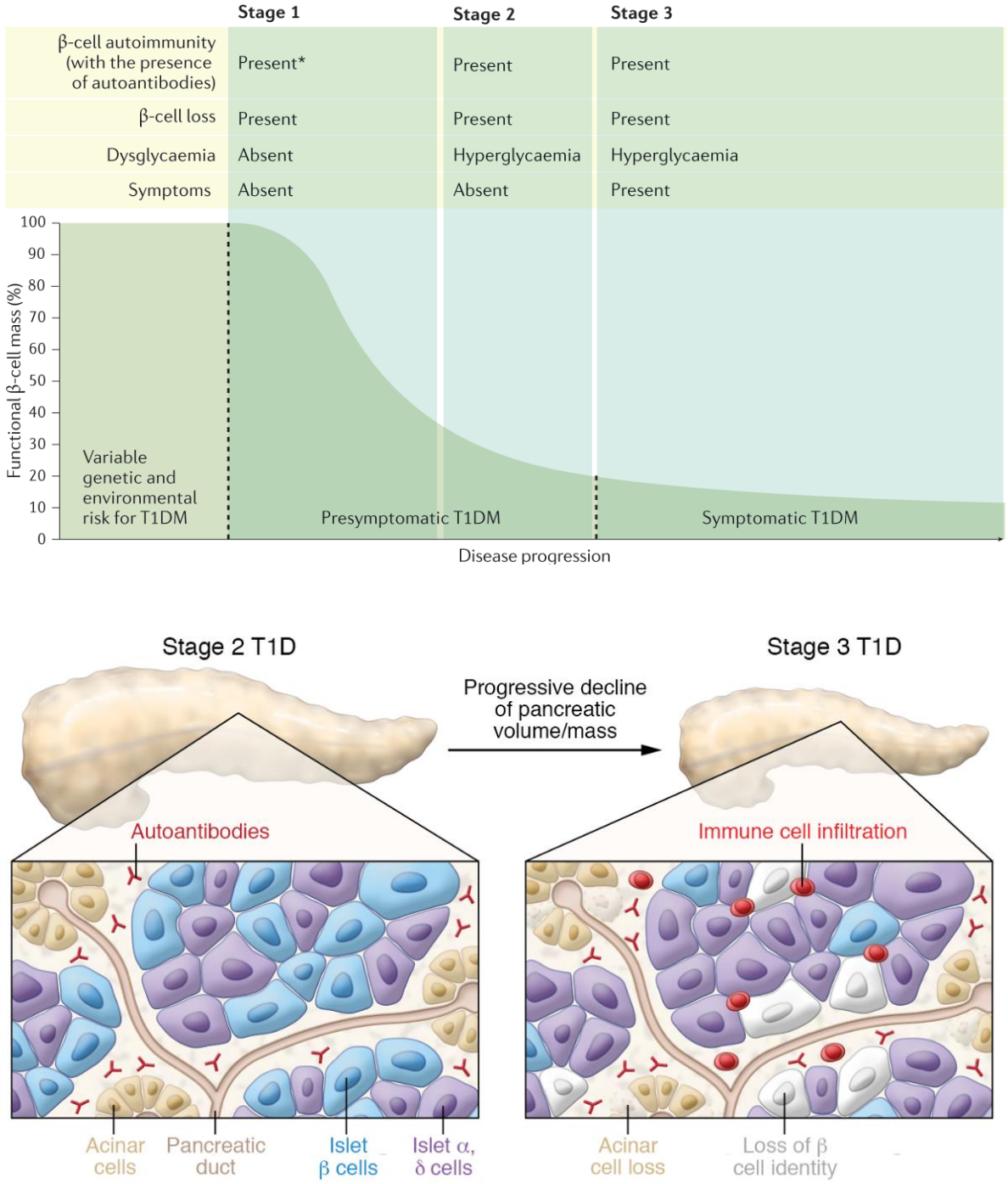

Figure 5: Stages in the progression of type 1 diabetes.

After a trigger event type 1 diabetes is developed. Three stages of disease progression have been identified. The first stage is asymptomatic and characterized by the presence of autoantibodies targeting insulin-producing β-cells, β-cells loss and euglycemia. The second stage also asymptomatic is characterized by increased accumulation of autoantibodies (bottom left panel), increasing β-cells loss and hyperglycemia. The third stage is symptomatic and characterized by a higher presence of autoantibodies, infiltration of immune cells, significant reduction in functional β-cell mass (upper panel) and pancreatic volume (bottom right panel), severe reduction in insulin secretion (not shown), and hyperglycemia. T1DM, type 1 diabetes mellitus. From Katsarou et al., 2017; Powers, 2021.

incidence has been attributed to puberty, which is typically earlier in girls than boys (Katsarou et al., 2017).
In adults with T1D, there is a different scenario. Examination of adult-onset T1D in 32 counties between 1973 and 2019 showed a higher incidence among men than women aged between 20 to 40 years (International Diabetes Federation, 2021).

2.1.2 Pathophysiology of type 1 diabetes

Type 1 diabetes is an immune-related disease characterized by the destruction of insulin-producing β-cells (DiMeglio et al., 2018; Katsarou et al., 2017). The progression of T1D and the reduction of functional β-cell mass occurs progressively (Figure 5).
Three stages of disease progression have been identified (Figure 5) (Katsarou et al., 2017). The first stage, usually presymptomatic, is characterized by the accumulation of two or more β-cell-targeting autoantibodies without dysglycaemia (DiMeglio et al., 2018; Katsarou et al., 2017). The first stage can be established months to years before β-cell loss (DiMeglio et al., 2018; Katsarou et al., 2017). The presence of autoantibodies is detected in 70-90% of people with T1D and is classified as type 1a diabetes (Katsarou et al., 2017). However, in a reduced group of individuals, no autoantibodies are detected, and the cause of β-cell loss is unknown; these cases are referred to as idiopathic T1D diabetes or type 1b diabetes (Katsarou et al., 2017).
The second stage, usually still presymptomatic, is characterized by the accumulation of β-cell-targeting autoantibodies, hyperglycemia, and loss of insulin release in a glucose tolerance test (Figure 5) (Katsarou et al., 2017). Although it is not currently known whether hyperglycemia and loss of GSIS response originate from β-cell loss and/or β-cell failure (Katsarou et al., 2017). The second stage can last more than a year before progressing to the third stage (Katsarou et al., 2017).
The third stage is also characterized by the presence of autoantibodies and hyperglycemia but is now symptomatic and corresponds to the time of clinical diagnosis in more than 95% of cases (Figure 5) (Katsarou et al., 2017).

The glucose-insulin axis is disrupted in people with T1D. In untreated T1D, insulin is no longer produced; therefore, insulin-stimulated glucose uptake is reduced, resulting in persistent hyperglycemia. Insulin deprivation triggers a catabolic state, affecting energy stores and protein mass (Hebert & Nair, 2010). Reduced glucose uptake triggers the use of alternative sources for energy production, such as the conversion of fatty acids into ketone bodies in the liver (Katsarou et al., 2017). Excessive production of ketone bodies leads to their accumulation and diabetic ketoacidosis (Katsarou et al., 2017).
In addition, people with T1D have elevated glucagon levels and increased energy expenditure, contributing to the overall catabolic state (Hebert & Nair, 2010). Increased glucagon levels in untreated or poorly treated T1D patients may increase gluconeogenesis, further contributing to hyperglycemia (Hebert & Nair, 2010). In the muscle, insulin deprivation results in increased protein breakdown and reduced protein synthesis (Hebert & Nair, 2010).

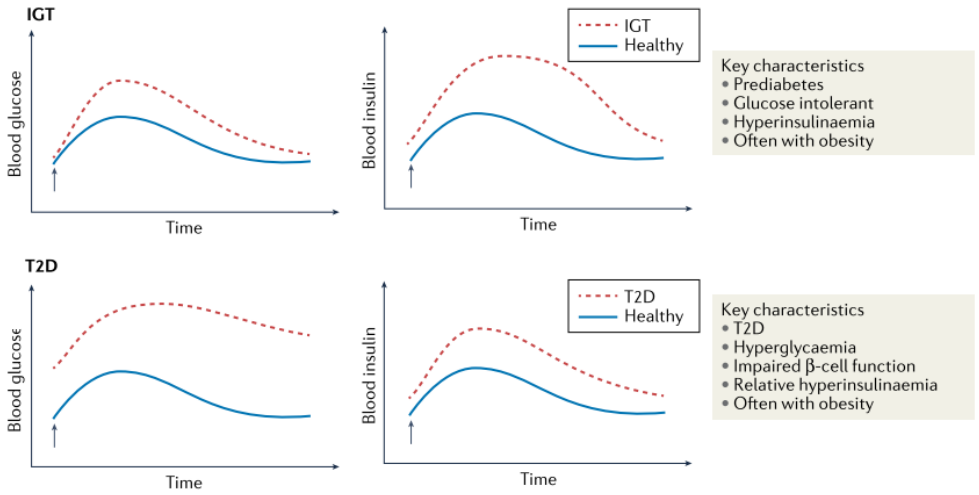

Figure 6: Disease progression of type 2 diabetes.
Progression from prediabetes states to T2D. Blood glucose (left panel) and insulin levels (right panel) after an oral glucose tolerance test (arrow) in healthy individuals (blue curve) versus individuals with impaired glucose tolerance (IGT) (upper red curve) or overt T2D (bottom red curve). Upper panel: Individuals with IGT show hyperinsulinemia compared to healthy individuals after an oral glucose load. Bottom panel: Individuals with T2D show higher fasting glucose levels, glucose intolerance and relative hyperinsulinemia insufficient to lower blood glucose levels compared to healthy individuals. Adapted from James et al., 2021.

		Prediabetes	
Screening test	**Healthy**	**Impaired fasting glucose**	**Impaired glucose tolerance**
Fasting plasma glucose	**5.6 - 6.1 mmol/L** (<100 – 110 mg/dL)	**IDF: 6.1 – 6.9 mmol/L** (110- 125 mg/dL) **ADA: 5.6 – 6.9 mmol/L** (100- 125 mg/dL)	**<7.0 mmol/L** (126 mg/dL)
		and	and if measured
Oral glucose tolerance test	**7.8 mmol/L** (<140 mg/dL)	**<7.8 mmol/L** (140 mg/dL)	**≥7.8 - <11.1 mmol/L** (140 – 200 mg/dL)
Glycated hemoglobin (HbA1c)	**<5.7-6.0%** (39 – 42 mmol/mol)	**5.7 – 6.4%** (39 – 47 mmol/mol)	

Table 2. Diagnostic criteria for prediabetes.
Prediabetes is diagnosed when impaired fasting glucose and/or impaired glucose tolerance detected, and/or when glycated hemoglobin values are above the normal threshold. Diagnostic criteria for impaired fasting glucose for the International Diabetes Federation (IDF) and American Diabetes Association (ADA) are shown. Adapted from International Diabetes Federation, 2021; DeFronzo et al., 2015; American Diabetes Association, 2021.

2.2 Type 2 diabetes

Type 2 diabetes is characterized by impaired insulin secretion by β-cell dysfunction and/or insulin resistance, resulting in hyperglycemia (Chatterjee et al., 2017; International Diabetes Federation, 2021). During the first stages of the disease, from prediabetes to overt T2D, insulin resistance results in enhanced insulin production as a compensatory mechanism to reduced blood glucose (Figure 6) (Chatterjee et al., 2017; International Diabetes Federation, 2021; James et al., 2021). Excessive insulin production leads to β-cell failure and loss (Chatterjee et al., 2017).

The causes of T2D are not entirely understood. Still, it is well established that overweight and obesity, sedentary lifestyle, energy-dense diets, increasing age, ethnicity, and genetic predisposition are risk factors for T2D (Chatterjee et al., 2017; International Diabetes Federation, 2021). From these, obesity is considered the leading risk factor for T2D development, mainly since 60% or, in some cases, up to 90% of people with T2D are obese and show insulin resistance (Chatterjee et al., 2017; Reed et al., 2021). The association between obesity and T2D is such that the term "diabesity" is often used (Reed et al., 2021).

Type 2 diabetes, when untreated or poorly intervened, can lead to severe complications, including cardiovascular disease, neuropathy, retinopathy, and nephropathy (Kaul et al., 2012). In addition, T2D is the leading cause of blindness and limb amputation and is a risk factor for Alzheimer's and Parkinson's diseases (Reed et al., 2021).

The development of T2D takes place progressively. Early metabolic imbalances such as hyperglycemia and/or hyperinsulinemia i.e., excess circulating insulin; can be present years before diagnosis of diabetes, a condition referred to as prediabetes.

2.2.1 Prediabetes

Metabolic dysregulations such as hyperglycemia and/or hyperinsulinemia especially in T2D, often appear years before symptoms. This scenario may explain, at least in part, the 25-50% of people with undiagnosed T2D (Chatterjee et al., 2017; International Diabetes Federation, 2021).

Intermediate hyperglycemia or most frequently known as prediabetes, is a high-risk factor for T2D (DeFronzo et al., 2015; International Diabetes Federation, 2021). Prediabetes is characterized by plasma glucose levels above the normal threshold but below the diagnosis criteria for T2D (International Diabetes Federation, 2021). The American Diabetes Association (ADA) the diagnostic criteria for prediabetes (Table 2) (American Diabetes Association, 2021; International Diabetes Federation, 2021). Prediabetes is diagnosed when the following criteria are met: diagnosis of impaired fasting glucose and/or impaired glucose tolerance, and/or glycated hemoglobin values are between 5.7 – 6.4% (39-47 mmol/mol) (Table 2) (American Diabetes Association, 2021; International Diabetes Federation, 2021).

According to the IDF 2021 report, both impaired fasting glucose and impaired glucose tolerance showed an alarming prevalence worldwide in 2021 and projection estimates for 2045 (International Diabetes Federation, 2021). In 2021, 6.2% and 10.6% of adults worldwide were estimated to have impaired fasting glucose and impaired glucose tolerance, respectively. Prevalence estimates for 2045 showed impaired

fasting glucose and impaired glucose tolerance would reach 6.9% and 11.4% rates worldwide, respectively. Furthermore, the prevalence of impaired fasting glucose is estimated to increase across all age groups by 2045, while the prevalence of impaired glucose tolerance is expected to increase in the young (45 years old or younger) and older adults (70 years or older) (International Diabetes Federation, 2021).

One in four young adults (19-34 years) have prediabetes in some countries, such as in the US (B. N. Hart et al., 2021). The increasing prevalence of prediabetes in young individuals includes women of reproductive age. In the US, prediabetes was diagnosed in 27.8% of the population aged between 18 and 44 years old (Centers for Disease Control and Prevention, 2021). Consistent with this, screening for the prevalence of chronic diseases in a fertility clinic in the US from 2011 to 2012 identified about 31% of women aged between 18 to 44 years had prediabetes (Robbins et al., 2013).
Additionally, there is an overall lack of follow-up and intervention after diagnosis of prediabetes. In a study of nearly 22,000 women of reproductive age, less than half of the women had a follow-up six months after the prediabetes diagnosis, and less than 1% underwent medical treatment (Marshall et al., 2017). The reduced response after diagnosis was overall attributed to the lack of medical guidance (Marshall et al., 2017).

It seems that prediabetes is not given the necessary attention it should. Indeed, a consensus regarding prediabetes definition and diagnostic criteria among organizations, including WHO, IDF, and ADA, is missing (Hollander & Spellman, 2012; International Diabetes Federation, 2021). As a result, standardized epidemiological data to assess global estimates of prediabetes prevalence and incidence is lacking.

People with prediabetes may present insulin resistance, β-cell dysfunction, oxidative stress, and inflammation years before the onset of T2D (DeFronzo et al., 2015; Luc et al., 2019). The estimated incidence of progression from prediabetes to T2D five years after the diagnosis of impaired fasting glucose and impaired glucose tolerance is 50% and 26%, respectively (International Diabetes Federation, 2021). Early lifestyle interventions (i.e., weight loss, physical activity, and medication) to normalize plasma glucose levels are critical to prevent or delay the development of T2D (American Diabetes Association, 2021).

2.2.2 Epidemiology of type 2 diabetes

Type 2 diabetes is the most frequent type of diabetes, representing 90% of all cases worldwide (International Diabetes Federation, 2021). The global increase in sedentary lifestyles, poor nutrition, and obesity has largely contributed to the increasing prevalence of T2D (Chatterjee et al., 2017). Increases in prevalence may also be due to early detection of the disease and improved medical care (International Diabetes Federation, 2021).

The global estimates of T2D prevalence in 2017 demonstrated that 4.4% of people aged between 15 and 49 years old had T2D (Khan et al., 2019). In high-income countries (i.e., USA, UK, Australia, and France), it has been recently shown that T2D incidence may be decreasing or remaining stable as a reflection of the prevention and screening strategies (Fuentes et al., 2020; International Diabetes Federation, 2021). However, studies in low-income countries are lacking to confirm this trend

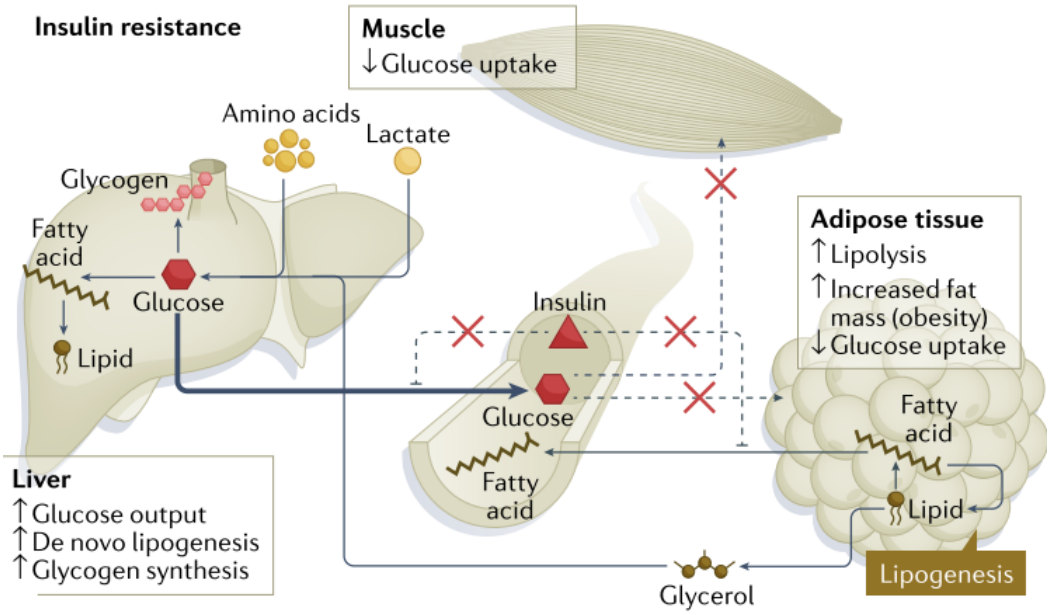

Figure 7: Pathophysiology of type 2 diabetes.

In type 2 diabetes, insulin resistance impairs energy metabolism in target tissues. Hyperglycemia is maintained by insulin resistance-resultant reduced glucose uptake in muscle and adipose tissue and increased liver gluconeogenesis. In addition, insulin resistance leads to increased lipogenesis and glycogenesis in the liver and, increased lipolysis and fatty acid release in the adipose tissue. Adapted from James et al., 2021.

(International Diabetes Federation, 2021). Overall global estimates of type 2 diabetes without the inclusion of type 1 diabetes cases are scarce.

Type 2 diabetes can be diagnosed at any age, but the highest risk is around 40-60 years old (Reed et al., 2021). Type 2 diabetes used to be considered an adult disease; however, T2D is becoming increasingly common in children and young individuals (International Diabetes Federation, 2021; Reed et al., 2021). The incidence of T2D is low in children but progressively increases at puberty, associated with the physiological decrease in insulin sensitivity during this stage (International Diabetes Federation, 2021; Kelsey & Zeitler, 2016). The increase in childhood overweight and obesity has resulted in more children and young adults developing T2D (International Diabetes Federation, 2021).

Diagnosis of T2D under 15-40 years of age is known as youth-onset T2D, a severe form of T2D in the young (Chatterjee et al., 2017; International Diabetes Federation, 2021). People with youth-onset T2D show rapid loss of β-cell function compared to later-onset T2D, have fewer treatment options and are thus at higher risk for complications (Magliano et al., 2020). Exposure to diabetes in the intrauterine environment as well as certain ethnic groups (i.e., Native American, Indigenous Australian, Pacific Islander, and First Nation Canadian), are highly associated with young-onset T2D (Magliano et al., 2020). A higher prevalence in girls than boys is also shown in youth-onset T2D (Magliano et al., 2020).

The prevalence of T2D in young adults, including women of reproductive age, is similarly increasing (Celik et al., 2022). Indeed, of five women with diabetes, two are of reproductive age (Celik et al., 2022). Examination of diagnosed and undiagnosed diabetes and prediabetes rates in women aged between 20 to 44 years in an interval of nearly 30 years, from 1976-1980 and 2007-2010, clearly showed the increasing prevalence of alterations in glucose metabolism in women of reproductive age (Szmuilowicz et al., 2019). Alarmingly, from 1976-1980 to 2007-2010, the rate of diagnosed T2D (from 1.2 to 2.3), undiagnosed T2D (from 1.2 to 2.6) or undiagnosed prediabetes (from 11.9 to 24.0) more than doubled in women of reproductive age (Szmuilowicz et al., 2019).

Concerning the impact of T2D on gender, global epidemiological data from 1990 to 2017 showed similar prevalence trends between males and female adult-onset T2D, but males showed a slightly higher T2D prevalence than females (Khan et al., 2019).

2.2.3 Pathophysiology of type 2 diabetes

In T2D, one of the main pathological conditions leading to the onset of the disease is the progressive impaired insulin secretion by pancreatic β-cells (DeFronzo et al., 2015). Pancreatic β-cell failure is probably due to insulin resistance in various tissues, including liver, muscle, and adipose tissue but also in the kidney, gastrointestinal tract, vasculature, brain, and pancreatic β-cells (DeFronzo et al., 2015).

Physiological responses during fasting-feeding cycles, notably the glucose-insulin axis, are completely altered in T2D and contribute greatly to permanent hyperglycemia (Figure 7). Insulin secretion is impaired, and β-cells are resistant to the stimulatory effect of gut incretin hormones to secrete insulin (DeFronzo et al., 2015). In the liver, during both fasting and feeding states, there are increased levels of

glucagon, basal gluconeogenesis, free fatty acids, lactate, glycerol, and AAs (DeFronzo et al., 2015). At the molecular level, increased gluconeogenesis results from the upregulation of transcription factor FOXO1, an insulin-signaling AKT-target, which drives the expression of gluconeogenesis genes (Czech, 2017). In parallel, while insulin fails to reduce gluconeogenesis, lipogenesis remains elevated and further exacerbates insulin resistance and/or its consequences (James et al., 2021).
In the muscle, altered insulin signaling results in reduced insulin-mediated glucose uptake (DeFronzo et al., 2015; James et al., 2021). Indeed, failure of GLUT-4 translocation to the plasma membrane in response to insulin is an early step of insulin resistance and T2D onset (Leto & Saltiel, 2012). In the adipose tissue, glucose uptake is similarly reduced (DeFronzo et al., 2015; James et al., 2021). Moreover, insulin resistance impairs the ability of energy storage of the white adipose tissue, leading to fatty acid release and ectopic accumulation in other tissues causing cellular stress and altered metabolism (Figure 7) (Scheja & Heeren, 2019). Altogether, impaired insulin secretion, reduced insulin-stimulated glucose uptake, increased gluconeogenesis, glucotoxicity, lipotoxicity, and chronic inflammation contribute to insulin resistance and are hallmarks of T2D (DeFronzo et al., 2015).

Different molecular mechanisms of insulin resistance have been described. One of them is the activation of serine/threonine kinases that inhibit the phosphorylation of different insulin-signaling molecules contributing to insulin resistance (Boucher et al., 2014). Similarly, several causes of insulin resistance have been attributed, including hyperglycemia, inflammation, lipotoxicity, mitochondrial dysfunction, oxidative stress, and ER stress (Boucher et al., 2014). Hyperglycemia alone can reduce insulin sensitivity of target tissues (i.e., muscle and adipose tissue) and decrease insulin secretion from β-cells (Boucher et al., 2014).

Hyperglycemia effects on insulin sensitivity are mostly linked to impairment of the insulin signaling pathway. Hyperglycemia leads to the hyperactivation of the protein phosphatase PP2A, a negative regulator of the several protein kinases essential for insulin action, including AKT, S6 kinase (S6K), and ERK (Boucher et al., 2014). Hyperactivation of PP2A, frequently observed in diabetes, reduces the phosphorylation of the IR and insulin-signaling molecules contributing to insulin resistance (Boucher et al., 2014).
Hyperinsulinemia has also been related to insulin resistance through hyperactivation of negative regulators of insulin action such as PHLPP1 and Grb14, which decrease the phosphorylation of AKT, and compete for IRS binding to IR (Boucher et al., 2014).

Moreover, increased levels of ROS, as a consequence of mitochondrial dysfunction frequently present in diabetes, lead to the serine phosphorylation of IRS protein by activation of stress kinases (Boucher et al., 2014).

Screening test	Healthy	T1D and T2D
Fasting plasma glucose	**5.6 - 6.1 mmol/L** (<100 – 110 mg/dL)	**≥7.0 mmol/L** (126 mg/dL)
Oral glucose tolerance test	**7.8 mmol/L** (<140 mg/dL)	**≥11.1 mmol/L** (200 mg/dL)
HbA1c	**<5.7-6.0%** (39 – 42 mmol/mol)	**6.5%** (≥48 mmol/mol)
Random plasma glucose	-	**≥11.1 mmol/L** (200 mg/dL)

Table 3. Diagnostic criteria for type 1 and type 2 diabetes.
Diabetes, both type 1 and type 2, is diagnosed when one or more of the four criteria are met. HbA1c, hemoglobin A1C. T1D, type 1 diabetes; T2D, type 2 diabetes. Adapted from International Diabetes Federation, 2021; DeFronzo et al., 2015.

2.3 Diagnosis of type 1 and type 2 diabetes

Despite having different etiology and pathophysiology, type 1 and type 2 diabetes diagnostic criteria is based on the detection of hyperglycemia, regardless of the age of onset and the presence or not of symptoms (Table 3) (DiMeglio et al., 2018; International Diabetes Federation, 2021; Katsarou et al., 2017).

Distinguishing T1D from T2D may be complicated and require additional testing, such as the screening of pancreatic autoantibodies, together with other features such as clinical symptoms, insulin deficiency, age of diagnosis, body mass index (BMI), and family history (DiMeglio et al., 2018; Katsarou et al., 2017). The sole presence of autoimmunity is not sufficient for T1D diagnosis since obese adolescents may present autoimmunity (Katsarou et al., 2017).

Hyperglycemia is diagnosed when one or more of the following conditions are met: fasting plasma glucose levels are equal to or higher than 7.0 mmol/L, oral glucose tolerance test values are equal to or higher than 11.1 mmol/L, glycated hemoglobin values are equal or higher to 6.5% (48 mmol/mol), random plasma glucose measurement is equal or higher than 11.1 mmol/L (Table 3) (International Diabetes Federation, 2021). In T1D, measurement of glycated hemoglobin (HbA1c) can be similarly used, but because hyperglycemia can occur rapidly, between days to weeks, in people with T1D, HbA1c tests may be less sensitive for T1D diagnosis (DiMeglio et al., 2018; International Diabetes Federation, 2021; Katsarou et al., 2017).

Together with hyperglycemia, classic symptoms of T1D and T2D can be present, including polyuria, i.e., excessive urination, polydipsia, i.e., excessive thirst, fatigue, sudden weight loss, and diabetic ketoacidosis (DiMeglio et al., 2018; International Diabetes Federation, 2021). However, people with T2D are more frequently asymptomatic or present less severe symptoms than people with T1D (International Diabetes Federation, 2021). Indeed, a long period can separate the onset of early metabolic perturbations and T2D diagnosis (International Diabetes Federation, 2021). This period is referred to as prediabetes, which will be described in this chapter.

The absence of symptoms has contributed to another alarming trend: the increasing rate of undiagnosed people with diabetes. Indeed, one in two adults (20-70 years), mainly with T2D, are undiagnosed (International Diabetes Federation, 2021). Deficient health systems and screening policies, especially in low-income countries, may also contribute to high rates of missed diagnosis (International Diabetes Federation, 2021).

2.4 Rare forms of diabetes

Other less common types of diabetes have been described. That is the case for monogenic diabetes, which is caused by single-gene mutations (International Diabetes Federation, 2021). Monogenic diabetes constitutes 1.5-2% of all diabetes cases (International Diabetes Federation, 2021). However, because the screening of this type of diabetes is uncommon, monogenic diabetes may be misdiagnosed as T1D or T2D (International Diabetes Federation, 2021; Kapur et al., 2019).

Risk factors for the diagnosis of Metabolic Syndrome (MetS)		
Obesity	**Waist circumference** Values vary according to ethnicity. Here values for European populations	≥80 cm in females ≥94 cm in males
Dyslipidemia	**HDL cholesterol**	1.3 mmol/L (<50 mg/dL) in females 1.0 mmol/L (<40 mg/dL) in males
	Triglycerides	1.7 mmol/L (≥150 mg/dL)
	or ongoing treatment for this condition	
Hyperglycemia	**Fasting plasma glucose**	≥5.6 mmol/L (≥100 mg/dL)
	or ongoing treatment for this condition	
Hypertension	**Systolic blood pressure**	≥ 130 mm Hg
	Diastolic blood pressure	≥ 85 mm Hg
	or ongoing treatment for this condition	

Table 4: Risk factors for the diagnosis of Metabolic Syndrome (MetS).
Metabolic syndrome is diagnosed when at least three of the following conditions are present: obesity, dyslipidemia, hyperglycemia and hypertension. Adapted from Lanktree & Hegele, 2017.

Monogenic diabetes can be classified as neonatal diabetes mellitus, maturity-onset diabetes of the young (MODY), and rare diabetes-associated syndromic diseases (International Diabetes Federation, 2021). At the same time, these types of diabetes can be classified into different subtypes, as is the case for MODY (International Diabetes Federation, 2021).

Other types of diabetes, mainly originating from diverse causes, have been described (International Diabetes Federation, 2021). These types of diabetes were known before as "secondary diabetes" and include diabetes caused by diseases (i.e., pancreatitis, pancreatic cancer, Cushing's syndrome), medical procedures (i.e., pancreatectomy), and by drugs that impair insulin secretion or action (International Diabetes Federation, 2021).

2.5 Hyperglycemia and hyperinsulinemia outside diabetes

Hyperglycemia and/or hyperinsulinemia are also associated with other contexts outside overt diabetes, such as metabolic syndrome (MetS), obesity, and polycystic ovary syndrome (PCOS).

Metabolic syndrome (MetS) is defined as the presence of at least three risk factors: obesity, dyslipidemia, hyperglycemia, and hypertension (Table 4) (Lanktree & Hegele, 2017). Although not a disease *per se*, MetS implies an underlying metabolic dysfunction and a higher risk for metabolic diseases. Indeed, MetS constitute a 5-fold higher risk for T2D and a 2-fold higher risk of cardiovascular disease (CVD) (International Diabetes Federation, 2006).

Risk factors associated with MetS are similarly associated with other diseases, notably women with PCOS or people with obesity. Polycystic ovary syndrome is a common endocrine disorder in women of reproductive age, characterized by ovarian dysfunction, hormonal imbalances, and, in most cases, insulin resistance (Moghetti & Tosi, 2021). Consequently, PCOS is associated with a higher risk for T2D (Moghetti & Tosi, 2021).
People with obesity, defined as body mass index (BMI) greater than or equal to 30 kg/m^2 by the World Health Organization, can present insulin resistance and/or hyperinsulinemia (World Health Organization, 2021b; A. M. Y. Zhang et al., 2021). Although there is some controversy about who influences the other between insulin resistance and hyperinsulinemia, it is generally considered that excess adiposity and insulin resistance lead to hyperinsulinemia (Czech, 2017; A. M. Y. Zhang et al., 2021). Over time, obesity-induced insulin resistance may lead to hyperglycemia, one of the last conditions of obesity progression to overt T2D (A. M. Y. Zhang et al., 2021).

2.6 Diabetes in pregnancy

Diabetes in pregnancy can originate from 1) diagnosed pre-existing diabetes referred to as pre-gestational diabetes (PGD), 2) gestational diabetes mellitus (GDM), or 3) diabetes first detected in pregnancy (International Diabetes Federation, 2021). Pre-gestational diabetes includes diagnosed type 1 and 2 and other forms of diabetes before conception (International Diabetes Federation, 2021). Gestational diabetes mellitus (GDM) corresponds to diabetes developed exclusively during pregnancy and which is expected to persist after delivery (International Diabetes Federation, 2021). Diabetes first

diagnosed in pregnancy corresponds to undiagnosed diabetes, most frequently detected in the first trimester, which is expected to persist after delivery (International Diabetes Federation, 2021).

Hyperglycemia affects one in six pregnancies (International Diabetes Federation, 2021). In 2021, 21.1 million (16.7%) of live births were affected by hyperglycemia in women aged between 20-49 years old (International Diabetes Federation, 2021). Of these, 80.3% of cases corresponded to GDM, while the remaining 10.6% and 9.1% were attributed to pre-existing diabetes, both type 1 and 2, and diabetes diagnosed during pregnancy (International Diabetes Federation, 2021).

Furthermore, prediabetes can also be detected during pregnancy. However, symptoms of hyperglycemia are not common and may be confused with those of pregnancy. As a consequence, detection of prediabetes can be easily neglected if screening is not performed (International Diabetes Federation, 2021).
Implementing screening policies before conception and during early pregnancy may help identify women with early metabolic disturbances. In New Zealand, the measurement of glycated hemoglobin is performed early in pregnancy to detect women with undiagnosed diabetes or prediabetes (Carris et al., n.d.; Hughes et al., 2018). Prediabetes in pregnancy has been associated with adverse pregnancy outcomes such as hypertensive disorders (Hughes et al., 2018). Despite potential impacts on both mother and offspring, prediabetes during pregnancy remains poorly characterized.

All forms of diabetes during pregnancy are associated with adverse pregnancy outcomes and short- and long-term consequences in the offspring, including a lifelong risk of chronic diseases. The implications of a diabetic intrauterine context in the offspring will be described in detail in Chapters 2 and 3.

2.6.1 Gestational diabetes mellitus (GDM)

Gestational diabetes mellitus (GDM) is characterized by hyperglycemia during pregnancy and may be accompanied by chronic insulin resistance and hyperinsulinemia (Hufnagel et al., 2022; Plows et al., 2018).

In most pregnancies, physiological and mild insulin resistance gradually develops due to the production of placental hormones, including placental lactogen, estrogen, progesterone, and leptin (Hjort et al., 2019; International Diabetes Federation, 2021; Plows et al., 2018; Vince et al., 2020). To compensate for the transient insulin resistance, insulin secretion increases to supply the fetus with the required glucose demands. Hyperglycemia and GDM arise when women cannot adapt to these metabolic changes (Vince et al., 2020). In approximately 80% of GDM cases, β-cell dysfunction is present prior to pregnancy (Plows et al., 2018). Thus, metabolic adaptations triggered by pregnancy are established upon an already dysfunctional maternal metabolism, contributing to chronic insulin resistance in GDM (Plows et al., 2018).

Although GDM is usually reversed after delivery, it has been shown that women who developed GDM and retained the gestational weight gain may present metabolic dysfunctions such as decreased insulin sensitivity and increased inflammation after the pregnancy (Catalano, 2014). In addition, women with GDM are at higher risk for T2D up to three to six years after a GDM episode (International Diabetes Federation, 2021).

A

Glucose concentration thresholds in pregnancy	Healthy
Preprandial glucose	**5.3 mmol/L** (≤95 mg/dL)
1-hour postprandial glucose	**7.8 mmol/L** (≤140 mg/dL)
2-hours postprandial glucose	**6.7 mmol/L** (≤120 mg/dL)

B

Screening test	GDM
Fasting plasma glucose	**5.1 mmol/L** (92 mg/dL)
1-hour Oral glucose tolerance test	**10 mmol/L** (180 mg/dL)
2-hours Oral glucose tolerance test	**8.5 mmol/L** (153 mg/dL)

Table 5. Glucose concentration in healthy diabetic women and diagnostic criteria for gestational diabetes mellitus.

A) Target glucose concentration thresholds in pregnancy in non-diabetic women. Adapted from American Diabetes Association, n.d. B) Gestational diabetes mellitus diagnostic criteria. Gestational diabetes mellitus is diagnosed when one or more criteria are met. GDM, gestational diabetes mellitus. Adapted from International Diabetes Federation, 2021.

GDM is usually screened in all women during the second to the third trimester (24–28 weeks) (Hufnagel et al., 2022). Nevertheless, women with GDM may present hyperglycemia from the first trimester, around weeks 9-10 (Desoye & Cervar-Zivkovic, 2020).
The recommended diagnostic criteria define GDM when fasting glucose is 5.1 mmol/L, and/or oral glucose tolerance test after one and two hours is 10 mmol/L and 8.5 mmol/L, respectively (Table 5) (American Diabetes Association, 2021; International Diabetes Federation, 2021).
These diagnostic criteria have been endorsed by the World Health Organization (WHO), the American Diabetes Association (ADA), the International Association of the Diabetes and Pregnancy Study Groups (IADPSG), and the International Federation of Gynaecology and Obstetrics (FIGO) (International Diabetes Federation, 2021). However, among countries, there is often a lack of consensus on the diagnostic criteria for GDM, which complicates the evaluation of epidemiological data (International Diabetes Federation, 2021; H. Wang et al., 2022).

A recent meta-analysis covering 45 countries and standardized by the IADPSG gestational diabetes mellitus diagnostic criteria assessed the prevalence of GDM globally and by regions. This study revealed a global 14% prevalence of GDM (H. Wang et al., 2022). Among regions, the highest GDM prevalence was observed in the Middle East and North Africa, with 27.6%, followed by South-East Asia, with 20.8% (H. Wang et al., 2022). In addition, a higher prevalence of GDM was observed in high-income countries (14.2%) when compared to middle- (9.2%) or low-income countries (12.7%) (H. Wang et al., 2022).

Gestational diabetes mellitus risk factors include obesity, overweight, excessive weight gain during pregnancy, advanced maternal age, previous history of GDM or family history of diabetes, PCOS, smoking, and adverse neonatal outcomes in previous pregnancies (International Diabetes Federation, 2021). Women with high-risk factors should be screened for GDM earlier in pregnancy (International Diabetes Federation, 2021).

2.6.2 Pre-gestational diabetes (PGD)

Pre-gestational diabetes (PGD) is characterized by hyperglycemia, impaired insulin secretion and/or insulin resistance, depending on the underlying diabetes type.

Together with the increasing incidence of diabetes in children and adolescents, the incidence of diabetes in women of reproductive age is similarly increasing (B. N. Hart et al., 2021; International Diabetes Federation, 2021). One in nine women has diabetes, and diabetes is increasing in women of reproductive age. Among new cases of diabetes, 35% correspond to women of reproductive age (B. N. Hart et al., 2021). Pre-gestational diabetes affects 1-2% of all pregnancies, but incidence rates are increasing (B. N. Hart et al., 2021).

Type 2 diabetes is the most frequent type of diabetes; consequently, most PGD cases correspond to women with T2D. Indeed, a study from 1996 to 2014 in the United States showed that 76% of women with PGD had T2D, whereas 24% had T1D (Peng et al., 2017).

Pre-gestational diabetes is considered a high-risk pregnancy, with a higher risk of complications for the mother and the offspring (B. N. Hart et al., 2021). To avoid or reduce the risk of pregnancy complications and adverse outcomes in the offspring, management of PGD is essential before conception (International Diabetes Federation, 2021). Before the discovery of insulin, the management of PGD was solely based on a low carbohydrate diet (Ornoy et al., 2021). Nowadays, PGD management implicates different approaches, including strict glycemic control, moderate exercise, diet, weight control, a higher dose of folic acid treatment, and insulin therapy (International Diabetes Federation, 2021; Ornoy et al., 2021).

Nevertheless, despite current treatments, maternal-fetal complications and adverse outcomes for both the mother and the offspring are still frequently associated with diabetic pregnancies. Indeed, women with pre-gestational diabetes, especially with T1D, are hyperglycemic from the first weeks of pregnancy (Desoye & Cervar-Zivkovic, 2020; Desoye & Nolan, 2016; Ornoy et al., 2021).

Chapter 2: The Developmental Origins of Health and Disease (DOHaD)

1. The emergence and definition of the Developmental Origins of Health and Disease (DOHaD)

The association between suboptimal environments during the early stages of life and poor heath in adulthood was suggested before the 1980s (M. A. Hanson & Gluckman, 2014). In 1977, Forsdahl and colleagues reported that nutritional deficiency due to poverty conditions during childhood and adolescence, followed by nutritional excess such as high fat consumption during adulthood, were associated with a higher risk of arteriosclerotic heart disease (Forsdahl, 1977).
In the late 1980s, epidemiological studies by professor David Barker and colleagues highlighted the association between placental and birth weight with adverse cardiovascular adult health (i.e., the prevalence of hypertension, coronary heart disease, and MetS) and proposed that future research should be focused towards the intrauterine environment (Barker, 1990; Barker et al., 1990). David Barker and colleagues proposed the hypothesis of "fetal programming" (Barker, 1990).
From there, the pioneer work from Barker and colleagues, together with the multiple experimental and human studies, highlighted how early life experiences, even before conception, were associated with programming, also referred to as "developmental programming" in the offspring (M. Hanson et al., 2004). The need to extend Barker's initial hypothesis arose and led to the emergence of the Developmental Origins of Health and Disease (DOHaD) concept, which better reflected the effects of environmental cues from pre-conception to childhood (M. Hanson et al., 2004; Hoffman et al., 2017; Suzuki, 2018).

Today, it is widely accepted that early life experiences (i.e., suboptimal parental nutrition, exposure to stress, pollution, smoking) during critical periods of development from pre-conception extending to post-natal life may shape the individual's future health and predispose them to a higher risk of non-communicable diseases (NCD) such as cardiovascular diseases, obesity, and T2D at later age (Fleming et al., 2018; Safi-Stibler & Gabory, 2020).

The offspring with poor metabolic health due to adverse early life experiences entering pregnancy may further feed a vicious cycle of the development of NCDs (Tarrade et al., 2015; Vambergue & Fajardy, 2011). For example, women exposed to diabetes during pregnancy may present impaired glucose tolerance at adult age, and upon the challenge of pregnancy, they may develop gestational diabetes (Vambergue & Fajardy, 2011).

The Developmental Origins of Health and Disease concept is based on the principles of developmental plasticity (Michels, 2017). The concept of developmental plasticity states that developing organisms adapt their phenotype under a changing and adverse environment to ensure survival (Michels, 2017). The adaptations and strategies to face this adverse environment may come with a price, leading to impaired developmental programs and poor health (A. J. Lea et al., 2017; Michels, 2017). Programming to disease risk later in life is assumed to occur when the adaptations and strategies put in place by the developing organism to a given environment do not match the future environment (A. J. Lea et al., 2017; Sun et al., 2016). The mismatch between the phenotype and this new environment may lead to disease later in life (A. J. Lea et al., 2017; Sun et al., 2016).

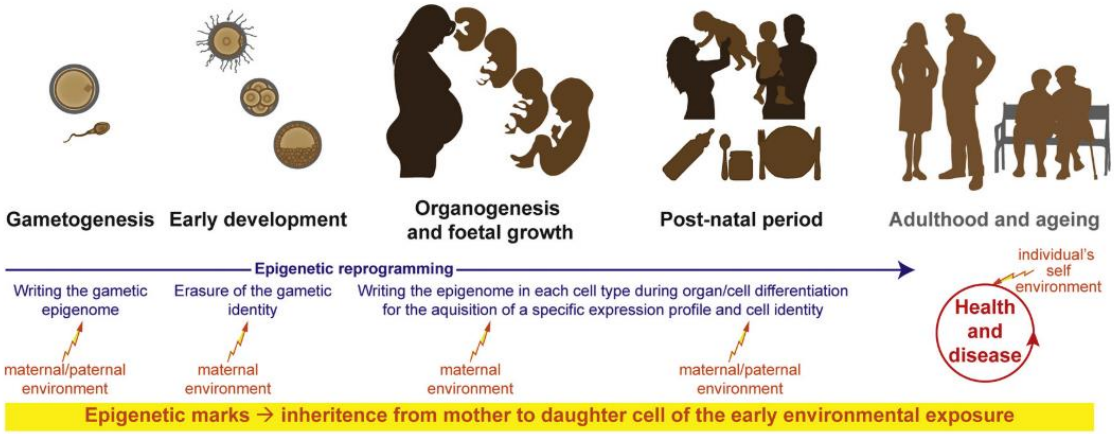

Figure 8: Critical and sensitive periods in development susceptible to programming.
The critical and sensitive developmental periods include the periconceptional period covering gametogenesis and preimplantation, fetal development and organogenesis, and post-natal development. These developmental windows are characterized by a series of epigenetic events (i.e., epigenetic reprogramming, differentiation events), making them sensitive to environmental cues and programming under suboptimal environments. From Safi-Stibler & Gabory, 2020.

Furthermore, developmental plasticity is considered to be greatest at the time of conception and to decrease thereafter, coinciding with the critical development periods shown to be susceptible to programming (Michels, 2017).

2. The critical and sensitive periods in development in the context of DOHaD

Initially, it was thought that the perturbation of life *in utero* could lead to developmental programming.
However, shortly thereafter, it was shown that environmental cues during the pre-conception period, involving maternal and paternal contribution, and/or during post-natal life were also sensitive periods susceptible to developmental programming (M. Hanson et al., 2004).
These sensitive periods are characterized by developmental plasticity, meaning that cells and tissues can respond and adapt to environmental cues to maximize the chances of survival (Langley-Evans, 2015). Moreover, these periods are characterized by highly dynamic epigenetic changes, which contribute to the establishment of cell-type identity, essential for cell and organ function (Jiménez-Chillarón et al., 2012). As will be discussed later, these epigenetic changes are sensitive to environmental cues, such as nutrient availability (Jiménez-Chillarón et al., 2012; Safi-Stibler & Gabory, 2020).

The sensitive windows in development include the periconceptional period covering gametogenesis and preimplantation development, the fetal period covering organogenesis and fetal development, and the post-natal period (Figure 8) (Safi-Stibler & Gabory, 2020; Suzuki, 2018).

Gametogenesis involves extensive genome-wide epigenetic reprogramming. Primordial germ cells, the common progenitor for both male and female gametes, undergo the erasure and the progressive and germ-specific re-establishment of epigenetic signatures (Cantone & Fisher, 2013; Safi-Stibler & Gabory, 2020). During this process, parent-of-origin epigenetic signatures that were also erased are re-established in an oocyte- and sperm-specific manner (Tucci et al., 2019).
Both oocyte and sperm have been shown to be impacted by environmental cues and shape the offspring's health. Oocytes from mice fed with a high-fat diet showed reduced expression of the protein Stella, implicated in inhibiting DNA demethylation mechanisms (L. Han et al., 2018). Reduced expression of Stella resulted in increased genome-wide DNA demethylation profiles in early embryos, which was associated with perturbated growth trajectories at the fetal stage and altered metabolic phenotype in the adult offspring (L. Han et al., 2018).
Although more studies addressing the contribution of the oocyte to developmental programming have been performed, the concept that the father’s environment may also affect the offspring's health has developed in recent years. Evidence has shown that poor paternal diet, metabolic imbalances, or stress may contribute directly through sperm or indirectly through the seminal plasma to a lifelong risk of NCDs in the offspring (Fleming et al., 2018; Watkins et al., 2018; Y. Zhang et al., 2019).
Indeed, the epigenome of the sperm may be influenced by environmental cues. The sperm of obese men shows different DNA methylation profiles and expression of small non-coding RNAs (Donkin et al., 2016). However, after weight loss treatments such as bariatric surgery, these epigenomic profiles were modified, demonstrating that the sperm epigenome responds to environmental cues.

The second sensitive period in development is preimplantation development. Preimplantation embryos are sensitive to changes in their surrounding environment, which strictly depend on maternal nutritional

and metabolic status (Fleming et al., 2021). In addition, during this short period of development, significant milestones take place, including the epigenetic reprogramming of parental genomes, the establishment of a totipotent state, the activation of the embryonic transcriptional program, and the first specification event, all of which constitute highly vulnerable events that will be covered in detail in Chapter 3 (Duranthon et al., 2008; Fleming et al., 2015).

After implantation of embryos, tissue differentiation, organogenesis, and fetal development initiate (Safi-Stibler & Gabory, 2020). The organogenesis period is another particularly sensitive window since perturbation of organ development can lead to long-term consequences in the structure and function (Fernandez-Twinn & Ozanne, 2010; Langley-Evans, 2015). Similarly, significant, fetal development is under placental control. Perturbations in placenta structure and function may act as an additional player in establishing developmental programming, as will be detailed in this chapter (Safi-Stibler & Gabory, 2020).

During the post-natal period, different organs reach maturation, including the intestine, liver, and nervous system (Safi-Stibler & Gabory, 2020). Moreover, nutrition changes occur, such as the transition from lactation to oral feeding accompanied by an increased diversity of nutrients, followed by the transition to solid foods (Safi-Stibler & Gabory, 2020). Optimal nutrition at this developmental stage, notably by optimal milk composition, is essential to prevent long-term adverse outcomes (Hue-Beauvais et al., 2017). Furthermore, another environmental factor important in this stage is parental care (Safi-Stibler & Gabory, 2020). Indeed, parental care, including the interaction during the lactation process and the social environment during post-natal development, is essential for the maturation of the nervous system (Safi-Stibler & Gabory, 2020).

Intergeneration and transgenerational transmission of the effects of parental early life exposures have also been described. Although these effects, due to the complexity of these studies, have been mostly demonstrated in animal models, i.e., rodents, *D. melanogaster*, *C. elegans*, and suggested in humans (Perez & Lehner, 2019). In humans, exposure to famine in utero was associated with increased neonatal adiposity until the F2 generation (Painter et al., 2008).
In rabbits, the offspring of embryos exposed to assisted reproductive technology (ART), precisely to cryopreservation-transfer procedures, showed altered growth trajectories, organ and liver weight, expression of common genes, and altered metabolic profile, along with an overall impaired liver function and zinc and fatty acid metabolism across the F1, F2 and F3 generations (Garcia-Dominguez et al., 2020).

It has been proposed that the window of exposure might be as important as the environmental cue (Fernandez-Twinn & Ozanne, 2010; Fleming et al., 2015; Langley-Evans, 2015). Indeed, the earlier the exposure in development, the more severe the phenotype may be in the offspring (Fernandez-Twinn & Ozanne, 2010; Fleming et al., 2015; Langley-Evans, 2015). Similarly, extended exposure periods may be associated with a broader range of perturbed organs and systems (Langley-Evans, 2015).

3. The role of the placenta in the DOHaD

The placenta constitutes the interface between the mother and the developing fetus (Maltepe & Fisher, 2015). Its main function is to supply nutrients, hormones, and oxygen to the fetus and remove waste products, thus regulating its development and growth (Maltepe & Fisher, 2015).

Environmental factors such as impaired maternal nutrition, pollution, and chemicals, among many others, have been shown to induce placental adaptations that adversely influence fetal development and growth (Tarrade et al., 2015). Indeed, impaired placenta structure and function is considered as programming agent (Safi-Stibler & Gabory, 2020; Tarrade et al., 2015).
Placental adaptations may vary according to the developmental window of exposure, the environmental factor, and the sex of the conceptus (Tarrade et al., 2015). These placental changes may include impaired placental development, reduced size, placental vascularity, blood flow, oxygen, and nutrient transfer to the fetus (Maltepe & Fisher, 2015).
Numerous studies have examined the correlation between placental and fetal size and weight (Maltepe & Fisher, 2015). It is considered that a large placenta may originate due to compensation mechanisms to maximize the transfer of nutrients, whereas a small placenta may originate due to deficient transfer capabilities (Langley-Evans, 2015; Maltepe & Fisher, 2015). Nevertheless, both low and high placental weight is associated with developmental programming to hypertension and cardiovascular disease in the offspring (Maltepe & Fisher, 2015).

Analysis of different environmental cues (e.g., famine, high-fat diet, PGD, obesity, or diesel engine exhaust) during pregnancy in human and animal models have demonstrated placental adaptions that may impair placental function and consequently impact the developing conceptus (Castillo-Castrejon et al., 2021; Rousseau-Ralliard, Valentino, et al., 2019; Tarrade et al., 2013).

This is the case for women with PGD or obesity (Gaillard, 2015; Vambergue & Fajardy, 2011). The placenta of women with PGD is heavier, hyper-vascularized, hyperproliferative, has reduced oxygen delivery to the fetus, and has an enlarged exchange surface to compensate for deficient transfer capabilities (Vambergue & Fajardy, 2011). In addition, the placenta of women with T2D precisely exhibited increased expression of transporters for glucose, AAs, and fatty acids, which may result in the increased delivery of macronutrients to the fetus, and thereby influence fetal growth and adiposity at birth in the offspring (Castillo-Castrejon et al., 2021).
Similarly, the placenta of women with pre-gestational obesity are frequently heavier and exhibit vascular dysfunction, inflammation, alteration of placental transporters, and mitochondrial activity (Gaillard, 2015).

4. The mechanisms behind DOHaD: the role of epigenetics

Early life experiences may result in disease risk later in life. However, the underlying mechanisms linking this first event to poor health in adulthood are not fully understood. To date, numerous studies suggest that epigenetic mechanisms are the most plausible candidate that could link early life exposures to environmental cues, the establishment and maintenance of short- and long-term consequences, and the memory of early life experiences throughout the life course of an individual (Portha et al., 2014; Waterland & Michels, 2007).

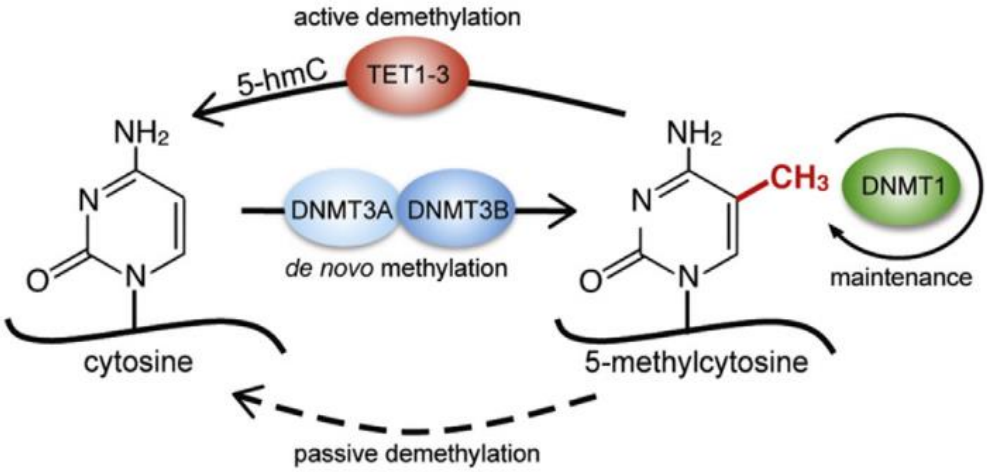

Figure 9: DNA methylation in eukaryotes.
The covalent binding of methyl moiety to the fifth carbon of cytosines generates the 5-methylcytosine (5mC). Deposition of the methyl moiety is catalyzed by the *de novo* DNA methyltransferases 3A (DNMT3A) or 3B (DNMT3B), whereas maintenance of DNA methylation patterns is catalyzed by the DNA methyltransferase 1 (DNTM1) through cell division. DNA demethylation can occur by active or passive mechanisms. Active DNA demethylation is in charge of DNA hydroxylates Ten-eleven translocation (TET) proteins 1-3, whereas passive DNA demethylation involves the absence of DNMT1 or its inhibition during successive rounds of cell division, leading to dilution of the methylation mark. From Ambrosi et al., 2017.

Moreover, several exogenous and endogenous cues may influence epigenetic mechanisms, such as nutrient availability, cellular metabolism, and cell signaling, among others.

4.1 Definition of epigenetics

In 1942, Conrad Waddington first defined "epigenetics" as the study of processes by which the genotype gives rise to the phenotype (Waddington, 2012). From there, modifications to the definition of epigenetics have been proposed by others (Cavalli & Heard, 2019). Currently, Cavalli G. and Heard E. have proposed a new definition of epigenetics as "the study of molecules and mechanisms that can perpetuate alternative gene activity states in the context of the same DNA sequence" (Cavalli & Heard, 2019).
This latest definition covers three important aspects: 1) the transgenerational and mitotic inheritance and the maintenance of gene activity or chromatin states, 2) the DNA sequence depends on the biological context, meaning that mitotic inheritance concerns the genomic sequence of individual cells, whereas, in transgenerational inheritance, it concerns the DNA of the whole organism, which may include its microbiota if it contributes to inheritance, and 3) it includes the regulatory processes related to known molecules implicated in epigenetic inheritance (Cavalli & Heard, 2019).

Carriers of epigenetic information and thus actors of epigenetic control include DNA methylation, post-translational modifications of histones and histone variants, non-coding RNAs (ncRNAs), and the 3D chromatin organization (Cavalli & Heard, 2019). Furthermore, these carriers, mainly referred to as "epigenetic marks," do not act independently but exhibit crosstalk between them (M. Kim & Costello, 2017). The regulation of epigenetic modifications is orchestrated by what is called in epigenetics "writers," the enzymes depositing the epigenetic modification, "erasers," the enzymes removing the epigenetic modification, and "readers," the effector proteins that recognize and bind the epigenetic modification (Atlasi & Stunnenberg, 2017).
The role of these epigenetic marks on gene expression regulation has been extensively described (Dai et al., 2020). In a simplified manner, epigenetic marks can change the local chromatin structure or promote the recruitment of non-histone protein effectors to chromatin (Dai et al., 2020).

4.1.1 DNA methylation

DNA methylation is a stable epigenetic mark generated by the covalent binding of a methyl moiety to the fifth carbon of cytosines generating the 5-methylcytosine (5mC) (Figure 9) (E. Li & Zhang, 2014). In mammals, DNA methylation participates in several processes, such as transcriptional regulation of gene expression, silencing of transposable elements, genomic imprinting, and X chromosome inactivation (E. Li & Zhang, 2014).

Cytosine methylation occurs specifically in CpG dinucleotides, which correspond to cytosine and guanine linked by a phosphate group on the same strand (E. Li & Zhang, 2014; Mattei et al., 2022). Across the genome, CpGs can be found in clusters known as CpG islands, which correspond to 200 bp to 2 kb in length, with more than 50% of CpG density, are predominantly situated upstream gene promoters, and are generally unmethylated (E. Li & Zhang, 2014). Methylation of a CpG island within a promoter region is associated with the transcriptional repression of the gene (E. Li & Zhang, 2014).

DNA methylation across promoters interferes with the binding of most transcription factors, and interacts with the methyl-CpG binding domain (MBD) family of proteins, triggering the recruitment of transcriptional repression complexes, thus resulting in transcriptional repression (E. Li & Zhang, 2014). Contrary to CpG islands, repetitive and transposable elements, intergenic DNA, and exons correspond to highly methylated genomic regions (E. Li & Zhang, 2014).

The "writers" of 5mC are the DNA methyltransferases (DNTMs) (Figure 9) (E. Li & Zhang, 2014). The *de novo* DNA methylation is in charge of DNMT3A and DNMT3B together with DNMT3L, while maintenance of DNA methylation patterns is in charge of the DNMT1 (Figure 9) (Atlasi & Stunnenberg, 2017; E. Li & Zhang, 2014). *De novo* DNA methylation comprises the addition of methyl groups to unmethylated CpGs through the action of DNAMT3A and DNMT3B, with their coactivator DNMT3L, which lacks the methyltransferase activity (Atlasi & Stunnenberg, 2017; E. Li & Zhang, 2014).
De novo DNA methylation is essential in development (Unoki, 2020). In mammals, during gametogenesis and embryogenesis, a genome-wide reprogramming event comprises a global erasure and restoration of DNA methylation patterns (M. Kim & Costello, 2017; Unoki, 2020). This restoring phase requires *de novo* DNA methylation (M. Kim & Costello, 2017; Unoki, 2020).
The mechanisms driving the *de novo* establishment of DNA methylation patterns are not fully understood (Unoki, 2020). In embryogenesis, transcription factor binding in active regions is believed to lead to the passive specification of DNA methylation regions, and ncRNAs may be involved in the specification process (Unoki, 2020). Furthermore, protection against *de novo* DNA methylation in specific regions of the genome may be accomplished through the enrichment of specific histone modifications (Millán-Zambrano et al., 2022).
The action of DNMT1 accomplishes the maintenance with high fidelity of global DNA methylation patterns through cell division (Ambrosi et al., 2017; M. Kim & Costello, 2017). During DNA replication, the E3 ubiquitin-protein ligase UHRF1 recognizes hemi-methylation sites and recruits DNMT1 to the replication fork (M. Kim & Costello, 2017). There, DNMT1 copies the methylation pattern from the hemi-methylated DNA strand to the newly synthesized DNA strand (Atlasi & Stunnenberg, 2017; Cavalli & Heard, 2019; M. Kim & Costello, 2017).

DNA methylation can be removed through either passive or active mechanisms (Figure 9) (Ambrosi et al., 2017; E. Li & Zhang, 2014). Passive DNA demethylation involves the absence of DNMT1 or its inhibition during successive rounds of cell division, thus diluting the methylation marks (Figure 9) (E. Li & Zhang, 2014). Active demethylation involves an enzymatic process by DNA hydroxylates such as the Ten-eleven translocation (TET) family of proteins, resulting in the removal of the methyl moiety (Figure 9) (E. Li & Zhang, 2014). TETs oxidize 5mC to 5-hydroxymethylcitosine (5hmC) and can be further oxidized to 5-formylcytosine and 5-carboxylcytosine (M. Kim & Costello, 2017). Active demethylation can then be accomplished by replication-dependent passive demethylation of the 5mC oxidation derivatives or through thymine-DNA glycosylase-mediated base excision repair mechanisms and thus be replaced by a new unmethylated cytosine (M. Kim & Costello, 2017; E. Li & Zhang, 2014).

DNA methylation constitutes a dynamic but stable process (M. Kim & Costello, 2017). On one side, DNA methylation is considered a cellular memory system, but on the other side, DNA methylation patterns are not permanent (E. Li & Zhang, 2014). Under physiological or pathophysiological contexts, DNA methylation may be subjected to changes in response to environmental cues (E. Li & Zhang, 2014).

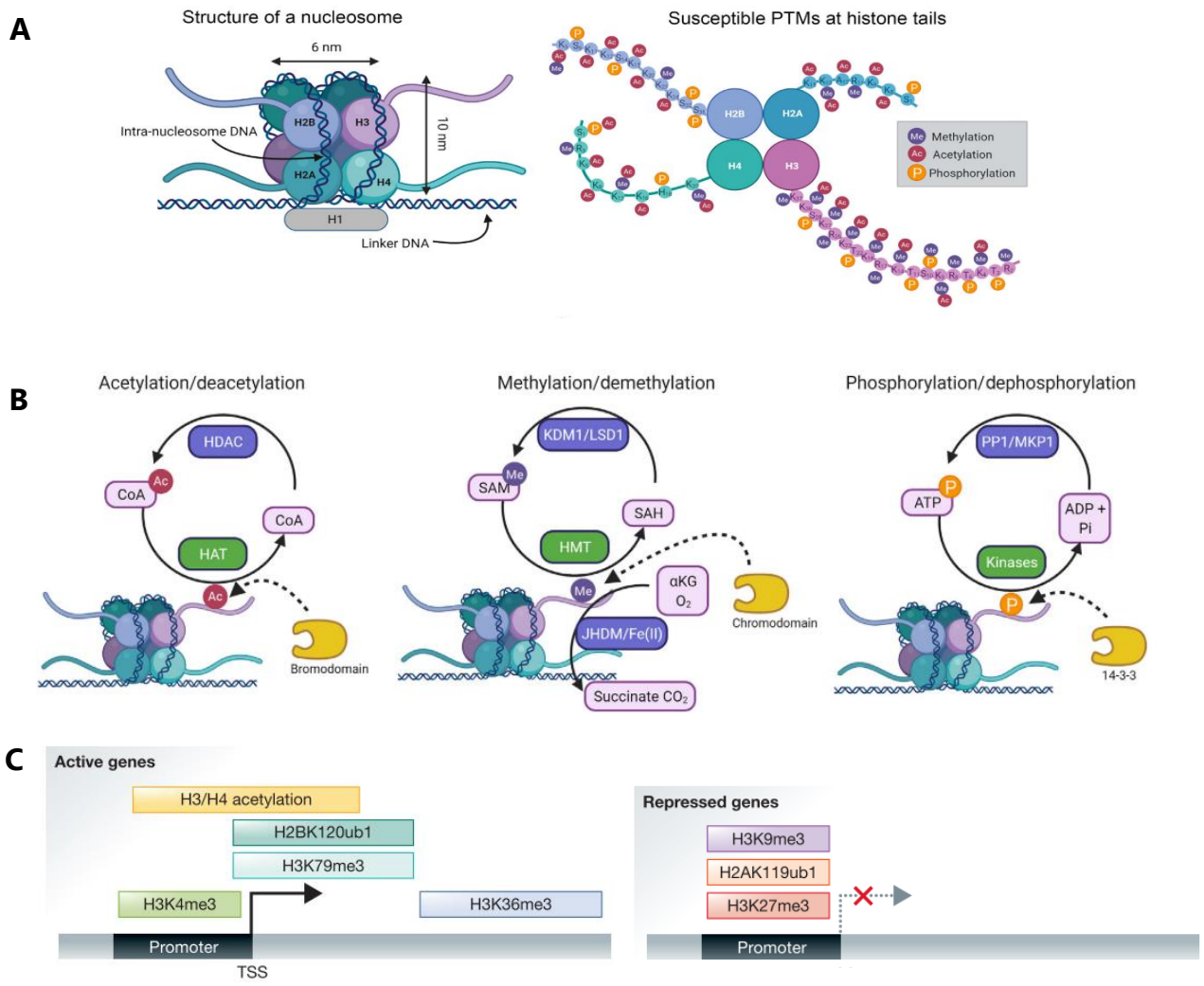

Figure 10: Post-translational modifications of histone tails, histone-modifying enzymes and histone post-translational modifications enriched in active and repressed genes.

A) In eukaryotes, 147 bp of DNA is wrapped around nucleosomes, constituted of a histone octamer of two copies of H2A, H2B, H3 and H4 stabilized by the H1. The amino acid residues within the N-terminal tail or in the globular core domains of these core histones are subject to multiple post-translational modifications (PTMs) such as histone methylation, acetylation and phosphorylation. Adapted from Torres-Perez et al., 2021. B) Deposition of histone PTMs is in charge of writers such as histone acetyltransferases (HATs), histone methyltransferases (HMTs) and kinases. Removal of histone modifications is accomplished by erasers, including histone deacetylases (HDACs), histone demethylases (HDMTs) and phosphatases. Readers proteins responsible for recognizing and bind histone PTMs include bromodomains-containing proteins for acetylation marks, chromodomain-containing proteins for methylated marks or 14-3-3-containing proteins for phosphorylation marks. Adapted from Torres-Perez et al., 2021. C) Active genes are associated with histone PTMs H3K4me3 within promoter regions, H3K79me3 and H2BK120ub1 and H3K36me3 in gene bodies. Transcriptionally repressed genes are associated with H3K27me3, H2AK119ub1 and H3K9me3 within promoter regions. Adapted from Zhang et al., 2015.

4.1.2 Histone post-translational modifications

In eukaryotes, DNA is packed around nucleosomes, the structural and functional unit of chromatin (Figure 10A) (Izzo & Schneider, 2010). Each nucleosome is constituted of a histone octamer with two copies of H2A, H2B, H3, and H4, in which 147 bp of DNA is wrapped around (Figure 10A) (Izzo & Schneider, 2010). To stabilize the DNA that enters and exists in the nucleosome, an additional histone, H1, acts as a linker between the DNA and the nucleosome (Figure 10A) (Izzo & Schneider, 2010; Torres-Perez et al., 2021).

The amino acid residues within the N-terminal tail or in the globular core domains of these core histones are subject to post-translational modifications (PTMs) (Figure 10A) (T. Zhang et al., 2015). Histone PTMs regulate chromatin structure and DNA-dependent processes by recruiting protein complexes (Millán-Zambrano et al., 2022). The combination of histone PTMs influences chromatin states locally, producing transcriptionally active or silent chromatin(Figure 10A) (Millán-Zambrano et al., 2022; T. Zhang et al., 2015). Moreover, crosstalk between histone PTMs and DNA methylation further influences chromatin states and, thus, gene activity (Du et al., 2015).
The most frequent histone PTMs are acetylation, methylation, phosphorylation, and ubiquitylation (T. Zhang et al., 2015). However, there is a large number of different histones PTMs, including sumoylation, glycosylation, and S-palmitoylation (Millán-Zambrano et al., 2022).

Like DNA methylation, histone PTMs constitute dynamic and reversible epigenetic marks, whose deposition, removal, and recognition are in charge of writers, erasers, and reader proteins (T. Zhang et al., 2015). Several of these histone-modifying enzymes depend on cofactors originating from cellular metabolic pathways, which will be presented in more detail in this chapter (Gut & Verdin, 2013; Millán-Zambrano et al., 2022).
The most extensively described histone-modifying enzymes include writers such as histone methyltransferases (HMTs) (e.g., SUV39H1, G9a, the Polycomb factor EZH2 or the Trithorax factor MLL), histone acetyltransferases (HATs) (e.g., p300/CBP, PCAF), and kinases (e.g., JAK2) (Figure 10B) (Allis & Jenuwein, 2016; Mahajan & Mahajan, 2013). Removal of histone modifications is accomplished by histone demethylases (HDMTs) (e.g., jumonji-domain containing LSD1), histone deacetylases (HDACs) (e.g., SIRT2 from the sirtuin protein family), and phosphatases (e.g., EYA) (Allis & Jenuwein, 2016; Mahajan & Mahajan, 2013). Effector or reader proteins can recognize histones in a modification-specific manner through recognition domains such as bromodomains for acetylated lysine or chromodomains for methylated lysine or arginine residues (Figure 10B) (Allis & Jenuwein, 2016; Sabari et al., 2017).

Functional regions across the genome, such as transcriptionally active or repressed genes and enhancers, are associated with a particular pattern of histone PTMs (Millán-Zambrano et al., 2022). Histone acetylation is generally associated with transcriptional activity primarily due to the neutralization of the positive charge of lysine residues, leading to a more decondensed chromatin state (Millán-Zambrano et al., 2022). Hence, histone acetylation is enriched on active promoters, enhancers, and other accessible regions of chromatin (Millán-Zambrano et al., 2022). Similarly, histone phosphorylation reduces the charge of histones, increasing DNA accessibility and thus facilitating transcription (Millán-Zambrano et al., 2022). Nevertheless, for histone methylation, the effects on transcriptional activity are more complex, site-specific, and may not directly influence nucleosome structure (Millán-Zambrano et al., 2022). For example, trimethylation of lysine 4 of H3 (H3K4me3) is enriched at most promoters of active genes

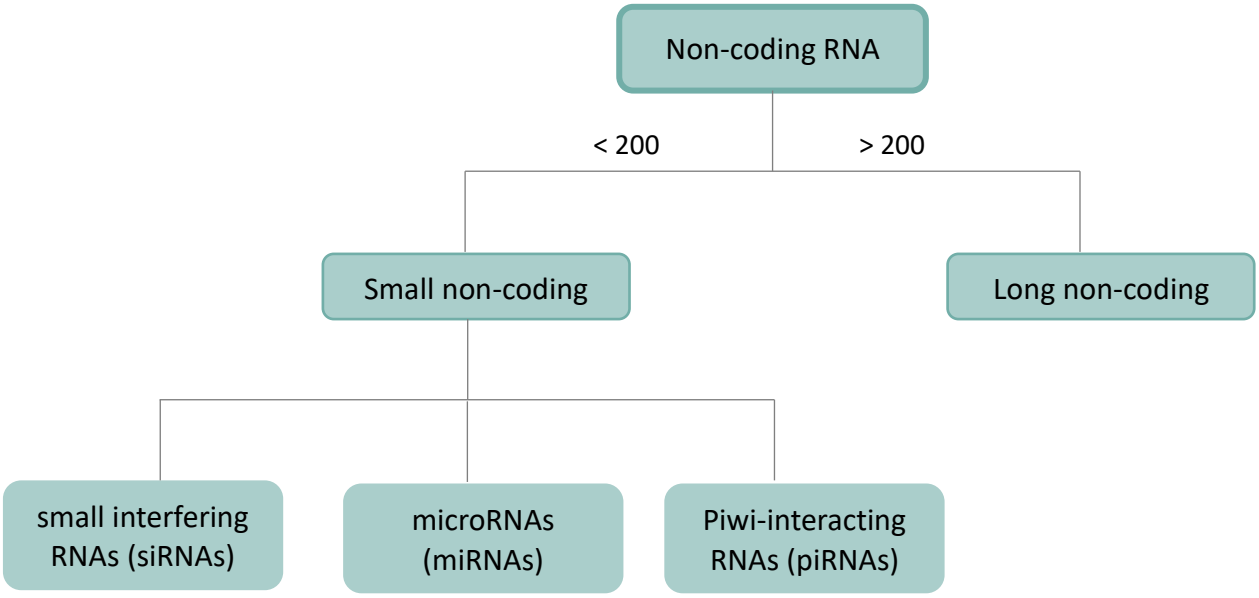

Figure 11: Simplified representation of the non-coding RNAs classification.
Non-coding RNAs can be classified by their size as short and long non-coding RNAs. Short ncRNAs are less than 200 nucleotides in length, and comprise small interfering RNAs (siRNAs), microRNAs (miRNAs) and Piwi-interacting RNAs (piRNAs). Long non-coding RNAs (lncRNAs), constitute transcripts longer than 200 nt in length.

around the TSS and is associated with transcription, whereas trimethylation on lysine 27 of H3 (H3K27me3) is associated with gene silencing (Millán-Zambrano et al., 2022).
Overall, most active genes are associated with lysine acetylation on H3 and H4 tails, H3K4me3, trimethylation of lysine 79 of H3 (H3K79me3), ubiquitylation on H2B, and trimethylation on lysine 36 of H3 (H3K36me3) (Figure 10C) (T. Zhang et al., 2015). Active enhancers are associated with mono-methylation on lysine 4 on H3 (H3K4me1) and acetylation on lysine 27 of H3 (H3K27ac) (Millán-Zambrano et al., 2022). Repressed genes are mostly associated with H3K27me3, ubiquitylation on lysine 119 of H2A (H2AK119ub1), and trimethylation on lysine 9 of H3 (H3K9me3) (Figure 10C) (T. Zhang et al., 2015).

Furthermore, histone variants, characterized by a different protein sequence such as H3.3, are also subject to histone PTMs, contributing to gene regulation, chromatin dynamics, DNA repair, and development (Martire & Banaszynski, 2020).

4.1.3 Non-coding RNAs

Non-coding RNAs (ncRNAs) are important transcriptional and post-transcriptional regulators (Fitz-James & Cavalli, 2022). They are primarily associated with gene expression repression, acting via histone modifications, chromatin-modifying enzymes, or DNA methylation, and through these interactions, they participate in epigenetic memory (Cavalli & Heard, 2019; Fitz-James & Cavalli, 2022). Moreover, ncRNAs are also implicated in regulating chromatin architecture (Cavalli & Heard, 2019).
Regulatory ncRNAs can be classified by their size as short and long non-coding RNAs (Figure 11) (P. Zhang et al., 2019). Short ncRNAs are less than 200 nucleotides in length and comprise small interfering RNAs (siRNAs), microRNAs (miRNAs), and Piwi-interacting RNAs (piRNAs) (Figure 11) (P. Zhang et al., 2019).

siRNAs are defined as double-stranded transcripts of 21-24 nt in length and are major regulators of gene silencing, whereas piRNAs are 21-30 nt in length and are mostly involved in the male germline (Fitz-James & Cavalli, 2022; Hombach & Kretz, 2016).
piRNAs maintain genome stability by repressing transposable and repetitive elements (Fitz-James & Cavalli, 2022; Hombach & Kretz, 2016). Interestingly, as shown in *Drosophila melanogaster*, the silencing mechanism of piRNAs implicates not only the post-transcriptional degradation of its target (e.g., transposable element) but also the recruitment of H3K9 heterochromatin to promote piRNAs transcription, here H3K9 differing from its known function as a repressive mark, and thus by this securing the maintenance of the silencing (Fitz-James & Cavalli, 2022). Moreover, this transposable element silencing mechanism is maintained across generations by transgenerational epigenetic inheritance (Fitz-James & Cavalli, 2022).
MicroRNAs, after a series of processing mechanisms, give rise to the mature single-stranded ~22 nt in length miRNAs, which is loaded into the RNA-induced silencing complex (RISC) to repress target mRNAs (Hombach & Kretz, 2016). miRNAs are responsible for the degradation of target mRNAs through binding to the 3′ UTR through base pair complementarity (Hombach & Kretz, 2016).

Regarding lncRNAs, they constitute transcripts longer than 200 nt in length, and can be classified into five subcategories depending on their position with respect to protein-coding genes (P. Zhang et al.,

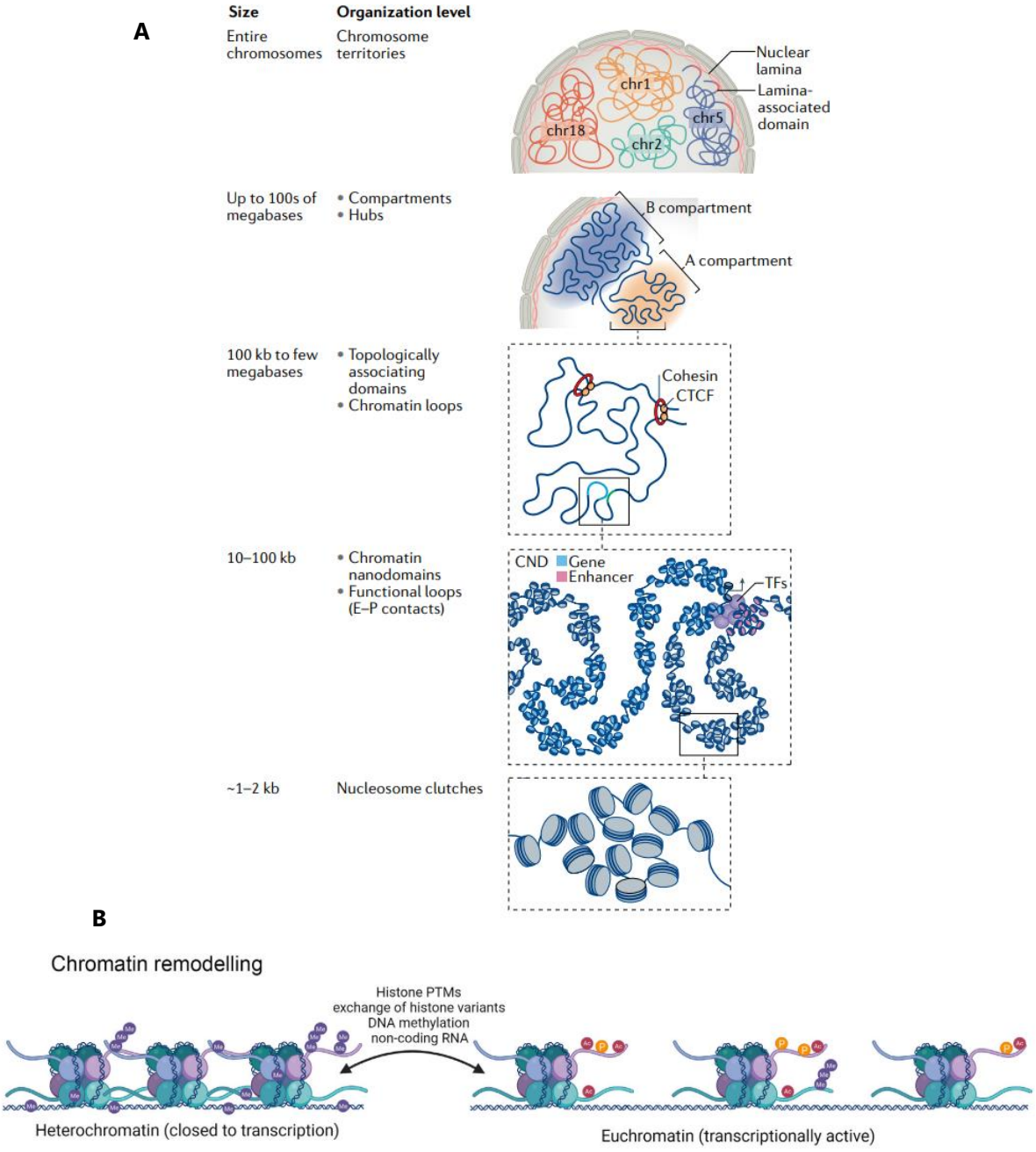

Figure 12: The 3D genome organization.

A) In the interphase nucleus, the genome follows a hierarchical organization in 3D structures. From the smallest to the biggest scale level the genome is organized by nucleosome clutches, chromatin nanodomains, chromatin loops referred to as topological associated domains (TADs), active and repressive compartments (A and B, respectively), and chromosomes territories. Adapted from Jerkovic´ & Cavalli, 2021. B) Simplified schematization of chromatin states. Open chromatin (euchromatin) generally within *cis*-regulatory elements (i.e., promoters, enhancers) is generally marked with H3K4me3 and H2AK119ub1 histone modifications, and is associated with active transcription. Closed chromatin (heterochromatin) is condensed, generally marked with H3K27me3 histone modification and is mostly associated with inactive transcription. Adapted from Torres-Perez et al., 2021.

2019). One of the most studied lncRNAs is the X-inactive specific transcript (Xist), essential for X chromosome inactivation in mammalian development (Cavalli & Heard, 2019).

4.1.4 Chromatin organization

In eukaryotes, the genome is organized and compartmentalized within the nucleus following a five levels high-order structure (Figure 12A) (Jerkovic´ & Cavalli, 2021; van Steensel & Furlong, 2019). This 3D organization that results in the formation of chromosomes includes folding by nucleosome clutches in which the DNA is wrapped around each one, followed by chromatin nanodomains where enhancer-promoter interactions take place, chromatin loops that form topological associated domains (TADs), gene-active (compartment A) and repressive (compartment B) compartments and finally into chromosomes territories (Figure 12A) (Jerkovic´ & Cavalli, 2021; van Steensel & Furlong, 2019).

At the smallest scale corresponding to the nucleosomes clutches, approximately 147 bp of DNA are tightly packed and wrapped around each nucleosome while maintaining finely-regulated chromatin accessibility capacity (Dai et al., 2020; Millán-Zambrano et al., 2022).

The 3D organization in compartments and domains is essential for biological processes, notably transcription (van Steensel & Furlong, 2019). At the same time, transcription, by forming subcompartments and subdomains and stabilizing enhancer-promoter interactions, further influences this organization (Figure 12A) (van Steensel & Furlong, 2019).
Based on their structural and biochemical properties, chromatin can be classified as heterochromatin and euchromatin (van Steensel & Furlong, 2019). Heterochromatin is considered condensed and is constituted of transcriptionally inactive or repressed genomic regions, whereas euchromatin is considered decondensed and constituted of transcriptionally active regions (van Steensel & Furlong, 2019).
Furthermore, the formation of heterochromatic or euchromatic regions depends on their associated epigenetic modifications (Dai et al., 2020; van Steensel & Furlong, 2019). Heterochromatin is associated with H3K27me3 or by H3K9me3 and H3K9me2, and is concentrated at the nuclear lamina and around the nucleoli (Figure 12B) (van Steensel & Furlong, 2019). Euchromatin, as it is associated with active genes and enhancer elements, is marked with different histone modifications, including H3K4me3, and is mostly situated in the nuclear interior (Figure 12B) (van Steensel & Furlong, 2019).
Heterochromatic and euchromatic regions are dynamic, especially during cell differentiation (van Steensel & Furlong, 2019). Transcriptional activation or gene silencing can induce genes situated at the nuclear lamina to be repositioned in the nuclear interior and vice versa (van Steensel & Furlong, 2019).
Nevertheless, for most genes, it is unclear whether the gene expression state induces repositioning of the gene or it is the repositioning that influences gene expression (van Steensel & Furlong, 2019).
The chromatin is capable of responding to specific cues, and thus for genomic regions to undergo DNA-templated processes such as transcription, recombination, replication, or repair, tightly condensed heterochromatin regions must decondense, thereby increasing accessibility to different components of the cellular machinery (Figure 12B) (Millán-Zambrano et al., 2022).

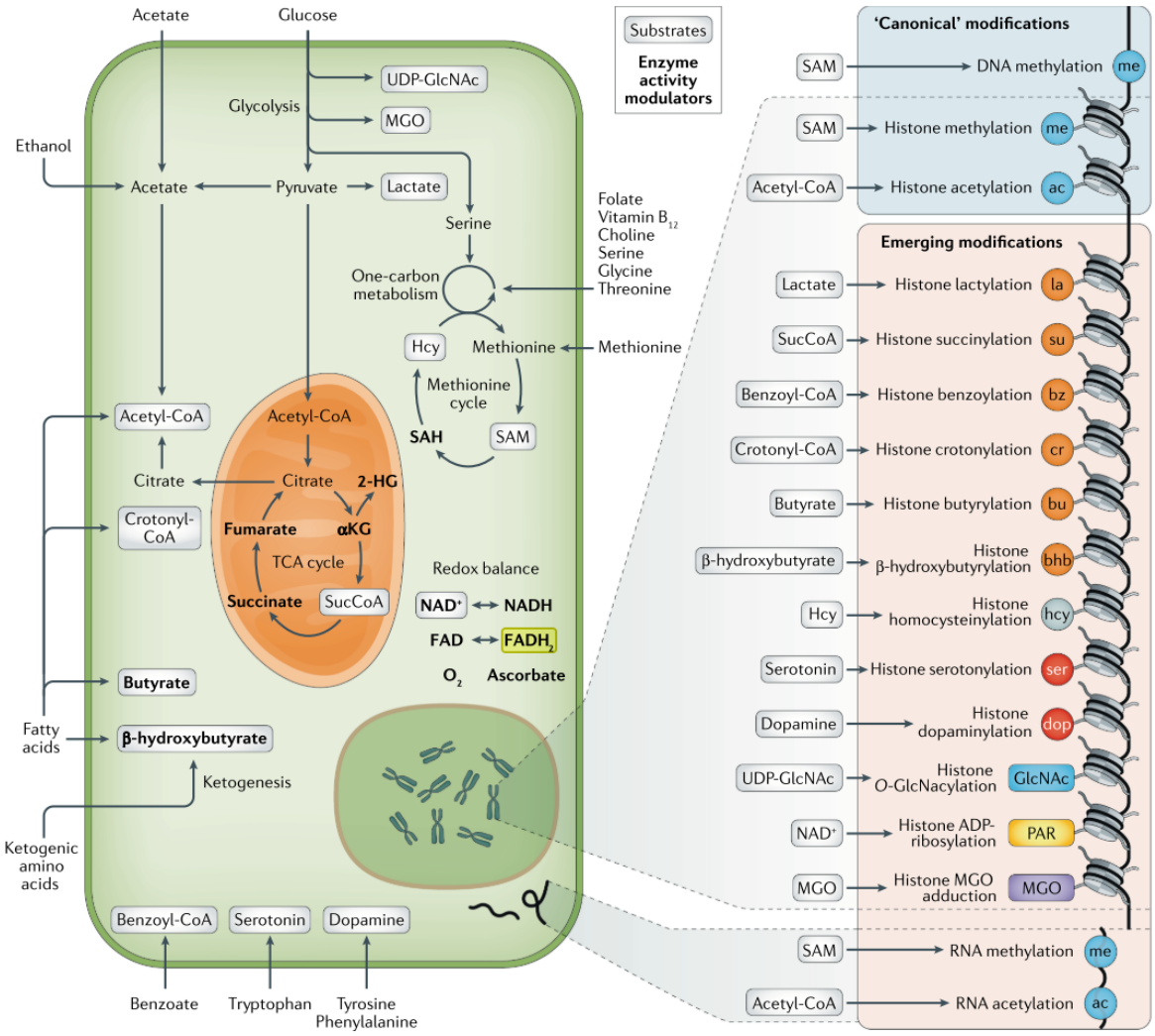

Figure 13: Metabolic pathways involved in the production of substrates and co-factors for epigenetic modifications.

Metabolism of dietary inputs such as glucose, fatty acids, amino acids and vitamins feed the intracellular pool of metabolites and regulate epigenetic modifications by supplying the substrates and co-factors for chromatin-modifying enzymes. Different metabolic pathways are implicated including glycolysis, the tricarboxylic acid (TCA) cycle, the one-carbon metabolism. Canonical modifications influenced by metabolic outputs include DNA and histone methylation, and histone acetylation. Emerging modifications similarly influenced include the constantly increasing group of histone post-translational modifications and RNA methylation and acetylation reactions. From Dai et al., 2020.

4.2 The interlink of cellular metabolism and epigenetics

The epigenome is sensitive to nutrient availability, and this is because chromatin-modifying enzymes use products of cellular metabolism as substrates and cofactors for epigenetic modifications (Figure 13) (Dai et al., 2020). The interlink between cellular metabolism and epigenetics has attracted more attention in recent years, not only because it contributes to our understanding of how cells respond to environmental cues but also because it opens the possibility of dietary and pharmacological interventions in pathological contexts.

There are numerous examples of the influence of intracellular metabolic status on the epigenome. One clear example is the methyl donor S-adenosylmethionine (SAM), implicated in all methylation reactions (Janke et al., 2015). SAM is produced through the one-carbon metabolism, a bi-cyclic pathway constituted of folate and methionine cycles that circulate carbon units and results in the production of several outputs, including SAM (Figure 13) (Locasale, 2013).
Dietary inputs directly influence and feed the one-carbon metabolism, such as methionine, which is almost exclusively supplied through diet in mammals (Dai et al., 2020).
Similarly, glycolysis-derived 3-phosphoglycerate (3PG) can be converted into serine, feeding the folate cycle and triggering its initiation (Locasale, 2013). Moreover, perturbations in methionine or the one-carbon metabolism affect SAM availability, which results in aberrant DNA and histone methylation profiles and gene expression changes (Dai et al., 2020).

DNA and histone methylation erasers TETs, jumonji-domain-containing demethylases (JHDMs), and amine oxidases are similarly influenced by the intracellular metabolic state. TETs and JHDMs require TCA-derived α-ketoglutarate as co-substrate, and its activity is inhibited by α-ketoglutarate analogs succinate and fumarate (Dai et al., 2020). Likewise, catalysis of TETs and JHMDs is activated by ascorbate, and requires ferrous iron as cofactor. On the other hand, the JHMDs LSD1 requires flavin adenine dinucleotide (FAD) as cofactor, and FAD is usually produced in the mitochondria and cytoplasm from riboflavin, also known as vitamin B2 (Etchegaray & Mostoslavsky, 2016). The ratio of FAD/$FADH_2$ dictates the level of nuclear FAD for epigenetic functions (Etchegaray & Mostoslavsky, 2016).
One-carbon metabolism may also be influenced by the cellular redox status (Dai et al., 2020; Locasale, 2013). In *C. elegans*, ROS generation leads to inhibition of H3K3 methyltransferases, reduced global levels of H3K4me3, and gene expression changes in long-term survival genes (Dai et al., 2020). Similarly, hypoxia and oxygen availability inhibited DNA and histone demethylases, and resulted in global changes in histone and DNA methylation (Dai et al., 2020).

The crosstalk between cellular metabolism and histone acetylation has also been extensively studied in different cellular contexts. In mammals, the breakdown of carbohydrates, notably glucose generates acetyl-CoA, which supplies the acetyl group for acetylation reactions (Dai et al., 2020).
More precisely, glucose metabolism results in the production of citrate, which is then exported back to the cytosol where it is converted to acetyl-CoA by the ATP-citrate lyase (ACLY) (Dai et al., 2020). Nevertheless, other sources can also produce acetyl-CoA, such as pyruvate, through *de novo* acetate production or by fatty acid β-oxidation (Figure 13) (Dai et al., 2020; Martínez-Reyes & Chandel, 2020).

Glucose abundance, enhanced glycolysis and consequently, acetate and acetyl-CoA production influence global levels of histone acetylation (Dai et al., 2020; Lu & Thompson, 2012). HDACs use

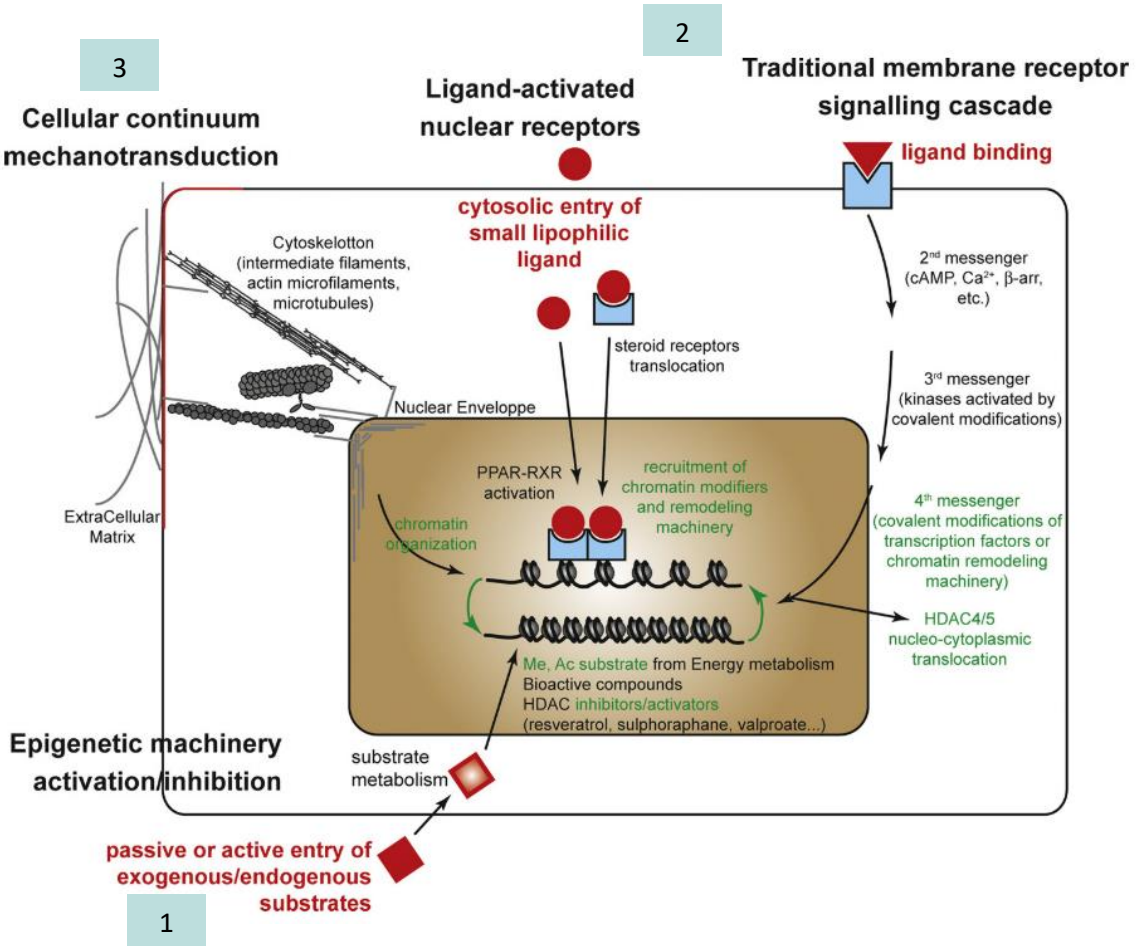

Figure 14: The potential mechanisms linking environmental cues, epigenetic mechanisms and developmental programming.

1) Changes in energy metabolism lead to alterations in substrate availability such as increased acetyl-CoA or SAM, thus impacting on histone post-translational modifications, chromatin dynamics and gene expression regulation. 2) Activation of signaling cascades through binding of ligands to membrane-bound or nuclear receptors may lead to gene expression regulation of downstream targets. Environmental insults such as endocrine disruptors can bind to nuclear receptors (i.e., estrogen receptors), similarly leading to gene expression regulation. 3) The extracellular matrix, the cytoskeleton and the nuclear envelope are connected. Changes in the extracellular matrix and/or the cytoskeleton may influence the nuclear envelope, leading to chromatin remodeling, which could itself influence gene expression. Adapted from Safi-Stibler & Gabory, 2020.

metabolites such as butyrate and β-hydroxybutyrate produced during fatty acid oxidation or ketogenesis, whereas sirtuins are affected by intracellular levels of NAD^+ (Dai et al., 2020). Glucose metabolism similarly impacts histone O-GlcNAcylation (Dai et al., 2020). The UDP-GlcNAc, a by-product of the HBP is used as a substrate for the β-N-acetylglucosamine (GlcNAc) in serine or threonine residues of histones (Dai et al., 2020).
Non-enzymatic chromatin modifications such histone methylglyoxal (MGO) adduction may also be influenced by metabolism since MGO, a precursor of AGE is a by-product of glycolysis, AA, and lipid metabolism (Figure 13) (Dai et al., 2020). Indeed, enhanced MGO glycation is correlated to increased glycolytic activity (Dai et al., 2020).

The role of metabolism on epigenetic modifications has been associated with different processes, especially in development, including lineage specification and induction and maintenance of pluripotency (Dai et al., 2020). In pluripotent human and mouse embryonic stem cells (ESCs), it was demonstrated that the first hours towards differentiation are characterized by loss of glucose-derived acetyl-CoA and acetate and subsequent loss of histone acetylation and that modulation of glycolysis, blocked histone deacetylation and differentiation (Moussaieff et al., 2015). Similarly, in proliferating muscle stem cells, low OXPHOS led to increased availability of glucose-derived acetyl-CoA and subsequent histone acetylation and chromatin accessibility at lineage-specific genes, but shift towards high OXPHOS during differentiation diminished histone acetylation levels (Yucel et al., 2019).

Noteworthy, it is unlikely that only the availability of a given metabolite is determinant for epigenetic changes. The local recruitment of chromatin-modifying enzymes to specific genomic regions, together with the distribution and availability of required substrates and co-factors in microdomains at the chromatin level, might contribute to the fine regulation of the epigenome (Katada et al., 2012). Reinforcing this hypothesis, both acetyl-CoA and SAM can localize in the nucleus within specific genomic loci to efficiently provide a sufficient source for chromatin-modifying enzymes (Dai et al., 2020).

4.3 Epigenetics as the candidate underlying mechanism of DOHaD

Epigenetic mechanisms are hypothesized to mediate the consequences of early life exposures, the memory of these exposures, and the high risk of NCDs later in life. Moreover, tightly-regulated epigenetic mechanisms are particularly crucial during the critical windows of development (i.e., periconceptional period, organogenesis, post-natal period); thus, alterations of the epigenome during development may contribute to programming (Safi-Stibler & Gabory, 2020).

The possible mechanisms by which epigenetics may respond to environmental cues and contribute to developmental programming have been proposed (Figure 14) (Safi-Stibler & Gabory, 2020). These mechanisms include 1) changes in substrate availability (i.e., acetyl-CoA or SAM) that may induce alterations in histone PTMs patterns at the genome-scale or locally, at gene-specific regions, thereby influencing chromatin dynamics and gene expression regulation (Safi-Stibler & Gabory, 2020). 2) Activating signaling cascades result in the gene expression regulation of downstream targets (Safi-Stibler & Gabory, 2020). For example, environmental insults such as endocrine-disrupting chemicals, frequently found in everyday items, bind to nuclear receptors such as estrogen receptors and influence the expression of downstream targets (Balaguer et al., 2019). 3)Through the crosstalk between the

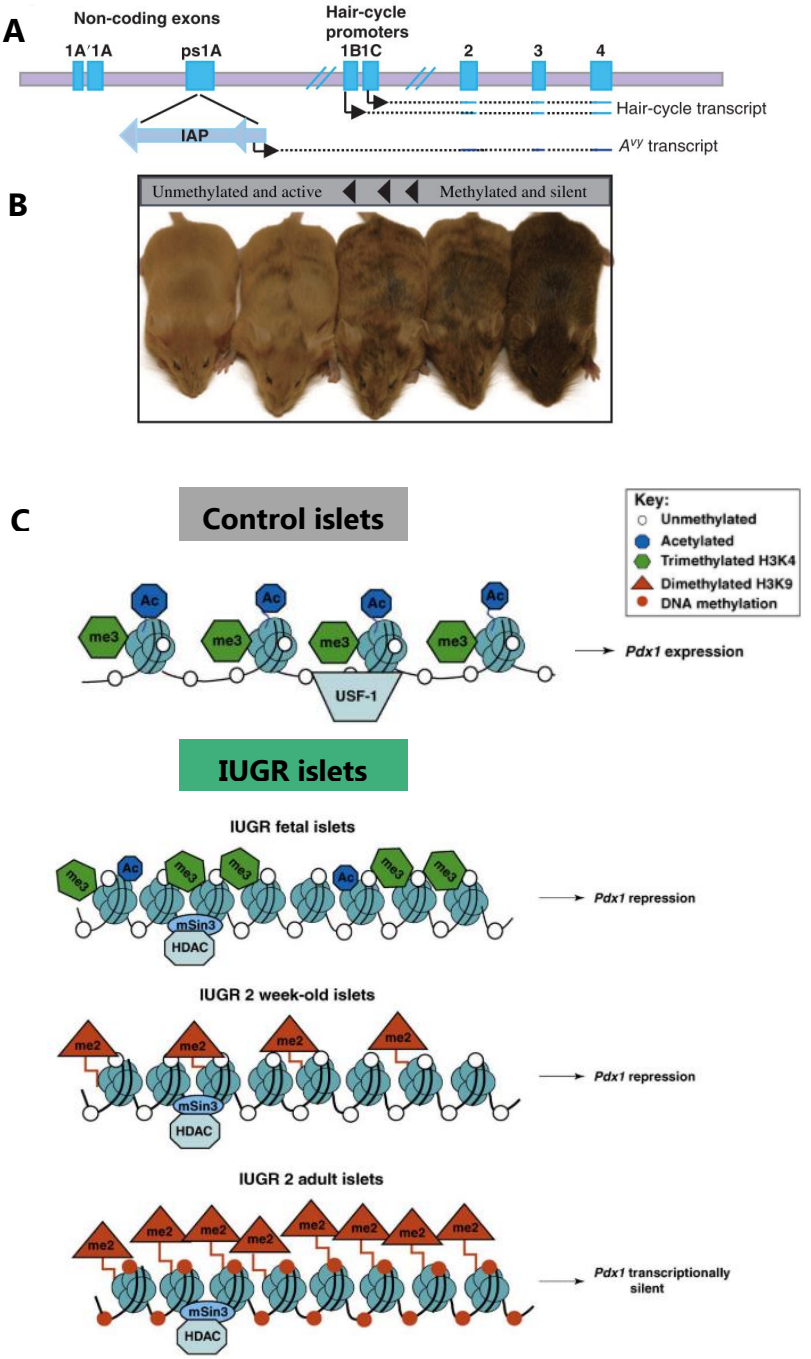

Figure 15: The agouti *A^{vy}* and IUGR-*Pdx1* mouse models.

A) The mutated *A^{vy}* allele is characterized by the insertion of the intracisternal A particle (IAP) retrotransposon between pseudo-exon 1A and exon 2 of the agouti gene, involved in the regulation of coat color. When the *A^{vy}* IAP is methylated, the agouti gene is transcribed from the hair-cycle promoters (exons 1B1C), leading to dark coat color. In contrast, unmethylated *A^{vy}* IAP leads to yellow coat color and altered metabolic phenotype in the adult offspring. B) Range of coat color according to the level of DNA methylation in the *A^{vy}* IAP allele. Adapted from Wang et al., 2017. C) IUGR causes progressive silencing of the *Pdx1* gene in pancreatic islets. In control pancreatic β-cells, the proximal promoter of *Pdx1* is unmethylated and in an open chromatin state with binding of the transcription factor USF-1 (gray box). In IUGR mice, from fetal to adult stages, *Pdx1* is progressively silenced, starting with the loss of histone acetylation and binding of USF-1, followed by H3K9me2 and DNA methylation positioning (green box). Adapted from Pinney & Simmons, 2010.

extracellular matrix, the cytoskeleton, and the nuclear envelope. Changes in the extracellular matrix or the nuclear envelope may influence chromatin dynamics and gene expression regulation (Figure 14) (Safi-Stibler & Gabory, 2020).

Numerous studies have shown an association between early life exposures to environmental cues and deregulated epigenetic mechanisms (H. S. Lee, 2015; Waterland & Michels, 2007).
In humans exposed to the Dutch Famine, aberrant methylation profiles were detected particularly in those exposed to famine during the first trimester of pregnancy, compared to their unexposed siblings (Heijmans et al., 2009; Tobi et al., 2014). Lower methylation levels were identified in the *IGF2* imprinted gene, an essential regulator of growth and development, while the methylation profile of seven other genes, including the leptin gene, an important regulator of energy metabolism, were associated with the famine exposure (Heijmans et al., 2009).
Interestingly, a second genome-scale analysis of individuals exposed to the Dutch famine identified that differentially methylated regions (DMRs) were mostly localized within regulatory regions next to DEGs (Tobi et al., 2014). Remarkably, these signatures were detected six decades after exposure to famine (Heijmans et al., 2009).

The influence of parental nutrition in the DNA methylation profiles on the offspring is shown in the agouti viable yellow mice (A^{vy}). The A^{vy} mice is a well-characterized mutation of the agouti gene, which regulates the coat color (Rosenfeld, 2009). The A^{vy} mice carry the insertion of the retrotransposon intracisternal A particle (IAP) upstream of the exon 2 of the agouti gene (Figure 15A) (Rosenfeld, 2009; Y. Wang et al., 2017). As a consequence, the expression of the agouti gene is regulated by a cryptic promoter of the IAP, whose expression is regulated by the level of DNA methylation (Rosenfeld, 2009). Therefore, different degrees of DNA methylation in the A^{vy} IAP result in different nuances of coat color, from yellow corresponding to hypomethylation of the A^{vy} IAP, brown corresponding to partial levels of DNA methylation in the A^{vy} IAP, to completely pseudo-agouti coat color (dark) corresponding to the complete methylation of the A^{vy} IAP (Figure 15B) (Rosenfeld, 2009; Y. Wang et al., 2017).
Supplementation with methyl donor through diet influences the methylation profile of the A^{vy} IAP in the offspring. When pregnant female A^{vy} mice were fed with a supplemented methyl donor diet, DNA methylation of the A^{vy} IAP increased, leading to pseudo-agouti dark coat color in the offspring compared to offspring from female A^{vy} mice fed with standard chow (Rosenfeld, 2009).
Moreover, when the A^{vy} IAP is completely demethylated (yellow coat color), the agouti gene is expressed in other organs than the skin and is associated with an altered metabolic phenotype characterized by obesity, hyperinsulinemia, and hyperglycemia (Rosenfeld, 2009). The DNA methylation profile and the altered metabolic phenotype in A^{vy} offspring can be maintained for up to two generations despite being fed normal diets (Y. Wang et al., 2017). Thus, by modulating maternal diet and increasing the methylation of the A^{vy} IAP, the altered metabolic phenotype can also be prevented. This is a clear example of parental diet, epigenetic changes, and disease risk in the offspring.

The IUGR model developed by Simmons and colleagues is another clear example of the contribution of epigenetic mechanisms in developing chronic diseases in adulthood (Park et al., 2008; Pinney & Simmons, 2010). Undernutrition by uteroplacental insufficiency *in utero* led to reduced expression of *Pdx1* from fetal stages (Figure 15C) (Park et al., 2008). *Pdx1* is a transcription factor key in the regulation of pancreas development, β-cell differentiation, and function (Park et al., 2008). In human and animal

models, reduced expression of *Pdx1* results in T2D, β-cell dysfunction, and impaired islet compensation under insulin resistance (Park et al., 2008).
In this model, the phenotype aggravated with age and was characterized by almost absent *Pdx1* expression and T2D development (Park et al., 2008). Assessment of fetal stages of this model demonstrated a coordinated and progressive silencing of *Pdx1* with age (Park et al., 2008). This progressive silencing initiated with the recruitment of HDAC1 and mSin3A to the proximal promoter of *Pdx1,* the deacetylation of H3 and H4, and the loss of binding of USF-1, the transcription factor implicated in *Pdx1* expression (Park et al., 2008). At two weeks of age, the proximal promoter of *Pdx1* showed loss of H3K4me3, a histone PTM associated with transcriptional activation, and methylation of H3K9me2, associated with the establishment and maintenance of heterochromatin (Figure 15C) (Park et al., 2008). Further, once the offspring developed T2D at a later age, characterization of the proximal promoter of *Pdx1* showed CpG island DNA methylation by DNMT1, ensuring the stable silencing of *Pdx1* (Park et al., 2008).
Interestingly, in two-weeks old animals, inhibition of HDACs but not DNA methylation partially restored *Pdx1* expression and reestablished USF-1 binding, thus opening the possibility for therapeutic interventions at this early stage, before the onset of T2D (Park et al., 2008).
A similar mechanism was demonstrated in macaques exposed to HFD during pregnancy (Aagaard-Tillery et al., 2008). The offspring showed hyperacetylation of hepatic tissues at the fetal stage, reduced HDAC1 expression, gene expression changes in key metabolic genes, increased liver triglycerides, and histological characteristics of non-alcoholic fatty liver disease (Aagaard-Tillery et al., 2008).

Nevertheless, few have demonstrated a clear mechanistic link between early life events, tissue-specific epigenetic dysregulation, and disease development later in life (Bianco-Miotto et al., 2017).

5. Environmental cues and their link to developmental programming

Experimental and epidemiological studies have provided a large amount of evidence regarding different types of environmental insults with a potential "programming" effect. Among those, we can highlight the exposure to chemical insults (i.e., parental smoking and alcohol consumption, air pollution), stress, assisted reproductive technology (ART) during the periconceptional period, and suboptimal maternal nutrition (i.e., under and overnutrition) and metabolic status. The consequences of suboptimal maternal nutrition and metabolic status in the offspring will be described in detail by the end of this section.

Exposure to chemicals, including parental smoking and exposure to air pollution, has been shown to affect pre- and post-natal development adversely. Pre-natal exposure to maternal smoking impairs growth trajectories in fetal development and is associated with lower birth weight, risk of asthma during childhood, obesity, T2D, and cancer (Cardenas et al., 2019; Vaiserman & Lushchak, 2019). Paternal smoking has been similarly associated with metabolic perturbations in the offspring, notably with accumulated body fat in males (Fernandez-Twinn et al., 2019).
In rats, alcohol ingestion during pregnancy was associated with insulin resistance and enhanced gluconeogenesis until adulthood (Vaiserman & Lushchak, 2019). These metabolic alterations were detected in the offspring even when maternal alcohol consumption occurred from four days prior to conception to four days during the pre-implantation period (Vaiserman & Lushchak, 2019).

Exposure to air pollution (i.e., carbon oxides, nitrogen oxides, ozone, polycyclic hydrocarbons, ultrafine particles, among others) *in utero* is associated with low birth weight, premature birth, cardiovascular disease, and respiratory diseases at adult age (Saenen et al., 2019). Experimental studies in rabbits exposed to diesel engine exhaust *in utero* showed an increased risk for insulin resistance and cardiovascular diseases in the offspring, but in a sex-specific manner, with the male offspring presenting a more severe phenotype characterized by MetS-like signatures (Rousseau-Ralliard et al., 2021).

Concerning psychological stress and mental health, numerous epidemiological studies have demonstrated that adverse childhood experiences such as neglect and physical and sexual abuse are positively associated with metabolic diseases such as T2D later in life (H. Huang et al., 2015).
Animal studies have demonstrated the same pattern. Wild-type mice separated from mothers after birth for three hours per day for ten days exhibited common features of obesity and T2D phenotypes at young adult age (Ilchmann-Diounou et al., 2019). The effects of maternal separation in the offspring included IGT, reduced insulin sensitivity, altered intestinal homeostasis including increased secretion of the satiety hormone ghrelin, and perturbed intestinal immune system, accompanied by microbiota dysbiosis, which is characterized by the loss of beneficial or expansion of harmful microorganisms (Ilchmann-Diounou et al., 2019). Several other studies using animal models have demonstrated that maternal nurturing behavior influences stress responses in the offspring (Portha et al., 2011). Offspring of rat mothers that showed a "high" nurturing behavior characterized by licking and grooming were less fearful, showed reduced anxiety, and reduced hypothalamic-pituitary-adrenal (HPA) response to stress compared to the offspring from "less" nurturing mothers (Portha et al., 2011).

Nutritional and metabolic imbalances, especially *in utero,* have been extensively studied in human and animal models. This next section will be dedicated to describing maternal nutritional and metabolic imbalances and their influence on the offspring.

5.1 The nutritional and metabolic context *in utero*

Suboptimal nutrition, i.e., under- and overnutrition *in utero,* alters the microenvironment of the conceptus and may lead to adaptations in the placenta and the developing fetus and lifelong increased risk for NCDs (Fleming et al., 2015). Moreover, human epidemiological studies and animal models have demonstrated that restricted and excessive nutrition and metabolic imbalances during development may lead to chronic diseases later in life (Fleming et al., 2015).
Analysis of human epidemiological data allows to demonstrate associations between a given environmental cue and phenotypes, but they remain rather limited in the search for underlying mechanisms and can be complex to interpret due to confounding effects. In this regard, animal models offer an opportunity to examine better the mechanisms underlying the different nutritional and metabolic challenges linked to predisposition to NCDs at a later age, to explore the different windows and duration of exposure, and to evaluate potential intervention strategies.

Hereafter, unless otherwise specified, I will focus on describing the effects of maternal diet and metabolic status *in utero*.

5.1.1 Undernutrition *in utero*

Undernutrition *in utero* may originate from the reduced bioavailability of nutrients due to suboptimal maternal diet, increased nutritional loss, or an impaired capacity of nutrient utilization from the conceptus (Velazquez & Fleming, 2013). Undernutrition *in utero* may result in fetal intrauterine growth retardation (IUGR), a common complication during pregnancy defined as the failure to achieve expected growth for a given gestational age (Armengaud et al., 2021; Martin-Gronert & Ozanne, 2007). Undernutrition and IUGR are associated with increased risk for NCDs in adulthood (Armengaud et al., 2021; Pinney, 2013).

Early life exposure to undernutrition and the potential adverse outcomes in the offspring have been extensively studied through retrospective analysis of well-documented periods of undernutrition, such as the Dutch famine in 1944 in the Netherlands, or through experimentation using animal models (Armengaud et al., 2021; Fleming et al., 2018).
In the following lines, I will present some examples of undernutrition *in utero* from human epidemiological and animal studies.

5.1.1.1 Human epidemiological studies of undernutrition *in utero*

Undernutrition in natural or human-induced settings has provided a unique opportunity to examine the short- and long-term effects of these stresses in the offspring.
One of the most extensively studied human-induced undernutrition settings is the Dutch famine, also referred to as the "Dutch Hunger Winter". The Dutch famine corresponds to an approximately six months period of food restriction that took place during the winter of 1944-1945, corresponding to the last months of the German occupation (Lumey et al., 2011). The Dutch famine occurred in a well-nourished population, but during this period, access to food was severely restricted, reaching 400 calories per day per person by the last months of the famine (Lumey et al., 2011; Peral-Sanchez et al., 2021; Roseboom, 2019).

Despite the geopolitical context, medical attention was maintained, and well-documented medical records were kept during this period, which has made it possible to retrospectively assess the effects of undernutrition during pre-natal life, and to precisely pinpoint the period of pregnancy impacted (Lumey et al., 2011; Roseboom, 2019).

These retrospective studies showed that the adult offspring exposed to the famine stresses *in utero* was associated with impaired metabolic, cardiovascular, and mental health (Roseboom, 2019).
All exposed periods of pregnancy led to increased total cholesterol, impaired glucose tolerance, especially when the exposure took place at late gestation, and increased prevalence of MetS and T2D in the adult offspring (~58 years old) (Lumey et al., 2011). Between men and women, some differences were observed. For example, women but not men showed increased triglyceride levels (Lumey et al., 2011).

When the timing of pregnancy exposed to the famine was explored in detail, a few differences were detected. Exposure in early gestation was associated with decreased DNA methylation in the imprinted

gene IGF-2, an important regulator of fetal development and growth; the increased prevalence of obesity increased antisocial personality and two-fold increased schizophrenia risk (Lumey et al., 2011; Peral-Sanchez et al., 2021). Exposure during mid-gestation was associated with an increased prevalence of mood disorders and antisocial personality, whereas exposure during late gestation was associated with decreased birth weight, increased prevalence of mood disorders, and higher mortality rates in the next generation (Lumey et al., 2011).

Furthermore, some specificities can be highlighted from the period of pregnancy impacted. Indeed, some have suggested that early pregnancy was the most vulnerable period to famine stresses (Roseboom, 2019). When compared to their non-exposed siblings, only early gestation was associated with changes in DNA methylation levels of IGF-2 in the ~59 years old offspring (Lumey et al., 2011). On the contrary, effects associated with altered size at birth were mostly found in late gestation exposure (Roseboom, 2019). Interestingly, when intergenerational effects were examined, only exposure during early- and mid-gestation but not late was associated with lower birth weight in the next generation (Lumey et al., 2011).

However, it is important to keep in mind that this period of undernutrition was also accompanied by other exposures such as the stress of the war and occupation, the extremely cold temperatures, and the use of food substitutes such as tulips bulbs, which can be quite toxic if ingested in their entirety (Lumey et al., 2011).

5.1.1.2 Animal models of undernutrition *in utero*

Animal models of IUGR can be generated through a low protein diet (LPD), total calorie restriction, or by induction of uteroplacental insufficiency through uterine artery ligation (Hoffman et al., 2017; Pinney, 2013). In this latter, both oxygenation and substrate availability is reduced (Hoffman et al., 2017; Pinney, 2013).

A clear example of how early life exposures to undernutrition may lead to developmental programming of T2D was shown in an IUGR rat model (Park et al., 2008). In the rat, IUGR caused by uteroplacental insufficiency at 18 days of gestation (4 days before term), resulted in β-cells alterations and T2D development in adults (Park et al., 2008). Searching the responsible mechanisms of IUGR-induced T2D onset revealed that IUGR fetuses had more than 50% reduced expression of *Pdx1* mRNA (Park et al., 2008). *Pdx1* is a transcription factor essential in pancreas development, β-cell differentiation, and function (Park et al., 2008). Reduced expression of *Pdx1* is associated with T2D, β-cell dysfunction, and impaired islet compensation under insulin resistance (Park et al., 2008).
Follow-up of *Pdx1* expression during development in the IUGR model showed that the offspring had reduced expression of *Pdx1* at birth but without perturbation of the β-cell mass (Park et al., 2008). However, IUGR offspring showed almost complete absence of Pdx1 expression at adult age, and the β-cell mass was severely reduced (Park et al., 2008).
As explained in section 4.3 of this chapter, further examination of the potential mechanisms deregulating *Pdx1* expression in this model showed a series of sequential events leading to the maintained silencing of *Pdx1* via epigenetic mechanisms, including the recruitment of chromatin-modifying enzymes, histone modifications, and DNA methylation at the proximal promoter of *Pdx1* (Park et al., 2008). These

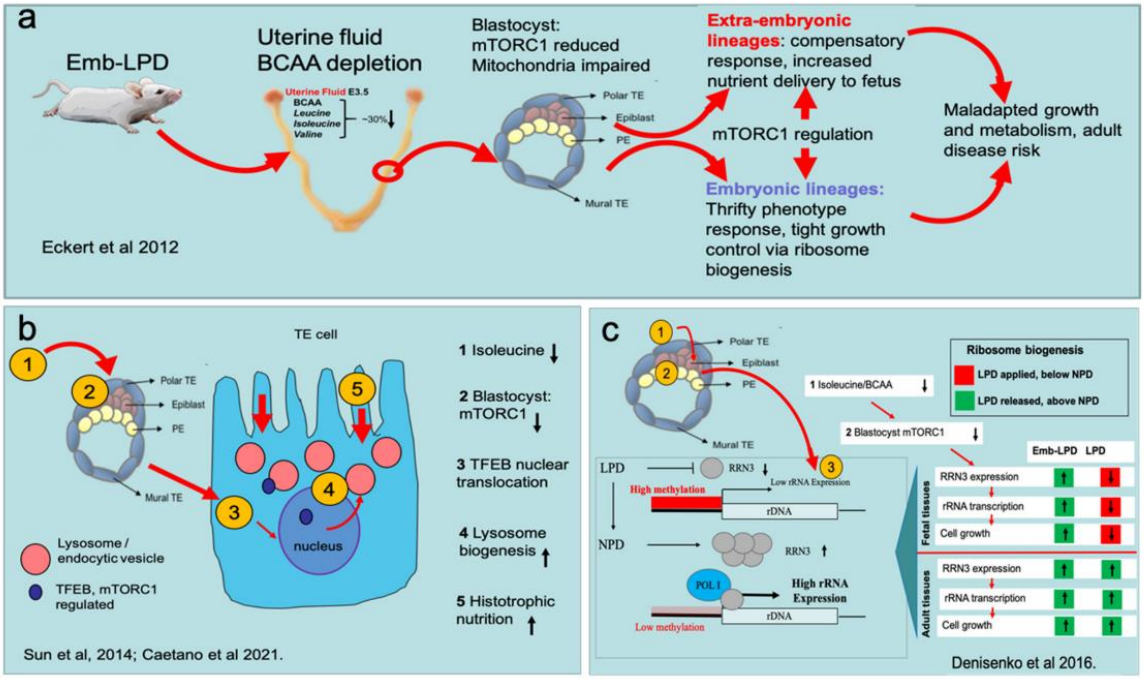

Figure 16: Undernutrition by a low protein diet during the preimplantation period results in altered embryo, fetal and adult phenotype.

a) Overview of the main responses in the Emb-LPD model. Maternal low protein diet during the preimplantation period reduced the level of branched amino acids within uterine fluids, leading to reduced mTORC1 signaling in early embryos. Extra-embryonic lineages triggered compensatory mechanisms to increase nutrient supply towards the embryo, while embryonic lineages resulted in altered ribosome biogenesis, implicated in growth regulation. These molecular and cellular responses within early embryos resulted in increased disease risk in adulthood. b) In both Emb-LPD and LPD models, the extra-embryonic lineage of early embryos, the trophectoderm (TE), activated compensatory mechanisms to enhance nutrient uptake. Reduced levels of isoleucine reduced mTORC1 signaling, stimulating the translocation of the transcription factor TFEB to regulate lysosome biogenesis and enhanced histotrophic nutrition. c) Embryonic lineages in early embryos, from both Emb-LPD and LPD models, modify rRNA transcription rates by regulating DNA methylation levels according to nutrient availability. In the Emb-LPD model, fetal and adult tissues increased rRNA transcription rates above control (NPD) levels, whereas, in the LPD model, fetal tissues reduced rRNA transcription rates, which subsequently increased in adult tissues. From Fleming et al., 2021.

sequential events occur progressively, from fetal stages until adult age, where the onset of T2D was detected (Park et al., 2008).

Another extensively studied model of undernutrition is the one developed by Fleming and colleagues (Figure 16) (Fleming et al., 2015, 2018). Different windows of development and both maternal and paternal contributions have been assessed in this model. The undernutrition challenge was accomplished by feeding rodents with an LPD diet consisting of 9% casein compared to the normal protein diet (NPD) composed of 18% casein (Fleming et al., 2015). Both diets contained the same level of macro- and micronutrients, with an increase of 14% in carbohydrates in the LPD to ensure both diets were isocaloric (Fleming et al., 2015).
Exposure of rodents to a low protein diet during the three to four days of the preimplantation period (Emb-LPD) or throughout gestation (LPD) led to embryonic, fetal, and adult altered phenotypes, but the impact during preimplantation development was overall more severe (Fleming et al., 2018, 2021). Indeed, the Emb-LPD triggered a multifactorial and sequential series of adaptations initiated in the preimplantation embryo (Figure 16) (Fleming et al., 2021). The low protein diet perturbated the composition of the maternal serum and uterine fluid, resulting in reduced AA, especially branched AA, mild hyperglycemia, and reduced insulin levels (Fleming et al., 2021). In response to these changes, early embryos triggered a series of molecular and cellular adaptations. Early embryos decreased mTORC1 signaling as a consequence of reduced branched AA and insulin levels and activated compensatory mechanisms in the extracellular lineages to enhance the delivery of nutrients (Figure 16) (Fleming et al., 2021). These compensatory mechanisms were maintained at post-implantation stages, possibly to protect fetal growth, even though at this period, a normal protein diet was restored (Fleming et al., 2021). As a result, increased fetal-to-placental weight ratio and birthweight was observed in the offspring (Fleming et al., 2021). Additionally, alterations in ribosome biogenesis were also identified, further influencing fetal growth (Figure 16) (Fleming et al., 2021).
The multiple responses initiated in the early embryo and further evolved during fetal and post-natal stages resulted in altered adult phenotypes at cardiometabolic, neurological, and skeletal levels (Fleming et al., 2021). Cardiometabolic perturbations included hypertension and reduced capacity for arterial dilatation in both male and female offspring, but with higher growth and adiposity observed in females (Fleming et al., 2021). Neurological perturbations in the adult offspring included reduced survival of neural stem cells and changes in neural networking capacity in the fetal brain, which resulted in changes in adult behavior affecting both locomotor and memory capacities (Fleming et al., 2021). Again, neurological alterations were mostly observed in the female offspring (Fleming et al., 2021). As for skeletal alterations, they involved increased fetal bone formation and reduced mineral density, characteristic of osteoporosis in humans; and were mostly observed in the male offspring (Fleming et al., 2021).

Compared to the LPD model, where the undernutrition stress was maintained throughout pregnancy, similar altered phenotypes were observed, notably the compensatory mechanisms in the extraembryonic lineages of the early embryo, an altered transcription rate of rRNA, and hypertension at adult stages (Fleming et al., 2018, 2021). However, contrary to Emb-LPD, LPD offspring showed reduced birthweight (Fleming et al., 2021).
Interestingly, the transcription rate of rRNA, which is coupled to ribosome biogenesis, mirrored nutrient availability and was affected in both Emb-LPD and LPD models. In the LPD model, rRNA transcription

rate was reduced in fetal tissues but upregulated after birth, whereas in the Emb-LPD model, rRNA transcription rate was upregulated in both fetal and adult tissues (Fleming et al., 2021). This model highlights how reducing nutrient availability during the preimplantation period was sufficient for the establishment of a series of irreversible responses in early embryos, responses that were either maintained or that progressed during pre-natal and post-natal life, contributing to poor cardiometabolic, neuronal, and skeletal health in the adult offspring. Compared to the LPD, it appears that the stress of nutrient deprivation *versus* nutrient availability *in utero* led to different responses in the Emb-LPD model, which may contribute to the adult phenotypes observed.

Furthermore, when maternal and paternal contributions were examined, different findings were observed. Exposure to LPD exclusively during oocyte maturation (Egg-LPD) also resulted in higher birthweight and hypertension in the adult offspring, as observed in the Emb-LPD model (Fleming et al., 2018). Indeed, all maternal models, Egg-LPD, Emb-LPD, and LPD, affected birthweight (Fleming et al., 2018). On the contrary, the paternal LPD model, consisting of males fed with LPD throughout all stages of spermiogenesis and spermatogenesis, did not affect birthweight or lead to hypertension but resulted in a higher heart-to-body weight ratio in the adult offspring (Fleming et al., 2018). Paternal LPD has also been associated with altered fetoplacental and adult phenotypes (Watkins et al., 2008), but it will not be further discussed to focus on the *in utero* influence on the offspring.

5.1.2 Overnutrition *in utero*: the context of obesity

Overnutrition *in utero* may originate from maternal obesity, suboptimal maternal diet, and excessive weight gain during pregnancy (Perng et al., 2019). As with undernutrition, overnutrition has been associated with poor pregnancy outcomes and lifelong NCDs risk and has been extensively studied using human epidemiological studies and animal models.

5.1.2.1 Obesity

The World Health Organization has defined overweight as a body mass index (BMI) greater than or equal to 25 kg/m^2 and obesity as a BMI greater than or equal to 30 kg/m^2 (World Health Organization, 2021b). The prevalence of obesity is continuously increasing and almost reaching epidemic proportions (Tarry-Adkins & Ozanne, 2017). In 2016, 650 million adults 18 years and older were obese, representing 13% of the world's adult population (World Health Organization, 2021b).
Obesity constitutes a risk for other NCDs such as T2D, cardiovascular diseases, hypertension, and cancer (Qasim et al., 2018).

Besides genetics, obesity originates from an energy imbalance between energy intake characterized by a high fat and high sugar diet and physical inactivity (Qasim et al., 2018; Schoonejans & Ozanne, 2021). Nevertheless, genetic predisposition or an unhealthy lifestyle cannot fully explain the increasing prevalence of obesity (Schoonejans & Ozanne, 2021). Confirmation of this was obtained by studies in siblings born before and after maternal weight loss through bariatric surgery (Schoonejans & Ozanne, 2021; J. Smith et al., 2009). Children born after maternal weight loss exhibited improved cardiometabolic markers and lower rates of obesity, insulin resistance, and hypertension compared to their siblings born before maternal weight loss (Schoonejans & Ozanne, 2021; J. Smith et al., 2009). In addition, despite

living in the same obesogenic environment, only certain individuals will develop obesity (Qasim et al., 2018). This predisposition to obesity, among other biological factors such as sex, age, and ethnicity, may originate from early-life exposures (Qasim et al., 2018).

5.1.2.1.1 Human epidemiological studies of obesity

Maternal obesity is associated with short- and long-term consequences such as higher birth weight, macrosomia, increased neonatal adiposity, and subsequent childhood obesity and metabolic disease in adulthood (Perng et al., 2019; Renault et al., 2015). In addition, maternal obesity is often associated with GDM, a combination of perinatal risk conditions that have been described as leading to more severe phenotypes than when only one of the conditions is present (Renault et al., 2015; Tarry-Adkins & Ozanne, 2017).

A meta-analysis of 45 observational studies showed an association between pre-gestational overweight and obesity with an increased risk for large for gestational age, higher birth weight, macrosomia with later overweight, and obesity in the offspring (Z. Yu et al., 2013). Moreover, several studies have reported that higher BMI in childhood, which originated from pre-gestational maternal obesity and excessive gestational weight gain, was accompanied by higher blood pressure, abnormal lipid levels, insulin resistance, and elevated inflammatory markers (Gaillard, 2015).
As expected, the window of exposure might be a determinant of the severity of the phenotype. Different studies have shown that, especially in early pregnancy (up to week 20 of gestation), weight gain was associated with more adverse phenotypes in childhood, including adiposity, cardio-metabolic profiles, higher diastolic blood pressure, and increased risk of overweight and obesity during childhood or adolescence (Renault et al., 2015).

Improvement of the quality of diet and/or reducing the amount of carbohydrate intake during pregnancy to minimize neonatal adiposity has been recommended for women with obesity (Renault et al., 2015). In a study of 222 pregnant women with pre-gestational BMI ≥30 kg/m^2, an assessment of their diet at weeks 11-14 (early gestation) and 36-37 (late gestation) of pregnancy showed that lower intake of digestible carbohydrates in late gestation but not in early resulted in lower fat mass at birth (Renault et al., 2015). This improved outcome was even observed in obese women with IGT but without GMD (Renault et al., 2015).

Obesity is a complex trait; thus, one major limitation of epidemiological studies is the incapacity to isolate the effects of obesity itself on the offspring from the consequences of obesity, such as exposure to low-grade inflammation and oxidative stress (Gaillard, 2015; Perng et al., 2019). In addition, when examining offspring obesity, it is difficult to separate the pathological responses that originate from obesity in the offspring from early-life exposures to obesity (Fernandez-Twinn et al., 2012). It is, therefore, essential to remember the presence of these confounding effects when interpreting data from epidemiological studies.

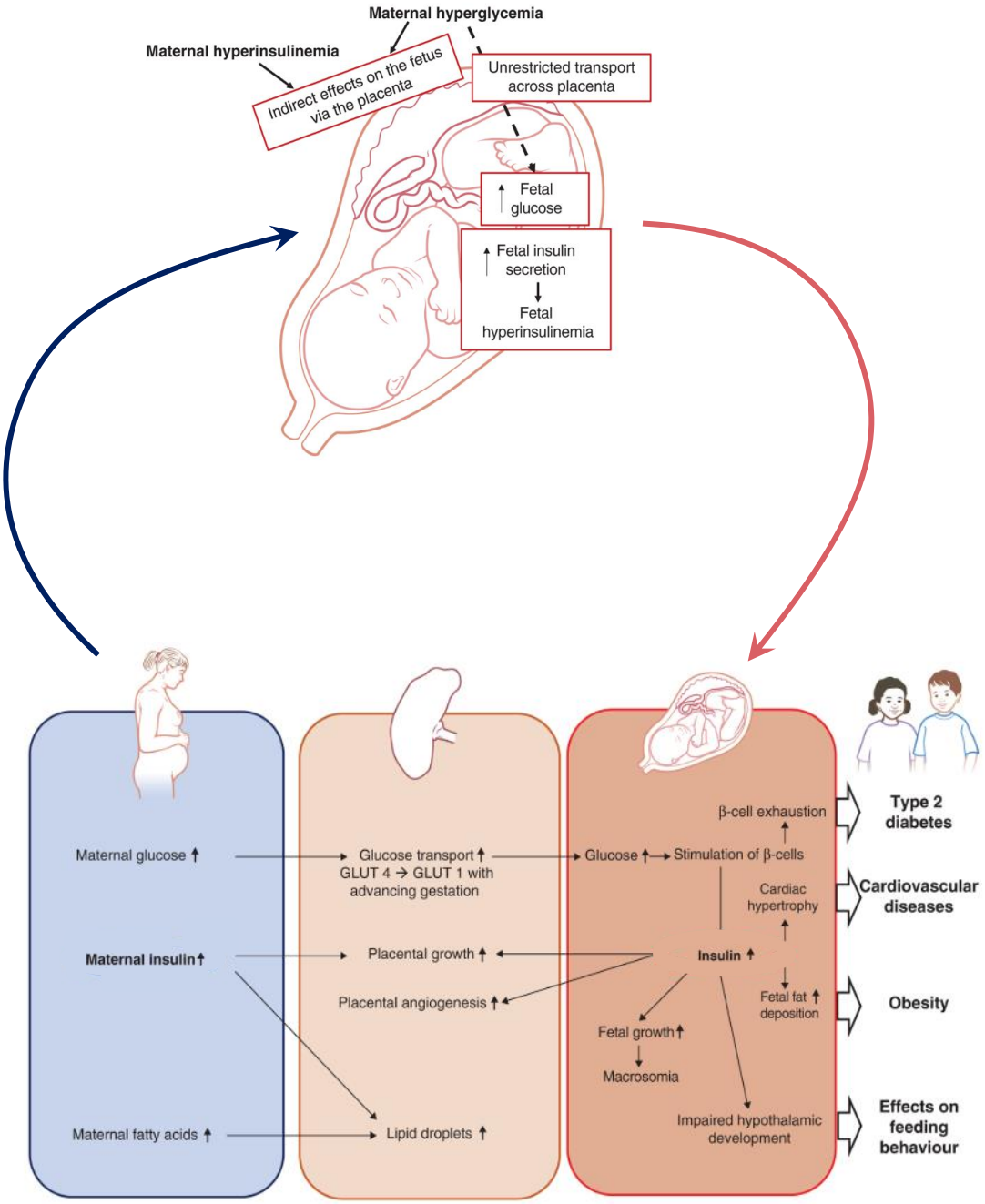

Figure 17: Diabetes in pregnancy influences the feto-placental phenotype and predispose the offspring to increased risk of non-communicable diseases.

Diabetes in pregnancy is characterized by maternal hyperglycemia and/or hyperinsulinemia. Other metabolic deregulations such as increased fatty acids may also be present. Maternal hyperglycemia and/or hyperinsulinemia may influence adaptations in the placenta, such as increased glucose transport, placental growth and angiogenesis and accumulation of lipids. These adaptations may affect the developing fetus, resulting in fetal hyperglycemia, hyperinsulinemia, impaired insulin secretion due to β-cell exhaustion, increased fetal growth, and fat deposition leading to macrosomia at birth. The offspring may also present neuronal and cardiometabolic altered phenotypes. Feto-placental adaptations may predispose the offspring to T2D and cardiometabolic disease risk later in life. Adapted from Hufnagel et al., 2022.

5.1.2.1.2 Animal models of obesity

Animal studies have reinforced evidence from epidemiological studies and provided more mechanistic insights into early life exposure to obesity and poor offspring health.
Using a C57BL/6J mouse model of maternal diet-induced obesity, it was shown that an obesogenic maternal environment adversely influences the metabolism and structure of the heart in the offspring, even before the establishment of adiposity (Fernandez-Twinn et al., 2012). Male offspring of mice fed with high fat, high sugar diet before conception and up until lactation were assessed at eight weeks before differences in body mass or body composition were detected (Fernandez-Twinn et al., 2012). At eight weeks, pups had higher heart weight, concomitant with structural changes, and increased expression of molecular markers of cardiac hypertropia and function (Fernandez-Twinn et al., 2012). In addition, pups exhibited increased insulin plasma levels, plausible insulin resistance due to reduced glucose to insulin ratio, increased insulin action through PI3K/MAPK and mTOR signaling pathways, and increased expression of oxidative stress markers (Fernandez-Twinn et al., 2012). Thus, early life exposure to diet-induced obesity results in cardiac hypertrophy, associated with hyperinsulinemia and increased insulin action, and all of that preceding detectable differences in body composition and adiposity in the offspring (Fernandez-Twinn et al., 2012).
The development of obesity in the offspring after early exposure to maternal obesity might be driven at least partly by adiposity hypertrophy and hyperplasia, a phenotype that precedes changes in body weight (Schoonejans & Ozanne, 2021).

In a meta-analysis of 123 studies that used different animal models to expose offspring to obesity exclusively *in utero*, the offspring showed a positive association with increased body weight, body fat percentage, and absolute fat mass (Schoonejans & Ozanne, 2021).
Furthermore, when the offspring exposed to obesity exclusively *in utero* was confronted with a second nutritional challenge through a high-fat diet (HFD) after birth, the effects were found to be additive with double-exposed offspring showing the highest adiposity values (Schoonejans & Ozanne, 2021).

5.1.3 Poor metabolic health *in utero*: diabetes in pregnancy

Diabetes in pregnancy is characterized by hyperglycemia and may be accompanied by other metabolic imbalances such as hyperinsulinemia, insulin resistance, inflammation, hyperleptinemia, i.e., high levels of leptin, a key hormone in food intake and systemic energy balance; and dyslipidemia (Hufnagel et al., 2022). These conditions, acting independently or in synergy, may be involved in the perturbation of the offspring's health.

Glucose is the main fuel for fetal nutrition and growth, freely crossing the placenta throughout pregnancy (Hufnagel et al., 2022). In a diabetic context, maternal hyperglycemia leads to increased glucose transfer to the fetus (Figure 17) (Ornoy et al., 2021). On the contrary, maternal circulating insulin cannot cross the placenta (Hufnagel et al., 2022). However, because insulin receptors are expressed in the placenta, insulin may exert its actions via binding to its receptor, thereby influencing the placenta metabolism, which in turn may influence the developing fetus (Figure 17) (Hufnagel et al., 2022).

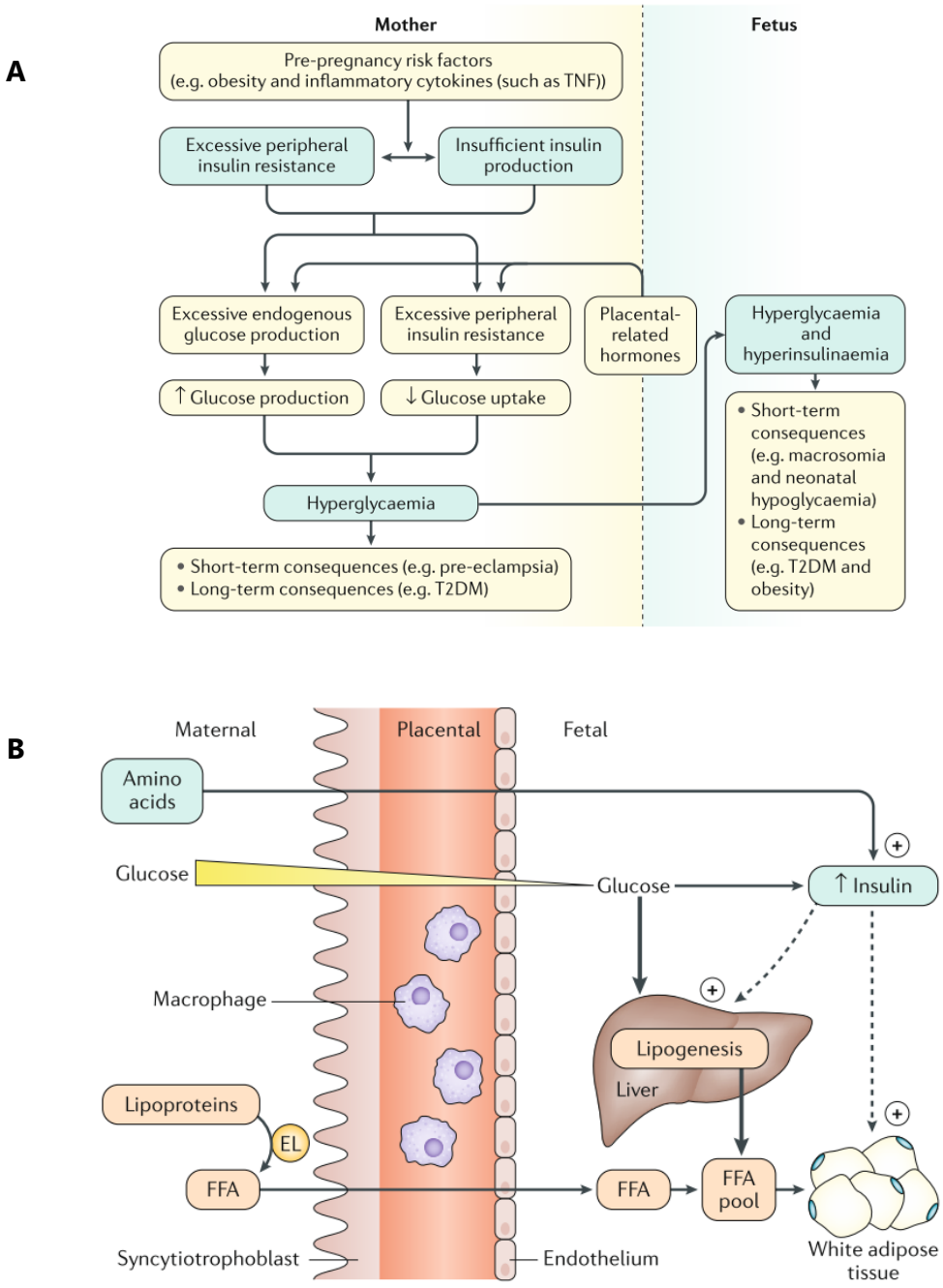

Figure 18: Gestational diabetes mellitus in the offspring.

A) Women with gestational diabetes mellitus (GDM) have insulin resistance, hyperglycemia and hyperinsulinemia. This results in increased glucose transfer to the fetus via the placenta, which stimulates fetal insulin production resulting in hyperinsulinemia. The short-term effects of fetal hyperglycemia and hyperinsulinemia are macrosomia and neonatal hypoglycemia, and the long-term effects are T2D and obesity. B) Increased maternal amino acids may also stimulate fetal hyperinsulinemia. High insulin stimulates triglyceride synthesis and fat storage in white adipocytes. Maternal free fatty acids (FFA) cross the placenta and increase the fetal free fatty acid pool. Increased glucose levels stimulate *de novo* lipogenesis in the liver, further contributing to the FFA fetal pool. Adapted from McIntyre et al., 2019.

Nevertheless, within the first trimester, precisely in the first days of pregnancy, the placenta is not yet fully developed, and the early embryo is bathed in both maternal glucose and insulin circulating levels within the intrauterine environment. This period in development will be covered in detail in Chapter 3.

Both hyperglycemia and/or hyperinsulinemia have been associated with adverse short- and long-term consequences in the offspring in different diabetes settings, including type 1 and type 2 diabetes and gestational diabetes mellitus (Figure 17) (Hufnagel et al., 2022; Ornoy et al., 2021). However, pre-gestational diabetes (PGD) and gestational diabetes mellitus (GDM) implicate different timing of exposure during pregnancy. A comparison of these two diabetic contexts in pregnancy has revealed some common and specific consequences in the offspring.

Here, I will describe both settings of diabetes in pregnancy, with special attention to pre-gestational diabetes in the offspring. A comparison of both settings will also be addressed.

5.1.3.1 Gestational diabetes mellitus and the offspring

Gestational diabetes mellitus develops in late gestation in women with subjacent metabolic dysfunctions prior to conception, as described in Chapter 1, section 2.6.1(Figure 18A) (Catalano, 2014).

The offspring exposed to GDM is associated with increased birth defects, especially cardiac malformations, adiposity, macrosomia, or large for gestational age (LGA), i.e., birthweight higher than 4 kg or when growth is higher than the 90th percentile at any gestational age (Ornoy et al., 2021; Wei et al., 2019). In addition, newborns can exhibit low calcium blood levels, increased bilirubin in blood serum, and respiratory distress (Catalano, 2010). Some of these conditions may result in complications during delivery, such as shoulder dystocia caused by macrosomia (Figure 18A, B) (Catalano, 2010).

Maternal hyperglycemia stimulates *de novo* lipogenesis in the fetal liver, contributing to the free fatty acid fetal pool (Figure 18B) (McIntyre et al., 2019). Additionally, the transfer of maternal free fatty acids further contributes to the free fatty acid fetal pool (Figure 18B) (McIntyre et al., 2019).
Furthermore, maternal hyperglycemia influences fetal insulin secretion, a process considered to mediate excessive growth in the offspring (Figure 18B). Glucose freely crosses the placenta towards the fetus. In diabetic contexts, maternal hyperglycemia increases the glucose gradient across the placenta to the fetus, resulting in fetal hyperglycemia (Ornoy et al., 2021). Increased fetal glucose then stimulates fetal insulin secretion resulting in fetal hyperinsulinemia, a condition known as the "Pedersen hypothesis" (Desoye & Nolan, 2016; Hjort et al., 2019). Other factors, such as AAs and fatty acids, may further stimulate fetal insulin secretion (Figure 18B) (Desoye & Nolan, 2016).
Fetal hyperinsulinemia leads to fetal hypoglycemia, further stimulating the placenta glucose gradient towards the fetus, a condition termed the "fetal glucose steal" (Desoye & Nolan, 2016; Hjort et al., 2019). Fetal hyperinsulinemia, via the metabolic and mitogenic actions of insulin, may contribute to excessive growth and macrosomia (Figure 18B) (Hjort et al., 2019). Moreover, increased insulin levels stimulate triglyceride synthesis and fat storage in fetal white adipocytes (Figure 18B) (McIntyre et al., 2019).
Fetal hyperinsulinemia may also lead to other complications after birth. Immediately after birth, once the excessive supply of maternal circulating glucose levels is stopped, persistent fetal hyperinsulinemia can lead to neonatal hypoglycemia (Desoye & Nolan, 2016). Neonatal hypoglycemia is a critical

condition that requires immediate intervention to avoid death or short- and long-term neurodevelopmental defects (Voormolen et al., 2018). The risk of hypoglycemia is such that special care is given to the offspring following delivery, including screening for neonatal hyperglycemia within the first 12h after delivery (Voormolen et al., 2018).

Gestational diabetes pregnancies are characterized by hyperglycemia and hyperinsulinemia (Hufnagel et al., 2022). Despite insulin's inability to cross the placenta, insulin can exert its action in the placenta, influencing the growth and metabolism of the placenta (Hufnagel et al., 2022). Insulin receptors are expressed in maternal- and fetal-facing portions of the human early and late gestation placenta (Hufnagel et al., 2022). Consequently, maternal hyperinsulinemia can stimulate placental growth and lipid levels, which could then influence the metabolism of the developing fetus (Hufnagel et al., 2022).

Offspring born from GDM pregnancies are at risk for higher blood pressure, impaired glucose tolerance, obesity, and potentially diabetes later in life (Metzger & Buchanan, 2018). A follow-up study of the offspring aged of 22 years old born from GDM pregnancies showed a 21% combined rate of T2D and prediabetes, characterized by impaired fasting glucose and impaired glucose tolerance, versus 4% in offspring not exposed to intrauterine hyperglycemia (Clausen et al., 2008).

Different studies have shown that treatment of mild GDM (i.e., glucose monitoring, diet, and medication if necessary) reduces adverse pregnancy and perinatal outcomes such as birth weight, macrosomia, preeclampsia, and gestational hypertension (Metzger & Buchanan, 2018; Szmuilowicz et al., 2019). Nevertheless, despite interventions, elevated C-peptide levels, i.e., an indicator of insulin production; in umbilical cords, were not reduced in GDM pregnancies, suggesting that fetal hyperinsulinemia was not normalized (Desoye & Nolan, 2016). Coherent with this, the risk for neonatal hypoglycemia is not reduced after GDM treatment, further reinforcing the presence of subjacent fetal metabolic dysregulations despite GDM management (Desoye & Nolan, 2016).

5.1.3.2 Pre-gestational diabetes and the offspring

Compared to GDM, pre-gestational diabetes involves exposure to overt diabetes throughout the pregnancy.
Although management of pre-gestational diabetes has greatly reduced the risk for congenital malformations, despite tight glycemic control and monitoring, pre-gestational diabetes is associated with short- and long-term consequences in the offspring (Ornoy et al., 2021; Vambergue & Fajardy, 2011).

5.1.3.2.1 Pre-gestational diabetes and the offspring: evidence from human studies

The offspring exposed to pre-gestational diabetes are at higher risk of congenital malformations, fetal and neonatal metabolic imbalances, and cardiovascular and metabolic disease risk later in life (Hufnagel et al., 2022; Ornoy et al., 2021).

Pre-gestational diabetes is associated with perturbation of growth trajectories in the offspring and can result in both low or high birth weight (Ornoy et al., 2021). This latter, also referred to as small for

gestational weight (SGA) is defined as birthweight less than 2,5 kg or growth under the 10th percentile (Wei et al., 2019). Small for gestational weight offspring is mostly associated with severe maternal diabetes contexts characterized by vascular complications, hypertension, or renal disease. As for fetal and/or neonatal, these are the most frequent consequence of diabetic pregnancies and are associated with complications for both the mother and the offspring (Ornoy et al., 2021). Indeed, compared to non-diabetic pregnancies, diabetic pregnancies have a 3-fold higher risk of macrosomia (Ornoy et al., 2021).

Like GDM pregnancies, maternal hyperglycemia in pre-gestational diabetes contexts is also associated with fetal hyperinsulinemia and a higher risk for fetal hypoglycemia at birth (Desoye & Nolan, 2016; Ornoy et al., 2021). In poorly controlled pre-gestational diabetes pregnancies, it is believed that even short periods of maternal hyperglycemia may stimulate fetal hyperinsulinemia (Desoye & Nolan, 2016).

Furthermore, diabetic pregnancies are associated with increased adiposity in the offspring (Perng et al., 2019). Insulin regulates both growth and metabolism. Fetal hyperinsulinemia has been proposed to be the origin of the excessive adiposity in the offspring through the stimulation of fetal mitogenic and anabolic pathways in muscles, connective and adipose tissues (Desoye & Nolan, 2016; Hjort et al., 2019; Ornoy et al., 2021). In overt diabetes, especially in T2D, other factors may be similarly involved, such as hyperlipidemia, oxidative stress, hypoxia, inflammation, and obesity if present (Hjort et al., 2019; Ornoy et al., 2021; Sies et al., 2017; Vambergue & Fajardy, 2011).

A diabetic environment *in utero* is also associated with long-term consequences in the offspring, including higher systolic and mean blood pressure in childhood, hypertension, MetS, obesity, cardiovascular diseases, and T2D (Higa et al., 2021; Y. Yu et al., 2019). A 40-year follow-up study in Denmark showed that offspring exposed to both type 1 and type 2 pre-gestational diabetes had higher rates of early onset of cardiovascular disease from childhood to at least early adulthood (Y. Yu et al., 2019). In addition, the increased risk was even greater when mothers had a history of CVD or diabetic complications (Y. Yu et al., 2019).

Maternal hyperglycemia alone or in the context of overt PGD is associated with short- and long-term consequences in the offspring. A large population-based cohort in China showed that both women with impaired fasting glucose and PGD were at higher risk of spontaneous abortion, preterm birth, macrosomia, and perinatal infant death (Wei et al., 2019). Women with impaired fasting glucose were also at higher risk of SGA offspring (Wei et al., 2019).
In addition, it was shown that maternal glucose levels within non-diabetic ranges influence glucose metabolism in the offspring. In the observational Hyperglycemia and Adverse Pregnancy Outcome Follow-up study (HAPO FUS), investigation of the maternal glucose spectrum at 28 weeks of gestation showed that exposure to higher glucose levels *in utero* despite being below the threshold of diabetes diagnostic criteria was associated with higher glucose levels and insulin resistance in childhood (10-14 years), independent on BMI and family history of diabetes (Scholtens et al., 2019). Therefore, these studies have shown that glucose levels and hyperglycemia alone may influence the metabolism of the offspring.

5.1.3.2.2 Pre-gestational diabetes and the offspring: evidence from animal studies

Mild or severe PGD, including T1D or T2D, can be induced in animal models using different approaches (Jawerbaum & White, 2010; Vambergue & Fajardy, 2011). These include partial pancreatectomy although is less frequently used nowadays, through diet (i.e., HFD), by the administration of drugs that target the destruction of β-cells (i.e., streptozotocin (STZ), alloxan), and by using genetic models in which diabetes develops spontaneously (i.e., the non-obese diabetic (NOD) as a T1D model in mice, the Goto Kakizaki (GK) as a T2D model in rats) (Jawerbaum & White, 2010; Vambergue & Fajardy, 2011).

One of the most used animal models of diabetes in pregnancy is the diabetes-induced model, frequently developed in rodents but also used in rabbits. In diabetes-induced models, by modulating the doses and period of drug administration, mild or severe diabetic phenotypes can be achieved(Jawerbaum & White, 2010). This allows to assess different degrees of severity of the disease (Jawerbaum & White, 2010). Because it is one of the most used animal models, this allows comparing findings between previous studies.
However, one limitation of induced-diabetes models, particularly those with a severe phenotype in certain strains and according to the experimental approach used, is the impaired fertility and reduced pregnancy rates (Jawerbaum & White, 2010). Diabetes-induced severe phenotypes may stop cycling after two to three weeks of STZ or alloxan treatment (Jawerbaum & White, 2010). There are some possibilities to overcome this limitation, such as using another strain, treating animals with insulin, or mating animals before the stop of cycling (Jawerbaum & White, 2010). However, these approaches may compromise the initial objective of the study itself.
Diabetes-induced models are considered a T1D-like model since the diabetic phenotype originates from the destruction of β-cells, not from insulin resistance (Jawerbaum & White, 2010). Although this model does not cover the genetic and immunological triggers that cause β-cell loss, it does present a proinflammatory phenotype after β-cells loss, similar to T1D in humans (Jawerbaum & White, 2010).

As for genetic models, inbreeding allows to select metabolic imbalances traits such as hyperglycemia and insulin resistance, which allow to obtain a range of phenotypes with different severities (Jawerbaum & White, 2010). However, the genetic background may be present in the offspring, thus it is important to identify the effects originating from a genetic background than those from the intrauterine environment (Jawerbaum & White, 2010). One way to achieve this is for example, using embryo transfer strategies (Jawerbaum & White, 2010).
Type 1 diabetes models, such as NOD in mice or the bio-breeding (BB) rats model, an immune attack to leads to β-cells destruction (Jawerbaum & White, 2010). Therefore, contrary to diabetes-induced models, β-cells loss is caused by an autoimmune reaction, therefore, the disease context is closer to T1D in humans (Jawerbaum & White, 2010). However, one limitation of the NOD model is that T1D-like phenotype mostly develops late, around 30 weeks of age, leading to older pregnant female mice in this model, with advanced age potentially adding confounding effects on the offspring (Jawerbaum & White, 2010). Concerning T2D models, there are plenty of diabetic models, but only a few have been used to assess diabetes in pregnancy. Many of these diabetic models originate from a polygenic background, such as the GK model in rats (Jawerbaum & White, 2010). These models have been frequently used to evaluate the effects of the diabetic intrauterine context in the offspring at different periods of development (Jawerbaum & White, 2010).

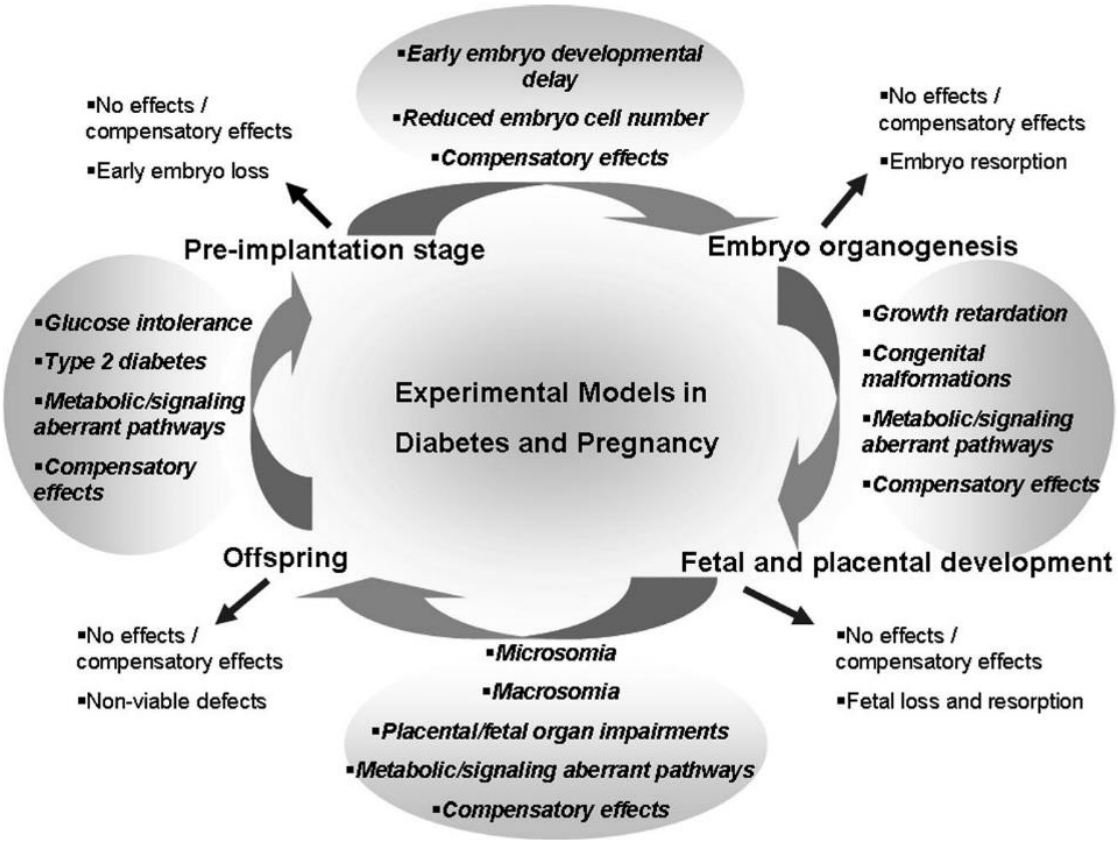

Figure 19: Possible outcomes in the offspring exposed to maternal diabetes in animal models. The possible outcomes for different developmental periods are shown. These may vary according to the degree of the maternal context and genetic and environmental factors. Gray arrows show the effects that can impact subsequent developmental stages and the next generation. Black arrows show the effects that would not lead to subsequent developmental impairments. From Jawerbaum & White, 2010.

Like diabetes in humans, in experimental models, the severity of β-cell dysfunction and insulin resistance dictates the maternal metabolic phenotype and long-term consequences in the offspring (Jawerbaum & White, 2010). Studies using these different models have described a wide range of alterations and adverse outcomes in the offspring during pre- and post-natal life (Figure 19) (Chavey et al., 2014; Vambergue & Fajardy, 2011).

During early gestation, precisely during the preimplantation period, both genetic and diabetes-induced models have shown delayed preimplantation development and apoptosis (Jawerbaum & White, 2010). The extent of the effects of a diabetic environment, particularly of a hyperglycemic and/or hyperinsulinemic environment, on preimplantation development will be de subject of Chapter 3.

At post-implantation stages, in both genetic and diabetes-induced models, congenital alterations have been frequently, such as neural tube defects, but also in the cardiovascular system and skeleton (Jawerbaum & White, 2010; Pavlinkova et al., 2009).

Oxidative stress, induced by the diabetic environment, is considered to contribute to the observed congenital malformations and apoptotic phenotypes, but other signaling pathways and alterations have also been suggested, such as low inositol uptake or folic acid deficiency (Jawerbaum & White, 2010).

Furthermore, altered gene expression changes have also been identified in post-implantation embryos, some of which have been associated with neural tube defects (Pavlinkova et al., 2009). The fetal offspring from STZ-induced diabetic mice showed altered expression levels of genes implicated in oxidative stress and hypoxia, two conditions associated with diabetic pregnancies (Pavlinkova et al., 2009). Interestingly, over 30% of differentially expressed genes (DEGs) were transcription factors, chromatin-modifying enzymes, or members of signaling pathways that influence gene expression (Pavlinkova et al., 2009).

Perturbations in mitochondrial activity driven by diabetes-induced oxidative stress have also been described. In STZ-induced diabetes rats, post-implantation embryos around the time of placentation showed altered expression of proteins involved in mitochondrial biogenesis, along with increased OXPHOS activity (Alcolea et al., 2007).

Exposure to a diabetic *in utero* environment, especially during organogenesis and fetal development, a critical period for endocrine pancreas development, has been shown to impair pancreatic β-cells. Several reports have shown that increased maternal glucose levels stimulate fetal islets hypertrophy and β-cell insulin production (Yessoufou & Moutairou, 2011), as described by the "Pedersen hypothesis" (Desoye & Nolan, 2016; Hjort et al., 2019).

Perturbations in β-cell mass persist at adult stages. Transferred oocytes from nondiabetic rats developed in the mild diabetic model GK/Par showed decreased β-cell mass in adult stages, indicating that the maternal intrauterine environment was sufficient to impair β-cell mass (Portha et al., 2011). Similarly, in diabetes-induced rodent models, both mild and severe hyperglycemic contexts led to impaired β-cell mass and insulin content in the offspring (Chavey et al., 2014). In the long-term, offspring exposed to mild hyperglycemia developed impaired insulin secretion in response to glucose, whereas offspring exposed to severe hyperglycemia developed insulin resistance (Chavey et al., 2014).

In rats, a T1D-like diabetic environment led to low birth weight and body weight gain, reduced glucose-stimulated insulin secretion in pancreatic islets, and reduced β-cell glucose metabolism, notably by the decreased enzymatic activity of PFK, pyruvate carboxylase (PC), and PDH at 15 weeks old (J. Han et al., 2007).

Other long-term perturbations have also been reported, notably on vascular and renal health after exposure to PGD (Rocha et al., 2005). In diabetic-induced rats, offspring showed systemic hypertension

and impaired kidney function characterized by decreased urinary flux and glomerular hypertrophy by three months of age (Rocha et al., 2005). By 12-months of age, the adult offspring showed a significant reduction in nephron number due to accelerated aging (Rocha et al., 2005).

5.1.3.3 The offspring of pre-gestational diabetes *versus* gestational diabetes mellitus

Pre-gestational diabetes and GDM are both associated with altered phenotypes and risk for NCDs later in life in the offspring. Because GDM develops around the second to third trimester after organogenesis, GDM does not put at risk the development during the first trimester (Jawerbaum & White, 2010).

It is considered that PGD is associated with more severe complications than GDM, but the earlier GDM onset, the more severe the outcomes in the offspring (Kapur et al., 2019; Ornoy et al., 2021). Indeed, the severity of the outcomes may differ depending on the duration and timing of exposure during pregnancy, with the most severe phenotypes associated with poor glycemic control in the first trimester (Kapur et al., 2019; Ornoy et al., 2021). Poor glycemic control before conception and during the first trimester in diabetic pregnancies is associated with congenital malformations in the offspring, including cardiac anomalies (i.e., cardiac enlargement, asymmetric hypertrophies) representing 40% of congenital malformations, and limb, musculoskeletal, and central nervous system defects such as sacral agenesis and hydrocephaly (Hufnagel et al., 2022; Ornoy et al., 2021).
Similar findings have been shown in animal models. Exposure to a diabetic environment, as early as during the preimplantation stage, i.e., during the first trimester, impacted the early embryo irreversibly, even when developed in a "healthy" intrauterine context. Transfer of control preimplantation embryos to develop in a NOD diabetic intrauterine environment or transfer of NOD-derived preimplantation embryos to develop in a control intrauterine environment led to a higher rate of malformations, including neural tube defects, abdominal wall defects, and limb anomalies (Otani et al., 1991; Wyman et al., 2008). Moreover, embryos from NOD-diabetic mice transferred to nondiabetic pseudopregnant female recipients mice also showed severe growth retardation (Wyman et al., 2008).

A study carried out comparing several types of congenital anomalies in the offspring born from PGD and GDM mothers in the U.S. showed a higher risk of congenital anomalies at birth in PGD than in GDM (Ornoy et al., 2021). A second cohort in which data of neonates born from 1999-2008 from PGD, GDM or nondiabetic pregnancies showed that 2.27 times higher risk for neonatal morbidity (i.e. respiratory distress syndrome and mechanical ventilation) than neonates born from GDM or nondiabetic pregnancies (Ornoy et al., 2021).

The severity of the outcomes in PGD compared to GDM may be associated to exposure of a diabetic environment during sensitive periods such as the preimplantation period and organogenesis. In humans, the development of the pancreas initiates four weeks after conception, and insulin deposits can be detected around weeks 7 and 8 (Desoye & Nolan, 2016). A pre-gestational diabetic context may affect fetal pancreas development and has been proposed to accelerate the maturation of β-cells, resulting in premature fetal insulin production (Desoye & Nolan, 2016).

Another potential contributing factor in the establishment of an altered phenotype in the offspring exposed to both PGD and GDM is the placenta. Indeed, a crosstalk between the developing fetus and the impaired placenta takes place. Fetal hyperinsulinemia, which may be developed in both PGD and GDM settings, influences placental growth (Starikov et al., 2014). Similarly, expression levels of IGF-I, IGF-II, and its receptors, along with the expression of GLUT-1, GLUT-4, and GLUT-9 are positively correlated with fetal macrosomia (Ornoy et al., 2021).
Both PGD and GDM have been associated with increased angiogenesis and "dysmaturity", corresponding to the immaturity of chorionic villi accompanied by increased villous capillaries (Ornoy et al., 2021; Starikov et al., 2014). Between PGD and GDM, one study found that GDM had a 7% incidence of delayed villous maturity, whereas a second study found a higher incidence (12.8%) in T2D pregnancies (Starikov et al., 2014).
Among PGD settings, both T1D and T2D in pregnancy are associated with preeclamptic placentas and impaired placental growth and development (Starikov et al., 2014). Among PGD type 1 and type 2, there may be a few dissimilarities. A comparison of 293 placentas of women with T1D and T2D showed that decidual vasculopathy and placental insufficiency were most frequently observed in women with T2D (Starikov et al., 2014). Decidual vasculopathy, which corresponds to morphological changes in the decidual spiral arteries, may be associated with the enhanced frequency of vascular complications in T2D (Starikov et al., 2014).

Growth trajectories are impacted by hyperglycemia from early gestation. Higher levels of glycosylated hemoglobin levels during the first and second trimesters were associated with LGA in the offspring compared to late pregnancy (Desoye & Nolan, 2016). Increased fetal growth prior to 30 weeks gestation is associated with more severe macrosomic phenotypes (Desoye & Nolan, 2016). It has been proposed that these perturbations may have their origin during oogenesis and may involve the oocyte's mitochondria and metabolism, subsequently impacting the early embryo and fetal growth trajectories (Desoye & Nolan, 2016).

As detailed in Chapter 1, there is an increasing prevalence of early metabolic imbalances, i.e., hyperglycemia and/or hyperinsulinemia, in the younger population, including women of reproductive age. These metabolic imbalances are often asymptomatic and can be present for several years before overt T2D develops (Chatterjee et al., 2017; International Diabetes Federation, 2021). Pregnancy in women with untreated early metabolic imbalances constitutes a risk for the offspring, especially during the first stage of pregnancy, when women are not yet aware of the pregnancy. Unfortunately, despite these risks, prediabetes in pregnancy remains poorly characterized.

Chapter 3: The periconceptional period, a critical window of development

1. The periconceptional period in the context of DOHaD

For more than twenty years, cumulative research has shown that the periconceptional period, corresponding to the time of conception and encompassing the preimplantation period until implantation of the developing embryo, is a highly vulnerable period of development when perturbated may lead to developmental programming in the offspring.

The early embryo harbors a limited pool of progenitor cells that will constitute all the tissues and organs of the future individual and give rise to the fetal portion of the placenta. These progenitors correspond to the inner cell mass (ICM) and trophectoderm (TE) within the blastocyst embryo.
Proper development of the two progenitors of the embryo proper is essential for subsequent development and is likely to be critical to ensure the appropriate structure and function of cells and organs of the future individual and the placenta.
The periconceptional period comprises tightly regulated fundamental events that enable the reprogramming of the gametes to give rise to the totipotent embryo, the transcriptional activation of the embryonic genome, and the progressive specification of the two key progenitors. These major events are characterized by a series of epigenetic, molecular, and cellular mechanisms that may be influenced by environmental cues. Moreover, the periconceptional period, notably the early embryo, is in immediate conctact with the oviduct and uterine fluid, which is strictly dependent on the maternal nutritional and metabolic status. Preimplantation embryos communicate with their surrounding environment. Previous research has shown that embryos can "sense" and respond to changes in their microenvironment, and these responses may contribute to developmental programming in the offspring.

The periconceptional period and precisely early embryos show a high level of developmental plasticity, which allows them to respond and adapt to a changing environment (Garcia-Dominguez et al., 2020). However, these changes may compromise the health of the offspring (A. J. Lea et al., 2017). Changes in the periconceptional environment, such as assisted reproductive techniques (ART), have been shown to alter the phenotype of the embryo and be associated with disease risk.
The development of assisted reproductive techniques (ART), such as in vitro fertilization or embryo in vitro culture, has assisted countless couples worldwide suffering from infertility issues. In France, nearly 30 000 births undergoing ART treatment were registered in 2019 (Agence de la biomédecine, 2019). However, several reports have highlighted the increased risk of adverse outcomes in the offspring born via ART (Fleming et al., 2018; R. Hart & Norman, 2013). These adverse outcomes include perturbations of growth trajectories, poor metabolic health such as impaired fasting glucose, insulin resistance, increased plasma lipids, increased total adiposity, higher blood pressure, vascular dysfunction in childhood and adolescence, and obesity (Fleming et al., 2018). Increased incidence of depression in children born from ART has also been described (R. Hart & Norman, 2013). Furthermore, ART has also been associated with an increased risk of imprinting disorders (Fleming et al., 2018). However, because in humans, there are multiple confounder factors present such as the origin of parental infertility, differences in post-natal environments, differences between ART techniques among facilities, in addition to the limited sample size, caution should be taken when interpreting these reports (Fleming et al., 2018).

The effects of ART have been addressed through animal models and further demonstrated how early embryos respond to these environmental cues.
In rabbits, *in vitro* embryo culture affects DNA methylation and hydroxymethylation patterns throughout preimplantation development (Salvaing et al., 2016). By comparing two different culture media frequently used media in ART to *in vivo* embryos, it was shown that both culture media resulted in different kinetics of DNA methylation and hydroxymethylation, along with the altered expression of TET1 and TET2 enzymes, implicated in DNA demethylation processes, and of ERVA and ERVB, two endogenous retroviral sequences known to be subjected to DNA methylation (Salvaing et al., 2016).
Media composition and manipulation affect early embryos and have been associated with altered phenotypes and disease risk in adulthood. In the mouse, the duration of embryo culture was shown to affect the offspring in a sex-specific manner (Aljahdali et al., 2020). Indeed, it was revealed that more extended periods of embryo culture were associated with poor cardiovascular health markers in males but not in females and embryo manipulation during critical periods of preimplantation development, such as embryonic genome activation (Aljahdali et al., 2020).
Moreover, embryo manipulation can lead to long-lasting signatures across generations. In rabbits, embryos that underwent vitrification and transfer procedures showed reduced growth, gene expression changes, altered metabolic profiles, and impaired liver metabolism, all maintained until three generations (Garcia-Dominguez et al., 2020).

Perturbations in maternal nutrition and its consequences on the uterine fluid composition have been shown to trigger responses in both oocyte and early embryos, and to result in disease later in life. Maternal undernutrition challenges have been extensively studied in rodents using the low protein diet (LPD) model. Both, Egg-LPD and Emb-LPD, that is, exposure during oocyte maturation or the preimplantation period were associated with perturbations of growth trajectories and cardiovascular disease in the adult offspring (Fleming et al., 2018, 2021). However, the Emb-LPD shows the most severe and drastic phenotype, with perturbations in cardiometabolic, neurological, and skeletal health (Fleming et al., 2021). At the embryo, both embryonic (epiblast) and extra-embryonic lineages (primitive endoderm and trophectoderm) showed adaptations to the undernutrition stress, with the activation of compensatory responses to enhanced nutrient uptake and protect the growth of the embryo (Fleming et al., 2021). These compensatory responses were maintained throughout development, despite normalization of the maternal diet, therefore highlighting that perturbation of the preimplantation period can lead to long-lasting and irreversible signatures associated with disease riks in adulthood.
Metabolic imbalances such as a T1D-like intrauterine environment exclusively during the periconceptional period resulted in an altered fetoplacental phenotype in the offspring. In the rabbit, exposure to an alloxan-induced diabetic environment exclusively during the periconceptional period, followed by transfer to non-diabetic recipients, was sufficient to alter the expression of genes involved in lipid metabolism along with specific fatty acid signatures in the placenta and hyperglycemic and dyslipidemic fetuses (Rousseau-Ralliard, Couturier-Tarrade, et al., 2019).

Taken together, it is clear that the periconceptional period is a highly vulnerable, sensitive, and critical window during development that can be affected by changes in its surrounding environment and trigger a series of adaptations that may compromise the health of the offspring.

1.1 The rabbit as a model organism to study the periconceptional period

The European rabbit, *Oryctolagus cuniculus*, is taxonomically classified in the Mammalia class, Lagomorpha order, and Leporidae family (Madeja et al., 2019). Rabbits are frequently used in research and are considered the third most used mammalian organism within the EU (Fischer et al., 2012). The use of rabbits in research has many advantages, including their relatively small size, short gestational period (29-31 days), female sexual maturity at 4-5 months of age, and the possibility to use gene-targeting tools such as the CRISPR/Cas9 system (Fischer et al., 2012; Madeja et al., 2019).

Moreover, lagomorphs, and thus rabbits, are genetically close to primates and share several common features, mainly in the early stages of development (Madeja et al., 2019).
Because rabbits share an overall similar embryonic and fetoplacental development to humans, they have been used extensively in embryology and reproduction biology (Fischer et al., 2012). In addition, the use of rabbits in reproduction biology has several advantages. In rabbits, ovulation is induced by mating; thus, the precise time of gestation and embryonic age can be easily followed (Fischer et al., 2012; Madeja et al., 2019). Moreover, superovulation of rabbits can be employed to reduce the number of animals needed, and embryo transfer after *in vitro* culture is possible (Fischer et al., 2012; Madeja et al., 2019).

Along with these advantages, several aspects of preimplantation development are closer between humans and rabbits than rodents. The duration and timing of key developmental events during preimplantation development are similar in humans and rabbits (Fischer et al., 2012). In particular, EGA takes place gradually, spanning several cell cycles, and is closer to the first specification event, as in humans (Leandri et al., 2008; Madeja et al., 2019). The inactivation of the X-chromosome, an essential process for dosage compensation, follows a similar timing and mechanism in human and rabbit embryos compared to rodents (Fischer et al., 2012; Okamoto et al., 2011). In rabbit and human embryos, *Xist* is expressed from maternal and paternal alleles and only shows a monoallelic expression at the blastocyst stage; thus, X-linked gene inactivation occurs at the blastocyst stage (Fischer et al., 2012). This could be particularly important considering several key metabolic genes are X-linked such as glucose 6-phosphate dehydrogenase (D. K. Gardner & Harvey, 2015).
Similarly, it was proposed that the need for rapid implantation in mouse embryos leads to a speeded TE differentiation (Piliszek & Madeja, 2018). The early specification of the TE in the mouse does not represent all mammalian species, including humans and rabbits (Piliszek & Madeja, 2018).
Furthermore, transcriptomic analysis of rabbit pluripotent cells shows many common characteristics with humans and non-human primates (Bouchereau et al., 2022). Moreover, the peri-gastrulation morphology of rabbit embryos corresponds to a flat disc, as in humans, and is different from the typical cup-shaped cylinder in rodents (Madeja et al., 2019). Regarding the placenta, both rabbits and humans at early stages show a discoid hemodichorial placenta, which makes the placenta structure of rabbits closer to that of humans and adequate for the study of placenta development and function (Chavatte-Palmer & Tarrade, 2016).

Moreover, although it is clear that animal models do not fully recapitulate the pathogenesis of human diseases, rabbits have shown to be a suitable model for studying atherosclerosis, diabetes, lipoprotein metabolism, and cardiovascular diseases, notably in the context of DOHaD (Madeja et al., 2019; Ramin et al., 2010; Rousseau-Ralliard, Couturier-Tarrade, et al., 2019).

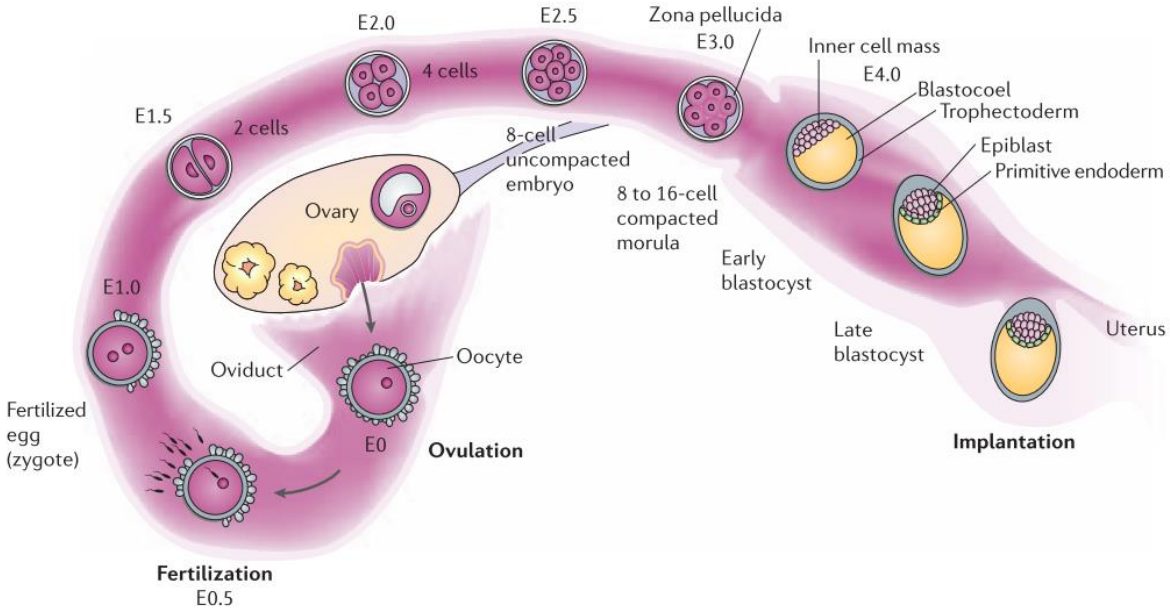

Figure 20: Overview of preimplantation development, example from the mouse.
Preimplantation development starts after fertilization. One-cell stage embryos (zygote) undergo a series of cleavage divisions without increasing volume while traveling through the oviduct. Embryos reach the morula stage and compaction and cell polarization takes place. This is followed by the first specification event giving rise to the inner cell mass (ICM) and the trophectoderm (TE) at the early blastocyst stage. Then, a second specification event takes place giving rise to the three lineages of the late blastocyst stage: the epiblast, the primitive endoderm and the TE. The late blastocyst reaches the uterus, hatches from the zona pellucida and is ready to implant into the uterine cavity. From Wang & Dey, 2006.

1.2 The preimplantation period

In sexually reproducing species, the fusion of two gametes, the egg, and the sperm, gives rise to a whole new organism (Figure 20) (Deneke & Pauli, 2021). After that, in mammals, the preimplantation period begins with a totipotent zygote undergoing a series of finely-tuned cellular and molecular processes leading to the implantation of a competent embryo, the blastocyst, into the uterine cavity (Figure 20) (H. Wang & Dey, 2006). This totipotent 1-cell embryo or zygote harbors the potential to produce all the cells and tissues of an organism, including the extra-embryonic tissues, in a temporally and spatially coordinated manner (Condic, 2014; Molè et al., 2020).

The newly formed zygote travels from the oviduct to the uterus while embryonic development occurs (Figure 20) (Gerri, Menchero, et al., 2020). A simplified overview of the morphological stages of preimplantation development can be broken down into cleavage, morula, and blastocyst stages. Throughout these stages, fundamental processes take place: the reprogramming of parental genomes, the embryonic genome activation (EGA), and the first specification event of the inner cell mass (ICM) and the trophectoderm (TE) (Shahbazi, 2020). The ICM corresponds to the pluripotent cluster of cells with the capacity to generate all tissues and cell types of the embryo proper, and the TE, to the first differentiated cell, progenitor of the fetal portion of the placenta (Duranthon et al., 2008; Ralston & Rossant, 2005).

Compared to post-implantation stages, the preimplantation period represents a pretty short period. The duration of the preimplantation period and the developmental timing of the three fundamental processes varies between species. In humans, preimplantation development takes~7 days; in the mouse ~5 days; in rabbits, 6.5 days and the bovine 21 days (Fischer et al., 2012; Shahbazi, 2020; Valadão et al., 2019).

1.2.1 From fertilization towards the cleavage embryo

At fertilization, the fusion of two specialized cells leads to the generation of a totipotent zygote (Cantone & Fisher, 2013). To accomplish this, the parental genomes, each characterized by its distinct epigenetic signatures, must undergo extensive chromatin remodeling to be reprogrammed into a totipotent state (Cantone & Fisher, 2013; Kimmins & Sassone-Corsi, 2005; Schulz & Harrison, 2019).

1.2.1.1 Reprogramming of parental genomes

Just after fertilization, parental genomes remain physically separated, each within a pronucleus, where they will undergo epigenetic reprogramming in an asymmetric manner (Cantone & Fisher, 2013). Before fertilization, the sperm genome is highly methylated and tightly packed in protamines, which consist of arginine-rich nuclear proteins that replace histones (Cantone & Fisher, 2013; Seah & Messerschmidt, 2018; Y. Wang et al., 2019). After fertilization, the paternal genome is rapidly decondensed, and protamines are replaced mainly through maternally-inherited histones (Cantone & Fisher, 2013; Okada & Yamaguchi, 2017). The protamine-to-histone exchange is essential for paternal genome reprograming (Okada & Yamaguchi, 2017). The newly added maternally-inherited histones

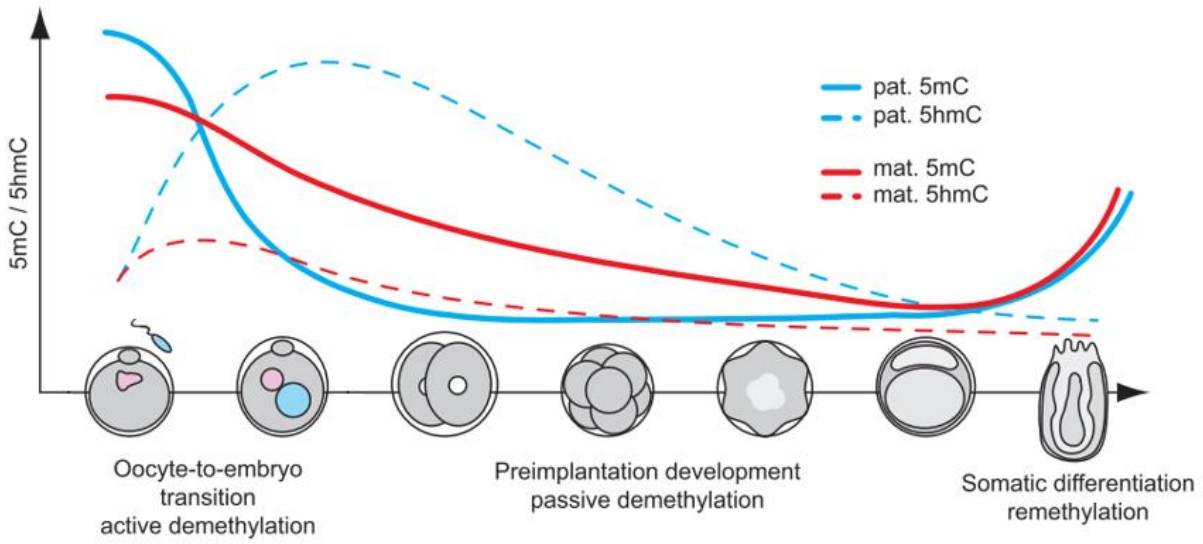

Figure 21: Epigenetic reprogramming of parental genomes, example from the mouse.
Upon fertilization parental genomes undergo a genome-wide wave of DNA demethylation in an asymmetric manner. The parental genome (in blue), overall more methylated than the maternal genome, follows an active DNA demethylation mechanism through the action of TET enzymes, leading to the formation of 5-hydroxymethylcitosine (5hmC) from 5-methylcytosine (5mC). In parallel, the maternal genome (in red) follows a passive DNA demethylation mechanism characterized by dilution of DNA methylation marks through cell division. The maternal genome can similarly be demethylated through active mechanisms, but to a much lower degree. Adapted from Seah & Messerschmidt, 2018.

carry acetylation marks in Lys5 and Lys12 on histone H4 and are hypomethylated (Cantone & Fisher, 2013).
Conversely, after fertilization, the maternal genome maintains the oocyte histone PTMs, including the repressive histone modifications H3K9me3 and H3K27me3 and the active ones such as H3K4me3 and H3K36me3 (Cantone & Fisher, 2013; Seah & Messerschmidt, 2018).
The maternal genome shows overall higher chromatin accessibility than the paternal genome due to its packaging with protamines (Y. Wang et al., 2019).

The reprogramming of parental genomes includes a genome-wide wave of DNA demethylation, which is generally considered active in the paternal genome and passive in the maternal genome (Figure 21). Active DNA demethylation, mostly associated with the parental genome, mainly occurs through the action of the Tet methylcytosine dioxygenase 3 (TET3) (Cantone & Fisher, 2013). Passive DNA demethylation, mostly associated with the maternal genome, occurs through the dilution of DNA methylation marks through cell division (Figure 21) (Cantone & Fisher, 2013).
However, variations in the DNA demethylation dynamics can be observed between species (Cantone & Fisher, 2013). The paternal genome is actively and extensively demethylated in the mouse during the first cycle (Reis e Silva et al., 2011). In contrast, the maternal genome undergoes passive DNA demethylation during the first cleavages (Reis e Silva et al., 2011). In humans, the sperm genome is more methylated than the oocyte genome (Y. Wang et al., 2019). After the 2-cell stage and up until post-implantation development, differences in demethylation dynamics between parental genomes lead to a lower DNA methylation level in the paternal genome than in the maternal genome (Y. Wang et al., 2019). In rabbits, the paternal genome is only partially demethylated during the first cycle, followed by the initiation of methylation maintenance during DNA replication (Reis e Silva et al., 2011). Conversely, methylation levels of the maternal genome remain stable in 1-cell embryos due to methylation maintenance during DNA replication (Reis e Silva et al., 2011).
Certain genomic regions escape the global DNA demethylation, notably the imprinting control regions (ICRs) of imprinted genes, which is essential to maintain parent-or-origin imprinted gene expression (Marcho et al., 2015; Okada & Yamaguchi, 2017; Y. Wang et al., 2019).

1.2.1.2 The cleavage stage embryo

The 1-cell embryo up to the blastocyst stage is surrounded by the zona pellucida, an outer envelope composed of glycoproteins (Zhu & Zernicka-Goetz, 2020). After fertilization, embryos undergo a series of cleavage divisions without increasing in volume, resulting in the 2-cell, 4-cell, and 8-cell embryos consecutively (Menchero et al., 2017; Shahbazi, 2020).

As development progresses, totipotent blastomeres progressively lose their totipotency potential (Kaneko, 2016). In rabbits and bovine embryos, totipotency in maintained until the 8-cell stage (Piliszek & Madeja, 2018). In contrast, in mouse embryos, heterogeneity between blastomeres may be present earlier, around the 2-cell or 4-cell stage (Molè et al., 2020; M. D. White et al., 2018; Zhu & Zernicka-Goetz, 2020). This heterogeneity may dictate whether some blastomeres may be biased toward one lineage compared to the other (M. D. White et al., 2018). Indeed, it has been proposed that enrichment in epigenetic modifications, especially higher levels of H3 methylation, precisely demethylation of

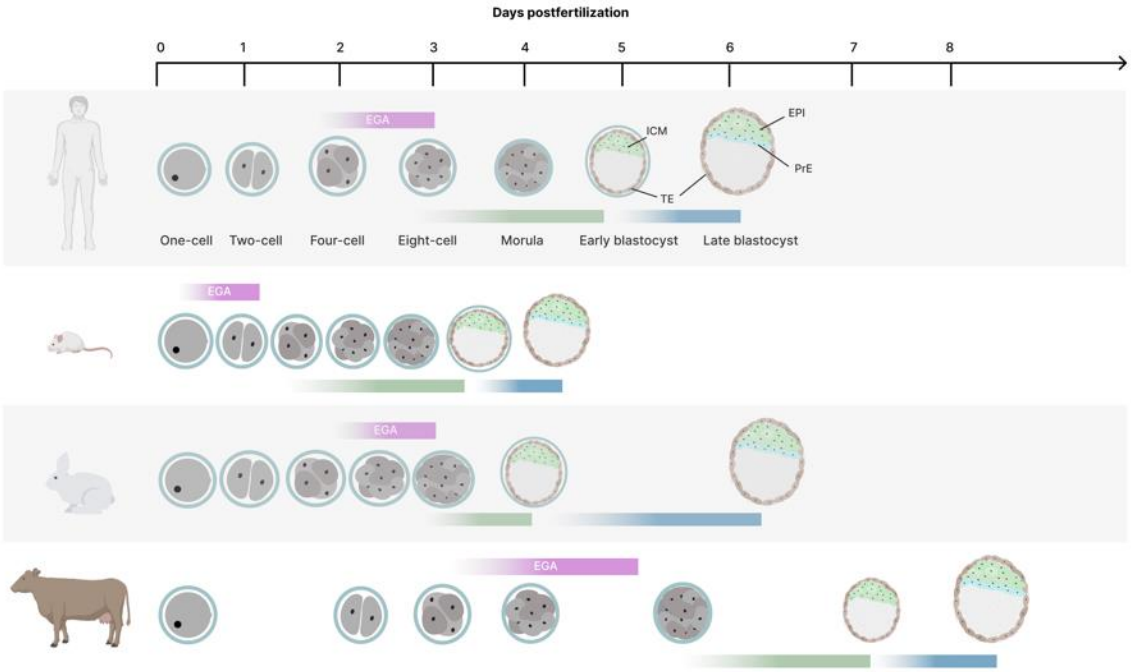

Figure 22: Comparison of preimplantation development in the human, mouse, rabbit and bovine. The developmental timing of key events taking place during preimplantation development is species-specific. The EGA (pink box), the first (green box) and the second specification (blue box) events are shown for each species. ICM, inner cell mass; TE, trophectoderm; EPI, epiblast; PrE, primitive endoderm.

arginines 17 and 26 of histone H3, influence cell fate decisions towards the ICM lineage (M. D. White et al., 2018).

During the cleavage stage, preimplantation embryos go from being transcriptionally silent to activating their transcriptional program to sustain subsequent development (Gerri, Menchero, et al., 2020). The series of events that enable embryonic genome activation (EGA) is known as the maternal-to-zygotic transition (MZT) (Gerri, Menchero, et al., 2020).

1.2.1.3 Maternal-to-zygotic transition

After fertilization, zygotes are transcriptionally silent and depend on the stock of maternal messenger RNAs (mRNAs) inherited proteins from the oocyte cytoplasm (Gerri, Menchero, et al., 2020; Leandri et al., 2008). During the first divisions, embryos rely on post-transcriptional gene regulation (Piliszek & Madeja, 2018). After one or more cleavage divisions depending on the species, the embryo progressively initiates its transcriptional control (Gerri, Menchero, et al., 2020).
The MZT enables maternal mRNAs, protein degradation, and EGA (Gerri, Menchero, et al., 2020; Jukam et al., 2017). EGA occurs gradually and is characterized by two transcriptional phases: the minor and major EGA (Schulz & Harrison, 2019).

The timing of EGA varies across species (Figure 22). In humans, EGA takes place around the transition from 4- to 8-cell stage (Shahbazi, 2020). In the mouse, EGA occurs between the early and late 2-cell stage, similar to the rat (Gerri, Menchero, et al., 2020). In rabbits, EGA occurs at the 8-cell stage, whereas in bovine embryos, EGA occurs between the 8- and 16-cell stage (Figure 22) (Manes, 1973; Christians et al.,, 1994; Piliszek & Madeja, 2018).
Nevertheless, previous reports indicate cleavage embryos may be slightly transcriptionally active before EGA (Piliszek & Madeja, 2018). That is the case of rabbit embryos, where transcription has been identified at the 2-cell stage (Piliszek & Madeja, 2018). Interestingly, as observed in human embryos, EGA in rabbits spans several cell cycles (Madeja et al., 2019).

1.2.2 From morula towards cell fate specification and blastocyst formation

After a series of cleavage divisions, embryos reach the morula stage, and compaction and cell polarization are established, an essential step towards the first specification event (Duranthon et al., 2008; Gerri, Menchero, et al., 2020).
Before compaction, blastomeres contacts are loose (Molè et al., 2020). Towards compaction, cell-cell communication increases between blastomeres through tight and adherens junctions, which is evident by the absence of cell boundaries (Gerri, Menchero, et al., 2020; Molè et al., 2020; Prados et al., 2012). During compaction, the outer cells become polarized while inner cells remain apolar (Gerri, Menchero, et al., 2020). The outer cells have an apical surface without cell-cell contacts and are exposed to the exterior (M. D. White et al., 2018). In contrast, inner cells are surrounded by a basolateral membrane and cell-cell contacts (M. D. White et al., 2018).

The timing and mechanisms of compaction differ between species, which has been better described in the mouse than in other mammalian species. In the mouse, compaction and polarization take place at

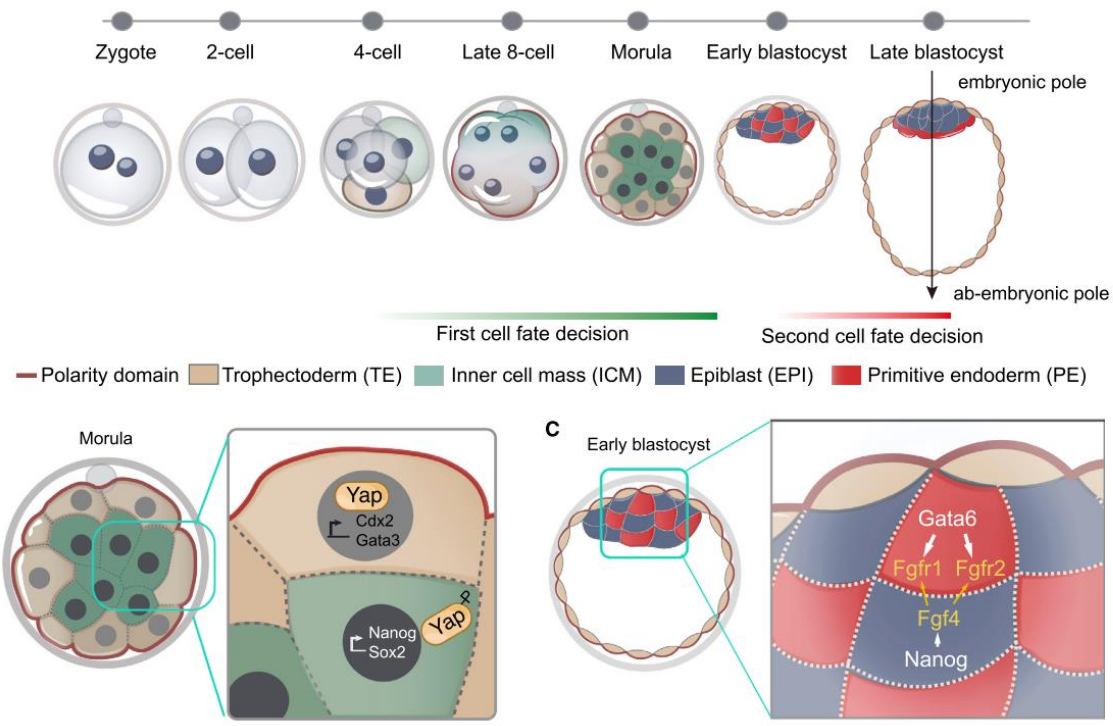

Figure 23: First and second specification events in the mouse preimplantation embryo.
The transition towards the blastocyst stage is associated with the first specification event leading the differentiation of the trophectoderm (TE) and the inner cell mass (ICM). Polarization of the outer triggers TE specification. In polarized outer cells, the TE program is initiated by the translocation of the transcription factor YAP1 to the nucleus, which regulates the expression of TE-specific transcription factors: *Cdx2* and *Gata3* and inhibits the expression of ICM-associated markers. In apolar inner cells, phosphorylation and degradation of YAP1 prevent its translocation to the nucleus, which increases the expression of pluripotency transcription factors, *Nanog* and *Sox2*, involved in the specification of the ICM. At early blastocyst stage, the specification of the epiblast (EPI) and primitive endoderm (PrE) takes place. At first, NANOG and GATA6 are expressed in a mutually exclusive manner between ICM cells, but the increased expression of NANOG and low expression of GATA6 in a group of cells leads to EPI specification. Consequently, the increased expression of GATA6 and low expression of NANOG, together with the increased signaling of FGF4 from cells with high Nanog expression, leads to PrE specification. From Zhu & Zernicka-Goetz, 2020.

the 8-cell stage and is characterized by the presence of E-cadherins and other major components of the tight and adherens junctions (Gerri, Menchero, et al., 2020; Zhu & Zernicka-Goetz, 2020). The apical domain contains the clustering of microvilli and the Par3-Par6-aPKC complex, while the basolateral domain is characterized by E-cadherins, Par-1, and the sodium-potassium pumps (Na^+/K^+-ATPase) (Gerri, Menchero, et al., 2020).
In humans, polarization is evident at the 8-cell stage and is characterized by the basolateral localization of E-cadherins, gap junctions, and apical microvilli (Gerri, Menchero, et al., 2020). In rabbits, compaction and polarization initiate around the 32-64 cell stage, at three days postfertilization (dpf); and the compacted morula is characterized by the presence of microvilli in the basolateral domain of outer cells (Gerri, Menchero, et al., 2020; Piliszek & Madeja, 2018). However, it was previously shown that not all blastomeres appeared polarized prior to blastocyst formation (Ziomek et al., 1990). In bovine embryos, the morula stage is reached at 16-32 cells, around the 5-6 dpf (Gerri, Menchero, et al., 2020).

The transition towards the blastocyst stage is associated with the first specification event leading to the differentiation of the TE and the formation of the ICM cluster of cells (Figure 23) (Gerri, Menchero, et al., 2020). Likewise, most of our knowledge related to this series of major events comes from studies in the mouse (Zhu & Zernicka-Goetz, 2020). In the mouse, establishing an apical domain in outer cells is key for initiating the first specification event, precisely to the TE initiation program (Gerri, McCarthy, et al., 2020; Zhu & Zernicka-Goetz, 2020). Inheritance of the apical domain asymmetrically between daughter cells instructs the polarization status: cells that inherit the apical component become polarized, and cells that do not become apolar (Zhu & Zernicka-Goetz, 2020). The polarity state is directly related to Hippo signaling, a key signaling pathway for the first specification event (Zhu & Zernicka-Goetz, 2020). Polarized cells have inactive Hippo signaling due to the restriction of key Hippo activators by the apical domain (Figure 23) (Zhu & Zernicka-Goetz, 2020). This results in the translocation of the transcription factor *Yap1* into the nucleus, where it interacts with the transcription factor TEAD4 to induce the expression of TE-specific transcription factors: *Cdx2* and *Gata3* (Zhu & Zernicka-Goetz, 2020). YAP1 also inhibits the expression of *Sox2*, triggering the initiation of the TE program (Gerri, Menchero, et al., 2020). Initially, *Cdx2* and *Oct4*, specific markers of TE and ICM, respectively, are co-expressed in all blastomeres (Bassalert et al., 2018). Upon polarization, outer cells expressing *Cdx2* inhibit *Oct4* expression, which is subsequently restricted to the ICM (Bassalert et al., 2018). *Sox2*, another pluripotency transcription factor, begins to be restricted to ICM cells (Bassalert et al., 2018). Unlike polarized cells, apolar cells have active Hippo signaling that leads to the phosphorylation and degradation of YAP1, preventing its translocation to the nucleus (Figure 23) (Piliszek & Madeja, 2018; Zhu & Zernicka-Goetz, 2020). This increases the expression of pluripotency transcription factors, *Nanog* and *Sox2*, involved in the specification of the ICM (Zhu & Zernicka-Goetz, 2020).

The first specification event has a position-dependent Hippo signaling (Hirate et al., 2013). However, Notch signaling acts in parallel to activate the TE program as early as the 4-cell stage (Gerri, Menchero, et al., 2020). TE specification in the mouse is completed at the 32-cell stage, which is followed by the onset of cavitation, marking the passage to the blastocyst stage (Gerri, Menchero, et al., 2020; Zhu & Zernicka-Goetz, 2020). The ratio of TE/ICM cells is different between species, but it is generally considered 3:1 (TE: ICM) (D. K. Gardner & Harvey, 2015).

Cavitation leads to the formation of the blastocoel, a fluid-filled cavity (H. Wang & Dey, 2006). Cavitation is initiated by the formation of microlumens that emerge in the intercellular space of the embryo (M. D. White et al., 2018). These microlumens are formed by the accumulation and exocytosis of vacuoles at the basal membrane of the outer cells of the compacted morula (M. D. White et al., 2018). In parallel, an osmotic gradient originating from the active transport of sodium ions across outer cells via transmembrane pumps allows fluid pumping into the embryo (M. D. White et al., 2018). Fluid pumping leads to the enlargement and coalescence of the various microlumens into a single cavity (M. D. White et al., 2018).
The pressure of cavitation affects the size and shape of the embryo and directs the ICM towards one pole, the embryonic pole (Gerri, Menchero, et al., 2020; M. D. White et al., 2018). Notably, an essential aspect of successful cavitation lies in the permeability barrier of the TE (M. D. White et al., 2018). Due to the establishment of tight junctions, the TE epithelium seals the embryo from the exterior and protects it from collapsing due to the increased pressure during cavitation and subsequent TE divisions (Firmin & Maître, 2021; M. D. White et al., 2018). However, whether the mechanisms of cavitation and the actors implicated in this process are conserved across species is unclear (Firmin & Maître, 2021).

1.2.3 The expanding blastocyst and the second specification event

In the mouse, the first specification event is followed by the second one corresponding to the specification of the ICM in the epiblast (EPI) and primitive endoderm (PrE) (Figure 23) (Zhu & Zernicka-Goetz, 2020). The EPI will give rise to the embryo proper, whereas the PrE participates in the yolk sac formation and patterning of the epiblast (Bassalert et al., 2018; Piliszek & Madeja, 2018). The PrE together with the TE, constitute the extra-embryonic tissues (Bassalert et al., 2018).

From the morula to the early blastocyst stage, NANOG and GATA6, two key transcription factors in EPI and PrE specification, respectively, are co-expressed in all blastomeres (Kang et al., 2013). In parallel, ICM cells secrete low levels of FGF4 (Bassalert et al., 2018). Subsequently, ICM cells initiate their specification towards the EPI or PrE fate (Bassalert et al., 2018). At this stage, NANOG and GATA6 begin to be expressed in a mutually exclusive manner between cells, following a salt-and-pepper pattern (Bassalert et al., 2018; Kang et al., 2013; Zhu & Zernicka-Goetz, 2020). At E3.75, either NANOG or GATA6 expression is lost between cells, resulting in cells with high expression of NANOG and low expression of GATA6 to be specified in EPI, and cells with high GATA6 expression, low NANOG expression to be further specified in PrE (Bassalert et al., 2018). Cells with higher NANOG expression increase FGF4 expression and secretion (Bassalert et al., 2018). This results in cells still in the precursor state with higher GATA6/NANOG ratio receiving increased levels of FGF4, which triggers commitment to the PrE fate through activation of the FGFR1/ERK signaling cascade (Bassalert et al., 2018). By E4.0 cells are either specified to EPI or PrE linages (Figure 23) (Bassalert et al., 2018).

1.2.4 Lineage specification in human and rabbit embryos

In human embryos, whether polarity states and the activity of the Hippo signaling pathway in inner and outer cells play a role in the first cell fate decisions has not been completely defined (Gerri, Menchero, et al., 2020). However, recent studies have reported similar patterns of expression of apical and basolateral proteins in morula stage embryos (Gerri, McCarthy, et al., 2020). Despite this, a few

Lineage	Gene / marker	Mouse	Reported function in mouse	Rabbit	Human	References
TE	CDX2	+	TE initiation	+	+	(Bouchereau et al., 2022; Gerri, Menchero, et al., 2020)
	GATA3	+	TE initiation	+	+	(Bouchereau et al., 2022; Gerri, Menchero, et al., 2020)
	YAP1	+	TE initiation	Not TE-specific*	+	(Gerri, McCarthy, et al., 2020; Gerri, Menchero, et al., 2020)
	TFAP2C	+	TE initiation	+	Not TE-specific	(Bouchereau et al., 2022; Pfeffer, 2018)
	KRT8	+	TE maintenance	+	+	(Bouchereau et al., 2022; Sozen et al., 2021; Wu et al., 2010)
EPI	POU5F1 (OCT4)	+	Pluripotency maintenance	+	+	(Bouchereau et al., 2022; Gerri, Menchero, et al., 2020)
	NANOG	+	Pluripotency maintenance	+	+	(Bouchereau et al., 2022; Gerri, Menchero, et al., 2020)
	SOX2	+	Pluripotency maintenance	+	+	(Bouchereau et al., 2022; Gerri, Menchero, et al., 2020)
	ESRRB	+	Pluripotency maintenance	+	Not detected	(Bouchereau et al., 2022; Gerri, Menchero, et al., 2020)
PrE	GATA6	+	PrE initiation	+	+	(Bouchereau et al., 2022; Gerri, Menchero, et al., 2020)
	GATA4	+	PrE maintenance	+	+	(Bouchereau et al., 2022; Gerri, Menchero, et al., 2020)
	SOX17	+	PrE maintenance	+	+	(Bouchereau et al., 2022; Gerri, Menchero, et al., 2020)

Table 6: Expression of lineage-specific markers in the mouse, rabbit and human preimplantation embryos. Adapted from Gerri et al., 2020.
*Unpublished RNA-seq data from *in vivo* rabbit preimplantation embryos.

similarities and divergencies of mouse early cell fate decisions compared to humans have been reported (Table 6). The initiation of the TE program starts as early as the morula stage, characterized by heterogenous expression of GATA3 and colocalization of GATA3 and YAP1 in outer cells (Gerri, McCarthy, et al., 2020). Later, YAP1, GATA3, and CDX2 expression is restricted to the TE (Gerri, Menchero, et al., 2020). However, CDX2 expression is exclusively detected after cavitation (Gerri, Menchero, et al., 2020). Another TE marker specific to human embryos is GATA2, although its expression is not detected at the morula stage (Gerri, McCarthy, et al., 2020). Similarly, KRT18 is found in outer cells and later restricted to the TE of blastocyst stage embryos (Gerri, McCarthy, et al., 2020). Overall the expression pattern of cell polarity proteins, the localized expression of GATA3, and the conserved expression of the Hippo signaling pathway components between human and mouse embryos suggest a functional link between cell polarity and TE initiation as early as the morula stage (Gerri, McCarthy, et al., 2020).

SOX2, a marker of ICM and EPI progenitors, is initially expressed in all cells of human embryos, with later restriction to the ICM of expanded blastocysts (Gerri, McCarthy, et al., 2020). This differs from the mouse, in which SOX2 is earlier restricted to the ICM (Gerri, McCarthy, et al., 2020).
Conversely, similar to mouse embryos, the EPI of human embryos express NANOG and SOX2, while SOX17 and GATA4 are confined to the PrE (Gerri, Menchero, et al., 2020). However, whether a salt-and-pepper pattern between EPI and PrE transcription factors is initially present in early human blastocysts is yet to be explored (Gerri, Menchero, et al., 2020). Conversely, EPI and PrE specification may involve mechanisms other than FGR receptors or MAPK signaling since its inhibition does not alter EPI and PrE specification (Gerri, Menchero, et al., 2020). Several species-specific markers identified in the mouse and implicated in the first and second specification events are similarly expressed in human embryos (Gerri, Menchero, et al., 2020). However, a few of them are lacking, while others are only expressed in human and not in mouse embryos (Gerri, Menchero, et al., 2020). This scenario suggests that in humans, lineage specification events may involve different mechanisms from what has been described in the mouse (Gerri, Menchero, et al., 2020).

The first and second specification mechanisms in rabbits have not been fully described (Gerri, Menchero, et al., 2020). Nevertheless, recent reports have revealed that lineage specification presents similarities to mouse and human embryos but also species-specific differences (Table 6). A recent study exploring the transcriptome of rabbit preimplantation embryos suggests that the TE program initiates as early as the morula stage, as seen in human embryos (Bouchereau et al., 2022). Morula embryos (E2.7) express both TE (GATA3, TFAP2C) and ICM markers (DDAP5, SOX15, KLF4, STAT3, KLF17, ESRBB) (Bouchereau et al., 2022). At the early and late blastocyst stage (E3.5-6.6), embryos showed enrichment in TE-specific markers TFAP2C and KRT18 (Bouchereau et al., 2022).

Unlike mouse embryos but similar to humans, CDX2 is expressed in rabbit TE but only after blastocyst formation (Gerri, Menchero, et al., 2020). This suggests CDX2 may be mostly implicated in the maintenance of the TE program rather than the initiation (Gerri, Menchero, et al., 2020). The ICM of early blastocysts (E3.5 to 4.0) shows the enrichment of pluripotency markers DPPA5, ESRRB, POUF5F1 (OCT4), and SOX2 (Bouchereau et al., 2022). Indeed, OCT4 is initially expressed in all blastomeres after EGA but becomes specific to the EPI at E5.0 (Bouchereau et al., 2022; Gerri, Menchero, et al., 2020). NANOG is expressed from the 2-cell stage until the blastocyst stage, which is restricted to the ICM (Piliszek & Madeja, 2018). Rabbit early blastocysts also show the enrichment of PrE markers (PDGFRA, GATA6,

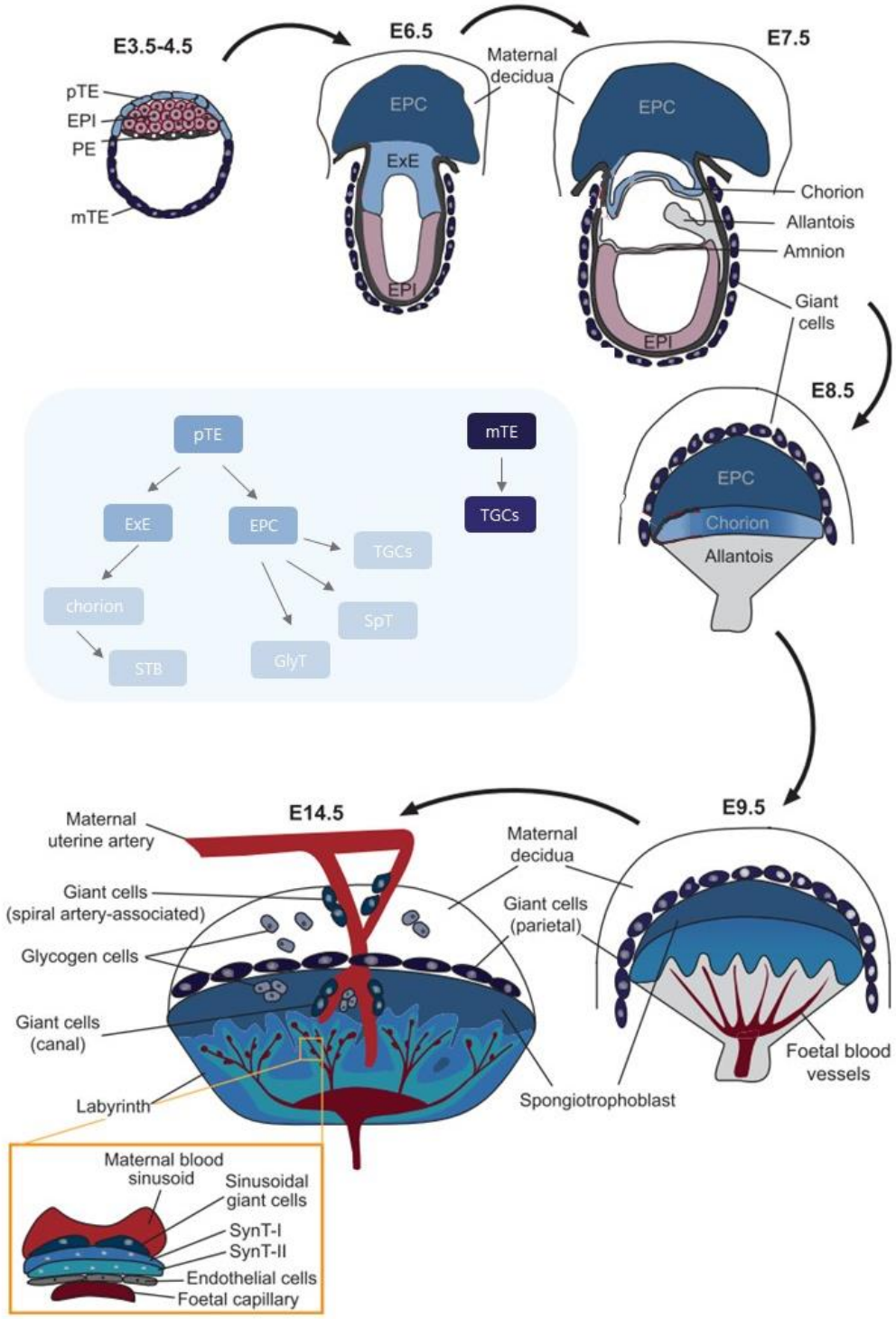

Figure 24: From blastocyst to the embryonic and placental development in the mouse.
Proliferation of pTE gives rise to ExE and the EPC. ExE cells next form the chorion, which is then fused to the mesoderm-derived allantois, forming the early placenta at E8.5. The placenta continues to develop and grow in size, yielding the mature placenta constituted of three principal layers: the labyrinth, the junctional zone and the TGCs layer. Trophoblast cell lineages are indicated in the blue box. pTE, polar TE; mTE, mural TE; ExE, extraembryonic ectoderm; EPC, ectoplacental cone; TGC, trophoblast giant cells; STB, syncytiotrophoblast; SpT, spongiotrophoblast; GlyT, glycogen trophoblast. Adapted from Latos & Hemberger, 2016.

HNF1B, FOXA2, RSPO3, SOX17), thus suggesting PrE specification begins as early as the E3.5 stage (Bouchereau et al., 2022; Piliszek & Madeja, 2018).
Interestingly, scRNA-seq analysis from different stages of rabbit preimplantation embryos showed that expression of SOX2 and GATA6, markers of EPI and PE respectively, become mutually exclusive at E4.0 and that the specification of EPI *vs.* PrE ends by E5.0 (Bouchereau et al., 2022). The expression of GATA6 and NANOG in a salt-and-pepper pattern described in the mouse is not present in rabbit ICM cells (Piliszek & Madeja, 2018). Thus, the mutual inhibition of GATA6 and NANOG may not be essential for initiating EPI and PrE specification in rabbits (Gerri, Menchero, et al., 2020; Piliszek & Madeja, 2018).

As described in the mouse, the FGF/MEK signaling cascade is essential in the specification of EPI *vs.* PrE (Piliszek & Madeja, 2018). In rabbit and human embryos, perturbations of the FGF/MEK pathway led to the same overall effect: inhibition of FGF4/MEK results in ablation of the PrE, and supplementation of FGF4 leads to ICM cells specified to PrE (Piliszek & Madeja, 2018). However, inhibition of the FGF/MEK pathway in human and rabbit embryos did not result in the complete absence of cells with PrE-specific markers, such as GATA6 and GATA4 in human embryos and GATA6 in rabbit embryos (Piliszek & Madeja, 2018). Thus, it suggests that a conserved global mechanism of the FGF/MEK pathway in EPI *versus* PrE specification is present in human and rabbit embryos. Still, some divergence is present in these species.

1.2.5 The TE, the first differentiated cell and placental development

The implantation process marks the initiation of placenta development (Aplin et al., 2020). The basic organization of the placenta, including a developing vascular network and the trophoblast as the nexus from the mother to the developing conceptus, is present by the third week of pregnancy (Aplin et al., 2020). However, the maternal-placenta blood supply initiates later on, by week 11 of pregnancy (Aplin et al., 2020). Before this, the conceptus relies on uterine secretions to support its development (Aplin et al., 2020).

Upon implantation, the TE will give rise to different specialized placental cell types, whereas the mesoderm, formed after gastrulation, participates in the formation of the umbilical cord and the fetal portion of the placental vascular network (Latos & Hemberger, 2016). The TE can be separated into polar TE, the TE in contact with the ICM at the early blastocyst stage, and the mural TE, in contact with the blastocoel (Figure 24) (Latos & Hemberger, 2016).

Placenta development in the mouse initiates with the differentiation of primary trophoblast giant cells (TGCs) from mural TE to help with the implantation process (Maltepe & Fisher, 2015). In parallel, the proliferation of the polar TE gives rise to the extraembryonic ectoderm (ExE) and the ectoplacental cone (EPC) (Hemberger et al., 2019). The outer cells of the EPC further differentiate into secondary TGCs (Hemberger et al., 2019). The secondary TGCs invade the maternal decidua, the transformed endometrial tissue, making contact with spiral arteries (Hemberger et al., 2019). Moreover, producing pro-angiogenic and vasodilatory factors allows the implantation site to be exposed to maternal blood, thus to nutrients and oxygen (Hemberger et al., 2019). Gastrulation occurs, and the three germ layers: the ectoderm, mesoderm, and endoderm, are established (Hemberger et al., 2019). Around gastrulation, the ExE forms the chorion later fused with the mesoderm-derived allantois, thus forming the early placenta (Figure 24) (Latos & Hemberger, 2016). Development of the chorion and EPC leads to the differentiation of various

trophoblast cell types and placental layers (Figure 24) (Latos & Hemberger, 2016). Among these cell types we can highlight the syncytiotrophoblast (STB) layers and the spongiotrophoblast (SpT) and glycogen trophoblast (GlyT) cells (Hemberger et al., 2019). The STB layers contribute to the formation of the vascular structure of the placental labyrinth and represent the principal site of nutrient and gas exchange, whereas the SpT and GlyTs are responsible for the endocrine function of the placenta (Hemberger et al., 2019). The EPC outer cells also differentiated into other specialized cell types: spiral-artery associated-TGCs, and the canal and parietal TGCs (Latos & Hemberger, 2016).

The placenta continues to develop and grow in size, yielding the mature placenta, consisting of three main layers: the labyrinth where the nutrient exchange takes place in rodents, the junctional zone, and the parietal TGCs layer, situated next to the maternal decidua (Figure 24) (Latos & Hemberger, 2016). In humans, the nutrient exchange takes place in the chorionic villi (Hemberger et al., 2019). The mature human placenta comprises expanded chorionic villi containing fetal vessels, a layer of cytotrophoblast cells, and STB cells, which are in direct contact with maternal blood (Hemberger et al., 2019).

1.3 The surrounding environment and energy metabolism of preimplantation embryos

The oviduct and uterine fluid correspond to the immediate microenvironment of the developing preimplantation embryo. The oviduct and uterine fluid play an essential role in preimplantation development, as it supplies the required nutrients to support embryonic development (Schindler, Pendzialek, et al., 2020).
The early embryo is in continuous crosstalk with its surrounding environment (Hu & Yu, 2017). Preimplantation embryos sense their environment and secretes autocrine and paracrine signals, while the surrounding tissue responds by adapting its secretory content (Hu & Yu, 2017). The crosstalk between preimplantation embryos and their surrounding environment has been recently shown in rabbits. The comparison of metabolomic profiles from uterine and blastocoelic fluids showed that of the 24 detected metabolites, 21 were present in both the uterine fluid and the embryo (Calderari et al., 2021).

The surrounding environment of preimplantation embryos is directly linked to early embryo energy metabolism. To sustain their development, preimplantation embryos uptake energy substrates, oxygen, proteins, antioxidants, ions, and other factors in the oviduct and uterine fluid. Therefore, changes in this microenvironment may influence preimplantation development.

1.3.1 The oviduct and uterine fluid

The oviduct and uterine fluid composition originate from a mixture of transudate components from the bloodstream and the secretion of epithelial cells (Aguilar & Reyley, 2005).
This composition may vary among species according to the estrous cycle stage and the specific location (oviduct *versus* uterine fluid) (Hu & Yu, 2017).

The oviduct and uterine fluid are composed of energy substrates (i.e., glucose, pyruvate, lactate, fructose), growth factors (i.e., EGF, IGF-1, IGF2, IR, TGF-α), lipids (i.e., prostaglandins, phospholipids, triglycerides), steroid hormones, AAs (i.e., glycine, methionine, lysine), proteins (i.e., albumin,

Substrate	Human		Rabbit		Mouse		Bovine	
	Oviduct fluid	Uterine fluid	Oviduct fluid	Uterine fluid	Oviduct fluid	Uterine fluid	Oviduct fluid	Uterine fluid
Glucose (mM)	0.5 - 3.1	0.5 – 3.2	-	0.5 - 2.6	1.7 – 5.2	0.6	0.02 - 3.2	3.8 - 4.6
Pyruvate (mM)	0.1 - 0.3	0.1 - 0.2	-	1.4	0.1 - 0.4	0.3	0.09 – 0.1	0.08 – 0.1
Lactate (mM)	5.4 - 10.5	5.9 - 8.6	-	-	4.3 - 11.7	9.4	5.4 – 6.7	1 – 1.1

Table 7: Composition of main energy substrates and growth factors in the oviduct and uterine fluid for human, rabbit, mouse and bovine in a physiological context.
References: Aguilar & Reyley, 2005; Calderari et al., 2021; Harris et al., 2005; Hu & Yu, 2017; Hugentobler et al., 2008; Saugandhika et al., 2022

immunoglobulin G, glycoproteins), ions (e.g., potassium, chloride, calcium, magnesium) (Aguilar & Reyley, 2005; Menezo & Guerin, 1997).
The concentration of main energy substrates in the oviduct and uterine fluid has been reported for different species (Table 7). The glucose concentrations in the human oviduct and uterine fluid ranged between 0.5 to 3.1 mM and 0.5 to 3.2 mM, respectively (Aguilar & Reyley, 2005; Harris et al., 2005; Hu & Yu, 2017; Saugandhika et al., 2022). Examining glucose concentrations in the oviduct fluid, humans and rabbits show closer maximal values (3.2 mM *versus* 2.6 mM, respectively) Table 7) (Aguilar & Reyley, 2005; Calderari et al., 2021; Harris et al., 2005; Hu & Yu, 2017; Saugandhika et al., 2022).

For pyruvate, the oviduct fluid concentration levels were quite close for the human, mouse, and bovine (Table 7) (Aguilar & Reyley, 2005; Harris et al., 2005; Hu & Yu, 2017; Hugentobler et al., 2008; Saugandhika et al., 2022). However, pyruvate concentrations in uterine fluids were higher for rabbits (1.4 mM) than for humans, mice, and bovines (Table 7) (Aguilar & Reyley, 2005; Calderari et al., 2021; Harris et al., 2005; Hu & Yu, 2017; Hugentobler et al., 2008; Saugandhika et al., 2022). Compared to glucose and pyruvate, lactate concentrations are higher in the oviduct and uterine fluids, reaching 10.5 mM in human oviduct fluids and 11.7 mM in the mouse (Table 7).

In addition, although insulin cannot cross the placental barrier, during the preimplantation period, maternal circulating glucose and insulin levels surround the developing embryo (Tarry-Adkins & Ozanne, 2017). Nevertheless, a complete assessment of oviduct and uterine fluid composition for several model organisms is lacking. In humans, measurement of insulin-like growth factor I (IGF-I) detected 8 nM and 10.9 nM in the oviduct and uterine fluid, respectively, and these concentrations corresponded to ~50% of serum concentrations (Lighten et al., 1998). In the rat oviduct, the mRNA of IGF-I and the insulin-like growth factor II (IGF-II) have been detected (Lighten et al., 1998). Nevertheless, little is known about insulin concentrations in physiological and pathological contexts. Mostly the presence but not the concentrations have been previously reported for humans and bovines (Aguilar & Reyley, 2005).

Glucose diffuses from the bloodstream (Aguilar & Reyley, 2005). Although usually below plasma concentrations, the composition and concentration of the oviduct and uterine fluid directly depend on the maternal nutritional and metabolic status (Aguilar & Reyley, 2005; Schindler, Pendzialek, et al., 2020). In a diabetic context, characterized by hyperglycemia and/or hyperinsulinemia, perturbations of the microenvironment surrounding preimplantation embryos are considered to contribute to adverse outcomes and developmental programming in the offspring. Indeed, in a rabbit T1D-like model, a 3.5-fold increase (1.75 mM) in uterine glucose levels was identified, together with altered metabolism and cellular homeostasis in exposed blastocysts (Fischer et al., 2017; Ramin et al., 2010).

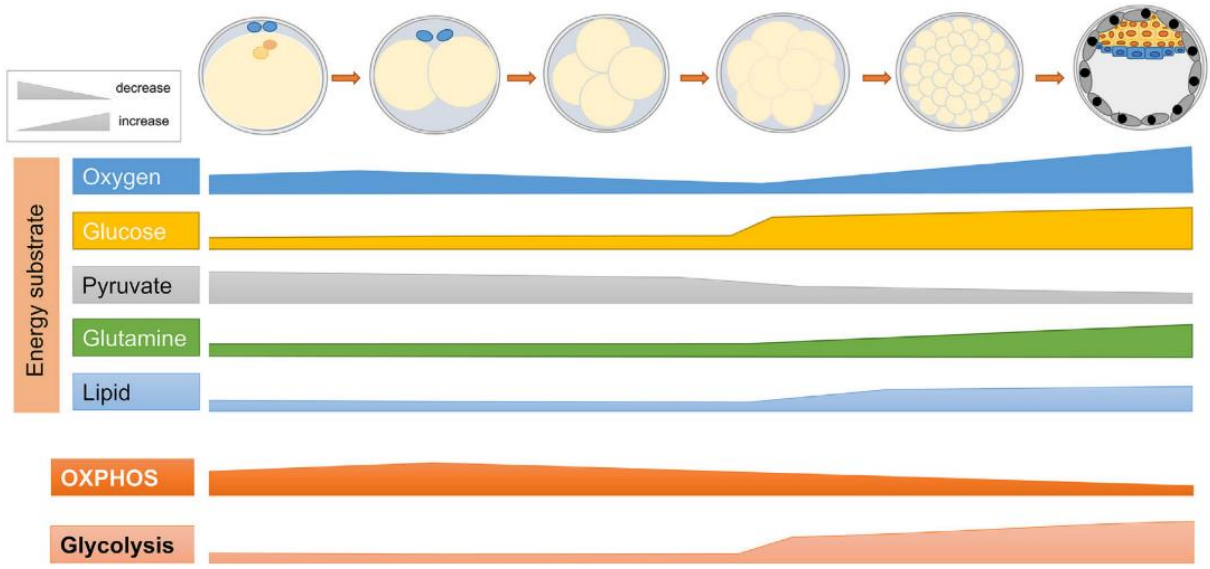

Figure 25: Preimplantation embryo energy metabolism.
The preimplantation metabolism can be divided into pre-compaction and post-compaction metabolism. Pre-compaction embryos have low energy demands, low oxygen consumption and glucose utilization and instead metabolize pyruvate and lactate as energy substrates through OXPHOS. As development continues and embryos reach the compaction and post-compaction stages, energy demands increase significantly to support cell division and blastocyst formation. Oxygen consumption increases, glucose is metabolized through glycolysis and fatty acid oxidation increases. From (Hu & Yu, 2017).

1.3.2 The preimplantation embryo energy metabolism

The requirements and metabolic signatures of preimplantation embryos can be divided into pre-compaction and post-compaction embryo metabolism.

During the pre-compaction stages, metabolic requirements and energy demands are low (Saugandhika et al., 2022). Embryos show low oxygen consumption levels, pyruvate oxidation, lactate and amino acids, glucose utilization capacity, and mitochondria activity (Figure 25) (D. K. Gardner & Harvey, 2015; Nagaraj et al., 2017; Saugandhika et al., 2022). Indeed, the intracellular high ATP/ADP ratio in pre-compaction stages suppresses glycolysis, among other mechanisms, by inhibiting glycolytic enzyme phosphofructokinase (PFK) (Kaneko, 2016; Saugandhika et al., 2022).

Pre-compaction embryos strictly utilize pyruvate and lactate as energy substrates through OXPHOS (Kaneko, 2016; Saugandhika et al., 2022). Indeed, in mouse 2-cell embryos, it was recently demonstrated that pyruvate entering the TCA cycle is virtually not glucose-derived (Sharpley et al., 2021).
The transport of pyruvate and lactate in preimplantation embryos is accomplished by monocarboxylate transporters (MCTs) (Purcell & Moley, 2009). In mouse embryos, the MCTs 1, 2, 3, and 4 expressions have been detected in all stages, whereas in human embryos, only MCTs 1 and 2 have been identified (Purcell & Moley, 2009). In preimplantation development, the role of pyruvate may extend from energy production purposes (Nagaraj et al., 2017). In the mouse, pyruvate is essential for EGA (Nagaraj et al., 2017). Pyruvate, key enzymes from pyruvate metabolism, and the TCA cycle are transiently localized in the nucleus of 1-cell to 2-cell mouse embryos (Nagaraj et al., 2017). The key enzymes of the TCA cycle, classified by the authors as "class I" metabolites, include pyruvate dehydrogenase, citrate synthase, aconitase 2 and isocitrate dehydrogenase 3A, which generate acetyl-CoA, citrate, isocitrate, and α-ketoglutarate, respectively (Nagaraj et al., 2017). These TCA-derived metabolites then participate in the regulation of epigenetic remodeling during EGA (Nagaraj et al., 2017). Failure to localize these TCA cycle-related enzymes results in aberrant histone modification profiles and EGA block (Nagaraj et al., 2017). Interestingly, this mechanism appears to be conserved in human embryos (Nagaraj et al., 2017).

As development continues and embryos reach the compaction and post-compaction stages, energy demands increase significantly, notably to support cell division and blastocyst formation (Figure 25) (D. K. Gardner & Harvey, 2015). Around the morula stage, the intracellular ATP/ADP ratio decreases, stimulating the activation of PFK and glucose utilization through aerobic glycolysis (Kaneko, 2016; Leese et al., 1993; Saugandhika et al., 2022). As shown in the mouse, glycolytic intermediates and gene expression patterns related to glycolysis are higher in blastocysts compared to the 2-cell embryo (Sharpley et al., 2021).
Glucose transporters are expressed in preimplantation embryos, although their expression may vary between species (Purcell & Moley, 2009). In the mouse, most GLUT transporters have been detected, including GLUT 1, 2, 3, 4, 8, 9, and 12, whereas in rabbit and human embryos, only GLUT 1, 4, 8, and GLUT1 and 14 have been detected, respectively (Purcell & Moley, 2009). GLUT1 expression is detected across all preimplantation stages (Purcell & Moley, 2009). After compaction, GLUT-1 is localized on the apical and mainly basolateral plasma membrane of the TE, and the plasma membrane of the ICM, suggesting transport of glucose from the outside towards the blastocoel and into the ICM (Purcell & Moley, 2009).

As for GLUT4 and GLUT8, both have been detected at the blastocyst stage (Purcell & Moley, 2009). GLUT4, although known to be insulin-dependent, is not translocated after stimulation with insulin or IGF-1 in preimplantation embryos (Purcell & Moley, 2009). Different from GLUT4 in the early embryo, GLUT8 has been reported to be insulin-sensitive in the mouse (Purcell & Moley, 2009).
Concomitant with an increased glycolytic flux, preimplantation embryos express both IR and IGF1R (Purcell & Moley, 2009). Insulin, which is not expressed by preimplantation embryos, is supplied by the maternal oviduct and uterine fluid, whereas IGF1 and IGF2 are both expressed by preimplantation embryos and supplied by the maternal intrauterine environment (Thieme et al., 2012).

It was widely accepted that post-compaction embryos did not completely oxidize glucose to ensure constant substrate availability for biosynthesis purposes (D. K. Gardner & Harvey, 2015). However, it has been recently shown that glucose oxidation may be less significant than previously thought by examining the carbon contribution of glucose and pyruvate/lactate during mouse preimplantation development (Sharpley et al., 2021). Glucose is indispensable for mouse embryos at the 8-cell stage, notably during the morula to blastocyst transition (F. Chi et al., 2020; Sharpley et al., 2021). However, glucose is hardly oxidized through the TCA cycle, as shown by the nearly absent carbon contribution from glucose to TCA-derived metabolites, acetyl-CoA, or amino acids (Sharpley et al., 2021). On the contrary, glucose is metabolized through the PPP and supplies nearly all ribose carbons in nucleotides (Sharpley et al., 2021). Carbon supply to acetyl-CoA and TCA-derived metabolites is rather in charge of pyruvate/lactate (Sharpley et al., 2021). Interestingly, pyruvate/lactate predominantly supplies carbons to one side of the TCA cycle-derived metabolites (Sharpley et al., 2021). This side of the TCA cycle corresponds to citrate, aconitate, and α-ketoglutarate, which are the class I metabolites previously described to be essential for EGA in the mouse and to be highly nutrition-sensitive (Nagaraj et al., 2017; Sharpley et al., 2021).

With an increased glucose influx, oxygen consumption increases at post-compaction stages, especially during cavitation, to support the activity of sodium-potassium pumps in the TE (Figure 25) (D. K. Gardner & Harvey, 2015).
Lipids are another energy source for preimplantation embryos (Hu & Yu, 2017). Human and mouse embryos have been shown to take up fatty acids during preimplantation development (Hu & Yu, 2017). Moreover, fatty acid oxidation increases from the 8-cell stage onwards, suggesting it to be essential for preimplantation development. Although early cleavage stages exhibit low fatty acid oxidation activity, its perturbation impairs blastocyst formation (Hu & Yu, 2017). Amino acids play important roles in preimplantation development (D. K. Gardner & Harvey, 2015). Glycine acts as a buffer to maintain the intracellular pH, and glutamine and aspartate are preferentially used as energy sources (D. K. Gardner & Harvey, 2015). Furthermore, activation of mTOR signaling by AA is essential for TE differentiation, invasive behavior, and embryo implantation (P. M. Martin, 2003).

In addition, in mouse blastocyst, it has been shown that ICM and TE show a few differences concerning energy metabolic pathways (D. K. Gardner & Harvey, 2015). The ICM relies on aerobic glycolysis to sustain proliferation, the maintenance of pluripotency, and prepare for the rapid increase of biomass by the time of implantation (Kaneko, 2016). The TE, on the other side, relies on OXPHOS to sustain the expansion and maintenance of the blastocoel (D. K. Gardner & Harvey, 2015; Kaneko, 2016).

Likewise, the ICM and TE mitochondria morphology further confirms their metabolic signatures (Kaneko, 2016). The ICM, similar to mouse embryonic stem cells (mESCs), shows spherical-shaped mitochondria with few cristae (Kaneko, 2016). Conversely, the TE shows elongated mitochondria with extensively folded cristae characteristic of active OXPHOS and a higher number of mitochondria than the ICM (Houghton, 2006; Kaneko, 2016).
Nevertheless, in light of the aforementioned recent findings, a more detailed assessment of glucose metabolism and carbon contribution in the ICM and TE in the mouse and other species is needed. In rabbits, the ICM and TE metabolism has not been extensively described. However, a recent study showed that similar to mouse, the TE of rabbit embryos exhibits higher OXPHOS activity than the ICM, while the ICM shows the expression of genes implicated in glucose uptake and glycolysis, indicative of active glucose utilization (Bouchereau et al., 2022).

Interestingly, glucose metabolism regulates TE specification in the mouse (F. Chi et al., 2020). Glucose metabolism through the Hexosamine Biosynthetic pathway (HBP) results in the translocation of YAP1 to the nucleus, while PPP, together with sphingolipid (S1P) signaling, activates mTOR signaling, thereby regulating *Tfap2c* translation (F. Chi et al., 2020). The YAP1 – TEAD4 – TFAP2C complex regulates the transcription of TE-specific genes (F. Chi et al., 2020).

1.3.3 Insulin action on preimplantation development

Insulin, IGF-1, and IGF2 are present in the oviduct and uterine fluid (Aguilar & Reyley, 2005; Thieme et al., 2012). In addition, both IGF1 and IGF2 are expressed by preimplantation embryos (Thieme et al., 2012). Preimplantation embryos express both IR and IGF1R, generally concomitant with the increase in glucose utilization and blastocyst formation (Rosenblum et al., 1986). Therefore, their expression may vary between species (Purcell & Moley, 2009). In the mouse, expression of IR and IGF1R has been detected around the 8-cell stage, whereas in the rabbit, IR is only detected at the blastocyst stage in both ICM and TE, while IGF1R is mainly found in the ICM (Navarrete Santos et al., 2008; Navarrete Santos, Tonack, Kirstein, Kietz, et al., 2004; Pantaleon & Kaye, 1996). In humans, IR is detected at the morula stage (Navarrete Santos et al., 2008).
Insulin and IGF-1 and IGF-2 can bind to both receptors but with higher affinity when bound to their corresponding receptor (Navarrete Santos et al., 2008).

Insulin mediates both metabolic and mitogenic actions through the activation of two branches: the MAPK (mitogenic actions) and the PI3K/AKT (metabolic actions) signaling pathways, as described in Chapter 1, section 1.2.
In preimplantation embryos, these downstream responses to insulin have also been described. In mouse blastocysts, insulin and IGF-1 stimulated glucose uptake via GLUT-1, but IGF-1 was more efficient than insulin (Pantaleon & Kaye, 1996). Interestingly, insulin or IGF-1 action on glucose uptake was mediated by the binding to IGF1R rather than IR (Pantaleon & Kaye, 1996).
Insulin signaling stimulates protein synthesis through phosphorylation of Eukaryotic Translation Initiation Factor 4E-Binding Protein 1 (4EBP1) and S6K, downstream targets of mTORC1 (Boucher et al., 2014). In compacted and blastocysts mouse preimplantation embryos, *in vitro* culture with insulin resulted in 90% increased protein synthesis (Harvey & Kaye, 1988). Although the mechanistic link

between insulin availability and activation of mTORC1 downstream insulin signaling leading to protein synthesis was not demonstrated, it is possible to speculate that this may be a plausible explanation.
In rabbits, more mechanistic insights on insulin's metabolic and mitogenic actions have been described. *In vitro* culture of rabbit blastocysts with insulin led to the activation of the insulin signaling pathway, as shown by the phosphorylation of MAPK ERK 1/2 (Navarrete Santos, Tonack, Kirstein, Pantaleon, et al., 2004). Insulin also enhanced the mRNA levels of IR and GLUT-4 4 (Navarrete Santos, Tonack, Kirstein, Pantaleon, et al., 2004). However, exposure to insulin did not result in the phosphorylation of PI3K, AKT, or changes in GLUT-8 mRNA levels, glucose uptake, or GLUT-4 translocation, all indicative that the Akt branch of the insulin signaling pathway was not activated (Navarrete Santos, Tonack, Kirstein, Pantaleon, et al., 2004). Based on these results, it was concluded that in rabbit blastocysts, insulin exerts mostly mitogenic than metabolic actions (Navarrete Santos, Tonack, Kirstein, Pantaleon, et al., 2004).
Further examination of insulin and IGF-1 actions on the ICM and TE of rabbit *in vivo* blastocysts showed a clearer picture and revealed lineage-specific responses.
The IR was expressed in both ICM and TE; however, IGF1R was mainly detected in the ICM (Navarrete Santos et al., 2008). Stimulation of blastocysts *in vitro* with either insulin or IGF-1 showed a cell-specific signaling response. Insulin mostly influenced the TE and triggered mitogenic and metabolic responses, including transcription of the MAPK target *c-fos* and inhibition of gluconeogenesis via downregulation of phosphoenolpyruvate carboxylase (PEPCK) by AKT (Navarrete Santos et al., 2008). On the contrary, insulin slightly influenced mitogenic responses in the ICM, but no activation of the PI3K/AKT brach was observed. However, IGF-1 stimulated mitogenic responses via binding to IGF1R exclusively in the ICM (Navarrete Santos et al., 2008).
Therefore, actions of the insulin/IGF-1 system occur in a lineage-specific manner *in vivo*- developed rabbit blastocyst (Navarrete Santos et al., 2008).
Several reports have described the mitogenic actions of insulin during preimplantation development in different species and in a lineage-specific manner. In the mouse, especially in the ICM (H. G. Gardner & Kaye, 1991; Harvey & Kaye, 1990) and in the bovine, especially in the TE (Augustin et al., 2003). In rabbit blastocysts, insulin promotes cell proliferation and reduces apoptosis (Herrler et al., 1998).

Preimplantation embryos are responsive to insulin levels, and both metabolic and mitogenic actions have been demonstrated. Moreover, lineage-specific responses have been described in rabbits, mice, and bovines. Thus, disturbances of the glucose and/or insulin axis, as in the context of prediabetes/diabetes in pregnancy, may influence preimplantation development and, most likely in a lineage-specific manner.

1.4 The periconceptional period in a diabetic context

Exposure to environmental insults such as a perturbed maternal metabolic status during critical periods of development can result in short- and long-term effects on the offspring, including a high risk for NCDs, as detailed in Chapter 2. One of these critical windows of development corresponds to the periconceptional period (i.e., from gametogenesis to preimplantation development). Maternal metabolic perturbations *in utero,* such as hyperglycemia, hyperinsulinemia and PGD during the periconceptional periods, have been shown to leave long-lasting signatures of this early life exposure, with repercussions for post-natal life. During preimplantation development, this is particularly critical since pregnancy at

this state is not yet recognized, and thus maternal metabolic perturbations may not be adequately monitored or intervened.

1.4.1 The effect of pre-gestational diabetes on the oocyte

Maternal diabetes impairs ovarian function and oocyte development, and diabetes is overall associated with subfertility in men and women (Ge et al., 2014; S. T. Kim & Moley, 2008). Indeed, male diabetic-induced mice showed altered sperm concentration and motility, altered expression of glucose transporters (i.e., GLUT8), lower fertilization rates, and reduced blastocyst formation (S. T. Kim & Moley, 2008). In a similar fashion, impaired expression of glucose transporters has been described in oocytes (Ge et al., 2014).

More importantly, these perturbations may propagate during embryonic development even when the initial insult is no longer present (Q. Wang et al., 2009). Embryo transfer experiments further confirmed this when 1-cell embryos from diabetic mice transferred to non-diabetic pseudo-pregnant recipients exhibited birth defects (i.e., neural tube defects) and growth retardation (Wyman et al., 2008).
Thus, indicating that the intrauterine environment during oogenesis is similarly a sensitive developmental window.

Mitochondria are known to be affected by a diabetic environment (Q. Wang et al., 2009). Similarly, in MII oocytes from diabetic-induced mice, mitochondria exhibited structural changes (i.e., narrow intermembrane space, rupture of outer membrane), increased number, reduced function, and altered distribution patterns during oocyte maturation (Q. Wang et al., 2009). Moreover, oocytes showed spindle defects, chromosome misalignments, and an increased incidence of aneuploidy (Q. Wang et al., 2009). Furthermore, because mitochondria are maternally-inherited in preimplantation embryos, faulty mitochondria could comprise embryo metabolism and development. Indeed, impaired mitochondria are considered to enhance apoptosis in preimplantation embryos from diabetic mice (Q. Wang et al., 2009).

Furthermore, a diabetic environment has also been associated with aberrant DNA methylation profiles in oocytes. Oocytes from diabetes-induce mice showed reduced DNA methylation in the imprinted genes *Peg3*, concomitant with reduced expression of DNMT1, DNMT3a, DNMT3b, and DNMT3L (Ge et al., 2014). Similar to these findings, global changes in histone acetylation patterns, in parallel with enhanced expression of HATs and decreased expression of HDACs, were also observed in oocytes from diabetic mice (Ding et al., 2012). Furthermore, recent findings have described a maternally-inherited IGT via oocyte TET3 insufficiency (B. Chen et al., 2022). In diabetes-induced mice, TET3 expression was found to be reduced in oocytes, as reported in people with diabetes (B. Chen et al., 2022). In diabetic mice, TET3 insufficiency in oocytes resulted in impaired demethylation in the paternal genome contributing to the hypermethylation of paternal alleles, including several insulin secretion genes (B. Chen et al., 2022). Aberrant DNA methylation patterns persisted until adulthood and were associated with IGT due to impaired glucose-stimulated insulin secretion (B. Chen et al., 2022).
The authors concluded that the predisposition to IGT in the offspring occurs through TET3 insufficiency in oocytes rather than through a direct perturbation in the oocyte epigenome (B. Chen et al., 2022).

The effect of hyperinsulinemia during *in vitro* oocyte maturation and its consequences on preimplantation development have been previously examined in the bovine. Analysis of D8 blastocysts developed from oocytes exposed to hyperinsulinemia during *in vitro* maturation impaired the developmental competence of blastocysts and resulted in increased cell numbers, changes in actin and mitochondrial patterns, and gene expression changes (Laskowski, Båge, et al., 2017; Laskowski, Sjunnesson, et al., 2017). Gene expression changes included the overexpression of genes involved in cell division, mitochondrial function, lipid metabolism, oxidative stress responses, and cell differentiation (Laskowski, Båge, et al., 2017; Laskowski, Sjunnesson, et al., 2017). Furthermore, assessment of the DNA methylation profile of those blastocysts further confirmed previously identified transcriptomic signatures and revealed DMRs in imprinted genes (i.e., insulin-like growth factor 2 receptor*, IGFR2*) and genes with an epigenetic-related function (Laskowski et al., 2018).

1.4.2 The preimplantation embryo in the context of diabetes

The preimplantation embryo constitutes a particularly sensitive period of development, as previously detailed. Exposure to a diabetic *in utero* environment exclusively during the preimplantation period can have long-lasting effects on the offspring. Due to obvious ethical reasons and technical limitations, research on human preimplantation embryos in a diabetic context is scarce. Hence, most, if not all, studies of preimplantation development under a diabetic environment come from studies in animal models using *in vivo* and *in vitro* strategies of exposure. Nevertheless, several studies have described that poor glycemic control in the first trimester is associated with the most severe outcomes in the offspring (Kapur et al., 2019; Ornoy et al., 2021).
From this section onwards, I will describe the effects of hyperglycemia, hyperinsulinemia and PGD exclusively on the preimplantation period.

1.4.2.1 The preimplantation embryo in a diabetic context: evidence from animal models

As detailed in Chapter 2, different animal models have been developed to study the effect of a maternal diabetic environment on the offspring. Likewise, to evaluate the preimplantation period, several of these models have been frequently used, especially those of induced- or spontaneously-developed diabetes (Jawerbaum & White, 2010). On the other hand, there is also the possibility of studying the effects of a diabetic context *in vitro.*

It is clear that both *in vivo* and *in vitro* strategies have advantages and limitations. *In vivo* strategies may represent a context closer to human pathophysiology. However, one cannot easily decorticate insult-specific effects. For example, in overt diabetes, not only hyperglycemia and/or hyperinsulinemia may be at the origin of adverse outcomes in the offspring, but so may be the presence of elevated ketones, triglycerides and free fatty acids, ROS, and proinflammatory cytokines (Fraser et al., 2007). *In vitro* models allow the analysis of each potential insult separately, such as hyperglycemia and/or hyperinsulinemia, and thus identify insult-specific effects. Moreover, most *in vivo* studies have addressed the whole periconceptional period, and therefore the impact on the oocyte and preimplantation embryos cannot be independently evaluated. Using *in vitro* strategies, one can better control the developmental stage to be examined (i.e., periconceptional versus preimplantation exposure, or before or after EGA), the duration, and the degree of the exposure. Nevertheless, both strategies are complementary and provide

useful evidence on possible mechanisms established in early embryos, mechanisms that could contribute to the developmental programming of the offspring in a diabetic intrauterine environment.

1.4.2.1.1 *In vivo* studies: induced and spontaneous animal model of diabetes

Depending on the model used and the severity of the diabetic context, either mild or severe, variation in the intrauterine diabetic context may be present. Diabetes-induced models (i.e., STZ or alloxan-induced) are overall hyperglycemic with plasma glucose concentrations between 18-30 mM, and hypoinsulinemic (Fischer et al., 2017; Ramin et al., 2010). However, these models require exogenous insulin administration to avoid the death of the animal by ketoacidosis (Fischer et al., 2017; Jawerbaum & White, 2010). Thus, the influence of hyperglycemia and insulin oscillating levels should be considered when interpreting the results. Similarly, the contribution of superovulation strategies that may influence embryonic development cannot be excluded.
Despite this variation, a few common perturbations have been described. These include developmental delay, apoptosis, metabolic dysfunctions, altered cell signaling, and metabolic stress (Fischer et al., 2017). It should be noted that the *in vivo* studies described here cover the periconceptional period (i.e., oocyte maturation, fertilization, and preimplantation development) and not exclusively the preimplantation period.

Maternal diabetes *in utero* leads to embryonic developmental delay, as shown in the offspring of rabbit-induced diabetes or the NOD mouse model (Jungheim & Moley, 2008; Ramin et al., 2010). Several metabolic perturbations have been described in preimplantation embryos from diabetic-induced animal models (Fischer et al., 2017; Gürke et al., 2016; Ramin et al., 2010). Blastocysts from diabetes-induced rabbits exhibited drastic reduced mRNA and protein levels of the IR, IGF-IR, and key glycolysis and gluconeogenesis enzymes such as hexokinase (HK) and PEPCK, respectively (Ramin et al., 2010). These results suggest reduced insulin sensitivity and insulin-stimulated glucose metabolism in early embryos (Ramin et al., 2010). By using the same T1D-like model, it was shown that rabbit blastocysts had an extensive accumulation of lipid droplets in both the ICM and TE, together with gene expression changes in lipogenic genes such as fatty acid transport protein 4 (FATP4) and the transcription factor sterol-regulated element binding protein 1 (SREBP1) (Schindler et al., 2014). Analysis of fatty acid metabolism between the ICM and TE in this model demonstrated different adaptative responses to a maternal diabetic environment (Schindler, Dannenberger, et al., 2020). The ICM showed higher levels of saturated fatty acids and decreased polyunsaturated fatty acids. In contrast, the TE showed lower levels of saturated fatty acids and higher levels of oleic acid. These metabolic signatures were associated with gene expression changes in key enzymes for fatty acid metabolism (Schindler, Dannenberger, et al., 2020). Moreover, glucose uptake is similarly affected by the hyperglycemic environment. Decreased expression of GLUT1, GLUT2, and GLUT3 were identified in mouse embryos exposed *in utero* to STZ-induced diabetes (Jungheim & Moley, 2008)

In blastocysts from diabetes-induced rabbits, mTORC1 signaling was activated concomitantly with increased protein synthesis, especially in the TE (Gürke et al., 2016). Activation of mTORC1 was hypothesized to be triggered by the high leucine concentration in the uterine fluid (Gürke et al., 2016). Moreover, reduced autophagy was similarly observed in exposed blastocysts (Gürke et al., 2016). Interestingly, this study demonstrated lineage-specific in blastocysts exposed to a diabetic environment

(Gürke et al., 2016). Moreover, increased formation of AGE was detected in the blastocoel of embryos recovered from diabetic rabbits (Haucke et al., 2014)

Furthermore, increased apoptosis has also been described in embryos exposed to maternal diabetes. Embryos recovered from mice in which diabetes was induced by STZ exhibited increased expression of the pro-apoptotic gene *Bax* at the mRNA and protein level and increased caspase-dependent apoptosis in both the ICM and TE (Moley, Chi, Knudson, et al., 1998). Similarly, in d6 blastocyst collected from diabetes-induced rabbits, 4.3-fold increased apoptosis in the ICM was detected concomitant with a 40% reduced transcription of the anti-apoptotic gene BCL2L1 (Ramin et al., 2010). Impaired glucose uptake and reduced intracellular levels of glucose have been proposed to trigger apoptosis in embryos exposed to maternal diabetes (Jungheim & Moley, 2008)

Exposure during the periconceptional period to maternal diabetes is sufficient to alter the fetoplacental phenotype (Rousseau-Ralliard, Couturier-Tarrade, et al., 2019). In rabbits, the offspring exposed exclusively during the periconceptional period to maternal diabetes, later transferred to pseudo-pregnant normoglycemic recipients, showed an altered fetoplacental phenotype (Rousseau-Ralliard, Couturier-Tarrade, et al., 2019). Analysis of the offspring 28d after conception showed decreased fetal weight, reduced weight in several organs such as the heart and kidney, and decreased weight in the whole placenta, including maternal and fetal portions (Rousseau-Ralliard, Couturier-Tarrade, et al., 2019). On one side, the fetal offspring exhibited hyperglycemia and dyslipidemia, decreased cholesterol, and altered fatty acid profiles. On the other side, the placenta from diabetic fetuses showed altered gene expression related to nutrient supply (i.e., overexpression of GLUT1) and lipid metabolism (i.e., overexpression of FASN), and structural changes such as decreased volume density of fetal vessels (Rousseau-Ralliard, Couturier-Tarrade, et al., 2019).

Moreover, it has been suggested that not only the degree and duration of hyperglycemia exposure are involved in the toxic effects of glucose but also the oscillating levels of glucose in the oviductal and uterine fluid (Fraser et al., 2007). Indeed, short episodes of hyperglycemia in rats during early but not late pregnancy led to increased fetal and placental weight (Ericsson et al., 2007).

1.4.2.1.2 Hyperglycemia *in vitro* exposure

Investigation of the effects of hyperglycemia *in vitro* during the preimplantation stage has demonstrated perturbations at different levels, from increased apoptosis gene expression changes, impaired cell signaling, and energy metabolism to reduced developmental competence.

Apoptosis has been frequently reported on the mouse and bovine embryos exposed to hyperglycemia, especially in the ICM (Jiménez et al., 2003; Keim et al., 2001). Accordingly, reduced total cell numbers and reduced cell numbers in either ICM or TE have been described (Bermejo-Alvarez et al., 2012; Fraser et al., 2007; Jiménez et al., 2003; Leunda-Casi et al., 2001).
Evaluation of the toxic effects of hyperglycemia in the mouse showed that it is mediated by an increased flux in the HBP and, consequently, by O-GlNAcylation (Pantaleon et al., 2010).
Mouse 1-cell embryos exposed to either 27 mM glucose or 0.2 mM hexosamine until the blastocyst stage showed increased HBP flux, *O*-GlNAcylation, and increased apoptosis concomitant with reduced

proliferation (Pantaleon et al., 2010). Interestingly, inhibition of *O*-GlNAcylation almost completely reversed the effects of hyperglycemia, with the exception of the proapoptotic effect (Pantaleon et al., 2010).

Furthermore, hyperglycemia may impact developmental competence, as most studies report decreased blastocyst formation upon high glucose exposure (Cagnone et al., 2012; Jiménez et al., 2003; Pantaleon et al., 2010). In addition, gene expression changes upon hyperglycemia exposure have also been described in preimplantation embryos (Cagnone et al., 2012). Bovine zygotes up until 8- to 16-cell stage exposed to 5mM glucose showed transcriptome changes at the blastocyst stage related to hypoxia signaling pathway, transforming growth factor beta (TGF-β) signaling, tumor necrosis factor (TNF) signaling, peroxisome proliferator-activated receptor alpha (PPARα) signaling, glutathione metabolism and oxidative stress response (Cagnone et al., 2012). Thus, suggesting perturbations in cell signaling and metabolism (Cagnone et al., 2012). As shown *in vivo*, impaired insulin sensitivity and insulin-stimulated glucose metabolism may be similarly impacted by hyperglycemia. Exposure to 10 to 25 mM glucose for 3 to 6 hours in rabbit d6 blastocysts led to reduced expression of IR and IGF-IR and glycolysis and gluconeogenesis enzymes HK and PEPCK, respectively (Ramin et al., 2010). Moreover, hyperglycemia led to the intracellular accumulation of lipid droplets, in parallel to gene expression changes of key lipogenic markers such as fatty acid synthase (FASN), key in *de novo* fatty acid synthesis and SREBP1, which also showed higher accumulation in the nucleus (Schindler et al., 2014).

Sexual dimorphism has also been described *in vitro* studies of hyperglycemia in preimplantation development (Jiménez et al., 2003). Nevertheless, findings on this matter are controversial (Bermejo-Alvarez et al., 2012; Cagnone et al., 2012; Jiménez et al., 2003). In addition, some have suggested that glucose levels (~5 mM versus ~20 mM) may affect one sex differently than the other (Jiménez et al., 2003).

Interestingly, some studies have described lineage-specific responses from exposure to hyperglycemia. In mouse embryos exposed to 6 to 28 mM glucose, an altered cell allocation to the ICM without evidence of apoptosis and an increased growth capacity of TEs were detected (Fraser et al., 2007; Leunda-Casi et al., 2001). Indeed, hyperglycemia led to impaired TE differentiation, probably due to reduced expression of FGF-4 in the ICM, a repressor protein of TE differentiation to TGC, and an essential player in the PrE/EPI specification event, as described earlier in this chapter (Bassalert et al., 2018; Leunda-Casi et al., 2001).

1.4.2.1.3 Hyperinsulinemia *in vitro* exposure

As with hyperglycemia, the effects of *in vitro* hyperinsulinemia exposure have been examined in preimplantation embryos. The effects described include increased proliferation or apoptosis, altered cell signaling, and energy metabolism, reduced developmental competence, and, as demonstrated by embryo-transfer experiments, perturbation of growth trajectories.
Nevertheless, the broad range of insulin concentrations used in previous studies complicates the comparison of findings.

Both increased proliferation and apoptosis have been described in preimplantation embryos exposed to

insulin concentrations. In the mouse, exposure to 1.7 pM to over 170nM insulin from the 2-cell stage to the blastocyst stage resulted in increased blastocyst total cell numbers and increased proliferation in the ICM (H. G. Gardner & Kaye, 1991; Harvey & Kaye, 1990). Similarly, bovine embryos exposed to 1.7 µM insulin from 1-cell to blastocyst stage showed total and TE increased cell numbers (Augustin et al., 2003). Rabbit embryos exposed to a range of insulin concentrations (68 nM – 6.8 µM) also showed increased proliferation and reduced apoptosis (Herrler et al., 1998). Conversely, Chi and colleagues reported extensive apoptosis in the ICM of mouse blastocysts exposed to 6 nM or 700 nM insulin from the 2-cell to the blastocyst stage (M. M.-Y. Chi et al., 2000).
Previous studies have described an increased blastocyst formation upon insulin exposure (Augustin et al., 2003; Harvey & Kaye, 1990; Herrler et al., 1998; Shao et al., 2007).

Coherent with an increased proliferation, rabbit embryos exposed to 170 nM insulin exhibited increased MAPK pathway activity but not stimulation of GLUT4 translocation or glucose uptake, thus suggesting that in this species, insulin acts as a growth factor than as a mediator of glucose homeostasis (Navarrete Santos, Tonack, Kirstein, Pantaleon, et al., 2004). Furthermore, exposure to 170 nM insulin in mouse morula and blastocysts stimulated protein synthesis and endocytosis exclusively in the TE (Dunglison et al., 1995; Harvey & Kaye, 1988).

Interestingly, the follow-up of mouse embryos exposed to 0.17 µM insulin from 2-cell to the blastocyst stage and later transferred to pseudo-pregnant recipients showed a 4 to 6% increase in fetal growth (Kaye & Gardner, 1999). Similarly, transfer of 2-cell stage mouse embryos was exposed to 40 nM insulin until the blastocyst stage and showed increased fetal and birth weight, in addition to aberrant DNA methylation of *Igf2* and *H19* imprinted genes, two important regulators of fetal and placental growth (Shao et al., 2007)

OBJECTIVES OF THE THESIS

Thus far, little is known about the effects of high glucose and/or high insulin on the first-specified lineages during preimplantation development, the ICM and TE as described in Chapter 3 section 1.4.2 of the Introduction of this thesis. Previous studies, particularly in the context of high insulin exposure, remain sparse, often focusing solely on whole embryos or in either of the first-specified lineages. More global approaches are needed to assess the effects of high glucose and/or high insulin during preimplantation development with a focus on both lineages. In addition, to our knowledge, no previous studies have explored the effects of both high glucose and high insulin, a condition frequently observed in prediabetic states, on preimplantation development.

Hence, the main objective of my thesis was to **investigate whether exposure to high glucose and high insulin alone or in combination during preimplantation development may affect the ICM and TE of early embryos by using an omics approach.**
To better address this question, we choose to use the rabbit model because of their different similarities to human preimplantation development, as stated in the Chapter 3, section 1.1 of the Introduction of this thesis. Furthermore, to decorticate the effects of high glucose and high insulin alone or in combination, we choose to develop an *in vitro* model which allows to control the microenvironment of preimplantation development better. Consequently, by using a rabbit embryo *in vitro* model, the first specific objective of this thesis was **to investigate the effects of exposure to high glucose, high insulin and high glucose and high insulin *in vitro* during preimplantation development on the ICM and TE gene expression programs** to obtain a global picture of the potential responses of each lineage to this perturbed metabolic environment.
The analysis of the gene expression programs of exposed embryos revealed that high insulin led to slight changes in the ICM and TE and that high glucose alone or in combination with high insulin led to more drastic gene expression changes. In this latter, among the changes observed, we identified the altered expression of genes implicated in chromatin remodeling and epigenetic mechanisms, which suggested potential changes in the epigenetic landscape of the ICM and TE of exposed embryos. Therefore, to further assess this hypothesis, we next decided to analyze the chromatin accessibility of the ICM and TE of embryos exposed to high glucose alone or in combination with high insulin to obtain the genome-wide view of the epigenomic landscape of these two lineages in response to this perturbed metabolic environment.
To pursue this, the second specific objective of my thesis was **to establish an ATAC-seq protocol for profiling chromatin accessibility in the ICM and TE of *in vitro*-developed embryos.** After the successful generation of ICM and TE ATAC-seq libraries from rabbit *in vitro*-developed embryos, the third and last objective of my thesis was **to investigate the effects of the exposure to high glucose alone or in combination with high insulin during *in vitro* preimplantation development on the ICM and TE chromatin accessibility genome-wide.**

To better present my thesis work, I have organized the following pages into **Part I** and **Part II** sections.
Part I will describe the development of the first specific objective related to the analysis of the gene expression programs of the ICM and TE after exposure to high glucose and/or high insulin. This part of my thesis work has resulted in the writing and publishing of a manuscript in the Journal *Cells* in

November 2022. In addition, I have included additional results that reflect the choice of the immunosurgery technique used in the subsequent analysis included in our published manuscript.

The **Part II** section will be consecrated to the development of the second and third specific objectives of my thesis. This section begins with a brief introduction and justification of this second part, followed by the description of a slightly-modified ATAC-seq protocol more suitable for our model and the generation and preliminary analysis of ICM and TE ATAC-seq libraries from embryos exposed to high glucose alone or in combination with high insulin. Because these results have not been published yet, the **Part II** section will end by a discussion and conclusion section.

Finally, the main results from **Part I** and **II** will be discussed in the General discussion section, followed by the conclusions and perspectives of this thesis.

MATERIAL AND METHODS

Only the materials and methods that are not present in the paper will be detailed here.

1. Immunostaining

Briefly, the zona pellucida was removed by pronase treatment, and blastocysts were permeabilized with Triton X-100, as described in the paper (Part I). Blastocysts were then incubated in blocking solution 2% BSA diluted in PBS for 45 min at RT. Embryos were then incubated with SOX2 (1:100 or 1:200, ABCAM) primary antibodies diluted in 2% BSA at 4°C overnight. Embryos were then rinsed three times in PBS with 0.5% polyvinylpyrrolidone (PVP) and incubated with secondary antibodies (1:200) anti-rabbit IgG Cy3 (Jackson ImmunoResearch) diluted in 2% BSA in PBS for 1 h at RT protected from light. Embryos were then rinsed three times in PBS with 0.5% PVP for 5 min. Embryos were mounted in Vectashield (Vector Laboratories) with 0.3 mg/mg DAPI (Invitrogen) for DNA counterstaining. For the SOX2-TUNEL assay, TUNEL was performed as described in the paper (Part I), followed by SOX2 immunostaining. Fluorescence microscopy and image analysis was performed as described in the paper (Part I).

2. Culture of mESCs and preparation for ATAC-seq

CD1 lines derived from ICM were cultured in Chemically Defined Medium (CDM) and supplemented with 0.7 µM PD0325901 (AxonMedCHem), 2.5 µM CHIR99201 (AxonMedChem), and 700 U/ml LIF (Cell Guidance Systems) medium referred to as "2i/LIF" at 37 °C, 5% CO_2 as previously described (Tosolini & Jouneau, 2015). Cells were sub-cultured every 3 days at 1:6 split ratio using 0.25% trypsin (1x) (Invitrogen). For ATAC-seq library preparation 50,000; 5000; 1000 and 500 cells were centrifuged at 500 rcf for 5 min. Cell pellets were washed once with 1 ml cold DPBS (Gibco) without Ca^{2+} or Mg^{2+}, and were centrifuged at 4 °C, 500 rcf for 5 min. The supernatant was carefully aspirated, and cell pellets were then resuspended in 1 ml cold ATAC-seq cell lysis buffer from Buenrostro et al., 2015, and centrifuged at 4 °C, 500 rcf for 10 min.

2. Preparation of ICM and TE for ATAC-seq

Two batches of ATAC-seq libraries were generated. The first batch consisted of ICM and TE ATAC-seq libraries in which the ATAC-seq protocol was tested a first time and will be referred to as "TEST" ATAC-seq libraries from hereon. These libraries were generated from 1-cell rabbit embryos developed *in vitro,* as detailed in the paper (Part I), with a few differences. Embryos were cultured *in vitro* in M199 medium and 20 0_2%, as there were donated from an ongoing project of the team. The second batch consisted of ICM and TE ATAC-seq libraries from rabbit embryos exposed to control (CNTRL), high glucose (HG), or high glucose and high insulin (HGI), as detailed in the paper (Part I).

For ICMs from TEST ATAC-seq libraries, dissociation tests were performed as follows: ICMs were transferred to a 40 µl drop of pre-heated 0.25% trypsin (1x) (Invitrogen) for 1 min or 1 min 30 s, or with TrypLE (1x) (Gibco) for 3 min 30 s on a warming plate while pipetting vigorously using a 50-60 µm glass capillary. Trypsin was then inactivated by transferring the group of isolated cells into a 50-60 µl drop of DPBS - 10% SVF. For ICM of exposed embryos ATAC-seq libraries, ICMs were transferred to a 40 µl drop of pre-heated 0.25% trypsin (1x) for 1 min 30 s on a warming plate while pipetting vigorously using a

50-60 µm glass capillary. Trypsin was then inactivated by transferring the group of isolated cells into a 50-60 µl drop of DPBS - 10% SVF. Immediately after, the 90-100 µl containing dissociated ICM cells were transferred to 1 ml cold DPBS, and were centrifuged at 4 °C, 500 rcf for 5 min. The supernatant was carefully aspirated, and cell pellets were then resuspended in 1 ml cold ATAC-seq cell lysis buffer and centrifuged at 4 °C, 500 rcf for 10 min. The supernatant was carefully aspirated to isolate nuclear pellets. Nuclear pellets were kept on ice. For the TE preparation, immediately after immunosurgery, TEs were transferred to 1 ml cold DPBS and centrifuged at 4 °C, 500 rcf for 5 min. The supernatant was carefully aspirated and cell pellets were then resuspended in 1 ml cold ATAC-seq cell lysis buffer and centrifuged at 4 °C, 500 rcf for 10 min. The supernatant was carefully aspirated to isolate nuclear pellets. Nuclear pellets were kept on ice.

3. ATAC-seq library construction for mESCs, ICM and TE

Nuclear pellets were resuspended in 50 µl transposition reaction mixture (25 µl TD buffer (Nextera DNA Library Prep Kit, Illumina), 2.5 µl TDE1 enzyme (Nextera DNA Library Prep Kit, Illumina), 22.5 µl nuclease free H_2O) and incubated for 60 min at 37 °C with shaking at 300 rpm. Transposed DNA was purified with MinElute PCR Purification Kit (Qiagen) and eluted in 10 µl buffer EB two times by repeating the elution step with the same volume. Libraries were PCR amplified in 50 µl reaction mixture: 25 µl SsoFast Evagreen supermix with low ROX (Bio-Rad, Hercules, CA), 1.25 µl 25 µM custom Nextera PCR primer 1 (i5), 1.25 µl 25 µM custom Nextera PCR barcoded primer 2 (i7) (demultiplexing by barcoded primers, dual-indexing strategy (Appendix 1), 12.5 µl nuclease free H_2O, 10 µl eluted DNA. PCR cycling conditions were as followed: 72 °C for 5 min, 98 °C for 30 s, followed by 12 cycles, 98 °C for 10 s, 63 °C for 30 s and 72 °C for 1 min. PCR-amplified libraries were again purified with the MinElute PCR Purification Kit (Qiagen) following the manufacturer's recommendations and eluted in 10 µl buffer EB two times by repeating the elution step with the same volume. Quality control of libraries (nucleosome laddering profiles) and DNA concentration were assessed with the Bioanalyzer 2100 DNA High Sensitivity chip (Agilent Technologies).
Once all libraries were generated, depending on the nucleosome laddering profiles and concentration, a final equimolar pool of 18 libraries was generated. To focus on open chromatin regions, the library pool was size-selected to keep 150-250 bp fragments corresponding of accessible DNA fragments. Size selection was performed by bead purification using a single-left sided bead purification strategy with Agencourt AMPure XP beads (Beckman Coulter) to eliminate primer dimers. Quality of the library pool was assessed again with the Bioanalyzer 2100 DNA High Sensitivity chip (Agilent Technologies). Libraries were then quantified by Qubit 2.0 with the dsDNA High Sensitivity Assay Kit (ThermoFisher Scientific).

3.1 Verification of ATAC-seq lysis buffer and transposition on mESCs

To verify the efficiency of the ATAC-seq lysis buffer prepared in-house, double staining with Hoechst 33342 1: 2000 (Invitrogen) and propidium iodide (PI) (1 mg/ml) 1:1000 was performed to assess cell viability. Hoechst is a fluorescent dye that preferentially binds adenine-thymine (A-T)-rich sequences of the minor grove of DNA and is cell-permeable. PI is a fluorescent dye that binds DNA by intercalating between bases and is not cell membrane-permeable, useful to detect dead cells. Two microtubes containing ~50, 000 cells were washed in 1 ml DPBS and centrifuged at 4 °C, 500 rcf for 5 min. The supernatant was carefully aspirated and 1 ml of fresh cold ATAC-seq lysis buffer or cold DPBS (negative control) was added into each microtube, respectively. Microtubes were then centrifuged at 4 °C, 500 rcf

for 10 min. The supernatant was carefully aspirated, pellets were then resuspended in 25 µl of DPBS and transferred to different wells in a 10-wells staining dish. To perform a double Hoechst/PI staining, 2 µl of Hoechst 1: 2000 and 1 µl of PI 1:1000 were diluted in 2 ml. In each well, 25µl of the Hoechst/PI mixture was added and incubated for 30 min protected from light at room temperature. Forty microliters of each well were mounted on slides, covered with a glass coverslip and observed in a fluorescence inverted Olympus IX71 microscope.
To verify the transposition, ~50, 000 cells were washed in 1 ml DPBS and centrifuged at 4 °C, 500 rcf for 5 min. The supernatant was carefully aspirated and 1 ml of fresh cold ATAC-seq lysis buffer was added and centrifuged at 4 °C, 500 rcf for 10 min. Nuclear pellets then were resuspended in the 50 µl transposition reaction mixture as previously detailed, or in 50 µl reaction mixture with 2.5 µl nuclease-free H_2O instead of 2.5 µl TDE1 enzyme (Nextera DNA Library Prep Kit, Illumina), and were incubated for 60 min at 37 °C with shaking at 300 rpm. Transposed DNA was purified with Wizard SV PCR Clean-Up System (Promega) an eluted in 15 µl nuclease-free H_2O following the manufacturer's recommendations. Libraries were PCR amplified in 50 µl reaction mixture as previously described with a slight modification. Sixteen PCR cycles were performed instead of 12, and a blank PCR with nuclease-free H_2O instead of DNA template was included. PCR-amplified libraries were next loaded in 2% agarose together with the HypperLadder of 50 – 2000 bp (Meridian Bioscience).

4. Sequencing, read alignment and peak calling of ICM and TE ATAC-seq libraries

Sequencing of ICM and TE ATAC-seq TEST libraries were performed in two steps: first, 1 M reads were sequenced on MiSeq Nano platform to generate 75 bp paired-end reads and assess the quality of the ATAC-seq libraries. Next, because control quality of ATAC-seq datasets were acceptable, we proceeded to sequencing on the NextSeq platform to generate 400 M of 75 bp paired-end reads of the pool, and 81 M mean sequenced reads per library.
Sequencing of ICM and TE ATAC-seq libraries from *in vitro*-exposed embryos to CNTRL, HG or HGI was performed on the NextSeq 2000 platform to generate 60 bp paired-end reads. All sequencing was performed by M. Monot, L. Lemée, Biomics Platform, C2RT, Institut Pasteur, Paris, France.

Bioinformatic analysis was performed on Unix/Linux operating system. Main steps of the ATAC-seq bioinformatic analysis pipeline is detailed in Appendix 2. In brief, raw sequencing reads were trimmed with Trim Galore (v0.6.5) and Cutadapt (v2.10) (M. Martin, 2011) to remove adapters and low quality ($q < 20$) ends, keeping unpaired reads and reads 10 or longer. Trimmed reads were aligned to the rabbit reference genome (Ensembl Oryctolagus cuniculus.OryCun2.0.104) with Burrow-Wheeler Aligner (BWA) tool (v0.7.17) (H. Li & Durbin, 2009) and indexed with SAMtools (v1.12) (H. Li et al., 2009).
PCR duplicates were removed with PicardTools (v2.20.7) (http://broadinstitute.github.io/picard/). Mitochondrial and low-quality alignments ($q<5$) were removed with SAMtools. Aligned reads were converted to bigWig files using bam-Coverage from DeepTools (v3.3.1) (Ramírez et al., 2016) with bins default values (50 bp) and normalized signal per Reads Per Kilobase Million (RPKM) for TEST ICM and TE ATAC-seq libraries, and Reads Per Million Reads (RPM) for ICM and TE libraries from exposed embryo. Bigwig files were loaded on the UCSC genome browser for track visualization and were used to generate multiBigWigSummary with DeepTools with bin size of 500 bp for library comparison.

MultiBigWigSummary was used to plot PCA and calculate the Pearson correlation coefficient between libraries with the deepTools functions plotPCA (options: --transpose, --log2, ntop 100000) and

plotCorrelation (options: --skipZeros and –removeOutliers). Plot of average signal on TSS and TES genomic regions was generated with deepTools plotProfile function by computeMatrix scale-regions generation (options: --beforeRegionStartLength 2000 --regionBodyLength 3000 --afterRegionStartLength 2000). Plot of fragment size distribution for each library were generated with bamPEFfragmentSize function from deepTools. Peaks were called with MACS2 (Feng et al., 2012) (v2.1.0) using the following parameters --nomodel, --shift -100 --extsize 200 and narrow peak cutoff of q <0.05. Differential chromatin accessibility regions (DARs) were identified with DESeq2 (Love et al., 2014) (v1.36.0) R package with adjusted p value < 0.01 and log2 fold change > 1. Variance stabilizing transformation (VST) was used to normalize raw signal in peaks for visualization. Heatmaps were generated with pheatmaps (v1.0.12) R package from z-scores generated from VST normalization. Among DARs, peaks ≥ 2000 bp from TSS were categorized as putative enhancers and peaks ≤ 2000 bp from TSS were categorized as putative promoters. Gene Ontology Biological Process of annotated genes within DARs was obtained with DAVID (D. W. Huang et al., 2009) (v2021). Motif enrichment analysis was performed with HOMER (v4.10.4) using findMotifsGenome.pl analysis with the following options: -size given – mask. Top "known motifs" output was used.

PART I: PAPER

Exposure to glucose and insulin during the preimplantation period in the rabbit: characterization of ICM and TE responses*

Romina Via y Rada, Nathalie Daniel, Catherine Archilla, Anne Aubert-Frambourg, Luc Jouneau, Yan Jaszczyszyn, Gilles Charpigny, Véronique Duranthon, Sophie Calderari

This article has been published in the **Journal *Cells*** (ISSN 2073-4409 - MDPI), ***Cells* 2022, *11*(23), 3766; https://doi.org/10.3390/cells11233766** in the section **Reproductive Cells and Development**, special issue: **Molecular and Clinical Advances in Understanding Early Embryo Development** (https://www.mdpi.com/journal/cells/special_issues/Embryo-Development).

*The differentially expressed genes (DEGs) identified in this study can be found in Appendices 3-8 of this manuscript.

cells

MDPI

Article

Identification of the Inner Cell Mass and the Trophectoderm Responses after an In Vitro Exposure to Glucose and Insulin during the Preimplantation Period in the Rabbit Embryo

Romina Via y Rada [1,2], Nathalie Daniel [1,2], Catherine Archilla [1,2], Anne Frambourg [1,2], Luc Jouneau [1,2], Yan Jaszczyszyn [3], Gilles Charpigny [1,2], Véronique Duranthon [1,2] and Sophie Calderari [1,2,*]

1 BREED INRAE, UVSQ, Université Paris-Saclay, 78350 Jouy-en-Josas, France
2 Ecole Nationale Vétérinaire d'Alfort, BREED, 94700 Maisons-Alfort, France
3 Institute for Integrative Biology of the Cell (I2BC), UMR 9198 CNRS, CEA, Paris-Sud University F, 91190 Gif-sur-Yvette, France
* Correspondence: sophie.calderari@inrae.fr

Abstract: The prevalence of metabolic diseases is increasing, leading to more women entering pregnancy with alterations in the glucose-insulin axis. The aim of this work was to investigate the effect of a hyperglycemic and/or hyperinsulinemic environment on the development of the preimplantation embryo. In rabbit embryos developed in vitro in the presence of high insulin (HI), high glucose (HG), or both (HGI), we determined the transcriptomes of the inner cell mass (ICM) and the trophectoderm (TE). HI induced 10 differentially expressed genes (DEG) in ICM and 1 in TE. HG ICM exhibited 41 DEGs involved in oxidative phosphorylation (OXPHOS) and cell number regulation. In HG ICM, proliferation was decreased ($p < 0.01$) and apoptosis increased ($p < 0.001$). HG TE displayed 132 DEG linked to mTOR signaling and regulation of cell number. In HG TE, proliferation was increased ($p < 0.001$) and apoptosis decreased ($p < 0.001$). HGI ICM presented 39 DEG involved in OXPHOS and no differences in proliferation and apoptosis. HGI TE showed 16 DEG linked to OXPHOS and cell number regulation and exhibited increased proliferation ($p < 0.001$). Exposure to HG and HGI during preimplantation development results in common and specific ICM and TE responses that could compromise the development of the future individual and placenta.

Keywords: preimplantation embryo; diabetes; DOHaD; rabbit

Citation: Via y Rada, R.; Daniel, N.; Archilla, C.; Frambourg, A.; Jouneau, L.; Jaszczyszyn, Y.; Charpigny, G.; Duranthon, V.; Calderari, S. Identification of the Inner Cell Mass and the Trophectoderm Responses after an In Vitro Exposure to Glucose and Insulin during the Preimplantation Period in the Rabbit Embryo. *Cells* **2022**, *11*, 3766. https://doi.org/10.3390/cells11233766

Academic Editor: Lon J. van Winkle

Received: 5 October 2022
Accepted: 18 November 2022
Published: 25 November 2022

1. Introduction

The worldwide prevalence of metabolic diseases such as diabetes is increasing at an alarming rate [1]. In 2021, the International Diabetes Federation estimated that 1 in 10 adults live with diabetes [1]. Type 2 diabetes (T2D) is a chronic metabolic disease characterized by hyperglycemia, insulin resistance, and/or impaired insulin secretion and accounts for 90% of diabetes cases [1]. In prediabetes and the early stages of T2D, impaired glucose tolerance, or hyperglycemia, is accompanied by compensatory hyperinsulinemia due to decreasing insulin sensitivity [1,2]. Unfortunately, these first signs of metabolic dysregulation are often asymptomatic, resulting in nearly half of T2D patients going undiagnosed and untreated [1]. Known before as adult-onset diabetes, the prevalence of T2D is increasing in younger people, including women of childbearing age [1,3]. Type 1 diabetes (T1D), an immune-related disease characterized by the destruction of insulin-producing cells, affects a young population [4]. In T1D, the glucose-insulin axis is disrupted. Insulin is no longer produced, and insulin-stimulated glucose uptake is reduced, resulting in persistent hyperglycemia [4]. One in six pregnancies is estimated to be affected by hyperglycemia [1]. Exposure in utero to a perturbed glucose-insulin homeostasis increases the risk of birth defects and metabolic deregulations such as enhanced growth, higher fasting glucose,

and lower insulin sensitivity in the offspring [5]. These metabolic dysregulations can be maintained throughout the life course of the individual, making it prone to developing cardiometabolic diseases such as obesity and T2D [3]. This is described by the Developmental Origins of Health and Disease (DOHaD) concept, which highlights that exposure to a suboptimal environment during critical periods of development predisposes the offspring to poor health later in life [6]. One key period of development sensitive to environmental insults is the preimplantation stage [7]. During the preimplantation stage, embryos undergo tightly regulated essential events such as the maternal-to-zygotic transition with the transcriptional activation of the embryonic genome (EGA) and the first lineage specification giving rise to the inner cell mass (ICM), the progenitor of the embryo proper, and the trophectoderm (TE), the progenitor of the embryonic portion of the placenta [8]. To sustain their development, embryos take advantage of the nutrients and growth factors present in the oviduct and uterine fluid [9,10]. The composition of these fluids varies according to maternal metabolic and hormonal status, as is the case for glucose and insulin, whose concentrations depend on maternal circulating plasma concentrations [9–11]. Preimplantation embryos are sensitive to perturbations in their surrounding microenvironment [7,8,11]. Variations in the environment of the early embryo, even restricted to the preimplantation period, result in irreversible defects in the adult offspring [12]. Studies in vivo and in vitro have demonstrated the susceptibility of preimplantation embryos to changes in glucose or insulin levels [13]. In diabetes-induced rabbit and mouse models, preimplantation embryos exposed to hyperglycemia resulted in perturbed insulin-mediated glucose metabolism, decreased glucose transport and utilization, reduced developmental competence and cell numbers, and increased apoptosis in the ICM [14–16]. In in vivo animal models, severe hyperglycemia was obtained by the chemical destruction of pancreatic β-cells, thus mimicking type 1 diabetes. Nevertheless, because insulin secretion was reduced or absent in these animals, frequent insulin injections were needed, which may have resulted in oscillating insulin levels in the intrauterine environment [15]. Unfortunately, insulin levels were not quantified in these studies; thus, it is impossible to identify whether the phenotypes described were the result of hyperglycemia or the combination of hyperglycemia and insulin. In vitro, exposure to high glucose alone led to impaired blastocyst development, reduced total cell numbers, decreased glycolytic activity, decreased insulin sensitivity, perturbed TE differentiation, and impaired capacity of trophoblast outgrowth in vitro—a marker of implantation potential [11,14,17]. Preimplantation embryos are exposed to insulin, which is present in the oviductal and uterine fluids at concentrations that depend on maternal insulin levels [14]. The extent of the cellular and molecular responses to insulin in early embryos has been less investigated [13]. Glucose and insulin, through the activation of signaling and metabolic pathways, are closely related [18]. In preimplantation embryos, glucose is used as an energy source, reaching the highest consumption rate at the blastocyst stage [19,20]. Furthermore, insulin receptors and insulin-responsive glucose transporters are expressed in mouse, rabbit, and human preimplantation embryos [21].

We hypothesized that the deregulation of glucose and insulin homeostasis present in an increasing number of women impacts the preimplantation embryo. Functionally different from the blastocyst stage, ICM and TE differ in their epigenetic, transcriptomic, and metabolic programs [20,22,23]. We hypothesized that exposure to this glucose-insulin altered environment affects ICM and TE differently and induces short- and long-term consequences not only in the future individual but also in the future placenta, a central element for fetal nutrition regulation, and whose structure and/or function adapt to suboptimal in utero environments [15,24,25]. Hence, to investigate the effects of high glucose and/or high insulin on preimplantation development, we used the rabbit model, a model with preimplantation development (i.e., EGA timing, gastrulation morphology), glucose metabolism at early stages, and a placental structure close to that of humans [26]. We established a model of one-cell stage rabbit embryos developed in vitro until the blastocyst stage with supplementation of glucose, insulin, or both to recreate a moderately

hyperglycemic and/or hyperinsulinemic environment [11,14,17,27] and addressed the specific gene expression responses of the ICM and TE.

2. Materials and Methods

2.1. Embryo In-Vitro Development

New Zealand White female rabbits (INRA line 1077) were superovulated as previously described [28] and mated with New Zealand White male rabbits. At 19 h post-coïtum (hpc), does were euthanized, and one-cell embryos were recovered from oviducts by flushing with phosphate buffer saline (PBS, Gibco, Thermo Fisher Scientific, Waltham, MA, USA). One-cell embryos were sorted in M199 HEPES (Sigma-Aldrich, Saint-Louis, MO, USA) supplemented with 10% fetal bovine serum (FBS, Gibco) and rinsed in Global medium (LifeGlobal Group, Guilford, CT, USA) supplemented with 10% human serum albumin (HSA, LifeGlobal Group). Embryos were then placed in 10 µL microdrops of Global-10% HSA medium supplemented with either glucose (Sigma-Aldrich G6152) and/or insulin (Sigma-Aldrich I9278) and covered with mineral oil (Sigma-Aldrich M8410) for a 72h culture at 38 °C, 5% CO_2, and 5% O_2 until the blastocyst stage. Four experimental groups were designed: Control (CNTRL): 0.18 mM of glucose without insulin; high insulin (HI): 0.18 mM of glucose and 1.7 µM of insulin; high glucose (HG): 15 mM of glucose without insulin; and high glucose and high insulin (HGI): 15 mM of glucose and 1.7 µM of insulin. After 72 h of culture, to determine the embryo's developmental competence in each group, embryos were classified into three categories: (i) arrested embryos; (ii) compacted embryos; (iii) blastocysts or cavitated embryos. The rate of arrested embryos (developmental arrest), compacted embryos, and blastocysts/cavitated embryos reported in percentage was calculated in fifteen to twenty-nine independent experiments from the total of one-cell embryos placed in culture. Blastocysts were recovered to proceed to ICM and TE isolation by moderate immunosurgery. To remove the zona pellucida, blastocysts were incubated for 1–3 min in 5 mg/mL Pronase (P5147, Sigma-Aldrich). Embryos were next incubated in anti-rabbit goat serum (R5131 Sigma-Aldrich) for 90 min at 37 °C and then incubated in guinea pig complement (S1639 Sigma-Aldrich) for 20 sec. The ICM was mechanically isolated from the TE by pipetting with a small-bore glass pipette (60–70-µm diameter). To clean the ICM to limit any contamination, several back and forth injections into the glass pipette were perfomed. ICM and their corresponding TE were then immediately stored at −80 °C for RNA sequencing analysis or fixed for microscopic analyses.

2.2. RNA Sequencing

ICM and their corresponding TE originating from the same blastocysts were used. Only one biological replicate from the HI group did not include the corresponding TE due to low total RNA quality. Total RNA was extracted from three biological replicates per culture condition, corresponding to pooled samples (n = 11–16 ICM or TE per replicate) using the Arcturus PicoPure RNA Isolation Kit (Applied Biosystems Life Technologies, Waltham, MA, USA). RNA quality was assessed using RNA 6000 Pico chips with an Agilent 2100 Bioanalyzer (Agilent Technologies, Santa Clara, CA, USA). All extracted samples had an RNA Integrity Number (RIN) $\geq$ 8 value. Seven hundred and fifty pictograms of total RNA were used for amplification using the SMART-Seq V4 ultra-low input RNA kit (Clontech, Takara, Saint-Germain-en-Laye, France) according to the manufacturer's recommendations with nine PCR cycles for cDNA pre-amplification. The cDNA quality was assessed with the Agilent Bioanalyzer 2100. Libraries were prepared as previously described [29]. Reads were mapped to the rabbit transcriptome reference (Ensembl 98 Oryctolagus cuniculus 2.0) using the splice junction mapper TopHat (v2.1.1) associated with the short-read aligner Bowtie2 (v2.3.4.1). To generate the gene count table, featureCounts (v1.6.0) was used. Hierarchical clustering was computed as previously described [29]. Data normalization and single-gene level analysis of the differential expression were performed using the DESeq2 package (v1.28.1) [30]. Differences were considered significant for adjusted p=values (Benjamini-Hochberg) < 0.05 and when the normalized expression counts

were more than 20 in two of the three biological replicates. Heatmaps were generated with the pheatmaps R package (v1.0.12), with the z-score calculation of the normalized expression counts obtained with DESeq2. Logarithm 2 Fold Change (Log2FC) of differentially expressed genes (DEG) was used to generate horizontal bar plots with R studio software (v1.2.5019). InteractiVenn [31] software was used for Venn diagram generation. Functional annotation of DEG with their associated Gene ontology (GO) Biological Process (BP) terms was performed using DAVID [32] (v6.8). Gene Set Enrichment Analysis (GSEA) [33] was performed using the GSEA Java Desktop application (v4.0.3) from the Broad Institute. Enrichment analysis was calculated using the normalized expression counts obtained with DESesq2 and the Molecular Signature Database (MSigDB, v7.0) gene set collections (Hallmarks [34], KEGG (Kyoto Encyclopedia of Genes and Genomes), Reactome [35], and GO BP [36,37]) by gene-set permutation. Gene sets were considered significant when the false discovery rate (FDR) was less than 0.05. Enrichment analysis results were analyzed with the R package SUMER [38] (v1.1.5) for the reduction of redundancy and condensation of gene sets. For cluster visualization, the clusterMaker2 [39] plugin from Cytoscape [40] (v3.8.2) was used.

2.3. Quantification of Total Cell Number in Whole Embryos

To quantify the total cell number in whole embryos, DAPI staining was assessed in in vitro-developed blastocysts. Blastocysts were recovered from in vitro culture, and the zona pellucida was removed as detailed above. Blastocysts were fixed in 4% paraformaldehyde (PFA, EMS) in PBS at room temperature (RT) for 20 min. Permeabilization was performed with 0.5% Triton X-100 (Sigma-Aldrich) in PBS with 0.5% polyvinylpyrrolidone (PVP) for 1 h at 37 °C in a humidified chamber. DNA was counterstained with 0.2 mg/mL DAPI (Invitrogen) in PBS for 15 min at RT. Blastocysts were analyzed by an inverted ZEISS AxioObserver Z1 microscope (Zeiss, Rueil Malmaison, France) equipped with an ApoTome slider (Axiovision software 4.8) using a 20X objective and a z-distance of 1.5 µm between optical sections at the MIMA2 platform (https://doi.org/10.15454/1.5572348210007727E12, accessed on 4 October 2022). The total number of DAPI-labeled nuclei was quantified manually using ImageJ software (1.53.j). Each condition was analyzed in five to nine independent experiments.

2.4. Quantification of Apoptotic and Proliferating Cells in ICM and TE

To quantify apoptotic and proliferating cells in ICM and TE, we first considered distinguishing the ICM and TE on whole embryos by immunostaining of known lineage-specific markers. CDX2 (CDX-2-88, Biogenex, Fremont, CA, USA), SOX2 (ab97959, Abcam, Cambridge, UK), and NANOG (14-5761-80, Invitrogen, Thermo Fisher Scientific, Waltham, MA, USA) antibodies were tested, but none showed sufficient specificity to consider differential counting (data not shown). Thus, determination of apoptotic and proliferating cell numbers was performed on isolated ICM and TE.

Detection of apoptotic cells was performed using the DeadEnd Fluorometric TUNEL System (Promega, Madison, WI, USA) in two to six independent experiments. Isolated ICM or TE were fixed in 4% PFA in PBS at RT for 20 min. Permeabilization was performed with 0.5% Triton X-100 in PBS with 0.5% PVP for 1 h at 37 °C in a humidified chamber. After rinsing in PBS with 0.5% PVP, a second fixation was performed in 4% PFA and 0.2% glutaraldehyde for 15 min at RT. As a positive control, ICM and TE were treated with 2 units of RQ1 RNase-free DNase (Promega) for 30 min. The TUNEL reaction was performed according to the manufacturer's directions. DNA was counterstained with 0.2 mg/mL DAPI in PBS for 15 min at RT.

Detection of proliferating cells was performed using the Click-iT® Edu Imaging Kit (Fisher Scientific, Waltham, MA, USA) in at least three independent experiments. Briefly, the zona pellucida was removed as detailed above, and then blastocysts were incubated with 10 µM EdU for 15 min at 38 °C, 5% CO_2, and 5% O_2. ICM and TE separation were performed by moderate immunosurgery. ICM and TE were fixed with 4% PFA at RT

for 20 min. EdU detection was performed according to the instructions provided by the manufacturer. DNA was counterstained with 0.2 mg/mL DAPI in PBS for 15 min at RT.

ICM and TE were analyzed by an inverted ZEISS AxioObserver Z1 microscope equipped with an ApoTome slider using a 20X objective and a z-distance of 1.5 µm between optical sections at the MIMA2 platform. The number of DAPI-labeled nuclei, TUNEL-positive nuclei, and EdU-positive nuclei were quantified manually using ImageJ software.

2.5. Statistical Analysis

Statistical analysis was carried out using the generalized linear mixed-effects model (GLMM) with the glmer function and the lme4 R package (v1.1-28). The total cell number was analyzed using the linear mixed-effects model (LMM) using the lmer function. The glucose and insulin concentrations were considered as fixed effects. No significant interaction between glucose and insulin was detected. The models applied in the analysis of developmental competence and total cell number did not include the interaction of glucose and insulin. The in vitro culture experiments and rabbits were considered to have random effects. Estimated marginal means (emmeans, also known as least-squares means) and post-hoc tests between conditions were performed using the emmeans R package (v1.7.3) with the emmeans and pairs functions. Results are shown as emmeans with standard errors. Differences were considered significant when p-values were < 0.05.

3. Results

To determine the effect of high glucose and/or high insulin during preimplantation development, one-cell rabbit embryos were cultured in vitro under control (CNTRL), high insulin (HI), high glucose (HG), or high glucose and high insulin (HGI) until the blastocyst stage (Figure 1). To evaluate the effect of these conditions on developmental competence, the mean percentage of arrested embryos, compacted morula, or expanded blastocysts at the end of the 72 h culture period was determined (Table 1). On blastocysts, ICM and their corresponding TE were separated by moderate immunosurgery (Figure 1), and specific transcriptomic responses to high glucose and/or high insulin were explored by RNA-sequencing. RNA-seq of three biological replicates per culture condition generated 102–145 million raw reads per sample. Clustering of the transcriptome datasets by Euclidean distance revealed a clear separation between the ICM and TE regardless of the condition (Figure 2A). Without excluding minimal contamination, these results underline the successful separation of these two compartments by immunosurgery. Principal component analysis (PCA) was performed separately on ICM (Figure 2B) and TE (Figure 2C) transcriptomic data. Comparison to the CNTRL resulted in the identification of differentially expressed genes (DEG) between ICM or TE from embryos developed in HI, HG, or HGI (Figure 3 and Supplementary Table S1). Functions of the identified DEGs were explored using GO terms annotations (Supplementary Table S1). To determine coordinated gene expression changes, we analyzed the gene expression datasets using GSEA with the Hallmarks gene set collections, KEGG, Reactome, and GO BP databases (Supplementary Table S2). Enrichment analysis results were then analyzed with SUMER for gene set condensation. The following paragraphs will describe the identified effects of high insulin or high glucose alone and then in combination in the ICM and TE of exposed embryos.

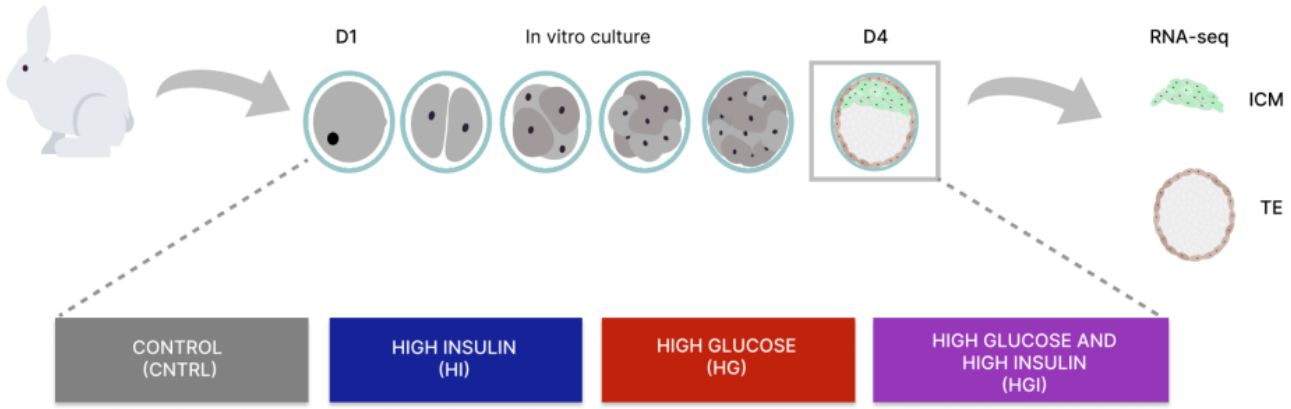

Figure 1. Schematic representation of the experimental workflow to analyze the in vitro exposure of preimplantation embryos from 1-cell to blastocyst stage for control, high insulin, high glucose, and high glucose and high insulin. The inner cell mass (ICM) and trophectoderm (TE) transcriptomes were determined by RNA-seq. D1, day 1. D4, day 4.

Table 1. Developmental competence of rabbit preimplantation embryos developed in vitro in CNTRL, HI, HG, or HGI conditions. Values are expressed as emmeans with standard errors in parenthesis. Different superscript letters (a, b) indicate significant differences within the same column ($p < 0.05$). CNTRL, control; HI, high insulin; HG, high glucose; HGI, high glucose and high insulin.

Condition	*N* Rabbits	*N* Embryos	Development Arrest Rate	Compacted Embryos Rate	Blastocyst Rate
CNTRL	60	1090	0.034 (0.009) [a]	0.303 (0.061) [a]	0.638 (0.057) [a]
HI	21	530	0.029 (0.009) [a]	0.309 (0.063) [a]	0.645 (0.059) [a]
HG	52	751	0.027 (0.008) [a]	0.228 (0.052) [b]	0.726 (0.051) [b]
HGI	35	519	0.023 (0.007) [a]	0.232 (0.053) [b]	0.732 (0.051) [b]

3.1. Impact of High Insulin In Vitro Exposure

The developmental competence of HI embryos showed no significant differences when compared to the CNTRL condition (Table 1). Quantification of total cell number by DAPI staining did not show significant changes in HI (262 ± 12, $n = 54$) versus CNTRL (240 ± 7, $n = 76$) blastocysts ($p < 0.05$, Supplementary Figure S1).

3.1.1. In ICM, High Insulin Induced Changes in Cellular Energy Metabolic Pathways

Transcriptome analysis by PCA and hierarchical clustering did not show a clear separation between HI ICM and CNTRL ICM (Figure 2). Differential analysis of HI ICM versus CNTRL ICM transcriptomes identified 10 DEG (3 overexpressed and 7 underexpressed) (Figure 3 and Supplementary Table S1). GSEA identified 37 significant positively enriched pathways (2 Hallmarks, 3 KEGG pathways, 14 GO BP, and 18 Reactome gene sets) and 8 negatively enriched (5 Hallmarks and 3 GO BP) pathways (Figure 4A and Supplementary Table S2).

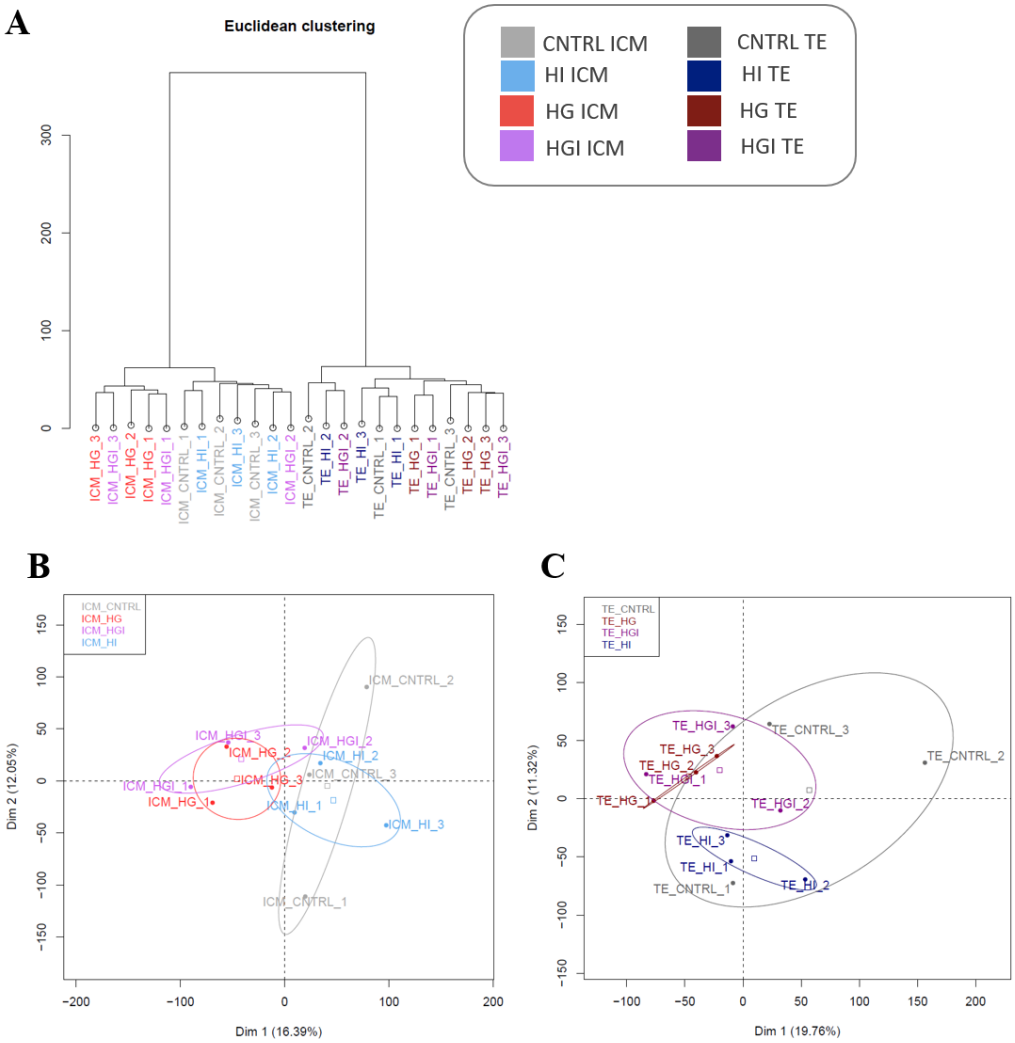

Figure 2. Transcriptome analysis of isolated ICM and TE from in vitro-developed blastocysts with high glucose and/or high insulin. (**A**). Clustering by Euclidean distance of the transcriptomic datasets of ICM and their corresponding TE developed in CNTRL, HI, HG, or HGI. Each group included three biological replicates which consisted of n = 11-16 ICM or TE. (**B**). Principal component analysis (PCA) of ICM groups. (**C**). PCA of TE groups. ICM, inner cell mass. TE, trophectoderm. CNTRL, control; HI, high insulin; HG, high glucose; HGI, high glucose and high insulin. Samples are color-coded according to the legend at the top (right).

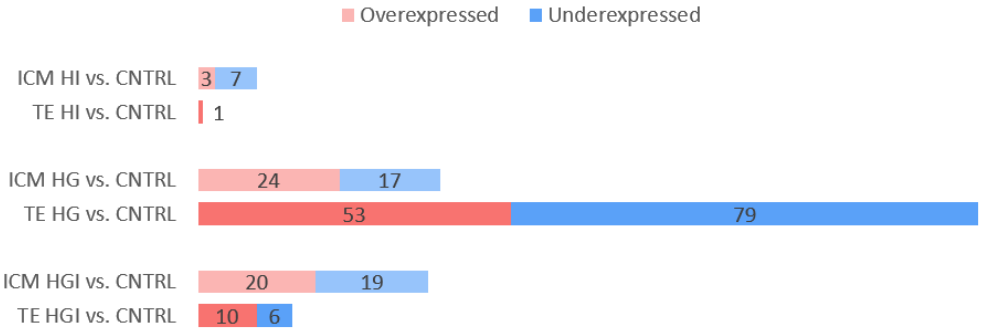

Figure 3. Differentially expressed genes (DEG) in ICM and TE of in vitro-developed blastocysts with HI, HG, or HGI compared to CNTRL. The number of overexpressed (red) and underexpressed (blue) DEGs with p-adjusted < 0.05 are shown. ICM, inner cell mass. TE, trophectoderm.

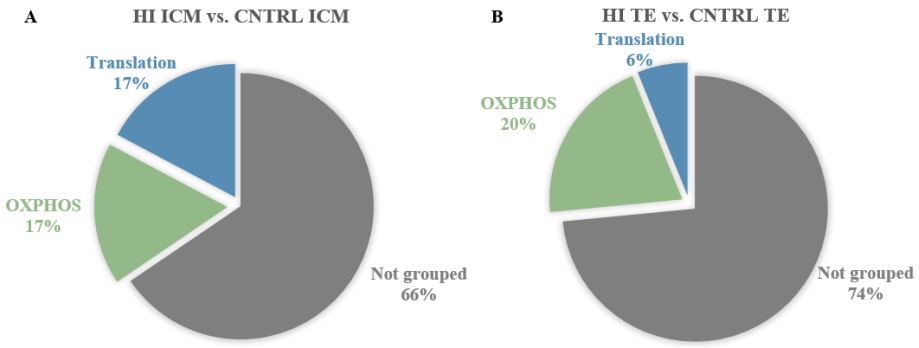

Figure 4. Significantly enriched gene sets (FDR < 0.05) in ICM and TE transcriptomes of in vitro-developed blastocysts with HI compared to CNTRL. Significantly enriched gene sets were identified by GSEA with the Molecular Signature Database (MSigDB) gene set collections: Hallmarks, KEGG, Reactome, and GO BP. GSEA was followed by SUMER analysis for gene set condensation. (**A**). Pie charts showing the enriched gene sets in HI ICM versus CNTRL ICM. (**B**). Pie charts showing the enriched gene sets in HI TE versus CNTRL TE. ICM, inner cell mass. TE, trophectoderm.

Enriched pathways included gene sets implicated in translation and oxidative phosphorylation (OXPHOS) (Figure 4A). Analysis of DEG and enrichment results in HI ICM transcriptomes compared to CNTRL ICM pointed out the perturbation of transcription and translation. Gene-by-gene statistical analysis identified DEG implicated in the regulation of transcription as *RC3H1* (ring finger and CCCH-type domains 1RC3H1, log2FC = −0.86) and *ICE1* (interactor of little elongation complex ELL subunit 1, log2FC = −0.71) (Supplementary Table S1). Concerning translation, enrichment analysis identified the overrepresentation of the "ribosome" KEGG pathway (normalized enrichment scores (NES) = 2.60), "translation" Reactome gene set (NES = 2.23), and the "translational elongation" and "translational termination" GO BP (NES = 1.98 and 2.06, respectively) (Supplementary Table S2). Enrichment results also highlighted the perturbation in OXPHOS. GSEA identified the significant positive enrichment of "oxidative phosphorylation" in Hallmark (NES = 1.98), KEGG (NES = 1.85), and GO terms (NES = 2.1), in addition to Reactome gene sets linked to OXPHOS as "NADH dehydrogenase complex assembly" (NES = 1.93) or "the citric acid cycle and respiratory electron transport" (NES = 2.22) (Supplementary Table S2). In line with these results, enrichment in "mitochondrial fatty acid (FA) β-oxidation" Reactome gene set (NES = 1.83) was also identified.

3.1.2. In TE, High Insulin Impacted Cellular Energy Metabolism and Oxidative Stress Pathways

Transcriptome analysis by PCA and hierarchical clustering showed no separation between HI TE and CNTRL TE (Figure 2). HI exposure resulted in the differential expression of only one gene, *PNLIP* (pancreatic lipase; log2FC = 5.1) (Figure 3 and Supplementary Table S1). However, GSEA analysis identified the significant positive enrichment of 83 gene sets (3 Hallmarks, 5 KEGG pathways, 20 GO BP, and 55 Reactome) and the significant negative enrichment of 7 gene sets (6 Hallmarks and 1 GO BP) (Supplementary Table S2).

Enriched pathways included gene sets implicated in translation and in OXPHOS (Figure 4B). Enrichment results highlighted a few gene sets implicated in translation, such as the "ribosome" KEGG pathway (NES = 1.82) or the "translation" Reactome gene set (NES = 1.82) (Figure 4B and Supplementary Table S2). Enrichment results related to OXPHOS included the overrepresentation of the "oxidative phosphorylation" gene sets in Hallmark (NES = 2.39), KEGG (NES = 2.27), and GO BP (NES = 2.11) or the Reactome gene set "respiratory electron transport" (NES = 2.30) (Figure 4B and Supplementary Table S2). In addition, reactive oxygen species (ROS) gene set "ROS and RNS production in phagocytes" (NES = 1.86) (Supplementary Table S2) and mitochondrial FA β-oxidation Reactome gene set (NES = 1.77) were identified. HI TE also showed the overrepresentation of acti-

vated NF-kB-related gene sets, including the Reactome FCERI-mediated NF-kB activation (NES = 1.94) (Supplementary Table S2).

3.1.3. High Insulin Induced Common Responses in ICM and TE

Between ICM and TE of high insulin-exposed embryos, whereas no common DEG was observed, 22 shared enriched GSEA gene sets were identified (Supplementary Tables S1 and S3). All shared gene sets exhibited the same level of enrichment. Among shared gene sets we highlighted translation, OXPHOS and FA β-oxidation. Enrichment of ROS and NF-kB signaling was only observed in HI TE.

3.2. Impact of High Glucose In Vitro Exposure

High glucose exposure led to a significant increase in blastocyst rate, mirrored by a significant reduction in the rate of compacted embryos compared to CNTRL embryos (Table 1). No significant differences were observed in the rate of arrested embryos after development with HG (Table 1). Quantification of total cell number showed a significantly increased cell number in HG (263 ± 9, $n = 75$) versus CNTRL (240 ± 7, $n = 76$) blastocysts ($p < 0.05$, Supplementary Figure S1).

3.2.1. In ICM, High Glucose Altered OXPHOS, Decreased Proliferation, Increased Apoptosis

Transcriptome analysis by PCA and hierarchical clustering showed the separation between HG ICM and CNTRL ICM (Figure 2). Differential analysis showed 41 DEG (24 upregulated and 17 downregulated) in the ICM of embryos exposed to HG compared to the CNTRL ICM (Figure 3 and Supplementary Table S1). GSEA analysis identified the significant positive enrichment of 73 functional gene sets (2 Hallmarks, 2 KEGG pathways, 11 GO BP, and 58 Reactome) (Supplementary Table S2).

Enrichment analyses identified 3 main clusters: translation, regulation of the cell number, and OXPHOS (Figure 5A). First, the protein translation cluster included KEGG "ribosome" (NES = 2.67), Reactome "metabolism of amino acids and derivatives" (NES = 1.79) and "translation" (NES = 2.51), and GO BP "translational initiation" (NES = 2.35) gene sets (Figure 5A, Supplementary Table S2). In addition, perturbation of transcription was also observed (Supplementary Table S1). Genes implicated in transcription were found to be differentially expressed, such as *KDM5A* (lysine demethylase 5A, log2FC = −0.35) and *GATA3* (GATA binding protein 3, log2FC = 1.05) (Supplementary Table S1). The second cluster highlighted alterations in the regulation of the cell number. GSEA revealed the enrichment of Hallmark "myc Target v1" (NES = 2.26), Reactome pathways such as "regulation of mitotic cell cycle" (NES = 1.89), and "regulation of apoptosis" (NES = 1.89). The differential analysis identified the overexpression of *LIN54* (lin-54 DREAM MuvB core complex component, log2FC = 0.65) and the underexpression of *CHP2* (calcineurin-like EF-hand protein 2, log2FC = −2.3) and *APC* (APC regulator of WNT signaling pathway, log2FC = −0.67) (Supplementary Table S1). To investigate cell proliferation and apoptosis at the cellular level, we performed EdU incorporation and the TUNEL assay (Figure 6 and Supplementary Figures S2–S5). Indeed, a reduced number of proliferating cells (Figure 6A and Supplementary Figure S2) and an increased proportion of apoptotic cells (Figure 6B and Supplementary Figure S4) were identified in HG ICM compared to CNTRL ICM. The third identified cluster concerning perturbations in energy metabolism included Hallmark "oxidative phosphorylation" (NES = 1.70), Reactome "respiratory electron transport" (NES = 2.23), GO BP "mitochondrial respiratory chain complex assembly" (NES = 2.02), and Reactome "cellular response to hypoxia" (NES = 1.81) (Figure 5A and Supplementary Table S2). In line with these results, HG ICM showed the overexpression of *FH* (fumarate hydratase, log2FC = 0.45) compared to CNTRL ICM (Supplementary Table S1).

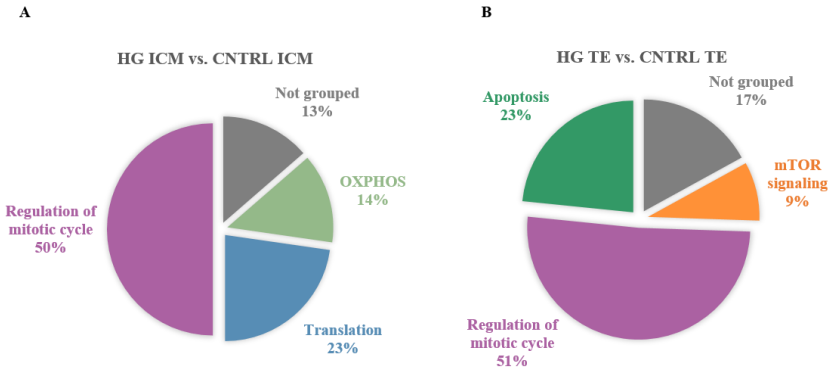

Figure 5. Significantly enriched gene sets (FDR < 0.05) in ICM and TE transcriptomes of in vitro-developed blastocysts with HG compared to CNTRL. Significantly enriched gene sets were identified by GSEA with the Molecular Signature Database (MSigDB) gene set collections: Hallmarks, KEGG, Reactome, and GO BP. GSEA was followed by SUMER analysis for gene set condensation. (**A**). Pie charts showing the enriched gene sets in HG ICM versus CNTRL ICM. (**B**). Pie charts showing the enriched gene sets in HG TE versus CNTRL TE. ICM, inner cell mass. TE, trophectoderm.

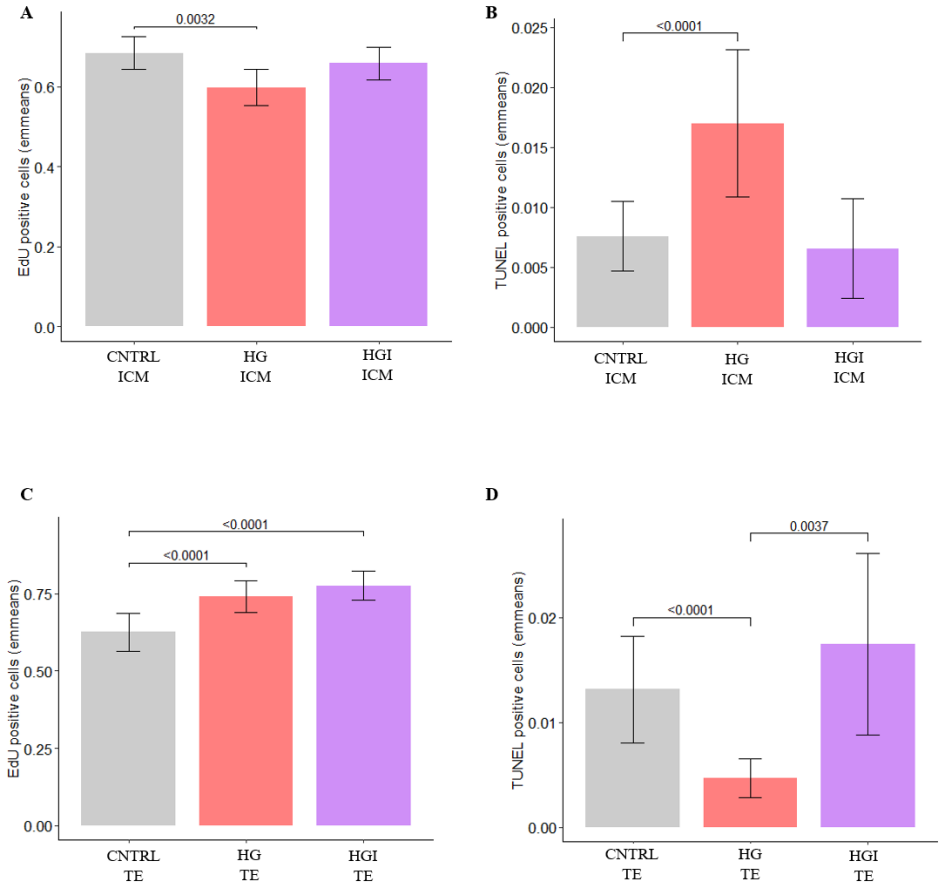

Figure 6. Quantification of proliferating and apoptotic cells in the ICM and TE of in-vitro-developed blastocysts with CNTRL, HG, and HGI by EdU incorporation and TUNEL assays. (**A**) Barplots showing the emmeans of proliferating cells in the ICM (n ICM = 16–38). (**B**) Barplots showing the emmeans percentage of apoptotic cells in the ICM (n ICM = 13–59). (**C**) Barplots showing the emmeans of proliferating cells in the TE (n TE = 16–24). (**D**) Barplots showing the emmeans of apoptotic cells in the TE (n TE = 18–52). Values are presented as emmeans ± S.E. Significant p values ($p < 0.05$) are shown. ICM, inner cell mass. TE, trophectoderm; CNTRL, control; HG, high glucose; HGI, high glucose and high insulin.

In addition to the main clusters, HG ICM transcriptomes showed perturbations in signaling pathways. HG ICM showed the overexpression of *REL* (REL proto-oncogene, NF-kB subunit, log2FC = 2.18) and the enrichment of gene sets related to NF-kB signaling, such as Reactome "FCERI mediated NF-kB activation" (NES = 1.84) (Supplementary Tables S1 and S2). Differential and enrichment analyses also showed dysregulations in the WNT signaling pathway. These results included the downregulation of *APC* (log2FC = −0.67) (Supplementary Table S1) and enrichment of Reactome "degradation of β-catenin by the destruction complex" (NES = 1.73) (Supplementary Table S2). Furthermore, gene-by-gene analysis of the HG ICM DEG revealed the overexpression of genes involved in the trophoblast lineage, such as GATA binding protein 3 (*GATA3*, log2FC = 1.05) and placenta expressed transcript 1 (*PLET1*, log2FC = 2.39) (Figure 7 and Supplementary Table S1).

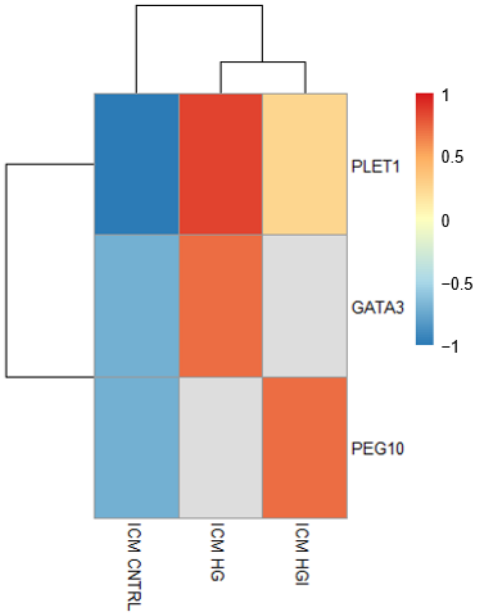

Figure 7. Heatmap showing the differential expression of genes (DEG) implicated in the TE lineage in HG and HGI ICM compared to CNTRL ICM. The mean normalized expression counts of n = 3 biological replicates, transformed to a Z-score, are represented by the color key. The gray color indicates the gene is not a DEG in that group. ICM, inner cell mass. TE, trophectoderm.

3.2.2. In TE, High Glucose Impacted Metabolic Pathways, Increased Proliferation, and Decreased Apoptosis

Transcriptome analysis by PCA and hierarchical clustering did not show a separation between HG TE and CNTRL TE (Figure 2). HG TE showed 132 DEG compared to CNTRL TE (53 overexpressed and 79 underexpressed) (Figure 3 and Supplementary Table S1). GSEA identified the enrichment of 78 functional gene sets, 76 of which were positively enriched (10 Hallmarks, 1 KEGG, and 65 Reactome), and 2 (GO BP) were negatively enriched (Supplementary Table S2).

Enriched pathways identified clusters related to metabolism and cell number regulation (Figure 5B). Concerning alterations in metabolism, enrichment results highlighted perturbations in mTOR signaling by the overrepresentation of Hallmarks "mTORC1 signaling" (NES = 1.68) and "PI3K-AKT-mTOR signaling" (NES = 1.61) (Figure 5B, Supplementary Table S2). Alteration of numerous genes involved in glycolysis, glycine, and lipid metabolism were identified such as *HK1* (hexokinase 1, log2FC = 0.53), *PHGDH* (phosphoglycerate dehydrogenase, log2FC = 0.85), *AACS* (acetoacetyl-CoA synthetase, log2FC = −1.48), *LDLR* (low density lipoprotein receptor, log2FC = −1.40, *GPAT3* (glycerol-3-phosphate acyltransferase 3, log2FC = 1.22), and *GPCPD1* (glycerophosphocholine phosphodiesterase 1, log2FC = 0.88) (Supplementary Table S1). The second main enrichment concerned the regulation of cell number (Figure 5B). Enriched pathways included Hallmark

"myc Target v1" (NES = 2.01), Reactome "mitotic G1-G1/S phases" (NES = 2.02), and "regulation of mitotic cell cycle" (NES = 2.08) gene sets (Supplementary Table S2). Consistent with these results, the HG TE transcriptome showed the altered expression of cell cycle progression genes, such as the underexpression of *CDKL4* (cyclin dependent kinase like 4, log2FC = −1.82) or *SMARCD3* (SWI/SNF related matrix associated actin dependent regulator of chromatin subfamily d member 3, log2FC = −3.00) or the overexpression of *GADD45A* (growth arrest and DNA damage inducible alpha, log2FC = 0.85) or *WEE1* (WEE1 G2 Checkpoint Kinase, log2FC = 0.97) (Supplementary Table S1). Assessment of cell proliferation by the EdU incorporation assay in HG TE further confirmed an increased number of proliferating cells compared to CNTRL TE (Figure 6C and Supplementary Figure S3). In parallel, enrichment results showed the overrepresentation of apoptosis-related gene sets such as Hallmarks "apoptosis" (NES = 1.73), "P53 pathway" (NES = 1.75), and the Reactome "regulation of apoptosis" (NES = 1.77) gene set (Supplementary Table S2). HG TE exhibited the differential expression of genes implicated in apoptosis, such as *CASP7* (caspase 7; log2FC = 1.13), *PDCD6* (programmed cell death 6; log2FC = 0.59), and *TRADD* (TNFRSF1A associated via death domain; log2FC = −1.37) (Supplementary Table S1). Investigation of apoptosis in HG TE by TUNEL assay showed a decrease in the number of apoptotic cells compared to CNTRL TE (Figure 6D and Supplementary Figure S5).

Beyond these main clusters, HG TE transcriptomes exhibited several other perturbations, as in the immune response. Enrichment and differential analysis identified the Hallmark "TGF-β signalling" (NES = 1.64) and "TNF-α signalling via NF-kB" (NES = 1.52) gene sets, and the underexpression of *ERC1* (ELKS/RAB6-interacting/CAST family member 1, log2FC = −0.91) (Supplementary Tables S1 and S2). The WNT signaling was identified as deregulated as highlighted by the enrichment of the Reactome "degradation of β-catenin by the destruction complex" (NES = 1.81) and "β-catenin independent WNT signaling" (NES = 1.79), and the underexpression of *ANKRD10* (ankyrin repeat domain 10; log2FC = −1.13) (Supplementary Tables S1 and S2). In addition, HG TE showed the enrichment of gene sets implicated in transcription and translation, such as the Reactome "transcriptional activity of SMAD2 SMAD3:SMAD4 heterotrimer" (NES = 1.9) and "translation" (NES = 1.88) (Supplementary Table S2). Along with these gene sets, gene-by-gene analysis and functional annotation by DAVID showed several DEG associated with transcriptional regulation, chromatin remodeling, and epigenetic mechanisms (Figure 8 and Supplementary Tables S1 and S4). Among the HG TE DEG, we highlighted the overexpression of *GADD45A*, *WEE1*, and *NPM3* (nucleophosmin/nucleoplasmin 3), and the underexpression of *SMARCD3*, *PADI2* (peptidyl arginine deiminase 2), *MOV10L1*, *ATF7* (activating transcription factor 7), *RESF1* (retroelement silencing factor 1), *BPTF* (bromodomain PHD finger transcription factor), and *NSD3* (nuclear receptor binding SET domain protein 3) (Figure 8 and Supplementary Tables S1 and S4).

3.2.3. High Glucose Induced Common and Specific Responses in ICM and TE

From the DEG identified in HG ICM (n = 41) and HG TE (n = 132), only 3 were shared: *ARRDC4* (arrestin domain containing 4) (log2FC = 2.07 and 2.02, respectively), *FAM3D* (family with sequence similarity 3 member D) (log2FC = 0.96 and 0.54, respectively), and *MOV10L1* (Mov10 RISC complex RNA helicase like 1) (log2FC = −1.26 and −1.57, respectively) (Supplementary Table S1). Despite the small amount of shared DEG, several processes were common, as shown by the 37 shared gene sets identified by GSEA, which are overrepresented in both ICM and TE (Supplementary Table S3). These gene sets were mainly related to the regulation of cell number. However, we identified opposite responses: the HG ICM exhibited decreased proliferation and increased apoptosis, whereas the HG TE showed increased proliferation and reduced apoptosis. Specific responses included transcriptome changes related to OXPHOS and lineage commitment in HG ICM and metabolism and epigenetic regulation in HG TE.

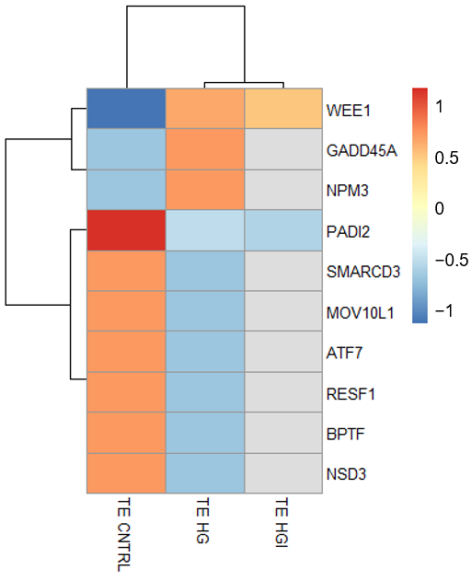

Figure 8. Heatmap showing the differential expression of genes (DEG) with a role in epigenetic regulation in HG and HGI TE compared to CNTRL TE. The mean normalized expression counts of $n = 3$ biological replicates, transformed to a z-score, are represented by the color key. The gray color indicates that the gene is not a DEG in that group. ICM, inner cell mass. TE, trophectoderm.

3.3. Impact of High Glucose and High Insulin In Vitro Exposure

High glucose and high insulin exposure led to a significant increase in blastocyst rate, mirrored by a significant reduction in the rate of compacted embryos compared to CNTRL embryos (Table 1). No significant differences were observed in the rate of arrested embryos after development with HGI (Table 1). Quantification of total cell number showed a significantly increased cell number in HGI (285 ± 14, $n = 50$) versus CNTRL (240 ± 7, $n = 76$) blastocysts ($p < 0.05$, Supplementary Figure S1).

As the development of HI embryos was not different from that of CNTRL embryos, a comparison of HGI vs. HI resulted in similar observations to HGI vs. CNTRL: no difference in the rate of arrested embryos, decrease in the rate of compacted embryos, and an increase of the rate of blastocysts and blastocyst total cell number (Table 1 and Supplementary Figure S1).

In comparison to high glucose, HGI embryos displayed similar development parameters: the rates of arrested, compacted, and blastocyst were similar in HGI compared to HG embryos. The cell number was also similar in HGI blastocysts in comparison to HG blastocysts (Table 1 and Supplementary Figure S1).

3.3.1. In ICM, Alteration of OXPHOS and ROS by High Glucose and High Insulin

Transcriptome analysis by PCA showed the separation between HGI ICM and CNTRL ICM (Figure 2). Differential analysis showed 39 DEG (20 overexpressed and 19 underexpressed) in comparison to CNTRL ICM (Figure 3 and Supplementary Table S1). GSEA analysis showed the significant positive enrichment of 107 gene sets (5 Hallmarks, 7 KEGG, 28 GO BP, and 66 Reactome) (Supplementary Table S2).

Enriched pathways highlighted two main clusters related to the regulation of gene expression and cellular energy metabolism (Figure 9A). Firstly, concerning the regulation of gene expression, several transcription factors were differentially expressed, such as *ELF2* (E74 like ETS transcription factor 2; log2FC = 0.71) and *SREBF2* (sterol regulatory element binding transcription factor 2; log2FC = −0.49). Overexpression of genes implicated in mRNA processing, such as *PTBP2* (polypyrimidine tract binding protein 2, log2FC = 0.96), was observed (Supplementary Table S1). Coherent with this, enrichment results highlighted transcriptome changes related to translation, including GO BP "translational initiation" (NES = 2.33), Reactome "mRNA splicing" (NES = 1.74), and KEGG

"ribosome" (NES = 2.85) (Figure 9A and Supplementary Table S2). The second identified cluster was related to OXPHOS. HGI ICM showed transcriptomic changes including Hallmark "oxidative phosphorylation" (NES = 2.02), KEGG (NES = 2.26), GO BP (NES = 2.55), and Reactome "mitochondrial fatty acid β oxidation" (NES = 1.82) gene sets (Figure 9A and Supplementary Table S2). Additionally, HG ICM showed the enrichment of ROS pathways, including Reactome "cellular response to hypoxia" (NES = 1.78) and Hallmark "reactive oxygen species" (NES = 1.73) (Figure 9A and Supplementary Table S2).

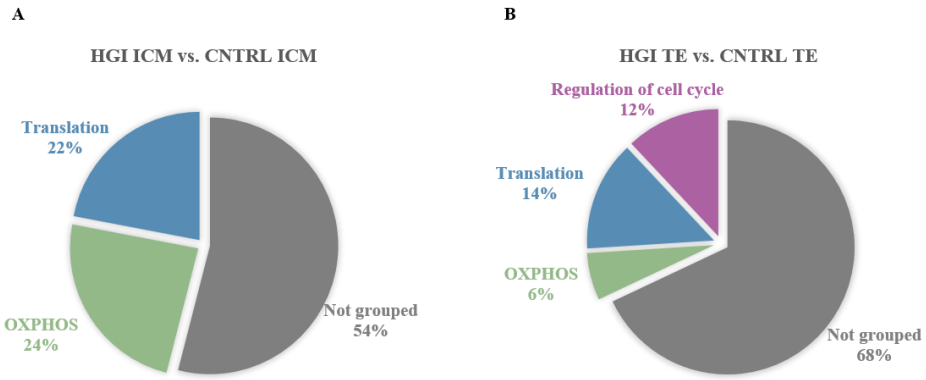

Figure 9. Significantly enriched gene sets (FDR < 0.05) in the ICM and TE transcriptomes of in vitro-developed blastocysts with HGI compared to CNTRL. Significantly enriched gene sets were identified by GSEA with the Molecular Signature Database (MSigDB) gene set collections: Hallmarks, KEGG, Reactome, and GO BP. GSEA was followed by SUMER analysis for gene set condensation. (**A**). Pie charts showing the enriched gene sets in HGI ICM versus CNTRL ICM. (**B**). Pie charts showing the enriched gene sets in HGI TE versus CNTRL TE. ICM, inner cell mass. TE, trophectoderm.

In addition to these main clusters, HGI ICM exhibited DEG and enriched gene sets implicated in cell number regulation. Among these, we can list the *APC* gene (log2FC = −0.74), the Hallmark "myc target v1" (NES = 2.02), and the Reactome "regulation of apoptosis" (NES = 1.73) (Supplementary Tables S1 and S3). We examined a possible imbalance in proliferation and apoptosis in HGI ICM and did not detect significant changes in the proportion of proliferating or apoptotic cells compared to CNTRL ICM (Figure 6A,B and Supplementary Figures S2 and S4). HGI ICM transcriptomes also showed enrichment in TNF-α signaling (Figure 9A and Supplementary Table S2). Among the DEG and gene sets implicated in this pathway, we highlighted the differential expression of *USP15* (ubiquitin specific peptidase 15, log2FC = 0.47), enriched Hallmark "TNFA signaling via NFKB" (NES = 1.70), and GO BP "cytokine metabolic process" (NES = 1.94) (Figure 9A and Supplementary Tables S1 and S2). Among the DEG identified, we also highlighted the differential expression of genes implicated in the trophoblast lineage and placenta development, such as *PLET1* (log2FC = 1.97) and *PEG10* (paternally expressed 10, log2FC = 1.79) (Figure 7 and Supplementary Table S1).

Then, the specific responses triggered by high glucose and high insulin in combination on the ICM were determined by the identification of common and specific transcriptomic changes between HGI versus CNTRL ICM and HI versus CNTRL ICM and between HGI versus CNTRL ICM and HG versus CNTRL ICM (Supplementary Figure S6A, Tables S1 and S3).

HGI ICM and HI ICM shared 2 DEG, including the protein-coding gene *RPS6KA3* (ribosomal protein S6 kinase A3) (log2FC = 0.77 and 0.88, respectively), and 29 gene sets, all with the same expression pattern (Supplementary Figure S6A, Tables S1 and S3). Shared changes in gene expression were related to the regulation of gene expression and OXPHOS (Supplementary Table S3).

HGI ICM and HG ICM shared 16 DEG and 62 gene sets, all with the same expression pattern (Supplementary Figure S6A, Tables S1 and S3). These shared transcriptome changes were related to the regulation of gene expression, OXPHOS, NF-kB signalling, and the

aberrant expression of TE genes. Despite the few shared gene sets involved in cell number regulation, the increased apoptosis and decreased proliferation identified in HG ICM were not found in HGI ICM. The enrichment in the ROS pathway was exclusively identified in HGI ICM.

3.3.2. In TE, Alteration of OXPHOS, ROS, and Proliferation by High Glucose and High Insulin

Transcriptome analysis by PCA and hierarchical clustering did not show a separation between HGI TE and CNTRL TE (Figure 2C). HGI TE exhibited 16 DEG (10 overexpressed and 6 underexpressed) in comparison to CNTRL TE (Figure 3 and Supplementary Table S1). Enrichment analysis in HGI TE identified 108 gene sets positively enriched (8 Hallmarks, 2 KEGG pathways, 11 GO BP, and 87 Reactome) (Supplementary Table S2).

Enriched pathways included gene sets related to transcription, translation, cell number regulation, and OXPHOS, as highlighted by the three main clusters (Figure 9B and Supplementary Table S2). Transcription and translation enriched gene sets included the Reactome "transcriptional regulation by MECP2" (NES = 1.89), KEGG "ribosome" (NES = 2.53), Reactome "translation" (NES = 2.10), and KEGG "proteasome" (NES = 2.17) (Supplementary Table S2). Enriched pathways implicated in the regulation of cell number included Hallmark "myc target v1" (NES = 2.30) and Reactome "regulation of mitotic cell cycle" (NES = 2.22) (Figure 9B and Supplementary Table S2). In line with these enriched gene sets, the differential analysis identified the significant overexpression of *TUBB* (tubulin beta class I, log2FC = 0.50) and *WEE1* (log2FC = 0.92), 2 genes implicated in the G2/M transition of the mitotic cell cycle (Supplementary Table S1). The EdU incorporation assay in HGI TE confirmed a significant increase in the proportion of proliferating cells compared to CNTRL TE (Figure 6C and Supplementary Figure S3). Despite identifying a small enrichment of gene sets implicated in apoptosis (Supplementary Table S2), the TUNEL assay in HGI TE did not detect significant differences in the proportion of apoptotic cells compared to CNTRL TE (Figure 6D and Supplementary Figure S5). The third identified cluster was related to energy metabolism, as indicated by the Hallmark "oxidative phosphorylation" (NES = 1.54), "ROS pathway" (NES = 1.79), Reactome "cellular response to hypoxia" (NES = 2.00), and GO BP "regulation of transcription from RNA polymerase II promoter in response to hypoxia" (NES = 2.04) (Figure 9B and Supplementary Table S2). In line with these enrichments, DEG in HGI TE included the overexpression of *TXNIP* (thioredoxin-interacting protein; log2FC = 1.81) (Supplementary Table S1).

Besides these clusters, transcriptome analysis showed perturbations in the immune response in HGI TE. Enriched pathways included the Hallmark "TGF-α signaling via NF-kB" (NES = 1.73), GO BP "positive regulation of cytokine biosynthetic process" (NES = 2.02), and TGF-β signaling (NES = 1.67) (Supplementary Table S2). Additionally, enrichment results showed perturbations of the WNT signaling pathway by the Reactome "degradation of β-catenin by the destruction complex" (NES = 1.80) (Supplementary Table S2).

The combination of high glucose and high insulin triggered specific responses in the TE. HI TE and HGI TE shared 1 DEG (*PNLIP*, log2FC = 5.08 and 4.71, respectively) and 43 overrepresented gene sets (Supplementary Figure S6B, Tables S1 and S3). These gene sets were related to translation, OXPHOS, ROS, and NF-kB signaling (Supplementary Table S3). In comparison to HG TE, 9 DEG and 53 gene sets shared the same expression pattern (Supplementary Figure S6B, Tables S1 and S3). Corresponding pathways were related to transcription and translation, NF-kB signaling and regulation of cell number. A higher number of proliferating cells was detected in both HG TE and HGI TE. Decrease in HG TE, apoptosis was not altered in HGI TE. The alteration of the metabolic pathway genes and the altered expression of genes involved in epigenetic mechanisms detected in HG TE were not identified in HGI TE. Inversely, OXPHOS and ROS pathways were only overrepresented in HGI TE (Supplementary Table S3).

3.3.3. High Glucose and High Insulin Induced Common and Specific Responses in ICM and TE

Between HGI ICM and HGI TE, whereas only one DEG was shared (*ARRDC4*, log2FC = 2.09 and 2.02, respectively), half (n = 54) of the enriched gene sets were shared and exhibited the same enrichment pattern (Supplementary Tables S1 and S3). Transcription, translation, OXPHOS, ROS, and NF-kB signaling were impacted in ICM and TE in response to HGI (Supplementary Table S2). Specific responses between compartments can be noticed, such as cell commitment dysregulations occurring exclusively in the ICM.

4. Discussion

Prediabetes and the early stages of T2D are characterized by hyperglycemia and hyperinsulinemia [1,2]. Unfortunately, these first metabolic dysregulations are often asymptomatic, resulting in nearly half of people with T2D being undiagnosed and untreated [1]. In the early stages of pregnancy, including the preimplantation period, women are not yet aware of their gestational status; therefore, in undiagnosed diabetic women, pregnancies are not adequately intervened. Increased glucose and insulin concentrations are reflected in oviductal and uterine fluids [9,11]. Preimplantation embryos are responsive to glucose and insulin through the activation of signaling and metabolic pathways [14,15,41–43]. The preimplantation period corresponds to a critical window of susceptibility during which variations in the environment can have a major impact on the offspring. Here, we have established an in vitro model using the rabbit to study the effects of high glucose and/or high insulin on preimplantation embryo development.

As growth factors, glucose and insulin are key regulators of proliferation and apoptosis. In the present study, the presence of high glucose stimulated blastocyst development and growth. Observations in mice and bovine embryos mainly described a negative impact of glucose on blastocyst development, obtained with glucose concentrations above 20 mM [11,44]. Here, we have shown that high glucose exposure led to the alteration of proliferation and apoptosis in mirror patterns. Consistent with our findings, mouse and rat embryos exposed to glucose showed increased apoptosis in the ICM [45,46]. Inversely to ICM, and to our knowledge first described here, proliferation was increased, and apoptosis decreased in the TE of embryos exposed to high glucose. When embryos were exposed to high levels of insulin alone, blastocyst rate and growth were not impacted, and changes in the expression of genes involved in proliferation and apoptosis were not identified. The mitogenic actions of insulin are well known [18]; however, in preimplantation embryos, this remains controversial [47–50]. Our findings show that when high levels of insulin were added in addition to high glucose, the increased rate and growth of blastocysts observed in the presence of high glucose alone persisted. Despite changes in the proliferation and apoptosis gene expression, only the proliferation rate remained increased in the TE. These results suggest a crosstalk between glucose and insulin in mediating growth-related effects.

Glucose and insulin play a central role in regulating energy homeostasis and metabolism [18,51]. Here, embryos developed in the presence of high glucose exhibited OXPHOS signatures in the ICM and mTORC1 signaling and glycolytic and lipid metabolism signatures in the TE. Glucose, via glycolysis and OXPHOS, leads to the production of cellular energy in the form of ATP [52]. Until the morula stage, preimplantation embryos metabolize lactate and pyruvate preferentially as an energy source through OXPHOS [51]. Around the morula stage and onward, glucose is preferentially metabolized, although the metabolic pathway used may differ between the ICM and TE [51,53]. Exposure to hyperglycemia in vitro and in vivo led to hyperactivation of mTORC1 signaling in rabbit blastocysts, especially in the TE [41]. The mTORC1 and mTORC2 complexes stimulate anabolic processes such as protein, lipid, and nucleotide synthesis and regulate glucose metabolism by favoring glycolysis over OXPHOS [54]. To sustain cell growth, the mTORC1 and mTORC2 complexes stimulate anabolic processes such as protein, lipid, and nucleotide synthesis, regulate glucose metabolism by favoring glycolysis over OXPHOS, and promote cell survival and proliferation [54]. In the present study, both ICM and TE developed

in an insulin-rich environment and exhibited OXPHOS gene expression signatures. The metabolic effects of insulin are well known, and insulin has been shown to stimulate the oxidative capacity of mitochondria [18,55]. In addition, the TE of embryos developed with high insulin showed ROS-related gene expression changes, suggesting insulin-mediated oxidative stress. ROS, mainly produced as a by-product of OXPHOS, plays a role in physiological cellular processes [56]. Here, in the presence of both high glucose and high insulin, OXPHOS and ROS gene expression signatures were also identified in the ICM and TE. In addition, transcriptome changes related to NF-kB and TNF-α signaling were identified in the ICM and TE. NF-kB signaling, central regulator of inflammation and immunity, also regulates multiple cellular processes, including mitochondrial respiration [57]. NF-kB is induced by environmental cues, including insulin and ROS [58,59]. Here, gene expression changes related to OXPHOS, ROS, and NF-kB suggest metabolic stress in the ICM and TE of embryos exposed to both high glucose and high insulin.

Interestingly, we identified the deregulation of a subset of genes implicated in chromatin remodeling and epigenetic regulation in the TE. Emerging research has underlined the crosslink between metabolism and chromatin dynamics and its influence on gene expression [60,61]. A clear example of this is the generation of regulators of chromatin-modifying enzymes through glucose metabolism [60,61]. Among the genes showing altered expression in the TE exposed to high glucose, we highlighted *GADD45A*, *BPTF*, *PADI2*, and *ATF7*. GADD45A mediates active DNA demethylation, facilitating transcriptional activation, and also regulates trophoblast cell migration and invasion during placentation [62,63]. BPTF encodes the largest subunit of the Nucleosome Remodeling Factor (NURF) chromatin remodeling complex and plays an essential role in extraembryonic lineage development [64,65]. As for PADI2, a catalyzer of histone citrullination, it regulates chromatin organization and transcriptional regulation of cell cycle progression, metabolism, and proliferation genes [66]. ATF7, a stress-responsive chromatin regulator that recruits histone methyltransferases to repress the transcription of metabolic genes, has been proposed to mediate paternal low protein diet-induced intergenerational programming by reducing H3K9me2 in target genes [67,68]. In the presence of both high glucose and high insulin, the number of epigenetic genes with altered expression was less than in embryos exposed to high glucose alone, whereas no gene with an epigenetic-related function showed differential expression in embryos exposed to high insulin alone. Thus, these results suggested a crosstalk between insulin and glucose in terms of epigenetic regulation, especially in the TE. Thus, the differential expression of these genes suggests alterations in the TE epigenetic landscape, alterations that could compromise trophoblast differentiation.

In addition to the altered expression of epigenetic genes in the TE, the ICM exhibited the overexpression of genes involved in the trophoblast lineage when exposed to high glucose alone or in combination with high insulin. GATA3 is a well-known transcription factor associated with TE initiation and trophoblast differentiation [69,70]. Overexpression of GATA3 was sufficient to induce trophoblast fate in mouse embryonic stem cells (ESCs) [69]. PLET1 is an epigenetically-regulated cell surface protein essential to drive the differentiation of the trophoblast lineage [71]. *PEG10*, a paternally expressed imprinted gene highly expressed in the placenta, is essential for placenta formation in early development [72]. In the mouse, it has been recently demonstrated that glucose metabolism is required for the specification of the TE lineage through the hexosamine biosynthetic pathway (HBP), the pentose phosphate pathway (PPP), and the activation of the mTOR pathway [70]. Furthermore, when human ESCs were cultured with high glucose, the differentiation of the definitive endoderm was impaired [73]. In addition, we observed the enrichment of NF-kB signatures on the ICM of embryos exposed to high glucose alone or in combination with high insulin, and the NF-kB signaling pathway is known to regulate trophoblast differentiation and function [74,75]. Moreover, the ICM of embryos exposed to high glucose alone or in combination with high insulin showed signatures of oxidative rather than glycolytic metabolism, which in the mouse has been described to be characteristic of the TE rather than of the ICM [20]. Our findings indicate a potential impairment

in cell commitment in the ICM. Perturbations in ICM cell allocation could directly influence the TE lineage [46,76]. Blastocysts with different amounts of ICM cells led to limited trophoblast proliferation, suggesting the necessity for cell allocation homeostasis between these two compartments [46,76]. Moreover, the crosstalk between ICM and TE influencing TE differentiation has been previously described [17].

In conclusion, exposure to high glucose and high insulin alone or in combination during preimplantation development results in lineage-specific responses in the progenitors of the future individual and the embryonic portion of the placenta. We showed here that in the presence of high insulin, the impact of high glucose was lowered in some cases, suggesting significant crosstalk between glucose metabolism and insulin signaling in the early embryo. These results suggested that a mismatch in the glucose and insulin axis represents a risk for early embryonic development and, thus, for offspring health. Moreover, despite being present in the preimplantation maternal environment, insulin is usually absent in in vitro culture systems. Integration of insulin may be useful in improving embryo culture media.

Supplementary Materials: The following supporting information can be downloaded at: https://www.mdpi.com/article/10.3390/cells11233766/s1, Figure S1: Quantification of total cell number in vitro-developed blastocysts with CNTRL, HI, HG or HGI; Table S1: Differentially expressed genes (DEGs) in Inner Cell Mass (ICM) and Trophectoderm (TE) of embryos developed with High Insulin (HI), High Glucose (HG) or High Glucose and high Insulin (HGI) versus Control (CNTRL); Table S2: Gene Set Enrichment Analysis (GSEA); Table S3: Shared gene sets; Table S4: Functional annotation of Differentially expressed genes (DEGs)

Author Contributions: Conceptualization, S.C. and V.D.; methodology, C.A., N.D., R.V.y.R. and S.C.; software, A.F., L.J. and R.V.y.R.; validation, S.C. and R.V.y.R.; formal analysis, A.F., C.A., G.C., R.V.y.R. and S.C.; investigation, N.D., R.V.y.R., S.C. and Y.J.; resources, N.D., R.V.y.R. and S.C.; data curation, A.F., C.A., L.J. and Y.J.; writing-original draft preparation, R.V.y.R. and S.C.; writing-review and editing, S.C. and V.D.; visualization, A.F. and R.V.y.R.; supervision, S.C. and V.D., project administration, S.C., funding acquisition, S.C. and V.D. All authors have read and agreed to the published version of the manuscript.

Funding: This research was funded by the Societé Francophone du Diabète (SFD), by the INRAE with dedicated help from the PhASE department (CI 2017), and by the Agence Nationale de la Recherche REVIVE LabEx (Investissement d'Avenir, ANR-10-LABX-73). RV is the recipient of a doctoral fellowship from the Ministère de l'Enseignement supérieur, de la Recherche et de l'Innovation (MESRI), from the INRAE PhASE department and from the REVIVE LabEx.

Institutional Review Board Statement: The animal study protocol was approved by the Ethics Committee of INRAE (approved protocol code APAFIS#2180-2015112615371038 v2, approved on 16 December 2015 and approved protocol code APAFIS#26907-2020070115104375 v3, approved on 1 October 2020).

Informed Consent Statement: Not applicable.

Data Availability Statement: The data are available under accession number GSE218009GEO.

Acknowledgments: We are grateful for the technical support provided by the INRAE animal experimentation unit (UE1298–SAAJ, INRAE Jouy-en-Josas, France). We thank the @BRIDGe facility (GABI, AgroParisTech, INRAE, Université Paris-Saclay, Jouy-en-Josas, France) for their valuable technical assistance in assessing total RNA quality. This work has benefited from the facilities and expertise of the high throughput sequencing core facility of I2BC (Centre de Recherche de Gif—http://www.i2bc.paris-saclay.fr/, accessed on 4 October 2022). We thank the MIMA2 platform (Microscopie et Imagerie des Microorganismes, Animaux et Aliments, https://doi.org/10.15454/1.5572348210007727E12, accessed on 4 October 2022) and particularly Pierre Adenot for his help on ApoTome microscopy observations. We thank Laura Hua, Virginie Marcinek, and Pierre Midrouillet for their help during their short-term internships. We thank Delphine Rousseau-Ralliard, Bertrand Duvillié, and Patrice Humblot for their helpful discussions on data analysis.

Conflicts of Interest: The authors declare no conflict of interest.

References

1. InteInternational Diabetes Federation. *IDF Diabetes Atlas*, 10th ed.; International Diabetes Federation: Brussels, Belgium, 2021; ISBN 978-2-930229-98-0.
2. Thomas, D.D.; Corkey, B.E.; Istfan, N.W.; Apovian, C.M. Hyperinsulinemia: An Early Indicator of Metabolic Dysfunction. *J. Endocr. Soc.* **2019**, *3*, 1727–1747. [CrossRef]
3. Hjort, L.; Novakovic, B.; Grunnet, L.G.; Maple-Brown, L.; Damm, P.; Desoye, G.; Saffery, R. Diabetes in Pregnancy and Epigenetic Mechanisms—How the First 9 Months from Conception Might Affect the Child's Epigenome and Later Risk of Disease. *Lancet Diabetes Endocrinol.* **2019**, *7*, 796–806. [CrossRef] [PubMed]
4. DiMeglio, L.A.; Evans-Molina, C.; Oram, R.A. Type 1 Diabetes. *Lancet* **2018**, *391*, 2449–2462. [CrossRef]
5. Francis, E.C.; Dabelea, D.; Ringham, B.M.; Sauder, K.A.; Perng, W. Maternal Blood Glucose Level and Offspring Glucose–Insulin Homeostasis: What Is the Role of Offspring Adiposity? *Diabetologia* **2020**, *64*, 83–94. [CrossRef]
6. Langley-Evans, S.C. Nutrition in Early Life and the Programming of Adult Disease: A Review. *J. Hum. Nutr. Diet.* **2015**, *28*, 1–14. [CrossRef]
7. Watkins, A.J.; Ursell, E.; Panton, R.; Papenbrock, T.; Hollis, L.; Cunningham, C.; Wilkins, A.; Perry, V.H.; Sheth, B.; Kwong, W.Y.; et al. Adaptive Responses by Mouse Early Embryos to Maternal Diet Protect Fetal Growth but Predispose to Adult Onset Disease1. *Biol. Reprod.* **2007**, *78*, 299–306. [CrossRef] [PubMed]
8. Velazquez, M.A. Impact of Maternal Malnutrition during the Periconceptional Period on Mammalian Preimplantation Embryo Development. *Domest. Anim. Endocrinol.* **2015**, *51*, 27–45. [CrossRef] [PubMed]
9. Kaye, P.L.; Gardner, H.G. Preimplantation Access to Maternal Insulin and Albumin Increases Fetal Growth Rate in Mice. *Hum. Reprod.* **1999**, *14*, 3052–3059. [CrossRef] [PubMed]
10. Acevedo, J.J.; Mendoza-Lujambio, I.; de la Vega-Beltrán, J.L.; Treviño, C.L.; Felix, R.; Darszon, A. KATP Channels in Mouse Spermatogenic Cells and Sperm, and Their Role in Capacitation. *Dev. Biol.* **2006**, *289*, 395–405. [CrossRef]
11. Fraser, R.B.; Waite, S.L.; Wood, K.A.; Martin, K.L. Impact of Hyperglycemia on Early Embryo Development and Embryopathy: In Vitro Experiments Using a Mouse Model. *Hum. Reprod.* **2007**, *22*, 3059–3068. [CrossRef] [PubMed]
12. Fleming, T.P.; Sun, C.; Denisenko, O.; Caetano, L.; Aljahdali, A.; Gould, J.M.; Khurana, P. Environmental Exposures around Conception: Developmental Pathways Leading to Lifetime Disease Risk. *Int. J. Environ. Res. Public Health* **2021**, *18*, 9380. [CrossRef] [PubMed]
13. Jungheim, E.S.; Moley, K.H. The Impact of Type 1 and Type 2 Diabetes Mellitus on the Oocyte and the Preimplantation Embryo. *Semin. Reprod. Med.* **2008**, *26*, 186–195. [CrossRef] [PubMed]
14. Ramin, N.; Thieme, R.; Fischer, S.; Schindler, M.; Schmidt, T.; Fischer, B.; Santos, A.N. Maternal Diabetes Impairs Gastrulation and Insulin and IGF-I Receptor Expression in Rabbit Blastocysts. *Endocrinology* **2010**, *151*, 4158–4167. [CrossRef]
15. Rousseau-Ralliard, D.; Couturier-Tarrade, A.; Thieme, R.; Brat, R.; Rolland, A.; Boileau, P.; Aubrière, M.-C.; Daniel, N.; Dahirel, M.; Derisoud, E.; et al. A Short Periconceptional Exposure to Maternal Type-1 Diabetes Is Sufficient to Disrupt the Feto-Placental Phenotype in a Rabbit Model. *Mol. Cell. Endocrinol.* **2019**, *480*, 42–53. [CrossRef] [PubMed]
16. Moley, K.H.; Chi, M.M.Y.M.-Y.; Mueckler, M.M. Maternal Hyperglycemia Alters Glucose Transport and Utilization in Mouse Preimplantation Embryos. *Am. J. Physiol. Metab.* **1998**, *275*, E38–E47. [CrossRef]
17. Leunda-Casi, A.; de Hertogh, R.; Pampfer, S. Decreased Expression of Fibroblast Growth Factor-4 and Associated Dysregulation of Trophoblast Differentiation in Mouse Blastocysts Exposed to High D-Glucose in Vitro. *Diabetologia* **2001**, *44*, 1318–1325. [CrossRef]
18. Boucher, J.; Kleinridders, A.; Kahn, C.R. Insulin Receptor Signaling in Normal and Insulin-Resistant States. *Cold Spring Harb. Perspect. Biol.* **2014**, *6*, a009191. [CrossRef]
19. Purcell, S.H.; Moley, K.H. Glucose Transporters in Gametes and Preimplantation Embryos. *Trends Endocrinol. Metab.* **2009**, *20*, 483–489. [CrossRef]
20. Gardner, D.K.; Harvey, A.J. Blastocyst Metabolism. *Reprod. Fertil. Dev.* **2015**, *27*, 638–654. [CrossRef]
21. Navarrete Santos, A.; Ramin, N.; Tonack, S.; Fischer, B. Cell Lineage-Specific Signaling of Insulin and Insulin-Like Growth Factor I in Rabbit Blastocysts. *Endocrinology* **2008**, *149*, 515–524. [CrossRef]
22. Canon, E.; Jouneau, L.; Blachère, T.; Peynot, N.; Daniel, N.; Boulanger, L.; Maulny, L.; Archilla, C.; Voisin, S.; Jouneau, A.; et al. Progressive Methylation of POU5F1 Regulatory Regions during Blastocyst Development. *Reproduction* **2018**, *156*, 145–161. [CrossRef] [PubMed]
23. Bouchereau, W.; Jouneau, L.; Archilla, C.; Aksoy, I.; Moulin, A.; Daniel, N.; Peynot, N.; Calderari, S.; Joly, T.; Godet, M.; et al. Major Transcriptomic, Epigenetic and Metabolic Changes Underlie the Pluripotency Continuum in Rabbit Preimplantation Embryos. *Development* **2022**, *149*, dev200538. [CrossRef] [PubMed]
24. Fleming, T.P.; Kwong, W.Y.; Porter, R.; Ursell, E.; Fesenko, I.; Wilkins, A.; Miller, D.J.; Watkins, A.J.; Eckert, J.J. The Embryo and Its Future. *Biol. Reprod.* **2004**, *71*, 1046–1054. [CrossRef] [PubMed]
25. Staud, F.; Karahoda, R. Trophoblast: The Central Unit of Fetal Growth, Protection and Programming. *Int. J. Biochem. Cell Biol.* **2018**, *105*, 35–40. [CrossRef]
26. Fischer, B.; Chavatte-Palmer, P.; Viebahn, C.; Navarrete Santos, A.; Duranthon, V. Rabbit as a Reproductive Model for Human Health. *Reproduction* **2012**, *144*, 1–10. [CrossRef]

27. Laskowski, D.; Sjunnesson, Y.; Humblot, P.; Sirard, M.A.; Andersson, G.; Gustafsson, H.; Båge, R. Insulin Exposure during in Vitro Bovine Oocyte Maturation Changes Blastocyst Gene Expression and Developmental Potential. *Reprod. Fertil. Dev.* **2017**, *29*, 876–889. [CrossRef]
28. Tarrade, A.; Rousseau-Ralliard, D.; Aubrière, M.C.; Peynot, N.; Dahirel, M.; Bertrand-Michel, J.; Aguirre-Lavin, T.; Morel, O.; Beaujean, N.; Duranthon, V.; et al. Sexual Dimorphism of the Feto-Placental Phenotype in Response to a High Fat and Control Maternal Diets in a Rabbit Model. *PLoS ONE* **2013**, *8*, e83458. [CrossRef]
29. Sanz, G.; Daniel, N.; Aubrière, M.C.; Archilla, C.; Jouneau, L.; Jaszczyszyn, Y.; Duranthon, V.; Chavatte-Palmer, P.; Jouneau, A. Differentiation of Derived Rabbit Trophoblast Stem Cells under Fluid Shear Stress to Mimic the Trophoblastic Barrier. *Biochim. Biophys. Acta-Gen. Subj.* **2019**, *1863*, 1608–1618. [CrossRef]
30. Love, M.I.; Huber, W.; Anders, S. Moderated Estimation of Fold Change and Dispersion for RNA-Seq Data with DESeq2. *Genome Biol.* **2014**, *15*, 1–21. [CrossRef]
31. Heberle, H.; Meirelles, V.G.; da Silva, F.R.; Telles, G.P.; Minghim, R. InteractiVenn: A Web-Based Tool for the Analysis of Sets through Venn Diagrams. *BMC Bioinform.* **2015**, *16*, 1–7. [CrossRef]
32. Huang, D.W.; Sherman, B.T.; Lempicki, R.A. Systematic and Integrative Analysis of Large Gene Lists Using DAVID Bioinformatics Resources. *Nat. Protoc.* **2009**, *4*, 44–57. [CrossRef]
33. Subramanian, A.; Tamayo, P.; Mootha, V.K.; Mukherjee, S.; Ebert, B.L.; Gillette, M.A.; Paulovich, A.; Pomeroy, S.L.; Golub, T.R.; Lander, E.S.; et al. Gene Set Enrichment Analysis: A Knowledge-Based Approach for Interpreting Genome-Wide Expression Profiles. *Proc. Natl. Acad. Sci. USA* **2005**, *102*, 15545–15550. [CrossRef] [PubMed]
34. Liberzon, A.; Birger, C.; Thorvaldsdóttir, H.; Ghandi, M.; Mesirov, J.P.; Tamayo, P. The Molecular Signatures Database Hallmark Gene Set Collection. *Cell Syst.* **2015**, *1*, 417–425. [CrossRef] [PubMed]
35. Jassal, B.; Matthews, L.; Viteri, G.; Gong, C.; Lorente, P.; Fabregat, A.; Sidiropoulos, K.; Cook, J.; Gillespie, M.; Haw, R.; et al. The Reactome Pathway Knowledgebase. *Nucleic Acids Res.* **2019**, *48*, D498–D503. [CrossRef] [PubMed]
36. Ashburner, M.; Ball, C.A.; Blake, J.A.; Botstein, D.; Butler, H.; Cherry, J.M.; Davis, A.P.; Dolinski, K.; Dwight, S.S.; Eppig, J.T.; et al. Gene Ontology: Tool for the Unification of Biology. *Nat. Genet.* **2000**, *25*, 25–29. [CrossRef] [PubMed]
37. Carbon, S.; Douglass, E.; Good, B.M.; Unni, D.R.; Harris, N.L.; Mungall, C.J.; Basu, S.; Chisholm, R.L.; Dodson, R.J.; Hartline, E.; et al. The Gene Ontology Resource: Enriching a GOld Mine. *Nucleic Acids Res.* **2021**, *49*, D325–D334. [CrossRef]
38. Savage, S.R.; Shi, Z.; Liao, Y.; Zhang, B. Graph Algorithms for Condensing and Consolidating Gene Set Analysis Results. *Mol. Cell. Proteomics* **2019**, *18*, S141–S152. [CrossRef] [PubMed]
39. Morris, J.H.; Apeltsin, L.; Newman, A.M.; Baumbach, J.; Wittkop, T.; Su, G.; Bader, G.D.; Ferrin, T.E. ClusterMaker: A Multi-Algorithm Clustering Plugin for Cytoscape. *BMC Bioinform.* **2011**, *12*, 1–14. [CrossRef]
40. Shannon, P. Cytoscape: A Software Environment for Integrated Models of Biomolecular Interaction Networks. *Genome Res.* **2003**, *13*, 2498–2504. [CrossRef]
41. Gürke, J.; Schindler, M.; Pendzialek, S.M.; Thieme, R.; Grybel, K.J.; Heller, R.; Spengler, K.; Fleming, T.P.; Fischer, B.; Navarrete Santos, A. Maternal Diabetes Promotes MTORC1 Downstream Signalling in Rabbit Preimplantation Embryos. *Reproduction* **2016**, *151*, 465–476. [CrossRef]
42. Shao, W.-J.; Tao, L.-Y.; Xie, J.-Y.; Gao, C.; Hu, J.-H.; Zhao, R.-Q. Exposure of Preimplantation Embryos to Insulin Alters Expression of Imprinted Genes. *Comp. Med.* **2007**, *57*, 482–486. [PubMed]
43. Schindler, M.; Pendzialek, S.M.; Grybel, K.; Seeling, T.; Santos, A.N. Metabolic Profiling in Blastocoel Fluid and Blood Plasma of Diabetic Rabbits. *Int. J. Mol. Sci.* **2020**, *21*, 919. [CrossRef] [PubMed]
44. Jiménez, A.; Madrid-Bury, N.; Fernández, R.; Pérez-Garnelo, S.; Moreira, P.; Pintado, B.; de la Fuente, J.; Gutiérrez-Adán, A. Hyperglycemia-Induced Apoptosis Affects Sex Ratio of Bovine and Murine Preimplantation Embryos. *Mol. Reprod. Dev.* **2003**, *65*, 180–187. [CrossRef] [PubMed]
45. Moley, K.H. Diabetes and Preimplantation Events of Embryogenesis. *Semin. Reprod. Endocrinol.* **1999**, *17*, 137–151. [CrossRef] [PubMed]
46. Pampfer, S. Apoptosis in Rodent Peri-Implantation Embryos: Differential Susceptibility of Inner Cell Mass and Trophectoderm Cell Lineages—A Review. *Placenta* **2000**, *21*, 3–10. [CrossRef]
47. Harvey, M.B.; Kaye, P.L. Insulin Increases the Cell Number of the Inner Cell Mass and Stimulates Morphological Development of Mouse Blastocysts in Vitro. *Development* **1990**, *110*, 963–967. [CrossRef]
48. Gardner, H.G.; Kaye, P.L. Insulin Increases Cell Numbers and Morphological Development in Mouse Pre-Implantation Embryos in Vitro. *Reprod. Fertil. Dev.* **1991**, *3*, 79–91. [CrossRef]
49. Augustin, R.; Pocar, P.; Wrenzycki, C.; Niemann, H.; Fischer, B. Mitogenic and Anti-Apoptotic Activity of Insulin on Bovine Embryos Produced in Vitro. *Reproduction* **2003**, *126*, 91–99. [CrossRef]
50. Chi, M.M.-Y.; Schlein, A.L.; Moley, K.H. High Insulin-Like Growth Factor 1 (IGF-1) and Insulin Concentrations Trigger Apoptosis in the Mouse Blastocyst via Down-Regulation of the IGF-1 Receptor. *Endocrinology* **2000**, *141*, 4784–4792. [CrossRef]
51. Kaneko, K.J. *Metabolism of Preimplantation Embryo Development: A Bystander or an Active Participant?* 1st ed.; Elsevier Inc.: Amsterdam, The Netherlands, 2016; Volume 120, ISBN 9780128014288.
52. May-Panloup, P.; Boguenet, M.; El Hachem, H.; Bouet, P.E.; Reynier, P. Embryo and Its Mitochondria. *Antioxidants* **2021**, *10*, 139. [CrossRef]

53. Leese, H.J.; Conaghan, J.; Martin, K.L.; Hardy, K. Early Human Embryo Metabolism. *BioEssays* **1993**, *15*, 259–264. [CrossRef] [PubMed]
54. Liu, G.Y.; Sabatini, D.M. MTOR at the Nexus of Nutrition, Growth, Ageing and Disease. *Nat. Rev. Mol. Cell Biol.* **2020**, *8*, 183–203. [CrossRef] [PubMed]
55. Cheng, Z.; Tseng, Y.; White, M.F. Insulin Signaling Meets Mitochondria in Metabolism. *Trends Endocrinol. Metab.* **2010**, *21*, 589–598. [CrossRef]
56. Sies, H.; Jones, D.P. Reactive Oxygen Species (ROS) as Pleiotropic Physiological Signalling Agents. *Nat. Rev. Mol. Cell Biol.* **2020**, *21*, 363–383. [CrossRef] [PubMed]
57. Albensi, B.C. What Is Nuclear Factor Kappa B (NF-KB) Doing in and to the Mitochondrion? *Front. Cell Dev. Biol.* **2019**, *7*, 154. [CrossRef] [PubMed]
58. Bertrand, F.; Philippe, C.; Antoine, P.J.; Baud, L.; Groyer, A.; Capeau, J.; Cherqui, G. Insulin Activates Nuclear Factor KB in Mammalian Cells through a Raf-1- Mediated Pathway. *J. Biol. Chem.* **1995**, *270*, 24435–24441. [CrossRef] [PubMed]
59. Morgan, M.J.; Liu, Z. Crosstalk of Reactive Oxygen Species and NF-KB Signaling. *Cell Res.* **2011**, *21*, 103–115. [CrossRef]
60. Reid, M.A.; Dai, Z.; Locasale, J.W. The Impact of Cellular Metabolism on Chromatin Dynamics and Epigenetics. *Nat. Cell Biol.* **2017**, *19*, 1298–1306. [CrossRef] [PubMed]
61. Martínez-Reyes, I.; Chandel, N.S. Mitochondrial TCA Cycle Metabolites Control Physiology and Disease. *Nat. Commun.* **2020**, *11*, 102. [CrossRef]
62. Arab, K.; Karaulanov, E.; Musheev, M.; Trnka, P.; Schäfer, A.; Grummt, I.; Niehrs, C. GADD45A Binds R-Loops and Recruits TET1 to CpG Island Promoters. *Nat. Genet.* **2019**, *51*, 217–223. [CrossRef]
63. Qian, X.; Zhang, Y. EZH2 Enhances Proliferation and Migration of Trophoblast Cell Lines by Blocking GADD45A-Mediated P38/MAPK Signaling Pathway. *Bioengineered* **2022**, *13*, 12583–12597. [CrossRef] [PubMed]
64. Goller, T.; Vauti, F.; Ramasamy, S.; Arnold, H.-H. Transcriptional Regulator BPTF/FAC1 Is Essential for Trophoblast Differentiation during Early Mouse Development. *Mol. Cell. Biol.* **2008**, *28*, 6819–6827. [CrossRef] [PubMed]
65. Landry, J.; Sharov, A.A.; Piao, Y.; Sharova, L.V.; Xiao, H.; Southon, E.; Matta, J.; Tessarollo, L.; Zhang, Y.E.; Ko, M.S.H.; et al. Essential Role of Chromatin Remodeling Protein Bptf in Early Mouse Embryos and Embryonic Stem Cells. *PLoS Genet.* **2008**, *4*, e1000241. [CrossRef]
66. Beato, M.; Sharma, P. Peptidyl Arginine Deiminase 2 (PADI2)-Mediated Arginine Citrullination Modulates Transcription in Cancer. *Int. J. Mol. Sci.* **2020**, *21*, 1351. [CrossRef]
67. Yoshida, K.; Maekawa, T.; Ly, N.H.; Fujita, S.; Muratani, M.; Ando, M.; Katou, Y.; Araki, H.; Miura, F.; Shirahige, K.; et al. ATF7-Dependent Epigenetic Changes are Required for the Intergenerational Effect of a Paternal Low-Protein Diet. *Mol. Cell* **2020**, *78*, 445–458.e6. [CrossRef] [PubMed]
68. Liu, Y.; Maekawa, T.; Yoshida, K.; Muratani, M.; Chatton, B.; Ishii, S. The Transcription Factor ATF7 Controls Adipocyte Differentiation and Thermogenic Gene Programming. *iScience* **2019**, *13*, 98–112. [CrossRef] [PubMed]
69. Ralston, A.; Cox, B.J.; Nishioka, N.; Sasaki, H.; Chea, E.; Rugg-Gunn, P.; Guo, G.; Robson, P.; Draper, J.S.; Rossant, J. Gata3 Regulates Trophoblast Development Downstream of Tead4 and in Parallel to Cdx2. *Development* **2010**, *137*, 395–403. [CrossRef]
70. Chi, F.; Sharpley, M.S.; Nagaraj, R.; Roy, S.S.; Banerjee, U. Glycolysis-Independent Glucose Metabolism Distinguishes TE from ICM Fate during Mammalian Embryogenesis. *Dev. Cell* **2020**, *53*, 9–26.e4. [CrossRef] [PubMed]
71. Murray, A.; Sienerth, A.R.; Hemberger, M. Plet1 Is an Epigenetically Regulated Cell Surface Protein That Provides Essential Cues to Direct Trophoblast Stem Cell Differentiation. *Sci. Rep.* **2016**, *6*, 25112. [CrossRef]
72. Ono, R.; Nakamura, K.; Inoue, K.; Naruse, M.; Usami, T.; Wakisaka-Saito, N.; Hino, T.; Suzuki-Migishima, R.; Ogonuki, N.; Miki, H.; et al. Deletion of Peg10, an Imprinted Gene Acquired from a Retrotransposon, Causes Early Embryonic Lethality. *Nat. Genet.* **2006**, *38*, 101–106. [CrossRef] [PubMed]
73. Chen, A.C.H.; Lee, Y.L.; Fong, S.W.; Wong, C.C.Y.; Ng, E.H.Y.; Yeung, W.S.B. Hyperglycemia Impedes Definitive Endoderm Differentiation of Human Embryonic Stem Cells by Modulating Histone Methylation Patterns. *Cell Tissue Res.* **2017**, *368*, 563–578. [CrossRef] [PubMed]
74. Armistead, B.; Kadam, L.; Drewlo, S.; Kohan-Ghadr, H.-R.R. The Role of NFκB in Healthy and Preeclamptic Placenta: Trophoblasts in the Spotlight. *Int. J. Mol. Sci.* **2020**, *21*, 1775. [CrossRef]
75. Marchand, M.; Horcajadas, J.A.; Esteban, F.J.; McElroy, S.L.; Fisher, S.J.; Giudice, L.C. Transcriptomic Signature of Trophoblast Differentiation in a Human Embryonic Stem Cell Model. *Biol. Reprod.* **2011**, *84*, 1258–1271. [CrossRef] [PubMed]
76. Ansell, J.D.; Snow, M.H.L. The Development of Trophoblast in Vitro from Blastocysts Containing Varying Amounts of Inner Cell Mass. *J. Embryol. Exp. Morphol.* **1975**, *33*, 177–185. [CrossRef] [PubMed]

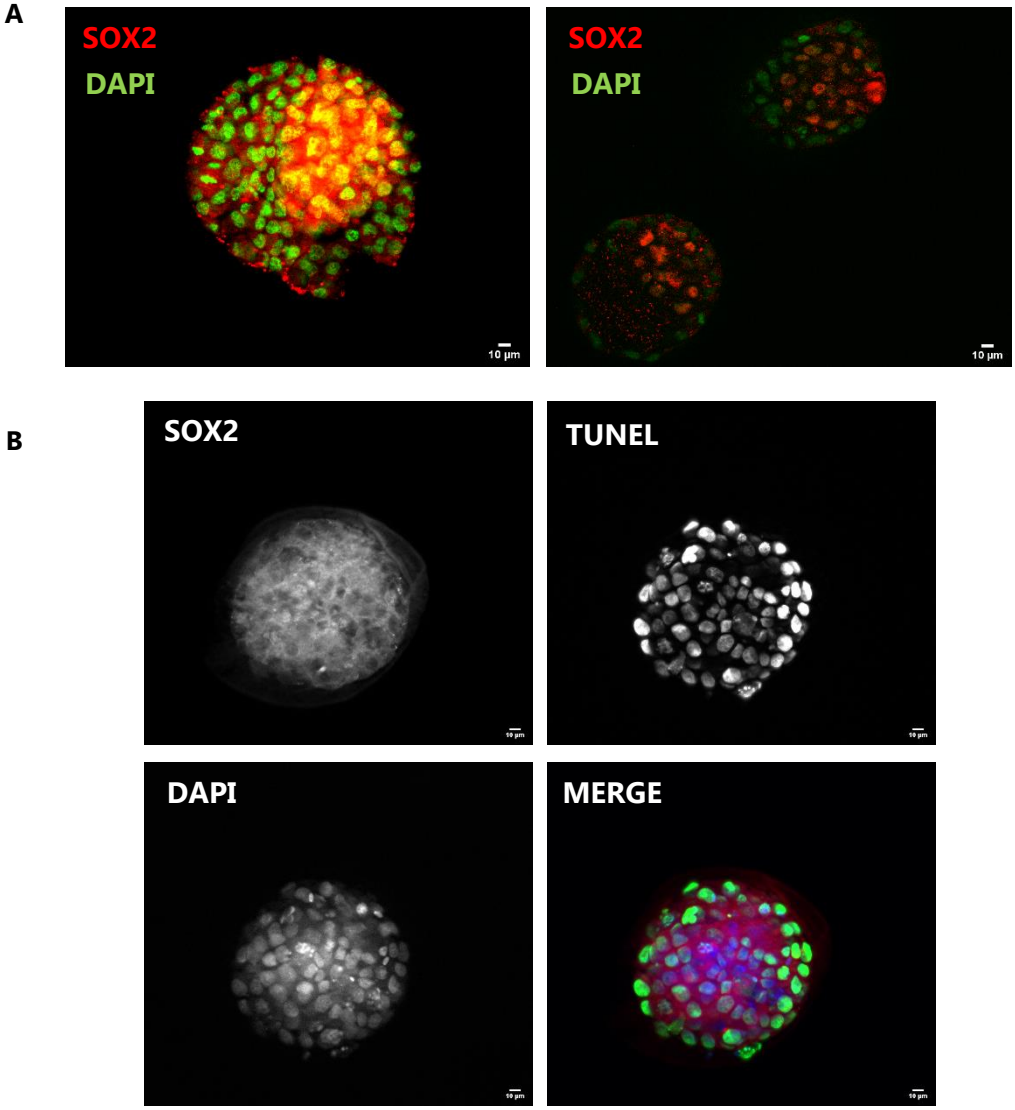

Figure 26: Immunostaining of SOX2 in rabbit *in vitro*-developed blastocysts.
A) *SOX2* (red) immunostaining counterstained with DAPI (green) in *in vitro*-developed blastocysts. *SOX2* dilution 1 :100 (left) or 1 :200 (right). B) *SOX2* immunostaining coupled with TUNEL assay in *in vitro*-developed blastocysts incubated with RNase-free DNase as a positive control. From left to right, *SOX2* (1:200), TUNEL positive cells, DAPI and merge of *SOX2* (red), TUNEL positive cells (green) and DAPI (bleu). Scale bar: 10 µm.

Additional results

1. Lineage-specific markers of rabbit early blastocysts

Exposure to HG or HGI led to increased total cell numbers at the blastocyst stage and gene expression changes related to cell proliferation and apoptosis in both ICM and TE.
Therefore, to assess cell proliferation and apoptosis in exposed embryos precisely in the ICM and TE, EdU incorporation and TUNEL assays were used.

Our initial objective was to use a marker of the ICM or TE to discriminate cells of both lineage and to include the immunostaining for the detection of this marker within the EdU and TUNEL protocols. However, despite our attempts, we were not able to identify a suitable marker. The results summarized here to describe the attempts to identify an ICM-specific marker.
First, we selected a few known ICM and TE markers identified in other mammalian species, as described in the Introduction (Chapter 3, section 1.2.2), such as CDX2 for the TE, and OCT4 (*POU5F1*), SOX2, and NANOG for the ICM.
Transcriptomic data generated in our model showed similar levels of *CDX2* transcripts between CNTRL ICM (RLOG = 6.7) and CNTRL TE (RLOG = 6.7) from *in vitro*-developed embryos. Based on these results, we focused on OCT4, SOX2, and NANOG as potential ICM markers. Transcriptomic data from *in vitro*-developed embryos showed that OCT4 transcript level were similar between CNTRL ICM (RLOG =15.6) and CNTRL TE (RLOG =15.3). However, SOX2 (CNTRL ICM, RLOG = 10.7 and CNTRL TE, RLOG =8.3) and NANOG (CNTRL ICM, RLOG = 12.8 and CNTRL TE, RLOG = 9.3) had slightly higher transcripts in CNTRL ICM than in CNTRL TE. Both SOX2 and NANOG had not yet been tested in *in vitro*-developed rabbit embryos in the team. *In vivo* and *in vitro* rabbit embryos present a certain delay in developmental timing, which could influence the expression of lineage-specific markers. Therefore, we tested SOX2 and NANOG by immunostaining to examine whether they showed specific staining in the ICM in *in vitro*-developed embryos.

Immunostaining of *SOX2* was performed in *in vitro*-developed rabbit blastocysts (Figure 26A). Despite an increased signal colocalizing with DAPI around the ICM, SOX2 staining was heterogeneous, with non-specific staining in a few TE cells (Figure 26A). Nevertheless, to test whether SOX2 immunostaining non-specific binding may be improved when coupled with TUNEL assay, *in vitro*-developed blastocysts were treated with DNAse I to induce DNA fragmentation (positive control), and TUNEL assay was followed by SOX2 immunostaining, as described in the paper and in the methods section (Figure 26B). SOX2 immunostaining coupled with TUNEL assay exhibited non-specific staining (Figure 26B). In parallel, immunostaining of NANOG was also performed in *in vitro*-developed blastocysts. However, a similar non-specific pattern as detected with SOX2 was observed (not shown).

Taken together these results, we decided not to pursue further the inclusion of lineage-specific markers in the assessment of cell proliferation and apoptosis by EdU incorporation and TUNEL assays. As an alternative, both protocols were tested and shown to be successful in isolated ICM and TE after immunosurgery, with minor modifications. Thus, the same experimental strategy used for RNA-seq was employed in these assays. Moreover, because the ICM of embryos exposed to HG or HGI showed

overexpression of TE genes (i.e., *PLET1*, *GATA3*, *PEG10*) as detailed in the Paper, the use of lineage-specific markers may lead to inconsistencies.

Summary of Part I

The prevalence of metabolic diseases is increasing worldwide, with more women entering pregnancy with metabolic dysregulations such as hyperglycemia and/or hyperinsulinemia.
Development in suboptimal environments, especially during critical periods, is associated with short-and long-term consequences in the offspring, as explained by the concept of DOHaD. The preimplantation embryo, corresponding to the first days of development, is highly sensitive to environmental cues and perturbations in its surrounding environment. Key processes take place at this developmental stage, including the reprogramming of parental genomes, the embryonic genome activation, and the first specification event giving rise to the ICM and TE, the progenitor of the future individual, and the embryonic portion of the placenta, respectively. Furthermore, preimplantation embryos strictly depend on the maternal nutritional and metabolic status through the oviduct and uterine fluid bathing the developing embryo. Both glucose and insulin are present in the oviduct and uterine fluid and are influenced by maternal circulating plasma concentrations.

The aim of this study was to investigate the effects of high glucose and/or high insulin exposure on preimplantation development. Thus, one-cell rabbit embryos were cultured *in vitro* until the blastocyst stage in control (CNTRL), high insulin (HI), high glucose (HG) or high glucose and high insulin (HGI) conditions. In *in vitro*-developed embryos, the developmental competence and total cell number at the blastocyst stage were determined. To investigate the effects of these conditions on the gene expression programs of both lineages of *in vitro*-developed blastocysts, the ICM and TE were isolated, and transcriptome analysis by RNA-seq was performed.

Analysis of developmental competence, total cell number, and transcriptome of the ICM and TE from exposed embryos showed the following common and exclusive responses:

- High insulin supplementation during preimplantation development in the rabbit did not affect the development competence nor the total cell number of blastocysts. However, minor transcriptome changes were identified in the ICM and TE. Both lineages exposed to high insulin showed gene expression changes related to transcription and translation and OXPHOS. In addition, the ICM and TE showed transcriptome changes related to β-oxidation and NF-kB signaling, respectively.

- High glucose supplementation during preimplantation development increased blastocyst formation and total cell number. Transcriptome analysis of both lineages showed gene expression changes related to transcription, translation, cell cycle, energy metabolism, more precisely OXPHOS in the ICM and glycolysis in the TE, and NF-kB and WNT signaling. In addition, the ICM showed the overexpression of two genes implicated in the trophoblast lineage, *GATA3* and *PLET1*, whereas the TE showed transcriptome changes related to mTOR signaling, epigenetic regulation, and TGF-β signaling. Assessment of cell proliferation and apoptosis in both lineages by EdU incorporation and TUNEL assays showed two opposite patterns. High glucose resulted in an increased number of apoptotic cells and a reduced number of proliferating cells in the ICM, whereas the TE showed an increased number of proliferating cells and a reduced number of apoptotic cells.

- High glucose and high insulin supplementation during preimplantation development led to increased blastocyst formation and total cell number. Transcriptome analysis of both lineages showed gene expression changes related to transcription, translation, cell cycle, OXPHOS, ROS, and NF-kB signaling. In addition, the ICM showed the overexpression of two genes implicated in the trophoblast lineage, *PEG10* and *PLET1*, whereas the TE showed transcriptome changes related to WNT signaling. Investigation of cell proliferation and apoptosis in both lineages by EdU incorporation and TUNEL assays did not show significant changes in the ICM, whereas the TE showed an increased number of proliferating cells.

Hence, this study demonstrated that preimplantation embryos exposed to high glucose or high insulin, alone or in combination, exhibit transcriptome changes in a lineage-specific manner. Overall the identified transcriptome changes in the ICM and TE suggest an altered embryo energy metabolism, cell signaling, and cellular homeostasis. High glucose and/or high insulin exposure as early as in the preimplantation period may compromise the development of future individual and placenta and may lead to short and long-term consequences in the offspring.

PART II: Accessible-chromatin profiling of rabbit preimplantation embryos developed in high glucose and/or high insulin

In mammals, there are two periods characterized by extensive epigenetic reprogramming and chromatin remodeling: gametogenesis and preimplantation development (Cantone & Fisher, 2013). In preimplantation embryos, changes in chromatin dynamics are associated with three major events: the reprogramming of parental genomes, EGA, and the lineage specification of the ICM and TE (Cantone & Fisher, 2013; Gerri, Menchero, et al., 2020). A finely tuned epigenetic regulation of each of these events is paramount to allow proper embryonic development.

Epigenetic mechanisms are interlinked with cellular metabolism and are sensitive to metabolic cues (Dai et al., 2020). Glucose, fatty acids, AAs entering metabolic pathways generate several metabolites that are used as substrates and cofactors for chromatin-modifying enzymes (Dai et al., 2020). This is the case of glucose-derived acetyl-CoA by supplying the acetyl group for acetylation of proteins, including histones (Dai et al., 2020). Moreover, as described in the Introduction of this thesis (Chapter 2, section 4.2), increased glucose availability and glycolysis enhances acetyl-CoA production and modules global histone acetylation levels and, consequently gene expression regulation (Dai et al., 2020).
Concerning insulin, its influence on epigenetic regulation has received less attention. It is no doubt that insulin, through the activation of the insulin signaling pathway, influences the downstream transcriptional regulation of target genes (Boucher et al., 2014), thus influencing the local chromatin configuration of its targets. Interestingly, it was recently shown that the insulin receptor (IR) translocates from the cell surface to the nucleus and associates with promoters and the RNA Polymerase II genome-wide to regulate the expression of genes related to insulin action such as lipid metabolism and protein synthesis (Hancock et al., 2019).
Thus, both glucose metabolism and insulin signaling influence epigenetic regulation. In skeletal muscle myoblasts, insulin in normal or hyperglycemic conditions led to methylation, phosphorylation and acetylation changes in histone H3 (Kabra et al., 2009). Similarly, ROS increased production by insulin and hyperglycemic conditions resulted in histone H3 PTMs changes (Kabra et al., 2009).

Our previous work (Part I, paper) has shown that rabbit embryos exposed to HI, HG or HGI exhibited changes in ICM and TE transcriptomes in a wide range of cellular processes. Of these, HG and HGI embryos showed the overrepresentation of transcription together with the differential expression of transcription factors and, especially in HG TE, of genes implicated in epigenetic regulation (i.e., chromatin remodelers and histone methyltransferases and demethylases) (Appendix 6). These results questioned us whether the epigenetic landscape of embryos exposed to a high glucose, or high glucose and high insulin environment may be impacted. Moreover, genes associated with the TE lineage, trophoblast differentiation, and placental development were overexpressed in HG or HGI ICM. Considering the recently described role of glucose metabolism in the specification of the TE in the mouse (F. Chi et al., 2020), it interrogated us whether commitment to the ICM would be similarly perturbed by the glucose-rich environment.

Furthermore, epigenetic mechanisms are hypothesized to orchestrate the memory of early life experiences such as development in a perturbed metabolic environment and to contribute to the short- and long-term consequences in the offspring, as described by the DOHaD. Therefore, investigation of

the epigenetic regulation of the two cell lineages in early embryos responsible for the development of the future individual and the fetal portion of the placenta, exposed to high glucose and/or high insulin, may contribute to understand the developmental programming of the offspring developed in a diabetic environment.

Perturbation in DNA methylation profiles has been frequently used to evaluate the effects of early life exposures in the offspring (P. Chen et al., 2017; Koeck et al., 2022; Shao et al., 2007). In our model, most of our findings suggest rather changes in chromatin dynamics associated with transcription regulation. Therefore, to examine chromatin dynamics in relationship with gene expression, we next decided to profile the chromatin accessibility of the ICM and TE of embryos exposed to high glucose, or high glucose and high insulin or developed in our control condition. Because minor transcriptome changes with no DEG implicated in epigenetic regulation were detected in ICM and TE exposed to HI, we decided to further investigate HG and HGI exposed embryos.
For this, we have implemented the Assay for Transposase-Accessible Chromatin using sequencing (ATAC-seq) protocol developed by Buenrostro et al., 2015 on rabbit embryos, and performed ATAC-seq on CNTRL, HG or HGI ICM and TE from *in vitro*-developed blastocysts.

Compared to other chromatin accessibility profiling methods such as DNase-seq, which requires around 1-10 million cells, ATAC-seq has high sensitivity on low-input cell numbers (500 – 50, 000 cells), ideal for studies with limited biological material (Minnoye et al., 2021). Indeed, adaptations of the ATAC-seq protocol using as few as 20 cells have been previously described (Wu et al., 2018). In addition, ATAC-seq has an overall simple and fast protocol that can be performed in less than a day, depending on the cell type (Minnoye et al., 2021). Another important advantage of this method is that ATAC-seq has been previously performed in mouse, bovine and human preimplantation embryos (Halstead et al., 2020; L. Liu et al., 2019; Ming et al., 2020; Wu et al., 2018).

Gene regulation influences chromatin states. Upon a given signal, i.e., development, growth, stress, nucleosome occupancy change within a genomic location to allow or restrict accessibility to *cis*-regulatory elements, i.e., enhancers and promoters, to transcriptional regulators such as transcription factors (Minnoye et al., 2021). Decreased nucleosome occupancy within *cis*-regulatory elements is suggestive of an active genomic region associated with transcriptional activation (C. K. Lee et al., 2004). On the contrary, increased nucleosome occupancy at *cis*-regulatory elements is associated with transcriptional repression. Mapping chromatin accessibility genome-wide allows to obtain a picture of the *cis*-regulatory elements that are potentially associated with transcription activity in a cell (C. K. Lee et al., 2004). By mapping chromatin accessibility in ICM and TE of exposed embryos, we may identify chromatin changes associated to promoters or putative enhancers that were influenced by high glucose and/or high insulin. Analysis of these regulatory elements and their correlation with transcriptome data could provide more insight into the molecular mechanisms behind the transcriptome changes previously identified and potentially identify core genes and/or signaling pathways that are involved in the response of the ICM and TE to high glucose alone or in combination with high insulin.

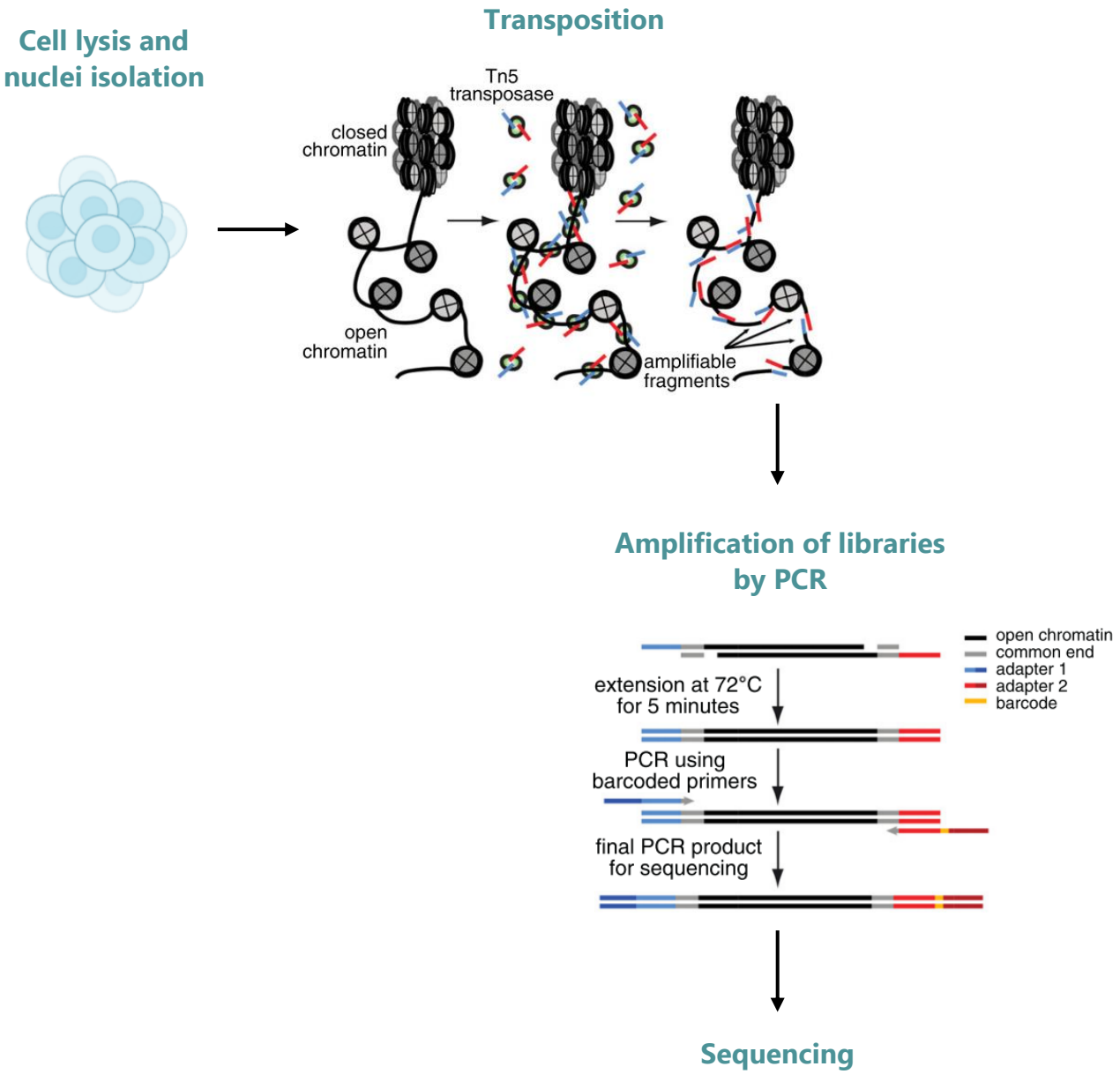

Figure 27: Transposase-accessible chromatin using sequencing (ATAC-seq) assay for chromatin accessibility profiling.

The main steps of the ATAC-seq protocol consist of the cell lysis and nuclei isolation, followed by the nuclei exposition to the hyperactive DNA transposase (Tn5) preloaded with sequencing adaptors that simultaneously cleaves and tags accessible chromatin regions (tagmentation, also referred to as transposition). Next, the generated library of fragments is purified, PCR-amplified and sequenced. Adapted from Buenrostro et al., 2013.

RESULTS

This second part of my thesis work will be divided into two parts. The first part corresponds to the attempts and subsequent establishment of an ATAC-seq protocol suitable for rabbit ICM and TE from *in vitro*-developed embryos. The second part corresponds to the chromatin profiling of ICM and TE from embryos exposed *in vitro* to CNTRL, HG or HGI.

The first step of the ATAC-seq protocol consists of cell lysis and nuclei isolation (Figure 27) (Buenrostro et al., 2013). Nuclei pellets are then exposed to the Tn5 transposase (Buenrostro et al., 2013). The Tn5 transposase consists on a genetically engineered hyperactive DNA transposase preloaded with high-throughput sequencing adaptors (Buenrostro et al., 2013, 2015). The Tn5 simultaneously cleaves and tags accessible chromatin regions, including nucleosome-depleted genomic regions, following a "cut and paste" mechanism (Buenrostro et al., 2013, 2015). The generated DNA fragments are then purified, PCR-amplified, and sequenced by next-generation sequencing techniques (Buenrostro et al., 2013, 2015) (Figure 27).

1. ATAC-seq library preparation on D6 *in vivo* rabbit embryos and mESCs

The initial objective was to test the ATAC-seq protocol published by Buenrostro et al., 2015 in *in vivo* D6 rabbit embryos since the mean total cell number (*n*= ~80 000 to 100 000, Fischer et al., 2012) would allow to perform several experiments without the need of a large number of embryos. Additionally, we could take advantage of these first assays to generate ATAC-seq libraries from the EPI, PrE and TE samples that would be useful for other ongoing research projects of the team. However, after two independent attempts to dissociate EPI, PrE and TE from dissected D6 embryos with 0.05% or 0.25% trypsin (1x), TrypLE (1x) or Accutase (Innovative Cell Technologies) for 5-10 min, we were unable to obtain nearly any cell dissociation of the three lineages. Although the TE appeared to dissociate slightly in trypsin 0.05%, long incubation periods with trypsin can lead to significant protein degradation and impact subsequent chromatin analysis. Compared to the early blastocyst stage, cell dissociation of D6 blastocysts lineages require particular treatment.

The ICM and TE of *in vitro*-developed blastocysts may not require such a time-consuming cell dissociation protocol. In addition, because implementing a new protocol may require a considerable amount of experiments and replicates, which would involve the use of a larger number of animals, we decided to work with mESCs, which were already available in the laboratory. Because our goal was to use the minimum amount of ICM and TE cells to obtain good quality ATAC-seq libraries, using mESCs allows to more easily quantify the number of cells and to test the protocol with different cell inputs.

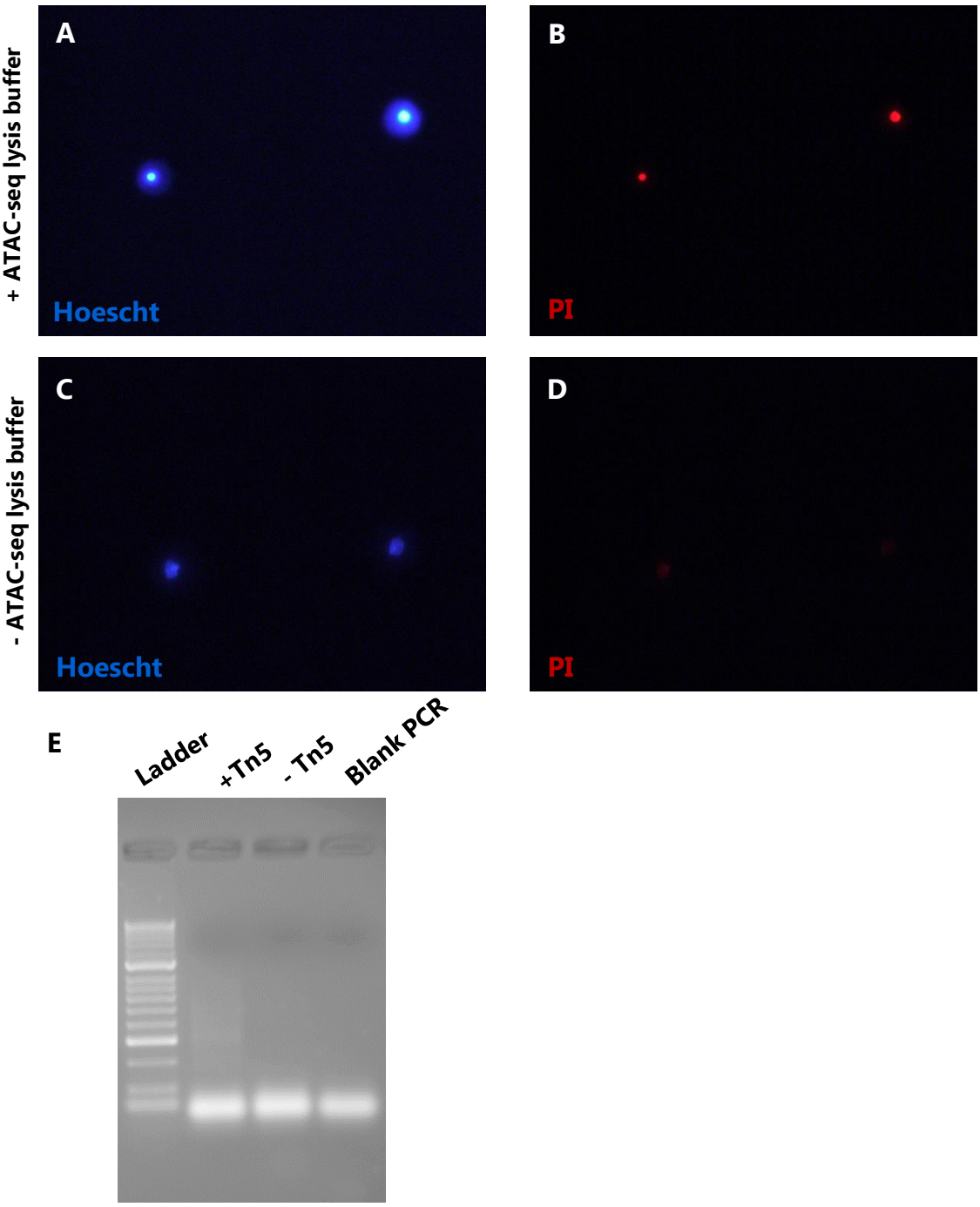

Figure 28: Verification of lysis and transposition of the ATAC-seq protocol on mESCs.
Mouse ESCs stained with Hoechst (left) and propodium iodide (PI) (right) after centrifugation with ATAC-seq cell lysis buffer (A-B) or DPBS (C-D) at 4 °C, 500 rcf for 10 min. E) Nuclear pellets from mESCs underwent transposition with TDE1 enzyme (Tn5 transposase from Nextera DNA Library Prep Kit, Illumina) or with nuclease-free H_2O. The transposed content was then amplified by PCR and run on 2% agarose gel. Lines correspond to: 1) HypperLadder (50 – 2000 bp, Meridian Bioscience), 2) PCR product from nuclear pellets transposed with Tn5 in the mix. 3) PCR product from nuclear pellets transposed with nuclease-free H_2O in the mix instead of Tn5, 4) Blank PCR.

1.1 Cell lysis and transposition for ATAC-seq library preparation using mESCs

The first step of the ATAC-seq protocol involves cell lysis. To confirm this first step, and because the ATAC-seq cell lysis buffer from Buenrostro et al., 2015 was prepared in-house, ~50,000 mESCs were either centrifuged with the ATAC-seq lysis buffer or with DPBS.
Next, we stained each lysate with Hoescht, a fluorescent dye that preferentially binds adenine-thymine (A-T)-rich sequences of the minor grove of DNA and is cell-permeable and with propidium iodide (PI), a fluorescent dye that binds DNA by intercalating between bases and is not cell membrane-permeable, to detect dead cells.
Nuclei from cells centrifuged with the ATAC-seq lysis buffer were Hoescht positive, PI positive. (Figure 28A, B). On the contrary, nuclei from cells centrifuged with DPBS were Hoescht positive, PI negative. Thus, these results confirmed the efficacity of the ATAC-seq lysis buffer (Figure 28C, D).

The next step was to confirm the transposition event. Nuclei from ~50,000 lysed mESCs underwent transposition with either the Tn5 transposase or with nuclease-free H_2O in the transposition reaction mixture (Figure 28E).
To examine whether the transposition with the Tn5 generated different fragments, each sample was PCR-amplified and run on 2% agarose gel. Nuclear pellets that underwent transposition with the Tn5 transposase Tn5 showed a slight smear on agarose gel (Figure 28E). Nuclear pellets that underwent transposition with nuclease-free H_2O instead of the Tn5, or the blank PCR did not show any smear on gel. This suggested the generated of fragments of different sizes by transposition with the Tn5 enzyme after cell lysis.

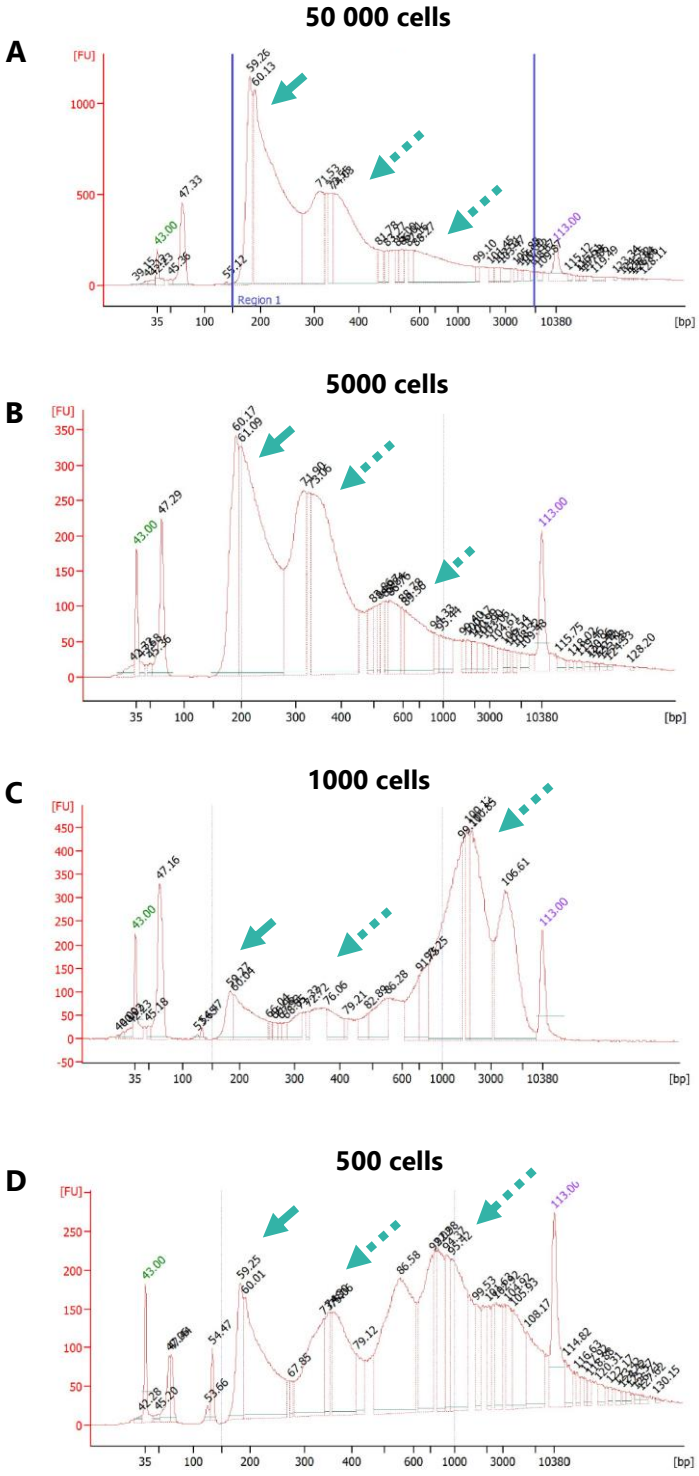

Figure 29: Electropherogram of mESCs ATAC-seq libraries using different cell inputs.
A-D) ATAC-seq libraries from 50 000, 5000, 1000 and 500 mESCs before size-selection. Electropherograms display fragment length in base pairs (bp) versus fluorescence intensity (FU). Lower and upper markers are shown in green and purple, respectively. In A-B, a higher enriched peak corresponding to nucleosome-free fragments of 150-250 bp (solid arrow) is shown, followed by a DNA laddering pattern indicative of poly-nucleosome fractions (mono-nucleosome, di-nucleosome, tri-nucleosome) (dotted arrow). In B-C, a lower enriched peak corresponding to nucleosome-free fragments is observed, followed by a higher enrichment of poly-nucleosome fractions.

1.2 Quality control of mESCs ATAC-seq libraries

After confirmation that cell lysis and transposition, two key steps for ATAC-seq library preparation worked as expected, we used the same conditions to generate ATAC-seq libraries from 50,000; 5000; 1000 and 500 mESCs.

To investigate whether the generated libraries had the expected DNA laddering profile, quality control of the libraries was performed using the Bioanalyzer (Figure 29). Electropherogram of ATAC-seq library from 50,000 and 5000 mESCs showed an enrichment in nucleosome-free fragments as shown by a higher peak of 150-250 bp, followed by the expected DNA laddering pattern indicative of poly-nucleosome fractions (mono-nucleosome, di-nucleosome, tri-nucleosome) (Figure 29A, B). The electropherogram of 1000 and 500 mESCs showed a lower enrichment in nucleosome-free fragments and higher enrichment of fragments of 600 to 1000 bp (Figure 29C, D). The ATAC-seq libraries from 1000 and 500 mESCs may be improved by performing a one-sided size selection to remove larger fragments (>1000 bp). Thus, ATAC-seq libraries prepared from mESCs showed an expected profile.

The next step was to test the protocol on a pool of ICMs and TEs from rabbit embryos developed *in vitro*. Based on Bioanalyzer traces of mESCs ATAC-seq libraries, we decided to use a cell number input between 1000 to 5000 cells to obtain a higher enrichment of nucleosome-free fragments.

2. ATAC-seq library preparation on rabbit ICM and TE from *in vitro*-developed blastocysts (TEST)

During our previous study (Part I paper), we estimated the mean total cell number of each lineage of control blastocysts developed *in vitro* (not shown). Mean total cell numbers were between *n*= 50-100 for ICM and *n*= 200-300 cells for the TE. To obtain between 1000 to 5000 cells per ICM and TE, we decided to pool a minimum of *n*=13-16 ICM or TE.

Pool of *n*=13-16 ICM and TE were obtained from *in vitro*-developed embryos. As performed in Part I, each pool contained ICM and TE originating from the same embryo.

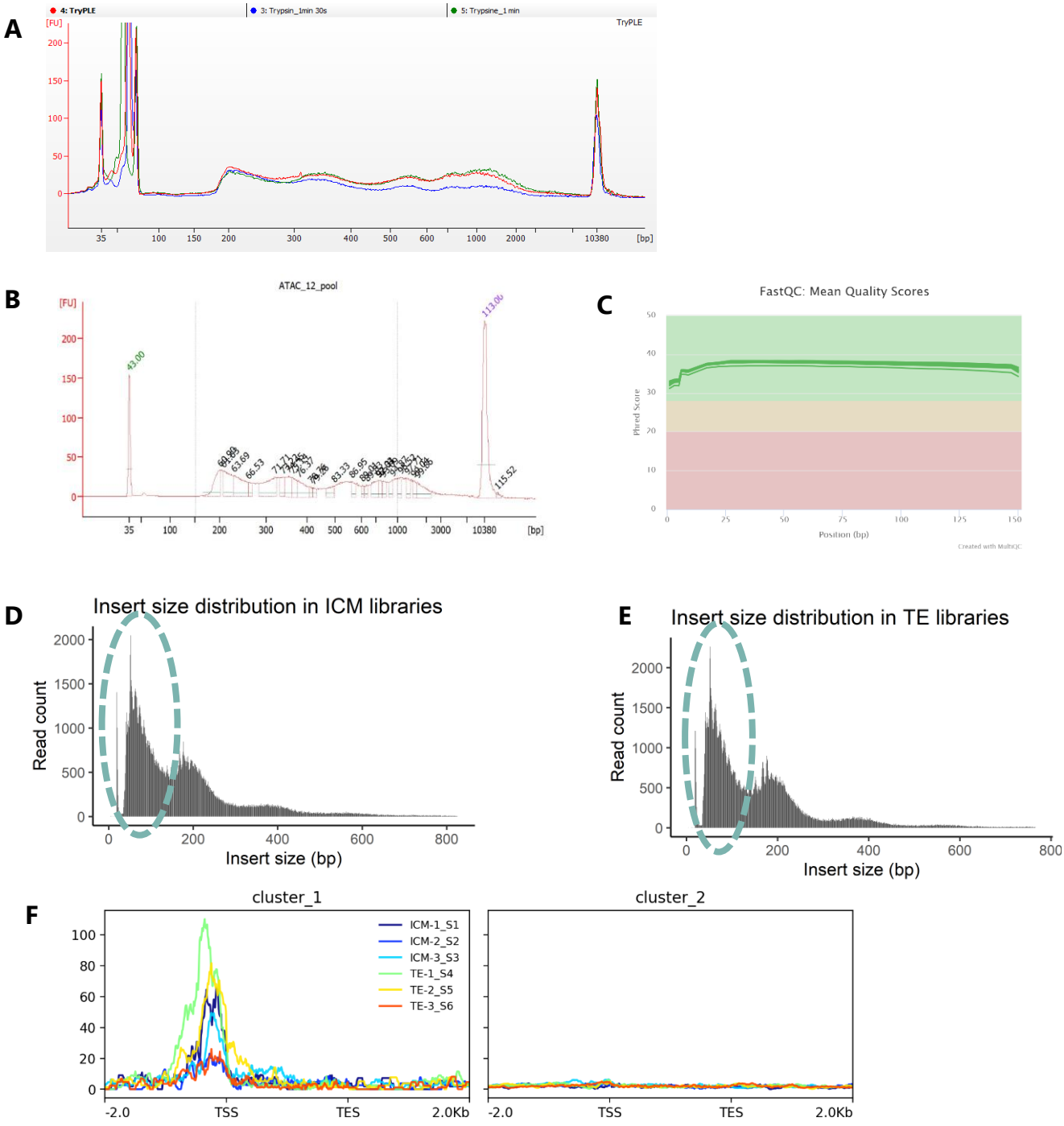

Figure 30: ICM dissociation treatments for preparation of ATAC-seq libraries and quality control of ICM and TE ATAC-seq TEST libraries.

A) Three strategies were performed to dissociate ICM samples: incubation of 0.25% trypsin (1x) for 1 min (green) or 1 min 30s (blue) or with TryPLE (1x) (red). The electropherogram shows three ATAC-seq ICM libraries generated from dissociation strategies. Electropherograms display fragment length in base pairs (bp) versus fluorescence intensity (FU). B) Electropherogram of six ICM and TE ATAC-seq libraries after size-selection. C) MultiQC plot from the control quality sequencing report showing the mean quality score of reads across samples. Phred Score indicates the base quality in sequencing. D-E) Insert size distribution of ICM and TE ATAC-seq datasets. Nucleosome-free inserts are indicated in a dashed circle. F) Average ATAC-seq signal enriched around the TSS (transcription start site) in a group of rabbit genes (cluster 1). TSS and transcription end sites (TES) are shown. ICM samples: ICM-1_S1, ICM dissociated with trypsin 1min 30s; ICM-2_S2; ICM dissociated with TryPLE, ICM-3_S3; ICM dissociated with trypsin 1min. TE samples, TE-1_S4, TE-2_S5, TE-3_S6.

2.1 Dissociation strategies for ICM of *in vitro*-developed embryos

After immunosurgery, the TE is like flat-shaped epithelium, thereby, no dissociation may be required for ATAC-seq library preparation. Therefore, TE ATAC-seq libraries were prepared directly. However, ICM constitutes a more compact cluster of cells, thus, for efficient lysis, three dissociation strategies were evaluated, including the use of trypsin and TryPLE.
Dissociation with trypsin for 1 min 30s or TryPLE resulted in dissociation of the ICM cluster of cells, whereas trypsin for 1 min only led to slight dissociation of ICM cells. A comparative electropherogram of the three ICM traces showed no remarkable changes among the three strategies (Figure 30A). However, incubation for 1 min 30 resulted in slightly lower enrichment in larger fragments (> 400 bp) (Figure 30A).

2.2 Sequencing quality control of ICM and TE TEST ATAC-seq libraries

The next step was to assess the quality of ATAC-seq libraries by sequencing. At the same time, we will be able to examine further the quality of the libraries between the different ICM dissociation strategies. Therefore, following the ATAC-seq protocol modifications presented above, six ATAC-seq TEST libraries were prepared from three ICM samples, which followed the three dissociation strategies and three TE samples. Libraries were pooled, size-selected, and sent to sequencing (Figure 30B and Appendix 9).

To assess the quality of the ATAC-seq libraries, first, we performed a MiSeq Nano Illumina sequencing of 1M reads from the ATAC-seq pool. This short sequencing depth allowed to do a quick overview of the quality of ATAC-seq libraries before proceeding to higher sequencing depth. Examination of the dataset by FastQC plot showed a good mean quality score from sequenced reads across samples (Figure 30C). Furthermore, the insert size distribution showed the enrichment of <200 bp fragments, together with the expected mono-nucleosome and di-nucleosome periodicity of ~200 bp fragments for ICM and TE libraries (Figure 30D, E).

To examine regulatory regions potentially associated with transcriptional activity we focused on promoter regions spanning 2 kb within annotated genes in each direction, potentially covering transcription start site (TSS) and transcription end site (TES).
Plotting of ATAC-seq signal over TSS and TES genomic regions showed enrichment of ATAC-seq signal on TSS of a group of genes suggesting highly open chromatin regions (cluster 1) (Figure 30F). On the contrary, cluster 2 showed genes without ATAC-seq signal enrichment over TSS suggestive of closed chromatin regions, potentially representing non-transcribed genomic regions (Figure 30F).

Taking into consideration the ATAC-seq typical nucleosomal laddering profile and the successful detection of accessible regions showed by the strong enrichment of ATAC-seq reads around TSS, we next proceeded to the sequencing of the six ATAC-seq libraries with higher sequencing depth (~400 M reads).

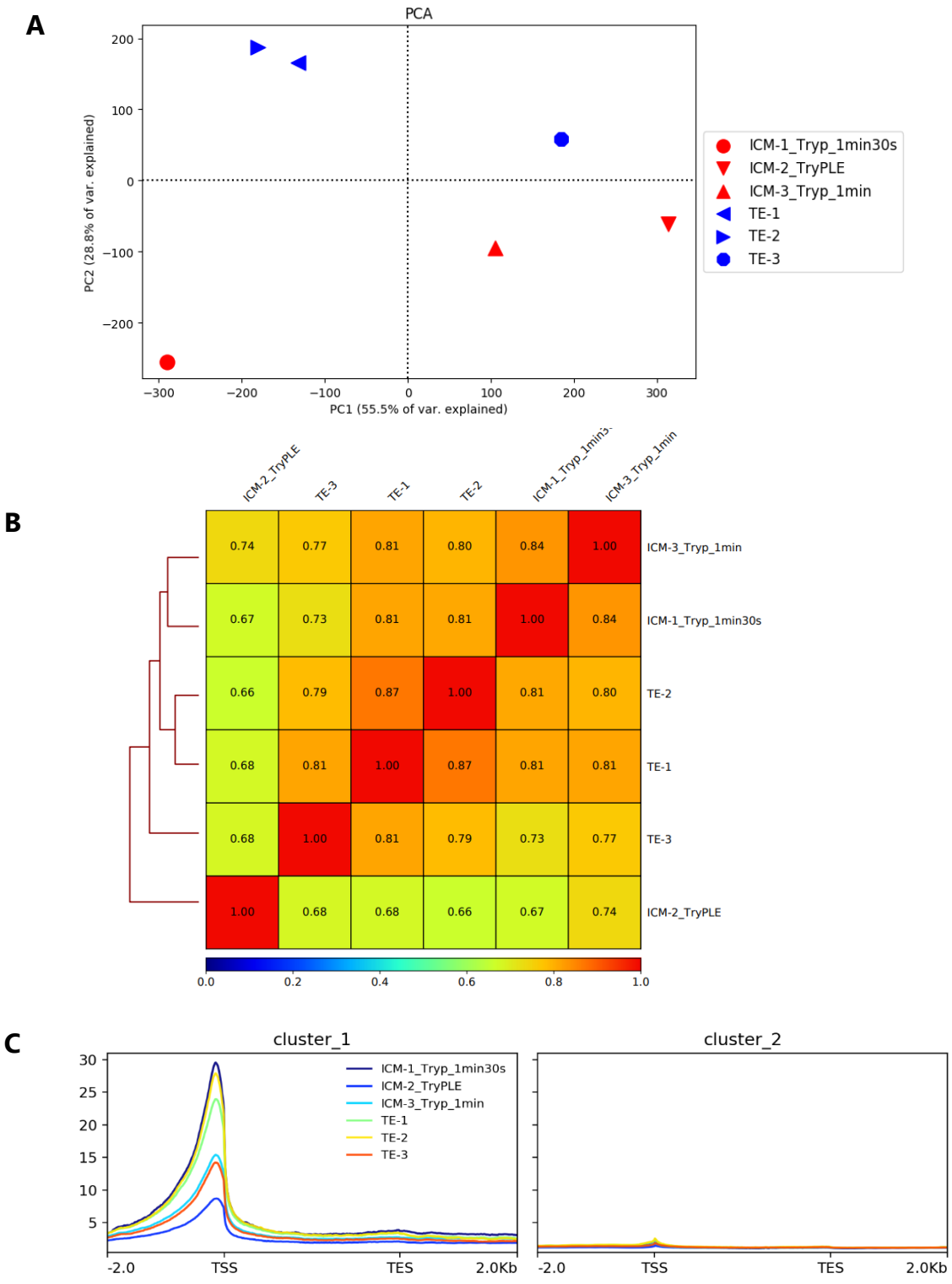

Figure 31: ATAC-seq on ICM and TE TEST libraries.

Principal component analysis (PCA) of ATAC-seq signal from three ICM and TE libraries, normalized by Reads Per Kilobase Million (RPKM). B) Heatmap of Pearson correlation coefficient of ATAC-seq signal between ICM and TE libraries. C) Average ATAC-seq signal enriched around the TSS in a group of rabbit genes (cluster 1). ICM samples: ICM-1_Tryp_1min30s, ICM dissociated with trypsin for 1 min 30 s; ICM-2_TryPLE, ICM dissociated with TryPLE; ICM-3_Tryp_1min, ICM dissociated with trypsin 1 min. TSS, transcription start site; TES, transcription end site.

Sequencing of ATAC-seq ICM and TE TEST libraries generated between 6 to 24 million nonmitochondrial uniquely mapped reads (Appendix 10). Principal component analysis (PCA) of ATAC-seq signal from ICM and TE libraries showed partial grouping of samples according to lineage (Figure 31A). Among ICM samples, ATAC-seq signal from ICM dissociated with TryPLE showed a reduced Pearson correlation coefficient, suggesting dissimilarity compared to ICM samples dissociated with trypsin (Figure 31B). On the contrary, ATAC-seq datasets from ICM samples dissociated with trypsin, or between TE samples showed higher similarity (Figure 31B). All ATAC-seq libraries showed TSS enrichment in a group of rabbit genes (cluster 1) (Figure 31C).
Altogether, these results indicate the feasibility of the ATAC-seq protocol from Buenrostro et al., 2015 with a few modifications to assess chromatin accessibility on ICM and TE from *in vitro*-developed rabbit embryos. Concerning the dissociation strategies tested in ICM samples, taking into consideration these results, the dissociation with trypsin for 1 min 30 s was chosen for subsequent experiments.

Although the main objective for the generation of this ATAC-seq dataset was to verify the quality of the libraries, this dataset can now be used for other purposes such as comparison of chromatin accessibility profiles between ICM and TE and with ICM and TE from D4-5 embryos, as well as between different culture medium (Global and M199) or conditions (20 O_2% and 5%O_2).

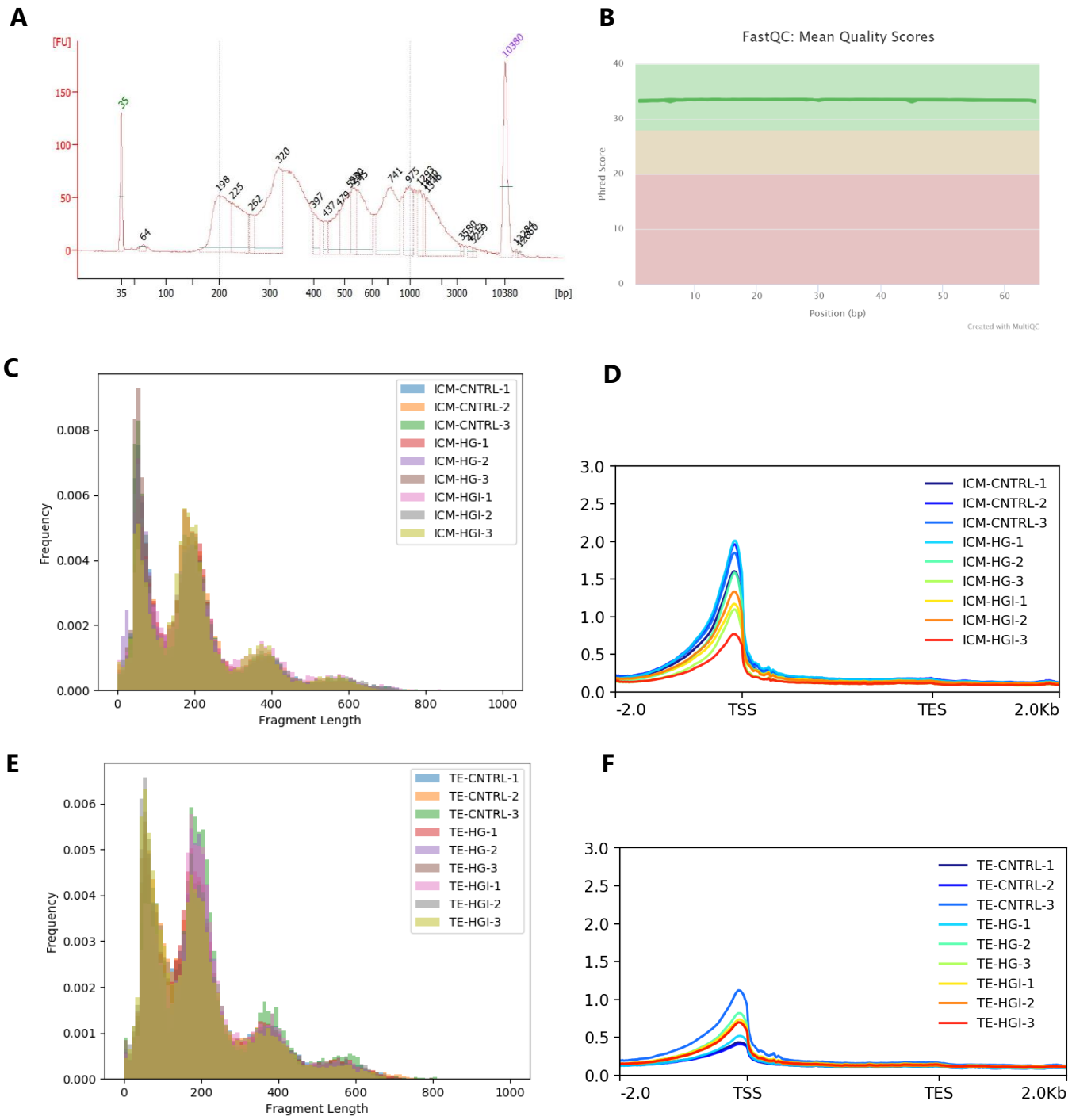

Figure 32: Quality control of ICM and TE ATAC-seq libraries from embryos exposed to CNTRL, HG and HGI.

A) Electropherogram of ATAC-seq ICM and TE pooled libraries after size selection. B) MultiQC plot from the control quality sequencing report showing the mean quality score of reads across samples. Phred Score indicates the base quality in sequencing. C) Frequency of fragment size from ICM CNTRL, HG and HGI libraries. D) Enrichment of ATAC-seq signal on TSS genomic regions of ICM from CNTRL, HG and HGI libraries. E) Frequency of fragment size from TE CNTRL, HG and HGI libraries. E) Enrichment of ATAC-seq signal on TSS genomic regions of TE from CNTRL, HG and HGI libraries. CNTRL, control; HG, high glucose; HGI, high glucose and high insulin; TSS, transcription start sites; TES, transcription end sites.

3. ATAC-seq libraries from ICM and TE exposed to control (CNTRL), high glucose (HG) and high glucose and high insulin (HGI)

Using mESCs and then ICM and TE from rabbit *in vitro*-developed embryos we were able to establish an ATAC-seq protocol suitable for our model. Thereby, the next step was to use the established protocol for the profiling of chromatin accessibility landscapes in ICM and TE from *in vitro*-developed embryos with high glucose and/or high insulin supplementation.

Eighteen ICM and TE ATAC-seq libraries from *in vitro*-developed embryos with CNTRL, HG or HGI were generated. Three biological replicates were included for each experimental condition, consisting of a pool of *n*=13-26 ICM and TE from blastocysts (±50% blastocoel) from 2-3 independent *in vitro* culture sessions (Appendix 11). With the exception to HGI libraries, attempts were made to generate ATAC-seq libraries from embryos from the same rabbit developed in different culture conditions.
All libraries were pooled, size-selected and sequenced (Figure 32A). Sequencing of ATAC-seq ICM and TE libraries generated between 23 to 70 million nonmitochondrial uniquely mapped reads (Appendix 4).

Data quality evaluated by FASTQC indicated good quality reads (Figure 32B). ICM and TE libraries from embryos exposed to CNTRL, HG or HGI showed the characteristic ATAC-seq library fragment size distribution with enrichment of <200 bp fragments followed by mono-nucleosome and di-nucleosome periodicity of ~200 bp fragments (Figure 32C, E). Similarly, plotting of ATAC-seq signal over TSS and TES genomic regions across ICM and TE libraries showed enriched ATAC-seq signal on the TSS of a group of genes (Figure 32D, F). PCA of ATAC-seq signal from ICM and TE libraries showed the presence of one outlier among CNTRL biological replicates (TE-CNTRL-3) and thus was not included in subsequent analysis (not shown).

To investigate possible differences in chromatin accessibility among embryos exposed to high glucose or high glucose and high insulin, ICM and TE ATAC-seq datasets were compared to CNTRL ICM or CNTRL TE. Results from the differential analysis will be presented in the following lines for each lineage and condition.

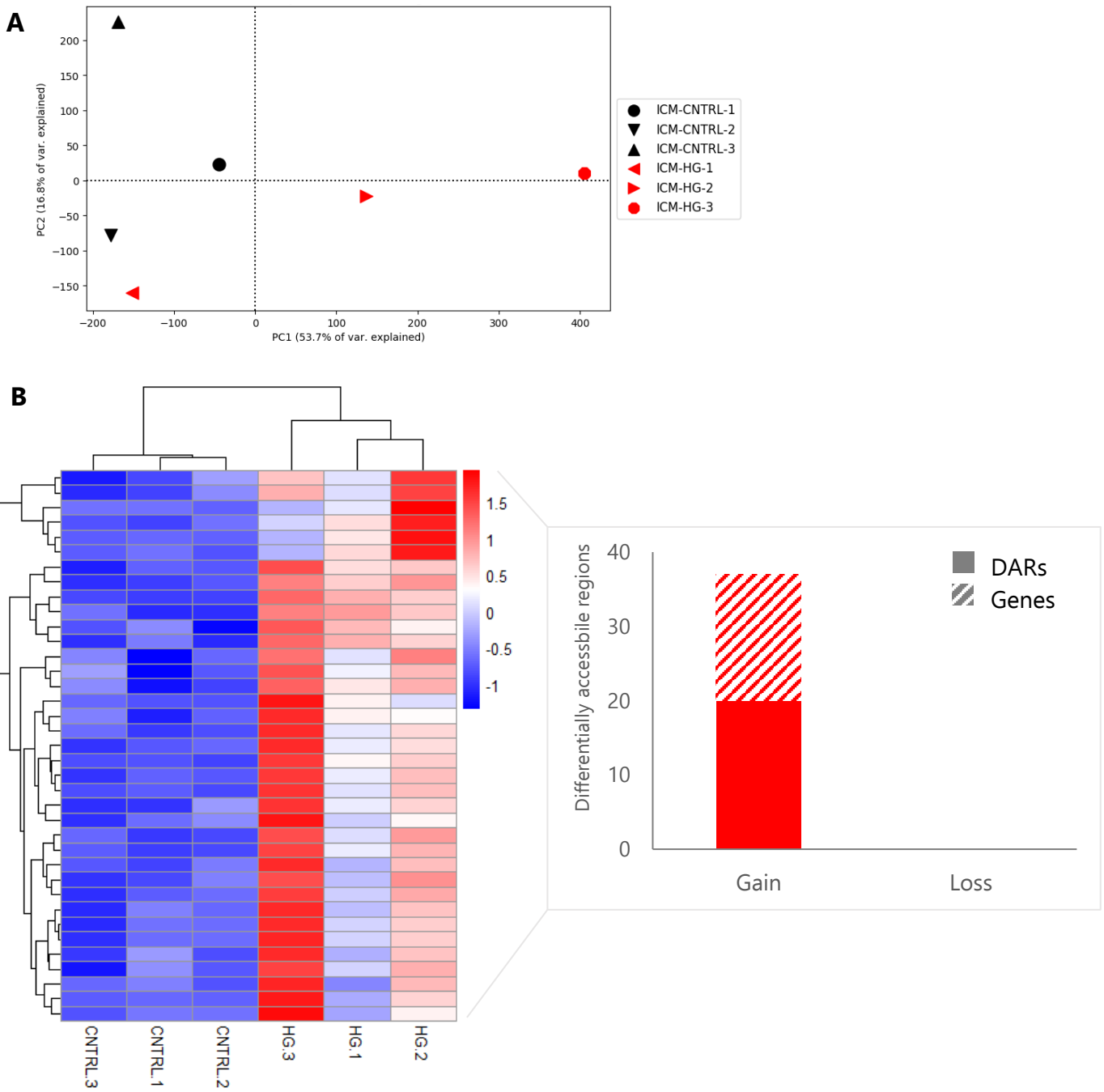

C

Genes located proximal to HG ICM DARs		
***n* genes**	***n* protein-coding**	**Gene symbol**
17	5	*CLCN6, DERA, SCFD2, SLIT3,* and one without an official gene symbol

Figure 33: Chromatin accessibility in the ICM embryos exposed to high glucose.
A) PCA of ATAC-seq signal from ICM from *in vitro*-developed embryos with CNTRL or HG. B) Heatmap showing log2 fold change significant DARs (adjusted p >0.01) between ICM of embryos developed with CNTRL or HG (left) and the stacked bar chart showing the gained and lost accessible chromatin regions and the number of associated genes in HG ICM (right). C) Rabbit genes located proximal to DAR (p >0.01) in HG ICM. Identified protein-coding genes are shown. CNTRL, control; HG, high glucose. DARs, differentially accessible regions.

3.1 Chromatin accessibility in the ICM and TE of embryos exposed to high glucose (HG)

In the ICM:

Comparison of ATAC-seq signal between ICM of embryos developed in HG or CNTRL by PCA showed closeness between CNTRL ICM biological replicates whereas HG biological replicates show more heterogeneity (Figure 33A).

Differential analysis between CNTRL and HG ICM showed 37 differentially accessible regions (DARs) (p >0.01). Of those, all 37 DARs were found in HG ICM indicative of gained accessible chromatin regions (Figure 33B).

We next investigated whether the identified DARs between HG and CNTRL ICM were proximal to regulatory regions such as gene promoters or putative enhancers.
From the 37 DARs in HG ICM, 17 corresponded to promoter regions of annotated rabbit genes (Figure 33C, Appendix 13). Of those, 5 were identified as protein-coding genes (Figure 33C, Appendix 13).
Next, we examine the functional annotation, precisely the gene ontology (GO) biological process of the 5 protein-coding genes that gained chromatin accessibility in the ICM of embryos exposed to high glucose.

The 5 genes included (Figure 33C, Appendix 13):

- Ras-GEF domain-containing protein (Ensembl ID ENSOCUG00000026272; no official gene symbol) involved in small GTPase mediated signal transduction (GO:0007264);
- Chloride voltage-gated channel 6 (*CLCN6*) involved in chloride transport (GO:0006821);
- Deoxyribose-phosphate aldolase (*DERA*) involved in deoxyribonucleotide catabolic process (GO:0009264);
- Sec1 family domain containing 2 (*SCFD2*) implicated in vesicle-mediated transport (GO:0016192);
- Slit guidance ligand 3 (*SLIT3*) associated with nervous system development (GO:0007399).

We next examined whether among the identified DARs between HG and CNTRL ICM corresponding to intergenic genomic regions harbored known motifs for transcription factor binding. Nevertheless, motif enrichment analysis did not show significantly enriched motifs in HG ICM or CNTRL ICM (Appendix 17).

Taken together, high glucose during preimplantation development caused a marked "open" chromatin in 37 genomic regions in the ICM of *in vitro*-developed blastocysts. The regions that gained chromatin accessibility in HG ICM were associated with genes implicated signal transduction, ion and protein transport, biosynthetic processes and development.

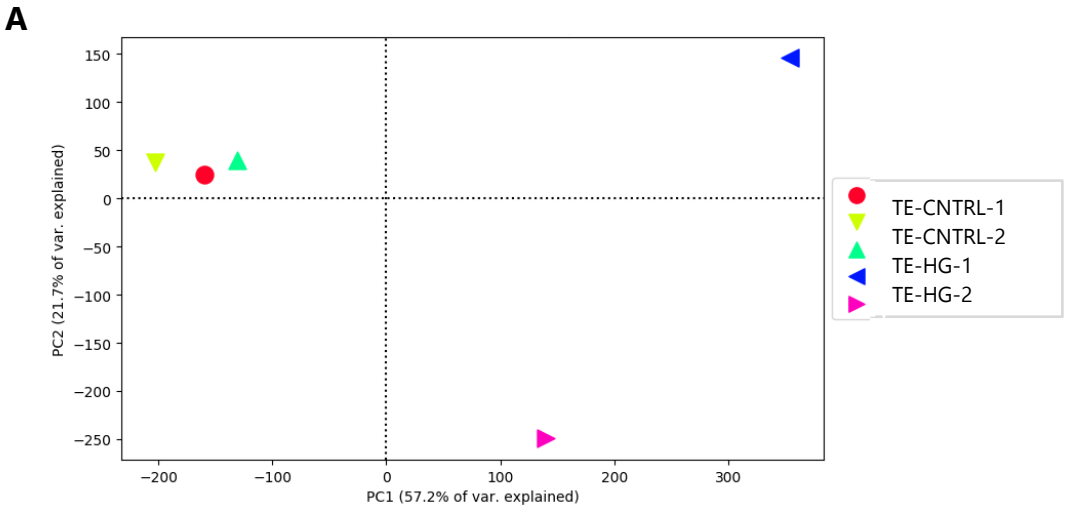

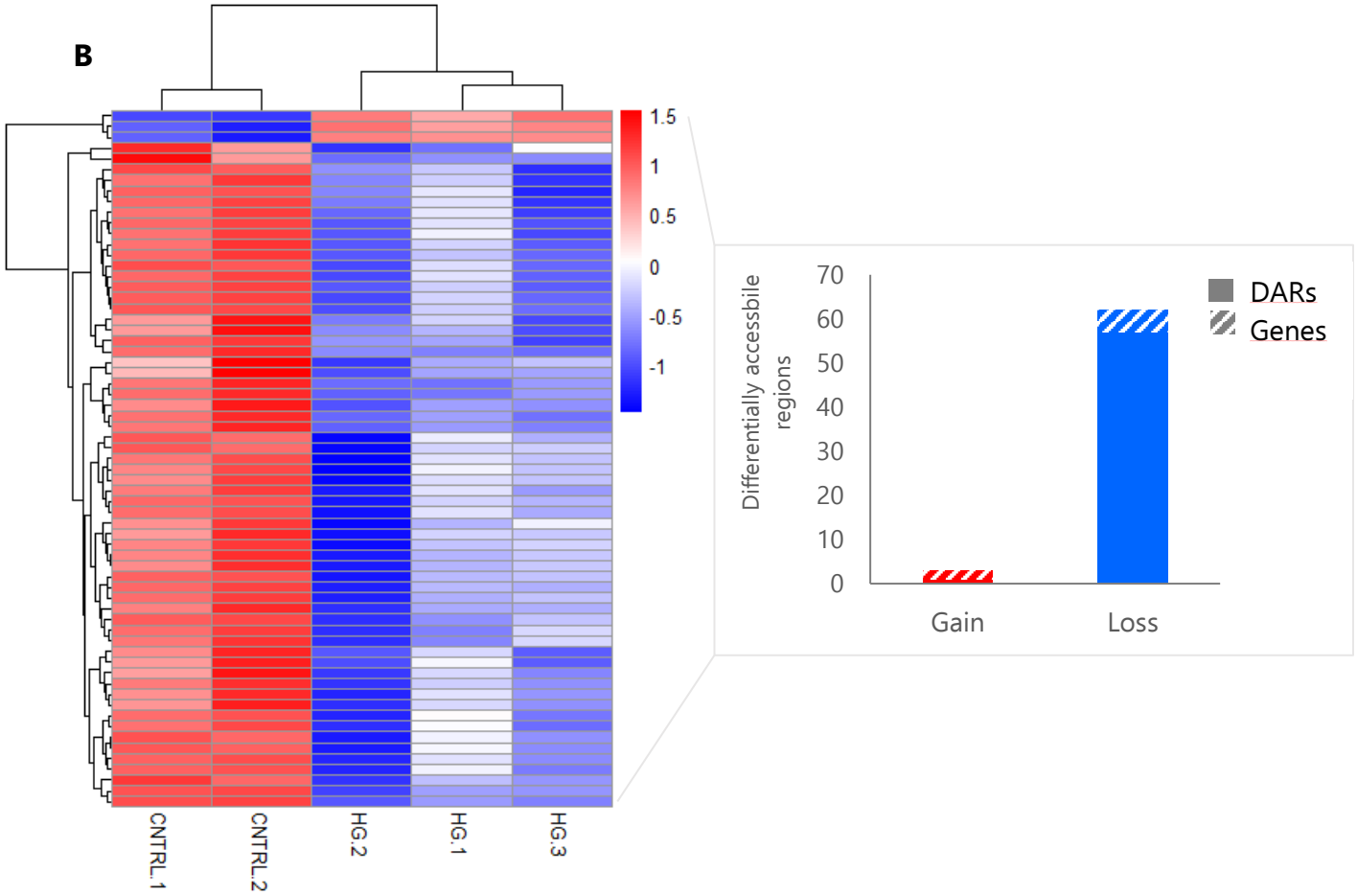

C

Genes located proximal to HG TE DAR		
***n* genes**	***n* protein-coding**	**Gene symbol**
2	1	*CENPU*

Genes located proximal to CNTRL TE DAR		
***n* genes**	***n* protein-coding**	**Gene symbol**
5	1	without an official gene symbol

Figure 34: Chromatin accessibility in the TE embryos exposed to high glucose.
A) PCA of ATAC-seq signal from TE from *in vitro*-developed embryos with CNTRL or HG. B) Heatmap showing log2 fold change significant DARs (adjusted p >0.01) between TE of embryos developed with CNTRL or HG (left) and the stacked bar chart showing the gained and lost accessible chromatin regions and the number of associated genes in HG TE (right). C) Rabbit genes located proximal to DAR (p >0.01) in HG TE. Identified protein-coding genes are shown. CNTRL, control; HG, high glucose. DARs, differentially accessible regions.

In the TE:

Comparison of ATAC-seq signal between the TE of embryos developed in HG or CNTRL by PCA showed CNTRL biological replicates grouped together, whereas HG TE replicates did not form a defined cluster. In addition, one of the HG TE biological replicates was grouped with CNTRL TE biological replicates (Figure 34A).

We next performed the differential analysis between CNTRL and HG TE and identified 65 differentially accessible regions (DARs) ($p > 0.01$). Of those, 3 DARs were found in HG TE indicative of gained accessible chromatin regions, whereas 62 DARs were accessible in CNTRL TE and thereby were lost in HG TE, suggestive of "closed" chromatin regions (Figure 34B).

We next searched whether the identified gained or lost accessible chromatin regions in HG TE were proximal to regulatory regions such as gene promoters or putative enhancers.
Of the 3 gained accessible chromatin regions in HG TE, only 2 corresponded to promoter regions of annotated rabbit genes (Figure 34C, Appendix 14). Of those, only 1 protein-coding gene was identified (Figure 34C, Appendix 14). From the 62 lost accessible chromatin regions in HG TE, only 5 corresponded to promoter regions of annotated rabbit genes (Figure 34C, Appendix 14). Of those, only 1 protein-coding gene was identified (Figure 34C, Appendix 14).

Next, we examined the functional annotation, GO biological process of the two protein-coding genes identified with gained and lost chromatin accessibility in the TE of embryos exposed to high glucose.
The protein-coding gene that showed chromatin accessibility in HG TE corresponded to centromere protein U (*CENPU*) gene associated to chromosome, centromeric region (GO:0000775) (Figure 34C, Appendix 14). The protein-coding gene that lost chromatin accessibility in HG TE corresponded to PseudoU_synth_2 domain-containing protein (Ensembl ID ENSOCUG00000027885; no official gene symbol), implicated in pseudouridine synthesis (GO:0001522) (Figure 34C, Appendix 14).

We next searched whether among the identified DARs between HG and CNTRL TE corresponding to intergenic genomic regions there were known motifs for transcription factor binding. Nevertheless, the enrichment analysis did not show significantly enriched motifs in HG ICM or CNTRL TE (Appendix 17).

In conclusion, high glucose during preimplantation development caused an overall marked "closed" chromatin with 62 loss and only 3 gained accessible chromatin regions in the TE of *in vitro*-developed blastocysts. Overall, the regions that gained and lost chromatin accessibility in HG TE were associated with genes implicated with chromosome centromeres and pseudouridine synthesis.

The comparison of ICM and TE of embryos exposed to high glucose shows lineage-specific responses. High glucose resulted in higher differentially accessible chromatin regions in HG TE compared to HG ICM. In the ICM, chromatin accessibility suggests responses related to signal transduction, cell transport, biosynthetic processes, and development, whereas the TE showed responses associated with chromosome centromeres and RNA modifications. Furthermore, a striking finding is that within DARs, HG ICM shows "open" chromatin, whereas HG TE shows an overall "closed" chromatin.

A

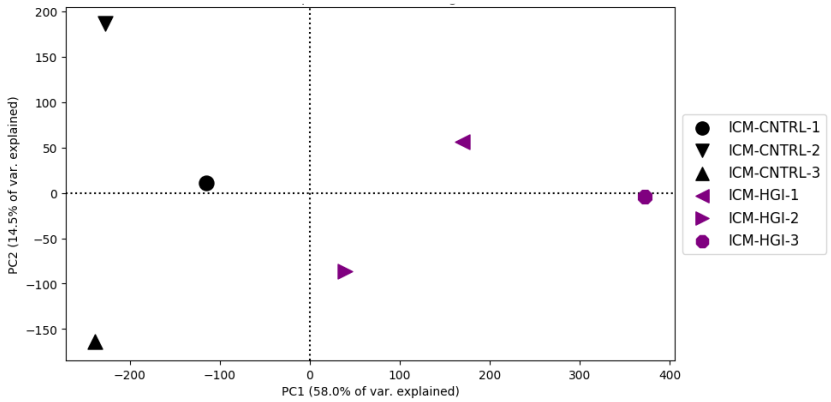

B

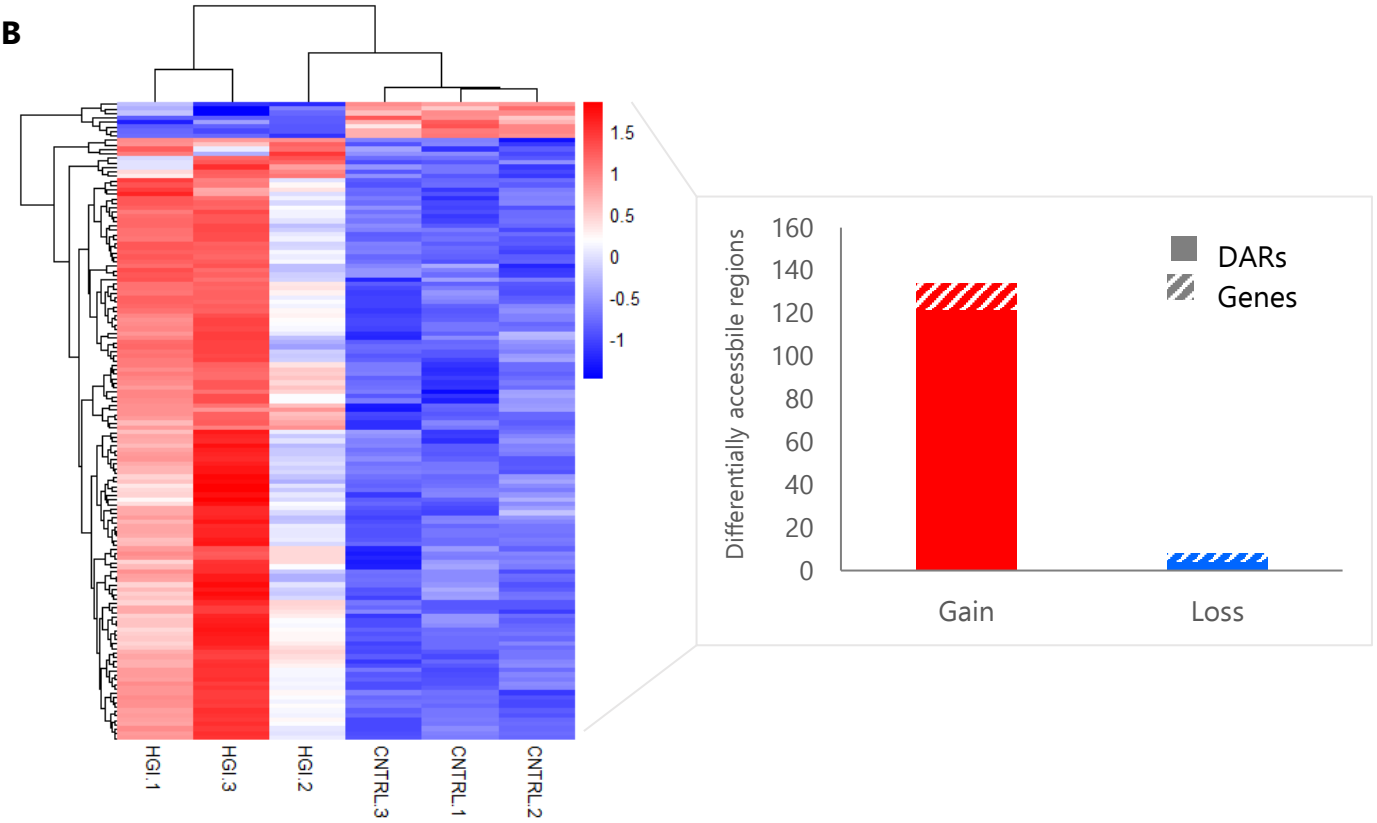

C

Genes located proximal to HGI ICM DARs		
***n* genes**	***n* protein-coding**	**Gene symbol**
12	7	*POC5, SOX1, MYO3B, PRKCB, SAMD8, ZC3HAV18,* an one without and official gene symbol

Genes located proximal to CNTRL ICM DARs		
***n* genes**	***n* protein-coding**	**Gene symbol**
4	3	*BABAM2, GSR, WHRN*

Figure 35: Chromatin accessibility in the ICM embryos exposed to high glucose and high insulin. A) PCA of ATAC-seq signal from ICM from *in vitro*-developed embryos with CNTRL or HGI. B) Heatmap showing log2 fold change significant DARs (adjusted p >0.01) between ICM of embryos developed with CNTRL or HGI (left) and the stacked bar chart showing the gained and lost accessible chromatin regions and the number of associated genes for each in HGI ICM (right). C) Rabbit genes located proximal to DAR (p >0.01) in HG ICM. Identified protein-coding genes are shown. CNTRL, control; HGI, high glucose and high insulin. DARs, differentially accessible regions.

3.2 Chromatin accessibility in the ICM and TE of embryos exposed to high glucose and high insulin (HGI)

In the ICM:

Comparison of ATAC-seq signal between ICM of embryos developed in CNTRL or HGI by PCA showed an overall separation of CNTRL ICM biological replicates and HGI biological replicates (Figure 35A).

Differential analysis between CNTRL and HGI ICM identified 142 differentially accessible regions (DARs) ($p > 0.01$). Of those, 134 DARs were found in HGI ICM indicative of gained accessible chromatin regions, whereas 8 DARs were accessible in CNTRL ICM, thus indicative of accessible chromatin regions lost in HGI ICM (Figure 35B).

We next examine whether the identified gained or lost accessible chromatin regions in HGI ICM were proximal to gene promoters or putative enhancers. Among the 134 gained accessible chromatin regions in HGI TE, 12 regions corresponded to promoters of annotated rabbit genes (Figure 35C, Appendix 15). Of those, 7 were known protein-coding genes (Figure 35C, Appendix 15). Regarding the 8 chromatin regions that lost accessibility in HGI ICM, 4 corresponded to the promoters of annotated rabbit genes (Figure 35C, Appendix 15). Of those, 3 were identified as protein-coding genes (Figure 35C, Appendix 15).

The 7 protein-coding genes that gained chromatin accessibility in the ICM of embryos exposed to high glucose and high insulin, and their functional annotation included (Figure 35C, Appendix 15):

- POC5 centriolar protein (*POC5*) implicated in cell cycle (GO:0007049);
- Ras-GEF domain-containing protein (Ensembl ID ENSOCUG00000026272; no official gene symbol), related to small GTPase mediated signal transduction (GO:0007264);
- SRY-box transcription factor 1 (*SOX1*) involved in regulation of transcription, DNA-templated (GO:0006355);
- Myosin IIIB (*MYO3B*) associated to response to stimulus (GO:0050896);
- Protein kinase C beta (*PRKCB*) implicated in regulation of transcription from RNA polymerase II promoter (GO:0006357);
- Sterile alpha motif domain containing 8 (*SAMD8*) related to sphingolipid metabolic process (GO:0006665);
- Zinc finger CCCH-type containing, antiviral 1 (*ZC3HAV1*) associated with the response to virus (GO:0009615).

Concerning the 3 protein-coding genes and their functional annotation that lost chromatin accessibility in the HGI ICM (Figure 35C, Appendix 15):

- BRISC and BRCA1 A complex member 2 (*BABAM2*) implicated in double-strand break repair (GO:0006302);
- Glutathione-disulfide reductase (*GSR*) involved in glutathione metabolic process (GO:0006749);
- Whirlin (*WHRN*) involved in the positive regulation of gene expression (GO:0010628).

Next, we examined whether among the remaining identified DARs that corresponded to intergenic genomic regions between HGI and CNTRL ICM there were known motifs for transcription factor binding.

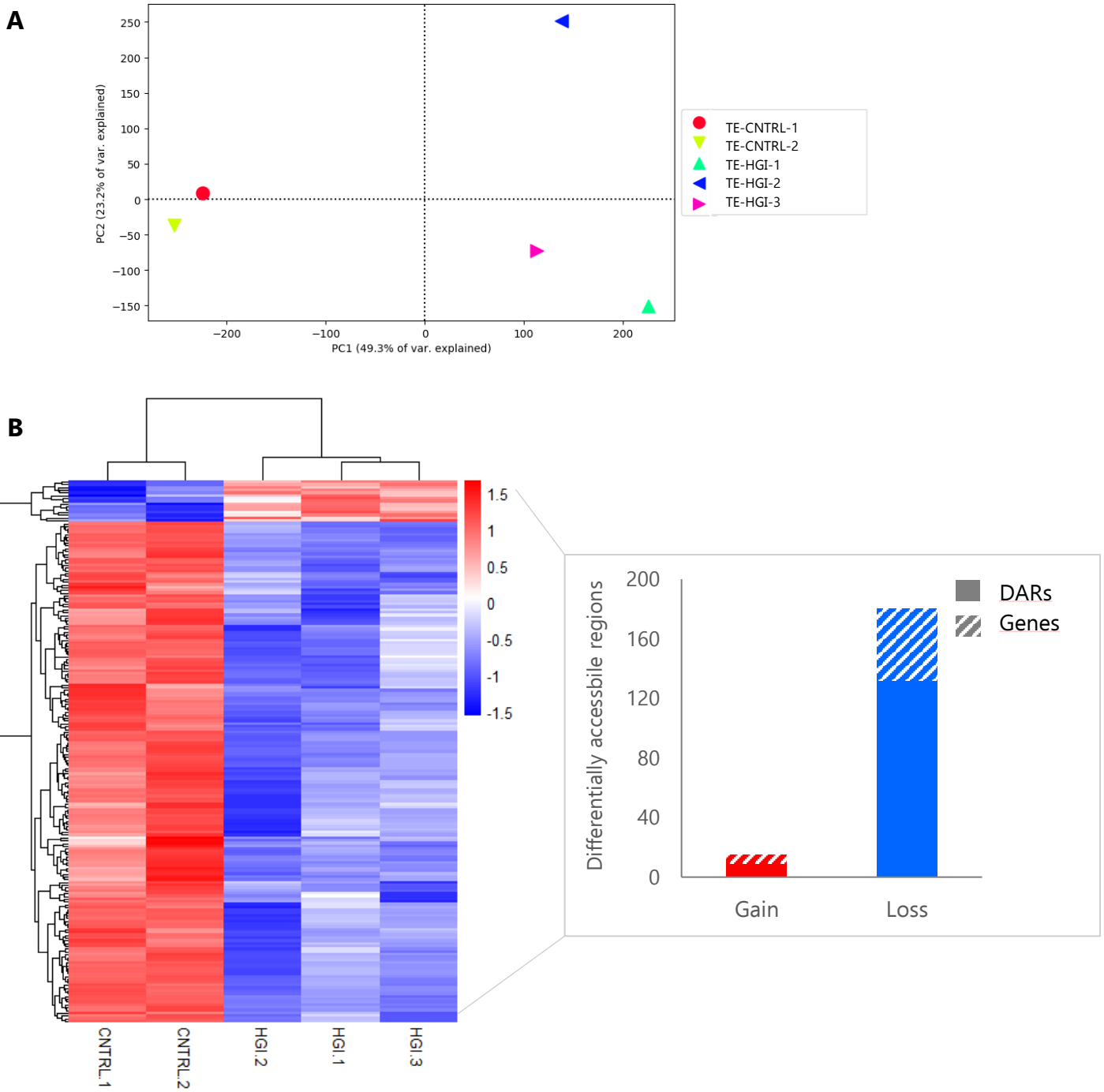

C

Genes located proximal to HGI TE DAR		
***n* genes**	***n* protein-coding**	**Gene symbol**
6	6	*BRD2, RFC4, RETREG1, UFM1* and 2 without an official gene symbol

Genes located proximal to CNTRL TE DAR		
***n* genes**	***n* protein-coding**	**Gene symbol**
48	11	*POC5, ASIC2, DYNC2I1,HOXC8, HTT, LPCAT2, PARD3, THBS4,* and 3 without an official gene symbol

Figure 36: Chromatin accessibility in the TE embryos exposed to high glucose and high insulin. A) PCA of ATAC-seq signal from TE from *in vitro*-developed embryos with CNTRL or HGI. B) Heatmap showing log2 fold change significant DARs (adjusted p >0.01) between TE of embryos developed with CNTRL or HGI (left) and the stacked bar chart showing the gained and lost accessible chromatin regions and the number of associated genes in HGI TE (right). C) Rabbit genes located proximal to DAR (p >0.01) in HGI TE. Identified protein-coding genes are shown. CNTRL, control; HGI, high glucose and high insulin. DARs, differentially accessible regions.

However, the enrichment analysis did not show significantly enriched motifs in DARs between HGI ICM or CNTRL ICM (Appendix 17).

Taken together, high glucose and high insulin during preimplantation development resulted in overall "open" chromatin in the ICM of *in vitro*-developed blastocysts, with 134 and 8 genomic regions that gained and lost chromatin accessibility, respectively. Genomic regions that gained chromatin accessibility in HGI ICM were associated with genes implicated in cell cycle, signal transduction, regulation of transcription, response to stimulus, immune response, and sphingolipid metabolism. Genomic regions that lost chromatin accessibility in HGI ICM were involved in DNA repair mechanisms, glutathione metabolism and gene expression regulation.

In the TE:

Comparison of ATAC-seq signal between TE of embryos developed in CNTRL or HGI by PCA showed the clear separation of CNTRL TE and HGI TE biological replicates (Figure 36A).

Differential analysis between CNTRL and HGI TE 195 differentially accessible regions (DARs) (p >0.01). Of those, 15 DARs were identified in HGI TE, indicative of gained accessible chromatin regions, whereas 180 DARs were accessible in CNTRL TE, thus indicative of accessible chromatin regions lost in HGI TE (Figure 36B).

We next examine whether the identified gained or lost DARs in HGI TE were within gene promoters or proximal to putative enhancers. Among the 15 accessible chromatin regions gained in HGI TE, 6 corresponded to promoters of annotated rabbit genes, and all 6 were known protein-coding genes (Figure 36C, Appendix 16). Concerning the 180 accessible chromatin regions lost in HGI TE, 48 corresponded to promoters of annotated rabbit genes (Figure 36C, Appendix 16). Of those, 11 were identified as protein-coding genes (Figure 36C, Appendix 16).

Examination of the identified protein-coding genes and their functional annotation showed (Figure 36C, Appendix 16):

- Bromodomain containing 2 (*BRD2*) involved in nucleosome assembly (GO:0006334);
- Replication factor C subunit 4 (*RFC4*) implicated in DNA replication (GO:0006260);
- Reticulophagy regulator 1 (*RETREG1*) associated to macromitophagy (GO:0000423);
- Ubiquitin fold modifier 1 (*UFM1*) involved in protein ufmylation (GO:0071569);
- Two uncharacterized proteins without official gene symbol involved in regulation of transcription, DNA-templated (GO:0006355).

Regarding the 11 protein-coding genes and their functional annotation that lost chromatin accessibility in the HGI TE (Figure 36C, Appendix 16):

- ATP synthase mitochondrial F1 complex assembly factor 2 (Ensembl ID ENSOCUG00000011529; no official gene symbol) involved in proton-transporting ATP synthase complex assembly (GO:0043461);
- POC5 centriolar protein (*POC5*) involved in cell cycle (GO:0007049);

- Acid sensing ion channel subunit 2 (*ASIC2*) involved in the regulation of systemic arterial blood pressure by aortic arch baroreceptor feedback (GO:0003026);
- Dynein 2 intermediate chain 1 (*DYNC2I1*) involved in embryonic skeletal system morphogenesis (GO:0048704);
- High mobility group protein B2 pseudogene (Ensembl ID ENSOCUG00000023376; no official gene symbol) related to innate immune response (GO:0045087);
- Homeobox C8 (*HOXC8*) involved in negative regulation of transcription from RNA polymerase II promoter (GO:0000122);
- Huntingtin (*HTT*) involved in establishment of mitotic spindle orientation (GO:0000132);
- Lysophosphatidylcholine acyltransferase 2 (*LPCAT2*) related to phosphatidylcholine acyl-chain remodeling (GO:0036151);
- Par-3 family cell polarity regulator (*PARD3*) involved in in cell cycle (GO:0007049);
- Thrombospondin 4 (*THBS4*) involved in cell adhesion (GO:0007155);
- One uncharacterized protein without official gene symbol, involved in regulation of transcription, DNA-templated (GO:0006355).

We next investigated whether among the remaining identified DARs that corresponded to intergenic genomic regions between HGI and CNTRL TE there were known motifs for transcription factor binding. The enrichment analysis did not show significantly enriched motifs in DARs between HGI TE or CNTRL TE (Appendix 17).

Taken together, high glucose and high insulin during preimplantation development caused an overall marked "closed" chromatin in the TE of *in vitro*-developed blastocysts with 180 loss and 15 gained accessible chromatin regions. Genomic regions that lost chromatin accessibility in HGI TE were associated with genes related to ATP synthase complex assembly, cell cycle, regulation of transcription, regulation of systemic arterial blood pressure, development, phosphatidylcholine metabolic process, immune response and cell adhesion. Genomic regions that gained chromatin accessibility in HGI TE were associated with genes implicated in the regulation of transcription, nucleosome assembly, DNA replication, macromitophagy, and protein ufmylation.

The comparison of ICM and TE of embryos exposed to high glucose and high insulin shows lineage-specific responses. High glucose and high insulin resulted in higher differentially accessible chromatin regions in HGI TE compared to HGI ICM. Interestingly, among the DARs identified, chromatin accessibility within the promoter of POC5 showed opposite patterns between HGI ICM and HGI TE. In HGI ICM, *PCO5* promoter gained chromatin accessibility, whereas, in HGI TE, it was lost (Figure 35C and 36C).
High glucose and high insulin lead to common (in bold) and specific (underlined) responses between ICM and TE:

- In the ICM, chromatin accessibility changes suggest responses related to **cell cycle**, signal transduction, **gene expression regulation**, **metabolism** and redox homeostasis, DNA repair mechanisms and **immune response**.

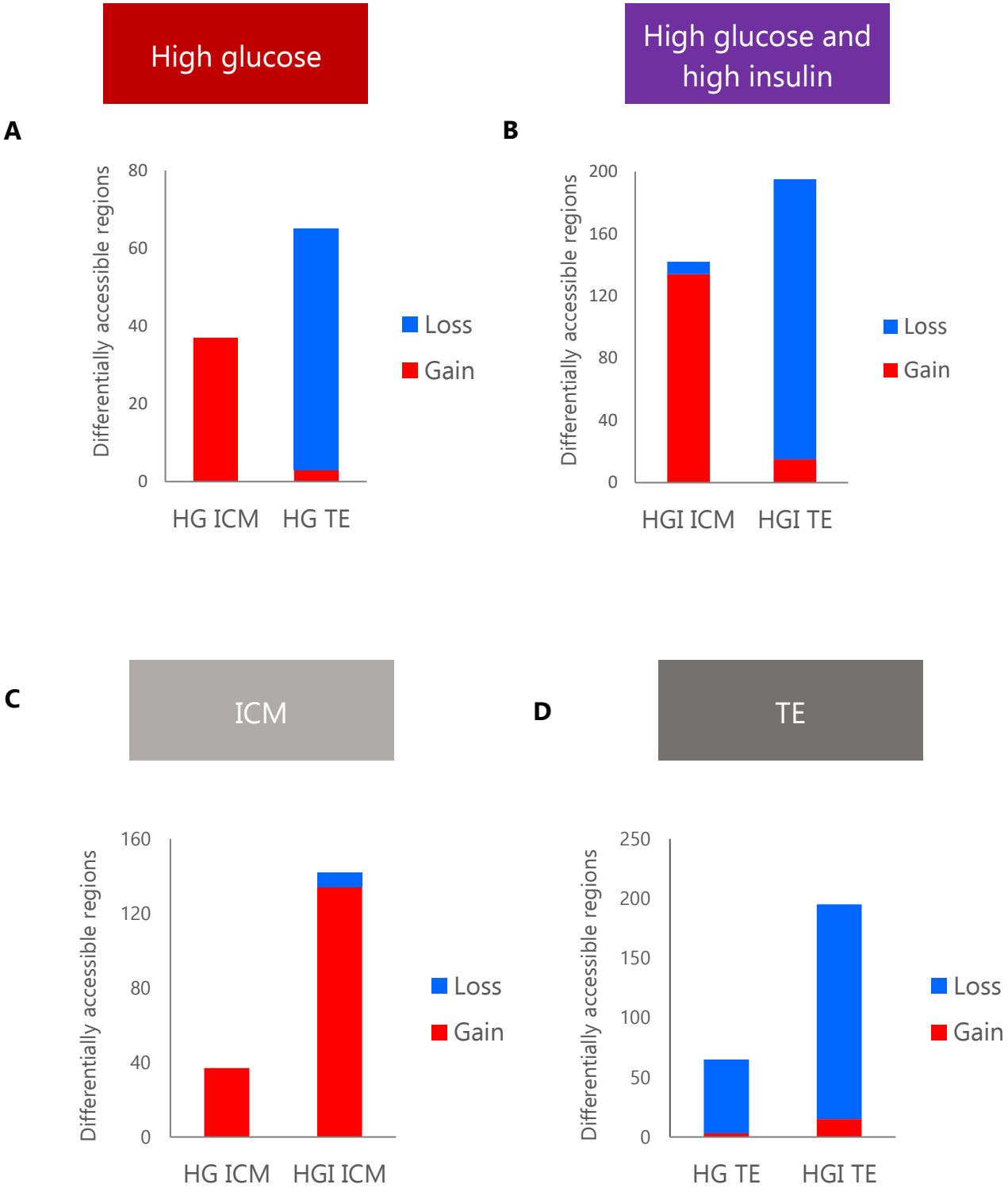

Figure 37: Comparison of chromatin accessibility in regulatory regions in the ICM and TE of embryos exposed to HG or HGI.

A-B) Stacked bar chart of DARs (adjusted p >0.01) showing gained and lost chromatin accessibility regions in ICM and TE of embryos exposed to high glucose (left) or high glucose and high insulin (right). C-D) Stacked bar chart of DARs (adjusted p >0.01) showing gained and lost chromatin accessibility regions in ICM (left) and TE (right) of embryos exposed to high glucose or high glucose and high insulin. HG, high glucose; HGI, high glucose and high insulin.

- In the TE, chromatin accessibility changes suggest responses related **cell cycle**, **gene expression regulation**, **metabolism**, mitochondrial quality control, development, cell adhesion, and **immune response**.

Within the identified DARs, HGI showed an overall "open" chromatin, whereas HGI TE showed an overall "closed" chromatin.

3.3 Comparison of chromatin accessibility changes between ICM and TE exposed to HG or HGI

Comparison of chromatin accessibility in regulatory regions genome-wide between CNTRL ICM or TE with the ICM and TE of embryos exposed to high glucose or high glucose and high insulin detected differentially accessible chromatin regions between lineages. We next compared the chromatin dynamics of each lineage of embryos exposed to HG or HGI, and a few remarkable findings were identified.

First, among the differentially accessible chromatin regions, only regulatory region was found in common between ICM and TE. High glucose and high insulin ICM exhibited gained chromatin accessibility within the promoter of *POC5*, but it was lost in the TE. Second, between lineages exposed to HG or HGI, both HG and HGI ICM showed gained chromatin accessibility within the promoter of Ras-GEF domain-containing protein (Ensembl ID ENSOCUG00000026272; no official gene symbol).
Third, high glucose alone or in combination with high insulin influences chromatin accessibility in specific regulatory regions in the ICM, whereas in the TE either condition rather stimulates an overall "closed" chromatin state (Figure 37A, B). Third, high glucose and high insulin trigger either gain or loss of chromatin accessibility in a higher number of regulatory genomic regions in both ICM and TE, compared to HG (Figure 37C, D).

Taken together, chromatin accessibility profiling shows that high glucose alone or in combination with high insulin induce lineage-specific chromatin changes, and that high glucose and high insulin induce more chromatin changes than high glucose alone in either lineage.

DISCUSSION PART II

1. Impact on the landscape of chromatin accessibility on embryos exposed to high glucose (HG) or high glucose and high insulin (HGI)

The cell modulates its gene expression program in response to external stimuli. Chromatin regulation by facilitating or inhibiting access to the transcriptional machinery is at the core of these responses. We have previously shown that exposure to high glucose and/or high insulin during preimplantation embryo in the rabbit caused gene expression changes related to energy metabolism, cell proliferation and apoptosis, inflammation, cellular stress responses, lineage specification, and in epigenetic regulation of gene expression. Some of these gene expression responses followed a lineage-specific pattern.

By mapping chromatin accessibility in the ICM and TE of embryos exposed to high glucose (HG) and high glucose and high insulin (HGI), we sought to identify chromatin changes within promoters or putative enhancers that were associated with the response of the ICM and TE to high glucose alone or in combination with high insulin. Chromatin accessibility profiles showed lineage-specific changes in response to HG or HGI.

Glucose metabolism has been shown to induce chromatin changes associated with gene regulation. Glucose-derived acetyl-CoA influences global histone acetylation levels, associated with "open" chromatin in transcriptionally active *cis*-regulatory elements, i.e., promoters and enhancers (Creyghton et al., 2010; Dai et al., 2020; Martínez-Reyes & Chandel, 2020). Histone acetylation neutralizes the positive charge of lysine residues weakening the interaction between histones and DNA, leading to a relaxed "open" chromatin configuration, permissive for transcription (Bannister & Kouzarides, 2011). Depending on the cellular context, changes in acetyl-CoA availability have been shown to influence specific loci (Yucel et al., 2019). In proliferating muscle stem cells, increased availability of glucose-derived acetyl-CoA led to increased histone acetylation, chromatin accessibility, and expression of stem and cell-cycle genes, thereby repressing differentiation (Yucel et al., 2019). However, in early differentiating myoblasts, glucose was rather metabolized through OXPHOS, leading to reduced glucose-derived acetyl-CoA levels, histone acetylation in stem and cell-cycle genes, and increased expression in lineage-specific genes (Yucel et al., 2019). This suggests crosstalk between acetyl-CoA availability, histone acetylation, and the activity of chromatin modifying enzymes and transcription factors that influence gene expression in specific genomic regions.

In parallel, glucose metabolism metabolites that act as substrates and cofactors for epigenetic modifications, such as TCA-derived α-ketoglutarate required to demethylases TETs and JHDMs, or the glycolysis derived-3PG that can be converted into serine and feed the one-carbon metabolism (Dai et al., 2020; Locasale, 2013).

As for insulin, its influence on chromatin changes and gene regulation may be mediated through direct activation of insulin signaling and transcriptional regulation of downstream targets (Boucher et al., 2014; Kabra et al., 2009) through translocation of the IR to the nucleus to regulate the expression of target genes (Hancock et al., 2019), although this mechanism has not been described in early embryos; or by insulin-stimulated glucose uptake and metabolism (Kabra et al., 2009). Thus, a crosstalk between glucose and insulin availability may influence chromatin changes and gene regulation.

To facilitate the discussion of the major findings of chromatin accessibility profiles between the ICM and TE from exposed embryos, I have divided this section into two parts. The first will be dedicated to the ICM exposed to HG and HGI, and the second will be dedicated to the TE exposed to HG and HGI.

1.1 Gain and loss of chromatin accessibility in the ICM of embryos exposed to high glucose (HG) or high glucose and high insulin (HGI)

The ICM of embryos exposed to high glucose showed differentially accessible regions, with all of them associated with an "open" chromatin state. Of those, the gene *DERA* was identified. *DERA* encodes for the enzyme in charge of the conversion of 2-deoxy-D-ribose-5-phosphate to glyceraldehyde-3-phosphate and acetaldehyde, which are then converted to acetyl-CoA to enter glycolysis and the TCA cycle, respectively (Salleron et al., 2014). Interestingly, *DERA* is part of the cellular stress responses (Salleron et al., 2014). Upon energy deprivation, mitochondrial or oxidative stress, DERA is recruited to stress granules and enables the use of deoxynucleosides as an energy source to maintain ATP levels and prevent apoptosis (Salleron et al., 2014). Overexpression of DERA in HeLa cells helped maintain ATP levels when cultured under glucose deprivation but in the presence of deoxyinosine, as an energy source (Salleron et al., 2014).
In line with stress-responsive chromatin changes, the gene *SCFD2* was also associated with open chromatin regions in HG ICM. The promoter of *SCFD2* was identified as a target of the p53 protein upon hypoxia and/or DNA damage cellular stress responses (Krieg et al., 2006).
High glucose ICM also exhibited accessible chromatin within the promoter of slit guidance ligand (SLIT3). SLIT ligands were mostly associated with axon guidance, but increasing evidence has positioned them together with their receptors, the ROBO proteins, in different cellular contexts, including inflammation, hypoxia, angiogenesis, and placental development and function (Hess et al., 2019; Liao et al., 2012). Indeed, SLIT3 was overexpressed in human umbilical vein endothelial cells (HUVEC) cultured under hypoxia (Liao et al., 2012). In addition, SLIT3 overexpression has been reported in preeclamptic placentas, and transcriptional regulation is mediated by the hypoxia marker, hypoxia-inducible factor 1 alpha (HIF-1α) (Fang et al., 2017). Interestingly, transcriptome data from HG ICM showed an overrepresentation of gene sets related to the regulation of expression of SLITs and ROBOs and signaling by ROBO receptors in HG ICM (not shown). Indeed, SLIT3 was the second most enriched gene in the Reactome Signaling by Robo receptors gene set (not shown). Thus, it would be interesting to examine further the role of SLIT3 and ROBO receptors in the ICM of embryos exposed to high glucose.

We previously identified transcriptomic changes in the ICM of embryos exposed to high glucose. Forty genes were found differentially expressed compared to CNTRL ICM, with 24/41 genes overexpressed and 15/41 underexpressed. In addition, 73 overrepresented gene sets were identified in HG ICM. These gene expression changes were related to transcription, translation, OXPHOS, WNT, and NF-kB signaling pathways, cell cycle regulation, apoptosis, and ICM lineage commitment. An increased number of apoptotic and reduced number of proliferating cells were also identified. The identified annotated genes that gained chromatin accessibility in HG ICM are overall consistent with our previous findings, such as altered energy metabolism, regulation of apoptosis and stress-responses, and inflammation.

The ICM of embryos exposed to high glucose and high insulin showed 142 differentially accessible regions, with most of them (134/142) associated with an "open" chromatin state and a few (8/142) mostly

associated with a "closed" chromatin state. Among the accessible chromatin regions in HGI ICM, a few interesting annotated genes were identified.

High glucose and high insulin ICM showed chromatin accessibility within the promoter of the protein kinase C beta (*PRKCB*) gene, a serine and threonine protein kinase isoform part of the large family of protein kinases C (PKC) (Turban & Hajduch, 2011). *PRKCB* belongs to the group of conventional PKC, and two beta isoforms, β1 and β2 have been described (Turban & Hajduch, 2011). Conventional isoforms of PKC are activated by growth factors and have been associated with positively regulating insulin signaling, although not much is known about the mechanistic aspects of PKCβ (Turban & Hajduch, 2011). In the muscle, the splicing of PRKCB is necessary for GLUT-4 translocation to the plasma membrane in insulin-mediated glucose uptake (Turban & Hajduch, 2011). Moreover, conventional isoforms of PKC have been associated with fatty-acid induced insulin resistance (Turban & Hajduch, 2011). Accumulation of lipids such as diacylglycerol and ceramides is thought to mediate with conventional PKC to phosphorylate IRS and inhibit insulin signaling (Turban & Hajduch, 2011). Activation of PKCβ has been described in different altered metabolic contexts, including hyperglycemia, saturated, high-fat diets, and obesity (Shu et al., 2021). In the ICM, gained accessibility in the promoter of *PRKCB* could indicate its transcriptional activation, most likely in response to insulin, which is coherent with embryos exposed to a high glucose and high insulin environment. Whether PKCβ is involved in the stimulation of insulin signaling and mediating its metabolic actions, i.e., glucose uptake, or by inhibiting insulin signaling requires further examination. Regarding the transcriptome of HGI ICM, at this stage, it is complicated to pinpoint the precise involvement of *PRKCB* in the responses identified. Further comparison of ATAC-seq and RNA-seq datasets could provide more information on the contribution of *PRKCB* in HGI ICM.

Another interesting gene that gained chromatin accessibility is the sterile alpha motif domain containing 8 (*SAMD8*), also known as SMSr. The ceramide phosphoethanolamine synthase SAMD8/SMSr is localized in the endoplasmic reticulum where it acts as a sensor of ceramide levels, regulates its production, and exerts an anti-apoptotic activity (Cabukusta et al., 2017; Tafesse et al., 2013). Inhibition of SMSr activity results in the accumulation of ER ceramides and their mistargeting to the mitochondria, which triggers the ceramide-induced mitochondrial pathway of apoptosis (Tafesse et al., 2013). The activity of SAMD8/SMSr is thereby essential to control ER ceramides levels and maintain cellular homeostasis. The explanation for SAMD8/SMSr gained chromatin accessibility is unclear at this stage but may suggest an underlying cellular response to modulate ER ceramide levels and protect ICM cells from apoptosis. Interestingly, both conventional PKC, such as *PRKCB,* which also gained chromatin accessibility in HGI ICM, and *SAMD8* have been associated with cellular responses against high ceramide levels. Transcriptome data on HGI ICM showed the overrepresentation of gene sets implicated in the "protein localization to the endoplasmic reticulum", however, *SAMD8* was not found enriched in those gene sets.

The neuroectodermal marker SRY-box transcription factor 1 (*SOX1*) was also identified in "open" chromatin regions in HGI ICM. In the mouse, *SOX1* participates in the differentiation of neural progenitors (Suter et al., 2009). High glucose was shown to impair neural lineage differentiation in GR-E14 mESC line, and *SOX1* expression, known to promote neurogenesis, was suppressed by high glucose (P. Yang et al., 2016). Impaired expression of early markers of neural fate, including *SOX1* were proposed by the authors to be associated with impaired neurogenesis, altered neurulation, and neural tube defects frequently observed in the offspring exposed to maternal diabetes (P. Yang et al., 2016). Our transcriptome data shows low levels of transcript in both CNTRL and HGI ICM with a slightly increase in HGI ICM, therefore is not clear why *SOX1* would have gained chromatin accessibility in HGI ICM. In rabbit *in vivo* blastocysts, *SOX1* is not expressed in the ICM (Duranthon, *et al.*, unpublished RNA-seq data). As

shown in the mouse, it is likely that *SOX1* is expressed at post-implantation stages in the rabbit, and thus altered *SOX1* gene expression regulation could affect neuroectodermal development. Interestingly, HGI ICM showed gained chromatin accessibility in the promoter of zinc finger CCCH-type containing antiviral 1 (*ZC3HAV1*). *ZC3HAV1* has been previously described to upregulated in the ICM of human and mouse embryos (Ozawa et al., 2012). However, our transcriptomic data shows that *ZC3HAV1* exhibits higher expression in the TE than in the ICM of CNTRL embryos. Similarly, RNA-seq data from rabbit *in vivo* blastocysts shows the rapid increase in *ZC3HAV1* expression in the TE (86 h.p.c.), expression that is then slightly increased in TE (96 h.p.c), and later maintained, although at lower levels in both extra-embryonic lineages (PrE and TE) (Duranthon, *et al.*, unpublished RNA-seq data). In these embryos, the ICM (96 h.p.c) shows higher expression than ICM (86 h.p.c), but still at a lesser level that in the TE (86-96 h.p.c), and *ZC3HAV1* expression is nearly absent in EPI (144 h.p.c) (Duranthon, *et al.*, unpublished RNA-seq data). In cancer cells, overexpression of *ZC3HAV1* via MAPK signaling and its role in promoting proliferation, migration, and invasion has been described (W. Huang et al., 2021). In our context, it is possible that insulin signaling and the downstream activation of the MAPK pathway may be involved in the regulation of *ZC3HAV1.* Furthermore, we previously showed that HGI ICM exhibited the overexpression of two genes involved in trophoblast differentiation and placental development, paternally expressed 10 (*PEG10*) and placenta expressed transcript 1 (*PLET1*). Thus, chromatin accessibility within the promoter of *ZC3HAV1* further reinforces our hypothesis that high glucose and high insulin may affect ICM cell commitment. Certainly, it would be interesting to examine this hypothesis further and to investigate the role of *ZC3HAV1* in HGI ICM, especially since the overexpression of *ZC3HAV1* results in migratory and invasive phenotypes, two features associated to the trophoblastic lineage.

High glucose and high insulin ICM also showed chromatin accessibility within the promoter of POC5 centriolar protein (*POC5*). *POC5* is a centriolar protein recruited to centrioles during the G2/M phase, essential for cell cycle progression (Azimzadeh et al., 2009). Transcriptome data in HGI ICM showed gene expression associated with proliferation and cell cycle. When cell proliferation was assessed by EdU incorporation assay, we did not identify significant changes compared to CNTRL ICM.

The ICM of embryos exposed to high glucose and high insulin also shows the loss of chromatin accessibility in a few regions. One of those is BRISC and BRCA1 A complex member 2 (*BABAM2*), implicated in the regulation of cell cycle progression and maintenance of pluripotency in mESCs (Chung et al., 2020). The *BABAM2* knockout in mESCs following DNA damage caused abnormal G1 phase retention along with the overexpression of p53, inhibition of NANOG expression by p53, reduced expression of pluripotency markers over time, loss of alkaline phosphatase activity associated with stemness, and increased expression of mesodermal and ectodermal differentiation markers (Chung et al., 2020). In HGI ICM, we previously showed the overexpression of genes associated with the trophoblastic lineage (*PEG10 and PLET1*). Moreover, ROS-related gene expression changes were identified and it is well known that overproduction of ROS can result in macromolecule damage. We can hypothesize that loss of *BABAM2* via ROS-induced damage, or by other factors may be involved in the regulation of pluripotency in HGI ICM and the overexpression of TE genes. Further analysis would be required to explore this hypothesis.

Another gene that lost chromatin accessibility within its promoter in HGI ICM is glutathione-disulfide reductase (GSR), or most frequently called glutathione reductase (GR) (Sies et al., 2017). GSR is an antioxidant enzyme key member of the glutathione system that catalyzes the reduction of oxidized glutathione disulfide (GSSG) using NADPH as a substrate to GSH, the reduced glutathione form (Couto

et al., 2016; Deponte, 2013). Glutathione is a powerful antioxidant molecule that participates in several cellular processes, notably in the maintenance of cellular redox homeostasis (Deponte, 2013). In preimplantation embryos, reduction of GSH levels has been associated with decreased developmental competence (Sánchez-Santos et al., 2018). The loss of chromatin accessibility within the GSR promoter may indicate the transcriptional repression of *GSR* in HGI ICM, which could compromise the redox balance in this lineage. Consistent with this, in HGI ICM we identified the overrepresentation of gene sets related to the "reactive oxygen species pathway", suggesting ROS-mediated cellular stress in HGI ICM.

Transcriptome analysis of HGI ICM previously showed 39 DEGs, with 20/39 overexpressed and 19/39 underexpressed. Enrichment analysis further showed 106 positively enriched gene sets, and 1 negatively enriched. These results showed gene expression changes related to transcription, translation, OXPHOS, ROS, fatty acid β-oxidation, NF-kB signaling, and ICM lineage commitment. Chromatin accessibility analysis results are in line with our previous finding, particularly with energy metabolism, ROS, and ICM cell commitment.

Altogether, high glucose and high insulin resulted in a higher number of differentially accessible regions in the ICM, compared to high glucose alone. Compared to our transcriptome analysis, we also showed a higher number of overrepresented gene sets in HGI ICM compared to HG ICM. One explanation for these differences could be that both glucose and insulin stimulate gene regulation. Chromatin accessibility in genes involved in the insulin signaling pathway such as *PRKCB* or potentially regulated by downstream pathways, such as *ZC3HAV1* may be indicative of the activity of this pathway. Together with ICM responses related to energy metabolism, both glucose and insulin availability may have triggered a higher number of cellular responses involving gene regulation than high glucose alone. Among the differentially accessible regions in HG and HGI, only the gained accessibility within the promoter of the gene Ras-GEF domain-containing protein (Ensembl ID ENSOCUG00000026272; no official gene symbol) was found in common. The remaining differentially accessible regions that are not associated to known annotated genes have yet to be examined to determine whether other differentially accessible regions, potentially corresponding to non-annotated genes or putative enhancers, are in common between HG ICM and HGI ICM.

1.2 Gain and loss of chromatin accessibility in the TE of embryos exposed to high glucose (HG) and high glucose and high insulin (HGI)

The TE of embryos exposed to high glucose showed differentially accessible regions, with most of them associated with a "closed" chromatin state. Among the differentially accessible regions identified in HG TE, only two annotated genes were identified, centromere protein U (*CENPU*) that gained chromatin accessibility and a second protein-coding gene, not characterized that gained lost chromatin accessibility. *CENPU* is component of the centromere and a transcriptional repressor (Deng et al., 2021). Overexpression of *CENPU* has been associated with several types of cancers (Deng et al., 2021). In addition, it was previously determined that *CENPU* is an upstream regulator of the high mobility group box 2 (HMGB2) nuclear protein, which is implicated in the regulation of glycolysis (Deng et al., 2021). In gastric cancer cells, the overexpression of *CENPU* stimulated cell proliferation and glycolysis via HMGB2 (Deng et al., 2021). In our model, we previously reported transcriptome changes related to increased

glycolysis and proliferation along with an increased number of proliferating cells in HG TE. Interestingly, HMGB2 is highly expressed in CNTRL and HG TE (not shown). Therefore, it would be interesting to further investigate whether CENPU and HMGB2 participate in the metabolic and cell number changes previously observed in HG TE.

Transcriptome analysis of HG TE revealed 132 DEGs, with 53/132 genes overexpressed and 79/132 genes underexpressed. Enrichment analysis showed 78 positively enriched gene sets. Changes in gene expression were related to transcription, translation, epigenetic regulation, glycolysis, mTORC signaling, WNT and NK-kB signaling, and cell cycle regulation and apoptosis. An increased number of proliferating and reduced number of apoptotic cells were also identified. Accessible chromatin profiles, despite the 65 differentially accessible regions identified, only two were annotated genes. Thus, it is difficult to compare previously identified altered functions with those revealed by accessible chromatin profiles. However, *CENPU* constitutes an interesting target possibly related to the increased metabolic and cell proliferation changes observed in HG TE.

Interestingly, accessible chromatin profiles were overall associated with a "closed" chromatin state. In our transcriptome study, among the DEGs in HG TE, we identified 9 DEGs implicated in epigenetic mechanisms. Of those 7/9 (*PADI2, SMARCD3, MOV10L1, ATF7, RESF1, BPTF and NSD3*) were found underexpressed compared to CNTRL TE. One explanation for the overall "closed" with few "open" chromatin states within differentially accessible regions may reside in the activity of these genes. In mammary gland stem cells, the bromodomain PHD finger transcription factor (*BPTF*), a subunit of the Nucleosome Remodeling Complex (NURF), was responsible for the maintenance of chromatin accessibility at enhancers and self-renewal capacity (Frey et al., 2017). Depletion of BPTF resulted in chromatin accessibility remodeling, with gained chromatin accessibility in regions proximal to genes associated with apoptosis and cell-cycle arrest (Frey et al., 2017). Similarly underexpressed, SWI/SNF related matrix associated actin dependent regulator of chromatin subfamily d member 3 (*SMARCD3*), also known as *Baf60c*, is a member of the SWI/SNF chromatin-remodeling complex, known to directly interact with transcriptional activators (P. Zhang et al., 2016). In parallel, we also identified the overexpression of growth arrest and DNA damage inducible alpha (*GADD45A*), associated with active DNA demethylation to facilitate transcriptional activation (Arab et al., 2019). Due to the function of these genes, and their expression levels in HG TE, it is possible that they had contributed to the overall chromatin changes identified. Certainly, identification of the remaining DARs, as they could be possible targets of these chromatin regulators could confirm this hypothesis.

Similar to HG TE, the TE of embryos exposed to high glucose and high insulin showed differentially accessible regions, with most of them associated with a "closed" chromatin state. Among those that gained chromatin accessibility in HGI TE there were a few interesting findings. The bromodomain containing 2 (*BRD2)* gene has been recently shown to have an active role in the accessible genome organization and to promote the spatial mixing and compartmentalization of active chromatin in the absence of Cohesin (L. Xie et al., 2022).
In mouse preimplantation development, BET proteins, including BRD2 were shown to be necessary for the specification and maintenance of the ICM and epiblast lineage but not for the formation of the TE or the PrE directly (Tsume-Kajioka et al., 2022). Furthermore, BRD2 regulates the expression of more than 1500 genes, including cyclin A, regulator of cell cycle progression (Deeney et al., 2016; Ruchat, 2015). In

addition, *BRD2* expression has been associated with different physiological and pathological contexts including obesity and T2D (Deeney et al., 2016; Ruchat, 2015). Interestingly, BRD2 has been proposed as a candidate gene in the fetal metabolic programming of offspring exposed to maternal hyperglycemia (Ruchat, 2015). BRD2 DNA methylation changes in placenta and cord blood were associated with variations in maternal glucose levels within a normal range (Ruchat, 2015). Due to the great number of *BRD2*-associated genes, including those involved in cell cycle, it would be possible to further investigate whether the HGI TE DEGs previously identified are among BRD2 known targets. *BRD2* is definitely a candidate target to further examine in our model due to its implication in developmental programming by maternal hyperglycemia.

Also implicated in cell cycle, the replication factor C subunit 4 (*RFC4*) gene showed chromatin accessibility in HGI TE. *RFC4* is involved in DNA replication and was proposed to act as a sensor in DNA checkpoints (H.-S. Kim & Brill, 2001). *RFC4* is upregulated in several types of cancers (J. Zhang et al., 2021). Inhibition of *RFC4* by siRNA in carcinoma cell line *in vitro* reduced the proliferation of cancerous cells (J. Zhang et al., 2021). In our model, we previously demonstrated increased proliferation in HGI TE. Therefore, *RFC4* could contribute to cell cycle regulation in HGI TE. Indeed, among the overrepresented genes identified in HGI TE involved in G2/M checkpoints, *RFC4* was found enriched (not shown).

In line with these findings, a few genes involved in cell cycle showed loss of chromatin accessibility in HGI TE, such as *PCO5* also identified in HGI ICM but with the opposite pattern, or par-3 family cell polarity regulator (*PARD3*). *PARD3* has been reported to inhibit proliferation and to acts as a tumor suppressor in certain cancers (J. Li et al., 2019). Consistent with a tumor-suppresor activity, silencing of *PARD3* enhanced proliferation, migration and invasion in a carcinoma cell line (L. Wang et al., 2017).

Another gene associated with accessible chromatin regions in HGI TE is the reticulophagy regulator 1 (*RETREG1*). RETREG1 gene codes for an ER-phagy receptor that was recently shown to mediate ER-phagy upon cellular glucose deprivation (Luo et al., 2022). In line with RETREG1, HGI TE also showed accessible chromatin within the promoter of ubiquitin fold modifier 1 (UFM1). UMF1 is similarly involved in ER-stress responses and has been associated with metabolic diseases such as T2D (Z. Xie et al., 2019). The transcriptome of HGI TE showed the overrepresentation of "establishment of protein localization to endoplasmic reticulum" and "cellular responses to stress" gene sets. Although *RETREG1* and *UFM1* were not found enriched in these gene sets, these results further reinforced the hypothesis of molecular stress in the TE induced by high glucose and high insulin.

Overall, the TE of embryos exposed to HGI showed the loss of chromatin accessible regions. Among these regions, several known protein-genes were identified, including the ATP synthase mitochondrial F1 complex assembly factor 2 (not official gene symbol), an orthologue of human *ATPAF2* gene. *ATPAF2*, a nuclear encoded mitochondrial protein, is implicated in the assembly and activity of the ATP synthase and consequently in mitochondrial respiration (Zhou et al., 2021). Transcriptome analysis of HGI TE revealed increased OXPHOS-related signatures, thereby it is possible *ATPAF2* (in human) may be involved in mitochondrial activity in HGI TE.

High glucose and high insulin TE showed the loss of chromatin accessibility within the promoter of high mobility group protein B2 pseudogene (not official gene symbol), which is an orthologues gene human and mouse *HMGB2* gene. As described in HG TE, *HMGB2* is a downstream factor regulated by *CENPU*, and participates in cell proliferation and glycolysis regulation (Deng et al., 2021). Loss of HMGB2 promoter chromatin accessibility suggests the transcriptional repression of HMGB2, which may be in line with our previous findings indicating OXPHOS rather than glycolytic signatures in HGI TE.

Interestingly, loss of chromatin accessibility in a few genes that may be implicated in placental development was identified. That is the case for the huntingtin (HTT) gene, which mutant *Htt*$^{-/-}$ mouse phenotype is characterized by disorganized extraembryonic membranes including morphological changes in the allantois, and the abnormal folding of the yolk sac (Sanders et al., 2015). Similarly, the homeobox C8 (*HOXC8*) was found to be greatly overexpressed in placental explants stimulated with the growth factor EG-VEGF (Murthi et al., 2015). EG-VEGF regulates trophoblast proliferation and invasion and is highly expressed in the placentas of IUGR offspring (Murthi et al., 2015). It is unclear whether the loss of chromatin accessibility within regulatory sequences of the *HTT* and *HOXC8* genes in HGI TE may involve deregulated gene expression. Nevertheless, because of their association with placental development and function, they are interesting targets for further evaluation.

Transcriptome analysis of HGI TE detected 16 DEGs, with 10/16 overexpressed and 6/10 underexpressed. Enrichment analysis of transcriptomes revealed 108 positively enriched gene sets. HGI TE showed gene expression changes related to transcription, translation, OXPHOS, ROS, NF-kB and TGF-β signaling and cell cycle. An increased number of proliferating cells were also identified. Here, accessible chromatin profiling has further confirmed these altered functions, especially those related to OXPHOS, stress responses, and cell cycle.

High glucose alone or in combination with high insulin leads to different responses in the TE. Accessible chromatin profiling shows that HGI resulted in a higher number of differentially accessible regions in the TE, compared to HG. Enrichment analysis from transcriptomes of HG TE and HGI TE similarly showed a higher number of overrepresented gene sets in HGI TE compared to HG TE. As with HGI ICM, these results suggest that the combined availability of glucose and insulin induces a higher number of cellular responses influencing gene regulation in the TE, compared to the exposition to HG. Among the differentially accessible regions identified in HG and HGI TE, no common annotated genes have been identified in common. The remaining differentially accessible regions have yet to be analyzed to search for common regions that correspond to non-annotated genes or putative enhancers.

One striking finding from the ATAC-seq analysis is the opposite patterns observed between the ICM and TE. It appears that within differentially accessible regions, in response to high glucose alone or in combination, the ICM shows an overall "open" chromatin compared to CNTRL ICM, whereas the HG and HGI TE shows an overall "closed" chromatin compared to CNTRL TE.
The ICM and TE are two distinct lineages with specific transcriptomic, epigenetic, and metabolic signatures as shown in several species, including the mouse, bovine, horse, rabbit and human (Bouchereau et al., 2022; G. Guo et al., 2010; Hosseini et al., 2015; Iqbal et al., 2014; L. Liu et al., 2019; Ozawa et al., 2012; M. Yang et al., 2020). These differences can be explained by the different fates of ICM and TE. The pluripotent ICM is expected to undergo a second round of specification and give rise to EPI and PrE (Ralston & Rossant, 2005). The EPI gives rise to the embryo proper, and the PrE becomes the extraembryonic endoderm, later contributing to the formation of the yolk sac (Ralston & Rossant, 2005). The fate of the multipotent TE is to undergo a series of specification events and give rise to the different cell types that constitute the fetal portion of the placenta (Ralston & Rossant, 2005).
Differences in chromatin accessibility between ICM and TE have been previously described in human embryos. Characterization of chromatin accessibility in the ICM and TE from human blastocysts by ATAC-seq revealed higher chromatin accessibility within promoters in the ICM, but higher chromatin

accessibility within distal intergenic regions, i.e., putative enhancers, in the TE (L. Liu et al., 2019; M. Yang et al., 2020). In the mouse, chromatin accessibility has been described to be progressively increased at poised enhancers throughout development, showing the highest level in the EPI after implantation (Crispatzu et al., 2021). However, because the TE was not included in this study, we are unable to compare this dynamic to that of the TE. Indeed, only a few studies have included the TE when assessing chromatin accessibility in preimplantation embryos.
Regarding DNA methylation in these two lineages, DNA methylation levels were found lower in the TE than in the ICM of human blastocysts (Olcha et al., 2021). These differences were attributed to the higher transcriptional activity in the TE, associated with its more advanced commitment to differentiation, compared to the pluripotent ICM (Olcha et al., 2021).
Considering the differences between the ICM and TE, it is not surprising that environmental cues lead to lineage-specific responses, as we have observed in the accessible chromatin and transcriptome profiles. To the best of my knowledge, the evaluation of chromatin accessibility in the ICM and TE after exposure to stresses or environmental cues has not been described yet. The reason behind the "open" chromatin in HG and HGI ICM, and "closed" in HG and HGI TE is not clear at this stage. Further examination of the differential accessible regions may help answer this question.

One potential hypothesis that emerges from these findings is that HG an HGI may have reduced the differences between the ICM and TE lineages from exposed embryos. Blunted differences between ICM and TE when exposed to a different environment have been previously described. In the mouse, *in vitro*-developed embryos showed a marked reduction in the number of DEGs between ICM and TE, compared to *in vivo* ICM and TE (Giritharan et al., 2012). The pathways impacted in *in vitro* ICM and TE included those related to embryonic stem cell pluripotency (Giritharan et al., 2012). Similar findings have been reported in the bovine. Transcriptomic signatures of ICM *versus* TE from *in vitro* and *in vivo* bovine embryos showed a dramatic reduction in the number of DEGs between these two lineages from *in vitro*-developed embryos (Hosseini et al., 2015). Among the genes that were impacted in the *in vitro* context, several were related to epigenetic regulation of pluripotency and cell differentiation, notably CDX2, FGFR2, DNMT1, GADD45A, and SMARCA2, among others (Hosseini et al., 2015). In our model, transcriptome analysis suggested deregulations in ICM cell commitment, with overexpression of *GATA3* and *PLET1* in HG ICM and *PEG10* and *PLET1* in HGI ICM. Analysis of the ICM accessible chromatin landscape in exposed embryos further reinforces this hypothesis. We have identified changes in the regulation of *BABAM2* and *ZC3HAV1* in HGI ICM. In the same way, the TE of exposed embryos exhibited gene expression changes in major signaling pathways involved in implantation and placental development, such as mTOR and TGF-β. Accessible chromatin profiles further revealed changes in the regulation of genes associated with placental development (*HTT and HOX8*) and epigenetic regulation (*BRD2*) in HGI TE.
Taken together, it is thus possible that ICM and TE gene expression programs and cell identity is impaired or delayed compared to CNTRL counterparts in embryos exposed to high glucose alone or in combination with high insulin. Indeed, the comparison of the number of DEGs between HG ICM *versus* HG TE and HGI ICM *versus* HGI TE, compared to their CNTRL counterparts, showed a reduction in the number of DEGs in the ICM *versus* TE exposed to HG or HGI (not shown). Evaluation of transcriptomic and accessible chromatin datasets between ICM *versus* TE in each condition (CNTRL, HG, and HGI) could help explore this hypothesis further.

A second hypothesis is that high glucose led to lineage-specific responses. Both ICM and both TE of exposed embryos overall showed the same pattern ("open" *versus* "closed", respectively) and since high glucose is the common factor in these two conditions, it is possible that it may have contributed to overall chromatin states observed in each lineage.
Glucose metabolism may have influenced gene regulation in a lineage-specific manner. Indeed, changes in glucose-derived acetyl-CoA availability have been shown to influence global histone acetylation (Martínez-Reyes & Chandel, 2020). In proliferating muscle stem cells, increased availability of glucose-derived acetyl-CoA led to increased histone acetylation, chromatin accessibility and expression of stem and cell-cycle genes inhibiting differentiation (Yucel et al., 2019). In early differentiating myoblasts, shifting towards OXPHOS metabolism reduced glucose-derived acetyl-CoA levels, histone acetylation in stem and cell-cycle genes and increased expression in lineage-specific genes (Yucel et al., 2019). Glucose metabolism via the TCA cycle may also generate substrates and co-factors for chromatin modifying enzymes, which in crosstalk with transcription factors may influence gene expression in specific genomic regions (Dai et al., 2020; Martínez-Reyes & Chandel, 2020). In our model, both transcriptomic and chromatin accessible changes suggest altered expression in metabolic pathways, notably OXPHOS and glycolysis. Indeed, together with OXPHOS gene expression signatures, HG ICM showed the overexpression of fumarate hydratase (FH) involved in the conversion of fumarate to malate in the TCA cycle, whereas HGI ICM showed fatty acid β-oxidation-related transcriptome changes, another source of acetyl-CoA. Accordingly, it is possible that different metabolites may have contributed to the changes observed in ICM and TE of exposed embryos. In HGI embryos, the addition of insulin could have further modulated these changes. In skeletal muscle myoblasts, insulin with hyperglycemic conditions led to methylation, phosphorylation, and acetylation changes in histone H3 (Kabra et al., 2009).
AKT, a core target of the insulin signaling pathway, has also been shown to modulate epigenetic changes influencing gene expression. In tumor cells, it was shown that oncogenic activation AKT leads to the constant acetyl-CoA availability via activation of the ACLY, responsible for the cleavage of citrate to generate acetyl-CoA and oxaloacetate (J. V. Lee et al., 2014). Increased acetyl-CoA led to changes in histone acetylation levels associated with the expression of genes favoring tumorigenesis (J. V. Lee et al., 2014).
Finally, transcriptomic analysis in ICM and TE of exposed embryos revealed a number of DEGs between lineages and conditions, with the highest number in HG TE. However, chromatin accessibility profiles revealed only two annotated genes impacted. Overall, among the differentially accessible regions identified, only a few corresponded to annotated genes, possibly due to the limited annotation of the rabbit genome. This is especially the case for enhancers elements, which are typically poorly characterized mostly due to their variable distance from target genes (Creyghton et al., 2010).

We can speculate that some of the differentially accessible regions correspond to enhancers that may have shifted from inactive to poised/active states and vice versa. Enhancers, key in regulating developmental programs, may be active or poised (Creyghton et al., 2010; Crispatzu et al., 2021). Active enhancers are distinctively enriched in H3K27ac, H3K4me1/2 and bound to histone acetyltransferase p300 (Creyghton et al., 2010). Conversely, poised enhancers harbor a combination of repressive and activating features, including high chromatin accessibility, enrichment in H3K4me1, H3K27me3, and are bound to transcriptions factors, co-activators, and Polycomb proteins, involved in transcriptional repression (Crispatzu et al., 2021). Moreover, the pool of poised enhancers may be more important than those in an active state. By comparing the enrichment in H3K27ac in distal enhancers, which

discriminates active from poised enhancers, an overall reduced pool of active enhancers was observed in mESCs and several different adult cell types (Creyghton et al., 2010).

Taken together, preliminary analysis of chromatin accessibility profiles in the ICM and TE exposed to HG and HGI is in agreement with our previous findings. However, due to the low annotation status of the rabbit genome, the majority of differentially accessible regions remained undetermined. Identification of the remaining differentially accessible regions and their functional significance, along with their correlation with RNA-seq data may provide more insight into gene-regulatory networks activated in the ICM and TE of embryos exposed to HG and HGI, and whether common and/or specific responses are influenced by high glucose alone or in combination with high insulin. Investigation of potentially impaired ICM and TE gene expression programs and their consequences further on development, such as during organogenesis, may shed light on the alterations observed in the offspring exposed to metabolic imbalances.

CONCLUSION PART II

This part of the thesis aimed to establish an ATAC-seq protocol for the profiling of chromatin accessibility in the ICM and TE of *in vitro*-developed embryos in the rabbit and to apply the developed protocol to investigate whether exposure to high glucose or high glucose and high insulin during *in vitro* preimplantation development impacted the accessible chromatin landscape of the ICM and TE.

We can conclude that:

- The ATAC-seq protocol developed by Buenrostro et al., 2015 and slightly modified here have allowed the evaluation of the accessible chromatin landscape of the ICM and TE of *in vitro*-developed embryos in the rabbit.

- The ICM of embryos exposed to high glucose gained chromatin accessibility within the promoter of genes involved in signal transduction, ion and protein transport, biosynthetic processes, and development. The TE of embryos exposed to high glucose gained and lost chromatin accessibility within the promoter of genes related to chromosome centromeres and pseudouridine synthesis.

- The ICM of embryos exposed to high glucose and high insulin gained chromatin accessibility within the promoter of genes involved in cell cycle, signal transduction, gene expression regulation, response to stimulus, immune response, and metabolism, and lost chromatin accessibility within the promoter of genes involved in DNA repair, glutathione metabolism and gene expression regulation. The TE of embryos exposed to high glucose and high insulin gained chromatin accessibility within the promoter of genes associated with gene expression regulation, nucleosome assembly, DNA replication, macromitophagy and protein post-translational modifications, and lost chromatin accessibility within the promoters of genes associated to mitochondrial activity, metabolism, cell cycle, gene expression regulation, regulation of systemic arterial blood pressure, development, immune response and cell adhesion.

- High glucose alone or in combination with high insulin led to lineage-specific chromatin changes with an overall marked "openness" and "closeness" in a group of chromatin regulatory regions in the ICM and TE, respectively.

- Exposure to high glucose and high insulin results in a higher number of differentially accessible chromatin regions in both the ICM and TE compared to high glucose.

- Among the differentially accessible chromatin regions identified in each lineage, only a few corresponded to annotated genes and thus several of these regions remained undetermined.

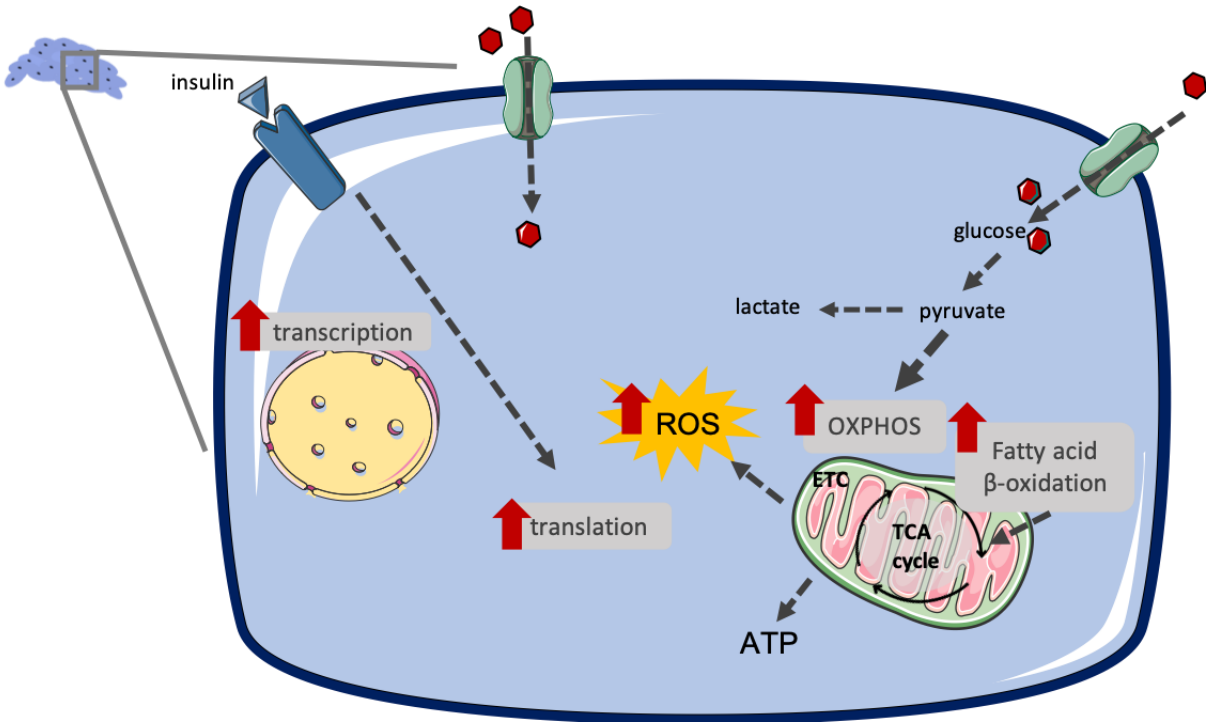

Figure 38: Schematic representation of the main responses in the ICM of embryos exposed to high insulin *in vitro*.

Grey boxes show the responses identified in this thesis by transcriptomic profiling. Red arrows indicate the hypothesized direction of expression changes. Dashed grey arrows show the hypothesized relationship among the different responses identified. ETC, electron transport chain; OXPHOS, oxidative phosphorylation; TCA, tricarboxylic acid.

GENERAL DISCUSSION

During this thesis, we aimed to investigate the effects of exposure to high glucose and high insulin, during the preimplantation period, with a particular interest in the ICM and TE, the progenitor lineages of the embryo proper, and the placenta. To obtain a global picture of the potential effects of high glucose and/or high insulin, we focused on the analysis of gene expression programs by transcriptome profiling and chromatin accessibility genome-wide of the ICM and TE of exposed embryos. We have shown that perturbation of the environment during preimplantation development by high glucose and/or high insulin results in common and lineage-specific significant changes in gene expression programs of the ICM and TE of early embryos.

To adresss the major findings of our work, the general discussion is divided into three sections: the first corresponding to the impact on energy metabolism on ICM and TE of exposed embryos, the second concerning the impact on cell number homeostasis in the ICM and TE of exposed embryos, and a third section where I situate our findings to the context of DOHaD.

1. Impact on energy metabolism in ICM and TE of embryos exposed to high glucose and/or high insulin

1.1 Impact on energy metabolism in the ICM

As energy demands increase prior to blastocyst formation, preimplantation embryos shift from an oxidative metabolism by use of pyruvate and lactate as main energy sources to a glycolytic metabolism by use of glucose as the main energy source (D. K. Gardner & Harvey, 2015; Kaneko, 2016).
Between the ICM and TE, slight differences in the fate of glucose may exist. The ICM of mouse blastocysts uses preferentially aerobic glycolysis, which leads to high lactate production from pyruvate by the enzyme lactate dehydrogenase (LDH) (D. K. Gardner & Harvey, 2015). In highly proliferative cells such as the ICM, it is considered that aerobic glycolysis is the preferred metabolic pathway over OXPHOS to support the energetic and biosynthetic needs (Krisher & Prather, 2012). This is known as the Warburg effect as was first described in cancer cells (Krisher & Prather, 2012). Preimplantation development has been frequently associated with the Warburg effect, especially for ICM (Kaneko, 2016; Krisher & Prather, 2012). Compared to the TE, the ICM has a relatively quiescent metabolism in terms of ATP production and oxygen consumption (Houghton, 2006; Kaneko, 2016). This is further reinforced by the reduced number and morphology of the mitochondria in the ICM compared to the TE (Houghton, 2006; Kaneko, 2016). In rabbits, recent findings suggest that glycolysis is similarly the preferred metabolic pathway in the ICM (Bouchereau et al., 2022).
In our study, exposure to high insulin (HI), high glucose (HG) or high glucose and high insulin (HGI) resulted in gene expression changes suggestive of OXPHOS in the ICM (Figure 38, 40 and 42). This indicates that the ICM of exposed embryos has increasing energetic demands. One explanation of increased energetic demands in the ICM may be a reduction of free glucose levels in the blastocoel of embryos exposed to high glucose and/or high insulin. The supply of glucose and/or insulin to the ICM is dependent on the transporting activity of the TE to the blastocoel (Harvey & Kaye, 1990; Houghton, 2006). Glucose is present in the blastocoel, as identified by metabolomic profiling of the blastocoel fluid

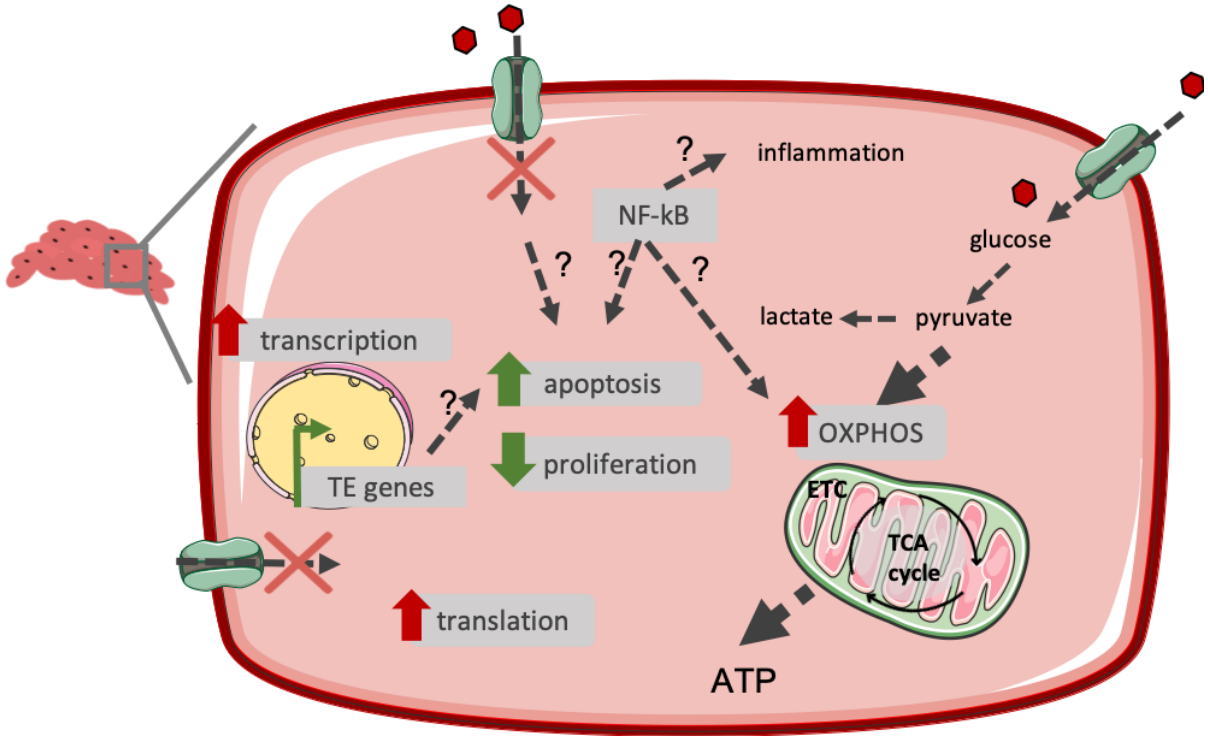

Figure 40: Schematic representation of the main responses in the ICM of embryos exposed to high glucose *in vitro*.

Grey boxes show the responses identified in this thesis by transcriptomic profiling and preliminary accessible chromatin analysis. Up and down green arrows show the direction of expression changes confirmed at the cellular level. Red arrows indicate the hypothesized direction of expression changes. Dashed grey arrows show the hypothesized relationship among the different responses identified. ETC, electron transport chain; OXPHOS, oxidative phosphorylation; TCA, tricarboxylic acid; TE, trophectoderm.

in *in vivo* rabbit blastocysts (Calderari et al., 2021). Reduced free glucose levels in the blastocoel of exposed embryos could have triggered OXPHOS. Indeed, arrestin domain-containing protein 4 (ARRDC4) gene was found overexpressed in HG ICM and HGI ICM. In addition, both HG TE and HGI TE showed the overexpression of ARRDC4 and thioredoxin-interacting protein (TXNIP). ARRDC4 and TXNIP are two glucose-responsive genes involved in the inhibition of glucose uptake (Richards et al., 2018). In human pancreatic β EndoC-βH1 cell line cultured with high glucose concentrations, both TXNIP and ARRDC4 were upregulated via nuclear translocation of their upstream regulator MondoA, and this resulted in reduced glucose uptake (Richards et al., 2018). Recently, in differentiated adipocytes, ARRDC4 has been shown to regulate insulin-stimulated glucose metabolism (Dagdeviren et al., 2020).
Although the role of TXNIP-ARRDC4 in preimplantation embryos in physiological or pathological contexts has not been described yet, based on previous findings, it is tempting to place the role of these two genes in glucose homeostasis regulation in early embryos. Reduced glucose uptake by both ICM and TE could have decreased free glucose levels, therefore shifting towards OXPHOS instead of glycolysis in the ICM to maintain high ATP intracellular levels. This metabolic shift has been previously shown in cancer cells. In the human astrocyte cancer cell line, culture under serum starvation resulted in enhanced TCA and OXPHOS activity and reduced glycolysis to maintain high ATP levels (Z. Liu et al., 2016). In the mouse, blastocysts, high glucose or high insulin have been associated with reduced expression of glucose transporters and insulin-stimulated glucose uptake (M. M.-Y. Chi et al., 2000; M. M. Y. Chi et al., 2000; Jiménez et al., 2003). Both *in vivo* and *in vitro* high glucose conditions decreased the expression of GLUT1, GLUT2, and GLUT3 and led to reduced intraembryonic free glucose levels (M. M. Y. Chi et al., 2000; Jiménez et al., 2003).
Insulin may also stimulate ATP synthesis via OPXHOS. A short insulin exposure in rat and human skeletal muscle cells led to increased oxidative phosphorylation and mitochondrial (Nisr & Affourtit, 2014).

In HI and HGI ICM, fatty acid β-oxidation transcriptomic signatures may be associated with OXPHOS gene expression changes (Figure 38 and 42). The β-oxidation of fatty acids generates ATP by coupling the TCA cycle with OXPHOS within mitochondria (Shi & Sirard, 2022). It has been proposed that early embryos rely on fatty acid β-oxidation for ATP production, thereby, glucose can be metabolized by aerobic glycolysis to supply metabolites for biosynthesis purposes (Krisher & Prather, 2012).

Shifting the fate of glucose towards its complete oxidation may reduce biosynthetic pathways in the ICM. Enhanced glycolysis enables the production of glycolytic intermediates to be directed to biosynthetic pathways, such as the pentose phosphate pathway (PPP) for the synthesis of ribose sugars for DNA and RNA synthesis, and NADPH required for lipid biosynthesis and glutathione and thioredoxin systems, essential for antioxidant responses (Sies & Jones, 2020; D. G. Smith & Sturmey, 2013). In addition, aerobic glycolysis results in the increase production and secretion of lactate (D. K. Gardner & Harvey, 2015). Increased lactate secretion and acidification of the extracellular environment have been proposed to facilitate implantation and modulate the local immune response to avoid the rejection of the embryo (D. K. Gardner & Harvey, 2015). Thus, limited supply to the PPP arm and reduced lactate production by ICM may alter biosynthetic pathways and potentially implantation. In the mouse it has been shown that the ICM consumes three times more glucose and produces six times more lactate than the TE (Moley, 1999). However, the contribution of the ICM to total lactate production to facilitate implantation has not been previously described. Identification of the contribution of the ICM could provide further insights in the context of lactate reduction under an abnormal metabolic activity.

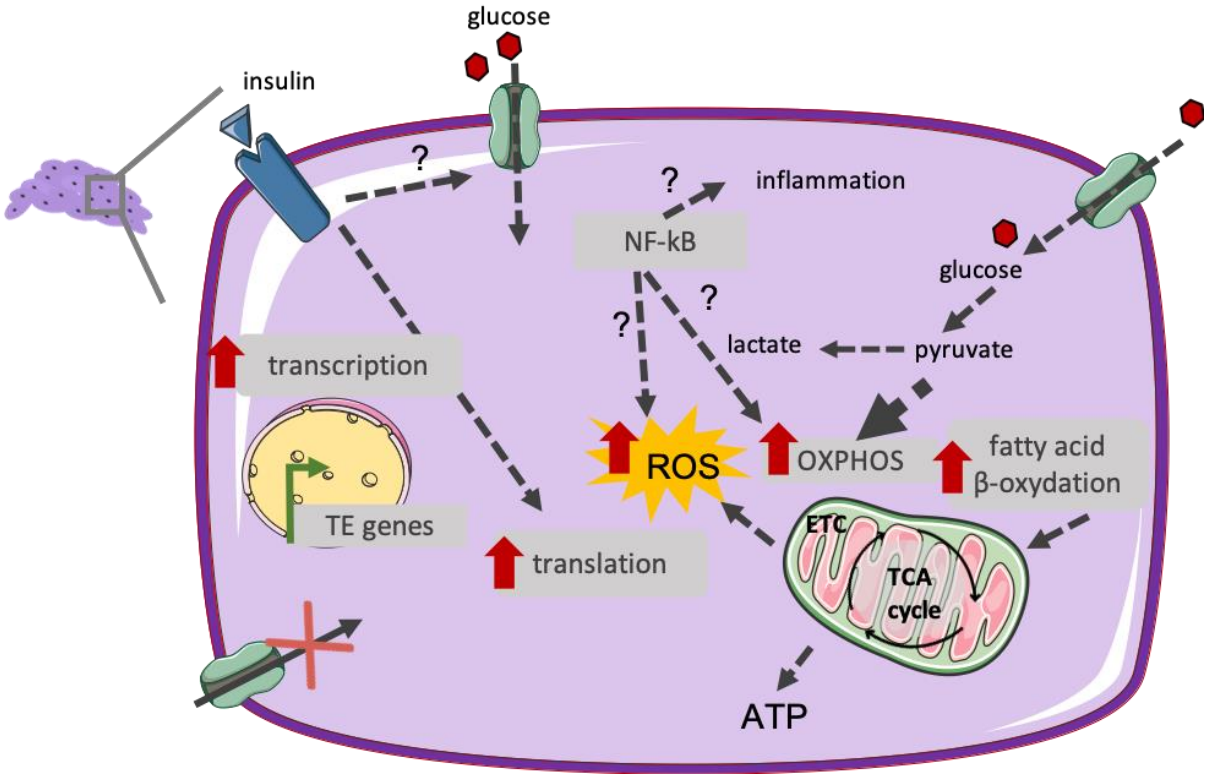

Figure 42: Schematic representation of the main responses in the ICM of embryos exposed to high glucose and high insulin *in vitro*.

Grey boxes show the responses identified in this thesis by transcriptomic profiling and preliminary accessible chromatin analysis. Red arrows indicate the hypothesized direction of expression changes. Dashed grey arrows show the hypothesized relationship among the different responses identified. ETC, electron transport chain; OXPHOS, oxidative phosphorylation; ROS, reactive oxygen species; TCA, tricarboxylic acid; TE, trophectoderm.

Increased ATP generation may be associated with increased protein synthesis in ICM of exposed embryos. Mammalian somatic cells use one-third of the produced ATP to support protein synthesis (Houghton, 2006). The ICM of exposed embryos showed transcriptome changes related to protein translation. It is then possible to speculate that ICM from embryos exposed to high glucose and/or high insulin completely oxidizes glucose to support protein synthesis.
In HI and HGI ICM, protein synthesis may be mediated by insulin. Insulin signaling via mTORC1 triggers the transcriptional activation of several targets, including genes involved in protein synthesis such as the p70 ribosomal S6 kinase (S6K) (Boucher et al., 2014).
In HG ICM, increased protein synthesis may have been trigged by glucose. In fast-twitch muscle fibers of pig neonates under insulin and amino acid fasting levels, post-prandial glucose levels stimulated protein synthesis with increased phosphorylation of PKB and formation of the eIF4E-eIF4G complex, independent of AMPK and mTOR nutrient-sensing pathways (Jeyapalan et al., 2007).
Interestingly, high glucose caused chromatin accessibility within the promoter region of *DERA*. Upon glucose deprivation in HG ICM cells, DERA transcriptional activation may have been regulated to enable the maintenance of ATP levels by using deoxynucleosides as energy sources (Salleron et al., 2014).

Additionally, increased OXPHOS may result in increased production of intermediates from the TCA cycle, required for anabolic processes such as esterols and fatty acids production from citrate, glutamate, glutamine, and proline production from α-ketoglutarate, and aspartate and asparagine production from oxaloacetate (DeBerardinis & Chandel, 2020). Increased OXPHOS could result in increased availability of TCA-derived metabolites that act as substrates and cofactors for chromatin-modifying enzymes such as acetyl-CoA, donor of the acetyl group for acetylation reactions (Dai et al., 2020). However, it was shown that glucose only contributes to minor amounts of carbon to TCA metabolites, and rather pyruvate/lactate supply most carbon units in mouse blastocysts (Sharpley et al., 2021). In mouse blastocysts, glucose is metabolized through the PPP and supplies nearly all ribose carbons in nucleotides (Sharpley et al., 2021). These evaluations were made on whole blastocysts, therefore, it is yet to be determined whether glucose follows the same fate in both cell lineages and across species and also in pathological settings, such as in high glucose and/or high insulin-rich environments. In our model, complete oxidation of glucose in the ICM, could perturb carbon contributions patterns in TCA-derived metabolites.

Increased OXPHOS in the ICM may come with a price, and the presence of both high glucose and high insulin in the ICM of exposed embryos may be a clear example. In HGI ICM, ROS-related gene expression changes were detected, possibly indicative of impaired mitochondrial function and metabolic stress (Figure 42). Reactive oxygen species are generated by various sources, including fatty acid β-oxidation and mitochondrial electron transport chain (ETC) (Liemburg-Apers et al., 2015; Sies & Jones, 2020). The mitochondrial ETC releases superoxide and hydrogen peroxide in physiological contexts, important actors of redox signaling (Sies & Jones, 2020). However, increased OXPHOS may lead to overproduction of ROS (Donnay et al., 1999; Liemburg-Apers et al., 2015).
Interestingly, chromatin accessibility profiling by ATAC-seq has further reinforced the hypothesis of metabolic stress in HGI ICM. Indeed, HGI ICM show loss of chromatin accessibility on the promoter of glutathione reductase (*GSR*) gene, an antioxidant enzyme key member of the glutathione system, downstream of NFE2 like bZIP transcription factor 2 (NRF2), the master regulator of cellular redox

homeostasis (Couto et al., 2016). In the ICM, as detailed above, it has been proposed that glycolysis and PPP contribute to the supply of NADPH for the synthesis of reduced glutathione (GSH) (D. K. Gardner & Harvey, 2015). Therefore, a shift towards complete oxidation of glucose may reduce the NADPH pool and, consequently, the activity of GSR, thereby eliminating a protective mechanism against oxidative stress.

Potential signatures of cellular stress have been detected in ICM from embryos exposed to HG or HGI (Figure 40 and 42). Both HG and HGI ICM showed gene expression signatures of NF-kB signaling. NF-kB signaling regulates different cellular processes including inflammatory responses, apoptosis, metabolism, and oxidative stress, with both anti- and pro-oxidant roles described in different cellular contexts (Lingappan, 2018; T. Liu et al., 2017). Interestingly, NF-kB has been shown to regulate the expression of OXPHOS genes and to upregulate OXPHOS in cancer cells, thereby suppressing the Warburg effect (Albensi, 2019). Transcriptome signatures of NF-kB in HG and HGI ICM may be associated with increased OXPHOS signatures but also in ROS production, especially in HGI ICM.

The suspected increase in cellular respiration and mitochondrial activity may distance ICM of exposed embryos from the optimal metabolic activity range, as stipulated by the "quiet embryo" hypothesis and the "Goldilocks Zone" concept proposed by Leese, et al. and colleagues (Leese, 2002; Leese et al., 2022). The "quiet embryo" hypothesis postulated that a "quiet" rather than "active" metabolism is associated with viability (Leese, 2002). Recently, this hypothesis has been revisited and the concept "Goldilocks Zone" has been added to better define the optimal ranges of metabolic activity (Leese et al., 2022). It has been now proposed that not "too quiescent" nor "too high" metabolic activity is suitable for developmental potential (Leese et al., 2022). It has been proposed that some of the responses of embryos, and in this case the ICM, to environmental stress that results in loss of "quietness" and upregulation of metabolism includes higher OXPHOS activity, protein synthesis and ROS production (Krisher & Prather, 2012; Leese et al., 2022). Both protein synthesis and OXPHOS were overrepresented in embryos exposed to high glucose and/or high insulin, and HGI ICM exhibited ROS-related transcriptome changes. Although developmental competence was not affected by high glucose and/or high insulin in *in vitro*-developed blastocysts, it is tempting to speculate that despite this, the ICM of these embryos was outside the optimal metabolic activity range as proposed by the "quiet embryo" revisited hypothesis (Leese et al., 2022). Maintenance of a "quiet" aerobic metabolism minimizing ROS production may contribute to pluripotency, self-renewing and proliferation capacity in the ICM (Leese et al., 2008).

1.2 Impact on energy metabolism in the TE

The trophectoderm, a differentiated polarized epithelium is the first differentiated lineage during embryonic development and within the embryo, has a different role than the ICM. The TE is in charge of blastocoel formation and the transcellular transport of substrates and growth factors for the use of ICM (Houghton, 2006). Indeed, the polar TE and the blastocoel are the immediate microenvironments of the ICM (Moley, 1999). To accomplish these main functions, a sufficient amount of ATP must be generated in the TE (Houghton, 2006). Studies in mouse embryos have shown that the TE metabolizes glucose, the main energy source at blastocysts stage, through OXPHOS (D. K. Gardner & Harvey, 2015). The notion that TE has increased mitochondrial activity and, thereby oxygen consumption is supported by the

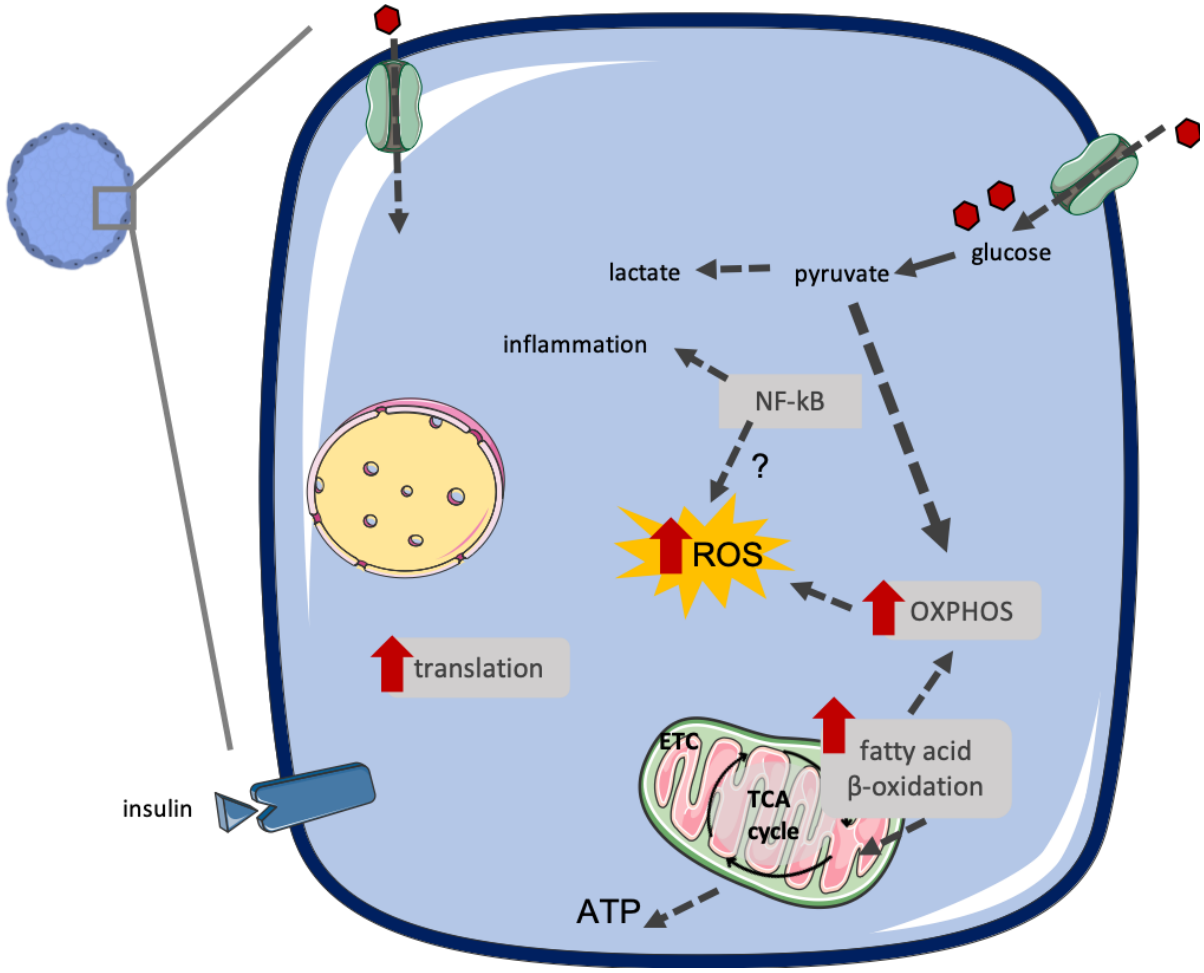

Figure 39: Schematic representation of the main responses in the TE of embryos exposed to high insulin *in vitro*.

Grey boxes show the responses identified in this thesis by transcriptomic profiling. Red arrows indicate the hypothesized direction of expression changes. Dashed grey arrows show the hypothesized relationship among the different responses identified. ETC, electron transport chain; OXPHOS, oxidative phosphorylation; ROS, reactive oxygen species; TCA, tricarboxylic acid.

increased number of mitochondria compared to the ICM, and the long, slender with, prominent cristae morphology of TE mitochondria (Houghton, 2006). Consequently, it is overall considered that TE has a more active metabolism than the ICM (Houghton, 2006). In the rabbit, transcriptome analysis and evaluation of mitochondrial membrane depolarization and OXPHOS-derived ROS revealed higher expression of OXPHOS genes, higher mitochondrial membrane depolarization and ROS generation in the TE from E3.5 onwards compared to ICM from *in vivo* embryos (Bouchereau et al., 2022).
In our model, the TE of embryos exposed to high insulin (HI) and high glucose and high insulin (HGI) showed transcriptome changes related to OXPHOS and ROS (Figure 39 and 43). In HI TE gene expression changes related to fatty acid β-oxidation were also identified. Oxidative metabolism in the rabbit TE is not unexpected. However, because its overrepresentation was highlighted when compared to CNTRL TE transcriptome, together with the enrichment of ROS-related pathways, it suggests an overactivation of OXPHOS and ROS generation. The electron transport chain coupled with OXPHOS is a well-known endogenous source of ROS, and excessive OXPHOS is associated with the overproduction of ROS (Donnay et al., 1999; Liemburg-Apers et al., 2015). Interestingly, HI TE also showed fatty acid β-oxidation-related gene expression changes, and fatty acid β-oxidation is another endogenous source of ROS (Liemburg-Apers et al., 2015). It is thereby possible to speculate that the TE of embryos exposed to high insulin alone or in combination with high glucose, as observed in the ICM, may present impaired mitochondrial function and be under metabolic stress.

The NF-kB signaling was also overrepresented in the TE of embryos exposed to high glucose and/or high insulin (Figure 39, 41 and 43). NF-kB has been associated with several processes, including its influence on OXPHOS over glycolysis in cancer cells and the response to ROS (Lingappan, 2018; T. Liu et al., 2017). In the TE, activation of NF-kB signaling may also influence trophoblast development and function (Armistead et al., 2020; Marchand et al., 2011). The NF-kB signaling pathway was found to be overrepresented during *in vitro* differentiation of the trophoblast lineage (Marchand et al., 2011). Indeed, NF-kB is essential during normal placental development, especially in the first trimester, to promote the invasion of extravillous cytotrophoblasts which derivate from the TE, and the trophoblast-decidual crosstalk (Armistead et al., 2020). However, hyperactivation of NF-kB in the placenta has been associated with preeclampsia (Armistead et al., 2020). Overproduction of pro-inflammatory cytokines may promote an inflammatory environment, lead to vascular dysfunction and impair the trophoblast-decidual crosstalk and invasion of the extravillous cytotrophoblasts (Armistead et al., 2020).

Different from the ICM, which is protected by the polar TE from the external environment, the TE is protected by the zona pellucida, making the TE more closely exposed to the external milieu. Elevated levels of glucose, as in the HG or HGI context, led to overexpression of both *ARRDC4* and *TXNIP* in HG and HGI TE. As described above, *ARRDC4* and *TXNIP* participate in the inhibition of glucose uptake and regulation of the cellular glucose homeostasis (Richards et al., 2018; Wilde et al., 2019).
Both high glucose and insulin-stimulated glucose upregulation of *TXNIP* and *ARRDC4* leading to inhibition of glucose uptake has been previously described (Dagdeviren et al., 2020; Richards et al., 2018). Glucose-6-phosphate, the first step after glucose entry to the cell, is the key signal for MondoA transcriptional activity, which includes the transcriptional activation of *ARRDC4* and *TXNIP* (Wilde et al., 2019). MondoA responds to both glycolysis and OXPHOS (Wilde et al., 2019). Interestingly, HG TE also showed overexpression of hexokinase 1 (*HK1*), the responsible enzyme phosphorylation of glucose after its entry into the cell yielding glucose-6-phosphate, the first step of glycolysis (Chandel, 2021a).

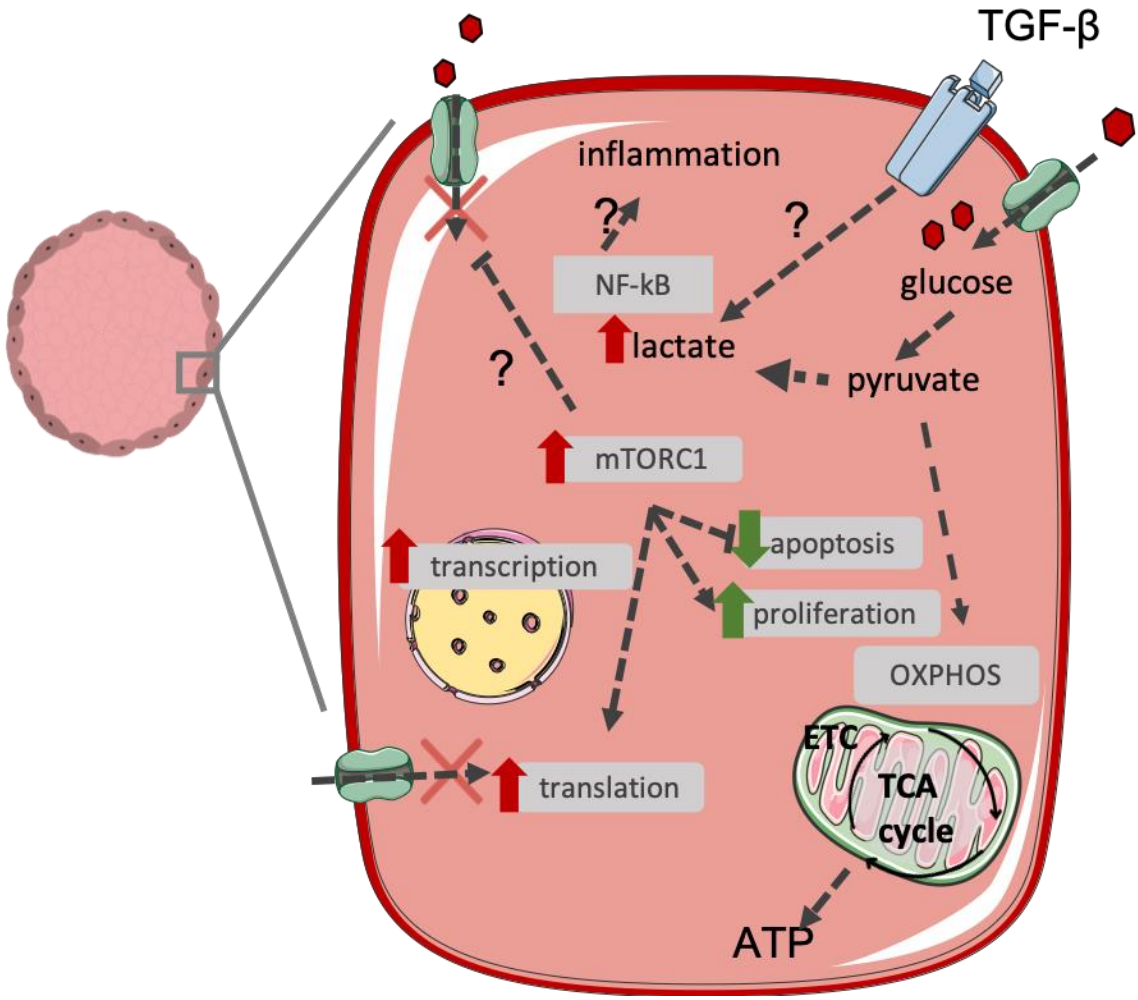

Figure 41: Schematic representation of the main responses in the TE of embryos exposed to high glucose *in vitro*.

Grey boxes show the responses identified in this thesis by transcriptomic profiling and preliminary accessible chromatin analysis. Up and down green arrows show the direction of expression changes confirmed at the cellular level. Red arrows indicate the hypothesized direction of expression changes. Dashed grey arrows show the hypothesized relationship among the different responses identified. ETC, electron transport chain; mTORC1, mechanistic target of rapamycin complex 1; OXPHOS, oxidative phosphorylation; TCA, tricarboxylic acid; TGF-β, transforming growth factor beta.

Overexpression of *ARRDC4* and *TXNIP* and potentially inhibition of glucose uptake in a glucose-rich environment suggests a negative regulatory feedback loop in HG and HGI TE potentially as a way to restore metabolic homeostasis. Reduced glucose uptake by the TE could lead to reduced free glucose levels in the blastocoel, influencing energy metabolism in the ICM as previously described.

Overexpression of *ARRDC4* and *TXNIP* upon increased glucose levels may not be a straight-forward response of the TE. Indeed, overexpression of mTORC1 was identified in HG TE (Figure 41). The mammalian target of rapamycin (mTOR) is a nutrient-sensing pathway responsive to various environmental cues, including oxygen, energy, nutrients, and growth factors to drive cell growth (Saxton & Sabatini, 2017). To facilitate growth, the mTOR protein complex mTORC1 stimulates glycolysis over OXPHOS (Saxton & Sabatini, 2017). In addition, previous reports have shown that mTOR is a negative regulator of TXNIP expression to stimulate glucose uptake and proliferation (Wilde et al., 2019).
Considering that HG TE showed increased proliferation, which will be discussed in the next section, along with *HK1*, *ARRDC4* and *TXNIP* overexpression, it is tempting to hypothesize that inhibition of glucose uptake is a downstream response to an increased glycolytic flux in order to restore glucose homeostasis in the TE exposed to high glucose.
An increased glycolytic flux in HG TE may also be associated with gene expression changes related to the transforming growth factor beta (TGF-β). Several studies have reported that in a high glucose context, TGF-β further facilitates glycolysis over OXPHOS, stimulates glucose uptake, lipid metabolism and fatty acid storage, ROS generation, among several other responses (H. Liu & Chen, 2022). Nevertheless, TGF-β signaling is involved in many cellular processes, including apoptosis, adhesion and migration, immunity, and differentiation, thus the involvement of TGF-β glucose metabolism in the TE of embryos exposed to high glucose requires further studies (H. Liu & Chen, 2022).
Exposure to hyperglycemia in *in vitro* and *in vivo* in diabetes-induced rabbits led to hyperactivation of mTORC1 signaling, especially in the TE, and has been proposed to be involved in the metabolic programming in the offspring exposed to a diabetic intrauterine environment (Gürke et al., 2016). Moreover, mTOR signaling is essential for TE specification, trophoblast differentiation and during the implantation process to by promoting invasive and migratory activity (P. M. Martin & Sutherland, 2001). In a high glucose context, hyperactivation of mTORC1, known to stimulate *de novo* lipid synthesis, may result in perturbated lipid profiles in the placenta. Rabbit blastocysts developed under an alloxan-induced diabetic environment exhibited increased lipid accumulation along with the differential expression of genes implicated in *de novo* lipid synthesis, lipid storage and fatty acid transport, and metabolism (Schindler et al., 2014). Similarly, exposure to an alloxan-induced diabetic environment exclusively during the periconceptional period, followed by transfer to non-diabetic recipients in the rabbit, was sufficient to alter the expression of genes involved in lipid metabolism and to induce specific fatty acid signatures in the placenta, adaptation that may have contributed to hyperglycemia and dyslipidemia detected in rabbit fetuses (Rousseau-Ralliard, Couturier-Tarrade, et al., 2019). Activation of mTOR signaling in the placenta, along with increased expression of glucose, fatty acids and amino acids transporters, has been proposed to contribute to the excessive nutrient transfer to the fetus and resultant impaired growth trajectories and adiposity in the offspring of T2D pregnancies (Castillo-Castrejon et al., 2021).

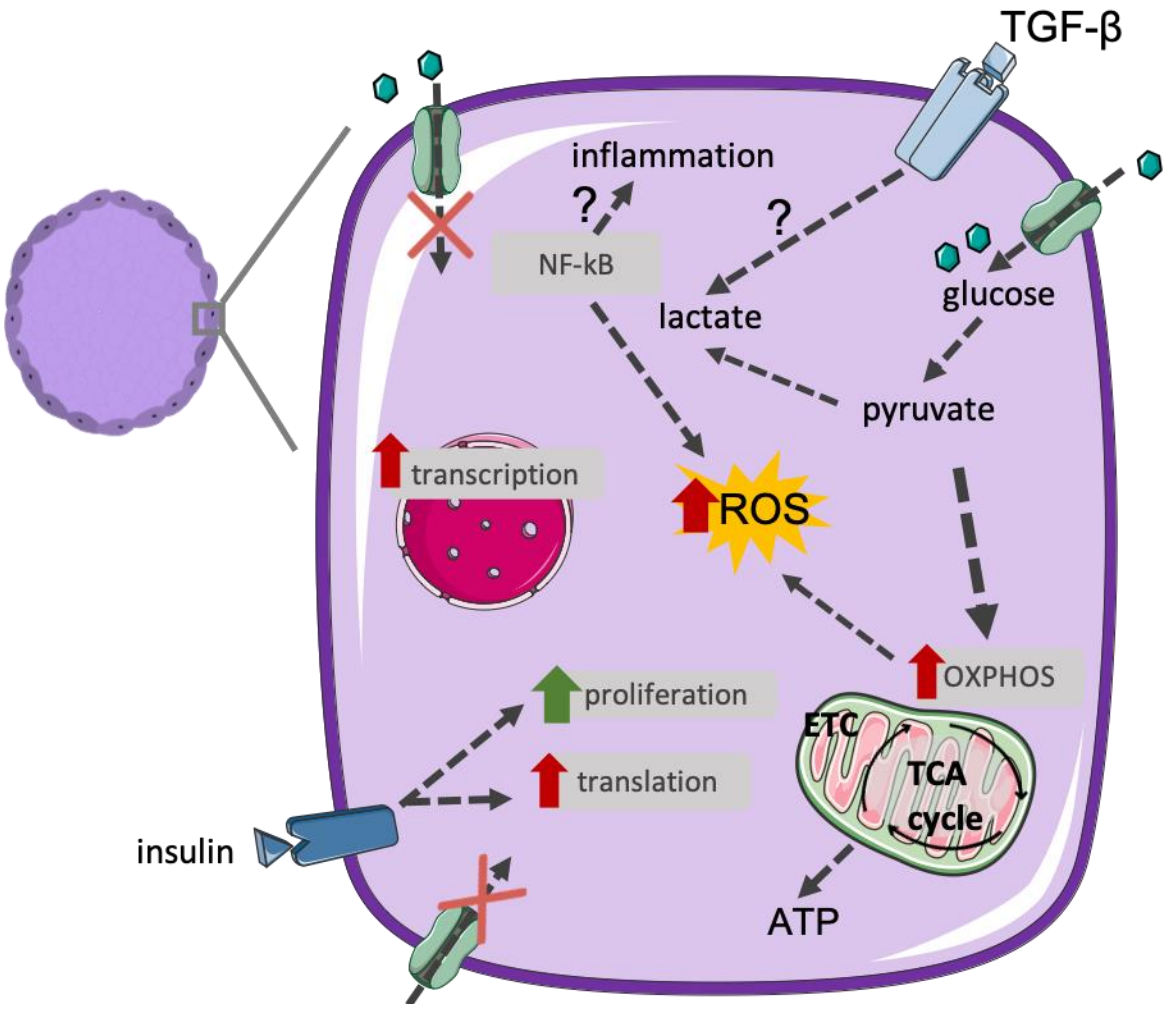

Figure 41: Schematic representation of the main responses in the TE of embryos exposed to high glucose and high insulin *in vitro*.

Grey boxes show the responses identified in this thesis by transcriptomic profiling and preliminary accessible chromatin analysis. The up green arrow shows the direction of expression changes confirmed at the cellular level. Red arrows indicate the hypothesized direction of expression changes. Dashed grey arrows show the hypothesized relationship among the different responses identified. ETC, electron transport chain; OXPHOS, oxidative phosphorylation; ROS, reactive oxygen species; TCA, tricarboxylic acid; TGF-β, transforming growth factor beta.

2. Impact on cell number homeostasis in the ICM and TE of exposed embryos

2.1 Impact on cell number homeostasis in the ICM of exposed embryos

Glucose and insulin have both been associated with the perturbation of growth trajectories in the offspring. In the embryo, exposure to insulin *in vitro* from the 2-cell stage was shown to increase total cell numbers in blastocysts, and this was due to increased proliferation and 23% enhanced cell numbers in the ICM (Harvey & Kaye, 1990). Transfer of insulin-exposed blastocysts and evaluation at E19-20 showed a 4-6% increase in fetal weight (Kaye & Gardner, 1999). Further investigation on the origin of increased fetal and birth weight in mouse embryos exposed *in vitro* to insulin exclusively during the preimplantation period revealed aberrant DNA methylation signatures of *Igf2* and *H19* imprinted genes, two important regulators of fetal and placental growth (Shao et al., 2007).
However, the mitogenic effects of insulin during preimplantation development remain controversial. Previous studies also in mice showed decreased cell numbers and extensive apoptosis in the ICM upon exposure to high insulin *in vitro* (M. M.-Y. Chi et al., 2000). In our study, exposure to high insulin did not affect total cell numbers of blastocysts, and transcriptome analysis did not show an overrepresentation of cell cycle and/or apoptosis gene expression changes. A plausible explanation for these differences may reside in the experimental strategies used (i.e., species, concentrations used, the timing of exposure, the manipulation techniques at critical stages such as the EGA, especially in the mouse).

On the contrary, high glucose alone or in combination with high insulin led to different responses in the ICM of exposed embryos. Both HG or HGI exposure led to increased blastocyst rate, reduced rate of compacted embryos, significantly higher total cell numbers, and transcriptome changes associated with cell proliferation and apoptosis (Figure 40 and 42). Interestingly, only the ICM from embryos exposed to HG showed increased number of apoptotic cells and reduced number of proliferating cells. Increased apoptosis triggered by hyperglycemia has been previously described in mouse, rat, bovine, and rabbit preimplantation embryos (M. M. Y. Chi et al., 2000; Hinck et al., 2003; Jiménez et al., 2003; Moley, Chi, & Mueckler, 1998; Moley, Chi, Knudson, et al., 1998; Ramin et al., 2010).
Interestingly, previous studies have shown increased apoptosis, precisely in the ICM of preimplantation embryos exposed to hyperglycemia and/or a diabetic intrauterine environment (R. G. Lea et al., 1996; Pampfer et al., 1990; Ramin et al., 2010). In the mouse, *in vitro* exposure to hyperglycemia *in vitro* led to reduced cell allocation to the ICM, but no signs of increased apoptosis were detected (Fraser et al., 2007). In the rabbit, alloxan-induced diabetes led to an increased expression of antiapoptotic gene *BCL2L1* also known as *bcl-x(L)* and 4.3-fold increase in apoptotic cells in the ICM of D6 blastocysts (Ramin et al., 2010). Similarly, using the spontaneously diabetic BB rat model, exposure to an intrauterine diabetic context resulted in a reduced number exclusively in the ICM (R. G. Lea et al., 1996).
Increased apoptosis upon exposure to *in vitro* or *in vivo* hyperglycemia has been attributed to a decrease in glucose uptake and intraembryonic free glucose (M. M. Y. Chi et al., 2000; Jiménez et al., 2003; Moley, Chi, & Mueckler, 1998). Streptozotocin-induced diabetes mice exhibited decreased expression of glucose transporter GLUT-1 and reduced glucose uptake resulting in decreased intraembryonic free glucose levels which was proposed to act as a cell death signal and trigger apoptosis via increased expression of the proapoptotic protein BAX (M. M. Y. Chi et al., 2000). In our model, we did not detect differential expression of GLUT transporters, but we rather identified overexpression of *ARRDC4*, as previously described, *ARRDC4* has been shown to inhibit glucose uptake in other cell systems, especially

in a high-glucose context (Dagdeviren et al., 2020; Richards et al., 2018). Therefore, we can hypothesize that increased apoptosis in HG ICM was possibly triggered by reduced glucose uptake and/or reduced intraembryonic free glucose levels since the TE, which supplies glucose for the ICM also showed overexpression of *ARRDC4* and *TXNIP* when exposed to high glucose alone or in combination with high insulin.

Contrary to HG ICM, in HGI ICM no signs of increased apoptosis or reduced proliferation were identified. It is possible that in the presence of both high glucose and high insulin, other transporters sensitive to insulin signals may compensate for reduced glucose uptake, such as GLUT-8, which has been shown to respond to insulin to regulate glucose uptake in the mouse (Purcell & Moley, 2009). In mouse embryos exposed to high glucose *in vitro*, GLUT-1 expression and glucose uptake were reduced (M. M.-Y. Chi et al., 2000). GLUT-1 is expressed by the basolateral plasma membrane of the TE and the plasma membrane of the ICM, and has been proposed to transport glucose from the outside towards the blastocoel and into the ICM (Purcell & Moley, 2009). However, the blocked expression of GLUT-1 using antisense oligonucleotides led to a reduction of 36% of intraembryonic free glucose (M. M.-Y. Chi et al., 2000), which suggests that other transporters also participate in glucose uptake.
A few reports have described that insulin treatment during preimplantation development in diabetic rats reduced the rate of malformations, and a reduced number of ICM cells has been associated with increased rate of malformations and reabsorptions in diabetic (M. M.-Y. Chi et al., 2000; Moley, 1999). Indeed, even a short interruption of insulin treatment in streptozotocin-induced diabetes rats during the preimplantation period resulted in increased rates of skeletal malformations, thus highlighting the importance of tight glycemic control during preimplantation development (Eriksson et al., 1983). It is thus possible that insulin may reduce the hyperglycemia-induced responses in preimplantation embryos, in this case, apoptosis. Indeed, insulin is known to exert anti-apoptotic actions (Boucher et al., 2014). However, other reports also using alloxan-induced or spontaneous diabetic models have reported higher rates of apoptosis in the ICM even in the presence of regular insulin supplementation (R. G. Lea et al., 1996; Ramin et al., 2010), therefore the role of insulin in protecting the ICM against apoptosis may be influenced by others factors such as the concentration of insulin.
Additionally, other mechanisms protecting HGI ICM cells against apoptosis may be in play. HGI ICM showed chromatin accessibility within the *SAMD8/SMSr* promoter, an ER-ceramide sensor that exerts an anti-apoptotic activity by modulating ceramide production under physiological contexts (Cabukusta et al., 2017; Tafesse et al., 2013). It would be interesting to examine further the expression and activity of *SAMD8/SMSr* under high glucose and high insulin conditions in the early embryo.

Surprisingly, the ICM of embryos exposed to high glucose alone or in combination with high insulin showed the overexpression of genes associated with the trophectoderm lineage (Figure 40 and 42). High glucose ICM showed overexpression of GATA binding protein 3 (*GATA3*) and *PLET1*. The transcription factor GATA3 is associated with TE initiation and trophoblast differentiation (F. Chi et al., 2020; Ralston et al., 2010). In mESCs, GATA3 overexpression was sufficient to induce trophoblast fate to drive trophoblast differentiation in TSCs (Ralston et al., 2010). In the rabbit*, GATA3* was found to be expressed in some cells from the morula stage, indication of an early onset of TE program (Bouchereau et al., 2022). Regarding PLET1, is an epigenetically-regulated cell surface protein essential to drive the differentiation of the trophoblast lineage (Murray et al., 2016). *In vitro*, it was shown that PLET1 expression alone was

not sufficient to induce a cell fate switch between embryonic stem cells (ESCs) to trophoblast stem cells (TSCs), but its overexpression promoted the differentiation of TSCs (Latos & Hemberger, 2016).
Concerning HGI ICM, overexpression of *PEG10* and also *PLET1* were identified. *PEG10* is a paternally expressed imprinted gene, highly expressed in the placenta and essential for placenta formation in early development (Ono et al., 2006). Additionally, HGI resulted in gained and loss of chromatin accessibility of genes potentially implicated in lineage specification. HGI resulted in chromatin accessibility within the promoter of *SOX1*, an early marker of neural progenitors that are not expressed in the ICM of rabbit *in vivo* blastocysts, and *ZC3HAV1,* which appears to be associated with the TE in the rabbit, contrary to other species (Ozawa et al., 2012). Conversely, HGI ICM loss chromatin accessibility within the promoter of *BABAM2*. Loss of *BABAM2* expression has been associated with progressively reduced expression of pluripotency markers and cell cycle progression blockage in mESCs. It is tempting to speculate that exposure to high glucose alone or in combination with high insulin may impair ICM cell commitment.
It has been recently shown by Chi, *et al.* and colleagues that glucose metabolism is essential in the TE specification program in the mouse (F. Chi et al., 2020). Glucose metabolism through the hexosamine biosynthetic pathway (HBP) controls YAP1 localization to the nucleus, while the pentose phosphate pathway (PPP) and mTOR drive the translation regulation and activation of TFAP2C, which together with YAP1 regulate the transcriptional activation of TE-specific markers such as *Cdx2* and *Gata3* to initiate the TE fate program (F. Chi et al., 2020; Gerri, Menchero, et al., 2020).
As detailed previously, one of our hypotheses is that ICM exposed to high glucose and/or high insulin increases the oxidation of glucose for energy production which could compromise biosynthetic pathways such as the PPP. Thus, one possible explanation for the expression of TE-genes in HG and HGI ICM would be that glucose metabolism through HBP and PPP metabolic pathways may have influenced the TE program in ICM cells. However, we have not identified transcriptome changes related to those metabolic pathways. In addition, Chi, *et al.* and colleagues also showed that the expression of the transcription factor *GATA3* frequently associated with TE fate initiation was not found to be glucose-responsive (F. Chi et al., 2020).
In human ESCs, culture with high glucose impaired the differentiation of the definitive endoderm, partly by disruption of histone methylation patterns on the promoters of definitive endoderm markers (A. C. H. Chen et al., 2017). Taking into consideration these elements, it is thereby possible that in our model, high glucose in the ICM may have trigger other signals leading to the overexpression of TE genes. Aberrant ICM gene expression programs, possibly by activation of TE potential, may trigger a cell death cascade in this lineage, as others have suggested (M. M.-Y. Chi et al., 2000; Pampfer, 2000).
At this time, it is unclear which signal may have triggered increased apoptosis in HG ICM and what may have protected from it in the presence of high glucose and high insulin. Further studies will be required to answer these questions.

Perturbation in ICM cell numbers may affect the TE lineage as well as future fetal development. Mouse blastocysts with different amounts of ICM cells led to limited trophoblast proliferation, suggesting the necessity for cell allocation homeostasis between these two lineages (Ansell & Snow, 1975; Pampfer, 2000). Concerning fetal development, an appropriate number of ICM cells has been shown to be required for normal fetal development, and it is considered to be essential for embryo health (Houghton, 2006; Lane & Gardner, 1997). Indeed, reduced ICM cell numbers have been proposed to be at the origin of malformations and/or perturbated growth trajectories, i.e., small for gestational weight frequently associated with diabetic pregnancies (R. G. Lea et al., 1996; Moley, 1999).

2.2 Impact on cell number homeostasis in the TE of exposed embryos

As recently described, the mitogenic effects of insulin on the preimplantation period are controversial, and this is true for both the ICM and TE.
In the bovine, *in vitro* supplementation of insulin resulted in increased blastocyst total cell numbers due to a significantly increase in TE cell numbers and decreased in the number of apoptotic cells (Augustin et al., 2003). In our study, transcriptome analysis in the TE of embryos exposed to high insulin did not show differential expression of genes implicated in cell cycle and/or apoptosis and only a few gene sets were identified by GSEA enrichment analysis. Additionally, blastocysts total cell numbers were not affected by high insulin. On the contrary, the TE of embryos exposed to high glucose alone or in combination with high insulin showed increased total cell numbers at blastocyst stage and increased proliferation in the TE (Figure 41 and 43). In addition, HG TE also showed reduced apoptosis (Figure 41). Consistent with our findings, accessible chromatin profiling identified an open chromatin region proximal to the promoter of *RFC4* gene, involved in DNA replication, in HGI TE. In parallel, CNTRL embryos compared to HGI TE showed open chromatin proximal to the promoter of *POC5* and *PARD3,* both associated with cell cycle.
Considering that no increased proliferation was observed in HG or HGI ICM, it is tempting to speculate that an increased total cell number in these embryos originated by an increased proliferation in the TE.

Increased cell numbers in the TE could explain the increased blastocyst rate observed in embryos exposed to HG or HGI, and it may have influenced the TE lineage. The pumping of the TE into the extracellular space results in the expansion of the blastocoel, which influences the size of the embryo (Zhu & Zernicka-Goetz, 2020). Continuous pumping by the TE creates pressure within the blastocyst, which deforms the TE and ICM lineages and stimulates the recruitment of tight junction proteins to TE cell contacts, further stimulating the cavitation process (Zhu & Zernicka-Goetz, 2020). Interestingly, if cavitation is perturbed, blastocysts are smaller and have increased ICM numbers, therefore the ICM: TE ratio is impacted (Zhu & Zernicka-Goetz, 2020). Although the mechanism linking cavitation and the ICM:TE ratio is not known, it is hypothesized to involve the reduction of cavity tension which influences the division pattern of TE cells (Zhu & Zernicka-Goetz, 2020). In our model, increased proliferation in the TE and possibly increased TE numbers may have stimulated the cavitation process, resulting in reduced compacted embryos and increased blastocysts rate after 72 h exposure to HG or HGI. The influence of increased proliferation in the TE on the ICM:TE ratio cannot be excluded. Here, we were not able to determine ICM and TE cell numbers, thus further studies will be required to confirm this hypothesis.

Between HG and HGI TE there may be different cellular responses governing an increased proliferation. In HG TE, glucose-driven activation of mTORC1 may participate in the regulation of a cascade of responses to support anabolism and cell proliferation (G. Y. Liu & Sabatini, 2020). The positive effects of insulin on proliferation have been well described in different cellular contexts, including the preimplantation embryo (Augustin et al., 2003; Boucher et al., 2014; H. G. Gardner & Kaye, 1991). In HGI TE, increased proliferation is most likely mediated by Raf/Ras/MEK/MAPK arm of the insulin pathway.
Increased proliferation in the TE, progenitor of the embryo portion of the placenta may have consequences for the placenta structure and function and consequently for the offspring. Placental development requires an adequate equilibrium between trophoblast proliferation, differentiation and invasion capacities, especially in early pregnancy (Aires, 2015). Indeed, placental development is most sensitive to perturbations in the first trimester, which is characterized by an intense growth rate (Desoye

& Cervar-Zivkovic, 2020; Vambergue & Fajardy, 2011). In altered metabolic intrauterine environments such as pre-gestational diabetes, both hyperglycemia and hyperinsulinemia may contribute to impaired placental growth (Desoye & Cervar-Zivkovic, 2020). Indeed, pre-gestational diabetes has been associated with increased placental weight (Aires, 2015; Desoye & Cervar-Zivkovic, 2020).
Interestingly, depending on the timing of metabolic imbalances during pregnancy, the effects on the placenta may vary (Desoye, 2018). During the first trimester, one of the described potential effects is impaired trophoblast proliferation (Desoye, 2018). Pre-gestational diabetes is overall associated with a reduction in trophoblast and placental growth due to oxidative and/or proinflammatory stress (Desoye, 2018). However, in the presence of high insulin, a different scenario may present, with insulin signaling rather stimulating placental growth (Desoye, 2018). In the preimplantation context, it remains to decipher the consequences of increased TE proliferation upon exposure to high glucose alone or in combination with high insulin. Further investigation of these responses may be of great relevance, considering that alterations in placental growth may directly influence fetal growth, birth weight, and the offspring's future health (Desoye, 2018; Rousseau-Ralliard, Couturier-Tarrade, et al., 2019).

2.3 The implications of ICM and TE responses to high glucose and/or high insulin on future development and offspring's health

The worldwide incidence of early metabolic imbalances, such as prediabetes and metabolic diseases, such as diabetes, is continuously increasing (International Diabetes Federation, 2021). More women of reproductive age enter pregnancy with poor metabolic health (B. N. Hart et al., 2021; International Diabetes Federation, 2021).
Metabolic imbalances *in utero*, such as pre-gestational diabetes, are associated with congenital malformations and fetal and neonatal metabolic imbalances (Hufnagel et al., 2022; Ornoy et al., 2021). At birth, some of the first signs of altered signatures include the perturbation of growth trajectories, characterized by macrosomia or SGA, depending on the severity of the diabetic context; and metabolic imbalances such as fetal hypoglycemia and hyperinsulinemia, and increased adiposity (Hufnagel et al., 2022; Ornoy et al., 2021). Later in life, offspring exposed to a diabetic environment *in utero* is associated with disease risk, including hypertension, MetS, obesity, cardiovascular diseases, and T2D (Higa et al., 2021; Y. Yu et al., 2019).
Here, we have shown that as early as the first days of embryonic development, glucose and/or insulin-rich environment is sensed by early embryos, and this triggers a series of adaptations, at least at the gene regulation level. These adaptations are suggestive of altered metabolism, cell number homeostasis, cell signaling, cell differentiation, and potentially metabolic stress. These perturbations could result in impaired metabolism, growth trajectories, adiposity, impaired organ development, and function and be traduced as disease risk in the offspring.
Furthermore, not only the future individual is affected by this environment, but also the future placenta. An impaired placental development and function constitute an additional stressor during life *in utero* (Tarrade et al., 2013). Indeed, women with pre-gestational diabetes show heavier, hyper-vascularized, hyperproliferative placentas, with impaired transfer capabilities towards the developing fetus (Gaillard, 2015; Vambergue & Fajardy, 2011).
Further examination of the lineage-specific responses identified here may contribute to understanding the mechanisms underlying developmental programming in the offspring after exposure to metabolic imbalances *in utero*.

STRENGTHS AND LIMITATIONS OF THE STUDY

We have shown that exposure of preimplantation embryos to high glucose and/or high insulin results in common and lineage-specific significant changes in gene expression programs of the ICM and TE. However, some limitations of our work should be acknowledged. At this stage, we have identified differences in transcript level and changes in chromatin accessibility in both ICM and TE exposed to high glucose and/or high insulin. However, these analyses and their interpretation require caution as we have not assessed the protein level or the activity of many of the gene candidates and/or signaling and metabolic pathways.

Rabbits constitute a suitable model for studying the preimplantation period, as detailed in the Introduction, Chapter 3 section 1.1. However, one of the main advantages of this model is the incomplete annotation status of the rabbit reference genome. This has undoubtedly resulted in a loss of information when assessing the differentially expressed genes and differentially accessible chromatin regions within promoters of annotated genes and proximal to putative enhancers, whose location within chromosomes is not well known.

Similarly, since most databases have not yet included the rabbit as a model organism, by using bioinformatics tools that are strictly based in other species we may additionally lose more information. For example, the Gene Set Enrichment Analysis (GSEA) database collections (Hallmarks, KEGG, Reactome) are based on human or mouse molecular signatures, or the bioinformatic tool HOMER used here for searching protein binding motifs within accessible regions of chromatin. Most of the known motifs have been defined in model organisms such as mouse, *Drosophila* and in human, however, the sequence of these motifs may vary between species.

Another aspect that was not included in our analyses but that could provide more information on the effects of high glucose and/or high insulin would be to determine the presence of sexual dimorphism in the responses between embryos. Especially considering that X-chromosome inactivation and dosage compensation initiates at the early blastocyst stage in the rabbit (Okamoto et al., 2011), and our study was performed precisely at this stage, but in in *vitro*-developed embryos, which may show a certain delay in the developmental timing compared to *in vivo* rabbit embryos.
In addition, we observed a certain degree of heterogeneity among biological replicates in both transcriptomic and chromatin accessibility analysis. A different ratio of female and male embryos within biological replicates may have contributed to the observed heterogeneity.

Working with preimplantation models, especially those developed *in vitro*, and in addition to performing each analysis by lineage means that biological material will be limited. This was particularly challenging for ATAC-seq library preparation because obtaining more than 5000 cells, especially for ICM samples, would have been difficult due to the variable number of zygotes obtained from superovulated rabbits between sessions, along with the number of embryos reaching the blastocyst stage with a well-defined blastocoel, and surviving the immunosurgery process.

Finally, we have focused this work on the study of high glucose and/or high insulin exclusively during the preimplantation period. This enables to identify the specific responses of high glucose alone or in

combination with high insulin, and by lineage. However, metabolic imbalances may exist prior to pregnancy as detailed in Introduction, Chapter 3 section 2.2.1, which implies that oocytes were already exposed to intrauterine metabolic imbalances. This may be especially important not only because of the potential epigenetic contribution of the female pronucleus to the embryo, but also considering that mitochondria are maternally-inherited and are one of the main organelles affected by metabolic imbalances and cellular stress. Therefore, it is possible that the contribution of the oocyte may exacerbate the responses of preimplantation embryos to high glucose and/or high insulin.

PERSPECTIVES

Exposure to high glucose and/or high insulin during the *in vitro* development of rabbit preimplantation embryos resulted in transcriptomic and chromatin accessibility changes in the ICM and TE. Several key questions with possible short and long-term perspectives have been generated from this work.

The short-term perspective of this study is to pursue the chromatin accessibility analysis and correlate RNA-seq and ATAC-seq datasets. This analysis could provide more understanding of the molecular responses and gene expression changes previously described. Moreover, it could provide a complete lineage-specific gene network that is activated by the influence of high glucose and/or high insulin, and to provide gene candidates implicated in the epigenetic regulation of gene expression that could be followed by future studies.

One of the main findings of the transcriptome analysis is the perturbation of genes implicated in metabolic pathways, i.e., OXPHOS versus glycolysis in both the ICM and TE of exposed embryos. It the ICM, exposure to high glucose or high insulin alone or combined resulted in OXPHOS-related gene expression changes. This is particularly interesting since previous reports from mouse and rabbit embryos suggest that the ICM is more glycolytic than oxidative. It would be interesting to confirm at the cellular level whether the ICM of exposed embryos shows increased OXPHOS activity while the ICM of *in vitro*-developed control embryos mainly uses aerobic glycolysis.
As it is considered that pre-compaction embryos use OXPHOS and then switch towards glycolysis in the ICM while remaining mostly oxidative in the TE, it would be interesting to, throughout preimplantation development, examine whether his metabolic switch did not take place in the ICM of exposed embryos, or whether it was switched back to oxidative metabolism at some point.
An oxidative metabolism in the ICM could be deleterious for the embryos since it may increase ROS production and compromise biosynthetic pathways such as the pentose phosphate pathway and NADPH pool essential for redox homeostasis.
In the TE of HG embryos, there were rather glycolysis-related gene expression changes, which shifts from the previously-reported preferred metabolic pathways in these lineages. To examine the metabolic pathways governing the ICM and TE of exposed embryos, different elements of cellular metabolism could be analyzed. For example, glucose uptake and consumption could be assessed by using noninvasive techniques such as radiolabeled glucose (D. K. Gardner, 2007). In addition, measurement of lactate production and the activity of mitochondria could provide more insight into the fate of pyruvate and OXPHOS activity in the cell. Mitochondrial activity may be examined by using the TMRE (tetramethylrhodamine, ethyl ester) dye, which is rapidly sequestered by active mitochondria, contrary to depolarized or inactive mitochondria, and which has been previously used in rabbit embryos (Bouchereau et al., 2022).
Furthermore, intracellular levels of ROS could also be examined in exposed embryos. Embryos exposed to high insulin or high glucose and high insulin showed transcriptomic and accessible chromatin changes related to cellular responses against ROS. Therefore, to investigate whether ROS production was enhanced, we could treat exposed embryos with the ROS-sensitive fluorescent probe CellROX.

Another interesting finding related to preimplantation energy metabolism is the strong overexpression of ARRDC4, a glucose uptake inhibitor in both ICM and TE of HG and HGI exposed embryos. To the best of our knowledge, no previous reports have described the role of ARRDC4 and TXNIP in energy metabolism during the preimplantation stage. Thus, it would be interesting to further examine ARRDC4 in physiological and pathological contexts during preimplantation development. For this, functional studies could be included, such as siRNA-mediated downregulation of ARRDC4 coupled with measurement of glucose uptake in preimplantation embryos developed in control and high glucose and/or high insulin conditions. In addition, we could perform immunostaining of MondoA, the transcription factor that regulates ARRDC4 and TXNIP expression, to identify the subcellular location upon the development of embryos in control or high glucose and/or high insulin conditions.

Several studies have described sexual dimorphism in the response of offspring exposed to different environmental cues such as high-fat or low-protein diet, high glucose, and ART (Duranthon & Chavatte-Palmer, 2018; Jiménez et al., 2003; Pérez-Cerezales et al., 2018; Tarrade et al., 2013; Watkins et al., 2007). Our model comprised *in vitro* culture of rabbit preimplantation embryos until the early blastocyst stage. In the rabbit, X-chromosome inactivation and dosage compensation initiate at the early blastocyst stage (96 h.p.c.), first in the TE and then progressively in the ICM (Okamoto et al., 2011). However, as indicated earlier, *in vitro*-developed embryos may show slight developmental delay compared to rabbit embryos *in vivo* (Salvaing et al., 2016). It is then possible that X-chromosome inactivation and dosage compensation in *in vitro*-developed embryos has not yet been initiated or may have taken place only in a few cells. Preimplantation embryos are exerted of the effect of sex hormones since gonadal differentiation takes place at post-implantation stages. However, the absence of dosage compensation or the heterogeneity of X-inactivation in *in vitro*-developed embryos may result in different expression levels of X-linked genes between female and male embryos, which could influence the response to environmental cues.

Indeed, it was previously shown in bovine embryos that exposure to high glucose *in vitro* affected male embryos, and female embryos appeared to be protected against hyperglycemia-induced apoptosis (Jiménez et al., 2003). These differences were attributed to the active X-chromosomes in female embryos since X-chromosome inactivation, and dosage compensation had not yet taken place in these embryos (Jiménez et al., 2003). Moreover, it was suggested that this could also explain the differences in the X-linked gene expression levels in these embryos, including the X-linked inhibitor of apoptosis protein (XIAP) gene, glucose 6-phosphate dehydrogenase (G6PD) key in the pentose phosphate pathway (PPP), and hypoxanthine phosphoribosyl transferase (HPRT) implicated in the detoxification of ROS and involved in growth regulation (Jiménez et al., 2003).
Interestingly, in rabbit embryos, two of these genes are also X-linked. According to Ensembl website and the current annotation of the rabbit reference genome, both XIAP and HPRT are situated within the X-chromosome. As for G6PD, current knowledge is that it is localized in the Scaffold GL018816; therefore, whether G6PD is X-linked in the rabbit is not known.
Taken together, it would be interesting to evaluate whether female and male embryos show the same responses after exposure to high glucose and/or high insulin. Especially since in mouse and human blastocysts, it has been described that female embryos have a higher glucose consumption than male embryos (D. K. Gardner & Harvey, 2015).

To investigate whether there is gender-specific responses, first we should confirm whether X-inactivation has not taken place in *in vitro*-developed embryos. For this, we could perform an RNA fluorescence *in situ* hybridization (FISH) of *Xist,* the regulatory RNA involved in the coating and silencing of the X-chromosome that expressed in both X-chromosomes in the rabbit and to coupled it the immunofluorescence of H3K27me3 which is known to be enriched in the X-inactive chromosome.
In case X-chromosome inactivation was not initiated or is not yet detected in all cells in these embryos, the next step would be to explore for example, whether there is increased apoptosis in female *versus* male embryos exposed to high glucose and/or high insulin. To do this, it would be necessary to sex embryos by performing qPCR of the *XIST* gene, and to determine the expression level of genes involved in apoptosis in individual male and female embryos. In addition, TUNEL assay coupled to *Xist* RNA FISH to discriminate female from male embryos could be performed.

Another finding that would be interesting to further explore is the presence of the overexpressed TE gene in ICM of embryos exposed to HG or HGI, and the altered expression of several genes and signaling pathways in the TE that could compromise subsequent placental development and function. To explore these results deeper, it would be interesting to examine the protein level of ICM and TE markers in these embryos, such as the recently identified naïve pluripotency markers in the rabbit (Bouchereau et al., 2022). Moreover, we could examine the capacity of ICM of exposed embryos to differentiate into EPI and PrE-lineages *in vitro*. Regarding the TE, rabbit trophoblast stem cells could be derived from exposed blastocysts as previously described (Sanz et al., 2019) to investigate the proliferative and invasive capacity of trophoblasts, and the differentiation potential into trophoblast-derived cells such as syncytiotrophoblasts.

Finally, we have shown that exposure to high glucose and/or high insulin influences the gene expression programs of both the ICM and TE. It would be important to examine whether these changes are maintained throughout development, including post-natal stages, and whether the observed changes at the preimplantation stage have influenced the adult phenotype (i.e., weight, blood glucose levels, insulin production and sensitivity in target organs, lipid profile, blood pressure, and other cardiovascular risk factors). Moreover, it would also be interesting to investigate whether the exposure exclusively during the preimplantation stage was sufficient for the onset of developmental programming in the offspring. If this is the case, interventions during the preimplantation stage or later in development could be explored with the intention to reverse or reduce the altered phenotypes.
In vitro-developed embryos exposed to high glucose and/or high insulin could be transferred to healthy normoglycemic rabbit recipients to continue development, a technique that is mastered in the team. By allowing the development of these embryos, different components and developmental stages could be assessed, such as fetal development and the placental structure and function during pregnancy, as well as the phenotype at birth, post-natal life, and adult stages.
Furthermore, because an increased overproduction of ROS is believed in exposed embryos, especially in those exposed to high insulin or high glucose and high insulin, it would be interesting to explore whether interventions during *in vitro* culture could alleviate or reverse the phenotypes identified in this study. These interventions could be examined immediately after culture, in the ICM and TE, but also at fetal and/or post-natal stages, by using the embryo transfer strategy. These interventions could consist on the supplementation of antioxidant enzymes to the culture media, such as the mitochondria-targeted antioxidant and anti-apoptotic agent MitoQ. MitoQ has been previously shown to reduce mitochondrial

oxidative stress and prevent hypoxia-induced developmental programming of cardiovascular disease in rats (Spiroski et al., 2021). Moreover, MitoQ has been previously used during *in vitro* maturation of mouse oocytes and was shown to reduce intracellular levels of ROS, and improve maturation rates and developmental competence of embryos, similar to *in vivo* embryos (Shirzeyli et al., 2020).

GENERAL CONCLUSIONS

This thesis aimed to investigate the effects of early metabolic imbalances such as hyperinsulinemia and/or hyperinsulinemia during the preimplantation period, one of the most vulnerable and often disregarded periods of development.
To this end, an *in vitro* model was generated in the rabbit to explore the potential effects of high glucose and/or high insulin supplementation during the preimplantation period, but more precisely in the two lineages specified during this developmental stage: the ICM, the progenitor of the all tissues and organs of the future individual, and in the TE, the first differentiated cell and progenitor of the fetal portion of the placenta, essential for the nutrition and growth of the developing fetus. Using genome-wide transcriptome and chromatin accessibility profiling techniques, we sought to obtain a comprehensive picture of the potential effects of this altered metabolic environment in the ICM and TE of *in vitro*-developed embryos.

Here, we showed that high insulin alone results in minor gene expression changes in both the ICM and TE of exposed embryos. In contrast, high glucose alone or in combination with high insulin influenced a series of common and lineage-specific responses at the chromatin, transcriptome, and cellular levels. Transcriptomic and chromatin changes were associated with metabolic pathways, cell number homeostasis, cell signaling, cellular stress responses, lineage commitment in the ICM, and gene expression regulation. Interestingly, although transcriptome analysis revealed that the TE of embryos exposed to high glucose exhibited altered expression of a subset of genes involved in epigenetic regulation, accessible chromatin profiling revealed that high glucose and high insulin results in more drastic changes in the accessible chromatin landscape in both the ICM and TE of exposed embryos. At the cellular level alone, high glucose led to increased apoptosis in the ICM and proliferation in the TE. However, in combination with high insulin, only the TE showed increased proliferation. The different results described here raise several questions for future studies that may contribute to a full understanding of the mechanisms put in place by the ICM and TE to adapt to glucose and/or insulin-rich environments.

Finally, our work highlights how disruption of the preimplantation microenvironment by high glucose and/or high insulin impacts both the inner cell mass and trophectoderm of preimplantation embryos, an impact that could compromise the development of the future individual and placenta and contribute to developmental programming of the offspring.

REFERENCES

Aagaard-Tillery, K. M., Grove, K., Bishop, J., Ke, X., Fu, Q., McKnight, R., & Lane, R. H. (2008). Developmental origins of disease and determinants of chromatin structure: Maternal diet modifies the primate fetal epigenome. *Journal of Molecular Endocrinology*, *41*(1–2), 91–102. https://doi.org/10.1677/JME-08-0025

Agence de la biomédecine. (2019). *Activité d 'Assistance Médicale à la Procréation*. https://rams.agence-biomedecine.fr/principaux-chiffres-de-lactivite#:~:text=ENFANTS ISSUS D'UNE AMP,nés de la population générale.

Aguilar, J., & Reyley, M. (2005). The uterine tubal fluid: secretion, composition and biological effects. *Animal Reproduction Science*, *2*(2), 91–105. https://doi.org/https://doi.org/10.1016/j.ydbio.2005.11.002

Aires, M. B. (2015). Effects of maternal diabetes on trophoblast cells. *World Journal of Diabetes*, *6*(2), 338. https://doi.org/10.4239/wjd.v6.i2.338

Albensi, B. C. (2019). What Is Nuclear Factor Kappa B (NF-κB) Doing in and to the Mitochondrion? *Frontiers in Cell and Developmental Biology*, *7*(JULY), 1–7. https://doi.org/10.3389/fcell.2019.00154

Alcolea, M. P., Lladó, I., García-Palmer, F. J., & Gianotti, M. (2007). Responses of mitochondrial biogenesis and function to maternal diabetes in rat embryo during the placentation period. *American Journal of Physiology-Endocrinology and Metabolism*, *293*(3), E636–E644. https://doi.org/10.1152/ajpendo.00120.2007

Aljahdali, A., Airina, R. K. R. I., Velazquez, M. A., Sheth, B., Wallen, K., Osmond, C., Watkins, A. J., Eckert, J. J., Smyth, N. R., & Fleming, T. P. (2020). The duration of embryo culture after mouse IVF differentially affects cardiovascular and metabolic health in male offspring. *Human Reproduction*, *35*(11), 2497–2514. https://doi.org/10.1093/humrep/deaa205

Allis, C. D., & Jenuwein, T. (2016). The molecular hallmarks of epigenetic control. *Nature Reviews Genetics*, *17*(8), 487–500. https://doi.org/10.1038/nrg.2016.59

Ambrosi, C., Manzo, M., & Baubec, T. (2017). Dynamics and Context-Dependent Roles of DNA Methylation. *Journal of Molecular Biology*, *429*(10), 1459–1475. https://doi.org/10.1016/j.jmb.2017.02.008

American Diabetes Association. (2021). 2. Classification and Diagnosis of Diabetes: Standards of Medical Care in Diabetes—2021. *Diabetes Care*, *44*(Supplement_1), S15–S33. https://doi.org/10.2337/dc21-S002

Andrali, S. S., Smapley, M. L., Vanderford, N. L., & Özcan, S. (2008). Glucose regulation of insulin gene expression in pancreatic β-cells. *Biochemical Journal*, *415*(1), 1–10. https://doi.org/10.1042/BJ20081029

Ansell, J. D., & Snow, M. H. L. (1975). The development of trophoblast in vitro from blastocysts containing varying amounts of inner cell mass. *Journal of Embryology and Experimental Morphology*, *33*(1), 177–185. https://doi.org/10.1242/dev.33.1.177

Aplin, J. D., Myers, J. E., Timms, K., & Westwood, M. (2020). Tracking placental development in health and disease. *Nature Reviews Endocrinology*. https://doi.org/10.1038/s41574-020-0372-6

Arab, K., Karaulanov, E., Musheev, M., Trnka, P., Schäfer, A., Grummt, I., & Niehrs, C. (2019). GADD45A binds R-loops and recruits TET1 to CpG island promoters. *Nature Genetics*, *51*(2), 217–223. https://doi.org/10.1038/s41588-018-0306-6

Armengaud, J. B., Yzydorczyk, C., Siddeek, B., Peyter, A. C., & Simeoni, U. (2021). Intrauterine growth restriction: Clinical consequences on health and disease at adulthood. *Reproductive Toxicology*, *99*(October 2020), 168–176. https://doi.org/10.1016/j.reprotox.2020.10.005

Armistead, B., Kadam, L., Drewlo, S., & Kohan-Ghadr, H.-R. R. (2020). The role of NFκB in healthy and preeclamptic placenta: Trophoblasts in the spotlight. *International Journal of Molecular Sciences*, *21*(5), 1775. https://doi.org/10.3390/ijms21051775

Aronoff, S. L., Berkowitz, K., Shreiner, B., & Want, L. (2004). Glucose Metabolism and Regulation: Beyond

Insulin and Glucagon. *Diabetes Spectrum*, *17*(3), 183–190. https://doi.org/10.2337/diaspect.17.3.183

Atlasi, Y., & Stunnenberg, H. G. (2017). The interplay of epigenetic marks during stem cell differentiation and development. *Nature Reviews Genetics*, *18*(11), 643–658. https://doi.org/10.1038/nrg.2017.57

Augustin, R., Pocar, P., Wrenzycki, C., Niemann, H., & Fischer, B. (2003). Mitogenic and anti-apoptotic activity of insulin on bovine embryos produced in vitro. *Reproduction*, *126*(1), 91–99. https://doi.org/10.1530/rep.0.1260091

Azimzadeh, J., Hergert, P., Delouvée, A., Euteneuer, U., Formstecher, E., Khodjakov, A., & Bornens, M. (2009). hPOC5 is a centrin-binding protein required for assembly of full-length centrioles. *Journal of Cell Biology*, *185*(1), 101–114. https://doi.org/10.1083/jcb.200808082

Balaguer, P., Delfosse, V., & Bourguet, W. (2019). Mechanisms of endocrine disruption through nuclear receptors and related pathways. *Current Opinion in Endocrine and Metabolic Research*, *7*, 1–8. https://doi.org/10.1016/j.coemr.2019.04.008

Bannister, A. J., & Kouzarides, T. (2011). Regulation of chromatin by histone modifications. *Cell Research*, *21*(3), 381–395. https://doi.org/10.1038/cr.2011.22

Bar-Even, A., Flamholz, A., Noor, E., & Milo, R. (2012). Rethinking glycolysis: on the biochemical logic of metabolic pathways. *Nature Chemical Biology*, *8*(6), 509–517. https://doi.org/10.1038/nchembio.971

Barker, D. J. P. (1990). The fetal and infant origins of adult disease. *BMJ*, *301*(6761), 1111–1111. https://doi.org/10.1136/bmj.301.6761.1111

Barker, D. J. P., Bull, A. R., Osmond, C., & Simmonds, S. J. (1990). Fetal and placental size and risk of hypertension in adult life. *BMJ*, *301*(6746), 259–262. https://doi.org/10.1136/bmj.301.6746.259

Bassalert, C., Valverde-Estrella, L., & Chazaud, C. (2018). Primitive Endoderm Differentiation: From Specification to Epithelialization. In *Current Topics in Developmental Biology* (Vol. 128, pp. 81–104). https://doi.org/10.1016/bs.ctdb.2017.12.001

Bermejo-Alvarez, P., Roberts, R. M., & Rosenfeld, C. S. (2012). Effect of glucose concentration during in vitro culture of mouse embryos on development to blastocyst, success of embryo transfer, and litter sex ratio. *Molecular Reproduction and Development*, *79*(5), 329–336. https://doi.org/10.1002/mrd.22028

Bianco-Miotto, T., Craig, J. M., Gasser, Y. P., van Dijk, S. J., & Ozanne, S. E. (2017). Epigenetics and DOHaD: from basics to birth and beyond. *Journal of Developmental Origins of Health and Disease*, *8*(5), 513–519. https://doi.org/10.1017/S2040174417000733

Bouché, C., Serdy, S., Kahn, C. R., & Goldfine, A. B. (2004). The cellular fate of glucose and its relevance in type 2 diabetes. *Endocrine Reviews*, *25*(5), 807–830. https://doi.org/10.1210/er.2003-0026

Boucher, J., Kleinridders, A., & Kahn, C. R. (2014). Insulin Receptor Signaling in Normal and Insulin-Resistant States. *Cold Spring Harbor Perspectives in Biology*, *6*(1), a009191–a009191. https://doi.org/10.1101/cshperspect.a009191191

Bouchereau, W., Jouneau, L., Archilla, C., Aksoy, I., Moulin, A., Daniel, N., Peynot, N., Calderari, S., Joly, T., Godet, M., Jaszczyszyn, Y., Pratlong, M., Severac, D., Savatier, P., Duranthon, V., Afanassieff, M., & Beaujean, N. (2022). Major transcriptomic, epigenetic and metabolic changes underlie the pluripotency continuum in rabbit preimplantation embryos. *Development*, *149*(17). https://doi.org/10.1242/dev.200538

Buenrostro, J. D., Giresi, P. G., Zaba, L. C., Chang, H. Y., & Greenleaf, W. J. (2013). Transposition of native chromatin for fast and sensitive epigenomic profiling of open chromatin, DNA-binding proteins and nucleosome position. *Nature Methods*, *10*(12), 1213–1218. https://doi.org/10.1038/nmeth.2688

Buenrostro, J. D., Wu, B., Chang, H. Y., & Greenleaf, W. J. (2015). ATAC-seq: A method for assaying chromatin accessibility genome-wide. *Current Protocols in Molecular Biology*, *2015*, 21.29.1-21.29.9. https://doi.org/10.1002/0471142727.mb2129s109

Cabukusta, B., Nettebrock, N. T., Kol, M., Hilderink, A., Tafesse, F. G., & Holthuis, J. C. M. (2017). Ceramide phosphoethanolamine synthase SMSr is a target of caspase-6 during apoptotic cell death.

Bioscience Reports, *37*(4), 1–13. https://doi.org/10.1042/BSR20170867

Cagnone, G. L. M., Dufort, I., Vigneault, C., & Sirard, M.-A. (2012). Differential Gene Expression Profile in Bovine Blastocysts Resulting from Hyperglycemia Exposure During Early Cleavage Stages1. *Biology of Reproduction*, *86*(2), 1–12. https://doi.org/10.1095/biolreprod.111.094391

Calderari, S., Daniel, N., Mourier, E., Richard, C., Dahirel, M., Lager, F., Marchiol, C., Renault, G., Gatien, J., Nadal-Desbarats, L., Chavatte-Palmer, P., & Duranthon, V. (2021). Metabolomic differences in blastocoel and uterine fluids collected in vivo by ultrasound biomicroscopy on rabbit embryos†. *Biology of Reproduction*, *104*(4), 794–805. https://doi.org/10.1093/biolre/ioab005

Campbell, J. E., & Newgard, C. B. (2021). Mechanisms controlling pancreatic islet cell function in insulin secretion. *Nature Reviews Molecular Cell Biology*, *22*(2), 142–158. https://doi.org/10.1038/s41580-020-00317-7

Cantone, I., & Fisher, A. G. (2013). Epigenetic programming and reprogramming during development. *Nature Structural & Molecular Biology*, *20*(3), 282–289. https://doi.org/10.1038/nsmb.2489

Cardenas, A., Lutz, S. M., Everson, T. M., Perron, P., Bouchard, L., & Hivert, M.-F. (2019). Placental DNA Methylation Mediates the Association of Prenatal Maternal Smoking on Birth Weight. *American Journal of Epidemiology*. https://doi.org/10.1093/aje/kwz184

Carris, N. W., Nwabuobi, C. K., He, M. S. W., Bullers, K., Wilson, A. R. E., Louis, M. P. H. J. M., & Magness, R. R. (n.d.). *Review of Prediabetes and Hypertensive Disorders of Pregnancy*. *33612*.

Castillo-Castrejon, M., Yamaguchi, K., Rodel, R. L., Erickson, K., Kramer, A., Hirsch, N. M., Rolloff, K., Jansson, T., Barbour, L. A., & Powell, T. L. (2021). Effect of type 2 diabetes mellitus on placental expression and activity of nutrient transporters and their association with birth weight and neonatal adiposity. *Molecular and Cellular Endocrinology*, *532*(May), 111319. https://doi.org/10.1016/j.mce.2021.111319

Catalano, P. M. (2010). The impact of gestational diabetes and maternal obesity on the mother and her offspring. *Journal of Developmental Origins of Health and Disease*, *1*(4), 208–215. https://doi.org/10.1017/S2040174410000115

Catalano, P. M. (2014). Trying to understand gestational diabetes. *Diabetic Medicine*, *31*(3), 273–281. https://doi.org/10.1111/dme.12381

Cavalli, G., & Heard, E. (2019). Advances in epigenetics link genetics to the environment and disease. *Nature*, *571*(7766), 489–499. https://doi.org/10.1038/s41586-019-1411-0

Celik, A., Forde, R., Racaru, S., Forbes, A., & Sturt, J. (2022). The Impact of Type 2 Diabetes on Women's Health and Well-being During Their Reproductive Years: A Mixed-methods Systematic Review. *Current Diabetes Reviews*, *18*(2). https://doi.org/10.2174/1573399817666210118144743

Centers for Disease Control and Prevention, C. (2021). *Prevalence of Prediabetes Among Adults*. https://www.cdc.gov/diabetes/data/statistics-report/prevalence-of-prediabetes.html

Chandel, N. S. (2021a). Carbohydrate Metabolism. *Cold Spring Harbor Perspectives in Biology*, *13*(1), a040568. https://doi.org/10.1101/cshperspect.a040568

Chandel, N. S. (2021b). Glycolysis. *Cold Spring Harbor Perspectives in Biology*, *13*(5), a040535. https://doi.org/10.1101/cshperspect.a040535

Chatterjee, S., Khunti, K., & Davies, M. J. (2017). Type 2 diabetes. *The Lancet*, *389*(10085), 2239–2251. https://doi.org/10.1016/S0140-6736(17)30058-2

Chavatte-Palmer, P., & Tarrade, A. (2016). Placentation in different mammalian species. *Annales d'Endocrinologie*, *77*(2), 67–74. https://doi.org/10.1016/j.ando.2016.04.006

Chavey, A., Ah Kioon, M.-D., Bailbé, D., Movassat, J., & Portha, B. (2014). Maternal diabetes, programming of beta-cell disorders and intergenerational risk of type 2 diabetes. *Diabetes & Metabolism*, *40*(5), 323–330. https://doi.org/10.1016/j.diabet.2014.02.003

Chen, A. C. H., Lee, Y. L., Fong, S. W., Wong, C. C. Y., Ng, E. H. Y., & Yeung, W. S. B. (2017). Hyperglycemia impedes definitive endoderm differentiation of human embryonic stem cells by modulating histone methylation patterns. *Cell and Tissue Research*, *368*(3), 563–578. https://doi.org/10.1007/s00441-017-2583-2

Chen, B., Du, Y.-R., Zhu, H., Sun, M.-L., Wang, C., Cheng, Y., Pang, H., Ding, G., Gao, J., Tan, Y., Tong, X., Lv,

P., Zhou, F., Zhan, Q., Xu, Z.-M., Wang, L., Luo, D., Ye, Y., Jin, L., … Huang, H. (2022). Maternal inheritance of glucose intolerance via oocyte TET3 insufficiency. In *Nature* (Vol. 605, Issue May). Springer US. https://doi.org/10.1038/s41586-022-04756-4

Chen, P., Piaggi, P., Traurig, M., Bogardus, C., Knowler, W. C., Baier, L. J., & Hanson, R. L. (2017). Differential methylation of genes in individuals exposed to maternal diabetes in utero. *Diabetologia*, *60*(4), 645–655. https://doi.org/10.1007/s00125-016-4203-1

Chi, F., Sharpley, M. S., Nagaraj, R., Roy, S. Sen, & Banerjee, U. (2020). Glycolysis-Independent Glucose Metabolism Distinguishes TE from ICM Fate during Mammalian Embryogenesis. *Developmental Cell*, *53*(1), 9-26.e4. https://doi.org/10.1016/j.devcel.2020.02.015

Chi, M. M.-Y., Schlein, A. L., & Moley, K. H. (2000). High Insulin-Like Growth Factor 1 (IGF-1) and Insulin Concentrations Trigger Apoptosis in the Mouse Blastocyst via Down-Regulation of the IGF-1 Receptor. *Endocrinology*, *141*(12), 4784–4792. https://doi.org/10.1210/endo.141.12.7816

Chi, M. M. Y., Pingsterhaus, J., Carayannopoulos, M., & Moley, K. H. (2000). Decreased glucose transporter expression triggers BAX-dependent apoptosis in the murine blastocyst. *Journal of Biological Chemistry*, *275*(51), 40252–40257. https://doi.org/10.1074/jbc.M005508200

Christians, E., Rao, V. H., & Renard, J. P. (1994). Sequential Acquisition of Transcriptional Control during Early Embryonic Development in the Rabbit. *Developmental Biology*, *164*(1), 160–172. https://doi.org/10.1006/dbio.1994.1188

Chung, C. Y. T., Lo, P. H. Y., & Lee, K. K. H. (2020). Babam2 Regulates Cell Cycle Progression and Pluripotency in Mouse Embryonic Stem Cells as Revealed by Induced DNA Damage. *Biomedicines*, *8*(10), 397. https://doi.org/10.3390/biomedicines8100397

Clausen, T. D., Mathiesen, E. R., Hansen, T., Pedersen, O., Jensen, D. M., Lauenborg, J., & Damm, P. (2008). High Prevalence of Type 2 Diabetes and Pre-Diabetes in Adult Offspring of Women With Gestational Diabetes Mellitus or Type 1 Diabetes. *Diabetes Care*, *31*(2), 340–346. https://doi.org/10.2337/dc07-1596

Condic, M. L. (2014). Totipotency: What it is and what it is not. *Stem Cells and Development*, *23*(8), 796–812. https://doi.org/10.1089/scd.2013.0364

Couto, N., Wood, J., & Barber, J. (2016). The role of glutathione reductase and related enzymes on cellular redox homoeostasis network. *Free Radical Biology and Medicine*, *95*, 27–42. https://doi.org/10.1016/j.freeradbiomed.2016.02.028

Creyghton, M. P., Cheng, A. W., Welstead, G. G., Kooistra, T., Carey, B. W., Steine, E. J., Hanna, J., Lodato, M. A., Frampton, G. M., Sharp, P. A., Boyer, L. A., Young, R. A., & Jaenisch, R. (2010). Histone H3K27ac separates active from poised enhancers and predicts developmental state. *Proceedings of the National Academy of Sciences of the United States of America*, *107*(50), 21931–21936. https://doi.org/10.1073/pnas.1016071107

Crispatzu, G., Rehimi, R., Pachano, T., Bleckwehl, T., Cruz-Molina, S., Xiao, C., Mahabir, E., Bazzi, H., & Rada-Iglesias, A. (2021). The chromatin, topological and regulatory properties of pluripotency-associated poised enhancers are conserved in vivo. *Nature Communications*, *12*(1), 4344. https://doi.org/10.1038/s41467-021-24641-4

Czech, M. P. (2017). Insulin action and resistance in obesity and type 2 diabetes. *Nature Medicine*, *23*(7), 804–814. https://doi.org/10.1038/nm.4350

Dagdeviren, S., Shah, A., Okawa, M., Melnik, V. Y., Sarikhani, M., Foot, N., Kumar, S., & Lee, R. T. (2020). Arrdc4 Regulates Insulin-Stimulated Glucose Metabolism. *Experimental Biology 220 Meeting*. https://doi.org/https://doi.org/10.1096/fasebj.2020.34.s1.05395

Dai, Z., Ramesh, V., & Locasale, J. W. (2020). The evolving metabolic landscape of chromatin biology and epigenetics. *Nature Reviews Genetics*, *21*(12), 737–753. https://doi.org/10.1038/s41576-020-0270-8

DeBerardinis, R. J., & Chandel, N. S. (2020). We need to talk about the Warburg effect. *Nature Metabolism*, *2*(2), 127–129. https://doi.org/10.1038/s42255-020-0172-2

Deeney, J. T., Belkina, A. C., Shirihai, O. S., Corkey, B. E., & Denis, G. V. (2016). BET Bromodomain proteins Brd2, Brd3 and Brd4 selectively regulate metabolic pathways in the pancreatic β-cell. *PLoS ONE*,

11(3), 1–16. https://doi.org/10.1371/journal.pone.0151329

DeFronzo, R. A., Ferrannini, E., Groop, L., Henry, R. R., Herman, W. H., Holst, J. J., Hu, F. B., Kahn, C. R., Raz, I., Shulman, G. I., Simonson, D. C., Testa, M. A., & Weiss, R. (2015). Type 2 diabetes mellitus. *Nature Reviews Disease Primers*, *1*(July), 1–23. https://doi.org/10.1038/nrdp.2015.19

Deneke, V. E., & Pauli, A. (2021). The Fertilization Enigma: How Sperm and Egg Fuse. *Annual Review of Cell and Developmental Biology*, *37*, 391–414. https://doi.org/10.1146/annurev-cellbio-120219-021751

Deng, T., Jiang, X., He, Z., Cai, M., Chen, C., & Xu, Z. (2021). Centromere protein U (CENPU) promotes gastric cancer cell proliferation and glycolysis by regulating high mobility group box 2 (HMGB2). *Bioengineered*, *12*(2), 10194–10202. https://doi.org/10.1080/21655979.2021.2002018

Deponte, M. (2013). Glutathione catalysis and the reaction mechanisms of glutathione-dependent enzymes. *Biochimica et Biophysica Acta - General Subjects*, *1830*(5), 3217–3266. https://doi.org/10.1016/j.bbagen.2012.09.018

Desoye, G. (2018). The human placenta in diabetes and obesity: Friend or foe? The 2017 Norbert Freinkel award lecture. *Diabetes Care*, *41*(7), 1362–1369. https://doi.org/10.2337/dci17-0045

Desoye, G., & Cervar-Zivkovic, M. (2020). Diabetes Mellitus, Obesity, and the Placenta. *Obstetrics and Gynecology Clinics of North America*, *47*(1), 65–79. https://doi.org/10.1016/j.ogc.2019.11.001

Desoye, G., & Nolan, C. J. (2016). The fetal glucose steal: an underappreciated phenomenon in diabetic pregnancy. *Diabetologia*, *59*(6), 1089–1094. https://doi.org/10.1007/s00125-016-3931-6

DiMeglio, L. A., Evans-Molina, C., & Oram, R. A. (2018). Type 1 diabetes. *The Lancet*, *391*(10138), 2449–2462. https://doi.org/10.1016/S0140-6736(18)31320-5

Ding, L., Pan, R., Huang, X., Wang, J. X., Shen, Y. T., Xu, L., Zhang, Y., Liu, Y., He, X. Q., Yang, X. J., Qi, Z. Q., & Wang, H. L. (2012). Changes in histone acetylation during oocyte meiotic maturation in the diabetic mouse. *Theriogenology*, *78*(4), 784–792. https://doi.org/10.1016/j.theriogenology.2012.03.026

Donkin, I., Versteyhe, S., Ingerslev, L. R., Qian, K., Mechta, M., Nordkap, L., Mortensen, B., Appel, E. V. R., Jørgensen, N., Kristiansen, V. B., Hansen, T., Workman, C. T., Zierath, J. R., & Barrès, R. (2016). Obesity and bariatric surgery drive epigenetic variation of spermatozoa in humans. *Cell Metabolism*, *23*(2), 369–378. https://doi.org/10.1016/j.cmet.2015.11.004

Donnay, I., Partridge, R. J., & Leese, H. J. (1999). Can embryo metabolism be used for selecting bovine embryos before transfer? *Reproduction Nutrition Development*, *39*(5–6), 523–533. https://doi.org/10.1051/rnd:19990501

Du, J., Johnson, L. M., Jacobsen, S. E., & Patel, D. J. (2015). DNA methylation pathways and their crosstalk with histone methylation. *Nature Reviews Molecular Cell Biology*, *16*(9), 519–532. https://doi.org/10.1038/nrm4043

Dunglison, G. F., Jane, S. D., McCaul, T. F., Chad, J. E., Fleming, T. P., & Kaye, P. L. (1995). Stimulation of endocytosis in mouse blastocysts by insulin: a quantitative morphological analysis. *Reproduction*, *105*(1), 115–123. https://doi.org/10.1530/jrf.0.1050115

Duranthon, V., & Chavatte-Palmer, P. (2018). Long term effects of ART: What do animals tell us? *Molecular Reproduction and Development*, *85*(4), 348–368. https://doi.org/10.1002/mrd.22970

Duranthon, V., Watson, A. J., & Lonergan, P. (2008). Preimplantation embryo programming: Transcription epigenetics, and culture environment. *Reproduction*, *135*(2), 141–150. https://doi.org/10.1530/REP-07-0324

Ericsson, A., Säljö, K., Sjöstrand, E., Jansson, N., Prasad, P. D., Powell, T. L., & Jansson, T. (2007). Brief hyperglycaemia in the early pregnant rat increases fetal weight at term by stimulating placental growth and affecting placental nutrient transport. *The Journal of Physiology*, *581*(3), 1323–1332. https://doi.org/10.1113/jphysiol.2007.131185

Eriksson, U. J., Dahlstrom, E., & Hellerstrom, C. (1983). Diabetes in pregnancy: skeletal malformations in the offspring of diabetic rats after intermittent withdrawal of insulin in early gestation. *Diabetes*, *32*(12), 1141–1145. https://doi.org/10.2337/diab.32.12.1141

Etchegaray, J.-P., & Mostoslavsky, R. (2016). Interplay between Metabolism and Epigenetics: A Nuclear

Adaptation to Environmental Changes. *Molecular Cell*, *62*(5), 695–711. https://doi.org/10.1016/j.molcel.2016.05.029

Fang, M., Du, H., Han, B., Xia, G., Shi, X., Zhang, F., Fu, Q., & Zhang, T. (2017). Hypoxia-inducible microRNA-218 inhibits trophoblast invasion by targeting LASP1: Implications for preeclampsia development. *International Journal of Biochemistry and Cell Biology*, *87*, 95–103. https://doi.org/10.1016/j.biocel.2017.04.005

Feng, J., Liu, T., Qin, B., Zhang, Y., & Liu, X. S. (2012). Identifying ChIP-seq enrichment using MACS. *Nature Protocols*, *7*(9), 1728–1740. https://doi.org/10.1038/nprot.2012.101

Fernandez-Twinn, D. S., Blackmore, H. L., Siggens, L., Giussani, D. A., Cross, C. M., Foo, R., & Ozanne, S. E. (2012). The Programming of Cardiac Hypertrophy in the Offspring by Maternal Obesity Is Associated with Hyperinsulinemia, AKT, ERK, and mTOR Activation. *Endocrinology*, *153*(12), 5961–5971. https://doi.org/10.1210/en.2012-1508

Fernandez-Twinn, D. S., Hjort, L., Novakovic, B., Ozanne, S. E., & Saffery, R. (2019). Intrauterine programming of obesity and type 2 diabetes. *Diabetologia*, *62*(10), 1789–1801. https://doi.org/10.1007/s00125-019-4951-9

Fernandez-Twinn, D. S., & Ozanne, S. E. (2010). Early life nutrition and metabolic programming. *Annals of the New York Academy of Sciences*, *1212*(1), 78–96. https://doi.org/10.1111/j.1749-6632.2010.05798.x

Firmin, J., & Maître, J.-L. L. (2021). Morphogenesis of the human preimplantation embryo: bringing mechanics to the clinics. *Seminars in Cell & Developmental Biology*, *120*(July), 22–31. https://doi.org/10.1016/j.semcdb.2021.07.005

Fischer, B., Chavatte-Palmer, P., Viebahn, C., Navarrete Santos, A., & Duranthon, V. (2012). Rabbit as a reproductive model for human health. *REPRODUCTION*, *144*(1), 1–10. https://doi.org/10.1530/REP-12-0091

Fischer, B., Schindler, M., Mareike Pendzialek, S., Gürke, J., Haucke, E., Grybel, K. J., Thieme, R., & Santos, A. N. (2017). *The Long-Term Effect of the Periconception Period on the Embryo's Epigenetic Profile and Phenotype: The Role of Maternal Disease Such as Diabetes and How the Effect Is Mediated (Example from a Rabbit Model)* (A. Fazeli & W. V. Holt (eds.); Vol. 1014, pp. 107–115). Springer International Publishing. https://doi.org/10.1007/978-3-319-62414-3_6

Fitz-James, M. H., & Cavalli, G. (2022). Molecular mechanisms of transgenerational epigenetic inheritance. *Nature Reviews Genetics*, *23*(6), 325–341. https://doi.org/10.1038/s41576-021-00438-5

Fleming, T. P., Sun, C., Denisenko, O., Caetano, L., Aljahdali, A., Gould, J. M., & Khurana, P. (2021). Environmental exposures around conception: Developmental pathways leading to lifetime disease risk. *International Journal of Environmental Research and Public Health*, *18*(17), 1–18. https://doi.org/10.3390/ijerph18179380

Fleming, T. P., Watkins, A. J., Sun, C., Velazquez, M. A., Smyth, N. R., & Eckert, J. J. (2015). Do little embryos make big decisions? How maternal dietary protein restriction can permanently change an embryo's potential, affecting adult health. *Reproduction, Fertility and Development*, *27*(4), 684–692. https://doi.org/10.1071/RD14455

Fleming, T. P., Watkins, A. J., Velazquez, M. A., Mathers, J. C., Prentice, A. M., Stephenson, J., Barker, M., Saffery, R., Yajnik, C. S., Eckert, J. J., Hanson, M. A., Forrester, T., Gluckman, P. D., & Godfrey, K. M. (2018). Origins of lifetime health around the time of conception: causes and consequences. *The Lancet*, *391*(10132), 1842–1852. https://doi.org/10.1016/S0140-6736(18)30312-X

Forsdahl, A. (1977). Are poor living conditions in childhood and adolescence an important risk factor for arteriosclerotic heart disease? *British Journal of Preventive and Social Medicine*, *31*(2), 91–95. https://doi.org/10.1136/jech.31.2.91

Fraser, R. B., Waite, S. L., Wood, K. A., & Martin, K. L. (2007). Impact of hyperglycemia on early embryo development and embryopathy: in vitro experiments using a mouse model. *Human Reproduction*, *22*(12), 3059–3068. https://doi.org/10.1093/humrep/dem318

Frey, W. D., Chaudhry, A., Slepicka, P. F., Ouellette, A. M., Kirberger, S. E., Pomerantz, W. C. K., Hannon, G.

J., & dos Santos, C. O. (2017). BPTF Maintains Chromatin Accessibility and the Self-Renewal Capacity of Mammary Gland Stem Cells. *Stem Cell Reports*, *9*(1), 23–31. https://doi.org/10.1016/j.stemcr.2017.04.031

Fuentes, S., Mandereau-Bruno, L., Regnault, N., Bernillon, P., Bonaldi, C., Cosson, E., & Fosse-Edorh, S. (2020). Is the type 2 diabetes epidemic plateauing in France? A nationwide population-based study. *Diabetes & Metabolism*, *46*(6), 472–479. https://doi.org/10.1016/j.diabet.2019.12.006

Gaillard, R. (2015). Maternal obesity during pregnancy and cardiovascular development and disease in the offspring. *European Journal of Epidemiology*, *30*(11), 1141–1152. https://doi.org/10.1007/s10654-015-0085-7

Garcia-Dominguez, X., Marco-Jiménez, F., Peñaranda, D. S., Diretto, G., García-Carpintero, V., Cañizares, J., & Vicente, J. S. (2020). Long-term and transgenerational phenotypic, transcriptional and metabolic effects in rabbit males born following vitrified embryo transfer. *Scientific Reports*, *10*(1), 11313. https://doi.org/10.1038/s41598-020-68195-9

Gardner, D. K. (2007). Noninvasive Metabolic Assessment of Single Cells. In *Methods in molecular medicine* (Vol. 132, pp. 1–9). https://doi.org/10.1007/978-1-59745-298-4_1

Gardner, D. K., & Harvey, A. J. (2015). Blastocyst metabolism. *Reproduction, Fertility and Development*, *27*(4), 638–654. https://doi.org/10.1071/RD14421

Gardner, H. G., & Kaye, P. L. (1991). Insulin increases cell numbers and morphological development in mouse pre-implantation embryos in vitro. *Reproduction, Fertility and Development*, *3*(1), 79–91. https://doi.org/10.1071/RD9910079

Ge, Z.-J., Zhang, C.-L., Schatten, H., & Sun, Q.-Y. (2014). Maternal Diabetes Mellitus and the Origin of Non-Communicable Diseases in Offspring: The Role of Epigenetics1. *Biology of Reproduction*, *90*(6), 1–6. https://doi.org/10.1095/biolreprod.114.118141

Gerri, C., McCarthy, A., Alanis-Lobato, G., Demtschenko, A., Bruneau, A., Loubersac, S., Fogarty, N. M. E., Hampshire, D., Elder, K., Snell, P., Christie, L., David, L., Van de Velde, H., Fouladi-Nashta, A. A., & Niakan, K. K. (2020). Initiation of a conserved trophectoderm program in human, cow and mouse embryos. *Nature*, *May 2019*. https://doi.org/10.1038/s41586-020-2759-x

Gerri, C., Menchero, S., Mahadevaiah, S. K., Turner, J. M. A., & Niakan, K. K. (2020). Human Embryogenesis: A Comparative Perspective. *Annual Review of Cell and Developmental Biology*, *36*(1), 411–440. https://doi.org/10.1146/annurev-cellbio-022020-024900

Giritharan, G., Piane, L. D., Donjacour, A., Esteban, F. J., Horcajadas, J. A., Maltepe, E., & Rinaudo, P. (2012). In vitro culture of mouse embryos reduces differential gene expression between inner cell mass and trophectoderm. *Reproductive Sciences*, *19*(3), 243–252. https://doi.org/10.1177/1933719111428522

Guo, G., Huss, M., Tong, G. Q., Wang, C., Li Sun, L., Clarke, N. D., & Robson, P. (2010). Resolution of Cell Fate Decisions Revealed by Single-Cell Gene Expression Analysis from Zygote to Blastocyst. *Developmental Cell*, *18*(4), 675–685. https://doi.org/10.1016/j.devcel.2010.02.012

Guo, S. (2014). Insulin signaling, resistance, and metabolic syndrome: Insights from mouse models into disease mechanisms. *Journal of Endocrinology*, *220*(2). https://doi.org/10.1530/JOE-13-0327

Gürke, J., Schindler, M., Pendzialek, S. M., Thieme, R., Grybel, K. J., Heller, R., Spengler, K., Fleming, T. P., Fischer, B., & Navarrete Santos, A. (2016). Maternal diabetes promotes mTORC1 downstream signalling in rabbit preimplantation embryos. *REPRODUCTION*, *151*(5), 465–476. https://doi.org/10.1530/REP-15-0523

Gut, P., & Verdin, E. (2013). The nexus of chromatin regulation and intermediary metabolism. *Nature*, *502*(7472), 489–498. https://doi.org/10.1038/nature12752

Haeusler, R. A., McGraw, T. E., & Accili, D. (2017). Biochemical and cellular properties of insulin receptor signalling. *Nature Reviews Molecular Cell Biology*. https://doi.org/10.1038/nrm.2017.89

Halstead, M. M., Ma, X., Zhou, C., Schultz, R. M., & Ross, P. J. (2020). Chromatin remodeling in bovine embryos indicates species-specific regulation of genome activation. *Nature Communications*, *11*(1). https://doi.org/10.1038/s41467-020-18508-3

Han, J., Xu, J., Long, Y. S., Epstein, P. N., & Liu, Y. Q. (2007). Rat maternal diabetes impairs pancreatic β-

cell function in the offspring. *American Journal of Physiology-Endocrinology and Metabolism*, *293*(1), E228–E236. https://doi.org/10.1152/ajpendo.00479.2006

Han, L., Ren, C., Li, L., Li, X., Ge, J., Wang, H., Miao, Y. L., Guo, X., Moley, K. H., Shu, W., & Wang, Q. (2018). Embryonic defects induced by maternal obesity in mice derive from Stella insufficiency in oocytes. *Nature Genetics*, *50*(3), 432–442. https://doi.org/10.1038/s41588-018-0055-6

Hancock, M. L., Meyer, R. C., Mistry, M., Khetani, R. S., Wagschal, A., Shin, T., Ho Sui, S. J., Näär, A. M., & Flanagan, J. G. (2019). Insulin Receptor Associates with Promoters Genome-wide and Regulates Gene Expression. *Cell*, 722–736. https://doi.org/10.1016/j.cell.2019.02.030

Hanson, M. A., & Gluckman, P. D. (2014). Early developmental conditioning of later health and disease: physiology or pathophysiology? *Physiological Reviews*, *94*(4), 1027–1076. https://doi.org/10.1152/physrev.00029.2013

Hanson, M., Gluckman, P., Bier, D., Challis, J., Fleming, T., Forrester, T., Godfrey, K., Nestel, P., & Yajnik, C. (2004). Report on the 2nd World Congress on Fetal Origins of Adult Disease, Brighton, U.K., June 7-10, 2003. *Pediatric Research*, *55*(5), 894–897. https://doi.org/10.1203/01.PDR.0000115682.23617.03

Harris, S. E., Gopichandran, N., Picton, H. M., Leese, H. J., & Orsi, N. M. (2005). Nutrient concentrations in murine follicular fluid and the female reproductive tract. *Theriogenology*, *64*(4), 992–1006. https://doi.org/10.1016/j.theriogenology.2005.01.004

Hart, B. N., Shubrook, J. H., & Mason, T. (2021). Pregestational Diabetes and Family Planning. *Clinical Diabetes*, *39*(3), 323–328. https://doi.org/10.2337/cd20-0062

Hart, R., & Norman, R. J. (2013). The longer-term health outcomes for children born as a result of ivf treatment: Part i-general health outcomes. *Human Reproduction Update*, *19*(3), 232–243. https://doi.org/10.1093/humupd/dms062

Harvey, M. B., & Kaye, P. L. (1988). Insulin stimulates protein synthesis in compacted mouse embryos. *Endocrinology*, *122*(3), 1182–1184. https://doi.org/10.1210/endo-122-3-1182

Harvey, M. B., & Kaye, P. L. (1990). Insulin increases the cell number of the inner cell mass and stimulates morphological development of mouse blastocysts in vitro. *Development*, *110*(3), 963–967. https://doi.org/10.1242/dev.110.3.963

Haucke, E., Santos, A. N., Simm, A., Henning, C., Glomb, M. A., Gürke, J., Schindler, M., Fischer, B., & Navarrete Santos, A. (2014). Accumulation of advanced glycation end products in the rabbit blastocyst under maternal diabetes. *Reproduction*, *148*(2), 169–178. https://doi.org/10.1530/REP-14-0149

Hebert, S. L., & Nair, K. S. (2010). Protein and energy metabolism in type 1 diabetes. *Clinical Nutrition*, *29*(1), 13–17. https://doi.org/10.1016/j.clnu.2009.09.001

Heijmans, B. T., Tobi, E. W., Lumey, L. H., & Slagboom, P. E. (2009). The epigenome: Archive of the prenatal environment. *Epigenetics*, *4*(8), 526–531. https://doi.org/10.4161/epi.4.8.10265

Hemberger, M., Hanna, C. W., & Dean, W. (2019). Mechanisms of early placental development in mouse and humans. *Nature Reviews Genetics*, *21*(January). https://doi.org/10.1038/s41576-019-0169-4

Herrler, A., Krusche, C. A., & Beier, H. M. (1998). Insulin and insulin-like growth factor-I promote rabbit blastocyst development and prevent apoptosis. *Biology of Reproduction*, *59*(6), 1302–1310. https://doi.org/10.1095/biolreprod59.6.1302

Hess, D. L., Kelly-Goss, M. R., Cherepanova, O. A., Nguyen, A. T., Baylis, R. A., Tkachenko, S., Annex, B. H., Peirce, S. M., & Owens, G. K. (2019). Perivascular cell-specific knockout of the stem cell pluripotency gene Oct4 inhibits angiogenesis. *Nature Communications*, *10*(1), 1–15. https://doi.org/10.1038/s41467-019-08811-z

Higa, R., Leonardi, M. L., & Jawerbaum, A. (2021). Intrauterine Programming of Cardiovascular Diseases in Maternal Diabetes. *Frontiers in Physiology*, *12*(November), 1–10. https://doi.org/10.3389/fphys.2021.760251

Hinck, L., Thissen, J. P., Pampfer, S., & De Hertogh, R. (2003). Effect of high concentrations of glucose on differentiation of rat trophoblast cells in vitro. *Diabetologia*, *46*(2), 276–283. https://doi.org/10.1007/s00125-002-1016-1

Hirate, Y., Hirahara, S., Inoue, K. I., Suzuki, A., Alarcon, V. B., Akimoto, K., Hirai, T., Hara, T., Adachi, M., Chida, K., Ohno, S., Marikawa, Y., Nakao, K., Shimono, A., & Sasaki, H. (2013). Polarity-dependent distribution of angiomotin localizes hippo signaling in preimplantation embryos. *Current Biology*, *23*(13), 1181–1194. https://doi.org/10.1016/j.cub.2013.05.014

Hjort, L., Novakovic, B., Grunnet, L. G., Maple-Brown, L., Damm, P., Desoye, G., & Saffery, R. (2019). Diabetes in pregnancy and epigenetic mechanisms—how the first 9 months from conception might affect the child's epigenome and later risk of disease. *The Lancet Diabetes and Endocrinology*, *7*(10), 796–806. https://doi.org/10.1016/S2213-8587(19)30078-6

Hoffman, D. J., Reynolds, R. M., & Hardy, D. B. (2017). Developmental origins of health and disease: current knowledge and potential mechanisms. *Nutrition Reviews*, *75*(12), 951–970. https://doi.org/10.1093/nutrit/nux053

Hollander, P., & Spellman, C. (2012). Controversies in Prediabetes: Do We Have a Diagnosis? *Postgraduate Medicine*, *124*(4), 109–118. https://doi.org/10.3810/pgm.2012.07.2562

Holman, G. D. (2020). Structure, function and regulation of mammalian glucose transporters of the SLC2 family. *Pflügers Archiv - European Journal of Physiology*, *472*(9), 1155–1175. https://doi.org/10.1007/s00424-020-02411-3

Hombach, S., & Kretz, M. (2016). Non-coding RNAs: Classification, Biology and Functioning. In *Advances in Experimental Medicine and Biology* (Vol. 937, pp. 3–17). https://doi.org/10.1007/978-3-319-42059-2_1

Hosseini, S. M., Dufort, I., Caballero, J., Moulavi, F., Ghanaei, H. R., & Sirard, M. A. (2015). Transcriptome profiling of bovine inner cell mass and trophectoderm derived from in vivo generated blastocysts. *BMC Developmental Biology*, *15*(1), 1–13. https://doi.org/10.1186/s12861-015-0096-3

Houghton, F. D. (2006). Energy metabolism of the inner cell mass and trophectoderm of the mouse blastocyst. *Differentiation*, *74*(1), 11–18. https://doi.org/10.1111/j.1432-0436.2006.00052.x

Hu, K., & Yu, Y. (2017). Metabolite availability as a window to view the early embryo microenvironment in vivo. *Molecular Reproduction and Development*, *84*(10), 1027–1038. https://doi.org/10.1002/mrd.22868

Huang, D. W., Sherman, B. T., & Lempicki, R. A. (2009). Systematic and integrative analysis of large gene lists using DAVID bioinformatics resources. *Nature Protocols*, *4*(1), 44–57. https://doi.org/10.1038/nprot.2008.211

Huang, H., Yan, P., Shan, Z., Chen, S., Li, M., Luo, C., Gao, H., Hao, L., & Liu, L. (2015). Adverse childhood experiences and risk of type 2 diabetes: A systematic review and meta-analysis. *Metabolism*, *64*(11), 1408–1418. https://doi.org/10.1016/j.metabol.2015.08.019

Huang, W., Hua, H., Xiao, G., Yang, X., Yang, Q., & Jin, L. (2021). ZC3HAV1 promotes the proliferation and metastasis via regulating KRAS in pancreatic cancer. *Aging*, *13*(14), 18482–18497. https://doi.org/10.18632/aging.203296

Hue-Beauvais, C., Miranda, G., Aujean, E., Jaffrezic, F., Devinoy, E., Martin, P., & Charlier, M. (2017). Diet-induced modifications to milk composition have long-term effects on offspring growth in rabbits. *Journal of Animal Science*, *95*(2), 761. https://doi.org/10.2527/jas2016.0847

Hufnagel, A., Dearden, L., Fernandez-Twinn, D. S., & Ozanne, S. E. (2022). Programming of cardiometabolic health: the role of maternal and fetal hyperinsulinaemia. *Journal of Endocrinology*, *253*(2), R47–R63. https://doi.org/10.1530/JOE-21-0332

Hugentobler, S. A., Humpherson, P. G., Leese, H. J., Sreenan, J. M., & Morris, D. G. (2008). Energy substrates in bovine oviduct and uterine fluid and blood plasma during the oestrous cycle. *Molecular Reproduction and Development*, *75*(3), 496–503. https://doi.org/10.1002/mrd.20760

Hughes, R. C. E., Rowan, J., & Williman, J. (2018). Prediabetes in pregnancy, can early intervention improve outcomes? A feasibility study for a parallel randomised clinical trial. *BMJ Open*, *8*(3), 1–8. https://doi.org/10.1136/bmjopen-2017-018493

Ilchmann-Diounou, H., Olier, M., Lencina, C., Riba, A., Barretto, S., Nankap, M., Sommer, C., Guillou, H., Ellero-Simatos, S., Guzylack-Piriou, L., Théodorou, V., & Ménard, S. (2019). Early life stress induces type 2 diabetes-like features in ageing mice. *Brain, Behavior, and Immunity*, *80*(April), 452–463.

https://doi.org/10.1016/j.bbi.2019.04.025
Ilonen, J., Lempainen, J., & Veijola, R. (2019). The heterogeneous pathogenesis of type 1 diabetes mellitus. *Nature Reviews Endocrinology*, *15*(11), 635–650. https://doi.org/10.1038/s41574-019-0254-y
International Diabetes Federation. (2006). *The IDF consensus worlwide definition of the Metabolic Syndrome*. https://idf.org/our-activities/advocacy-awareness/resources-and-tools/60:idfconsensus-worldwide-definitionof-the-metabolic-syndrome.html
International Diabetes Federation. (2021). *IDF Diabetes Atlas* (Tenth edit).
Iqbal, K., Chitwood, J. L., Meyers-Brown, G. A., Roser, J. F., & Ross, P. J. (2014). RNA-seq transcriptome profiling of equine inner cell mass and trophectoderm. *Biology of Reproduction*, *90*(3), 1–9. https://doi.org/10.1095/biolreprod.113.113928
Izzo, A., & Schneider, R. (2010). Chatting histone modifications in mammals. *Briefings in Functional Genomics*, *9*(5–6), 429–443. https://doi.org/10.1093/bfgp/elq024
James, D. E., Stöckli, J., & Birnbaum, M. J. (2021). The aetiology and molecular landscape of insulin resistance. *Nature Reviews Molecular Cell Biology*, *22*(11), 751–771. https://doi.org/10.1038/s41580-021-00390-6
Janke, R., Dodson, A. E., & Rine, J. (2015). Metabolism and Epigenetics. *Annual Review of Cell and Developmental Biology*, *31*(1), 473–496. https://doi.org/10.1146/annurev-cellbio-100814-125544
Jawerbaum, A., & White, V. (2010). Animal models in diabetes and pregnancy. *Endocrine Reviews*, *31*(5), 680–701. https://doi.org/10.1210/er.2009-0038
Jerkovic´, I., & Cavalli, G. (2021). Understanding 3D genome organization by multidisciplinary methods. *Nature Reviews Molecular Cell Biology*, *22*(8), 511–528. https://doi.org/10.1038/s41580-021-00362-w
Jeyapalan, A. S., Orellana, R. A., Suryawan, A., O'Connor, P. M. J., Nguyen, H. V., Escobar, J., Frank, J. W., & Davis, T. A. (2007). Glucose stimulates protein synthesis in skeletal muscle of neonatal pigs through an AMPK- and mTOR-independent process. *American Journal of Physiology - Endocrinology and Metabolism*, *293*(2). https://doi.org/10.1152/ajpendo.00121.2007
Jiménez-Chillarón, J. C., Díaz, R., Martínez, D., Pentinat, T., Ramón-Krauel, M., Ribó, S., & Plösch, T. (2012). The role of nutrition on epigenetic modifications and their implications on health. *Biochimie*, *94*(11), 2242–2263. https://doi.org/10.1016/j.biochi.2012.06.012
Jiménez, A., Madrid-Bury, N., Fernández, R., Pérez-Garnelo, S., Moreira, P., Pintado, B., de la Fuente, J., & Gutiérrez-Adán, A. (2003). Hyperglycemia-induced apoptosis affects sex ratio of bovine and murine preimplantation embryos. *Molecular Reproduction and Development*, *65*(2), 180–187. https://doi.org/10.1002/mrd.10286
Jukam, D., Shariati, S. A. M., & Skotheim, J. M. (2017). Zygotic Genome Activation in Vertebrates. *Developmental Cell*, *42*(4), 316–332. https://doi.org/10.1016/j.devcel.2017.07.026
Jungheim, E., & Moley, K. (2008). The Impact of Type 1 and Type 2 Diabetes Mellitus on the Oocyte and the Preimplantation Embryo. *Seminars in Reproductive Medicine*, *26*(2), 186–195. https://doi.org/10.1055/s-2008-1042957
Kabra, D. G., Gupta, J., & Tikoo, K. (2009). Insulin induced alteration in post-translational modifications of histone H3 under a hyperglycemic condition in L6 skeletal muscle myoblasts. *Biochimica et Biophysica Acta - Molecular Basis of Disease*, *1792*(6), 574–583. https://doi.org/10.1016/j.bbadis.2009.03.003
Kaneko, K. J. (2016). Metabolism of Preimplantation Embryo Development: A Bystander or an Active Participant? In *Current Topics in Developmental Biology* (1st ed., Vol. 120). Elsevier Inc. https://doi.org/10.1016/bs.ctdb.2016.04.010
Kang, M., Piliszek, A., Artus, J., & Hadjantonakis, A. K. (2013). FGF4 is required for lineage restriction and salt-and-pepper distribution of primitive endoderm factors but not their initial expression in the mouse. *Development (Cambridge)*, *140*(2), 267–279. https://doi.org/10.1242/dev.084996
Kapur, A., McIntyre, H. D., & Hod, M. (2019). Type 2 Diabetes in Pregnancy. *Endocrinology and Metabolism Clinics of North America*, *48*(3), 511–531. https://doi.org/10.1016/j.ecl.2019.05.009

Katada, S., Imhof, A., & Sassone-Corsi, P. (2012). Connecting threads: Epigenetics and metabolism. *Cell*, *148*(1–2), 24–28. https://doi.org/10.1016/j.cell.2012.01.001

Katsarou, A., Gudbjörnsdottir, S., Rawshani, A., Dabelea, D., Bonifacio, E., Anderson, B. J., Jacobsen, L. M., Schatz, D. A., & Lernmark, A. (2017). Type 1 diabetes mellitus. *Nature Reviews Disease Primers*, *3*, 1–18. https://doi.org/10.1038/nrdp.2017.16

Kaul, K., Tarr, J. M., Ahmad, S., Kohner, E. M., & Chibber, R. (2012). Chapter 1 Introduction To Diabetes Mellitus. *Diabetes: An Old Disease, a New Insight*, 1–11.

Kaye, P. L., & Gardner, H. G. (1999). Preimplantation access to maternal insulin and albumin increases fetal growth rate in mice. *Human Reproduction*, *14*(12), 3052–3059. https://doi.org/10.1093/humrep/14.12.3052

Keim, A. L., Chi, M. M.-Y., & Moley, K. H. (2001). Hyperglycemia-induced apoptotic cell death in the mouse blastocyst is dependent on expression of p53. *Molecular Reproduction and Development*, *60*(2), 214–224. https://doi.org/10.1002/mrd.1080

Kelsey, M. M., & Zeitler, P. S. (2016). Insulin Resistance of Puberty. *Current Diabetes Reports*, *16*(7). https://doi.org/10.1007/s11892-016-0751-5

Khan, M. A. B., Hashim, M. J., King, J. K., Govender, R. D., Mustafa, H., & Al Kaabi, J. (2019). Epidemiology of Type 2 Diabetes – Global Burden of Disease and Forecasted Trends. *Journal of Epidemiology and Global Health*, *10*(1), 107. https://doi.org/10.2991/jegh.k.191028.001

Kim, H.-S., & Brill, S. J. (2001). Rfc4 Interacts with Rpa1 and Is Required for Both DNA Replication and DNA Damage Checkpoints in Saccharomyces cerevisiae . *Molecular and Cellular Biology*, *21*(11), 3725–3737. https://doi.org/10.1128/mcb.21.11.3725-3737.2001

Kim, M., & Costello, J. (2017). DNA methylation: An epigenetic mark of cellular memory. *Experimental and Molecular Medicine*, *49*(4). https://doi.org/10.1038/emm.2017.10

Kim, S. T., & Moley, K. H. (2008). Paternal effect on embryo quality in diabetic mice is related to poor sperm quality and associated with decreased glucose transporter expression. *REPRODUCTION*, *136*(3), 313–322. https://doi.org/10.1530/REP-08-0167

Kimmins, S., & Sassone-Corsi, P. (2005). Chromatin remodelling and epigenetic features of germ cells. *Nature*, *434*(7033), 583–589. https://doi.org/10.1038/nature03368

Koeck, R. M., Busato, F., Tost, J., Consten, D., van Echten-Arends, J., Mastenbroek, S., Wurth, Y., Remy, S., Langie, S., Nawrot, T. S., Plusquin, M., Alfano, R., Bijnens, E. M., Gielen, M., van Golde, R., Dumoulin, J. C. M., Brunner, H., van Montfoort, A. P. A., & Zamani Esteki, M. (2022). Methylome-wide analysis of IVF neonates that underwent embryo culture in different media revealed no significant differences. *Npj Genomic Medicine*, *7*(1), 39. https://doi.org/10.1038/s41525-022-00310-3

Krieg, A. J., Hammond, E. M., & Giaccia, A. J. (2006). Functional Analysis of p53 Binding under Differential Stresses. *Molecular and Cellular Biology*, *26*(19), 7030–7045. https://doi.org/10.1128/mcb.00322-06

Krisher, R. L., & Prather, R. S. (2012). A role for the Warburg effect in preimplantation embryo development: Metabolic modification to support rapid cell proliferation. *Molecular Reproduction and Development*, *79*(5), 311–320. https://doi.org/10.1002/mrd.22037

Lane, M., & Gardner, D. K. (1997). Differential regulation of mouse embryo development and viability by amino acids. *Journal of Reproduction and Fertility*, *109*(1), 153–164. https://doi.org/10.1530/jrf.0.1090153

Langley-Evans, S. C. (2015). Nutrition in early life and the programming of adult disease: A review. *Journal of Human Nutrition and Dietetics*, *28*(s1), 1–14. https://doi.org/10.1111/jhn.12212

Lanktree, M. B., & Hegele, R. A. (2017). Metabolic Syndrome. *Genomic and Precision Medicine: Primary Care: Third Edition*, *43*(1), 283–299. https://doi.org/10.1016/B978-0-12-800685-6.00015-1

Laskowski, D., Båge, R., Humblot, P., Andersson, G., Sirard, M. A., & Sjunnesson, Y. (2017). Insulin during in vitro oocyte maturation has an impact on development, mitochondria, and cytoskeleton in bovine day 8 blastocysts. *Theriogenology*, *101*, 15–25. https://doi.org/10.1016/j.theriogenology.2017.06.002

Laskowski, D., Humblot, P., Sirard, M.-A., Sjunnesson, Y., Jhamat, N., Båge, R., & Andersson, G. (2018).

DNA methylation pattern of bovine blastocysts associated with hyperinsulinemia in vitro. *Molecular Reproduction and Development*, *85*(7), 599–611. https://doi.org/10.1002/mrd.22995

Laskowski, D., Sjunnesson, Y., Humblot, P., Sirard, M. A., Andersson, G., Gustafsson, H., & Båge, R. (2017). Insulin exposure during in vitro bovine oocyte maturation changes blastocyst gene expression and developmental potential. *Reproduction, Fertility and Development*, *29*(5), 876–889. https://doi.org/10.1071/RD15315

Latos, P. A., & Hemberger, M. (2016). From the stem of the placental tree: Trophoblast stem cells and their progeny. *Development (Cambridge)*, *143*(20), 3650–3660. https://doi.org/10.1242/dev.133462

Lea, A. J., Tung, J., Archie, E. A., & Alberts, S. C. (2017). Developmental plasticity. *Evolution, Medicine, and Public Health*, *2017*(1), 162–175. https://doi.org/10.1093/emph/eox019

Lea, R. G., McCracken, J. E., McIntyre, S. S., Smith, W., & Baird, J. D. (1996). Disturbed development of the preimplantation embryo in the insulin-dependent diabetic BB/E rat. *Diabetes*, *45*(11), 1463–1470. https://doi.org/10.2337/diabetes.45.11.1463

Leandri, R. D., Archilla, C., Bui, L. C., Peynot, N., Liu, Z., Cabau, C., Chastellier, A., Renard, J. P., & Duranthon, V. (2008). Revealing the dynamics of gene expression during embryonic genome activation and first differentiation in the rabbit embryo with a dedicated array screening. *Physiological Genomics*, *36*(2), 98–113. https://doi.org/10.1152/physiolgenomics.90310.2008

Lee, C. K., Shibata, Y., Rao, B., Strahl, B. D., & Lieb, J. D. (2004). Evidence for nucleosome depletion at active regulatory regions genome-wide. *Nature Genetics*, *36*(8), 900–905. https://doi.org/10.1038/ng1400

Lee, H. S. (2015). Impact of maternal diet on the epigenome during in utero life and the developmental programming of diseases in childhood and adulthood. *Nutrients*, *7*(11), 9492–9507. https://doi.org/10.3390/nu7115467

Lee, J. V., Carrer, A., Shah, S., Snyder, N. W., Wei, S., Venneti, S., Worth, A. J., Yuan, Z. F., Lim, H. W., Liu, S., Jackson, E., Aiello, N. M., Haas, N. B., Rebbeck, T. R., Judkins, A., Won, K. J., Chodosh, L. A., Garcia, B. A., Stanger, B. Z., … Wellen, K. E. (2014). Akt-dependent metabolic reprogramming regulates tumor cell Histone acetylation. *Cell Metabolism*, *20*(2), 306–319. https://doi.org/10.1016/j.cmet.2014.06.004

Leese, H. J. (2002). Quiet please, do not disturb: A hypothesis of embryo metabolism and viability. *BioEssays*, *24*(9), 845–849. https://doi.org/10.1002/bies.10137

Leese, H. J., Baumann, C. G., Brison, D. R., McEvoy, T. G., & Sturmey, R. G. (2008). Metabolism of the viable mammalian embryo: Quietness revisited. *Molecular Human Reproduction*, *14*(12), 667–672. https://doi.org/10.1093/molehr/gan065

Leese, H. J., Brison, D. R., & Sturmey, R. G. (2022). The Quiet Embryo Hypothesis: 20 years on. *Frontiers in Physiology*, *13*(May), 1–6. https://doi.org/10.3389/fphys.2022.899485

Leese, H. J., Conaghan, J., Martin, K. L., & Hardy, K. (1993). Early human embryo metabolism. *BioEssays*, *15*(4), 259–264. https://doi.org/10.1002/bies.950150406

Leto, D., & Saltiel, A. R. (2012). Regulation of glucose transport by insulin: traffic control of GLUT4. *Nature Reviews Molecular Cell Biology*, *13*(6), 383–396. https://doi.org/10.1038/nrm3351

Leunda-Casi, A., De Hertogh, R., & Pampfer, S. (2001). Decreased expression of fibroblast growth factor-4 and associated dysregulation of trophoblast differentiation in mouse blastocysts exposed to high D-glucose in vitro. *Diabetologia*, *44*(10), 1318–1325. https://doi.org/10.1007/s001250100633

Li, E., & Zhang, Y. (2014). DNA Methylation in Mammals. *Cold Spring Harbor Perspectives in Biology*, *6*(5), a019133–a019133. https://doi.org/10.1101/cshperspect.a019133

Li, H., & Durbin, R. (2009). Fast and accurate short read alignment with Burrows-Wheeler transform. *Bioinformatics*, *25*(14), 1754–1760. https://doi.org/10.1093/bioinformatics/btp324

Li, H., Handsaker, B., Wysoker, A., Fennell, T., Ruan, J., Homer, N., Marth, G., Abecasis, G., & Durbin, R. (2009). The Sequence Alignment/Map format and SAMtools. *Bioinformatics*, *25*(16), 2078–2079. https://doi.org/10.1093/bioinformatics/btp352

Li, J., Xu, H., Wang, Q., Fu, P., Huang, T., Anas, O., Zhao, H., & Xiong, N. (2019). Pard3 suppresses glioma

invasion by regulating RhoA through atypical protein kinase C/NF-κB signaling. *Cancer Medicine*, *8*(5), 2288–2302. https://doi.org/10.1002/cam4.2063

Liao, W. X., Laurent, L. C., Agent, S., Hodges, J., & Chen, D. bao. (2012). Human placental expression of slit/robo signaling cues: Effects of preeclampsia and hypoxia. *Biology of Reproduction*, *86*(4), 1–7. https://doi.org/10.1095/biolreprod.110.088138

Liemburg-Apers, D. C., Willems, P. H. G. M., Koopman, W. J. H., & Grefte, S. (2015). Interactions between mitochondrial reactive oxygen species and cellular glucose metabolism. *Archives of Toxicology*, *89*(8), 1209–1226. https://doi.org/10.1007/s00204-015-1520-y

Lighten, A. D., Moore, G. E., Winston, R. M. L., & Hardy, K. (1998). Routine addition of human insulin-like growth factor-I ligand could benefit clinical in-vitro fertilization culture. *Human Reproduction*, *13*(11), 3144–3150. https://doi.org/10.1093/humrep/13.11.3144

Lingappan, K. (2018). NF-κB in oxidative stress. *Current Opinion in Toxicology*, *7*, 81–86. https://doi.org/10.1016/j.cotox.2017.11.002

Liu, G. Y., & Sabatini, D. M. (2020). mTOR at the nexus of nutrition, growth, ageing and disease. *Nature Reviews Molecular Cell Biology*, *8*. https://doi.org/10.1038/s41580-019-0199-y

Liu, H., & Chen, Y. G. (2022). The Interplay Between TGF-β Signaling and Cell Metabolism. *Frontiers in Cell and Developmental Biology*, *10*(March), 1–14. https://doi.org/10.3389/fcell.2022.846723

Liu, L., Leng, L., Liu, C., Lu, C., Yuan, Y., Wu, L., Gong, F., Zhang, S., Wei, X., Wang, M., Zhao, L., Hu, L., Wang, J., Yang, H., Zhu, S., Chen, F., Lu, G., Shang, Z., & Lin, G. (2019). An integrated chromatin accessibility and transcriptome landscape of human pre-implantation embryos. *Nature Communications*, *10*(1), 364. https://doi.org/10.1038/s41467-018-08244-0

Liu, T., Zhang, L., Joo, D., & Sun, S.-C. (2017). NF-κB signaling in inflammation. *Signal Transduction and Targeted Therapy*, *2*(1), 17023. https://doi.org/10.1038/sigtrans.2017.23

Liu, Z., Sun, Y., Tan, S., Liu, L., Hu, S., Huo, H., Li, M., Cui, Q., & Yu, M. (2016). Nutrient deprivation-related OXPHOS/glycolysis interconversion via HIF-1α/C-MYC pathway in U251 cells. *Tumor Biology*, *37*(5), 6661–6671. https://doi.org/10.1007/s13277-015-4479-7

Locasale, J. W. (2013). Serine, glycine and one-carbon units: cancer metabolism in full circle. *Nature Reviews Cancer*, *13*(8), 572–583. https://doi.org/10.1038/nrc3557

Love, M. I., Huber, W., & Anders, S. (2014). Moderated estimation of fold change and dispersion for RNA-seq data with DESeq2. *Genome Biology*, *15*(12), 1–21. https://doi.org/10.1186/s13059-014-0550-8

Lu, C., & Thompson, C. B. (2012). Metabolic regulation of epigenetics. *Cell Metabolism*, *16*(1), 9–17. https://doi.org/10.1016/j.cmet.2012.06.001

Luc, K., Schramm-Luc, A., Guzik, T. J., & Mikolajczyk, T. P. (2019). Oxidative stress and inflammatory markers in prediabetes and diabetes. *Journal of Physiology and Pharmacology*, *70*(6), 809–824. https://doi.org/10.26402/jpp.2019.6.01

Lumey, L. H., Stein, A. D., & Susser, E. (2011). Prenatal Famine and Adult Health. *Annual Review of Public Health*, *32*(1), 237–262. https://doi.org/10.1146/annurev-publhealth-031210-101230

Luo, R., Liang, H., Zhang, W., Li, G., Zhao, K., Hua, W., Song, Y., & Yang, C. (2022). RETREG1-mediated ER-phagy activation induced by glucose deprivation alleviates nucleus pulposus cell damage via ER stress pathway. *Acta Biochimica et Biophysica Sinica*, *54*(4), 524–536. https://doi.org/10.3724/abbs.2022024

Madeja, Z. E., Pawlak, P., & Piliszek, A. (2019). Beyond the mouse: Non-rodent animal models for study of early mammalian development and biomedical research. *International Journal of Developmental Biology*, *63*(3–5), 187–201. https://doi.org/10.1387/ijdb.180414ap

Magliano, D. J., Sacre, J. W., Harding, J. L., Gregg, E. W., Zimmet, P. Z., & Shaw, J. E. (2020). Young-onset type 2 diabetes mellitus — implications for morbidity and mortality. *Nature Reviews Endocrinology*, *16*(6), 321–331. https://doi.org/10.1038/s41574-020-0334-z

Mahajan, K., & Mahajan, N. P. (2013). WEE1 tyrosine kinase, a novel epigenetic modifier. *Trends in Genetics*, *29*(7), 394–402. https://doi.org/10.1016/j.tig.2013.02.003

Maltepe, E., & Fisher, S. J. (2015). Placenta: The Forgotten Organ. *Annual Review of Cell and Developmental Biology*, *31*(1), 523–552. https://doi.org/10.1146/annurev-cellbio-100814-125620

Manes, C. (1973). The participation of the embryonic genome during early cleavage in the rabbit. *Developmental Biology*, *32*(2), 453–459. https://doi.org/10.1016/0012-1606(73)90254-6

Marchand, M., Horcajadas, J. A., Esteban, F. J., McElroy, S. L., Fisher, S. J., & Giudice, L. C. (2011). Transcriptomic signature of trophoblast differentiation in a human embryonic stem cell model. *Biology of Reproduction*, *84*(6), 1258–1271. https://doi.org/10.1095/biolreprod.110.086413

Marcho, C., Cui, W., & Mager, J. (2015). Epigenetic dynamics during preimplantation development. *Reproduction*, *150*(3), R109–R120. https://doi.org/10.1530/REP-15-0180

Marshall, C., Adams, S., Dyer, W., & Schmittdiel, J. (2017). Opportunities to Reduce Diabetes Risk in Women of Reproductive Age: Assessment and Treatment of Prediabetes within a Large Integrated Delivery System. *Women's Health Issues*, *27*(6), 666–672. https://doi.org/10.1016/j.whi.2017.06.001

Martin-Gronert, M. S., & Ozanne, S. E. (2007). Experimental IUGR and later diabetes. *Journal of Internal Medicine*, *261*(5), 437–452. https://doi.org/10.1111/j.1365-2796.2007.01800.x

Martin, M. (2011). Cutadapt removes adapter sequences from high-throughput sequencing reads. *EMBnet.Journal*, *17*(1), 10. https://doi.org/10.14806/ej.17.1.200

Martin, P. M. (2003). Amino Acid Transport Regulates Blastocyst Implantation. *Biology of Reproduction*, *69*(4), 1101–1108. https://doi.org/10.1095/biolreprod.103.018010

Martin, P. M., & Sutherland, A. E. (2001). Exogenous amino acids regulate trophectoderm differentiation in the mouse blastocyst through an mTOR-dependent pathway. *Developmental Biology*, *240*(1), 182–193. https://doi.org/10.1006/dbio.2001.0461

Martínez-Reyes, I., & Chandel, N. S. (2020). Mitochondrial TCA cycle metabolites control physiology and disease. *Nature Communications*, *11*(1), 102. https://doi.org/10.1038/s41467-019-13668-3

Martire, S., & Banaszynski, L. A. (2020). The roles of histone variants in fine-tuning chromatin organization and function. *Nature Reviews Molecular Cell Biology*, *21*(9), 522–541. https://doi.org/10.1038/s41580-020-0262-8

Mattei, A. L., Bailly, N., & Meissner, A. (2022). DNA methylation: a historical perspective. *Trends in Genetics*, *38*(7), 676–707. https://doi.org/10.1016/j.tig.2022.03.010

McIntyre, H. D., Catalano, P., Zhang, C., Desoye, G., Mathiesen, E. R., & Damm, P. (2019). Gestational diabetes mellitus. *Nature Reviews Disease Primers*, *5*(1), 47. https://doi.org/10.1038/s41572-019-0098-8

Menchero, S., Rayon, T., Andreu, M. J., & Manzanares, M. (2017). Signaling pathways in mammalian preimplantation development: Linking cellular phenotypes to lineage decisions. *Developmental Dynamics*, *246*(4), 245–261. https://doi.org/10.1002/dvdy.24471

Menezo, Y., & Guerin, P. (1997). The mammalian oviduct: Biochemistry and physiology. *European Journal of Obstetrics and Gynecology and Reproductive Biology*, *73*(1), 99–104. https://doi.org/10.1016/S0301-2115(97)02729-2

Metzger, B. E., & Buchanan, T. A. (2018). Gestational Diabetes. In *Diabetes in America*. http://www.ncbi.nlm.nih.gov/pubmed/33651565

Mezger, A., Klemm, S., Mann, I., Brower, K., Mir, A., Bostick, M., Farmer, A., Fordyce, P., Linnarsson, S., & Greenleaf, W. (2018). High-throughput chromatin accessibility profiling at single-cell resolution. *Nature Communications*, *9*(1), 6–11. https://doi.org/10.1038/s41467-018-05887-x

Michels, K. B. (2017). Developmental plasticity. *Evolution, Medicine, and Public Health*, *2017*(1), 183–184. https://doi.org/10.1093/emph/eox022

Millán-Zambrano, G., Burton, A., Bannister, A. J., & Schneider, R. (2022). Histone post-translational modifications — cause and consequence of genome function. *Nature Reviews Genetics*, *0123456789*. https://doi.org/10.1038/s41576-022-00468-7

Ming, H., Sun, J., Pasquariello, R., Gatenby, L., Herrick, J., Yuan, Y., Pinto, C., Bondioli, K. R., Krisher, R. L., & Jiang, Z. (2020). The landscape of accessible chromatin in bovine oocytes and early embryos. *Epigenetics*, *16*(3), 1–13. https://doi.org/10.1080/15592294.2020.1795602

Minnoye, L., Marinov, G. K., Krausgruber, T., Pan, L., Marand, A. P., Secchia, S., Greenleaf, W. J., Furlong, E. E. M., Zhao, K., Schmitz, R. J., Bock, C., & Aerts, S. (2021). Chromatin accessibility profiling methods. *Nature Reviews Methods Primers*, *1*(1), 1–3. https://doi.org/10.1038/s43586-020-00008-9

Moghetti, P., & Tosi, F. (2021). Insulin resistance and PCOS: chicken or egg? *Journal of Endocrinological Investigation*, *44*(2), 233–244. https://doi.org/10.1007/s40618-020-01351-0

Molè, M. A., Weberling, A., & Zernicka-Goetz, M. (2020). Comparative analysis of human and mouse development: From zygote to pre-gastrulation. In *Current Topics in Developmental Biology* (1st ed., Vol. 136). Elsevier Inc. https://doi.org/10.1016/bs.ctdb.2019.10.002

Moley, K. H. (1999). Diabetes and preimplantation events of embryogenesis. *Seminars in Reproductive Endocrinology*, *17*(2), 137–151. https://doi.org/10.1055/s-2007-1016221

Moley, K. H., Chi, M. M.-Y., Knudson, C. M., Korsmeyer, S. J., & Mueckler, M. M. (1998). Hyperglycemia induces apoptosis in pre-implantation embryos through cell death effector pathways. *Nature Medicine*, *4*(12), 1421–1424. https://doi.org/10.1038/4013

Moley, K. H., Chi, M. M.-Y., & Mueckler, M. M. (1998). Maternal hyperglycemia alters glucose transport and utilization in mouse preimplantation embryos. *American Journal of Physiology-Endocrinology and Metabolism*, *275*(1), E38–E47. https://doi.org/10.1152/ajpendo.1998.275.1.E38

Moussaieff, A., Rouleau, M., Kitsberg, D., Cohen, M., Levy, G., Barasch, D., Nemirovski, A., Shen-Orr, S., Laevsky, I., Amit, M., Bomze, D., Elena-Herrmann, B., Scherf, T., Nissim-Rafinia, M., Kempa, S., Itskovitz-Eldor, J., Meshorer, E., Aberdam, D., & Nahmias, Y. (2015). Glycolysis-mediated changes in acetyl-CoA and histone acetylation control the early differentiation of embryonic stem cells. *Cell Metabolism*, *21*(3), 392–402. https://doi.org/10.1016/j.cmet.2015.02.002

Murray, A., Sienerth, A. R., & Hemberger, M. (2016). Plet1 is an epigenetically regulated cell surface protein that provides essential cues to direct trophoblast stem cell differentiation. *Scientific Reports*, *6*(January), 1–14. https://doi.org/10.1038/srep25112

Murthi, P., Brouillet, S., Pratt, A., Borg, A., Kalionis, B., Goffin, F., Tsatsaris, V., Munaut, C., Feige, J. J., Benharouga, M., Fournier, T., & Alfaidy, N. (2015). An EG-VEGF-dependent decrease in homeobox gene NKX3.1 contributes to cytotrophoblast dysfunction: A possible mechanism in human fetal growth restriction. *Molecular Medicine*, *21*(4), 645–656. https://doi.org/10.2119/molmed.2015.00071

Nagaraj, R., Sharpley, M. S., Chi, F., Braas, D., Zhou, Y., Kim, R., Clark, A. T., & Banerjee, U. (2017). Nuclear Localization of Mitochondrial TCA Cycle Enzymes as a Critical Step in Mammalian Zygotic Genome Activation. *Cell*, *168*(1–2), 210-223.e11. https://doi.org/10.1016/j.cell.2016.12.026

Navarrete Santos, A., Ramin, N., Tonack, S., & Fischer, B. (2008). Cell Lineage-Specific Signaling of Insulin and Insulin-Like Growth Factor I in Rabbit Blastocysts. *Endocrinology*, *149*(2), 515–524. https://doi.org/10.1210/en.2007-0821

Navarrete Santos, A., Tonack, S., Kirstein, M., Kietz, S., & Fischer, B. (2004). Two insulin-responsive glucose transporter isoforms and the insulin receptor are developmentally expressed in rabbit preimplantation embryos. *Reproduction*, *128*(5), 503–516. https://doi.org/10.1530/rep.1.00203

Navarrete Santos, A., Tonack, S., Kirstein, M., Pantaleon, M., Kaye, P., & Fischer, B. (2004). Insulin acts via mitogen-activated protein kinase phosphorylation in rabbit blastocysts. *Reproduction*, *128*(5), 517–526. https://doi.org/10.1530/rep.1.00204

Nisr, R. B., & Affourtit, C. (2014). Insulin acutely improves mitochondrial function of rat and human skeletal muscle by increasing coupling efficiency of oxidative phosphorylation. *Biochimica et Biophysica Acta (BBA) - Bioenergetics*, *1837*(2), 270–276. https://doi.org/10.1016/j.bbabio.2013.10.012

Okada, Y., & Yamaguchi, K. (2017). Epigenetic modifications and reprogramming in paternal pronucleus: sperm, preimplantation embryo, and beyond. *Cellular and Molecular Life Sciences*, *74*(11), 1957–1967. https://doi.org/10.1007/s00018-016-2447-z

Okamoto, I., Patrat, C., Thépot, D., Peynot, N., Fauque, P., Daniel, N., Diabangouaya, P., Wolf, J. P., Renard, J. P., Duranthon, V., & Heard, E. (2011). Eutherian mammals use diverse strategies to initiate X-chromosome inactivation during development. *Nature*, *472*(7343), 370–374. https://doi.org/10.1038/nature09872

Olcha, M., Dong, X., Feil, H., Hao, X., Lee, M., Jindal, S., Buyuk, E., & Vijg, J. (2021). A workflow for simultaneous DNA copy number and methylome analysis of inner cell mass and trophectoderm

cells from human blastocysts. *Fertility and Sterility*, *115*(6), 1533–1540. https://doi.org/10.1016/j.fertnstert.2020.11.007

Ono, R., Nakamura, K., Inoue, K., Naruse, M., Usami, T., Wakisaka-Saito, N., Hino, T., Suzuki-Migishima, R., Ogonuki, N., Miki, H., Kohda, T., Ogura, A., Yokoyama, M., Kaneko-Ishino, T., & Ishino, F. (2006). Deletion of Peg10, an imprinted gene acquired from a retrotransposon, causes early embryonic lethality. *Nature Genetics*, *38*(1), 101–106. https://doi.org/10.1038/ng1699

Ornoy, A., Becker, M., Weinstein-Fudim, L., & Ergaz, Z. (2021). Diabetes during pregnancy: A maternal disease complicating the course of pregnancy with long-term deleterious effects on the offspring. a clinical review. *International Journal of Molecular Sciences*, *22*(6), 1–38. https://doi.org/10.3390/ijms22062965

Otani, H., Tanaka, O., Tatewaki, R., Naora, H., & Yoneyama, T. (1991). Diabetic environment and genetic predisposition as causes of congenital malformations in NOD mouse embryos. *Diabetes*, *40*(10), 1245–1250. https://doi.org/10.2337/diab.40.10.1245

Ozawa, M., Sakatani, M., Yao, J., Shanker, S., Yu, F., Yamashita, R., Wakabayashi, S., Nakai, K., Dobbs, K. B., Sudano, M. J., Farmerie, W. G., & Hansen, P. J. (2012). Global gene expression of the inner cell mass and trophectoderm of the bovine blastocyst. *BMC Developmental Biology*, *12*, 1–13. https://doi.org/10.1186/1471-213X-12-33

Painter, R. C., Osmond, C., Gluckman, P., Hanson, M., Phillips, D. I. W., & Roseboom, T. J. (2008). Transgenerational effects of prenatal exposure to the Dutch famine on neonatal adiposity and health in later life. *BJOG: An International Journal of Obstetrics and Gynaecology*, *115*(10), 1243–1249. https://doi.org/10.1111/j.1471-0528.2008.01822.x

Pampfer, S. (2000). Apoptosis in rodent peri-implantation embryos: Differential susceptibility of inner cell mass and trophectoderm cell lineages - A review. *Placenta*, *21*(SUPPL.1), 3–10. https://doi.org/10.1053/plac.1999.0519

Pampfer, S., De Hertogh, R., Vanderheyden, I., Michels, B., & Vercheval, M. (1990). Decreased inner cell mass proportion in blastocysts from diabetic rats. *Diabetes*, *39*(4), 471–476. https://doi.org/10.2337/diab.39.4.471

Pantaleon, M., & Kaye, P. L. (1996). IGF-I and insulin regulate glucose transport in mouse blastocysts via IGF-I receptor. *Molecular Reproduction and Development*, *44*(1), 71–76. https://doi.org/10.1002/(SICI)1098-2795(199605)44:1<71::AID-MRD8>3.0.CO;2-Q

Pantaleon, M., Tan, H. Y., Kafer, G. R., & Kaye, P. L. (2010). Toxic Effects of Hyperglycemia Are Mediated by the Hexosamine Signaling Pathway and O-Linked Glycosylation in Early Mouse Embryos1. *Biology of Reproduction*, *82*(4), 751–758. https://doi.org/10.1095/biolreprod.109.076661

Park, J. H., Stoffers, D. A., Nicholls, R. D., & Simmons, R. A. (2008). Development of type 2 diabetes following intrauterine growth retardation in rats is associated with progressive epigenetic silencing of Pdx1. *Journal of Clinical Investigation*, *118*(6), 2316–2324. https://doi.org/10.1172/JCI33655

Pavlinkova, G., Michael, J. M., & Kappen, C. (2009). Maternal diabetes alters transcriptional programs in the developing embryo. *BMC Genomics*, *10*, 1–12. https://doi.org/10.1186/1471-2164-10-274

Peng, T. Y., Ehrlich, S. F., Crites, Y., Kitzmiller, J. L., Kuzniewicz, M. W., Hedderson, M. M., & Ferrara, A. (2017). Trends and racial and ethnic disparities in the prevalence of pregestational type 1 and type 2 diabetes in Northern California: 1996–2014. *American Journal of Obstetrics and Gynecology*, *216*(2), 177.e1-177.e8. https://doi.org/10.1016/j.ajog.2016.10.007

Peral-Sanchez, I., Hojeij, B., Ojeda, D. A., Steegers-Theunissen, R. P. M., & Willaime-Morawek, S. (2021). Epigenetics in the Uterine Environment: How Maternal Diet and ART May Influence the Epigenome in the Offspring with Long-Term Health Consequences. *Genes*, *13*(1), 31. https://doi.org/10.3390/genes13010031

Pérez-Cerezales, S., Ramos-Ibeas, P., Rizos, D., Lonergan, P., Bermejo-Alvarez, P., & Gutiérrez-Adán, A. (2018). Early sex-dependent differences in response to environmental stress. *Reproduction*, R39–R51. https://doi.org/10.1530/REP-17-0466

Perez, M. F., & Lehner, B. (2019). Intergenerational and transgenerational epigenetic inheritance in animals. *Nature Cell Biology*, *21*(2), 143–151. https://doi.org/10.1038/s41556-018-0242-9

Perng, W., Oken, E., & Dabelea, D. (2019). Developmental overnutrition and obesity and type 2 diabetes in offspring. *Diabetologia*, *62*(10), 1779–1788. https://doi.org/10.1007/s00125-019-4914-1

Petersen, M. C., & Shulman, G. I. (2018). Mechanisms of insulin action and insulin resistance. *Physiological Reviews*, *98*(4), 2133–2223. https://doi.org/10.1152/physrev.00063.2017

Piffaretti, C., Mandereau-Bruno, L., Guilmin-Crepon, S., Choleau, C., Coutant, R., & Fosse-Edorh, S. (2019). Trends in childhood type 1 diabetes incidence in France, 2010–2015. *Diabetes Research and Clinical Practice*, *149*(Id), 200–207. https://doi.org/10.1016/j.diabres.2018.11.005

Piliszek, A., & Madeja, Z. E. (2018). Pre-implantation Development of Domestic Animals. In *Current Topics in Developmental Biology* (1st ed., Vol. 128, pp. 267–294). Elsevier Inc. https://doi.org/10.1016/bs.ctdb.2017.11.005

Pinney, S. E. (2013). Intrauterine growth retardation – a developmental model of type 2 diabetes. *Drug Discovery Today: Disease Models*, *10*(2), e71–e77. https://doi.org/10.1016/j.ddmod.2013.01.003

Pinney, S. E., & Simmons, R. A. (2010). Epigenetic mechanisms in the development of type 2 diabetes. *Trends in Endocrinology and Metabolism*, *21*(4), 223–229. https://doi.org/10.1016/j.tem.2009.10.002

Pizzagalli, M. D., Bensimon, A., & Superti-Furga, G. (2021). A guide to plasma membrane solute carrier proteins. *FEBS Journal*, *288*(9), 2784–2835. https://doi.org/10.1111/febs.15531

Plows, J. F., Stanley, J. L., Baker, P. N., Reynolds, C. M., & Vickers, M. H. (2018). The pathophysiology of gestational diabetes mellitus. *International Journal of Molecular Sciences*, *19*(11), 1–21. https://doi.org/10.3390/ijms19113342

Portha, B., Chavey, A., & Movassat, J. (2011). Early-life origins of type 2 diabetes: Fetal programming of the beta-cell mass. *Experimental Diabetes Research*, *2011*. https://doi.org/10.1155/2011/105076

Portha, B., Fournier, A., Ah Kioon, M. D., Mezger, V., & Movassat, J. (2014). Early environmental factors, alteration of epigenetic marks and metabolic disease susceptibility. *Biochimie*, *97*(1), 1–15. https://doi.org/10.1016/j.biochi.2013.10.003

Prados, F. J., Debrock, S., Lemmen, J. G., & Agerholm, I. (2012). The cleavage stage embryo. *Human Reproduction (Oxford, England)*, *27 Suppl 1*, 50–71. https://doi.org/10.1093/humrep/des224

Purcell, S. H., & Moley, K. H. (2009). Glucose transporters in gametes and preimplantation embryos. *Trends in Endocrinology & Metabolism*, *20*(10), 483–489. https://doi.org/10.1016/j.tem.2009.06.006

Qasim, A., Turcotte, M., de Souza, R. J., Samaan, M. C., Champredon, D., Dushoff, J., Speakman, J. R., & Meyre, D. (2018). On the origin of obesity: identifying the biological, environmental and cultural drivers of genetic risk among human populations. *Obesity Reviews*, *19*(2), 121–149. https://doi.org/10.1111/obr.12625

Ralston, A., Cox, B. J., Nishioka, N., Sasaki, H., Chea, E., Rugg-Gunn, P., Guo, G., Robson, P., Draper, J. S., & Rossant, J. (2010). Gata3 regulates trophoblast development downstream of Tead4 and in parallel to Cdx2. *Development*, *137*(3), 395–403. https://doi.org/10.1242/dev.038828

Ralston, A., & Rossant, J. (2005). Genetic regulation of stem cell origins in the mouse embryo. *Clinical Genetics*, *68*(2), 106–112. https://doi.org/10.1111/j.1399-0004.2005.00478.x

Ramin, N., Thieme, R., Fischer, S., Schindler, M., Schmidt, T., Fischer, B., & Santos, A. N. (2010). Maternal Diabetes Impairs Gastrulation and Insulin and IGF-I Receptor Expression in Rabbit Blastocysts. *Endocrinology*, *151*(9), 4158–4167. https://doi.org/10.1210/en.2010-0187

Ramírez, F., Ryan, D. P., Grüning, B., Bhardwaj, V., Kilpert, F., Richter, A. S., Heyne, S., Dündar, F., & Manke, T. (2016). deepTools2: a next generation web server for deep-sequencing data analysis. *Nucleic Acids Research*, *44*(W1), W160–W165. https://doi.org/10.1093/NAR/GKW257

Reed, J., Bain, S., & Kanamarlapudi, V. (2021). A review of current trends with type 2 diabetes epidemiology, aetiology, pathogenesis, treatments and future perspectives. *Diabetes, Metabolic Syndrome and Obesity: Targets and Therapy*, *14*, 3567–3602. https://doi.org/10.2147/DMSO.S319895

Reis e Silva, A. R., Adenot, P., Daniel, N., Archilla, C., Peynot, N., Lucci, C. M., Beaujean, N., & Duranthon, V. (2011). Dynamics of DNA methylation levels in maternal and paternal rabbit genomes after

fertilization. *Epigenetics*, *6*(8), 987–993. https://doi.org/10.4161/epi.6.8.16073

Renault, K. M., Carlsen, E. M., Nørgaard, K., Nilas, L., Pryds, O., Secher, N. J., Cortes, D., Jensen, J. E. B., Olsen, S. F., & Halldorsson, T. I. (2015). Intake of carbohydrates during pregnancy in obese women is associated with fat mass in the newborn offspring. *American Journal of Clinical Nutrition*, *102*(6), 1475–1481. https://doi.org/10.3945/ajcn.115.110551

Richards, P., Rachdi, L., Oshima, M., Marchetti, P., Bugliani, M., Armanet, M., Postic, C., Guilmeau, S., & Scharfmann, R. (2018). MondoA is an essential glucose-responsive transcription factor in human pancreatic β-cells. *Diabetes*, *67*(3), 461–472. https://doi.org/10.2337/db17-0595

Robbins, C. L., Keyserling, T. C., Pitts, S. B. J., Morrow, J., Majette, N., Sisneros, J. A., Ronay, A., Farr, S. L., Urrutia, R. P., & Dietz, P. M. (2013). *Screening Low-Income Women of Reproductive Age for Cardiovascular Disease Risk Factors*. *22*(4), 314–321. https://doi.org/10.1089/jwh.2012.4149

Rocha, S. O., Gomes, G. N., Forti, A. L. L., Pinho Franco, M. D. C., Fortes, Z. B., Cavanal, M. D. F., & Gil, F. Z. (2005). Long-term effects of maternal diabetes on vascular reactivity and renal function in rat male offspring. *Pediatric Research*, *58*(6), 1274–1279. https://doi.org/10.1203/01.pdr.0000188698.58021.ff

Roseboom, T. J. (2019). Epidemiological evidence for the developmental origins of health and disease: Effects of prenatal undernutrition in humans. *Journal of Endocrinology*, *242*(1), T135–T144. https://doi.org/10.1530/JOE-18-0683

Rosenblum, I. Y., Mattson, B. a, & Heyner, S. (1986). Stage-specific insulin binding in mouse preimplantation embryos. *Developmental Biology*, *116*, 261–263.

Rosenfeld, C. S. (2009). Animal Models to Study Environmental Epigenetics1. *Biology of Reproduction*, *82*(3), 473–488. https://doi.org/10.1095/biolreprod.109.080952

Rousseau-Ralliard, D., Couturier-Tarrade, A., Thieme, R., Brat, R., Rolland, A., Boileau, P., Aubrière, M.-C., Daniel, N., Dahirel, M., Derisoud, E., Fournier, N., Schindler, M., Duranthon, V., Fischer, B., Santos, A. N., & Chavatte-Palmer, P. (2019). A short periconceptional exposure to maternal type-1 diabetes is sufficient to disrupt the feto-placental phenotype in a rabbit model. *Molecular and Cellular Endocrinology*, *480*(April 2018), 42–53. https://doi.org/10.1016/j.mce.2018.10.010

Rousseau-Ralliard, D., Richard, C., Hoarau, P., Lallemand, M. S., Morillon, L., Aubrière, M. C., Valentino, S. A., Dahirel, M., Guinot, M., Fournier, N., Morin, G., Mourier, E., Camous, S., Slama, R., Cassee, F. R., Couturier-Tarrade, A., & Chavatte-Palmer, P. (2021). Prenatal air pollution exposure to diesel exhaust induces cardiometabolic disorders in adulthood in a sex-specific manner. *Environmental Research*, *200*. https://doi.org/10.1016/j.envres.2021.111690

Rousseau-Ralliard, D., Valentino, S. A., Aubrière, M., Dahirel, M., Lallemand, M., Archilla, C., Jouneau, L., Fournier, N., Richard, C., Aioun, J., Vitorino Carvalho, A., Jérôme, L., Slama, R., Duranthon, V., Cassee, F. R., Chavatte-Palmer, P., & Couturier-Tarrade, A. (2019). Effects of first-generation in utero exposure to diesel engine exhaust on second-generation placental function, fatty acid profiles and foetal metabolism in rabbits: preliminary results. *Scientific Reports*, *9*(1), 9710. https://doi.org/10.1038/s41598-019-46130-x

Ruchat, S. (2015). Genes in Fetal Metabolic Programming of Newborns Exposed To Maternal Hyperglycemia. *Epigenomics*, *7*, 1111–1122.

Sabari, B. R., Zhang, D., Allis, C. D., & Zhao, Y. (2017). Metabolic regulation of gene expression through histone acylations. *Nature Reviews Molecular Cell Biology*, *18*(2), 90–101. https://doi.org/10.1038/nrm.2016.140

Saenen, N. D., Martens, D. S., Neven, K. Y., Alfano, R., Bové, H., Janssen, B. G., Roels, H. A., Plusquin, M., Vrijens, K., & Nawrot, T. S. (2019). Air pollution-induced placental alterations: An interplay of oxidative stress, epigenetics, and the aging phenotype? *Clinical Epigenetics*, *11*(1), 1–14. https://doi.org/10.1186/s13148-019-0688-z

Safi-Stibler, S., & Gabory, A. (2020). Epigenetics and the Developmental Origins of Health and Disease: Parental environment signalling to the epigenome, critical time windows and sculpting the adult phenotype. *Seminars in Cell & Developmental Biology*, *97*(March), 172–180. https://doi.org/10.1016/j.semcdb.2019.09.008

Salleron, L., Magistrelli, G., Mary, C., Fischer, N., Bairoch, A., & Lane, L. (2014). DERA is the human deoxyribose phosphate aldolase and is involved in stress response. *Biochimica et Biophysica Acta - Molecular Cell Research*, *1843*(12), 2913–2925. https://doi.org/10.1016/j.bbamcr.2014.09.007

Salvaing, J., Peynot, N., Bedhane, M. N., Veniel, S., Pellier, E., Boulesteix, C., Beaujean, N., Daniel, N., & Duranthon, V. (2016). Assessment of "one-step" versus "sequential" embryo culture conditions through embryonic genome methylation and hydroxymethylation changes. *Human Reproduction*, *31*(11), 2471–2483. https://doi.org/10.1093/humrep/dew214

Sánchez-Santos, A., Martínez-Hernández, M. G., Contreras-Ramos, A., Ortega-Camarillo, C., & Baiza-Gutman, L. A. (2018). Hyperglycemia-induced mouse trophoblast spreading is mediated by reactive oxygen species. *Molecular Reproduction and Development*, *85*(4), 303–315. https://doi.org/10.1002/mrd.22965

Sanders, S. S., Hou, J., Sutton, L. M., Garside, V. C., Mui, K. K. N., Singaraja, R. R., Hayden, M. R., & Hoodless, P. A. (2015). Huntingtin interacting proteins 14 and 14-like are required for chorioallantoic fusion during early placental development. *Developmental Biology*, *397*(2), 257–266. https://doi.org/10.1016/j.ydbio.2014.11.018

Sanz, G., Daniel, N., Aubrière, M. C., Archilla, C., Jouneau, L., Jaszczyszyn, Y., Duranthon, V., Chavatte-Palmer, P., & Jouneau, A. (2019). Differentiation of derived rabbit trophoblast stem cells under fluid shear stress to mimic the trophoblastic barrier. *Biochimica et Biophysica Acta - General Subjects*, *1863*(10), 1608–1618. https://doi.org/10.1016/j.bbagen.2019.07.003

Saugandhika, S., Sharma, V., & Khatak, K. (2022). Illustrating the past, present and future perspective of Human Embryo Culture Media. *Animal Reproduction Update*, *2*(1), 90–107. https://doi.org/10.48165/aru.2022.2106

Saxton, R. A., & Sabatini, D. M. (2017). mTOR Signaling in Growth, Metabolism, and Disease. *Cell*, *168*(6), 960–976. https://doi.org/10.1016/j.cell.2017.02.004

Scheja, L., & Heeren, J. (2019). The endocrine function of adipose tissues in health and cardiometabolic disease. *Nature Reviews Endocrinology*, *15*(9), 507–524. https://doi.org/10.1038/s41574-019-0230-6

Schindler, M., Dannenberger, D., Nuernberg, G., Pendzialek, M., Grybel, K., Seeling, T., & Navarrete Santos, A. (2020). Embryonic fatty acid metabolism in diabetic pregnancy: the difference between embryoblasts and trophoblasts. *Molecular Human Reproduction*, *26*(11), 837–849. https://doi.org/10.1093/molehr/gaaa063

Schindler, M., Pendzialek, M., Navarrete Santos, A., Plösch, T., Seyring, S., Gürke, J., Haucke, E., Knelangen, J. M., Fischer, B., & Santos, A. N. (2014). Maternal Diabetes Leads to Unphysiological High Lipid Accumulation in Rabbit Preimplantation Embryos. *Endocrinology*, *155*(4), 1498–1509. https://doi.org/10.1210/en.2013-1760

Schindler, M., Pendzialek, S. M., Grybel, K., Seeling, T., & Santos, A. N. (2020). Metabolic profiling in blastocoel fluid and blood plasma of diabetic rabbits. *International Journal of Molecular Sciences*, *21*(3), 1–21. https://doi.org/10.3390/ijms21030919

Scholtens, D. M., Kuang, A., Lowe, L. P., Hamilton, J., Lawrence, J. M., Lebenthal, Y., Brickman, W. J., Clayton, P., Ma, R. C., McCance, D., Tam, W. H., Catalano, P. M., Linder, B., Dyer, A. R., Lowe, W. L., Metzger, B. E., Deerochanawong, C., Tanaphonpoonsuk, T., Chotigeat, S. B. U., … Grave, G. (2019). Hyperglycemia and Adverse Pregnancy Outcome Follow-up Study (HAPO FUS): Maternal Glycemia and Childhood Glucose Metabolism. *Diabetes Care*, *42*(3), 381–392. https://doi.org/10.2337/dc18-2021

Schoonejans, J. M., & Ozanne, S. E. (2021). Developmental programming by maternal obesity: Lessons from animal models. *Diabetic Medicine*, *38*(12), 1–11. https://doi.org/10.1111/dme.14694

Schulz, K. N., & Harrison, M. M. (2019). Mechanisms regulating zygotic genome activation. *Nature Reviews Genetics*, *20*(4), 221–234. https://doi.org/10.1038/s41576-018-0087-x

Seah, M. K. Y., & Messerschmidt, D. M. (2018). From Germline to Soma: Epigenetic Dynamics in the Mouse Preimplantation Embryo. In *Current Topics in Developmental Biology* (1st ed., Vol. 128, pp. 203–235). Elsevier Inc. https://doi.org/10.1016/bs.ctdb.2017.10.011

Seshadri, N., & Doucette, C. A. (2021). Circadian regulation of the pancreatic beta cell. *Endocrinology (United States)*, *162*(9), 1–11. https://doi.org/10.1210/endocr/bqab089

Shahbazi, M. N. (2020). Mechanisms of human embryo development: From cell fate to tissue shape and back. *Development (Cambridge)*, *147*(14). https://doi.org/10.1242/dev.190629

Shao, W.-J., Tao, L.-Y., Xie, J.-Y., Gao, C., Hu, J.-H., & Zhao, R.-Q. (2007). Exposure of preimplantation embryos to insulin alters expression of imprinted genes. *Comparative Medicine*, *57*(5), 482–486. http://www.ncbi.nlm.nih.gov/pubmed/17974131

Sharpley, M. S., Chi, F., Hoeve, J. ten, & Banerjee, U. (2021). Metabolic plasticity drives development during mammalian embryogenesis. *Developmental Cell*, *56*(16), 2329-2347.e6. https://doi.org/10.1016/j.devcel.2021.07.020

Shi, M., & Sirard, M.-A. (2022). Metabolism of fatty acids in follicular cells, oocytes, and blastocysts. *Reproduction and Fertility*, *3*(2), R96–R108. https://doi.org/10.1530/raf-21-0123

Shirzeyli, M. H., Amidi, F., Shamsara, M., Nazarian, H., Eini, F., Shirzeyli, F. H., Zolbin, M. M., Novin, M. G., & Joupari, M. D. (2020). Exposing mouse oocytes to mitoq during in vitro maturation improves maturation and developmental competence. *Iranian Journal of Biotechnology*, *18*(3), 12–21. https://doi.org/10.30498/ijb.2020.154641.2454

Shu, Y., Hassan, F., Ostrowski, M. C., & Mehta, K. D. (2021). Role of hepatic PKCβ in nutritional regulation of hepatic glycogen synthesis. *JCI Insight*, *6*(19), 1–15. https://doi.org/10.1172/jci.insight.149023

Sies, H., Berndt, C., & Jones, D. P. (2017). Oxidative Stress. *Annual Review of Biochemistry*, *86*(2), 715–748. https://doi.org/10.1146/annurev-biochem-061516-045037

Sies, H., & Jones, D. P. (2020). Reactive oxygen species (ROS) as pleiotropic physiological signalling agents. *Nature Reviews Molecular Cell Biology*, *21*(July). https://doi.org/10.1038/s41580-020-0230-3

Smith, D. G., & Sturmey, R. G. (2013). Parallels between embryo and cancer cell metabolism. *Biochemical Society Transactions*, *41*(2), 664–669. https://doi.org/10.1042/BST20120352

Smith, J., Cianflone, K., Biron, S., Hould, F. S., Lebel, S., Marceau, S., Lescelleur, O., Biertho, L., Simard, S., Kral, J. G., & Marceau, P. (2009). Effects of maternal surgical weight loss in mothers on intergenerational transmission of obesity. *Journal of Clinical Endocrinology and Metabolism*, *94*(11), 4275–4283. https://doi.org/10.1210/jc.2009-0709

Spiroski, A., Niu, Y., Nicholas, L. M., Austin-Williams, S., Camm, E. J., Sutherland, M. R., Ashmore, T. J., Skeffington, K. L., Logan, A., Ozanne, S. E., Murphy, M. P., & Giussani, D. A. (2021). Mitochondria antioxidant protection against cardiovascular dysfunction programmed by early-onset gestational hypoxia. *The FASEB Journal*, *35*(5), 1–15. https://doi.org/10.1096/fj.202002705R

Starikov, R., Inman, K., Chen, K., Lopes, V., Coviello, E., Pinar, H., & He, M. (2014). Comparison of placental findings in type 1 and type 2 diabetic pregnancies. *Placenta*, *35*(12), 1001–1006. https://doi.org/10.1016/j.placenta.2014.10.008

Sun, C., Velazquez, M. A., & Fleming, T. P. (2016). DOHaD and the Periconceptional Period, a Critical Window in Time. In *The Epigenome and Developmental Origins of Health and Disease* (pp. 33–47). Elsevier. https://doi.org/10.1016/B978-0-12-801383-0.00003-7

Suter, D. M., Tirefort, D., Julien, S., & Krause, K.-H. (2009). A Sox1 to Pax6 Switch Drives Neuroectoderm to Radial Glia Progression During Differentiation of Mouse Embryonic Stem Cells. *Stem Cells*, *27*(1), 49–58. https://doi.org/10.1634/stemcells.2008-0319

Suzuki, K. (2018). The developing world of DOHaD. *Journal of Developmental Origins of Health and Disease*, *9*(3), 266–269. https://doi.org/10.1017/S2040174417000691

Szmuilowicz, E. D., Josefson, J. L., & Metzger, B. E. (2019). Gestational Diabetes Mellitus. *Endocrinology and Metabolism Clinics of North America*, *48*(3), 479–493. https://doi.org/10.1016/j.ecl.2019.05.001

Tafesse, F. G., Vacaru, A. M., Bosma, E. F., Hermansson, M., Jain, A., Hilderink, A., Somerharju, P., & Holthuis, J. C. M. (2013). Sphingomyelin synthase-related protein SMSr is a suppressor of ceramide-induced mitochondrial apoptosis. *Journal of Cell Science*, *127*(2), 445–454. https://doi.org/10.1242/jcs.138933

Taniguchi, C. M., Emanuelli, B., & Kahn, C. R. (2006). Critical nodes in signalling pathways: insights into

insulin action. *Nature Reviews Molecular Cell Biology*, *7*(2), 85–96. https://doi.org/10.1038/nrm1837

Tarrade, A., Panchenko, P., Junien, C., & Gabory, A. (2015). Placental contribution to nutritional programming of health and diseases: epigenetics and sexual dimorphism. *Journal of Experimental Biology*, *218*(1), 50–58. https://doi.org/10.1242/jeb.110320

Tarrade, A., Rousseau-Ralliard, D., Aubrière, M. C., Peynot, N., Dahirel, M., Bertrand-Michel, J., Aguirre-Lavin, T., Morel, O., Beaujean, N., Duranthon, V., & Chavatte-Palmer, P. (2013). Sexual dimorphism of the feto-placental phenotype in response to a high fat and control maternal diets in a rabbit model. *PLoS ONE*, *8*(12). https://doi.org/10.1371/journal.pone.0083458

Tarry-Adkins, J. L., & Ozanne, S. E. (2017). Nutrition in early life and age-associated diseases. *Ageing Research Reviews*, *39*, 96–105. https://doi.org/10.1016/j.arr.2016.08.003

Thieme, R., Schindler, M., Ramin, N., Fischer, S., Mühleck, B., Fischer, B., & Navarrete Santos, A. (2012). Insulin growth factor adjustment in preimplantation rabbit blastocysts and uterine tissues in response to maternal type 1 diabetes. *Molecular and Cellular Endocrinology*, *358*(1), 96–103. https://doi.org/10.1016/j.mce.2012.03.007

Thomas, D. D., Corkey, B. E., Istfan, N. W., & Apovian, C. M. (2019). Hyperinsulinemia: An early indicator of metabolic dysfunction. *Journal of the Endocrine Society*, *3*(9), 1727–1747. https://doi.org/10.1210/js.2019-00065

Thorens, B., & Mueckler, M. (2010). Glucose transporters in the 21st Century. *American Journal of Physiology - Endocrinology and Metabolism*, *298*(2), 141–145. https://doi.org/10.1152/ajpendo.00712.2009

Tobi, E. W., Goeman, J. J., Monajemi, R., Gu, H., Putter, H., Zhang, Y., Slieker, R. C., Stok, A. P., Thijssen, P. E., Müller, F., Van Zwet, E. W., Bock, C., Meissner, A., Lumey, L. H., Eline Slagboom, P., & Heijmans, B. T. (2014). DNA methylation signatures link prenatal famine exposure to growth and metabolism. *Nature Communications*, *5*. https://doi.org/10.1038/ncomms6592

Tokarz, V. L., MacDonald, P. E., & Klip, A. (2018). The cell biology of systemic insulin function. *Journal of Cell Biology*, *217*(7), 1–17. https://doi.org/10.1083/jcb.201802095

Torres-Perez, J. V., Irfan, J., Febrianto, M. R., Di Giovanni, S., & Nagy, I. (2021). Histone post-translational modifications as potential therapeutic targets for pain management. *Trends in Pharmacological Sciences*, *42*(11), 897–911. https://doi.org/10.1016/j.tips.2021.08.002

Tosolini, M., & Jouneau, A. (2015). Acquiring ground state pluripotency:Switching mouse embryonic stem cells from Serum/LIF medium to 2I/LIF medium. *Methods in Molecular Biology*, *1341*(3), 41–48. https://doi.org/10.1007/7651_2015_207

Tsume-Kajioka, M., Kimura-Yoshida, C., Mochida, K., Ueda, Y., & Matsuo, I. (2022). BET proteins are essential for the specification and maintenance of the epiblast lineage in mouse preimplantation embryos. *BMC Biology*, *20*(1), 64. https://doi.org/10.1186/s12915-022-01251-0

Tucci, V., Isles, A. R., Kelsey, G., Ferguson-Smith, A. C., Bartolomei, M. S., Benvenisty, N., Bourc'his, D., Charalambous, M., Dulac, C., Feil, R., Glaser, J., Huelsmann, L., John, R. M., McNamara, G. I., Moorwood, K., Muscatelli, F., Sasaki, H., Strassmann, B. I., Vincenz, C., & Wilkins, J. (2019). Genomic Imprinting and Physiological Processes in Mammals. *Cell*, *176*(5), 952–965. https://doi.org/10.1016/j.cell.2019.01.043

Turban, S., & Hajduch, E. (2011). Protein kinase C isoforms: Mediators of reactive lipid metabolites in the development of insulin resistance. *FEBS Letters*, *585*(2), 269–274. https://doi.org/10.1016/j.febslet.2010.12.022

Unoki, M. (2020). Recent Insights into the Mechanisms of De Novo and Maintenance of DNA Methylation in Mammals. In *DNA Methylation Mechanism* (p. 13). IntechOpen. https://doi.org/10.5772/intechopen.89238

Vaiserman, A., & Lushchak, O. (2019). Developmental origins of type 2 diabetes: Focus on epigenetics. *Ageing Research Reviews*, *55*(August), 100957. https://doi.org/10.1016/j.arr.2019.100957

Valadão, L., Moreira da Silva, H., & Moreira da Silva, F. (2019). Bovine Embryonic Development to Implantation. *Embryology - Theory and Practice*, 1–10. https://doi.org/10.5772/intechopen.80655

Vambergue, A., & Fajardy, I. (2011). Consequences of gestational and pregestational diabetes on placental function and birth weight. *World Journal of Diabetes*, *2*(11), 196. https://doi.org/10.4239/wjd.v2.i11.196

van Steensel, B., & Furlong, E. E. M. (2019). The role of transcription in shaping the spatial organization of the genome. *Nature Reviews Molecular Cell Biology*. https://doi.org/10.1038/s41580-019-0114-6

Velazquez, M. A., & Fleming, T. P. (2013). Maternal Diet, Oocyte Nutrition and Metabolism, and Offspring Health. In *Oogenesis* (pp. 329–351). Springer London. https://doi.org/10.1007/978-0-85729-826-3_22

Vince, K., Perković, P., & Matijević, R. (2020). What is known and what remains unresolved regarding gestational diabetes mellitus (GDM). *Journal of Perinatal Medicine*, *48*(8), 757–763. https://doi.org/10.1515/jpm-2020-0254

Voormolen, D. N., de Wit, L., van Rijn, B. B., DeVries, J. H., Heringa, M. P., Franx, A., Groenendaal, F., & Lamain-de Ruiter, M. (2018). Neonatal Hypoglycemia Following Diet-Controlled and Insulin-Treated Gestational Diabetes Mellitus. *Diabetes Care*, *41*(7), 1385–1390. https://doi.org/10.2337/dc18-0048

Waddington, C. H. (2012). The epigenotype. 1942. *International Journal of Epidemiology*, *41*(1), 10–13. https://doi.org/10.1093/ije/dyr184

Wang, H., & Dey, S. K. (2006). Roadmap to embryo implantation: clues from mouse models. *Nature Reviews Genetics*, *7*(3), 185–199. https://doi.org/10.1038/nrg1808

Wang, H., Li, N., Chivese, T., Werfalli, M., Sun, H., Yuen, L., Ambrosius, C., Elise, C., & Immanuel, J. (2022). IDF Diabetes Atlas : Estimation of Global and Regional Gestational Diabetes Mellitus Prevalence for 2021 by International Association of Diabetes in Pregnancy Study Group ' s Criteria. *Diabetes Research and Clinical Practice*, *183*, 109050. https://doi.org/10.1016/j.diabres.2021.109050

Wang, L., Zhang, H., Hasim, A., Tuerhong, A., Hou, Z., Abdurahmam, A., & Sheyhidin, I. (2017). Partition-defective 3 (PARD3) regulates proliferation, apoptosis, migration, and invasion in esophageal squamous cell carcinoma cells. *Medical Science Monitor*, *23*, 2382–2390. https://doi.org/10.12659/MSM.903380

Wang, Q., Ratchford, A. M., Chi, M. M. Y., Schoeller, E., Frolova, A., Schedl, T., & Moley, K. H. (2009). Maternal Diabetes Causes Mitochondrial Dysfunction and Meiotic Defects in Murine Oocytes. *Molecular Endocrinology*, *23*(10), 1603–1612. https://doi.org/10.1210/me.2009-0033

Wang, Y., Liu, H., & Sun, Z. (2017). Lamarck rises from his grave: parental environment-induced epigenetic inheritance in model organisms and humans. *Biological Reviews*, *92*(4), 2084–2111. https://doi.org/10.1111/brv.12322

Wang, Y., Liu, Q., Tang, F., Yan, L., & Qiao, J. (2019). *Epigenetic Regulation and Risk Factors During the Development of Human Gametes and Early Embryos*. 1–20.

Waterland, R. A., & Michels, K. B. (2007). Epigenetic Epidemiology of the Developmental Origins Hypothesis. *Annual Review of Nutrition*, *27*(1), 363–388. https://doi.org/10.1146/annurev.nutr.27.061406.093705

Watkins, A. J., Dias, I., Tsuro, H., Allen, D., Emes, R. D., Moreton, J., Wilson, R., Ingram, R. J. M., & Sinclair, K. D. (2018). Paternal diet programs offspring health through sperm- and seminal plasma-specific pathways in mice. *Proceedings of the National Academy of Sciences*, *115*(40), 10064–10069. https://doi.org/10.1073/pnas.1806333115

Watkins, A. J., Ursell, E., Panton, R., Papenbrock, T., Hollis, L., Cunningham, C., Wilkins, A., Perry, V. H., Sheth, B., Kwong, W. Y., Eckert, J. J., Wild, A. E., Hanson, M. A., Osmond, C., & Fleming, T. P. (2007). Adaptive Responses by Mouse Early Embryos to Maternal Diet Protect Fetal Growth but Predispose to Adult Onset Disease1. *Biology of Reproduction*, *78*(2), 299–306. https://doi.org/10.1095/biolreprod.107.064220

Watkins, A. J., Wilkins, A., Cunningham, C., Perry, V. H., Seet, M. J., Osmond, C., Eckert, J. J., Torrens, C., Cagampang, F. R. A., Cleal, J., Gray, W. P., Hanson, M. A., & Fleming, T. P. (2008). Low protein diet fed exclusively during mouse oocyte maturation leads to behavioural and cardiovascular

abnormalities in offspring. *Journal of Physiology*, *586*(8), 2231–2244. https://doi.org/10.1113/jphysiol.2007.149229

Wei, Y., Xu, Q., Yang, H., Yang, Y., Wang, L., Chen, H., Anderson, C., Liu, X., Song, G., Li, Q., Wang, Q., Shen, H., Zhang, Y., Yan, D., Peng, Z., He, Y., Wang, Y., Zhang, Y., Zhang, H., & Ma, X. (2019). Preconception diabetes mellitus and adverse pregnancy outcomes in over 6.4 million women: A population-based cohort study in China. *PLoS Medicine*, *16*(10), 1–15. https://doi.org/10.1371/journal.pmed.1002926

White, M. D., Zenker, J., Bissiere, S., & Plachta, N. (2018). Instructions for Assembling the Early Mammalian Embryo. *Developmental Cell*, *45*(6), 667–679. https://doi.org/10.1016/j.devcel.2018.05.013

White, M. F. (2003). Insulin Signaling in Health and Disease. *Science*, *302*(5651), 1710–1711. https://doi.org/10.1126/science.1092952

Wilde, B. R., Ye, Z., Lim, T.-Y., & Ayer, D. E. (2019). Cellular acidosis triggers human MondoA transcriptional activity by driving mitochondrial ATP production. *ELife*, *8*, 1–25. https://doi.org/10.7554/eLife.40199

Wood, I. S., & Trayhurn, P. (2003). Glucose transporters (GLUT and SGLT): expanded families of sugar transport proteins. *British Journal of Nutrition*, *89*(1), 3–9. https://doi.org/10.1079/bjn2002763

World Health Organization. (2021a). *Diabetes*. https://www.who.int/news-room/fact-sheets/detail/diabetes

World Health Organization. (2021b). *Obesity and overweight*. https://www.who.int/news-room/fact-sheets/detail/obesity-and-overweight

Wu, J., Xu, J., Liu, B., Yao, G., Wang, P., Lin, Z., Huang, B., Wang, X., Li, T., Shi, S., Zhang, N., Duan, F., Ming, J., Zhang, X., Niu, W., Song, W., Jin, H., Guo, Y., Dai, S., … Sun, Y. (2018). Chromatin analysis in human early development reveals epigenetic transition during ZGA. *Nature*, *557*(7704), 256–260. https://doi.org/10.1038/s41586-018-0080-8

Wyman, A., Pinto, A. B., Sheridan, R., & Moley, K. H. (2008). One-cell zygote transfer from diabetic to nondiabetic mouse results in congenital malformations and growth retardation in offspring. *Endocrinology*, *149*(2), 466–469. https://doi.org/10.1210/en.2007-1273

Xie, L., Dong, P., Qi, Y., Hsieh, T.-H. S., English, B. P., Jung, S., Chen, X., De Marzio, M., Casellas, R., Chang, H. Y., Zhang, B., Tjian, R., & Liu, Z. (2022). BRD2 compartmentalizes the accessible genome. *Nature Genetics*, *54*(4), 481–491. https://doi.org/10.1038/s41588-022-01044-9

Xie, Z., Fang, Z., & Pan, Z. (2019). Ufl1/RCAD, a Ufm1 E3 ligase, has an intricate connection with ER stress. *International Journal of Biological Macromolecules*, *135*, 760–767. https://doi.org/10.1016/j.ijbiomac.2019.05.170

Yang, M., Tao, X., Titus, S., Zhao, T., Scott, R. T., & Seli, E. (2020). Analysis of accessible chromatin landscape in the inner cell mass and trophectoderm of human blastocysts. *Molecular Human Reproduction*, *26*(9), 702–711. https://doi.org/10.1093/molehr/gaaa048

Yang, P., Shen, W., Albert Reece, E., Chen, X., & Yang, P. (2016). High glucose suppresses embryonic stem cell differentiation into neural lineage cells. *Biochemical and Biophysical Research Communications*, *472*(2), 306–312. https://doi.org/10.1016/j.bbrc.2016.02.117

Yessoufou, A., & Moutairou, K. (2011). Maternal diabetes in pregnancy: Early and long-term outcomes on the offspring and the concept of "metabolic memory." *Experimental Diabetes Research*, *2011*. https://doi.org/10.1155/2011/218598

Yu, Y., Arah, O. A., Liew, Z., Cnattingius, S., Olsen, J., Sørensen, H. T., Qin, G., & Li, J. (2019). Maternal diabetes during pregnancy and early onset of cardiovascular disease in offspring: Population based cohort study with 40 years of follow-up. *The BMJ*, *367*(Cvd), 1–4. https://doi.org/10.1136/bmj.l6398

Yu, Z., Han, S., Zhu, J., Sun, X., Ji, C., & Guo, X. (2013). Pre-Pregnancy Body Mass Index in Relation to Infant Birth Weight and Offspring Overweight/Obesity: A Systematic Review and Meta-Analysis. *PLoS ONE*, *8*(4). https://doi.org/10.1371/journal.pone.0061627

Yucel, N., Wang, Y. X., Mai, T., Porpiglia, E., Lund, P. J., Markov, G., Garcia, B. A., Bendall, S. C., Angelo, M., & Blau, H. M. (2019). Glucose Metabolism Drives Histone Acetylation Landscape Transitions that Dictate Muscle Stem Cell Function. *Cell Reports*, *27*(13), 3939-3955.e6. https://doi.org/10.1016/j.celrep.2019.05.092

Zhang, A. M. Y., Wellberg, E. A., Kopp, J. L., & Johnson, J. D. (2021). *Hyperinsulinemia in Obesity , Inflammation , and Cancer*. 285–311.

Zhang, J., Wang, L., & Xie, X. (2021). RFC4 promotes the progression and growth of Oral Tongue squamous cell carcinoma in vivo and vitro. *Journal of Clinical Laboratory Analysis*, *35*(5), 1–8. https://doi.org/10.1002/jcla.23761

Zhang, P., Li, L., Bao, Z., & Huang, F. (2016). Role of BAF60a/BAF60c in chromatin remodeling and hepatic lipid metabolism. *Nutrition and Metabolism*, *13*(1), 1–13. https://doi.org/10.1186/s12986-016-0090-1

Zhang, P., Wu, W., Chen, Q., & Chen, M. (2019). Non-Coding RNAs and their Integrated Networks. *Journal of Integrative Bioinformatics*, *16*(3), 1–12. https://doi.org/10.1515/jib-2019-0027

Zhang, T., Cooper, S., & Brockdorff, N. (2015). The interplay of histone modifications – writers that read. *EMBO Reports*, *16*(11), 1467–1481. https://doi.org/10.15252/embr.201540945

Zhang, Y., Shi, J., Rassoulzadegan, M., Tuorto, F., & Chen, Q. (2019). Sperm RNA code programmes the metabolic health of offspring. *Nature Reviews Endocrinology*, *15*(8), 489–498. https://doi.org/10.1038/s41574-019-0226-2

Zhou, Z., Zhang, K., Liu, Z., Gao, X., Huang, K., Chen, C., Wang, D., Yang, Q., & Long, Q. (2021). ATPAF1 deficiency impairs ATP synthase assembly and mitochondrial respiration. *Mitochondrion*, *60*, 129–141. https://doi.org/10.1016/j.mito.2021.08.005

Zhu, M., & Zernicka-Goetz, M. (2020). Principles of Self-Organization of the Mammalian Embryo. *Cell*, *183*(6), 1467–1478. https://doi.org/10.1016/j.cell.2020.11.003

Ziomek, C. A., Chatot, C. L., & Manes, C. (1990). Polarization of blastomeres in the cleaving rabbit embryo. *Journal of Experimental Zoology*, *256*(1), 84–91. https://doi.org/10.1002/jez.1402560111

APPENDICES

Appendix 1: ATAC-seq primers.

Sequences from Buenrostro et al., 2013 and Mezger et al., 2018 (List of primer 1 and 2, respectively).

Primer 1		
	Index (i5)	**Sequence**
Ad1.1	TAGATCGC	AATGATACGGCGACCACCGAGATCTACACTAGATCGCTCGTCGGCAGCGTCAGATGTGTAT

Primer 2		
Ad2.*	**Index (i7)**	**Sequence**
Ad2.2	CGTACTAG	CAAGCAGAAGACGGCATACGAGATCTAGTACGGTCTCGTGGGCTCGGAGATGTG
Ad2.3	AGGCAGAA	CAAGCAGAAGACGGCATACGAGATTTCTGCCTGTCTCGTGGGCTCGGAGATGTG
Ad2.4	TCCTGAGC	CAAGCAGAAGACGGCATACGAGATGCTCAGGAGTCTCGTGGGCTCGGAGATGTG
Ad2.5	GGACTCCT	CAAGCAGAAGACGGCATACGAGATAGGAGTCCGTCTCGTGGGCTCGGAGATGTG
Ad2.6	TAGGCATG	CAAGCAGAAGACGGCATACGAGATCATGCCTAGTCTCGTGGGCTCGGAGATGTG
Ad2.7	CTCTCTAC	CAAGCAGAAGACGGCATACGAGATGTAGAGAGGTCTCGTGGGCTCGGAGATGTG
Ad2.9	GCTACGCT	CAAGCAGAAGACGGCATACGAGATAGCGTAGCGTCTCGTGGGCTCGGAGATGT
Ad2.12	GTAGAGGA	CAAGCAGAAGACGGCATACGAGATTCCTCTACGTCTCGTGGGCTCGGAGATGT
Ad2.13	GTCGTGAT	CAAGCAGAAGACGGCATACGAGATATCACGACGTCTCGTGGGCTCGGAGATGT
Ad2.14	ACCACTGT	CAAGCAGAAGACGGCATACGAGATACAGTGGTGTCTCGTGGGCTCGGAGATGT
Ad2.15	TGGATCTG	CAAGCAGAAGACGGCATACGAGATCAGATCCAGTCTCGTGGGCTCGGAGATGT
Ad2.16	CCGTTTGT	CAAGCAGAAGACGGCATACGAGATACAAACGGGTCTCGTGGGCTCGGAGATGT
Ad2.17	TGCTGGGT	CAAGCAGAAGACGGCATACGAGATACCCAGCAGTCTCGTGGGCTCGGAGATGT
Ad2.18	GAGGGGTT	CAAGCAGAAGACGGCATACGAGATAACCCCTCGTCTCGTGGGCTCGGAGATGT
Ad2.19	AGGTTGGG	CAAGCAGAAGACGGCATACGAGATCCCAACCTGTCTCGTGGGCTCGGAGATGT
Ad2.20	GTGTGGTG	CAAGCAGAAGACGGCATACGAGATCACCACACGTCTCGTGGGCTCGGAGATGT
Ad2.21	TGGGTTTC	CAAGCAGAAGACGGCATACGAGATGAAACCCAGTCTCGTGGGCTCGGAGATGT
Ad2.24	CCACTCCT	CAAGCAGAAGACGGCATACGAGATAGGAGTGGGTCTCGTGGGCTCGGAGATGT

Appendix 2: ATAC-seq bioinformatic analysis pipeline.

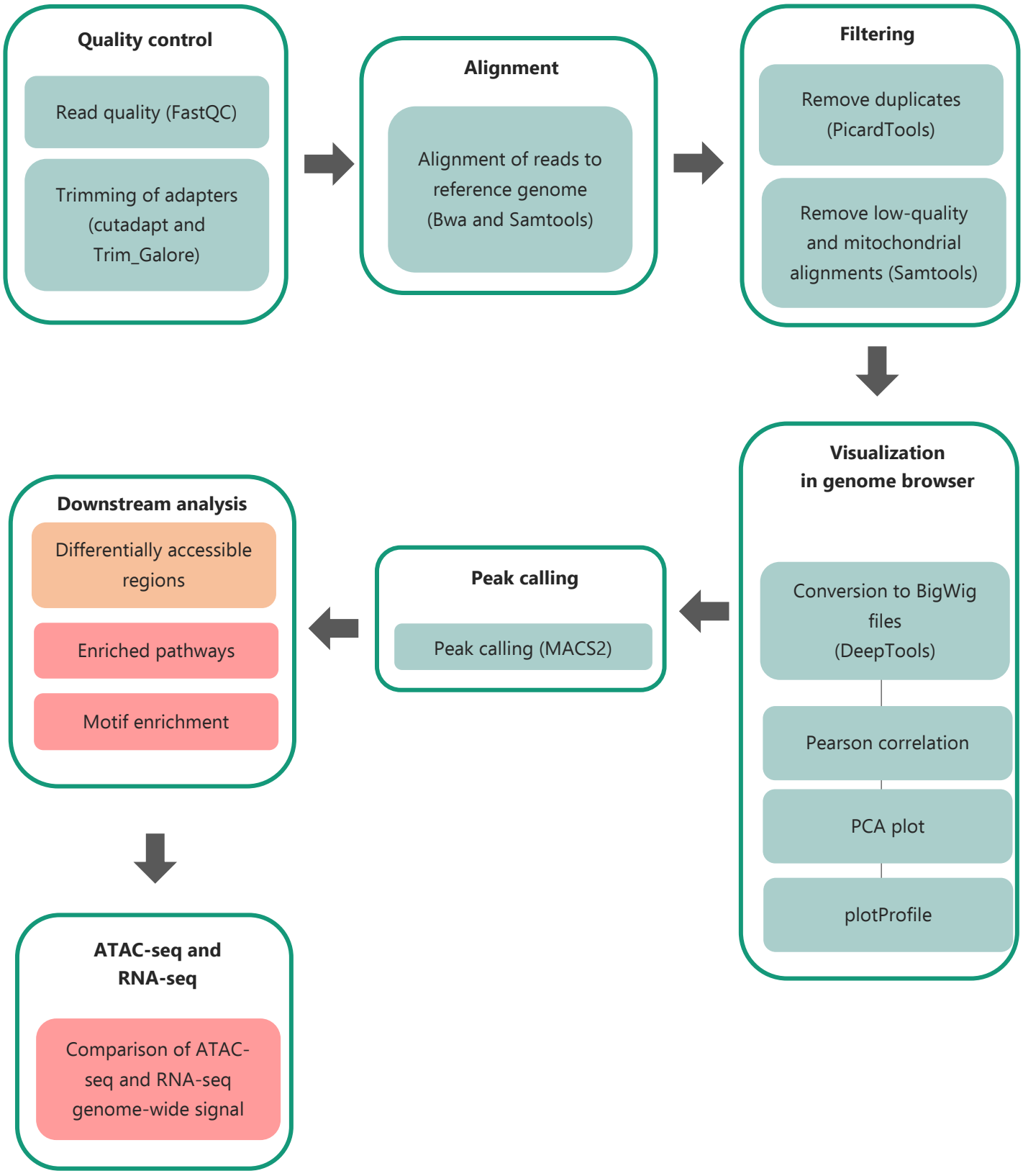

Appendix 3: Differentially expressed genes (DEGs) in inner cell mass (ICM) of embryos developed with high insulin (HI) versus control (CNTRL).

Geneid	Gene symbol	Gene name	Gene type	Log_2FC	adj *P* value	Gene Ontology Biological Process Term	Gene Ontology Biological Process Term 2	DEG shared between ICM comparisons to CNTRL	DEG shared between TE comparisons to CNTRL
ENSOCUG00000003208	DOCK8	dedicator of cytokinesis 8	protein_coding	4,91	4,18E-02	GO:0001771~immunological synapse formation	GO:0007264~small GTPase mediated signal transduction		
ENSOCUG00000017763	TLR3	toll like receptor 3	protein_coding	3,89	4,80E-02	GO:0002224~toll-like receptor signaling pathway	GO:0002282~microglial cell activation involved in immune response		
ENSOCUG00000025948	RPS6KA3	ribosomal protein S6 kinase A3	protein_coding	0,88	1,13E-02	GO:0001501~skeletal system development	GO:0002224~toll-like receptor signaling pathway	ICM HG vs CNTRL and ICM HGI vs CNTRL	
ENSOCUG00000022005	ICE1	interactor of little elongation complex ELL subunit 1	protein_coding	-0,71	3,71E-02	GO:0031334~positive regulation of protein complex assembly	GO:0042795~snRNA transcription from RNA polymerase II promoter	ICM HG vs CNTRL	
ENSOCUG00000005008	SPTBN1	spectrin beta, non-erythrocytic 1	protein_coding	-0,85	1,13E-02	GO:0000165~MAPK cascade	GO:0000281~mitotic cytokinesis		
ENSOCUG00000004930	RC3H1	ring finger and CCCH-type domains 1	protein_coding	-0,86	1,13E-02	GO:0000288~nuclear-transcribed mRNA catabolic process, deadenylation-dependent decay	GO:0000956~nuclear-transcribed mRNA catabolic process		
ENSOCUG00000035140			protein_coding	-0,89	1,11E-03			ICM HG vs CNTRL and ICM HGI vs CNTRL	
ENSOCUG00000016761	DOP1B	DOP1 Leucine Zipper Like Protein B	protein_coding	-1,02	3,81E-02				
ENSOCUG00000016929	APBB1	amyloid beta precursor protein binding family B member 1	protein_coding	-1,59	3,81E-02	GO:0006302~double-strand break repair	GO:0006351~transcription, DNA-templated	ICM HG vs CNTRL	
ENSOCUG00000014767	PAG1	phosphoprotein membrane anchor with glycosphingolipid microdomains 1	protein_coding	-3,05	4,94E-02	GO:0002250~adaptive immune response	GO:0007165~signal transduction		

Appendix 4: Differentially expressed genes (DEGs) in trophectoderm (TE) of embryos developed with high insulin (HI) versus control (CNTRL).

Geneid	Gene symbol	Gene name	Gene type	Log_2FC	adj *P* value	Gene Ontology Biological Process Term	Gene Ontology Biological Process Term 2	DEG shared between ICM comparisons to CNTRL	DEG shared between TE comparisons to CNTRL
ENSOCUG00000029602	PNLIP	pancreatic lipase	protein_coding	5,08	7,25E-03	GO:0001523~retinoid metabolic process	GO:0016042~lipid catabolic process		TE HG vs CNTRL and TE HGI vs CNTRL

Appendix 5: Differentially expressed genes (DEGs) in inner cell mass (ICM) of embryos developed with high glucose (HG) versus control (CNTRL).

Geneid	Gene symbol	Gene name	Gene type	Log_2FC	adj *P* value	Gene Ontology Biological Process Term	Gene Ontology Biological Process Term 2	DEG shared between ICM comparisons to CNTRL	DEG shared between TE comparisons to CNTRL
ENSOCUG00000002492	CD36	CD36 molecule	protein_coding	8,34	4,26E-02	GO:0000122~negative regulation of transcription from RNA polymerase II promoter	GO:0001954~positive regulation of cell-matrix adhesion		
ENSOCUG00000016898	PLEKHG1	pleckstrin homology and RhoGEF domain containing G1	protein_coding	8,08	4,15E-02	GO:0035023~regulation of Rho protein signal transduction	GO:0043547~positive regulation of GTPase activity		
ENSOCUG00000035276			protein_coding	7,11	3,87E-02				
ENSOCUG00000023725	RGN	regucalcin	protein_coding	2,54	8,27E-04	GO:0001822~kidney development	GO:0006469~negative regulation of protein kinase activity	ICM HGI vs CNTRL	
ENSOCUG00000009672	PLET1	placenta expressed transcript 1	protein_coding	2,39	1,96E-03	GO:0001953~negative regulation of cell-matrix adhesion	GO:0030154~cell differentiation	ICM HGI vs CNTRL	
ENSOCUG00000004968	REL	REL proto-oncogene, NF-kB subunit	protein_coding	2,18	1,58E-02	GO:0000122~negative regulation of transcription from RNA polymerase II promoter	GO:0006366~transcription from RNA polymerase II promoter		
ENSOCUG00000009737	ARRDC4	arrestin domain containing 4	protein_coding	2,07	7,54E-06	GO:0051443~positive regulation of ubiquitin-protein transferase activity,		ICM HGI vs CNTRL	TE HG vs CNTRL and TE HGI vs CNTRL
ENSOCUG00000012132	CHST2	carbohydrate sulfotransferase 2	protein_coding	1,42	2,74E-05	GO:0005975~carbohydrate metabolic process	GO:0006044~N-acetylglucosamine metabolic process	ICM HGI vs CNTRL	
ENSOCUG00000017821	GATA3	GATA binding protein 3	protein_coding	1,05	2,41E-02	GO:0000122~negative regulation of transcription from RNA polymerase II promoter	GO:0001701~in utero embryonic development		
ENSOCUG00000025948	RPS6KA3	ribosomal protein S6 kinase A3	protein_coding	1,04	1,65E-04	GO:0001501~skeletal system development	GO:0002224~toll-like receptor signaling pathway	ICM HI vs CNTRL and ICM HGI vs CNTRL	
ENSOCUG00000002770	FAM3D	family with sequence similarity 3 member D	protein_coding	0,96	8,27E-04	GO:0046676~negative regulation of insulin secretion		ICM HGI vs CNTRL	TE HG vs CNTRL
ENSOCUG00000014919	SNX12	sorting nexin 12	protein_coding	0,95	1,25E-02	GO:0010629~negative regulation of gene expression	GO:0010955~negative regulation of protein processing	ICM HGI vs CNTRL	
ENSOCUG00000022246	SYDE2	synapse defective Rho GTPase homolog 2	protein_coding	0,82	3,97E-03	GO:0007165~signal transduction	GO:0043087~regulation of GTPase activity		
ENSOCUG00000017608	PTBP2	polypyrimidine tract binding protein 2	protein_coding	0,80	3,59E-02	GO:0006376~mRNA splice site selection	GO:0006397~mRNA processing	ICM HGI vs CNTRL	
ENSOCUG00000025017			protein_coding	0,76	2,79E-02			ICM HGI vs CNTRL	
ENSOCUG00000012516	LIN54	lin-54 DREAM MuvB core complex component	protein_coding	0,65	1,85E-02	GO:0006351~transcription DNA-templated	GO:0006355~regulation of transcription DNA-templated		
ENSOCUG00000014647	USP15	ubiquitin specific peptidase 15	protein_coding	0,53	1,17E-02	GO:0006511~ubiquitin-dependent protein catabolic process	GO:0007179~transforming growth factor beta receptor signaling pathway	ICM HGI vs CNTRL	
ENSOCUG00000000348	GPLD1	glycosylphosphatidylinositol specific phospholipase D1	protein_coding	0,51	3,87E-02	GO:0001503~ossification	GO:0002042~cell migration involved in sprouting angiogenesis		

ENSOCUG00000007924	DUSP12	dual specificity phosphatase 12	protein_coding	0,49	4,84E-02	GO:0006464~cellular protein modification process	GO:0016311~dephosphorylation		
ENSOCUG00000010385			pseudogene	0,46	4,34E-02				
ENSOCUG00000021494	FH	fumarate hydratase	protein_coding	0,45	4,80E-02	GO:0006099~tricarboxylic acid cycle	GO:0006106~fumarate metabolic process		
ENSOCUG00000015783	CDKN2AIPNL	CDKN2A interacting protein N-terminal like	protein_coding	0,44	4,60E-02	GO:0006355~regulation of transcription, DNA-templated	GO:0007165~signal transduction	ICM HGI vs CNTRL	
ENSOCUG00000013581	GGPS1	geranylgeranyl diphosphate synthase 1	protein_coding	0,43	3,86E-02	GO:0006695~cholesterol biosynthetic process	GO:0006720~isoprenoid metabolic process	ICM HGI vs CNTRL	
ENSOCUG00000013200	FKBP1A	FK506 binding protein 1A	protein_coding	0,43	1,45E-02	GO:0000413~protein peptidyl-prolyl isomerization	GO:0001933~negative regulation of protein phosphorylation		
ENSOCUG00000012946	KDM5A	lysine demethylase 5A	protein_coding	-0,35	4,26E-02	GO:0000122~negative regulation of transcription from RNA polymerase II promoter	GO:0006366~transcription from RNA polymerase II promoter	ICM HGI vs CNTRL	
ENSOCUG00000016501	SEC61A1	Sec61 translocon alpha 1 subunit	protein_coding	-0,47	1,68E-02	GO:0006614~SRP-dependent cotranslational protein targeting to membrane	GO:0006620~posttranslational protein targeting to membrane	ICM HGI vs CNTRL	
ENSOCUG00000011763	MCOLN1	mucolipin 1	protein_coding	-0,56	2,79E-02	GO:0006812~cation transport	GO:0033572~transferrin transport		
ENSOCUG00000015620	APC	APC, WNT signaling pathway regulator	protein_coding	-0,67	4,22E-02	GO:0000281~mitotic cytokinesis	GO:0001708~cell fate specification	ICM HGI vs CNTRL	
ENSOCUG00000035140			protein_coding	-0,68	3,87E-02			ICM HI vs CNTRL and ICM HGI vs CNTRL	
ENSOCUG00000025569	CCR7	C-C motif chemokine receptor 7	protein_coding	-0,70	4,22E-02	GO:0001768~establishment of T cell polarity	GO:0001954~positive regulation of cell-matrix adhesion		
ENSOCUG00000016165	STK38	serine/threonine kinase 38	protein_coding	-0,71	1,17E-02	GO:0006464~cellular protein modification process	GO:0006468~protein phosphorylation		
ENSOCUG00000022005	ICE1	interactor of little elongation complex ELL subunit 1	protein_coding	-0,73	1,26E-02	GO:0031334~positive regulation of protein complex assembly	GO:0042795~snRNA transcription from RNA polymerase II promoter	ICM HI vs CNTRL	
ENSOCUG00000013580	MOV10L1	Mov10 RISC complex RNA helicase like 1	protein_coding	-1,26	3,70E-02	GO:0007141~male meiosis I	GO:0007275~multicellular organism development		TE HG vs CNTRL
ENSOCUG00000016929	APBB1	amyloid beta precursor protein binding family B member 1	protein_coding	-1,44	4,84E-02	GO:0006302~double-strand break repair	GO:0006351~transcription, DNA-templated	ICM HI vs CNTRL	
ENSOCUG00000005770	MFSD13A		protein_coding	-1,73	4,15E-02				
ENSOCUG00000022794	F2R	coagulation factor II thrombin receptor	protein_coding	-1,78	4,22E-02	GO:0000186~activation of MAPKK activity	GO:0002248~connective tissue replacement involved in inflammatory response wound healing		
ENSOCUG00000021735	ITGA7	integrin subunit alpha 7	protein_coding	-2,15	3,86E-02	GO:0007155~cell adhesion	GO:0007160~cell-matrix adhesion		
ENSOCUG00000000793	CHP2	calcineurin like EF-hand protein 2	protein_coding	-2,30	4,84E-02	GO:0008284~positive regulation of cell proliferation	GO:0010922~positive regulation of phosphatase activity		
ENSOCUG00000032142			protein_coding	-2,62	4,22E-02				
ENSOCUG00000014011	GRIP1	glutamate receptor interacting protein 1	protein_coding	-4,15	8,32E-04	GO:0008104~protein localization	GO:0016358~dendrite development		
ENSOCUG00000026960	U2		snRNA	-4,15	4,26E-02				TE HG vs CNTRL

Appendix 6: Differentially expressed genes (DEGs) in trophectoderm (TE) of embryos developed with high glucose (HG) versus control (CNTRL).

Geneid	Gene symbol	Gene name	Gene type	Log_2FC	adj *P* value	Gene Ontology Biological Process Term 1	Gene Ontology Biological Process Term 2	DEG shared between ICM comparisons to CNTRL	DEG shared between TE comparisons to CNTRL
ENSOCUG00000008772	FANK1		protein_coding	6,57	4,07E-02				
ENSOCUG00000007730	LAD1	ladinin 1	protein_coding	5,33	2,43E-02	GO:0098609~cell-cell adhesion			
ENSOCUG00000029602	PNLIP	pancreatic lipase	protein_coding	4,39	6,23E-03	GO:0001523~retinoid metabolic process	GO:0016042~lipid catabolic process		TE HI vs CNTRL and TE HGI and CNTRL
ENSOCUG00000016684	SLC25A15	solute carrier family 25 member 15	protein_coding	2,90	1,46E-02	GO:0000050~urea cycle	GO:0000066~mitochondrial ornithine transport		
ENSOCUG00000003010	TXNIP	thioredoxin interacting protein	protein_coding	2,38	4,27E-09	GO:0000122~negative regulation of transcription from RNA polymerase II promoter	GO:0006351~transcription		TE HGI vs CNTRL
ENSOCUG00000013558	CCDC172		protein_coding	2,07	8,02E-04				
ENSOCUG00000009737	ARRDC4	arrestin domain containing 4	protein_coding	2,02	1,74E-06	GO:0051443~positive regulation of ubiquitin-protein transferase activity,		ICM HG vs CNTRL and ICM HGI vs CNTRL	TE HGI vs CNTRL
ENSOCUG00000010195	ZC2HC1C		protein_coding	2,00	3,73E-02				
ENSOCUG00000006347	FAM117B		protein_coding	1,72	2,50E-02				
ENSOCUG00000024295	TRIB1	tribbles pseudokinase 1	protein_coding	1,67	1,19E-02	GO:0006468~protein phosphorylation	GO:0006469~negative regulation of protein kinase activity		
ENSOCUG00000034448			lncRNA	1,58	5,76E-03				
ENSOCUG00000026893	C1orf115		protein_coding	1,54	1,31E-02				
ENSOCUG00000022701	LOC103351872		protein_coding	1,27	3,08E-02				
ENSOCUG00000012071	GPAT3	glycerol-3-phosphate acyltransferase 3	protein_coding	1,22	1,96E-04	GO:0006654~phosphatidic acid biosynthetic process	GO:0016024~CDP-diacylglycerol biosynthetic process		

ENSOCUG00000016003	KCNK1	potassium two pore domain channel subfamily K member 1	protein_coding	1,20	1,59E-02	GO:0006813~potassium ion transport	GO:0030322~stabilization of membrane potential	
ENSOCUG00000004826	SLC40A1	solute carrier family 40 member 1	protein_coding	1,18	3,08E-02	GO:0002260~lymphocyte homeostasis	GO:0003158~endothelium development	
ENSOCUG00000011041	CASP7	caspase 7	protein_coding	1,13	3,57E-02	GO:0006508~proteolysis	GO:0006915~apoptotic process	
ENSOCUG00000014855	MCU	mitochondrial calcium uniporter	protein_coding	1,08	3,73E-02	GO:0006851~mitochondrial calcium ion transport	GO:0019722~calcium-mediated signaling	
ENSOCUG00000004199	CYP2J1		protein_coding	1,07	1,56E-02			
ENSOCUG00000006634	FAM107B	family with sequence similarity 107 member B	protein_coding	1,07	6,67E-03	GO:0007605~sensory perception of sound		
ENSOCUG00000012518	DSC2	desmocollin 2	protein_coding	1,05	1,05E-06	GO:0007155~cell adhesion	GO:0007156~homophilic cell adhesion via plasma membrane adhesion molecules	TE HGI vs CNTRL
ENSOCUG00000005956	ALDH18A1	aldehyde dehydrogenase 18 family member A1	protein_coding	1,05	4,30E-04	GO:0006536~glutamate metabolic process	GO:0006561~proline biosynthetic process	
ENSOCUG00000013074	WEE1	WEE1 G2 checkpoint kinase	protein_coding	0,97	6,74E-03	GO:0000086~G2/M transition of mitotic cell cycle	GO:0000226~microtubule cytoskeleton organization	TE HGI vs CNTRL
ENSOCUG00000007765	PSAT1	phosphoserine aminotransferase 1	protein_coding	0,96	3,28E-02	GO:0006564~L-serine biosynthetic process	GO:0008615~pyridoxine biosynthetic process	
ENSOCUG00000001142	SNX13	sorting nexin 13	protein_coding	0,95	2,52E-04	GO:0006886~intracellular protein transport	GO:0009968~negative regulation of signal transduction	TE HGI vs CNTRL
ENSOCUG00000017748	SPART		protein_coding	0,94	1,24E-02			
ENSOCUG00000015960	ACO1	aconitase 1	protein_coding	0,93	1,46E-02	GO:0006099~tricarboxylic acid cycle	GO:0006101~citrate metabolic process	

ENSOCUG00000024010	GPCPD1	glycerophosphocholine phosphodiesterase 1	protein_coding	0,88	3,29E-02	GO:0006629~lipid metabolic process	GO:0007519~skeletal muscle tissue development
ENSOCUG00000014223	UVRAG		protein_coding	0,87	6,74E-03		
ENSOCUG00000000466	MIOS	meiosis regulator for oocyte development	protein_coding	0,86	4,87E-02	GO:0032008~positive regulation of TOR signaling	GO:0034198~cellular response to amino acid starvation
ENSOCUG00000005759	PHGDH	phosphoglycerate dehydrogenase	protein_coding	0,85	2,89E-02	GO:0006541~glutamine metabolic process	GO:0006544~glycine metabolic process
ENSOCUG00000008954	GADD45A	growth arrest and DNA damage inducible alpha	protein_coding	0,81	3,30E-02	GO:0000079~regulation of cyclin-dependent protein serine/threonine kinase activity	GO:0000185~activation of MAPKKK activity
ENSOCUG00000014213	CTNND1	catenin delta 1	protein_coding	0,74	1,56E-02	GO:0006351~transcription, DNA-templated	GO:0006355~regulation of transcription
ENSOCUG00000003961	TXNRD1	thioredoxin reductase 1	protein_coding	0,73	4,61E-02	GO:0000302~response to reactive oxygen species	GO:0000305~response to oxygen radical
ENSOCUG00000004001	CNDP2	CNDP dipeptidase 2	protein_coding	0,73	4,86E-02	GO:0000096~sulfur amino acid metabolic process	GO:0006508~proteolysis
ENSOCUG00000011114	CCNJ		protein_coding	0,73	5,85E-03		
ENSOCUG00000010589	FBXO30	F-box protein 30	protein_coding	0,72	6,74E-03	GO:0016567~protein ubiquitination	
ENSOCUG00000009019	ZNF821	zinc finger protein 821	protein_coding	0,68	4,61E-02	GO:0006351~transcription, DNA-templated,	GO:0045944~positive regulation of transcription from RNA polymerase II promoter
ENSOCUG00000012552	SLC10A7	solute carrier family 10 member 7	protein_coding	0,65	9,17E-03	GO:0006814~sodium ion transport	GO:0055085~transmembrane transport
ENSOCUG00000002581	RAD21	RAD21 cohesin complex component	protein_coding	0,61	8,66E-03	GO:0006302~double-strand break repair	GO:0006310~DNA recombination

ENSOCUG0000008180	MAP4K4	mitogen-activated protein kinase kinase kinase kinase 4	protein_coding	0,59	6,67E-03	GO:0006468~protein phosphorylation	GO:0023014~signal transduction by protein phosphorylation	
ENSOCUG0000022971	PDCD6	programmed cell death 6	protein_coding	0,59	4,04E-02	GO:0001525~angiogenesis	GO:0001938~positive regulation of endothelial cell proliferation	
ENSOCUG0000016788	FAM114A2		protein_coding	0,59	1,46E-02			
ENSOCUG0000010587	APP	amyloid beta precursor protein	protein_coding	0,57	4,21E-02	GO:0001878~response to yeast	GO:0001967~suckling behavior	
ENSOCUG0000037023	GINS2	GINS complex subunit 2	protein_coding	0,54	3,08E-02	GO:0000727~double-strand break repair via break-induced replication	GO:0006260~DNA replication	
ENSOCUG0000002770	FAM3D	family with sequence similarity 3 member D	protein_coding	0,54	1,56E-02	GO:0046676~negative regulation of insulin secretion		ICM HG vs CNTRL and ICM HGI vs CNTRL
ENSOCUG0000006697	HK1	hexokinase 1	protein_coding	0,53	2,51E-02	GO:0001678~cellular glucose homeostasis	GO:0006096~glycolytic process	
ENSOCUG0000027508	RTN3	reticulon 3	protein_coding	0,52	4,41E-02	GO:0006915~apoptotic process	GO:0007268~chemical synaptic transmission	
ENSOCUG0000000734	YWHAZ	tyrosine 3-monooxygenase/tryptophan 5-monooxygenase activation protein zeta	protein_coding	0,51	4,17E-02	GO:0006605~protein targeting	GO:0007165~signal transduction	
ENSOCUG0000011891	TLE4	transducin like enhancer of split 4	protein_coding	0,50	3,73E-02	GO:0000122~negative regulation of transcription from RNA polymerase II promoter	GO:0006351~transcription	
ENSOCUG0000014826	CLTB	clathrin light chain B	protein_coding	0,47	5,41E-03	GO:0006886~intracellular protein transport	GO:0016192~vesicle-mediated transport	
ENSOCUG0000016819	NPM3	nucleophosmin/nucleoplasmin 3	protein_coding	0,46	2,43E-02	GO:0006364~rRNA processing	GO:0009303~rRNA transcription	

ENSOCUG0 0000015017	MRPS9	mitochondria l ribosomal protein S9	protein_coding	0,40	3,08E-02	GO:0000462~matu ration of SSU-rRNA from tricistronic rRNA transcript (SSU-rRNA 5.8 rRNA LSU-rRNA)	GO:0006412~tra nslation
ENSOCUG0 0000015866	BPTF	bromodomai n PHD finger transcription factor	protein_coding	-0,42	2,43E-02	GO:0000122~nega tive regulation of transcription from RNA polymerase II promoter	GO:0001892~em bryonic placenta development
ENSOCUG0 0000006746	SRPK2	SRSF protein kinase 2	protein_coding	-0,44	4,32E-02	GO:0000245~splic eosomal complex assembly	GO:0001525~an giogenesis
ENSOCUG0 0000004806	PCNT	pericentrin	protein_coding	-0,45	3,81E-02	GO:0000086~G2/ M transition of mitotic cell cycle	GO:0000226~mic rotubule cytoskeleton organization
ENSOCUG0 0000014835	SMC4	structural maintenance of chromosome s 4	protein_coding	-0,48	4,61E-02	GO:0000070~mito tic sister chromatid segregation	GO:0007076~mit otic chromosome condensation
ENSOCUG0 0000016542	NSD3		protein_coding	-0,54	2,43E-02		
ENSOCUG0 0000021154	EIF5B	eukaryotic translation initiation factor 5B	protein_coding	-0,55	3,93E-02	GO:0006413~trans lational initiation	GO:0006446~reg ulation of translational initiation
ENSOCUG0 0000016828	PRR14L		protein_coding	-0,55	3,14E-02		
ENSOCUG0 0000004640	ZRANB2	zinc finger RANBP2-type containing 2	protein_coding	-0,62	1,36E-03	GO:0006355~regu lation of transcription, DNA template	GO:0006397~mR NA processing
ENSOCUG0 0000013504	C15orf39		protein_coding	-0,69	2,27E-02		
ENSOCUG0 0000003769	MSMO1	methylsterol monooxygen ase 1	protein_coding	-0,71	1,56E-02	GO:0006631~fatty acid metabolic process	GO:0006695~cho lesterol biosynthetic process
ENSOCUG0 0000029385			protein_coding	-0,74	4,61E-02		

ENSOCUG00000009041	BOD1L1	biorientation of chromosomes in cell division 1 like 1	protein_coding	-0,74	4,26E-02	GO:0006281~DNA repair	GO:0006974~cellular response to DNA damage stimulus
ENSOCUG00000030035			pseudogene	-0,77	3,39E-02		
ENSOCUG00000014408	TASOR2		protein_coding	-0,79	8,66E-03		
ENSOCUG00000023782	il11ra	interleukin 11 receptor subunit alpha	protein_coding	-0,81	2,43E-02	GO:0007566~embryo implantation	GO:0019221~cytokine-mediated signaling pathway
ENSOCUG00000029282			protein_coding	-0,82	1,61E-02		
ENSOCUG00000027709			protein_coding	-0,84	4,87E-02		
ENSOCUG00000034985	FAM133B		protein_coding	-0,84	1,29E-03		
ENSOCUG00000029378			protein_coding	-0,85	3,11E-02		
ENSOCUG00000002765	LUC7L3	LUC7 like 3 pre-mRNA splicing factor	protein_coding	-0,86	2,52E-04	GO:0006376~mRNA splice site selection	GO:0008380~RNA splicing
ENSOCUG00000037990			lncRNA	-0,87	7,06E-03		
ENSOCUG00000004591	ZFC3H1	zinc finger C3H1-type containing	protein_coding	-0,88	3,62E-05	GO:0006396~RNA processing	
ENSOCUG00000012457	GOLGB1	golgin B1	protein_coding	-0,90	2,50E-02	GO:0006355~regulation of transcription, DNA-templated	GO:0006888~ER to Golgi vesicle-mediated transport
ENSOCUG00000005707	ATF7	activating transcription factor 7	protein_coding	-0,91	1,61E-02	GO:0000122~negative regulation of transcription from RNA polymerase II promoter	GO:0006351~transcription, DNA-templated
ENSOCUG00000002928	ERC1	ELKS/RAB6-interacting/CAST family member 1	protein_coding	-0,91	3,11E-02	GO:0006355~regulation of transcription, DNA template	GO:0007252~I-kappaB phosphorylation
ENSOCUG00000038951			lncRNA	-0,92	4,88E-02		
ENSOCUG00000007048	KSR1	kinase suppressor of ras 1	protein_coding	-0,95	2,18E-02	GO:0000165~MAPK cascade	GO:0007265~Ras protein signal transduction

ENSOCUG00000000924	PIGW	phosphatidylinositol glycan anchor biosynthesis class W	protein_coding	-0,99	3,73E-02	GO:0006505~GPI anchor metabolic process	GO:0006506~GPI anchor biosynthetic process	
ENSOCUG00000025173	TMCO3	transmembrane and coiled-coil domains 3	protein_coding	-1,01	3,28E-02	GO:1902600~hydrogen ion transmembrane transport		
ENSOCUG00000000806	TTC14		protein_coding	-1,04	2,07E-05			TE HGI vs CNTRL
ENSOCUG00000039327			lncRNA	-1,12	4,88E-02			
ENSOCUG00000007521	ANKRD10	ankyrin repeat domain 10	protein_coding	-1,13	2,66E-02	GO:0060828~regulation of canonical Wnt signaling pathway		
ENSOCUG00000025401	PPP1R35	protein phosphatase 1 regulatory subunit 35	protein_coding	-1,16	3,69E-02	GO:0010923~negative regulation of phosphatase activity		
ENSOCUG00000032049			lncRNA	-1,16	8,66E-03			
ENSOCUG00000022097	SNORD81		snoRNA	-1,17	2,05E-02			
ENSOCUG00000010107	ADA	adenosine deaminase	protein_coding	-1,20	7,59E-03	GO:0001666~response to hypoxia	GO:0001821~histamine secretion	
ENSOCUG00000031783			lncRNA	-1,24	4,40E-03			
ENSOCUG00000029489			lncRNA	-1,25	1,61E-02			
ENSOCUG00000029108	ND4	NADH dehydrogenase, subunit 4	protein_coding	-1,26	4,86E-02	GO:0001666~response to hypoxia	GO:0001701~in utero embryonic development	
ENSOCUG00000013854	CEP85L		protein_coding	-1,28	1,31E-02			
ENSOCUG00000033607			lncRNA	-1,30	4,64E-03			
ENSOCUG00000029084			Mt_rRNA	-1,30	5,71E-03			
ENSOCUG00000011856	AGRP	agouti related neuropeptide	protein_coding	-1,36	2,89E-02	GO:0007218~neuropeptide signaling pathway	GO:0007623~circadian rhythm	
ENSOCUG00000025249	TRADD	TNFRSF1A associated via death domain	protein_coding	-1,37	8,66E-03	GO:0006915~apoptotic process	GO:0006919~activation of cysteine-type endopeptidase activity involved in apoptotic process	

ENSOCUG00000032429			protein_coding	-1,39	1,29E-03				
ENSOCUG00000000651	LDLR	low density lipoprotein receptor	protein_coding	-1,40	2,51E-02	GO:0006629~lipid metabolic process	GO:0006897~endocytosis		
ENSOCUG00000029090	ND2	MTND2	protein_coding	-1,41	1,31E-02	GO:0006120~mitochondrial electron transport, NADH to ubiquinone	GO:0032981~mitochondrial respiratory chain complex I assembly		
ENSOCUG00000032540			protein_coding	-1,42	3,20E-02				
ENSOCUG00000029112	ND5	NADH dehydrogenase, subunit 5	protein_coding	-1,43	6,67E-03	GO:0001666~response to hypoxia	GO:0006120~mitochondrial electron transport		
ENSOCUG00000029144	ZNF260	zinc finger protein 260	protein_coding	-1,47	7,99E-04	GO:0006351~transcription, DNA-templated	GO:0006355~regulation of transcription, DNA-templated,		TE HGI vs CNTRL
ENSOCUG00000033708			protein_coding	-1,48	1,02E-02				
ENSOCUG00000013476	AACS	acetoacetyl-CoA synthetase	protein_coding	-1,48	3,63E-03	GO:0001889~liver development	GO:0006629~lipid metabolic process		
ENSOCUG00000006589	RESF1		protein_coding	-1,49	9,48E-03				
ENSOCUG00000017794	TULP2	tubby like protein 2	protein_coding	-1,53	4,81E-02	GO:0007601~visual perception	GO:0097500~receptor localization to nonmotile primary cilium		
ENSOCUG00000013580	MOV10L1	Mov10 RISC complex RNA helicase like 1	protein_coding	-1,57	1,56E-02	GO:0007141~male meiosis I	GO:0007275~multicellular organism development	ICM HG vs CNTRL	
ENSOCUG00000032024			lncRNA	-1,57	2,52E-04				
ENSOCUG00000029051	LOC103346187		protein_coding	-1,60	1,56E-02				
ENSOCUG00000036373			lncRNA	-1,60	9,71E-04				
ENSOCUG00000010163	ACSBG2	acyl-CoA synthetase bubblegum family member 2	protein_coding	-1,62	1,29E-03	GO:0001676~long-chain fatty acid metabolic process	GO:0006631~fatty acid metabolic process		
ENSOCUG00000031581			protein_coding	-1,71	1,56E-02				
ENSOCUG00000021686	LOC100339134		protein_coding	-1,72	4,30E-02				
ENSOCUG00000025334	LENG8	Leukocyte Receptor Cluster Member 8	protein_coding	-1,80	3,96E-03			ICM HGI vs CNTRL	

ENSOCUG00000001117	CDKL4	cyclin dependent kinase like 4	protein_coding	-1,82	1,31E-02	GO:0006468~protein phosphorylation	GO:0051726~regulation of cell cycle		
ENSOCUG00000026713	5_8S_rRNA		rRNA	-2,20	4,49E-08				
ENSOCUG00000014777	PADI2	peptidyl arginine deiminase 2	protein_coding	-2,25	8,02E-04	GO:0006325~chromatin organization	GO:0010848~regulation of chromatin disassembly		TE HGI vs CNTRL
ENSOCUG00000034529			rRNA	-2,31	3,54E-04				
ENSOCUG00000026960	U2		snRNA	-2,41	4,61E-02			ICM HG vs CNTRL	
ENSOCUG00000008452	FSTL4	follistatin like 4	protein_coding	-2,47	1,29E-03	GO:0031549~negative regulation of brain-derived neurotrophic factor receptor signaling pathway	GO:0048671~negative regulation of collateral sprouting		
ENSOCUG00000036803	TMEM132B		protein_coding	-2,51	1,36E-03				
ENSOCUG00000030457			lncRNA	-2,53	2,18E-02				
ENSOCUG00000009424	LAMA1	laminin subunit alpha 1	protein_coding	-2,72	1,52E-02	GO:0007155~cell adhesion	GO:0007166~cell surface receptor signaling pathway		
ENSOCUG00000000249	SMARCD3	SWI/SNF related, matrix associated, actin dependent regulator of chromatin, subfamily d, member 3	protein_coding	-3,00	1,99E-03	GO:0002052~positive regulation of neuroblast proliferation	GO:0003139~secondary heart field specification		
ENSOCUG00000003112	STRC	stereocilin	protein_coding	-3,18	2,06E-02	GO:0007160~cell-matrix adhesion	GO:0007605~sensory perception of sound		
ENSOCUG00000012232	KIRREL1		protein_coding	-3,21	7,30E-03				
ENSOCUG00000023301			protein_coding	-3,98	7,02E-05				
ENSOCUG00000035685			lncRNA	-4,28	3,81E-02				
ENSOCUG00000018288			snoRNA	-4,41	2,31E-02				
ENSOCUG00000006022	MINDY4		protein_coding	-5,43	9,71E-04				
ENSOCUG00000003142	AR	androgen receptor	protein_coding	-6,85	3,08E-02	GO:0001701~in utero embryonic development	GO:0003073~regulation of systemic arterial blood pressure		

Appendix 7: Differentially expressed genes (DEGs) in inner cell mass (ICM) of embryos developed with high glucose and high insulin (HGI) versus control (CNTRL).

Geneid	Gene symbol	Gene name	Gene type	Log_2FC	adj *P* value	Gene Ontology Biological Process Term 1	Gene Ontology Biological Process Term 2	DEG shared between ICM comparisons to CNTRL	DEG shared between TE comparisons to CNTRL
ENSOCUG00000009737	ARRDC4	arrestin domain containing 4	protein_coding	2,09	5,50E-06	GO:0051443~positive regulation of ubiquitin-protein transferase activity		ICM HG vs CNTRL	TE HG vs CNTRL and TE HGI vs CNTRL
ENSOCUG00000023725	RGN	regucalcin	protein_coding	1,98	3,09E-02	GO:0001822~kidney development	GO:0006469~negative regulation of protein kinase activity	ICM HG vs CNTRL	
ENSOCUG00000009672	PLET1	placenta expressed transcript 1	protein_coding	1,98	2,82E-02	GO:0001953~negative regulation of cell-matrix adhesion	GO:0030154~cell differentiation	ICM HG vs CNTRL	
ENSOCUG00000027535	PEG10	paternally expressed 10	protein_coding	1,80	2,89E-02	GO:0001890~placenta development	GO:0006915~apoptotic process		
ENSOCUG00000014919	SNX12	sorting nexin 12	protein_coding	1,22	5,50E-05	GO:0010629~negative regulation of gene expression	GO:0010955~negative regulation of protein processing	ICM HG vs CNTRL	
ENSOCUG00000014568	MTMR2	myotubularin related protein 2	protein_coding	1,21	5,22E-03	GO:0002091~negative regulation of receptor internalization,	GO:0006470~protein dephosphorylation		
ENSOCUG00000012132	CHST2	carbohydrate sulfotransferase 2	protein_coding	0,98	2,82E-02	GO:0005975~carbohydrate metabolic process	GO:0006044~N-acetylglucosamine metabolic process	ICM HG vs CNTRL	
ENSOCUG00000017608	PTBP2	polypyrimidine tract binding protein 2	protein_coding	0,96	2,20E-03	GO:0006376~mRNA splice site selection	GO:0006397~mRNA processing	ICM HG vs CNTRL	
ENSOCUG00000022135	NME1	NME/NM23 nucleoside diphosphate kinase 1	protein_coding	0,90	4,28E-02	GO:0002762~negative regulation of myeloid leukocyte differentiation	GO:0006163~purine nucleotide metabolic process		
ENSOCUG00000002770	FAM3D	family with sequence similarity 3 member D	protein_coding	0,87	4,02E-03	GO:0046676~negative regulation of insulin secretion		ICM HG vs CNTRL	TE HG vs CNTRL
ENSOCUG00000025017			protein_coding	0,84	5,22E-03			ICM HG vs CNTRL	
ENSOCUG00000025948	RPS6KA3	ribosomal protein S6 kinase A3	protein_coding	0,77	2,82E-02	GO:0001501~skeletal system development	GO:0002224~toll-like receptor signaling pathway	ICM HI vs CNTRL and ICM HG vs CNTRL	
ENSOCUG00000003711	ELF2	E74 like ETS transcription factor 2	protein_coding	0,71	3,07E-03	GO:0006351~transcription, DNA-templated	GO:0006357~regulation of transcription from RNA polymerase II promoter		
ENSOCUG00000003228	CLK4	CDC like kinase 4	protein_coding	0,61	4,50E-02	GO:0018108~peptidyl-tyrosine phosphorylation,	GO:0043484~regulation of RNA splicing		

ENSOCUG00000015783	CDKN2AIPNL	CDKN2A interacting protein N-terminal like	protein_coding	0,53	3,07E-03	GO:0006355~regulation of transcription, DNA-templated	GO:0007165~signal transduction	ICM HG vs CNTRL	
ENSOCUG00000023095	TRMT13	tRNA methyltransferase 13 homolog	protein_coding	0,52	2,82E-02	GO:0030488~tRNA methylation			
ENSOCUG00000014647	USP15	ubiquitin specific peptidase 15	protein_coding	0,47	3,17E-02	GO:0006511~ubiquitin-dependent protein catabolic process	GO:0007179~transforming growth factor beta receptor signaling pathway	ICM HG vs CNTRL	
ENSOCUG00000013581	GGPS1	geranylgeranyl diphosphate synthase 1	protein_coding	0,45	1,60E-02	GO:0006695~cholesterol biosynthetic process	GO:0006720~isoprenoid metabolic process	ICM HG vs CNTRL	
ENSOCUG00000008020	EYA3	EYA transcriptional coactivator and phosphatase 3	protein_coding	0,40	2,82E-02	GO:0006302~double-strand break repair	GO:0006351~transcription, DNA-templated		
ENSOCUG00000012446			protein_coding	0,34	4,96E-02				
ENSOCUG00000012946	KDM5A	lysine demethylase 5A	protein_coding	-0,35	3,84E-02	GO:0000122~negative regulation of transcription from RNA polymerase II promoter	GO:0006366~transcription from RNA polymerase II promoter	ICM HG vs CNTRL	
ENSOCUG00000021131	SMUG1	single-strand-selective monofunctional uracil-DNA glycosylase 1	protein_coding	-0,46	2,82E-02	GO:0006284~base-excision repair	GO:0045008~depyrimidination,		
ENSOCUG00000003178	SREBF2	sterol regulatory element binding transcription factor 2	protein_coding	-0,49	4,01E-02	GO:0000122~negative regulation of transcription from RNA polymerase II promoter,	GO:0006351~transcription, DNA-templated,		
ENSOCUG00000016501	SEC61A1	Sec61 translocon alpha 1 subunit	protein_coding	-0,53	2,26E-03	GO:0006614~SRP-dependent cotranslational protein targeting to membrane	GO:0006620~post translational protein targeting to membrane	ICM HG vs CNTRL	
ENSOCUG00000013941	CEP250	centrosomal protein 250	protein_coding	-0,64	3,09E-02	GO:0000086~G2/M transition of mitotic cell cycle	GO:0000278~mitotic cell cycle		
ENSOCUG00000015620	APC	APC, WNT signaling pathway regulator	protein_coding	-0,74	1,10E-02	GO:0000281~mitotic cytokinesis	GO:0001708~cell fate specification	ICM HG vs CNTRL	
ENSOCUG00000035140			protein_coding	-0,83	2,20E-03			ICM HI vs CNTRL and ICM HG vs CNTRL	
ENSOCUG00000010743	BICD2	BICD cargo adaptor 2	protein_coding	-0,88	1,37E-02	GO:0000042~protein targeting to Golgi	GO:0006890~retrograde vesicle-mediated transport, Golgi to ER		
ENSOCUG00000012438	NBEAL2	neurobeachin like 2	protein_coding	-0,93	3,02E-02	GO:0030220~platelet formation,			
ENSOCUG00000001592	SAFB2	scaffold attachment factor B2	protein_coding	-0,94	5,29E-03	GO:0006351~transcription, DNA-templated	GO:0006357~regulation of transcription from RNA polymerase II promoter,		
ENSOCUG00000025334	LENG8	Leukocyte Receptor Cluster Member 8	protein_coding	-1,09	2,47E-02				TE HG vs CNTRL

ENSOCUG00000007384	RNF17	ring finger protein 17	protein_coding	-1,16	2,20E-03	GO:0007275~multicellular organism development,	GO:0007286~spermatid development,
ENSOCUG00000015669	ARAP2	ArfGAP with RhoGAP domain, ankyrin repeat and PH domain 2	protein_coding	-1,39	1,94E-02	GO:0007165~signal transduction,	GO:0043547~positive regulation of GTPase activity
ENSOCUG00000008235	TSHZ1	teashirt zinc finger homeobox 1	protein_coding	-1,43	7,74E-03	GO:0000122~negative regulation of transcription from RNA polymerase II promoter	GO:0006351~transcription, DNA-templated
ENSOCUG00000004015	ZNF407	zinc finger protein 407	protein_coding	-1,46	8,63E-03	GO:0006351~transcription, DNA-templated,	GO:0006355~regulation of transcription, DNA-templated,
ENSOCUG00000000017	LIPE	lipase E, hormone sensitive type	protein_coding	-1,51	5,22E-03	GO:0006468~protein phosphorylation,	GO:0008152~metabolic process
ENSOCUG00000038768			lncRNA	-1,53	1,94E-02		
ENSOCUG00000022392	PIGZ	phosphatidylinositol glycan anchor biosynthesis class Z	protein_coding	-3,21	5,22E-03	GO:0006506~GPI anchor biosynthetic process	GO:0097502~mannosylation,
ENSOCUG00000029203	ZFP37	ZFP37 zinc finger protein	protein_coding	-6,08	2,04E-03	GO:0006351~transcription, DNA-templated	GO:0006355~regulation of transcription, DNA-templated,

Appendix 8: Differentially expressed genes (DEGs) in trophectoderm (TE) of embryos developed with high glucose and high insulin (HGI) versus control (CNTRL).

Geneid	Gene symbol	Gene name	Gene type	Log_2FC	adj *P* value	Gene Ontology Biological Process Term 1	Gene Ontology Biological Process Term 2	DEG shared between ICM comparisons to CNTRL	DEG shared between TE comparisons to CNTRL
ENSOCUG00000029602	PNLIP	pancreatic lipase	protein_coding	4,71	7,08E-03	GO:0001523~retinoid metabolic process	GO:0016042~lipid catabolic process		TE HI vs CNTRL and TE HG vs CNTRL
ENSOCUG00000025532			protein_coding	4,63	1,03E-02				
ENSOCUG00000003010	TXNIP	thioredoxin interacting protein	protein_coding	1,81	2,78E-04	GO:0000122~negative regulation of transcription from RNA polymerase II promoter	GO:0006351~transcription		TE HG vs CNTRL
ENSOCUG00000009737	ARRDC4	arrestin domain containing 4	protein_coding	1,37	3,36E-02	GO:0051443~positive regulation of ubiquitin-protein transferase activity,		ICM HG vs CNTRL and ICM HGI vs CNTRL	TE HG vs CNTRL
ENSOCUG00000001142	SNX13	sorting nexin 13	protein_coding	0,93	1,18E-03	GO:0006886~intracellular protein transport	GO:0009968~negative regulation of signal transduction		TE HG vs CNTRL
ENSOCUG00000013074	WEE1	WEE1 G2 checkpoint kinase	protein_coding	0,92	4,54E-02	GO:0000086~G2/M transition of mitotic cell cycle	GO:0000226~microtubule cytoskeleton organization		TE HG vs CNTRL
ENSOCUG00000012518	DSC2	desmocollin 2	protein_coding	0,84	1,18E-03	GO:0007155~cell adhesion	GO:0007156~homophilic cell adhesion via plasma membrane adhesion molecules		TE HG vs CNTRL
ENSOCUG00000014912	ANKRD49	ankyrin repeat domain 49	protein_coding	0,61	1,57E-02	GO:0007283~spermatogenesis	GO:0030154~cell differentiation		
ENSOCUG00000002187	TUBB	tubulin beta class I	protein_coding	0,50	3,36E-02	GO:0000086~G2/M transition of mitotic cell cycle	GO:0006928~movement of cell or subcellular component		
ENSOCUG00000008111	LRRC42		protein_coding	0,46	4,54E-02				
ENSOCUG00000016799	CYB5R1	cytochrome b5 reductase 1	protein_coding	-0,79	3,36E-02	GO:0002576~platelet degranulation	GO:0015701~bicarbonate transport		
ENSOCUG00000000806	TTC14		protein_coding	-0,85	6,22E-03				TE HG vs CNTRL
ENSOCUG00000000446	BCAT2	branched chain amino acid transaminase 2	protein_coding	-1,03	1,03E-02	GO:0006532~aspartate biosynthetic process	GO:0006550~isoleucine catabolic process		
ENSOCUG00000029144	ZNF260	zinc finger protein 260	protein_coding	-1,20	4,81E-02	GO:0006351~transcription, DNA-templated	GO:0006355~regulation of transcription, DNA-templated,		TE HG vs CNTRL
ENSOCUG00000008127	CALD1	caldesmon 1	protein_coding	-1,70	1,26E-02	GO:0006928~movement of cell or subcellular component	GO:0006936~muscle contraction		
ENSOCUG00000014777	PADI2	peptidyl arginine deiminase 2	protein_coding	-2,47	4,87E-04	GO:0006325~chromatin organization	GO:0010848~regulation of chromatin disassembly		TE HG vs CNTRL

Appendix 9: ICM and TE samples from *in vitro*-developed blastocysts for TEST ATAC-seq library generation.

Three samples were included for each lineage. For ICM samples, samples corresponded to dissociation strategies. For TE, three biological replicates were included.

Lineage	Condition or biological replicate	*n* pool	Concentrarion (nM)
ICM	Trypsin 1 min 30s	16	5.3
	TryPLE	16	5.4
	Trypsin 1 min	16	4.8
TE	1	18	6.5
	2	12	7.5
	3	18	15.1

Appendix 10: ICM and TE ATAC-seq TEST dataset for sequencing assay.

Raw reads, percentage of aligned reads (including mitochondrial DNA) and final informative reads (excluding duplicate reads, mitochondrial DNA, low quality reads) from ATAC-seq datasets.

Sample	Condition	Reads after trimming	Aligned reads (%)	Final informative reads
ICM	Trypsin 1min 30s	74729067	95.53%	6129550
ICM	TryPLE	61838368	96.45%	22080465
ICM	Trypsin 1 min	103464906	96.18%	24254126
TE	pool 1	84066395	96.85%	13178690
TE	pool 2	83363578	96.12%	7558850
TE	pool 3	79548110	96.21%	15961446

Appendix 11: ICM and TE samples from *in vitro*-developed blastocysts with CNTRL, HG or HGI for ATAC-seq library generation.

Three biological replicates were included for each experimental condition. Embryos from two *in vitro* culture session were distributed in at least CNTRL and HG experimental conditions. Pool between 13-26 ICM and TE were used for ATAC-seq library preparation. CNTRL, control; HG, high glucose; HGI, high glucose and high insulin.

Condition	Biological replicate	*In vitro* culture	*n* pool	ICM libraries (nM)	TE libraries (nM)
CNTRL	**1**	IVC-1	15	19.2	17.4
	2	IVC-1	26	13.4	9.8
	3	IVC-2	19	28.0	5.6
HG	**1**	IVC-1	15	13.1	7.8
	2	IVC-2	15	18.2	19.1
	3	IVC-2	15	13.7	10.5
HGI	**1**	IVC-3	13	7.0	8.4
	2	IVC-4	16	13.9	6.6
	3	IVC-5	14	7.8	12.1

Appendix 12: ICM and TE ATAC-seq dataset from embryos exposed to CNTRL, HG or HGI.

Raw reads, percentage of aligned reads (including mitochondrial DNA) and final informative reads (excluding duplicate reads, mitochondrial DNA, low quality reads) from eighteen ICM and TE ATAC-seq datasets from exposed embryos.

Sample	Condition	Biological replicate	Reads after trimming	Aligned reads (%)	Final informative reads
ICM	CNTRL	1	145821805	98.06%	40994553
		2	158379744	97.66%	32178616
		3	190491043	98.12%	44049620
TE	CNTRL	1	149441589	97.34%	52324339
		2	122640251	98.02%	53279895
		3	123972185	96.76%	23379204
ICM	HG	1	185246654	96.52%	47360653
		2	134916380	90.05%	36277037
		3	153522964	96.79%	39990290
TE	HG	1	159731917	97.47%	70152491
		2	147754313	97.35%	53389051
		3	134082794	96.78%	32128013
ICM	HGI	1	114809049	95.26%	26527095
		2	155360782	94.41%	35161650
		3	138064720	95.94%	29610163
TE	HGI	1	134740200	97.09%	46908442
		2	178782150	95.29%	37125472
		3	140454959	96.38%	45294381

Appendix 13: List of genes and its functional annotation (GO biological process) whose promoters were identified between differentially accessible regions (DARs) in HG ICM compared to CNTRL ICM.

Comparison	Condition	Gene symbol	Gene Name	GO BP term 1	GO BP term 2	GO BP term 3
HGvsCNTRL	Acessible in HG ICM	No official gene symbol	Ras-GEF domain-containing protein	GO:0007264~small GTPase mediated signal transduction		
		CLCN6	chloride voltage-gated channel 6	GO:0006821~chloride transport		
		DERA	deoxyribose-phosphate aldolase	GO:0009264~deoxyribonucleotide catabolic process	GO:0046121~deoxyribonucleoside catabolic process	GO:0046386~deoxyribose phosphate catabolic process
		SCFD2	sec1 family domain containing 2	GO:0016192~vesicle-mediated transport		
		SLIT3	slit guidance ligand 3	GO:0007399~nervous system development		

Appendix 14: List of genes and its functional annotation (GO biological process) whose promoters were identified between differentially accessible regions (DARs) in HG TE compared to CNTRL TE.

Comparison	Condition	Gene symbol	Gene Name	GO BP term 1	GO BP term 2	GO BP term 3
HGvsCNTRL	**Accessible in HG TE**	CENPU	centromere protein U	GO:0000775~chromosome, centromeric region	GO:0005634~nucleus	
HGvsCNTRL	**Accessible in CNTRL TE**	No official gene symbol	PseudoU_synth_2 domain-containing protein	GO:0001522~pseudouridine synthesis		

Appendix 15: List of genes and its functional annotation (GO biological process) whose promoters were identified between differentially accessible regions (DARs) in HGI ICM compared to CNTRL ICM.

Comparison	Condition	Gene symbol	Gene Name	GO BP term 1	GO BP term 2	GO BP term 3
HGIvsCNTRL	Acessible in HGI ICM	POC5	POC5 centriolar protein	GO:0007049~cell cycle		
		No official gene symbol	Ras-GEF domain-containing protein	GO:0007264~small GTPase mediated signal transduction		
		SOX1	SRY-box transcription factor 1	GO:0006355~regulation of transcription, DNA-templated	GO:0007399~nervous system development	
		MYO3B	myosin IIIB	GO:0007601~visual perception	GO:0050896~response to stimulus	
		PRKCB	protein kinase C beta	GO:0002250~adaptive immune response	GO:0006357~regulation of transcription from RNA polymerase II promoter	GO:0006915~apoptotic process
		SAMD8	sterile alpha motif domain containing 8	GO:0006665~sphingolipid metabolic process		
		ZC3HAV1	zinc finger CCCH-type containing, antiviral 1	GO:0009615~response to virus	GO:0045071~negative regulation of viral genome replication	GO:0061014~positive regulation of mRNA catabolic process
HGIvsCNTRL	Acessible in CNTRL ICM	BABAM2	BRISC and BRCA1 A complex member 2	GO:0006302~double-strand break repair	GO:0006325~chromatin organization	GO:0006915~apoptotic process
		GSR	glutathione-disulfide reductase	GO:0006749~glutathione metabolic process	GO:0045454~cell redox homeostasis	
		WHRN	whirlin	GO:0001895~retina homeostasis	GO:0007605~sensory perception of sound	GO:0010628~positive regulation of gene expression

Appendix 16: List of genes and its functional annotation (GO biological process) whose promoters were identified between differentially accessible regions (DARs) in HGI TE compared to CNTRL TE.

Comparison	Condition	Gene symbol	Gene Name	GO BP term 1	GO BP term 2	GO BP term 3
HGIvsCNTRL	Acessible in HGI TE	No official gene symbol	Uncharacterized protein	GO:0006355~regulation of transcription, DNA-templated		
		No official gene symbol	Uncharacterized protein	GO:0006355~regulation of transcription, DNA-templated		
		BRD2	bromodomain containing 2	GO:0001843~neural tube closure	GO:0006334~nucleosome assembly	GO:0006357~regulation of transcription from RNA polymerase II promoter
		RFC4	replication factor C subunit 4	GO:0006260~DNA replication	GO:1900264~positive regulation of DNA-directed DNA polymerase activity	
		RETREG1	reticulophagy regulator 1	GO:0000423~macromitophagy	GO:0019233~sensory perception of pain	GO:0043524~negative regulation of neuron apoptotic process
		UFM1	ubiquitin fold modifier 1	GO:0071569~protein ufmylation		

		No official gene symbol	ATP synthase mitochondrial F1 complex assembly factor 2	GO:0043461~proton-transporting ATP synthase complex		
		POC5	POC5 centriolar protein	GO:0007049~cell cycle		
		No official gene symbol	Uncharacterized protein	GO:0006355~regulation of transcription, DNA-templated		
		ASIC2	acid sensing ion channel subunit 2	GO:0003026~regulation of systemic arterial blood pressure by aortic arch baroreceptor	GO:0007602~phototransduction	GO:0007605~sensory perception of sound
		DYNC2I1	dynein 2 intermediate chain 1	GO:0035721~intraciliary retrograde transport	GO:0048704~embryonic skeletal system morphogenesis	GO:0060271~cilium assembly
HGIvsCNTRL	**Acessible regions CNTRL TE**	No official gene symbol	high mobility group protein B2 pseudogene	GO:0045087~innate immune response		
		HOXC8	homeobox C8	GO:0000122~negative regulation of transcription from RNA polymerase Ⅱ	GO:0009952~anterior/posterior pattern specification	GO:0030182~neuron differentiation
		HTT	huntingtin	GO:0000132~establishment of mitotic spindle orientation	GO:0006890~retrograde vesicle-mediated transport, Golgi to ER	GO:0007030~Golgi organization
		LPCAT2	lysophosphatidylcholine acyltransferase 2	GO:0006663~platelet activating factor biosynthetic	GO:0036151~phosphatidylcholine acyl-chain remodeling	GO:0061024~membrane organization
		PARD3	par-3 family cell polarity regulator	GO:0007049~cell cycle	GO:0051301~cell division	
		THBS4	thrombospondin 4	GO:0001938~positive regulation of endothelial cell proliferation	GO:0007155~cell adhesion	GO:0016525~negative regulation of angiogenesis

Appendix 17: HOMER protein-binding motifs enrichment analysis from intergenic regions identified between differentially accessible regions (DARs) in ICM and TE of embryos exposed to HG or HGI.

Comparison	Condition	Motif Name	P-value	q-value (Benjamini)
HGvsCNTRL	Acessible in HG ICM	PAX5(Paired,Homeobox),condensed/GM12878-PAX5-ChIP-Seq(GSE32465)/Homer	1,00E-02	1.0000
		CTCF-SatelliteElement(Zf?)/CD4+CTCF-ChIP-Seq(Barski_et_al.)/Homer	1,00E-02	1.0000
HGvsCNTRL	Accessible in HG TE	CUX1(Homeobox)/K562-CUX1-ChIP-Seq(GSE92882)/Homer	1,00E-03	0.1673
		ZNF143|STAF(Zf)/CUTLL-ZNF143-ChIP-Seq(GSE29600)/Homer	1,00E-03	0.1673
		IRF1(IRF)/PBMC-IRF1-ChIP-	1,00E-03	0.2689
		PRDM10(Zf)/HEK293-PRDM10.eGFP-ChIP-Seq(Encode)/Homer	1,00E-02	0.6791
		AGL95(ND)/col-AGL95-DAP-	1,00E-02	0.9230
HGIvsCNTRL	Acessible in HGI ICM	Rfx1(HTH)/NPC-H3K4me1-ChIP-Seq(GSE16256)/Homer	1,00E-03	0.3396
		PSE(SNAPc)/K562-mStart-Seq/Homer	1,00E-02	1.0000
HGIvsCNTRL	Acessible in CNTRL ICM	Chop(bZIP)/MEF-Chop-ChIP-	1,00E-04	0.0165
		Atf4(bZIP)/MEF-Atf4-ChIP-	1,00E-04	0.0183
		AARE(HLH)/mES-cMyc-ChIP-Seq/Homer	1,00E-03	0.1485
		HLF(bZIP)/HSC-HLF.Flag-ChIP-	1,00E-03	0.1485
		CEBP:CEBP(bZIP)/MEF-Chop-ChIP-Seq(GSE35681)/Homer	1,00E-03	0.1485
HGIvsCNTRL	Acessible in HGI TE	NFY(CCAAT)/Promoter/Homer	1,00E-02	1.0000
		NRF1(NRF)/MCF7-NRF1-ChIP-Seq(Unpublished)/Homer	1,00E-02	1.0000
		Tbx21(T-box)/GM12878-TBX21-ChIP-Seq(Encode)/Homer	1,00E-02	1.0000
		E2F6(E2F)/Hela-E2F6-ChIP-	1,00E-02	1.0000
		TOD6?/SacCer-Promoters/Homer	1,00E-02	1.0000
HGIvsCNTRL	Acessible in CNTRL TE	DUX4(Homeobox)/Myoblasts-DUX4.V5-ChIP-Seq(GSE75791)/Homer	1,00E-03	0.7011
		ARE(NR)/LNCAP-AR-ChIP-	1,00E-02	1.0000
		Rfx1(HTH)/NPC-H3K4me1-ChIP-Seq(GSE16256)/Homer	1,00E-02	1.0000
		Duxbl(Homeobox)/NIH3T3-Duxbl.HA-ChIP-Seq(GSE119782)/Homer	1,00E-02	1.0000
		CUX1(Homeobox)/K562-CUX1-ChIP-Seq(GSE92882)/Homer	1,00E-02	1.0000

RESUME SUBSTANTIEL DE LA THESE EN FRANÇAIS

La prévalence mondiale des maladies métaboliques telles que le diabète de type 2 ne cesse d'augmenter. De plus, près de la moitié des personnes atteintes d'un diabète de type 2 ne sont pas diagnostiquées et, par conséquent, ne sont pas traitées. Cette prévalence croissante a pour conséquence qu'un plus grand nombre de femmes entament leur grossesse avec une mauvaise santé métabolique. Les premiers signes de déséquilibres métaboliques, souvent asymptomatiques, tels que l'hyperglycémie et/ou l'hyperinsulinémie, sont de plus en plus fréquents chez les femmes en âge de procréer. En 2021, la Fédération Internationale du Diabète a établi qu'une naissance sur six était affectée par une hyperglycémie pendant la grossesse.

Le concept des origines développementales de la santé et des maladies (DOHaD pour *Developmental Origins of Health and Disease*) souligne que les expositions à des perturbations de l'environnement, telles qu'un statut métabolique maternel dérégulé pendant des étapes critiques du développement, sont associées à des conséquences à court et à long terme chez la progéniture, avec notamment un risque accru de maladies à l'âge adulte (non-transmissibles à la descendance). De nombreuses études épidémiologiques chez l'humain et sur des modèles animaux ont étayé le concept de DOHaD. Ces études ont surligné des fenêtres de développement critiques et particulièrement sensibles aux perturbations de l'environnement. L'une de ces fenêtres correspond à la période préimplantatoire.

L'embryon préimplantatoire est particulièrement sensible aux perturbations de son environnement. Au cours des premiers jours du développement, l'embryon suit une série d'événements clés dont la régulation fine implique des mécanismes épigénétiques. Ces événements incluent la reprogrammation des génomes parentaux pour donner lieu à un embryon totipotent, l'activation transcriptionnelle du génome embryonnaire, et de la première spécification de lignages qui aboutit à la définition de la masse cellulaire interne (MCI) et du trophectoderme (TE), respectivement progéniteurs de l'embryon proprement dit et du futur placenta.
Le développement précoce couvre la fenêtre de temps au cours de laquelle l'embryon progresse de l'oviducte à l'utérus où il s'implantera. Pendant cette période, l'embryon est donc entouré du fluide oviductal puis du fluide utérin, fluides qui fournissent tous les nutriments nécessaires au développement de l'embryon, notamment les substrats énergétiques comme le glucose et les facteurs de croissance comme l'insuline. La composition de ces fluides est directement influencée par le statut nutritionnel et métabolique maternel. Par conséquent, une composition altérée de cet environnement, comme cela a été démontré dans les modèles animaux de diabète, peut impacter le développement préimplantatoire. De la même manière, les défis nutritionnels tels qu'une sous- et surnutrition, et les techniques d'assistance médicale à la procréation (AMP) ont démontré que l'embryon préimplantatoire est sensible à son environnement, et qu'une perturbation de ce dernier peut déclencher une série de réponses moléculaires et cellulaires, réponses qui peuvent contribuer à un phénotype altéré au cours de la vie pré- et post-natal et à un risque accru de maladies à l'âge adulte. L'utilisation des modèles animaux a notamment mis en évidence que la perturbation de la période préimplantatoire exclusivement est suffisante pour induire des adaptations irréversibles et de longue durée conduisant à une prédisposition de maladies à l'âge adulte.

Le diabète prégestationnel, c'est-à-dire le diabète manifeste avant la conception, est associé à des complications et des effets délétères sur le nouveau-né tels que des malformations, une macrosomie fœtale, une hypoglycémie et un poids élevé à la naissance, ainsi qu'à un risque accru de maladies métaboliques telles qu'une obésité et/ou un diabète de type 2 à l'âge adulte. Plus le contrôle glycémique est mauvais pendant la grossesse, spécialement au cours du premier trimestre, plus les effets indésirables pourront être présents chez le nouveau-né.
Au cours des premiers jours de grossesse, le développement préimplantatoire a lieu. Pendant cette période, les femmes ne sont pas encore conscientes de leur grossesse. Par conséquent, les femmes ayant une mauvaise santé métabolique ne peuvent pas bénéficier des interventions nécessaires, exposant ainsi l'embryon précoce à un environnement métabolique altéré.

Les mécanismes par lesquels l'hyperglycémie et/ou l'hyperinsulinémie peuvent impacter le développement préimplantatoire et contribuer à la programmation n'ont pas encore été complètement élucidés. Ainsi, les modèles animaux, en particulier les stratégies de culture d'embryons *in vitro*, offrent une bonne opportunité d'étudier les effets de l'hyperglycémie et/ou de l'hyperinsulinémie exclusivement pendant la période préimplantatoire.

L'objectif de cette thèse était d'étudier les effets d'une exposition à un taux élevé de glucose et/ou d'insuline pendant le développement préimplantatoire. Nous avons choisi d'utiliser l'embryon précoce de lapin car son développement préimplantatoire est proche de celui de l'humain.
Ainsi, des embryons de lapin prélevés au stade 1cellule ont été cultivés *in vitro* jusqu'au stade blastocyste dans des conditions contrôle (CNTRL), d'insuline élevée (HI pour *high insulin*), de glucose élevé (HG pour *high glucose*) ou de glucose élevé et d'insuline élevée (HGI pour *high glucose and high insulin*). Nous avons analysé la compétence développementale des embryons cultivés *in vitro,* et nous avons déterminé le nombre total de cellules au stade blastocyste.
Au cours du développement préimplantatoire, la MCI et le TE, progéniteurs du futur individu et du futur placenta, sont spécifiés et chaque lignage possède des signatures épigénétiques, transcriptomiques et métaboliques spécifiques. Afin d'évaluer les effets d'une exposition à un taux élevé de glucose et/ou d'insuline sur le programme d'expression génique de ces deux lignages, nous avons séparé la MCI et le TE et effectué une analyse transcriptomique par RNA-seq.
Ainsi, nous avons montré que l'exposition à un un taux élevé de glucose et/ou d'insuline sur le développement préimplantatoire chez le lapin a induit des réponses communes et spécifiques dans chaque lignage.

- Une supplémentation élevée en insuline pendant le développement préimplantatoire n'a pas impacté la compétence de développement ni le nombre total de cellules des blastocystes exposés. Cependant, des changements mineurs du transcriptome ont été identifiés dans la MCI et le TE. Les deux lignages exposés à une forte dose d'insuline ont montré des changements dans l'expression des gènes liés à la transcription,à la traduction, et à la phosphorylation oxydative. En outre, la MCI et le TE ont montré des changements transcriptomiques liés à la β-oxydation et à la signalisation de la voie NF-kB, respectivement.

- Une supplémentation élevée en glucose pendant le développement préimplantatoire a conduit à une augmentation de la formation de blastocystes et du nombre total de cellules. L'analyse

du transcriptome des deux lignages a montré des changements d'expression génique liés à la transcription, à la traduction, au cycle cellulaire, au métabolisme énergétique, plus précisément à la phosphorylation oxydative dans la MCI et à la glycolyse dans le TE, ainsi qu'à la signalisation de la voie NF-kB et WNT. En outre, la MCI a montré la surexpression de deux gènes impliqués dans le lignage trophoblastique, *GATA3* et *PLET1*, tandis que le TE a montré des changements transcriptomiques liés à la signalisation de la voie mTOR, à la régulation épigénétique et à la signalisation de la voie TGF-β. L'évaluation de la prolifération cellulaire et de l'apoptose dans ces deux lignages, déterminée respectivement par incorporation d'EdU et des analyses TUNEL, a montré deux réponses opposées. Une exposition à un taux élevée en glucose a entraîné une augmentation du nombre de cellules apoptotiques et une réduction du nombre de cellules en prolifération dans la MCI, tandis que le TE a montré une augmentation du nombre de cellules en prolifération et une réduction du nombre de cellules en apoptose.

- Une supplémentation élevée en glucose et en insuline pendant le développement préimplantatoire a entraîné une augmentation de la formation de blastocystes et du nombre total de cellules. L'analyse du transcriptome des deux lignages a révélé des changements dans l'expression des gènes liés à la transcription, à la traduction, au cycle cellulaire, à la phosphorylation oxydative, aux ROS et à la signalisation de la voie NF-kB. En outre, la MCI a montré la surexpression de deux gènes impliqués dans le lignage trophoblastique, *PEG10* et *PLET1*, tandis que le TE a montré des changements transcriptomiques liés à la voie de signalisation WNT. L'étude de la prolifération cellulaire et de l'apoptose dans ces deux lignages, évaluée par incorporation d'EdU et des analyses TUNEL, n'a pas montré de changements significatifs dans la MCI, alors que le TE a montré un nombre accru de cellules en prolifération.

Cette étude a donc démontré que les embryons préimplantatoires exposés à un taux élevé de glucose ou d'insuline, seul ou en combinaison, présentent des modifications du transcriptome d'une manière spécifiques du lignage. Globalement, les modifications du transcriptome identifiées dans la MCI et le TE suggèrent une altération du métabolisme énergétique, de la signalisation cellulaire et de l'homéostasie du nombre de cellules de l'embryon.

De façon intéressante, le transcriptome des embryons exposés à un taux de glucose élevé seul ou avec une insuline élevée a montré une expression altérée des gènes impliqués dans des mécanismes épigénétiques, en particulier dans le TE exposé à un taux de glucose élevé, tandis que la MCI a montré des changements suggérant une perturbation de la spécification de ce lignage.

Par conséquent, afin d'évaluer si un taux deglucose élevé seul ou en combinaison avec un taux élevé d'insuline peut entrainer des modifications du paysage épigénétique de la MCI et du TE des embryons exposés, nous avons évalué l'accessibilité de la chromatine par ATAC-seq.

Nous avons d'abord établi un protocole d'ATAC-seq mieux adapté au modèle d'étude, protocole qui a ensuite été utilisé pour évaluer l'accessibilité de la chromatine de la MCI et du TE des embryons exposés aux conditions HG, HGI et CNTRL.

Ainsi, nous avons montré que l'exposition à une un taux élevé de glucose seul ou en combinaison avec l'insuline élevée a induit des réponses communes et spécifique dans la MCI et le TE des embryons exposés.

- Une supplémentation élevée en glucose dans la MCI a induit un gain en accessibilité chromatinienne au sein des promoteurs des gènes impliqués dans la signalisation cellulaire, le transport des ions et des protéines, les processus de biosynthèse et le développement. Par contre, le TE des embryons exposés a gagné et perdu de l'accessibilité chromatinienne dans le promoteur des gènes liés aux centromères des chromosomes et à la synthèse de la pseudouridine.

- Une supplémentation élevée en glucose et en insuline a induit dans la MCI le gain en accessibilité chromatinienne au sein des promoteurs des gènes impliqués dans le cycle cellulaire, la signalisation cellulaire, la régulation de l'expression génique, la réponse au stimulus, la réponse immunitaire et le métabolisme, et a perdu en accessibilité chromatinienne au sein des promoteurs des gènes impliqués dans la réparation de l'ADN, le métabolisme du glutathion et la régulation de l'expression génique. Le TE des embryons exposés a gagné en accessibilité chromatinienne au niveau des promoteurs des gènes associés à la régulation de l'expression génique, à l'assemblage des nucléosomes, à la réplication de l'ADN, à la macromitophagie et aux modifications post-traductionnelles des protéines, et a perdu l'accessibilité chromatinienne des promoteurs des gènes associés à l'activité mitochondriale, au métabolisme, au cycle cellulaire, à la régulation de l'expression génique, à la régulation de la pression artérielle systémique, au développement, à la réponse immunitaire et à l'adhésion cellulaire.

- Un taux élevé de glucose, seul ou combiné à une insuline élevée, a entraîné des modifications de la chromatine spécifiques à chaque lignage, avec plutôt une " ouverture " dans la MCI et une " fermeture " dans le TE pour certaines régions régulatrices de la chromatine.

- L'exposition à un taux élevé de glucose et d'insuline entraîne un nombre plus élevé de régions chromatiniennes différentiellement accessibles dans la MCI et le TE par rapport à la condition HG.

- Parmi les régions chromatiniennes différentiellement accessibles identifiées dans chaque lignage, seules quelques-unes correspondaient à des gènes annotés et donc plusieurs de ces régions restent à être identifiées.

L'ensemble de ces résultats a donc montré qu'une forte dose d'insuline entraîne des modifications mineures de l'expression génétique dans la MCI et le TE des embryons exposés. En revanche, un taux élevé de glucose seul ou en combinaison avec un taux élevé d'insuline entraîne une série de réponses communes et spécifiques à chaque lignage au niveau de la régulation de la chromatine, de l'expression génique et de l'homéostasie du nombre de cellules. Les changements transcriptomiques et chromatiniens étaient associés aux voies métaboliques, à l'homéostasie du nombre de cellules, à la signalisation cellulaire, aux réponses au stress cellulaire, à l'engagement de la lignée dans la MCI et à la régulation de l'expression génétique. Il est intéressant de noter que, bien que l'analyse du transcriptome ait révélé que le TE des embryons exposés à un taux élevé de glucose présentait une expression altérée d'un sous-ensemble de gènes impliqués dans la régulation épigénétique, le profil d'accessibilité de la chromatine a révélé qu'un taux élevé de glucose et d'insuline entraînait des changements plus radicaux dans le paysage chromatinien accessible dans la MCI et le TE des embryons exposés. Au niveau cellulaire,

seul le glucose élevé a entraîné une augmentation de l'apoptose dans la MCI et de la prolifération dans le TE. Cependant, en combinaison avec l'insuline élevée, seul le TE a montré une prolifération cellulaire accrue. Les différents résultats décrits ici soulèvent plusieurs questions pour des études futures qui pourraient contribuer à une compréhension plus complète des mécanismes mis en place par la MCI et le TE pour s'adapter à des environnements riches en glucose et/ou en insuline.

Enfin, notre travail met en évidence la façon dont la perturbation du microenvironnement préimplantatoire par un taux élevé de glucose et/ou d'insuline a un impact sur la masse cellulaire interne et le trophectoderme des embryons préimplantatoires, un impact qui pourrait compromettre le développement du futur individu et du placenta, et contribuer à la programmation dans la descendance.

COMMUNICATIONS

ORAL COMMUNICATIONS

Via y Rada, R., Daniel, N., Archilla, C., Aubert-Frambourg, A., Jouneau, L., Duranthon, V., Calderari, S. *"Impact d'un environnement (pré)-diabétique sur le développement embryonnaire précoce".* 5ème colloque de la Société Francophone pour la recherche et l'éducation sur les Origines Développementales, Environnementales et Epigénétiques de la Santé et des Maladies (SF-DOHaD). November 17-19, 2021. Jouy-en-Josas, France [Online]

Via y Rada, R., Daniel, N., Archilla, C., Aubert-Frambourg, A., Jouneau, L., Duranthon, V., Calderari, S. *"Epigenetic programming of the rabbit preimplantation embryo in a diabetic context".* Domestic Animal DOHaD & Epigenetics Meeting (DADE). October 12-13, 2021, Québec City, Canada [Online]

Via y Rada, R., Daniel, N., Archilla, C., Aubert-Frambourg, A., Jouneau, L., Duranthon, V., Calderari, S. *"Impact d'un environnement diabétique sur le développement embryonnaire précoce".* Congrès de la Société Francophone du Diabète (SFD). March 23-26, 2021, Marseille, France. [Online]

POSTERS

Via y Rada, R., Daniel, N., Archilla, C., Aubert-Frambourg, A., Jouneau, L., Duranthon, V., Calderari, S. *"Metabolic environment and epigenetic programming of the early embryo in rabbit".* Biosigne doctoral school day. November 19, 2019. Paris, France.

Via y Rada, R., Daniel, N., Archilla, C., Aubert-Frambourg, A., Jouneau, L., Duranthon, V., Calderari, S. *"Metabolic environment and epigenetic programming of the early embryo in rabbit".* Young Researchers symposium. March 28 2019. Jouy-en-Josas, France.

Via y Rada, R., Daniel, N., Archilla, C., Aubert-Frambourg, A., Jouneau, L., Duranthon, V., Calderari, S. *"Metabolic environment and epigenetic programming of the early embryo in rabbit".* Epigenetics: Physics of the nucleus 15th edition international course, Institut Curie, March 14-15, 2019. Paris, France.